Title

Determining the Origin of Functional Group Compatibility of the Iridium Trisboryl Complex

ISBN

9798293893546

Author

Guo, Xuelei

Publication Date

2025-08-01

Peer reviewed|Thesis/dissertation

Determining the Origin of Functional Group Compatibility of the Iridium Trisboryl Complex

by

Xuelei Guo

A dissertation submitted in partial satisfaction of the

requirements for the degree of

Doctor of Philosophy

in

Chemistry

in the

Graduate Division

of the

University of California, Berkeley

Committee

Professor John F. Hartwig, Chair

Professor Brooks Abel

Professor Markita Landry

Summer 2025

Abstract

Determining the Origin of Functional Group Compatibility of the Iridium Trisboryl Complex

Xuelei Guo

Doctor of Philosophy in Chemistry

University of California, Berkeley

Professor John F. Hartwig, Chair

The following dissertation reveals the modes of reactivity of varying classes of organic compounds with the iridium trisboryl complex. The fundamental principles guiding these modes of reactivity are elucidated.

Chapter 1 first presents a high-yielding, pure, and most importantly, reliable synthesis of the iridium trisboryl complex, (COE)(dtbpy)Ir(Bpin)$_3$, which is the cornerstone for the entirety of the research. Then, the selectivity of a series of varying classes of organic compounds for coordination to either the iridium center or the Bpin ligand of the iridium trisboryl complex is presented, collectively, highlighting the fundamental principles which divide these classes into three main categories of reactivity: reactivity at iridium, reactivity at a Bpin ligand, and ambident reactivity. While these classes are evaluated via stoichiometric reactions with the iridium trisboryl complex, the corresponding catalytic reaction is compared against the stoichiometric reaction in key cases where a difference in selectivity is seen.

Chapter 2 extends the utility of the catalytic C—H borylation of arenes via a mild and facile deprotection of the boronic ester products into the corresponding boronic acids. Many boronic acid selective reactions (which do not function well with boronic esters as substrates) are discovered and successfully applied to the boronic ester products of the catalytic C—H borylation of arenes after their deprotection.

Table of Contents

CHAPTER 1: Determining the Origin of Functional Group Compatibility of the Iridium Trisboryl Complex

Acknowledgements

Throughout this journey, I have been very fortunate to have had the support of many wonderful people. Oftentimes, people inspire from afar but their impact is immense and forever. I chose chemistry because once upon a time it was a true joy learning quantum mechanics from Professor Birgitta Whaley, chemical biology from Professor Matt Francis, physical organic chemistry from Professor Bob Bergman, and thermodynamics from the late Professor Phil Geissler. I am grateful to have had as wonderful of an undergraduate advisor as Professor Richmond Sarpong who upheld a culture of enthusiasm and rigor. I am also grateful to Professor Viresh Rawal for his sincere support throughout the years.

I have known intimately and many times over that a specific environment can make or break you. It was in the nurturing, open and supportive environment of BMS that I kindled an interest in catalysis and developed as a chemist. I am so grateful to Dr. Jake Janey for being such an incredibly supportive and benevolent leader. Most of all, I am forever indebted to Dr. Eric Simmons for all the generosity he has shown me. In addition to being a model of passion, knowledge, and measured problem solving, Eric fostered an environment of freedom and understanding because of which my interests and abilities thrived.

I would like to sincerely thank Professor John F. Hartwig for his support for the past four years. While it is easy to support someone when things are going well, John has been a source of support during challenging times. He has shown a vested interest in my progress as a graduate student and in my development as a chemist. Consistently, he has been an example of integrity when it comes to experimental design and critical thinking. I'm grateful to have a PI who has always made himself available and who pushes for the advancement of my career.

To my lab mates (and friends) who have shown me infinite support, inspiration, and laughs I would like to thank Dr. Jason Ma, Dr. Isaac Yu, Dr. Christina Pierson, Dr. John Brunn, Dr. Jeremy Nicolai, Dr. Takahiro Suto, Chris La, Sukriyo Chakraborty, Andrew Quest, Gabe Herrera, Yi Cheng Kang, Dr. Willi Amberg, Dr. Ian Rinehart, Dr. Molly McFadden, and certainly the group at large. I would also like to thank the members of my qualifying committee and dissertation committee for their time and support: Professors Dean Toste, Tom Maimone, Brooks Abel, Clayton Radke and Markita Landry. I am enormously grateful to Dr. Tim Boller for the discussions and advice on the synthesis of the iridium trisboryl complex.

Most importantly, I would like to thank my parents. They have made every sacrifice for me and with them I share every instance of achievement, joy and growth. Lastly, to my beloved art form, thank you for the greatest joy of my life, helping me through the tougher times, and providing me with a very clear identity when I had otherwise felt lost.

CHAPTER 1: Determining the Origin of Functional Group Compatibility of the Iridium Trisboryl Complex

1.1 Introduction

The C—H activation and borylation of arenes is a well-established methodology of high synthetic value.[1,2,3,4] It is ubiquitous in the chemistry community with widespread use in both academic and industrial settings.[5,6] The first mild catalytic system to enable the efficient borylation of simple arenes was achieved in 2002, employing an Ir/dtbpy system[7] (although the first catalytic system for the C—H borylation of arenes was achieved in 1999, employing a $Cp^*Ir(PMe_3)(H)(Bpin)$ catalyst with a high reaction temperature of 150 °C)[8]. It was also at this time that the COE-capped catalyst for the reaction was isolated (Figure 1.1). As such, this publication marked important first steps for the reaction from both a methodological as well as mechanistic stance.

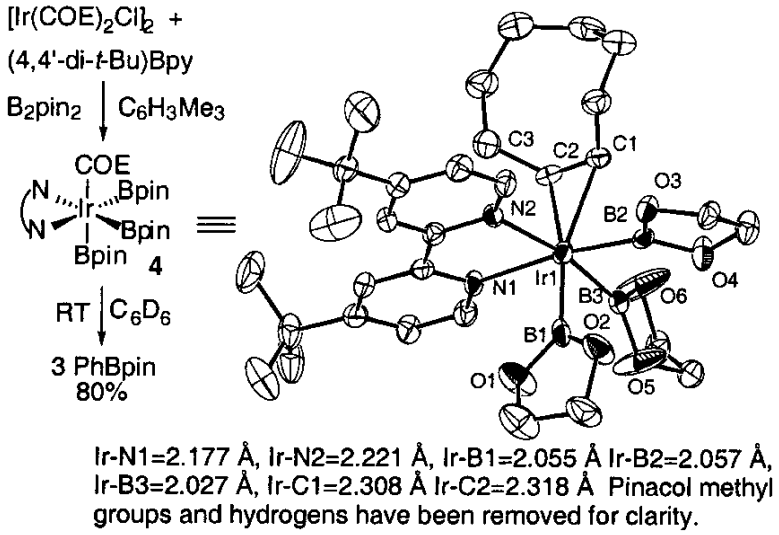

Figure 1.1 Crystal structure of the COE-capped iridium trisboryl complex[7]; Reprinted (adapted) with permission from J. Am. Chem. Soc. 2002, 124, 3, 390–391. Copyright 2002 American Chemical Society

In 2005, Boller and coworkers conducted kinetic studies to reveal the currently accepted reaction mechanism of an Ir(III)/Ir(V) cycle (Figure 1.2).[9] The active catalyst, $(dtbpy)Ir(Bpin)_3$, can either be generated in-situ from the standard catalytic conditions employing $[Ir(COD)X]_2$/ligand/B_2pin_2 (Figure 1.4) or from the dissociation of COE from the independently synthesized iridium trisboryl complex $(dtbpy)Ir(COE)(Bpin)_3$. Oxidative addition of a $C(sp^2)$—H bond generates the 7-coordinate intermediate $(dtbpy)Ir(Ar)(H)(Bpin)_3$. Subsequent reductive elimination furnishes the ArBpin product and $(dtbpy)Ir(Bpin)_2H$. Then, oxidative addition of B_2pin_2 followed by reductive elimination of HBpin regenerates the active catalyst.

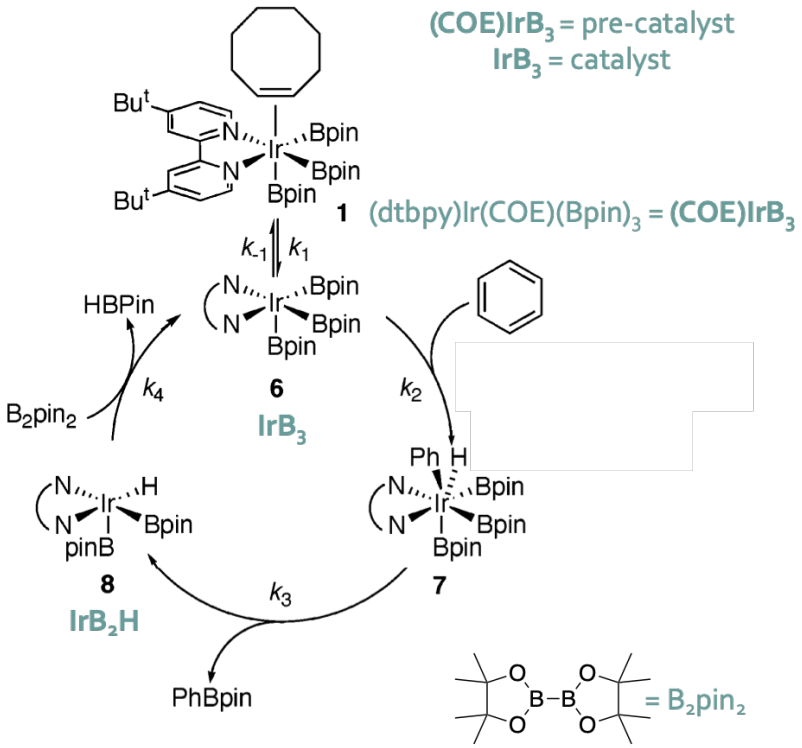

Figure 1.2 Mechanism of arene borylation[9]; Reprinted (adapted) with permission from J. Am. Chem. Soc. 2005, 127, 41, 14263–14278. Copyright 2005 American Chemical Society

Since the 2002 seminal publication, and for the next two decades, two Ir(III) systems have been established for undirected arene borylation: (dtbpy)Ir(III) and (tmphen)Ir(III) (Figure 1.3).[10] Complementary to these Ir(III) systems which select for sterically free sites, Furukawa and Chatani and coworkers developed a [Pt(NHC)] catalyst which selects for sterically congested sites.[11] While both Ir(III) systems are high performing and commonly used, for some substrates (tmphen)Ir(III) is superior. The origin of this difference was elucidated in 2019 by Oeschger and coworkers.[10] They demonstrated that tmphen binds tighter to Ir than does dtbpy. For slow reacting arenes, dtbpy dissociates from Ir before 100% conversion of the arene to its borylated product. Moreover, the free dtbpy itself can also be borylated resulting in catalyst deactivation.

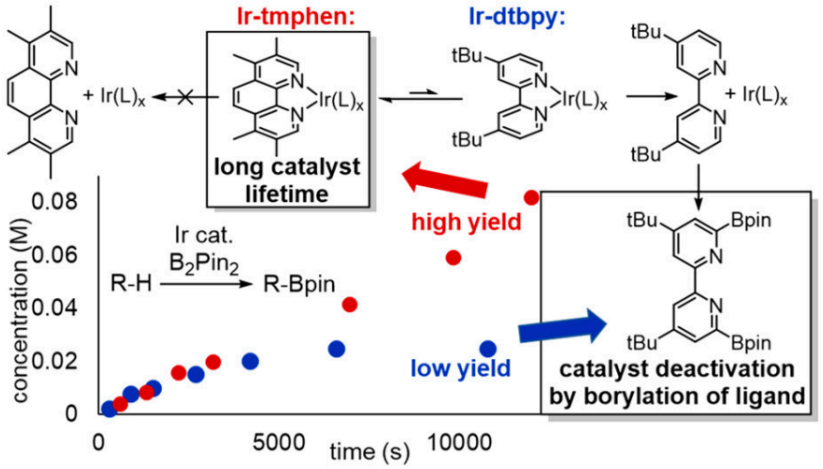

Figure 1.3 Catalyst lifetime: Ir-tmphen versus Ir-dtbpy[10]; Reprinted (adapted) with permission from J. Am. Chem. Soc. 2019, 141, 41, 16479–16485. Copyright 2019 American Chemical Society

In 2014, Larsen and Hartwig evaluated the methodology against several classes of heteroarenes spanning benzoxazoles, benzothiazoles, pyrimidines, benzimidazoles (Figure 1.4), pyrazoles and azaindoles.[12] A combination of empirical and mechanistic evaluations led to the establishment of a general set of rules for the regioselectivity of the borylation of different heteroarenes (Figure 1.5). Certain regioselectivity rules for heteroarenes mimic those for simple arenes: borylation selects for sterically free sites[11] and for C—H bonds of increased acidity.

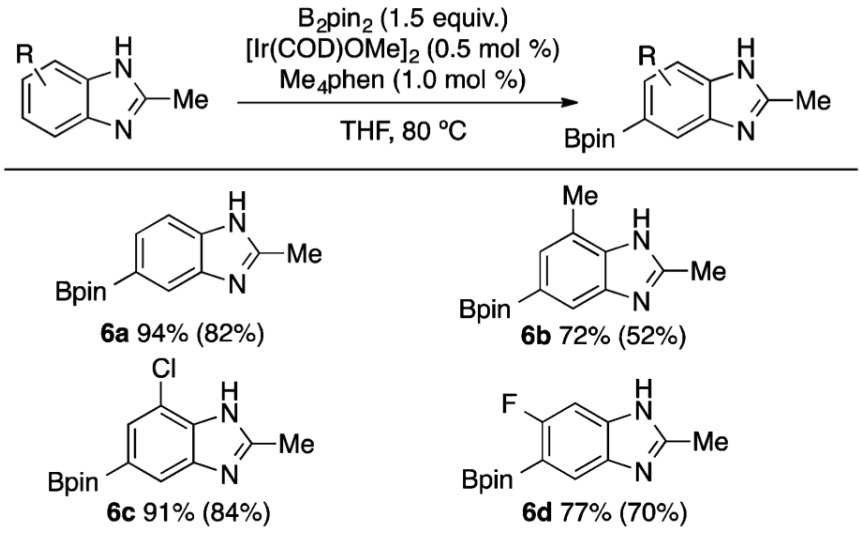

Figure 1.4 C—H borylation of benzimidazoles[12]; Reprinted (adapted) with permission from J. Am. Chem. Soc. 2014, 136, 11, 4287–4299. Copyright 2014 American Chemical Society

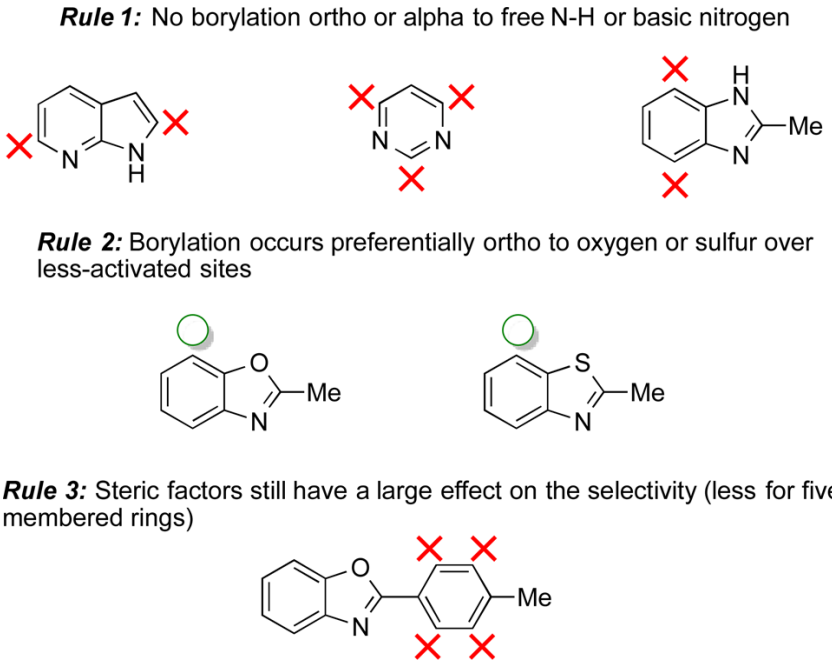

Figure 1.5 Regioselectivity rules for C—H borylation[12]; Reprinted (adapted) with permission from J. Am. Chem. Soc. 2014, 136, 11, 4287–4299. Copyright 2014 American Chemical Society

Larsen and Hartwig conducted kinetic studies to determine the rate equation for the reaction of 3-methylpyridine.[12] They revealed a zero-order dependence in 3-methylpyridine which contrasts the first-order dependence in arene previously determined by Boller[9]. As such, 3-methylpyridine was proposed to react via an alternative mechanism whereby the nitrogen atom of 3-methylpyridine binds to the iridium center of the iridium trisboryl complex to make for a (3-methylpyridine)(dtbpy)Ir(Bpin)$_3$ resting state which, upon dissociation from the iridium center and rearrangement to a C—H σ-complex, can undergo the turnover-limiting C—H activation (oxidative addition) (Figure 1.6).

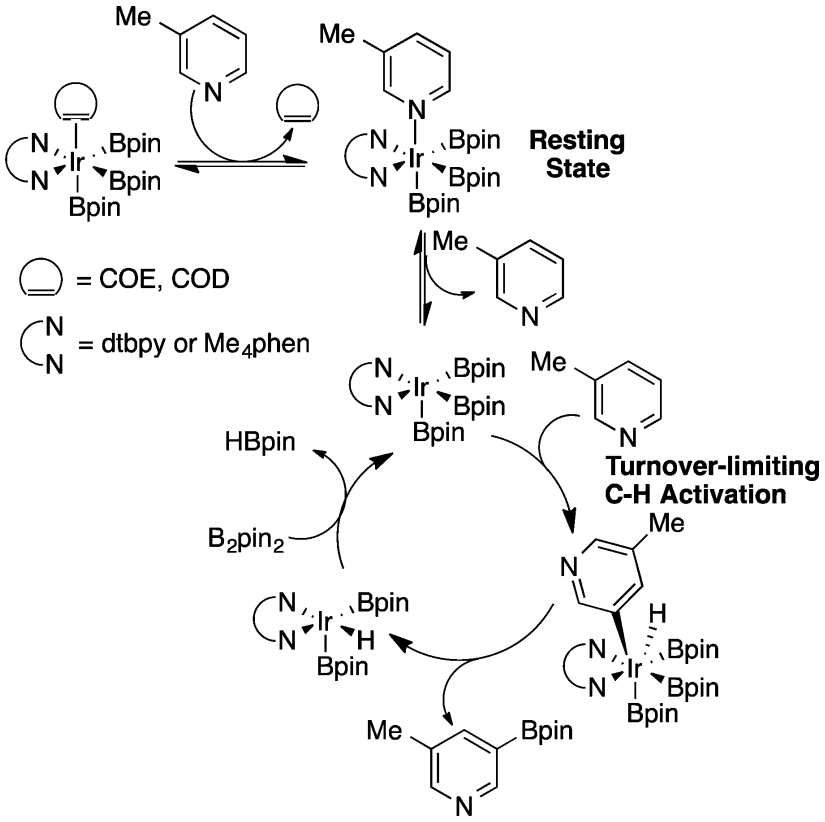

Figure 1.6 Proposed mechanism for the borylation of 3-methylpyridine[12]; Reprinted (adapted) with permission from J. Am. Chem. Soc. 2014, 136, 11, 4287–4299. Copyright 2014 American Chemical Society

At present, a mild and robust catalytic reaction is in place for the borylation of a variety of arenes and heteroarenes. The mechanism of arene borylation is well-established, and empirical rules have been delineated for regioselectivity. In an effort to fortify the methodology in the course of complex molecule synthesis, Hamel and Hartwig subjected the reaction to a robustness screen developed by Glorius[13] (unpublished, Figure 1.7). Arene and heteroarene borylations were conducted in the presence of varying classes of small molecules that mimic functional groups present on a complex molecule as it undergoes arene borylation (Figure 1.7). The Glorius robustness screen revealed many classes of compounds not tolerated by the arene borylation reaction (unpublished, Figure 1.8). Clearly, compounds other than arenes and heteroarenes react with the iridium trisboryl complex. Understanding the mechanism by which different classes of compounds react with the iridium trisboryl complex may reveal the fundamental principles for the functional group compatibility of the iridium trisboryl complex.

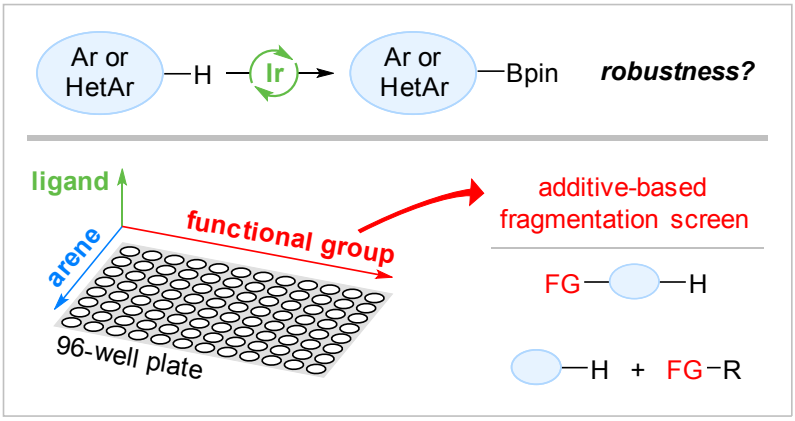

Figure 1.7 Glorius robustness screen for C—H borylation

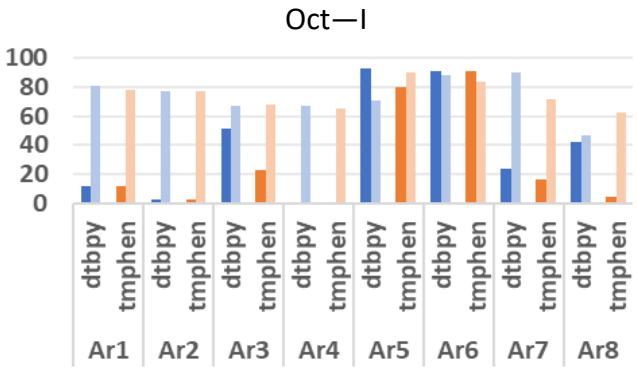

Figure 1.8 Representative Glorius robustness screen result for additive = octyliodide

1.2 Results and Discussion

1.2.1 Simplified, Reproducible and High-Yielding Large-Scale Synthesis of the Purified Iridium Trisboryl Complex (dtbpy)Ir(Bpin)$_3$ [IrB$_3$]

In 2005, Boller and co-workers reported the gram-scale synthesis of the COE-capped iridium trisboryl complex [IrB$_3$] (62% yield), as well as its purification (in 20% yield) for kinetic studies.[9] While an instrumental stepping stone for enabling stoichiometric experiments, this synthesis proved challenging to reproduce. The 20% yield of the purified material highlights both the amount of impurities present from the synthesis and the difficulty in separating the iridium trisboryl complex from these impurities.

In their work, Boller and co-workers evaluated several syntheses in order to find one whose order of addition provided the fewest impurities. In this work, practical improvements were implemented to further decrease impurity formation. Boller's synthesis employed mildly increased temperature (40 °C) for 20 minutes for the reaction which necessitated removal from the inert atmosphere of a glovebox and careful adaptation to an inert system outside the glovebox for heating. Instead, allowing the reaction to progress at ambient temperature inside the glovebox overnight obviates the risk of oxygen exposure from glovebox removal as well as

the risk of impurities formation at elevated temperature while ensuring full reaction completion with extended reaction time.

Boller's synthesis also made extended use of elevated temperatures (40 °C) for concentration of the reaction mixture. Here, the reaction mixture was concentrated at ambient temperature under vacuum and then allowed to sit in an open vessel overnight inside the glovebox to ensure full evaporation of residual solvent. For purification, Boller and co-workers used a series of cold (-30 °C) pentane and tetramethylsilane washes. In this work, it was found that cold (-30 °C) or ambient temperature washes of pentane or tetramethylsilane were equally effective or ineffective depending on the yield of the reaction. A high yielding reaction (75%), which is reliably obtained in this modified synthesis, only necessitated ambient temperature washes with tetramethylsilane, albeit with exhaustive amounts (100 mL employed for a gram-scale synthesis). The pure iridium trisboryl complex (a bright yellow powder, Figure 1.9) does not dissolve in tetramethylsilane. Because impurities increase the solubility of the iridium trisboryl complex in tetramethylsilane, any low-yielding reaction has proven nearly impossible to purify, even with Boller's purification at low temperatures.

Boller's work laid the foundation for the synthesis of the iridium trisboryl complex. Although the modifications made in this work are largely practical, they are significant for the reliable synthesis of the iridium trisboryl complex and its use in stoichiometric reactions. The purified iridium trisboryl complex, a bright yellow powder, can be reproducibly obtained in high yield (75%) and high purity as evidenced by ^{1}H-NMR spectroscopy of the isolated material (Figure 1.9).

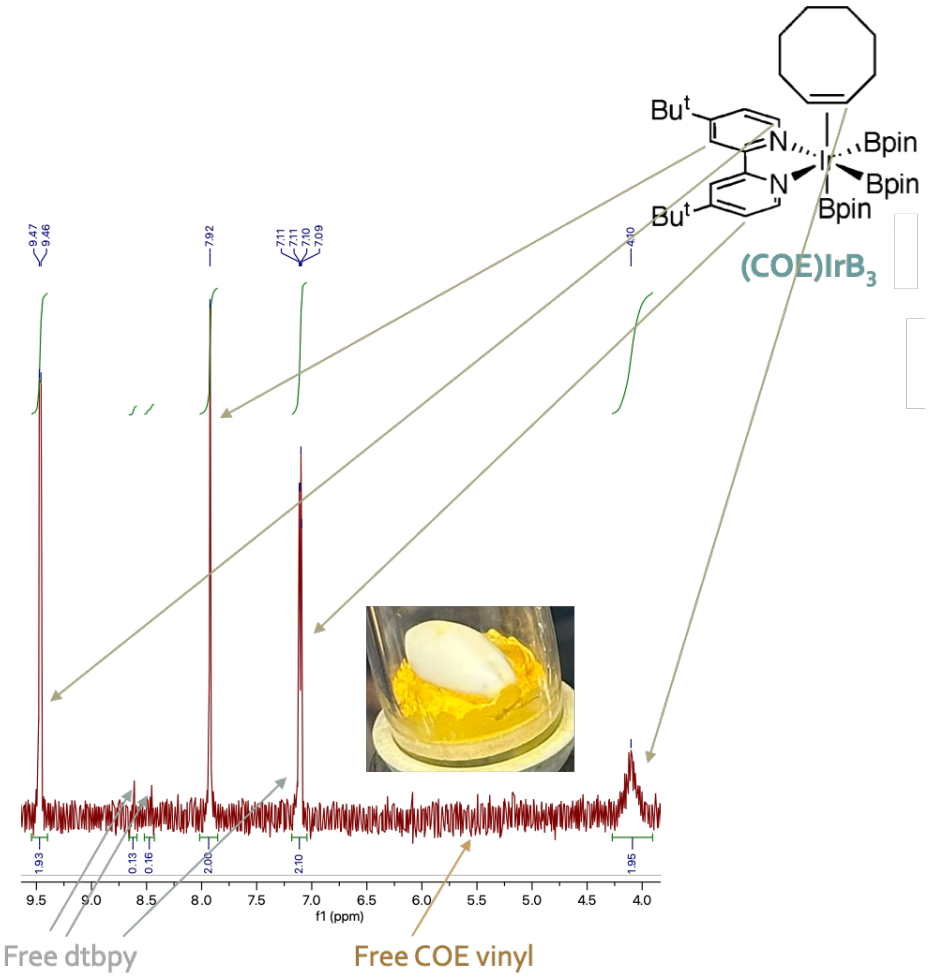

Figure 1.9 ^{1}H-NMR spectrum of the iridium trisboryl complex [IrB_3] at 25 °C

1.2.2 Characterization of (dtbpy)Ir(Bpin)$_2$H [IrB_2H] & (dtbpy)Ir(Bpin)H$_2$ [$IrBH_2$]

In their 2005 publication, Boller and coworkers also reported the ^{1}H-NMR spectroscopic characterization of iridium bisboryl monohydride and iridium monoboryl dihydride (Figure 1.10). The characterization was obtained from the stoichiometric reaction between the iridium trisboryl complex and 1,3-bis(trifluoromethyl)benzene at 0 °C. As such, the competency of both the iridium trisboryl complex as well as the iridium bisboryl monohydride as an intermediate in the borylation of arenes was demonstrated.

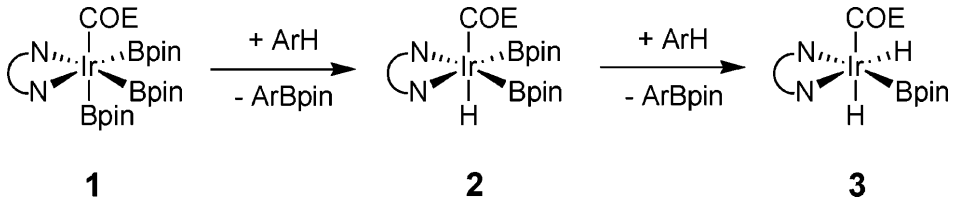

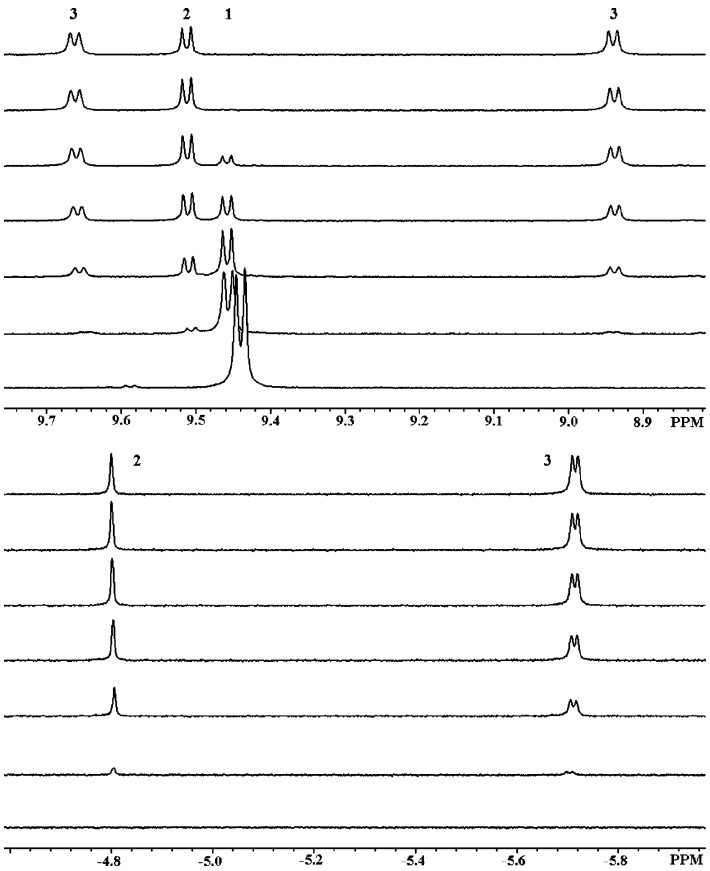

Figure 1.10 ^{1}H-NMR spectrum of (dtbpy)Ir(Bpin)$_3$, (dtbpy)Ir(Bpin)$_2$H and (dtbpy)Ir(Bpin)H$_2$ at 0 °C[9]; Reprinted (adapted) with permission from J. Am. Chem. Soc. 2005, 127, 41, 14263–14278. Copyright 2005 American Chemical Society

In this work, a clearer ^{1}H-NMR spectroscopic characterization of the iridium bisboryl monohydride was obtained, one in which the iridium bisboryl monohydride was the major component of the reaction mixture (Figure 1.11). This characterization was obtained during the stoichiometric reaction between the iridium trisboryl complex and nitrocyclopentane. Because nitrocyclopentane reacts more slowly than 1,3-bis(trifluoromethyl)benzene with the iridium trisboryl complex, the characterization of the iridium bisboryl monohydride was able to be conducted at 25 °C.

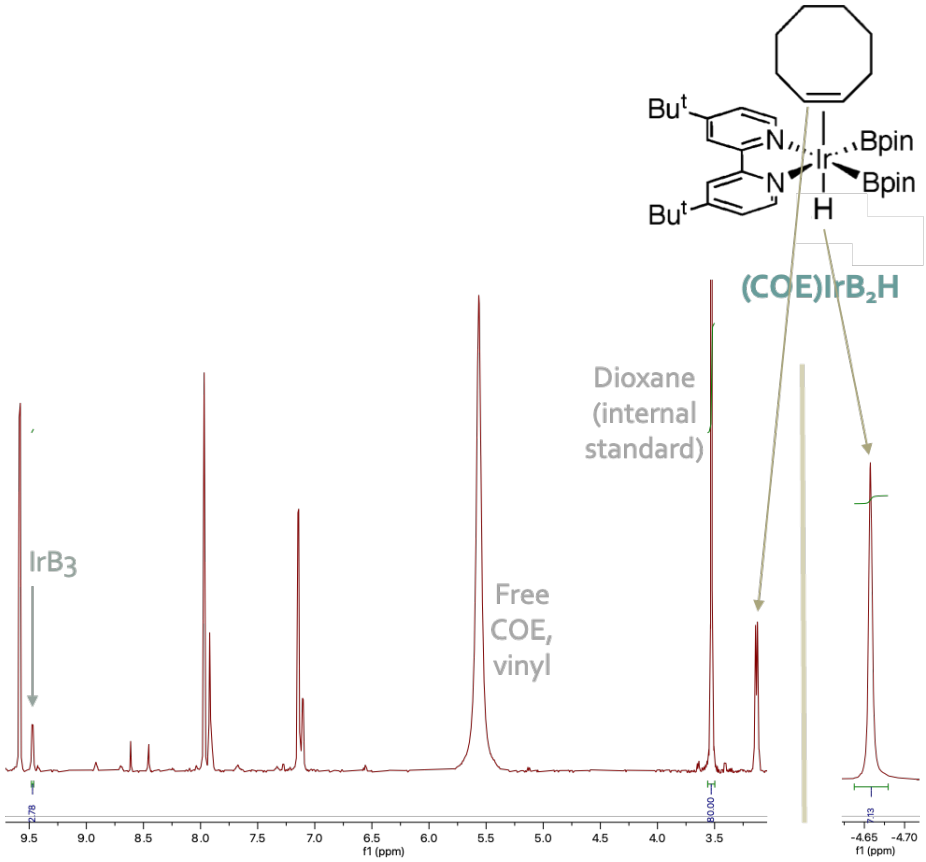

Figure 1.11 ^{1}H-NMR spectrum of (dtbpy)Ir(Bpin)$_2$H at 25 °C

The iridium monoboryl dihydride was generated from the stoichiometric reaction between the iridium trisboryl complex (less than 1 equivalent) and boc-pyrazole in the presence of an added 5 equivalents of COE and was characterized at 25 °C by ^{1}H-NMR spectroscopy (Figure 1.12). In the course of the borylation of boc-pyrazole, upon full consumption of the iridium trisboryl complex, the iridium bisboryl hydride byproduct becomes the borylating agent, generating the iridium monoboryl dihydride byproduct. During the course of this work, it was commonly observed that the iridium bisboryl monohydride gradually decomposed but that it is more stable in the presence of a higher concentration of COE. The added 5 equivalents of COE maintain a higher concentration of the iridium bisboryl monohydride so that a higher concentration of the iridium monoboryl dihydride byproduct is formed upon reaction of the bisboryl monohydride with boc-pyrazole.

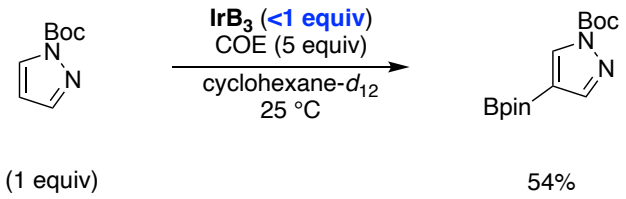

(1 equiv)

54%

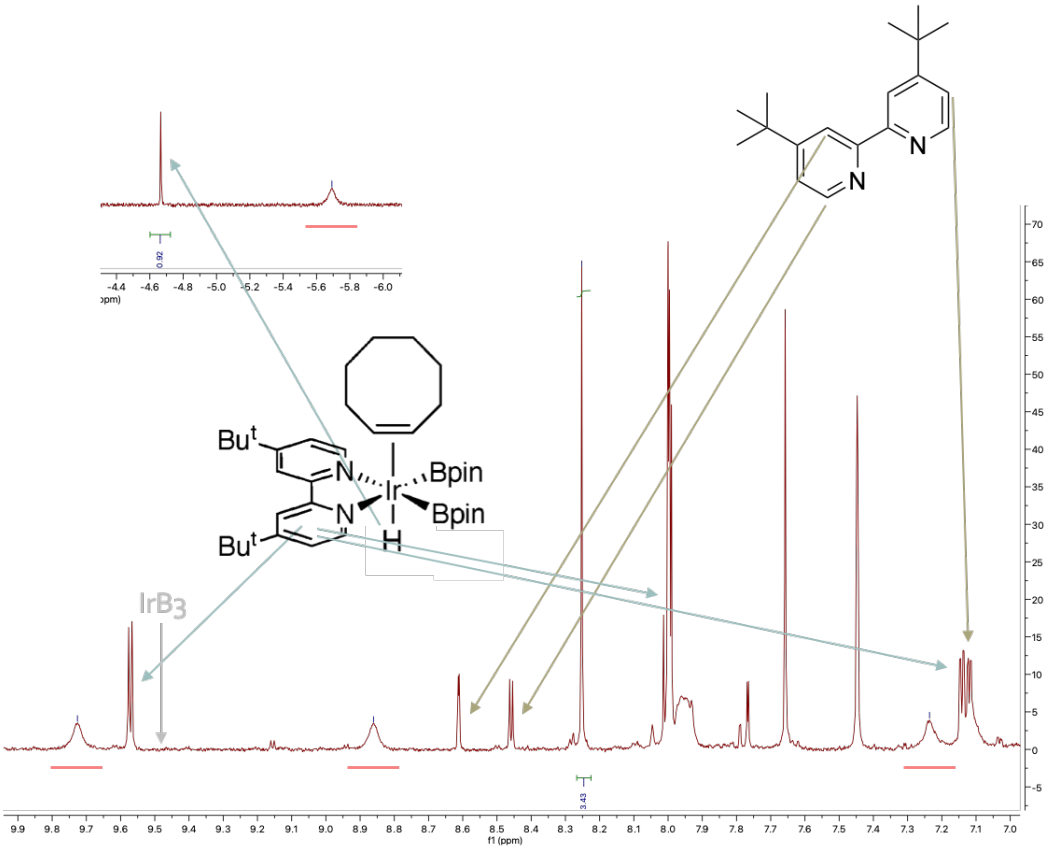

Figure 1.12 ^{1}H-NMR spectrum of (dtbpy)Ir(Bpin)H_2 (broad peaks underlined in red) at 25 °C

Gaining evidence for the iridium bisboryl monohydride and the iridium monoboryl dihydride by ^{1}H-NMR spectroscopy at 25 °C is important because the majority of the stoichiometric reactions in this study are conducted at 25 °C.

1.2.3 Reactivity at Bpin Ligand

1.2.3.1 Primary Alcohols, Amines and Thiols

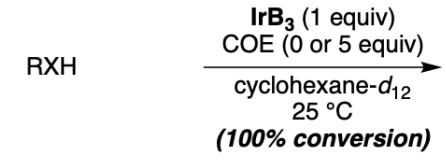

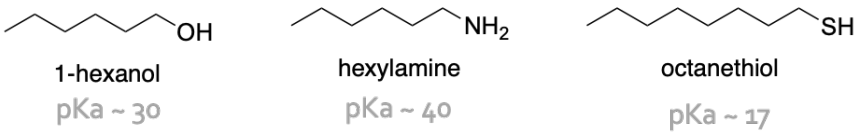

Figure 1.13 Borylation of RX—H bonds in the presence or absence of added COE (5 equiv). pKa of 1-hexanol approximated against the measured value of 29.8 for ethanol[14]. pKa of hexylamine approximated against the measured value of 41 for ammonia[15] and 44 for pyrrolidine[15]. pKa of octanethiol approximated against the measured value of 17.1 for butanethiol[16].

The reactivity of the iridium trisboryl complex is well-established to undergo oxidative addition of C—H bonds at the iridium center, leading to C—H functionalization.[9] In his 2005 publication, Boller showed that the borylation of 1,2-dichlorobenzene in the presence of added COE is slower than the borylation of 1,2-dicholorbenzene in the absence of added COE.[9] Added COE increases the concentration of the COE-bound iridium trisboryl complex and decreases the concentration of the active catalyst (non-COE-bound) that is competent for oxidative addition.

What had previously been unexplored is the case in which added COE does not affect the rate of borylation. Such a case is observed with primary alcohols, amines and thiols (Figure 1.13). With or without an added five equivalents of COE, primary alcohols (Figures 1.14 & 1.15), primary amines (Figures 1.16 & 1.17), and primary thiols (Figures 1.18 & 1.19) fully converted to their corresponding RX—Bpin products by the initial sampling (5 minutes). Therefore, whether the rate of borylation of primary alcohols, amines and thiols is affected by added COE needs to be determined at lower temperature.

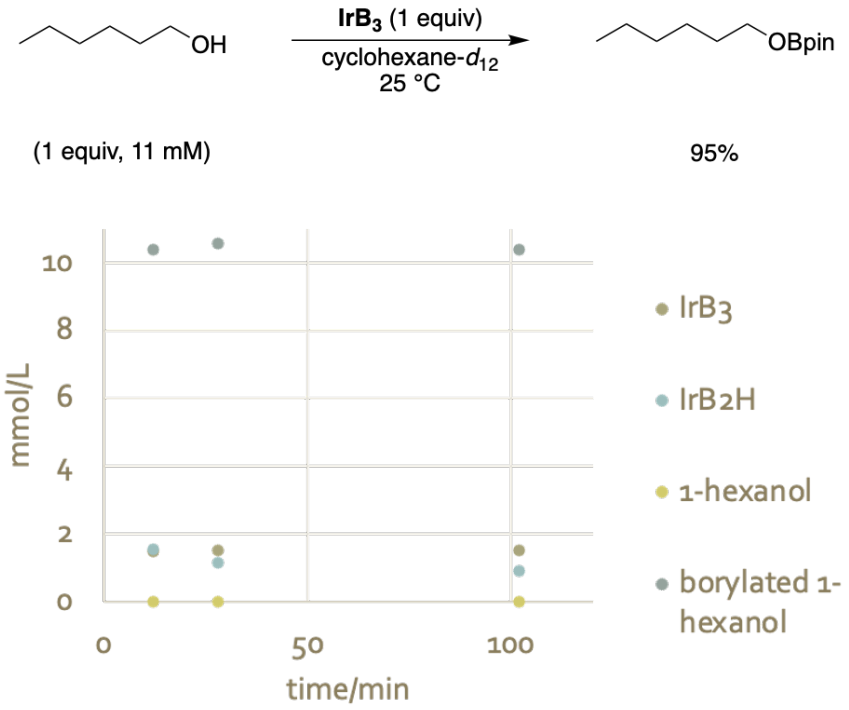

Figure 1.14 Borylation of 1-hexanol in the absence of added COE; IrB_3 = (dtbpy)(COE)Ir(Bpin)$_3$

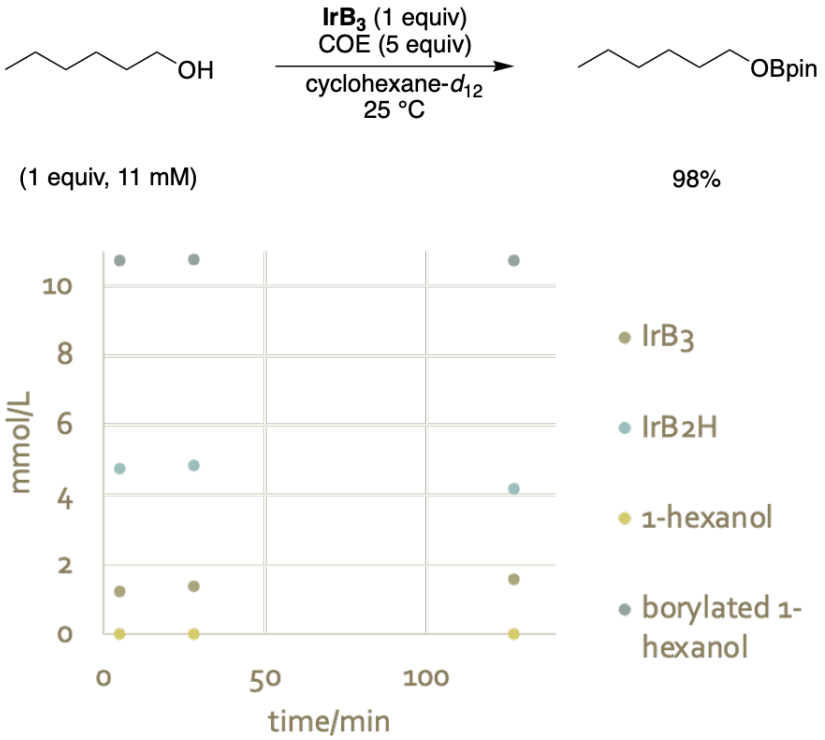

Figure 1.15 Borylation of 1-hexanol in the presence of added COE (5 equiv); IrB_3 = $(dtbpy)(COE)Ir(Bpin)_3$

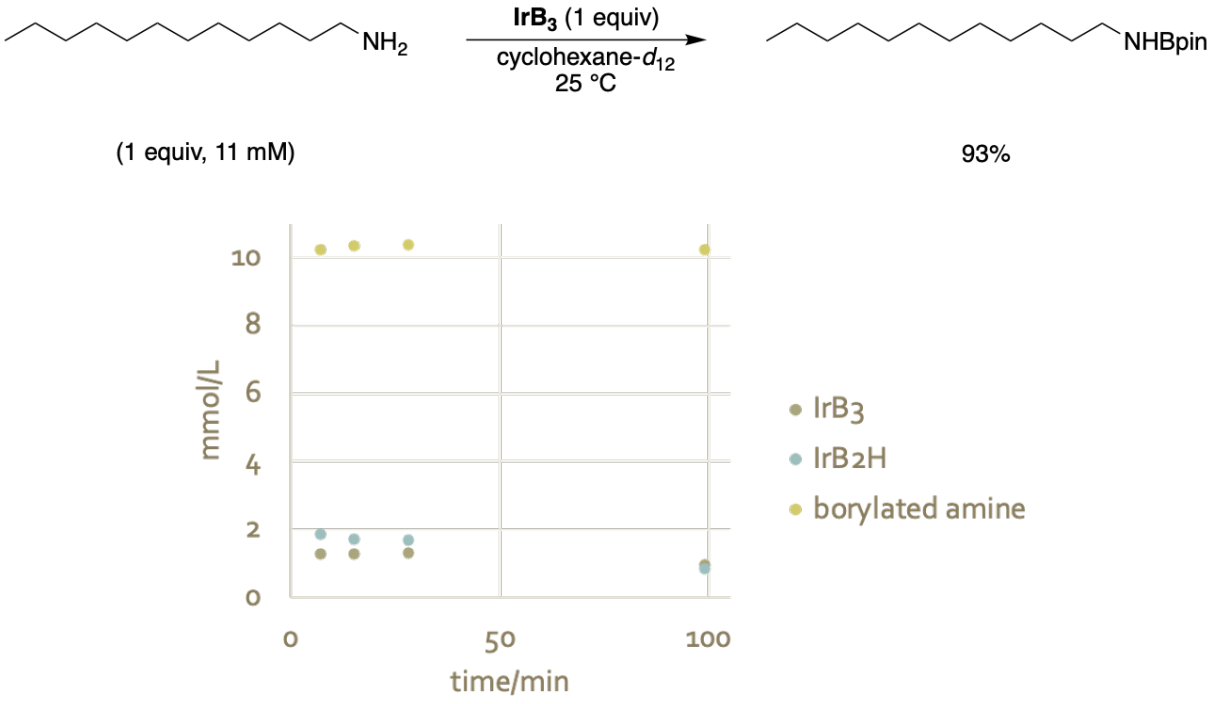

Figure 1.16 Borylation of dodecylamine in the absence of added COE; IrB_3 = $(dtbpy)(COE)Ir(Bpin)_3$

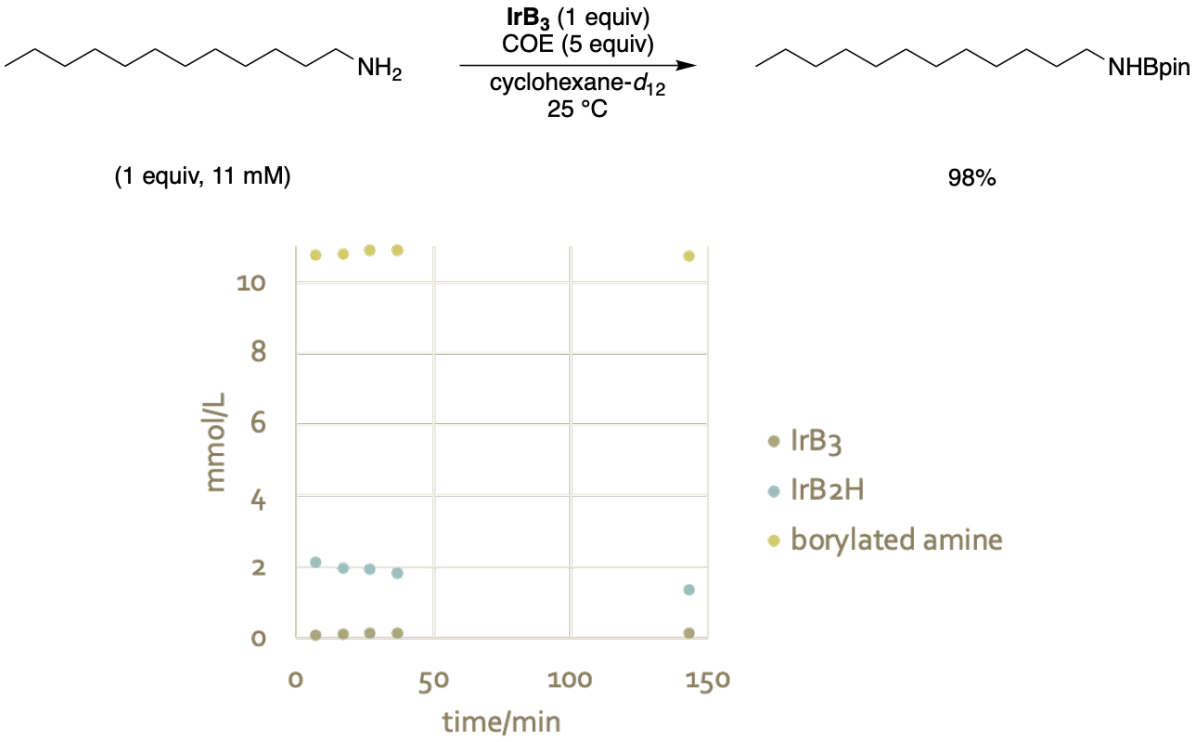

Figure 1.17 Borylation of dodecylamine in the presence of added COE (5 equiv); IrB_3 = $(dtbpy)(COE)Ir(Bpin)_3$

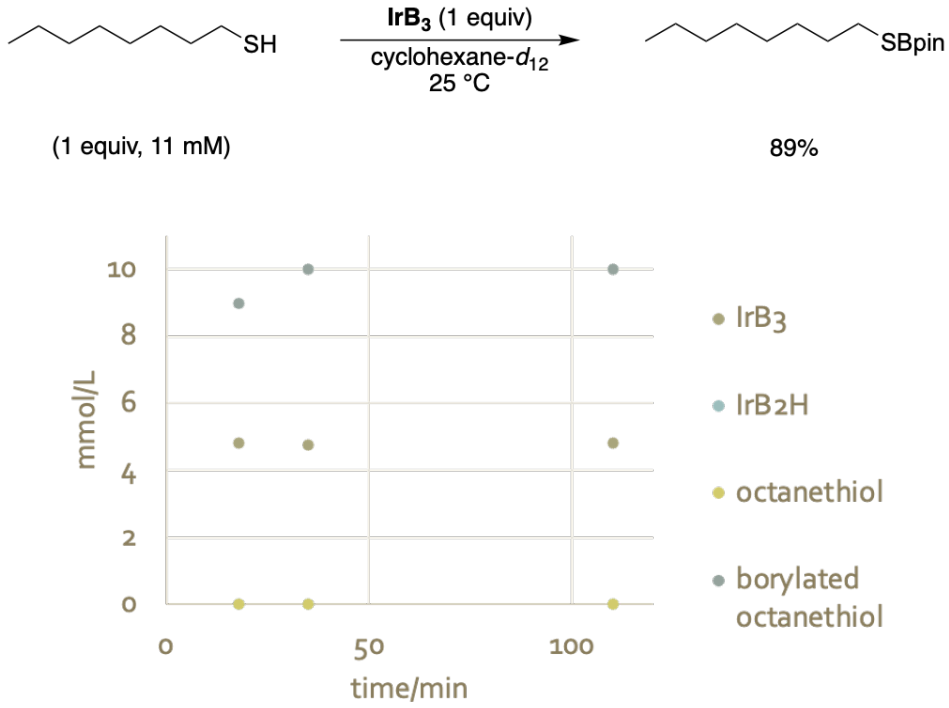

Figure 1.18 Borylation of octanethiol in the absence of added COE; IrB_3 = $(dtbpy)(COE)Ir(Bpin)_3$

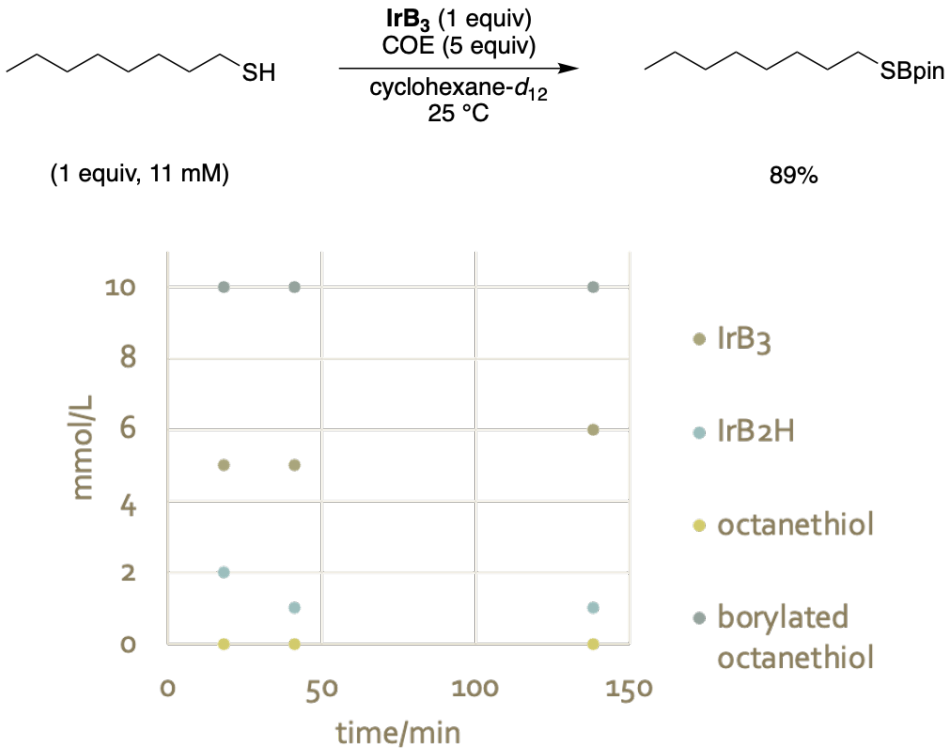

Figure 1.19 Borylation of octanethiol in the presence of added COE (5 equiv); IrB_3 = $(dtbpy)(COE)Ir(Bpin)_3$

1.2.3.2 Amide [pKa ~ 24]

Primary alcohol, amine and thiol with electron-donating alkyl chains all react rapidly with the Ir-trisboryl complex. N-methylbutyramide, on the other hand, reacts more slowly. Unlike the reactions of primary alcohol, amine and thiol, which occur within 5 min time at room temperature, the reactions of N-methylbutyramide occur over the course of 24 hours at 50 °C (Figure 1.20). Similar to the rate of the borylation of primary alcohol, amine and thiol, the rate of the borylation of N-methylbutyramide is the same in the presence or absence of added COE (Figure 1.20). Therefore, like for primary alcohol, amine and thiol, it is hypothesized that N-methylbutyramide borylates by coordination to the Bpin ligand of the iridium trisboryl complex (not by oxidative addition at the iridium center).

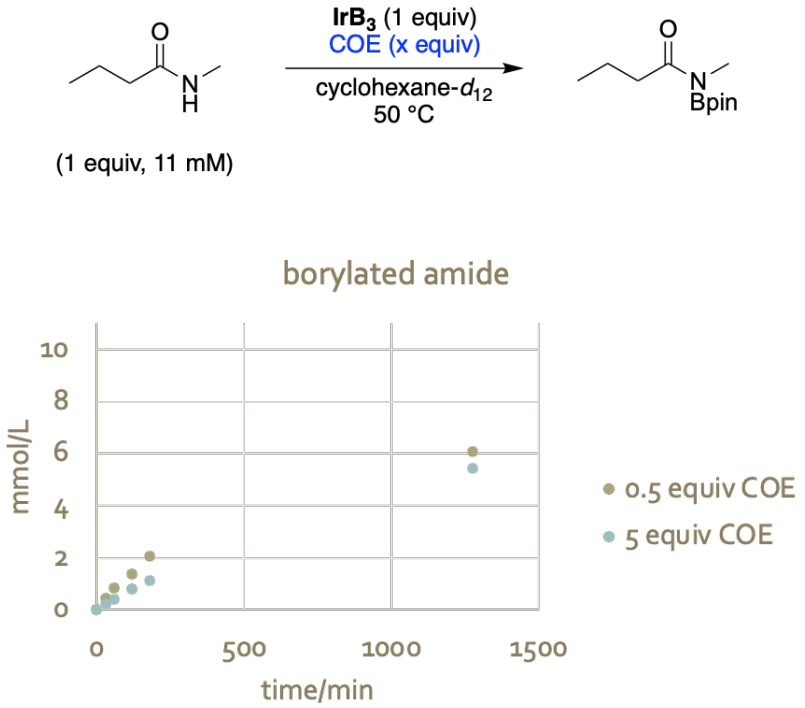

Figure 1.20 Borylation of N-methylbutyramide in the presence or absence of added COE (5 equiv); IrB_3 = (dtbpy)(COE)Ir(Bpin)$_3$. pKa of N-methylbutyramide approximated against the measured value of 25.9 for N-methylacetamide[17].

1.2.4 Reactivity at Iridium

1.2.4.1 Arenes [pKa ~ 37]

The borylation of aryl C—H bonds catalyzed by the iridium trisboryl complex is a reaction whose regioselectivity is well-established to be dictated by steric control.[7] This selectivity was also presented in the 2014 publication by Larsen and Hartwig, wherein a variety of heteroarenes also demonstrated sterically-driven regioselectivity for borylation.[12] Borylation of five- or six-membered rings preferentially occurs distal from a substituent – a sterically driven regioselectivity that is less pronounced for five membered rings.

This less pronounced steric control over regioselectivity in five- versus six-membered rings is delineated in this work in stoichiometric experiments (Figure 1.21). The borylation of tert-butyl 1H-pyrazole-1-carboxylate (boc-pyrazole) and of 2-chloro-4-fluoro-1-methylbenzene exclusively produce single isomeric products whose installed Bpin have no ortho-substitution (the ortho-fluoro substituent in 2-(4-chloro-2-fluoro-5-methylphenyl)-4,4,5,5-tetramethyl-1,3,2-dioxaborolane is of comparable size to that of a hydrogen atom). The C—H bond undergoing activation for each substrate is approximated to have the same pKa value of 37 (the pKa of boc-pyrazole was predicted to be 37.1 by the first-principle method by Shen and coworkers[18]; the pKa of 2-(4-chloro-2-fluoro-5-methylphenyl)-4,4,5,5-tetramethyl-1,3,2-dioxaborolane was approximated as the predicted value of 36.8 for fluorobenzene by the first-principle method by Shen and coworkers[18]). Yet the borylation of 2-chloro-4-fluoro-1-methylbenzene is much slower

than that of tert-butyl 1H-pyrazole-1-carboxylate (which is borylated within the first 5 minutes). The steric encumbrance of a neighboring C—H bond of a six membered arene is much greater than that of a neighboring C—H bond of a five membered arene and is a possible explanation for the drastic difference in the rate of borylation between the two substrates.

Moreover, the lower rate of borylation for each arene with added COE than without COE suggests that the mechanism of the borylation of each arene occurs by oxidative addition of the C—H bond at the iridium center of the iridium trisboryl complex (Figure 1.21).

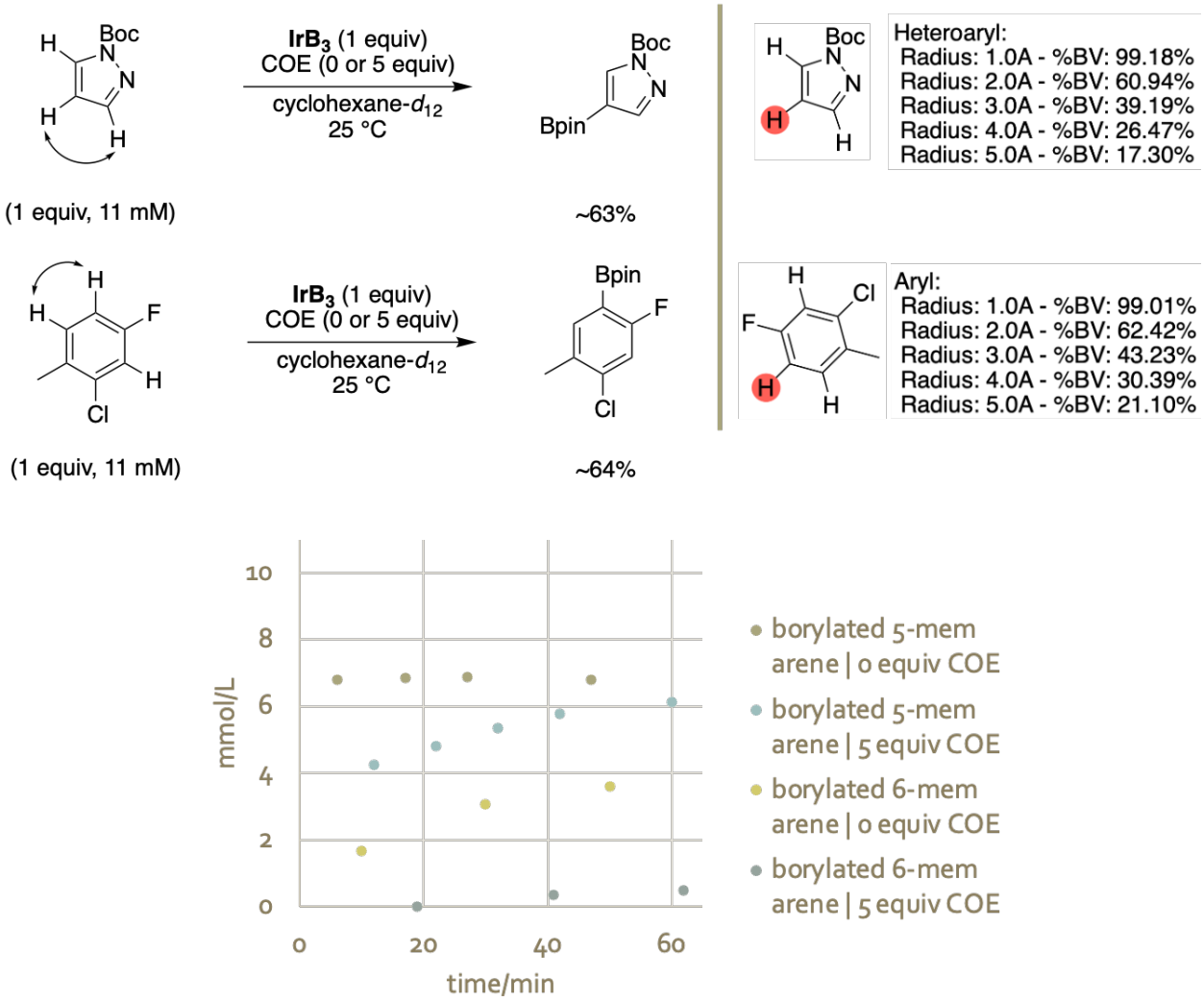

Figure 1.21 Difference in the rate of borylation of 5- versus 6-membered arenes of predicted[18] pKa 37, and calculated %buried volume[59]; IrB_3 = (dtbpy)(COE)Ir(Bpin)$_3$

1.2.4.2 m-Xylene [pKa ~ 46]

While the borylation of the C–H bond with a pKa of 37 on six membered aromatic rings without ortho-substitution progresses gradually at ambient temperature (Figure 1.21), the borylation of a C—H bond with a pKa of 46 (approximated by the predicted value of 44.7 for

benzene by the first-principle method by Shen and coworkers[18]) on a six-membered aromatic ring, also without ortho-substitution, does not proceed at all at ambient temperature (Figure 1.22), and exceeds the upper pKa limit for oxidative addition for a C(sp^2)—H bond at 25 °C.

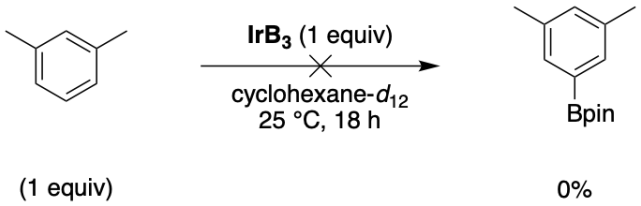

Figure 1.22 Borylation of m-xylene; IrB_3 = (dtbpy)(COE)Ir(Bpin)$_3$

1.2.4.3 Ketones [pKa ~ 27]

The iridium trisboryl complex also reacts with C(sp^3)—H bonds. Similar to C—H activation of C(sp^2)—H bonds, C—H activation of C(sp^3)—H bonds is sensitive to the steric environment of the substrate, as demonstrated by reactions of ketones (Figure 1.23). While both 2-methylheptan-3-one and cyclooctanone have secondary positions alpha to the carbonyl group (with C—H bonds of pKa values of approximately 27; the pKa of 2-methylheptan-3-one is approximated by the measured value of 27.1 for pentan-3-one[19]; the pKa of cyclooctanone is approximated against the measured value of 25.8 for cyclopentanone[20]), the secondary position of 2-methylheptan-3-one is more sterically congested with access blocked by the adjacent isopropyl group. As such, 2-methylheptan-3-one does not undergo borylation with the iridium trisboryl complex at ambient temperature after 18 hours. On the other hand, the secondary position of cyclooctanone alpha to the carbonyl is less sterically congested. The stoichiometric reaction of the iridium trisboryl complex with cyclooctanone forms the O—borylated product in 19% yield after 18 hours at ambient temperature (Figures 1.23 & 1.24).

Moreover, after 18 hours at 25 °C, the C(sp^3)—H bond of cyclooctanone (pKa ~ 27) borylated to 19% yield with the remainder mass balance being cyclooctanone (Figure 1.24). By comparison, the borylation of the C(sp^2)—H bond with a pKa value of 37 in 2-chloro-4-fluoro-1-methylbenzene yielded 64% of the borylated product under the same conditions (Figure 1.21). For a given C—H bond, an increased steric environment hinders C—H activation, a lower pKa value facilitates C—H activation, and increased s-character facilitates C—H activation. As is seen, these fundamental principles apply to all reactions of C—H bonds.

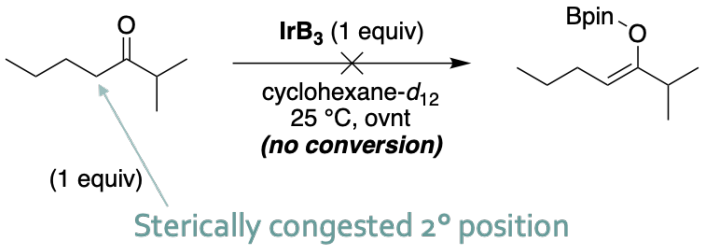

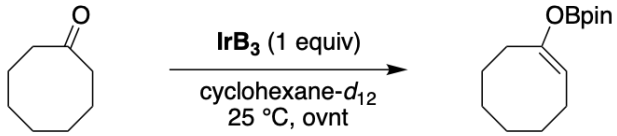

Figure 1.23 Borylation of C(sp^3)—H bonds of pKa ~ 27 [ketones][19,20]; IrB_3 = (dtbpy)(COE)Ir(Bpin)$_3$

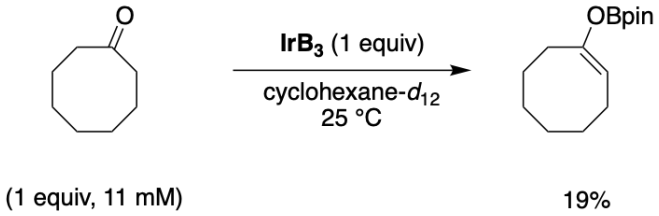

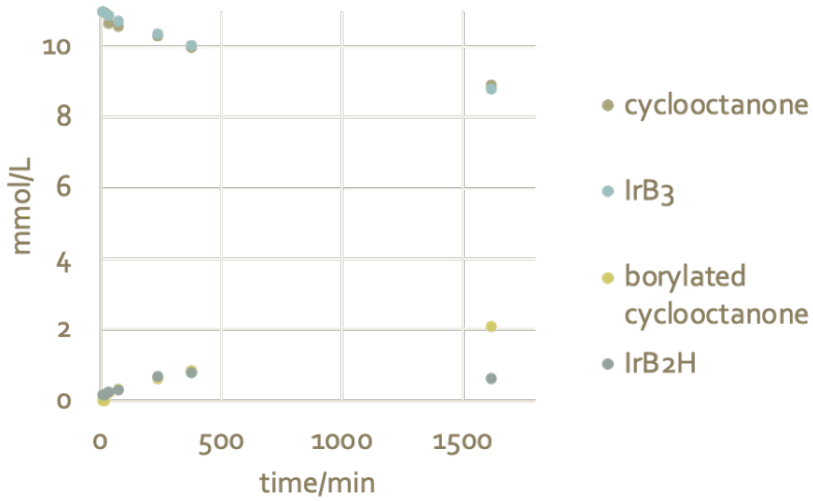

Figure 1.24 Time course for the borylation of cyclooctanone; IrB_3 = (dtbpy)(COE)Ir(Bpin)$_3$

1.2.4.4 Ester [pKa ~ 30] & Amide [pKa ~ 35]

These trends in reactivity apply to reactions of ketones (pKa 27)[19,20] (Figure 1.23), esters (pKa 30; approximated against the measured value of 29.5 for ethylacetate[21]) (Figure 1.25) and amides (pKa 35; approximated against the measured value of 35 for N,N-diethylacetamide[22])

(Figure 1.25). Neither methyl propionate nor *N,N*-dimethylpropionamide undergoes borylation with the iridium trisboryl complex at ambient temperature after 18 hours. Both compounds contain C—H bonds alpha to the carbonyl with pKa values higher than that of 2-methylheptan-3-one, which also does not react with the iridium trisboryl complex (**IrB$_3$**) under the same conditions (Figure 1.25). The steric environment of the C—H bond alpha to the carbonyl of *N,N*-dimethylpropionamide is comparable to that of 2-methylheptan-3-one, and the pKa value is higher. Therefore, it does not undergo borylation under ambient conditions. The C—H bond alpha to the carbonyl of methyl propionate is more sterically hindered than that of the C—H bond of 2-methylheptan-3-one, but the pKa value of the C—H bond is higher. Therefore, it does not undergo borylation under ambient conditions.

Elevated temperatures showed clearly the difference in reactivity between the alpha C—H bonds of methyl propionate and *N,N*-dimethylpropionamide. The reaction at 100 °C for 1 hour yielded 16% product from beta-borylation of methyl propionate, whereas the same conditions led to no conversion of *N,N*-dimethylpropionamide. The lack of borylation at the alpha position of methyl propionate suggests that the steric properties of that position inhibit the reaction more than the pKa value of the C(sp^3)—H bond. The lack of reaction of *N,N*-dimethylpropionamide, even at the beta position, suggests that a pKa value of approximately >40 prohibits C—H activation of a C(sp^3)—H bond by IrB_3. By contrast, as exemplified by tert-butyl 1H-pyrazole-1-carboxylate and 2-chloro-4-fluoro-1-methylbenzene, C(sp^2)—H bonds with the same pKa value do react with **IrB$_3$** (Figure 1.21).

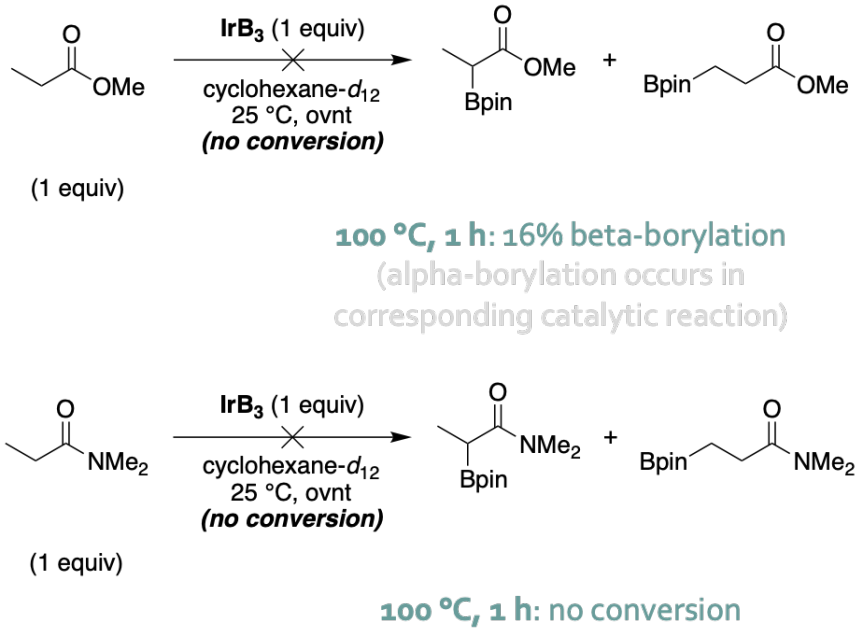

Figure 1.25 Borylation of C(sp^3)—H bonds of pKa ~ 30 & 35;[21,22] IrB_3 = (dtbpy)(COE)Ir(Bpin)$_3$

1.2.4.5 Difference in Selectivity between Catalytic and Stoichiometric Borylations of Methyl Propionate

The iridium trisboryl complex undergoes selective borylation of the C—H bond beta to the carbonyl in methyl propionate (Figure 1.25) by selective C—H activation of the methyl C—H bond over the methylene C—H bond. Moreover, borylation of the beta C—H bond in methyl propionate occurs in only 16% yield after 1 hour at 100 °C, at which point 0% IrB_3 remains, and the remaining mass balance is methyl propionate. By contrast, the corresponding catalytic reaction (whose active catalyst is the iridium trisboryl complex) proceeds more rapidly, converting 59% methyl propionate to the corresponding alpha borylated compound after 2 days at 50 °C (Figure 1.26). This selectivity for reaction at the alpha position was not observed in the corresponding stoichiometric reaction under more stringent conditions. Therefore, while the iridium trisboryl complex is generated in-situ in the catalytic reaction, the mechanism of borylation of methyl propionate in the catalytic reaction appears to be different than that of the corresponding stoichiometric reaction and is at present unknown.

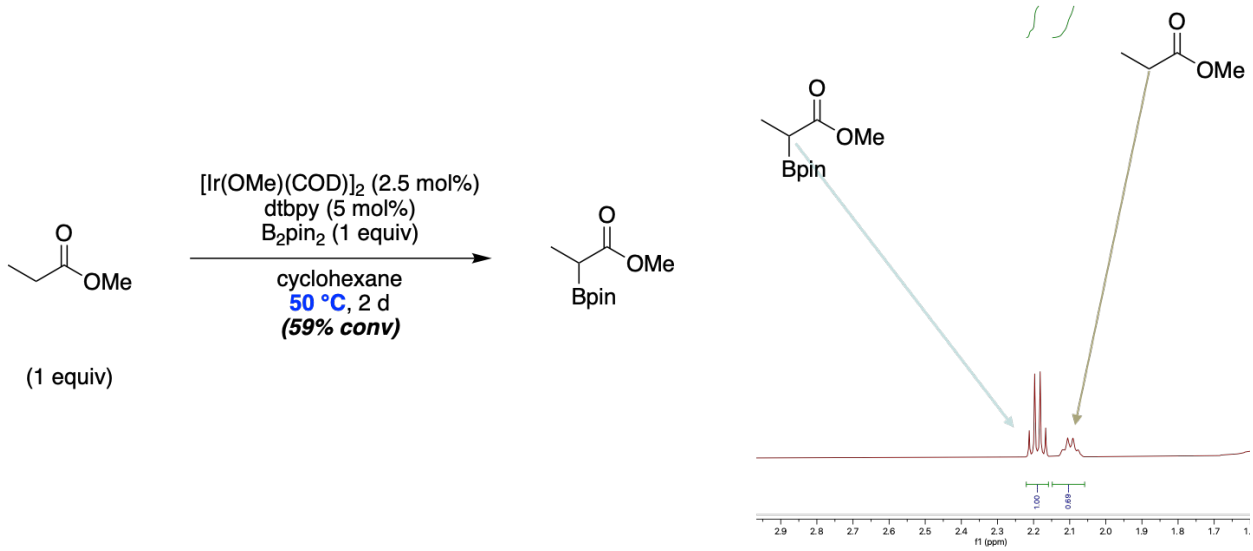

Figure 1.26 Catalytic borylation of methyl propionate [alpha-selective]

To confirm that the iridium trisboryl complex reacts selectively at the beta C—H bond in methyl propionate, the stoichiometric reaction was conducted at lower temperature (Figure 1.27). After 7 days at 50 °C (for full consumption of the iridium trisboryl complex), the beta borylated product was formed in 15% yield (diagnostic peak at 2.27 ppm, Figure 1.27), with the remaining mass balance (85%) the starting methyl propionate (diagnostic peak at 2.19 ppm, Figure 1.27).

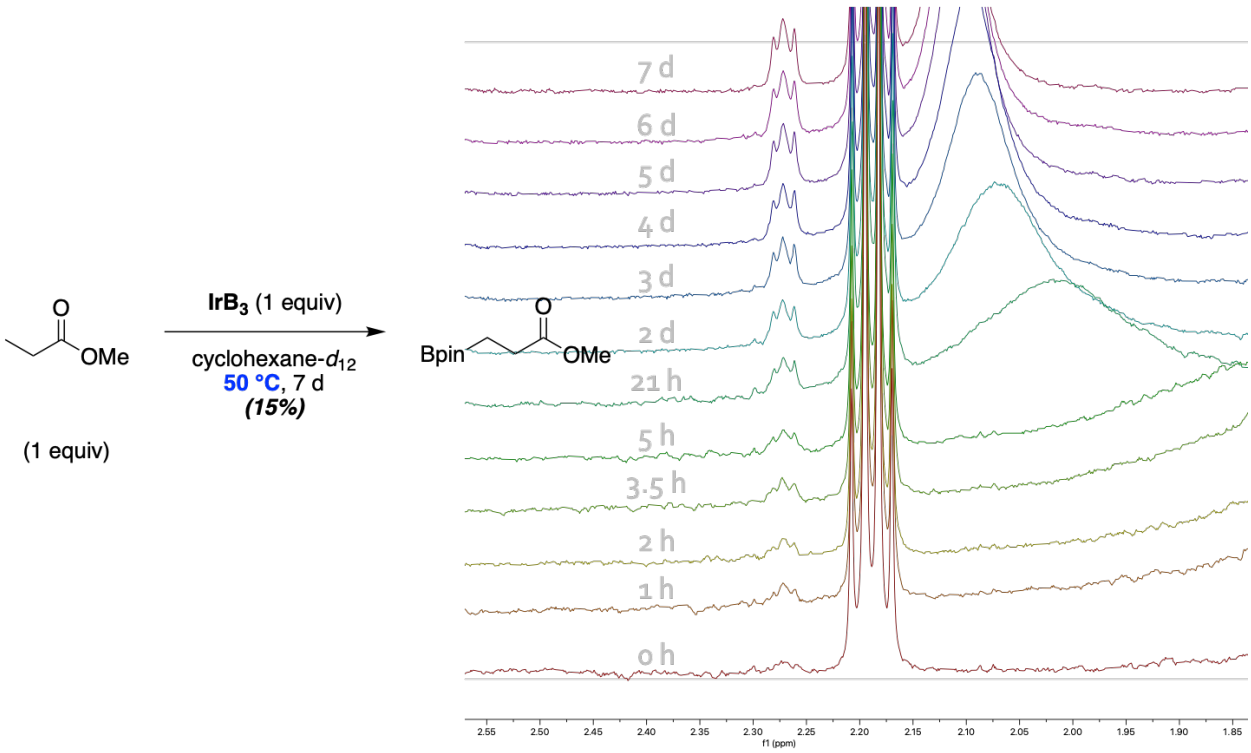

Figure 1.27 Stoichiometric borylation of methyl propionate [beta-selective]; IrB_3 = $(dtbpy)(COE)Ir(Bpin)_3$

1.2.4.6 Alkyl Bromides [pKa ~ 40]

The pKa of the alpha C(sp^3)—H bonds in alkyl bromides is approximated to be 40 (approximated against the measured value of 39 for 1,3-dithiane[20]; 1,3-dithiane chosen for the relative electronegativities between sulfur and bromine). *N,N*-dimethylpropionamide, which contains alpha C(sp^3)—H bonds with a predicted pKa of 35,[22] did not undergo borylation, even at 100 °C for 1 hour (Figure 1.25). Therefore, it is unsurprising that the alpha C(sp^3)—H bond of 1-bromopropane does not react with **IrB_3**, even at 100 °C for 1 hour (Figure 1.28). By contrast, when the s-character of a C—H bond is higher, as is that of the C–H bonds in bromocyclopropane, oxidative addition at the iridium center of the iridium trisboryl complex is facilitated. For bromocyclopropane, 13% of the beta-borylated product is formed after two days at 50 °C (Figures 1.28 & 1.29). The C—H bond alpha to bromide is inaccessible due to steric effects. However, even though the pKa of the C—H bond beta to bromide should be >40,[20] it undergoes oxidative addition because of the high s-character in the C–H bond; increased s-character leads to a stronger carbon-metal bond in the resulting oxidative addition complex because a C(sp^2)—M bond is stronger than a C(sp^3)—M bond[26,27]. The oxidative addition complex with the stronger carbon-metal bond would be more stable, and therefore oxidative addition of the C—H bond with the greater s-character occurs.[23]

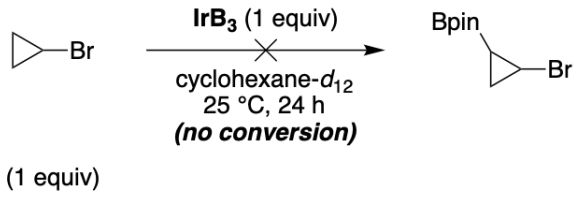

50 °C, 2 d *(time course)*: 13% beta-borylation
(alpha-borylation occurs in corresponding catalytic reaction)

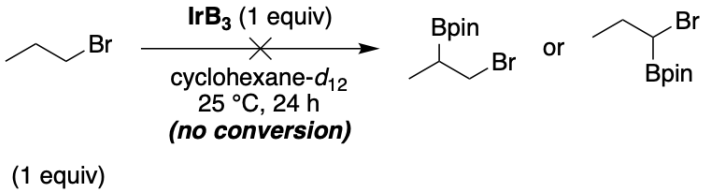

100 °C, 1 h: no conversion

Figure 1.28 Borylation of C(sp^3)—H bonds of pKa ~ 40;[20] IrB_3 = (dtbpy)(COE)Ir(Bpin)$_3$

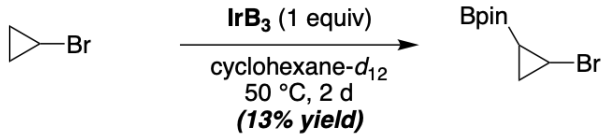

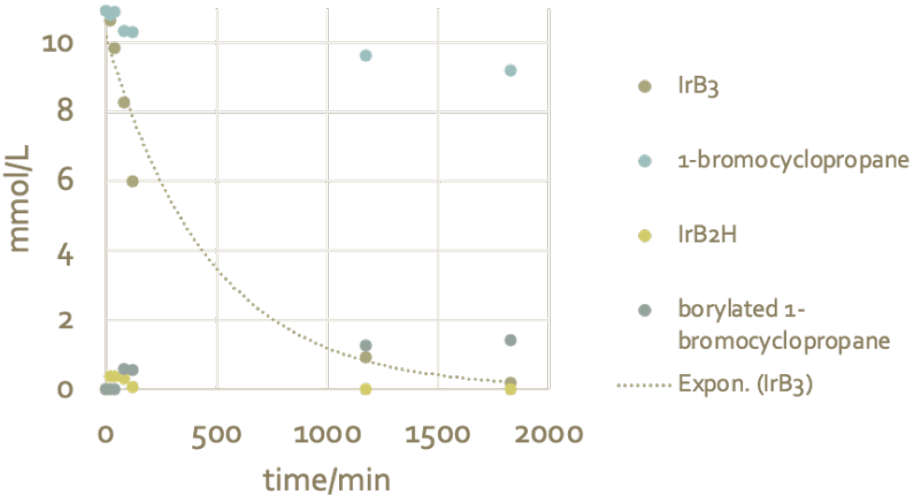

Figure 1.29 Time course for the borylation of bromocyclopropane at 50 °C; IrB_3 = (dtbpy)(COE)Ir(Bpin)$_3$

Similar to the case of methyl propionate, the corresponding catalytic borylation of bromocyclopropane occurs with a selectivity that is different from that of the stoichiometric reaction. In contrast to the borylation of the C—H bond beta to bromine from the reaction of

bromocyclopropane with stoichiometric amounts of **IrB_3**, the borylation of the C—H bond alpha to bromine occurs in the catalytic reaction of bromocyclopropane with B_2pin_2 catalyzed by the in-situ generated iridium trisboryl complex (Figures 1.30 – 1.35, characterization by ^{1}H-NMR, ^{13}C-NMR, HSQC and DEPT spectroscopy).

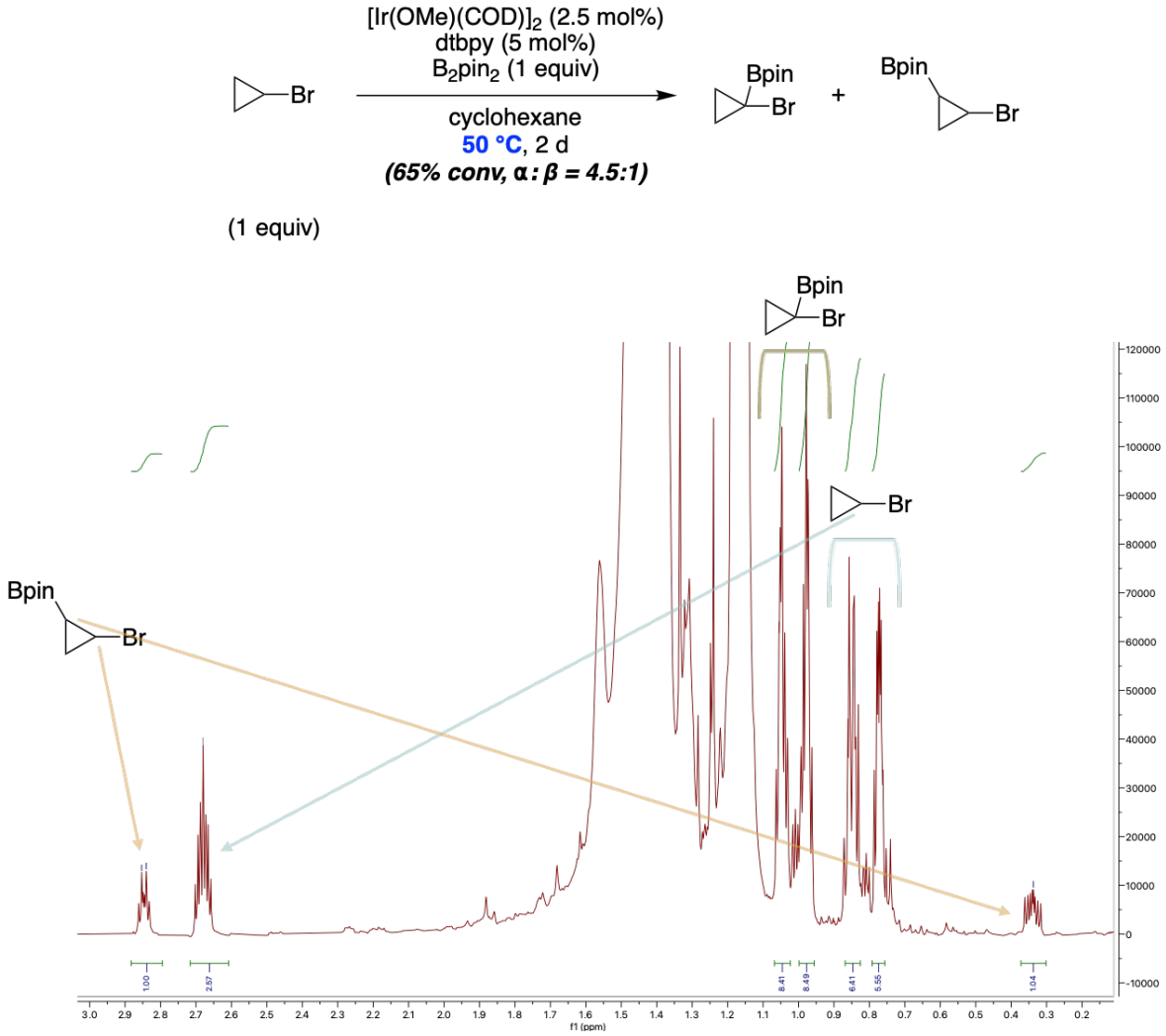

Figure 1.30 In-situ ^{1}H-NMR spectrum of the catalytic borylation of bromocyclopropane [2 days]. Note: 2-cyclopropyl-4,4,5,5-tetramethyl-1,3,2-dioxaborolane is not observed, as determined by comparing this spectrum to the published spectrum of the pure boryl bromocyclopropane.[24]. Beta borylated product matches the literature characterization of the known compound.[25] In-situ sample diluted with cyclohexane-d_{12} for ^{1}H-NMR spectroscopic analysis.

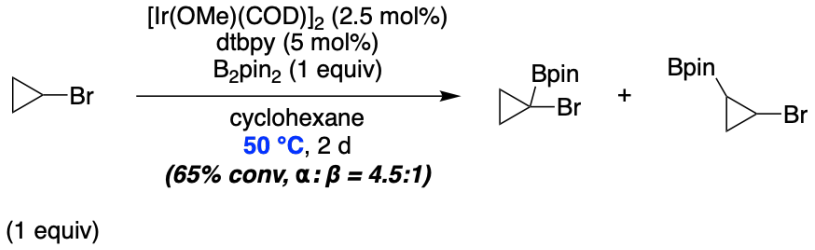

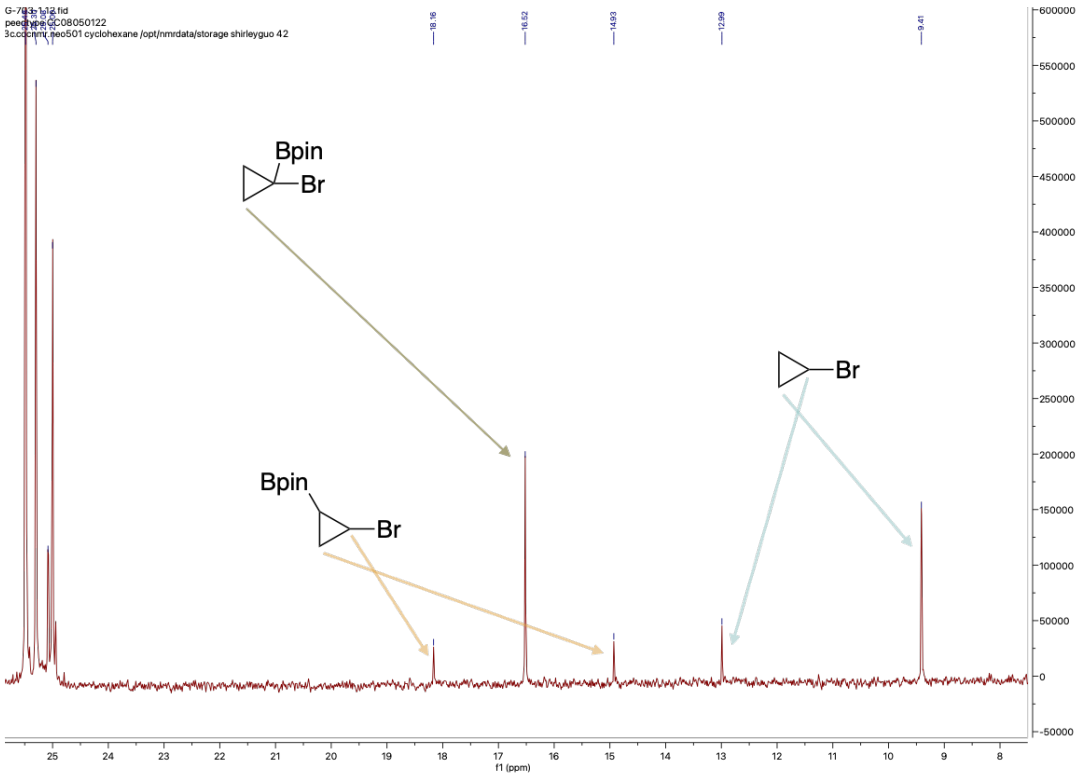

Figure 1.31 In-situ ^{13}C-NMR spectrum of the catalytic borylation of bromocyclopropane. Note: do not observe 2-cyclopropyl-4,4,5,5-tetramethyl-1,3,2-dioxaborolane when comparing to literature reference of known compound[24]. Beta borylated product matches the literature characterization of the known compound.[25] In-situ sample diluted with cyclohexane-d_{12} for ^{1}H-NMR spectroscopic analysis.

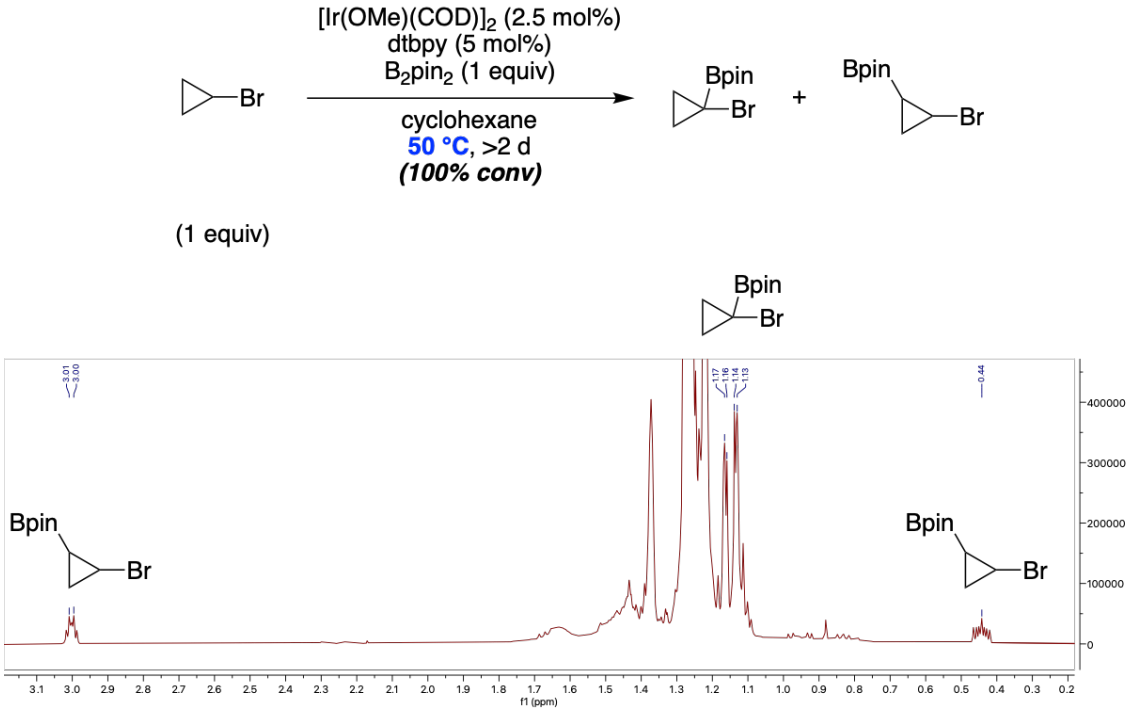

Figure 1.32 In-situ ^{1}H-NMR spectrum of the catalytic borylation of bromocyclopropane [>2 days]. Note: do not observe 2-cyclopropyl-4,4,5,5-tetramethyl-1,3,2-dioxaborolane when comparing to literature reference of known compound[24]. Beta borylated product matches the literature characterization of the known compound.[25] In-situ sample diluted with $CDCl_3$ for ^{1}H-NMR spectroscopic analysis. Some cyclohexane-d_{12} observed.

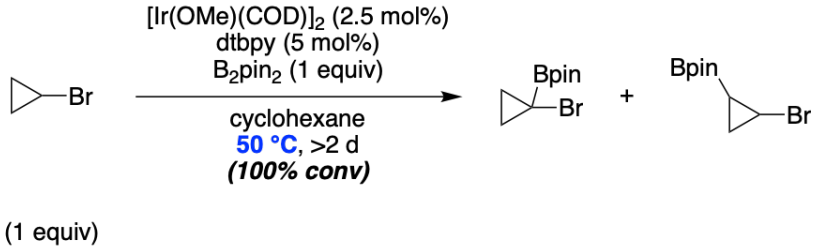

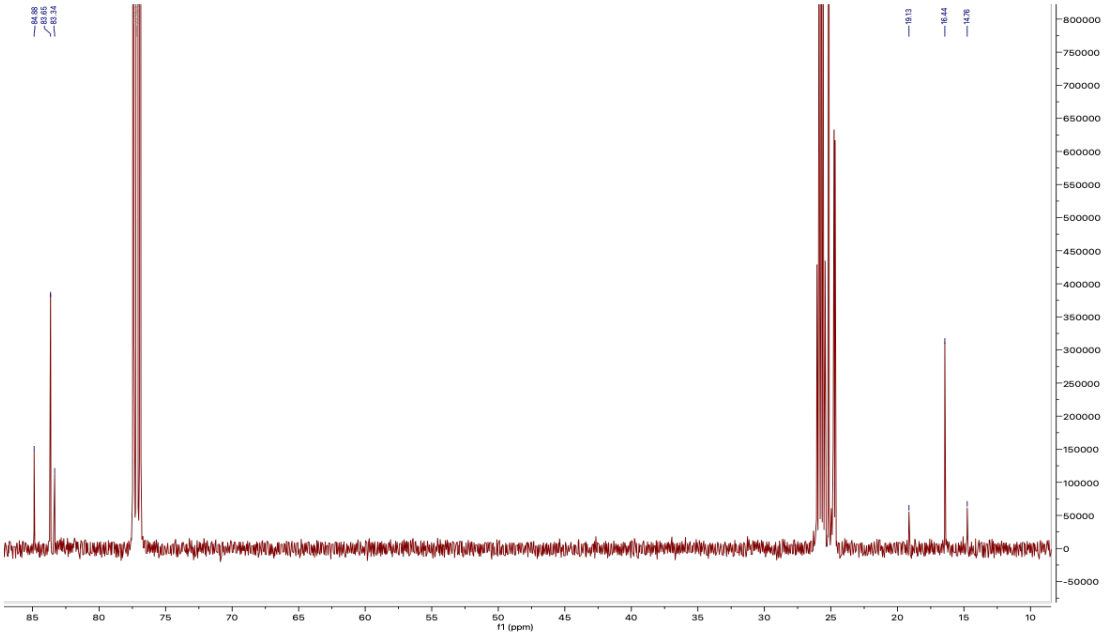

Figure 1.33 In-situ ^{13}C-NMR spectrum of the catalytic borylation of bromocyclopropane [>2 days]. Note: do not observe 2-cyclopropyl-4,4,5,5-tetramethyl-1,3,2-dioxaborolane when comparing to literature reference of known compound[24]. Beta borylated product matches the literature characterization of the known compound.[25] In-situ sample diluted with $CDCl_3$ for NMR spectroscopic analysis. Some cyclohexane-d_{12} observed.

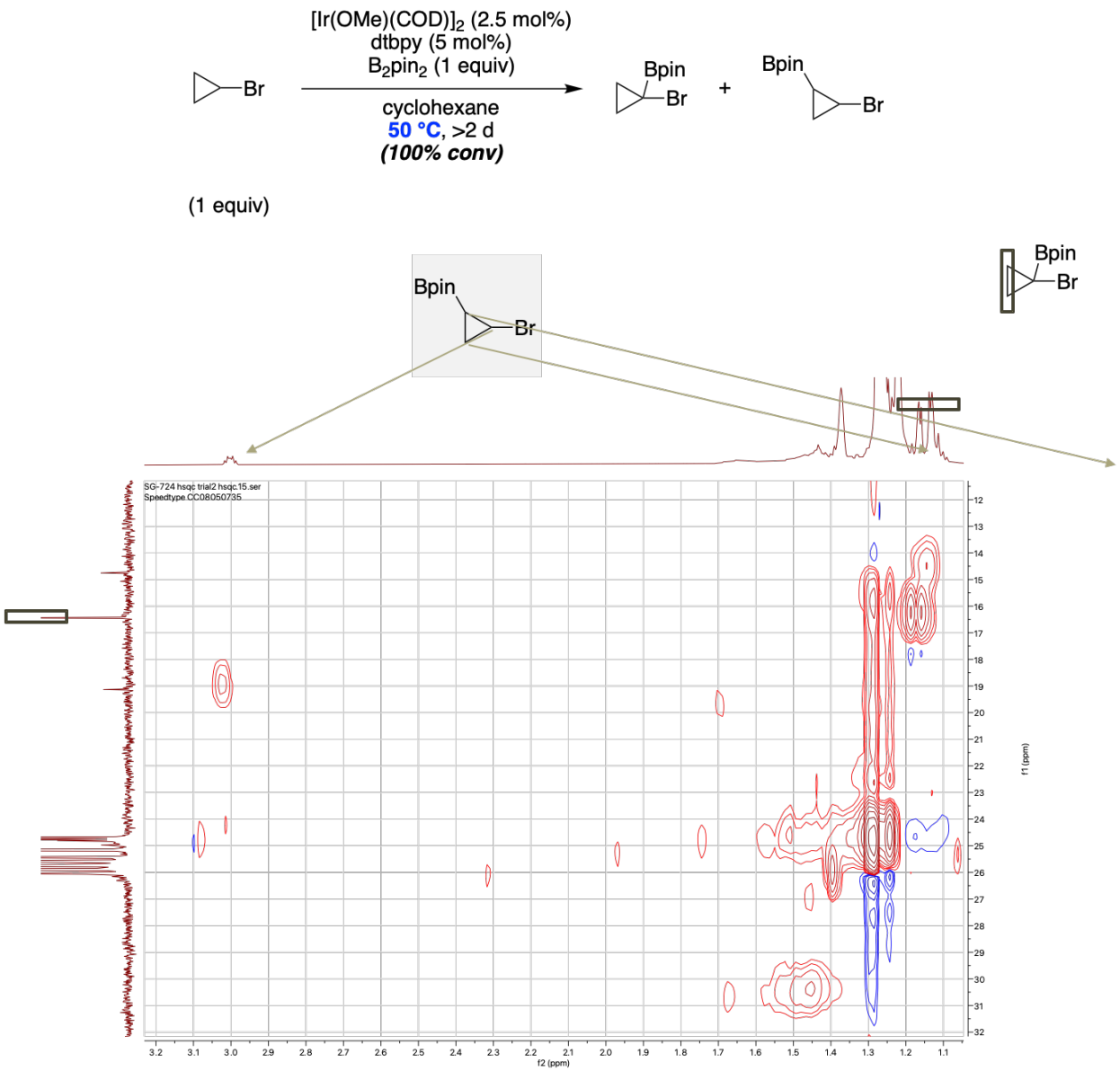

Figure 1.34 In-situ HSQC spectrum of the catalytic borylation of bromocyclopropane [>2 days]. In-situ sample diluted with $CDCl_3$ for NMR spectroscopic analysis. Some cyclohexane-d_{12} observed.

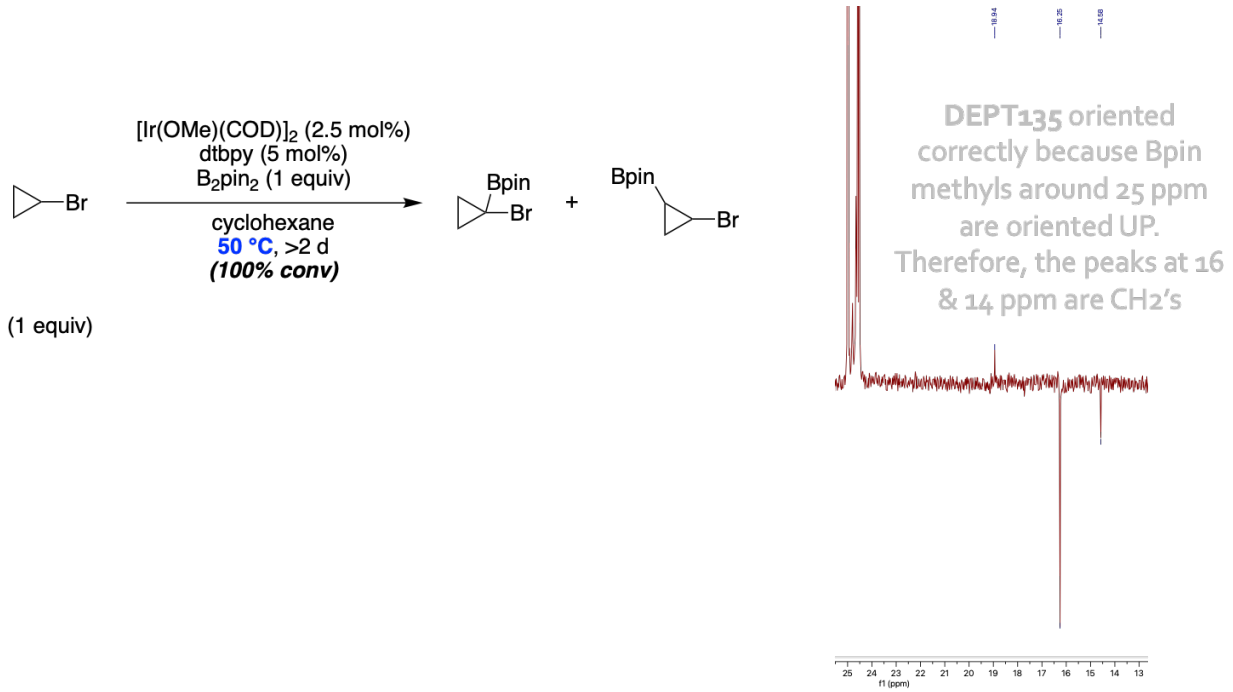

Figure 1.35 In-situ DEPT spectrum of the catalytic borylation of bromocyclopropane [>2 days]. In-situ sample diluted with $CDCl_3$ for NMR spectroscopic analysis. Some cyclohexane-d_{12} observed.

1.2.4.7 Phenylacetylene [pKa ~ 29]

The s-character of the C(sp)—H bond in phenylacetylene is the highest of the C—H bonds in the substrates evaluated (Figure 1.36). The reaction of phenylacetylene with the trisboryl complex **IrB₃** was conducted at 25 °C. After <5 min, phenylacetylene was fully consumed. However, the corresponding borylacetylene formed in only 11% yield and is likely generated via unknown minor decomposition pathways. The main products are two different forms of $Ir(Bpin)_n(alkynyl)_m$. As can be seen in the ^{1}H-NMR spectrum, there are two new sets of phenylacetylene aryl peaks (different from those of free phenylacetylene or those of borylacetylene) which correspond to two new sets of dtbpy aryl peaks (different from those of free dtbpy) (Figure 1.36). Furthermore, these new phenylacetylene aryl peaks do not result from borylation of the phenyl ring. No new hydride peaks are observed. Given that the number of boryl groups attached to iridium cannot be determined by NMR spectroscopy, these two new species can only be designated as $Ir(Bpin)_n(alkynyl)_m$, with an unknown number of boryl or alkynyl ligands, and therefore an unknown oxidation state for the metal.

The pKa of the C(sp)—H bond in phenylacetylene[20] is 29, which is two units higher than that of cyclooctanone[20] (pK_a = 27) (Figure 1.23). Nevertheless, phenylacetylene reacts within 5 minutes (Figure 1.36), whereas cyclooctanone reactcs slowly (Figure 1.23). The greater s-character of the C(sp)—H bond in phenylacetylene presumably facilitates reaction at the C—H bond; increased s-character leads to a stronger carbon-metal bond in the resulting oxidative addition complex since a C(sp)—M bond is stronger than a C(sp^2)—M bond[26,27,60], which is in

turn stronger than a C(sp^3)—M bond[23]. The complex with the stronger carbon-metal bond would be more stable, and therefore oxidative addition of the C—H bond with the greater s-character would occur.[23] No functionalization of the arene of the acetylene was observed, likely due to the lower s-character and higher pKa than the values of the C(sp)—H bond of the acetylene.

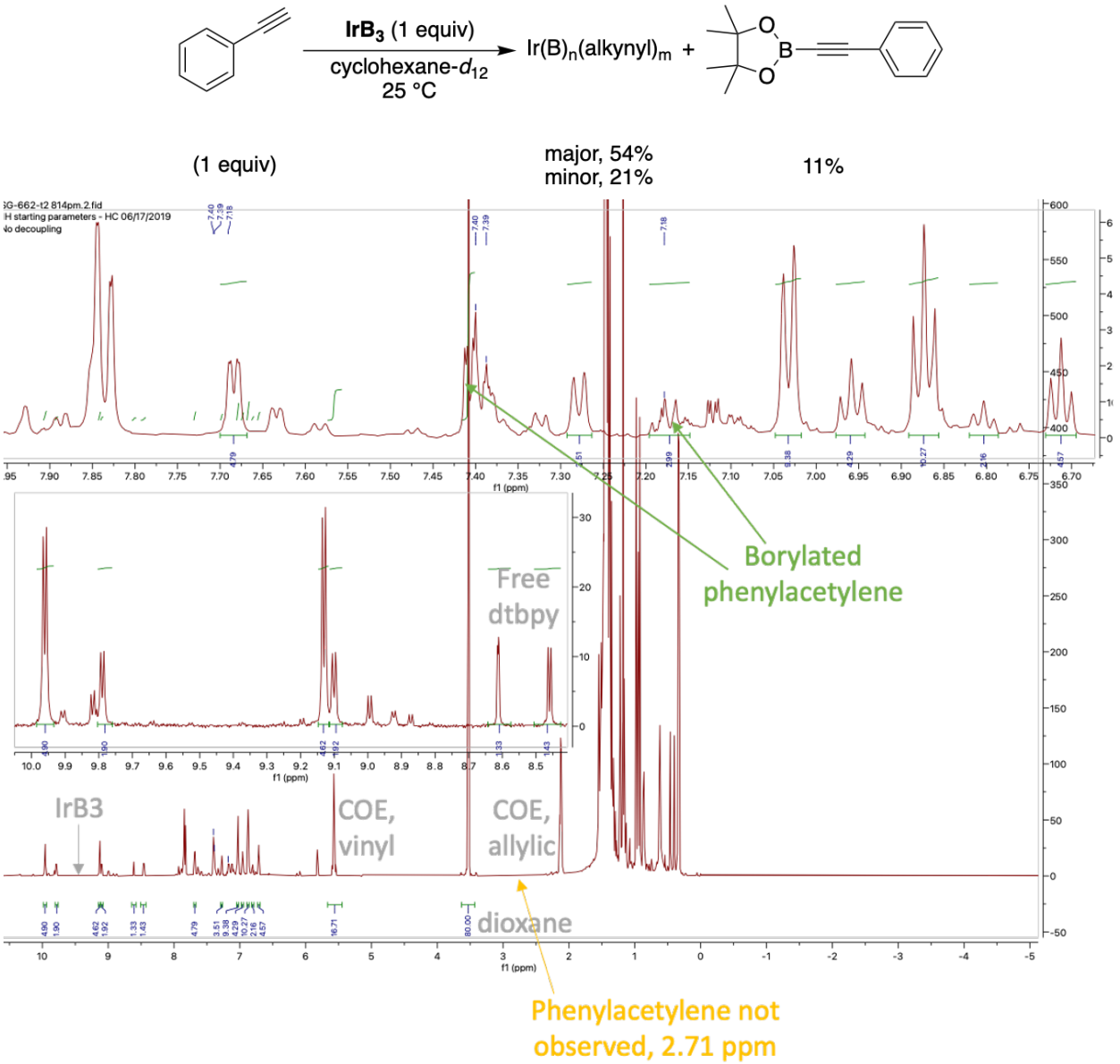

Figure 1.36 Reaction of phenylacetylene containing a C(sp)—H bond of pKa 29,[20] t = 5 minutes; IrB_3 = (dtbpy)(COE)Ir(Bpin)$_3$

1.2.4.8 Origin of Selectivity for Oxidative Addition

The iridium trisboryl complex selects for oxidative addition of the C—H bonds of greater s-character, increased acidity, and in sterically uncongested environments.[11,12] These principles

are already known. The Ir/dtbpy system selectively catalyzes the borylation of aryl C–H bonds over alkyl C–H bonds,[9] likely because of the selectivity of the catalyst for C—H bonds of increased s-character.[23] In this work, this principle is extended to C(sp)—H bonds which, as expected, undergo C—H activation faster than C(sp^2)—H bonds: while two new $Ir(Bpin)_n(alkynyl)_m$ species (which comprise the majority mass balance) are formed within 5 minutes, likely from oxidative addition of the C(sp)—H bond of phenylacetylene, no borylation of the C(sp^2)—H bonds of the phenyl group is observed (Figures 1.36 & 1.37). While alkane borylation can still take place if the C(sp^3)—H bond is of a low pKa and is in a sterically free environment (cyclooctanone, Figures 1.23 & 1.37), it does not easily occur with Ir/dtbpy, as it does with Hartwig's Ir/2-mphen[28] or Ir/tmphen[29]; or Schley's Ir/2,2'-dipyridylarylmethane[30].

And while it is known that the iridium trisboryl complex selects for oxidative addition of C—H bonds of increased acidity[7], here, a greater range of pKa values for both C(sp^2)—H and C(sp^3)—H bonds is evaluated (Figure 1.37). And while it is known that ortho substitution on the arene of a given C—H bond hinders the oxidative addition of that C—H bond,[7] here, the significant steric effect of an ortho C—H bond is demonstrated by the drastic difference in rate of borylation of boc-pyrazole and 2-chloro-4-fluoro-1-methylbenzene (Figures 1.21 & 1.37). For carbonyl compounds, C—H activation of the α C—H bond is hindered by increased substitution at the α' atom for ketones, esters and amides (Figures 1.23, 1.25 & 1.37).

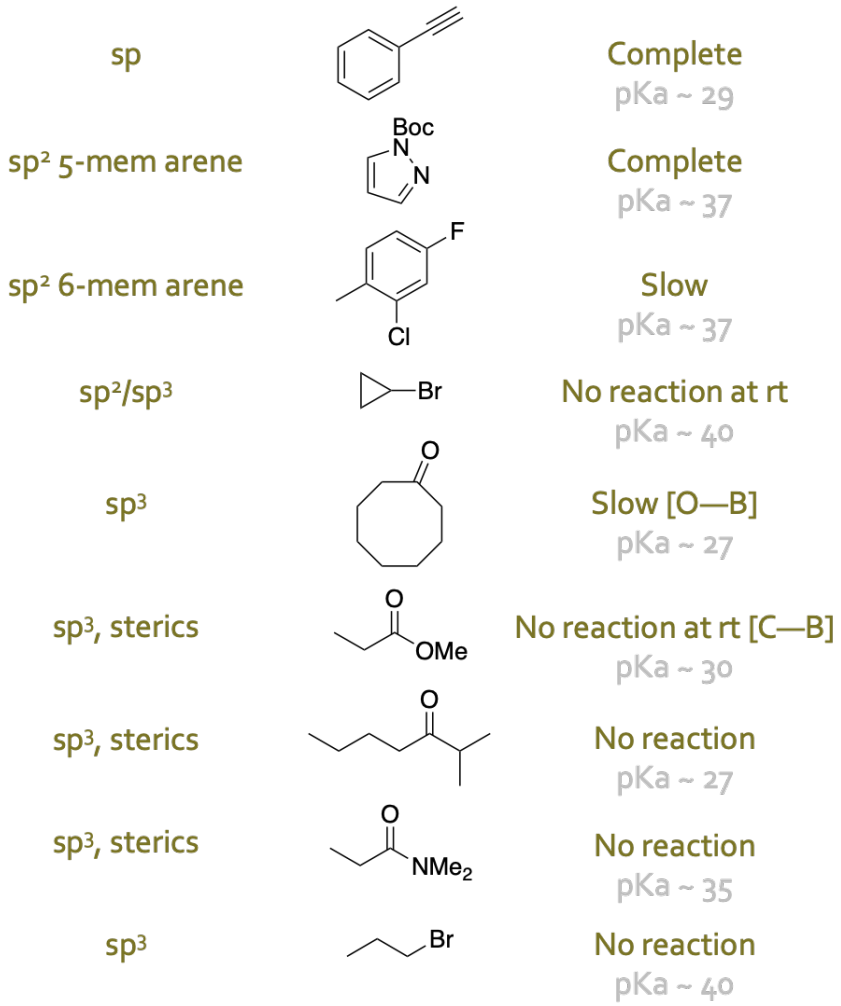

Figure 1.37 Order of reactivity at C—H bond based on s-character, pKa and sterics

1.2.5 Ambident Reactivity: Iridium Versus Bpin Ligand

1.2.5.1 Ethers, Dialkylamines and Thioethers

The previous classes of compounds are proposed to interact with the iridium trisboryl complex exclusively at either the Bpin ligand or at the iridium center. The following classes of compounds demonstrate ambident reactivity, and their selectivity for either the Bpin ligand or the iridium center highlights iridium's selectivity for soft Lewis bases.

Firstly, while the previous classes of compounds have undergone oxidative addition when reacting with the iridium center of the iridium trisboryl complex, there is another mode of reactivity that is demonstrated by the example of dithiane – Lewis base binding to iridium (Figure 1.38). In the stoichiometric experiment between dithiane and the iridium trisboryl complex, dithiane displaces COE and binds to iridium to make the complex (dithiane)(dtbpy)Ir(Bpin)$_3$ in Figures 1.38 & 1.39. By contrast, dioxane does not bind to iridium and is used as the internal standard for the stoichiometric reactions. Iridium is more thiophilic than oxophilic and selects for the softer Lewis base.

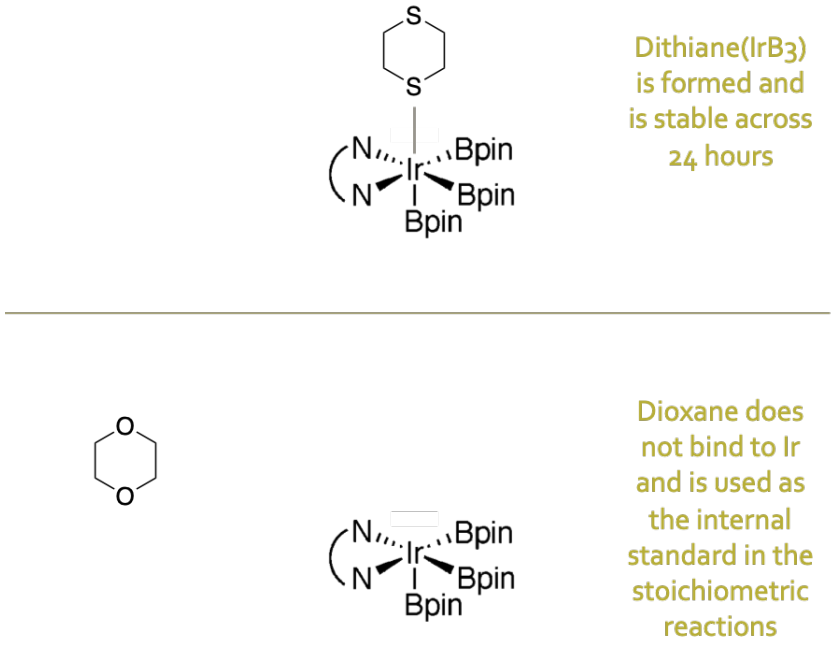

Figure 1.38 Selectivity of Ir for soft Lewis bases

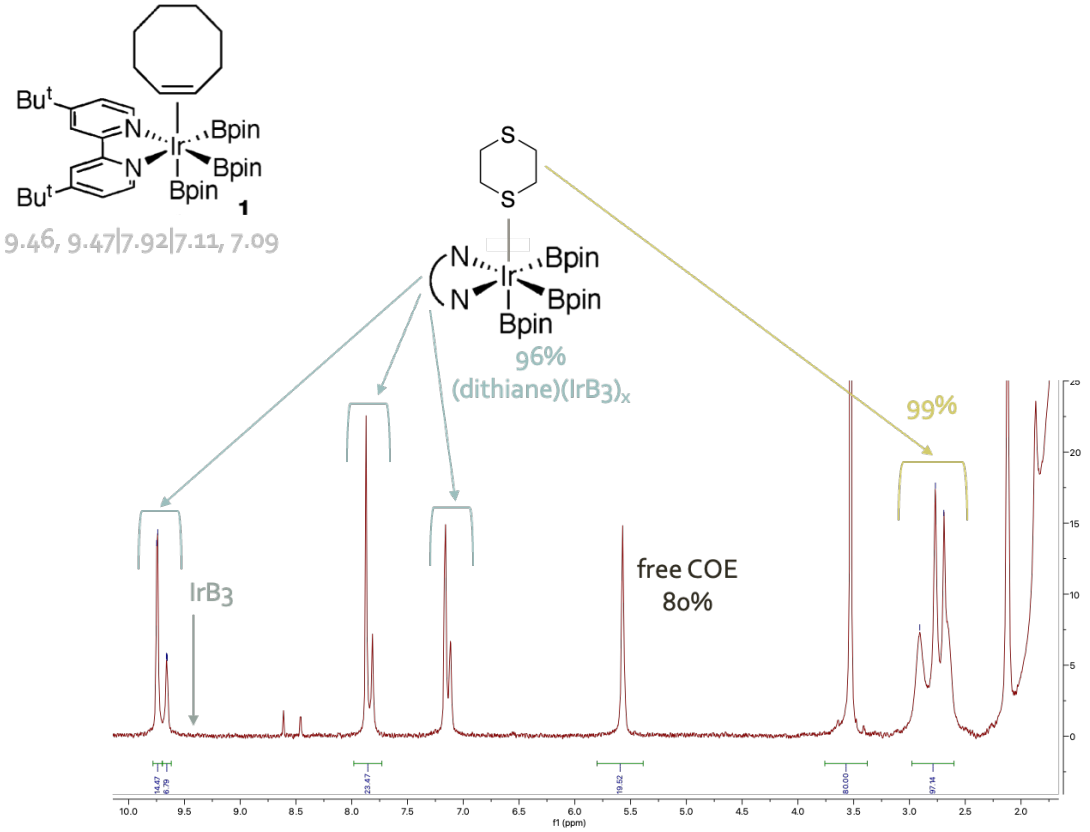

Figure 1.39 ^{1}H-NMR spectrum of stoichiometric reaction between (dtbpy)Ir(Bpin)$_3$ (1 equiv) and dithiane (1 equiv) at t = 24 h (same as profile at t = 5 min, see SI). Major species is (dithiane)(dtbpy)Ir(Bpin)$_3$ and minor species is (dithiane)[(dtbpy)Ir(Bpin)$_3$]$_2$.

Moreover, after dithiane binds to iridium, the remaining unbound sulfur atom functions as a Lewis base to a second iridium trisboryl fragment to form the dinuclear complex (dithiane)[(dtbpy)Ir(Bpin)$_3$]$_2$ (Figure 1.40).

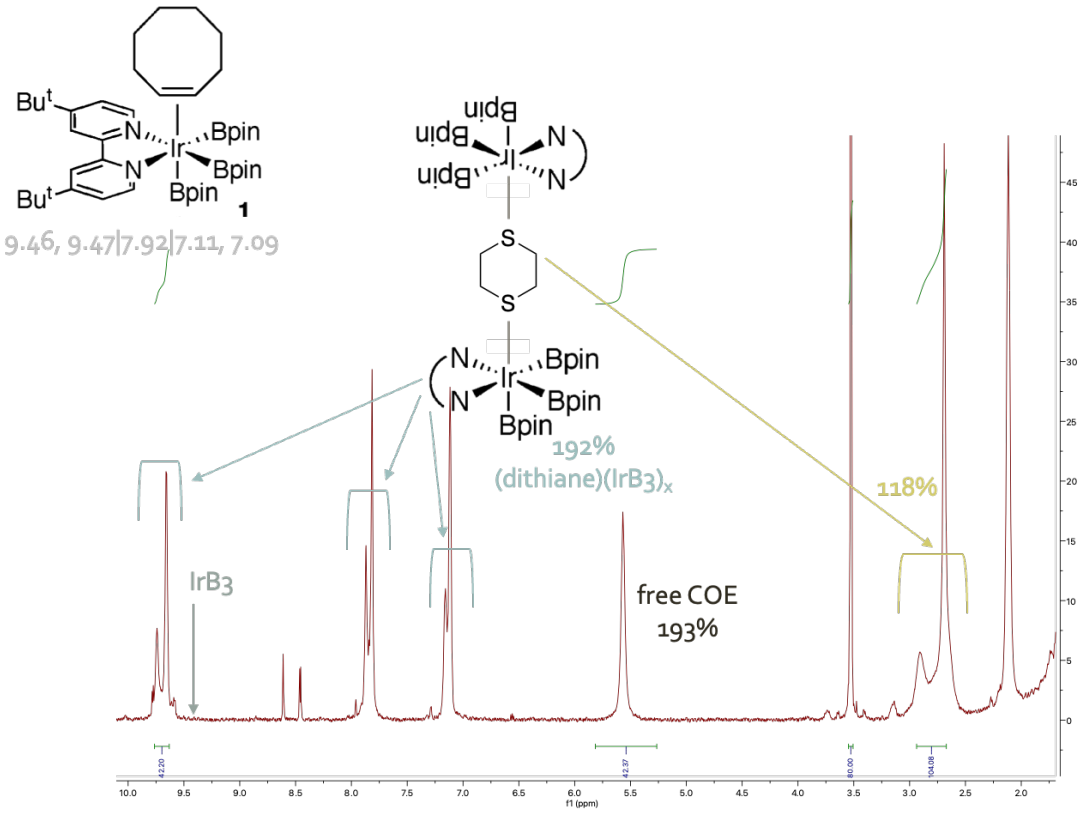

Figure 1.40 ^{1}H-NMR spectrum of stoichiometric reaction between (dtbpy)Ir(Bpin)$_3$ (2 equiv) and dithiane (1 equiv) at t = 5 min. Major species is (dithiane)[(dtbpy)Ir(Bpin)$_3$]$_2$ and minor species is (dithiane)(dtbpy)Ir(Bpin)$_3$.

1.2.5.2 Dialkylamine [pKa ~ 44]

While dithiane binds to iridium (displacing COE) (Figure 1.39) and dioxane does not (see Supporting Information), dialkylamines are proposed to bind to both the iridium center and the Bpin ligand of the iridium trisboryl complex. This ambident reactivity of dialkylamine is illustrated by the stoichiometric reactions with the iridium trisboryl complex in the absence and presence of added COE (Figure 1.41). While the standard stoichiometric experiment conducted without added COE progresses gradually to form the N—borylated product, the corresponding stoichiometric reaction with an added 5 equivalents of COE is much faster and is complete in 5 minutes (Figure 1.41). An increased concentration of COE results in displaced dialkylamine; this displacement is observed when comparing the ^{1}H-NMR spectrum of the stoichiometric reaction without added COE at 5 minutes wherein (dihexylamine)(dtbpy)Ir(Bpin)$_3$ is seen (Figure 1.42) versus the ^{1}H-NMR spectrum of the stoichiometric reaction with added COE at 5 minutes, wherein (dihexylamine)(dtbpy)Ir(Bpin)$_3$ is not seen (see Supporting Information).

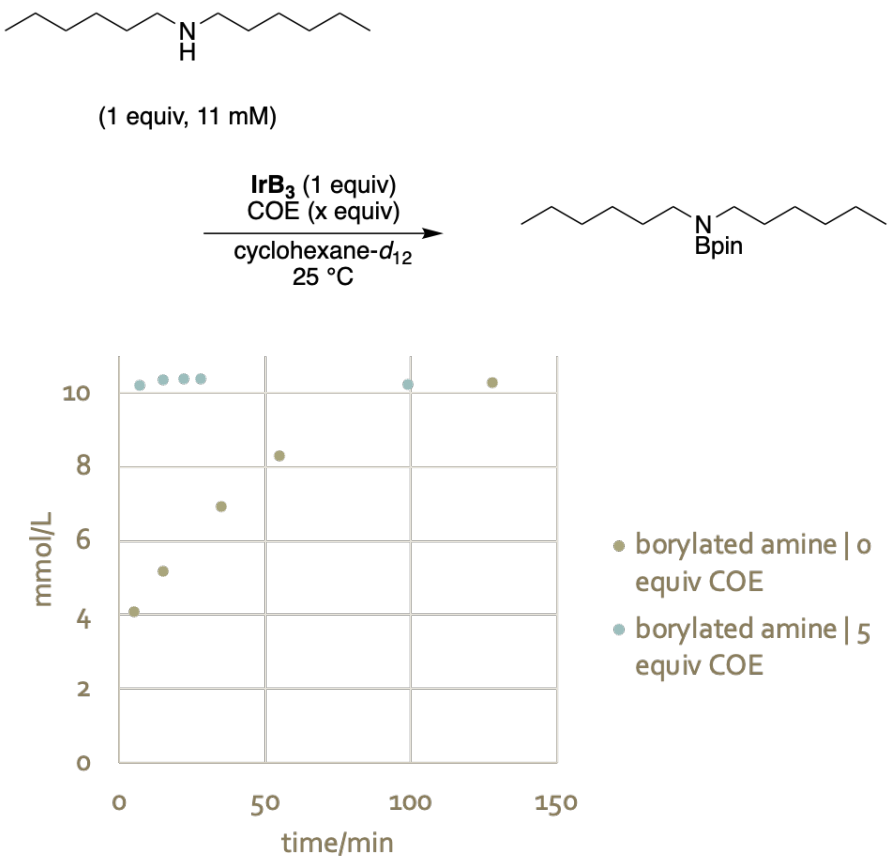

Figure 1.41 Time course for the stoichiometric reaction between dihexylamine (pKa ~ 44; pKa approximated against the measured value of 44 for pyrrolidine[15]) and IrB_3 with and without added COE; IrB_3 = (dtbpy)(COE)Ir(Bpin)$_3$

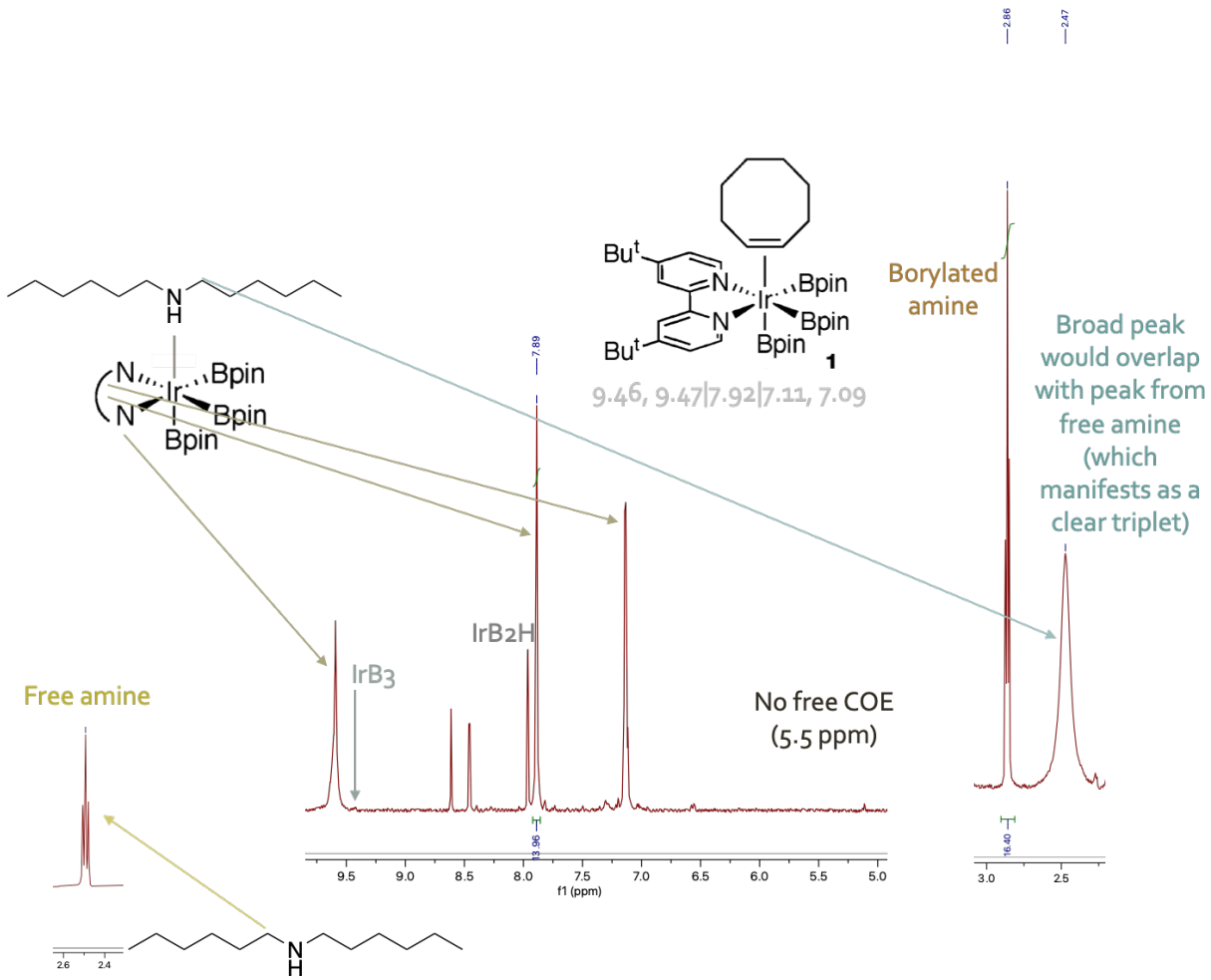

Figure 1.42 ^{1}H-NMR spectrum of stoichiometric reaction between (dtbpy)Ir(Bpin)$_3$ and dihexylamine at t = 5 min. (dihexylamine)(dtbpy)Ir(Bpin)$_3$: the original doublet at 9.47 & 9.46 ppm for the bound dtbpy of (COE)(dtbpy)Ir(Bpin)$_3$ shifted downfield and broadened into a singlet for the bound dtbpy of (dihexylamine)(dtbpy)Ir(Bpin)$_3$; and the original triplet at 2.5 ppm of the alpha proton of the free dialkylamine is now a broad singlet for a bound dialkylamine on (dihexylamine)(dtbpy)Ir(Bpin)$_3$.

It is proposed that while a primary alkylamine borylates via coordination to the Bpin ligand (Figures 1.16 & 1.17), a dialkylamine binds to iridium and only coordinates to the Bpin ligand upon displacement from iridium by a high concentration of COE (Figures 1.41 & 1.42). When free from binding to iridium, the more electron rich dialkylamine readily borylates in under 5 minutes (Figure 1.41). While octanethiol borylates within 5 minutes, likely via coordination to the Bpin ligand (Figures 1.18 & 1.19) (Kumar and coworkers have reported the binding of primary thiols to boron Lewis acids[31]), a thioether exhibits binding to iridium to make a complex that is stable for 18 hours (Figure 1.39). The increased electron density of ethers (as compared to primary alcohols), however, is still insufficient for dioxane to bind to iridium. Iridium selects for soft Lewis bases.

1.2.5.3 Phenol, Aniline and Thiophenol

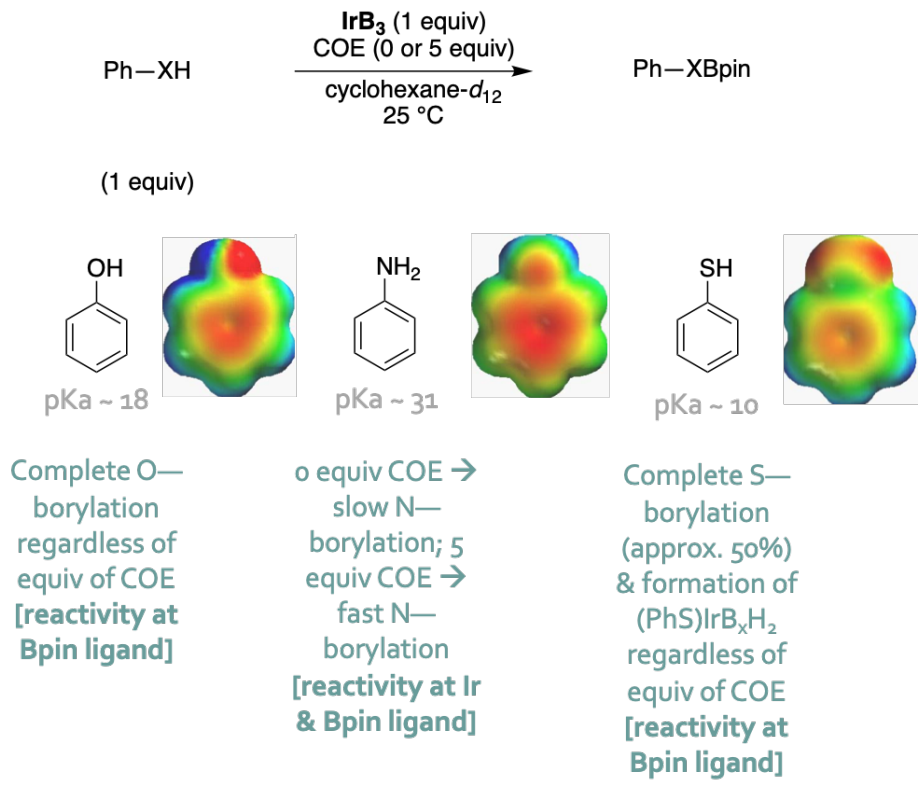

Figure 1.43 Stoichiometric reactions between IrB_3 and Ph—XH; IrB_3 = (dtbpy)(COE)Ir(Bpin)$_3$. pKa values for phenol[32], aniline[33] and thiophenol[16] are measured values obtained from literature.

An examination of the more electron-poor phenol, aniline and thiophenol, as compared to ether, dialkylamine and thioether, was also conducted (Figure 1.43). While phenol is more electron poor than alcohols, it is still proposed to be a functional Lewis base[34], coordinating to the Bpin ligand of the iridium trisboryl complex, resulting in the formation of the O—borylated product (Figure 1.43).

The initial rate of the stoichiometric reaction between the iridium trisboryl complex and aniline with an added 5 equivalents of COE is greater than the initial rate of the corresponding stoichiometric reaction without added COE (Figure 1.44). Similar to the case with dialkylamine (Figure 1.41), an increased rate of borylation in the presence of added COE is proposed to signify an increased concentration of COE displacing the otherwise bound Lewis base (in this case, aniline[35]). In contrast to the case with dialkylamine, in which there was a drastic increase in the rate of borylation with added COE (Figure 1.41), the increase in the rate of borylation with added COE in the case of aniline is small (Figure 1.44). An increased concentration of COE displaces bound aniline, and free aniline functions as a poor Lewis base in its coordination to the Bpin ligand of the iridium trisboryl complex.

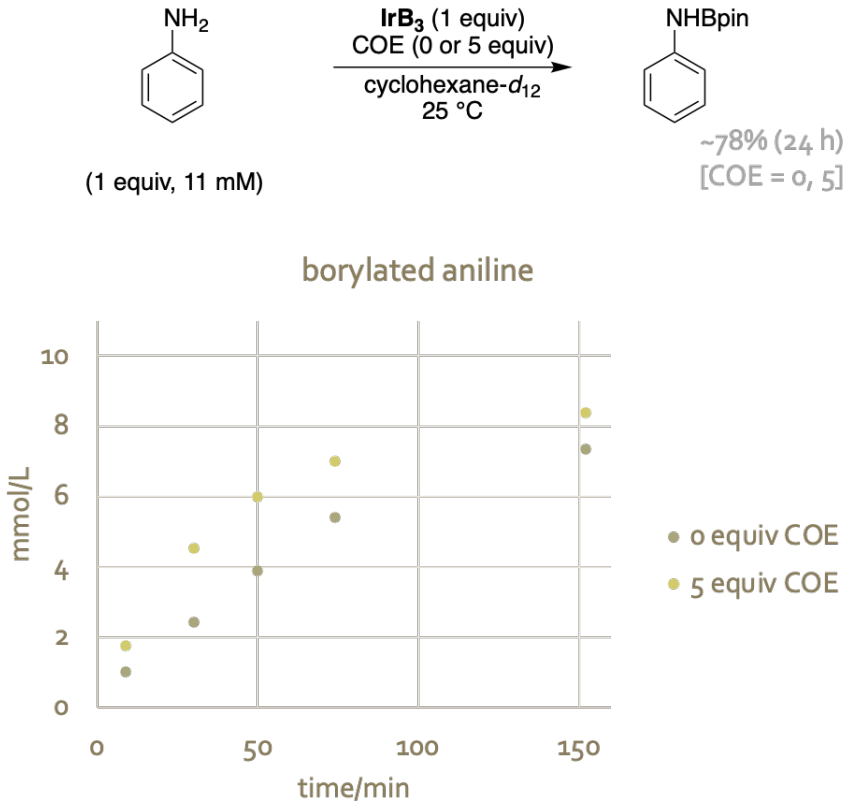

Figure 1.44 Time course for the stoichiometric reaction between aniline and IrB_3 with and without added COE; IrB_3 = (dtbpy)(COE)Ir(Bpin)$_3$

The initial ^{1}H-NMR spectrum of the stoichiometric reaction in the absence of added COE suggests that aniline binds to iridium (Figure 1.45). The ^{1}H-NMR spectrum of the reaction after 5 minutes reveals a shift in the peaks of the iridium trisboryl complex (as most diagnostically represented by the bound dtbpy ligand peaks) and of aniline (see Supporting Information for the ^{1}H-NMR spectrum of free aniline).

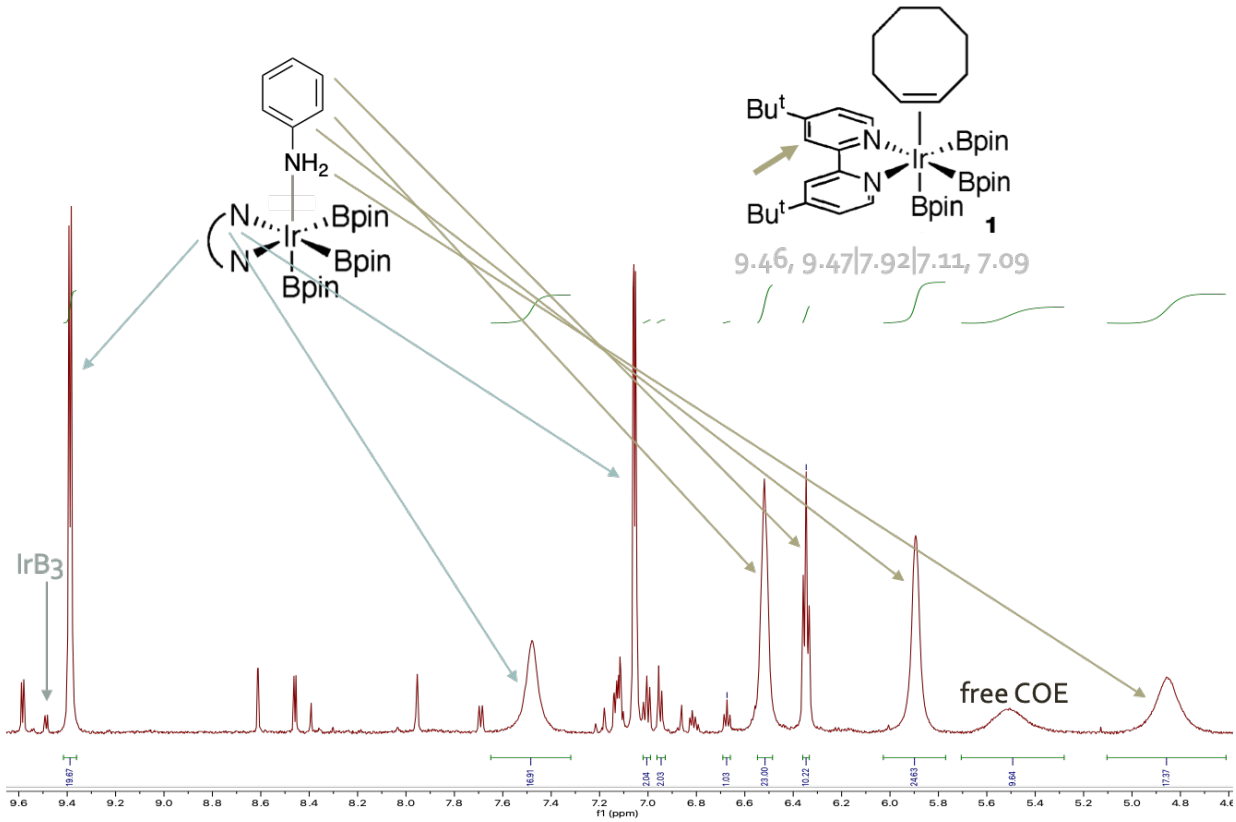

Figure 1.45 ^{1}H-NMR spectrum of the stoichiometric reaction between (dtbpy)Ir(Bpin)$_3$ (1 equiv) and aniline (1 equiv) at t = 5 min

Lastly, the more electron poor thiophenol (as compared to octanethiol) reacts at the Bpin ligand of the iridium trisboryl complex by a new mode (Figures 1.46 – 1.48). In contrast to phenol, which reacts rapidly with **IrB$_3$**, and aniline, which reacts with **IrB$_3$** to give 78% of the N—borylated product after 24 h, thiophenol reacts rapidly at room temperature to form only 50% yield of PhSBpin (Figures 1.46 – 1.48). The remainder of the thiophenol is present in the new iridium complex (PhS)(dtbpy)Ir(Bpin)$_2$H$_2$ (Figures 1.46 – 1.48).

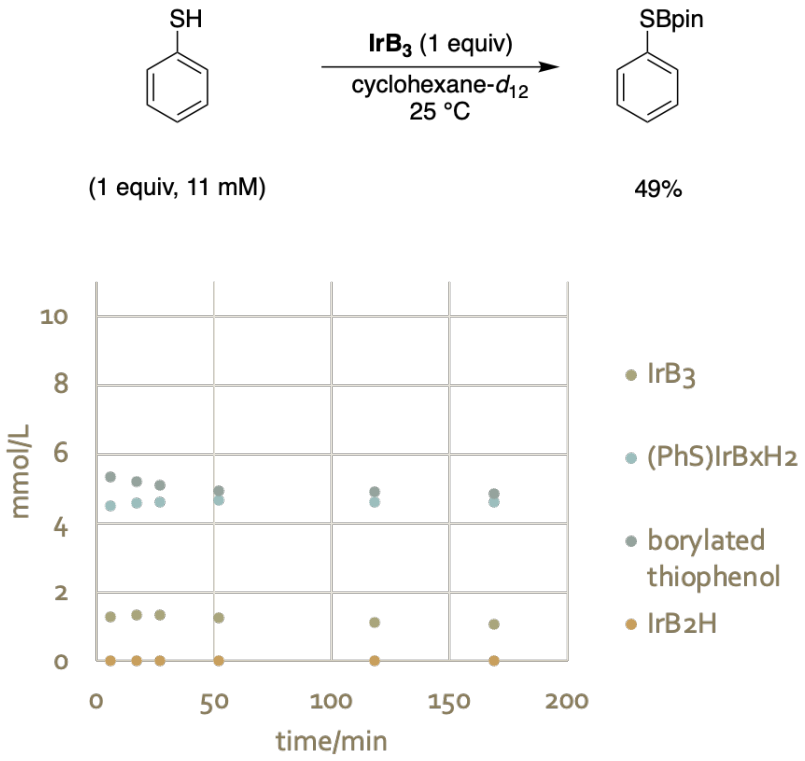

Figure 1.46 Time course for the stoichiometric reaction between thiophenol and IrB_3; IrB_3 = $(dtbpy)(COE)Ir(Bpin)_3$

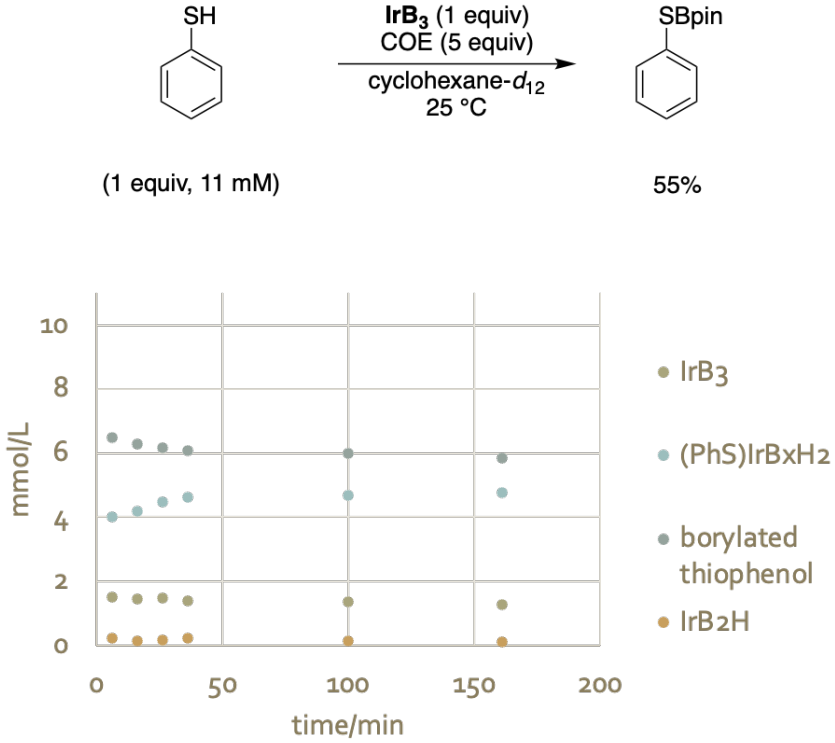

Figure 1.47 Time course for the stoichiometric reaction between thiophenol and IrB_3 with added COE; IrB_3 = (dtbpy)(COE)Ir(Bpin)$_3$

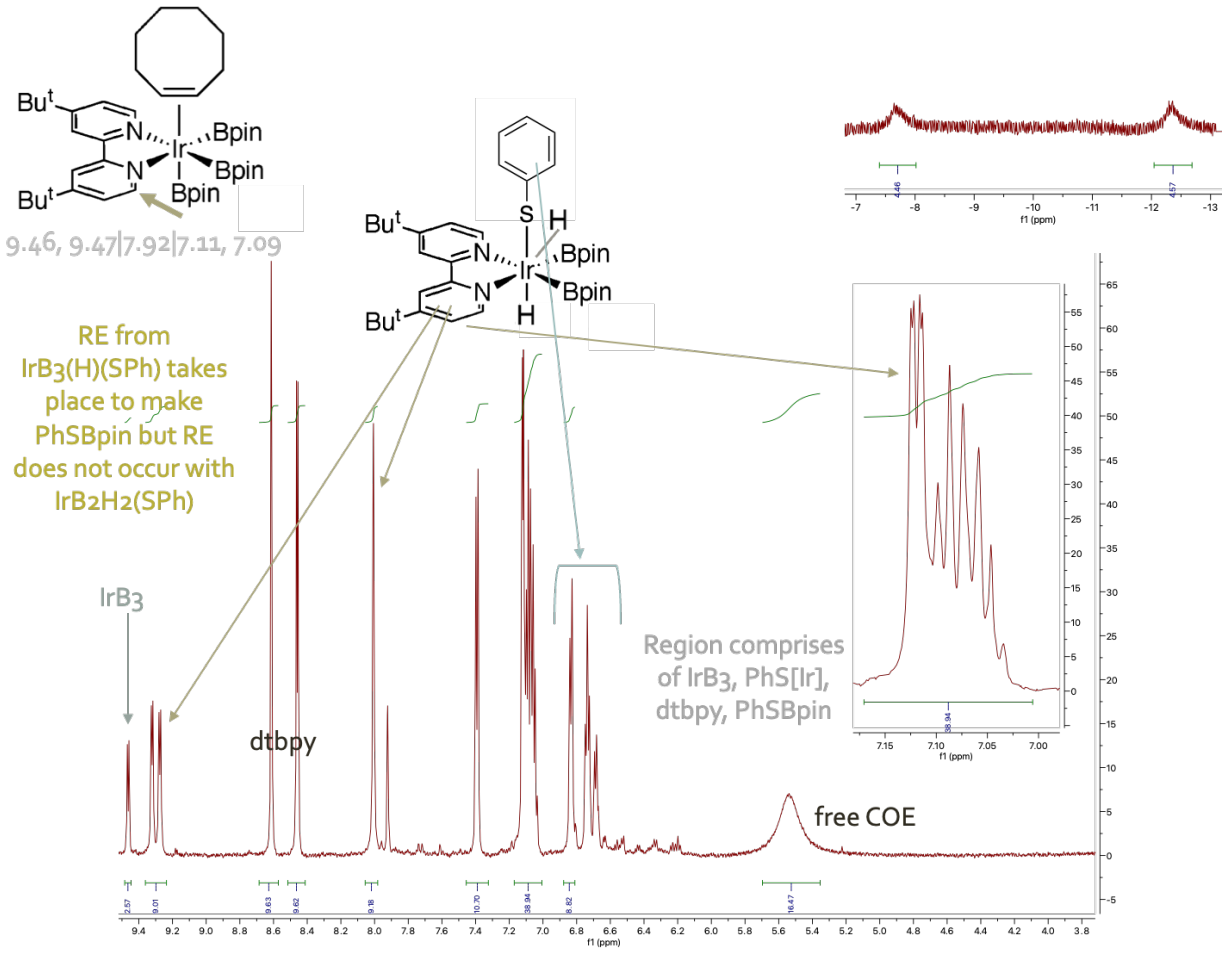

Figure 1.48 ^{1}H-NMR spectrum of the stoichiometric reaction between (dtbpy)Ir(Bpin)$_3$ (1 equiv) and thiophenol (1 equiv)

1.2.5.4 The Ambident Reactivity of Nitrogen Compounds

Figure 1.49 summarizes the ability of nitrogen compounds to function as Lewis bases to Ir or Bpin ligand of the iridium trisboryl complex. From these collective compounds, it is clear that protic nitrogen compounds will borylate at nitrogen, likely via coordination to the Bpin ligand of the iridium trisboryl complex. Unsurprisingly, nitrogen compounds with electron-rich alkyl groups readily borylate, whereas those with electron-poor acyl or phenyl groups slowly borylate.

What is unpredictable is which substituents make a nitrogen compound a functional Lewis base for binding to the iridium center of the iridium trisboryl complex. That aniline binds to iridium (as is observed in the ^{1}H-NMR spectrum, Figure 1.45), whereas N-methylbutyramide does not (as is observed in the ^{1}H-NMR spectrum, Supporting Information), is surprising. That

aniline binds to iridium whereas the primary alkylamine does not (Figures 1.16 & 1.17) likely stems from the fact that the primary alkylamine is a harder Lewis base than aniline, and iridium selects for the softer Lewis base. In their evaluation of the Lewis basicity of amines on the Legault iodonium Lewis acidity scale, Stuart and coworkers determined aniline to have lesser Lewis basicity than acyclic primary and secondary amines.[36] The lesser Lewis basicity of aniline may correspond to a softer Lewis base which, for the iridium trisboryl complex, would select for iridium over the Bpin ligand.

That the dialkylamine binds to iridium (as is observed in the ^{1}H-NMR spectrum, Figure 1.42) whereas the primary alkylamine does not (Figures 1.16 & 1.17) is the most surprising. In their evaluation of the Lewis basicity of amines using a zinc(II) Schiff-base complex as reference Lewis acid, Di Bella and coworkers determined the primary amine, n-propylamine, to be a stronger Lewis base than the secondary amine, pyrrolidine.[37] The lesser Lewis basicity of the secondary amine (in our case, dihexylamine) may correspond to a softer Lewis base which, for the iridium trisboryl complex, would select for iridium over the Bpin ligand.

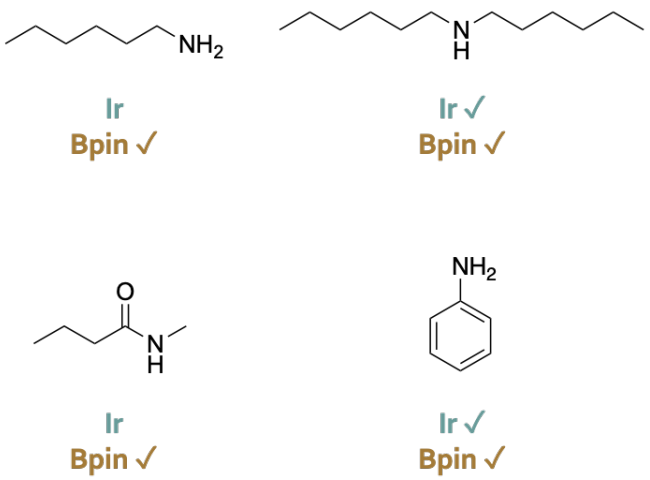

Figure 1.49 Nitrogen compounds and their ability to function as Lewis bases to Ir or Bpin ligand of the iridium trisboryl complex

1.2.5.5 3-Methylpyridine

The electron pair in the sp^2 orbitals of nitrogen atoms also function as Lewis bases binding to the iridium center of the iridium trisboryl complex.[12] The Lewis basicity of this class of compounds is well established and well represented by the dtbpy-ligated iridium trisboryl complex itself.

3-Methylpyridine, a representative compound of this class, has been previously studied by Larsen and Hartwig.[12] In this work, initial rates for the borylation of 3-methylpyridine indicated that the reaction was first-order in the concentration of the catalyst, zero-order in the concentration of B_2pin_2, and zero-order in the concentration of 3-methylpyridine (Figure 1.50). These results led to the proposed mechanistic cycle shown in Figure 1.51 wherein a 3-

methylpyridine bound iridium trisboryl complex is the resting state of the catalyst. They propose that rearrangement of 3-methylpyridine from a nitrogen ligand to a C—H σ-complex then allows oxidative addition (C—H activation).

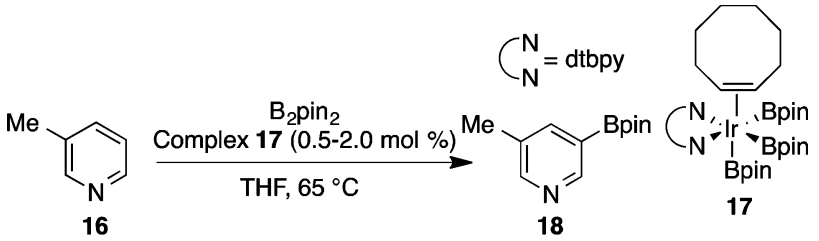

entry	$[B_2pin_2]$ (M)	3-picoline (M)	[catalyst] (M)	initial rate ($M \cdot s^{-1}$)
1	0.50	0.50	0.0025	$1.6 \pm 0.1 \times 10^{-6}$
2	0.50	0.50	0.0050	$3.6 \pm 0.1 \times 10^{-6}$
3	0.50	0.50	0.010	$7.6 \pm 0.4 \times 10^{-6}$
4	1.5	0.50	0.010	$7.9 \pm 0.3 \times 10^{-6}$
5	0.50	1.5	0.010	$8.2 \pm 0.3 \times 10^{-6}$

[a]Reactions were conducted on a 0.25 mmol scale. The formation of product **18** was observed by gas chromatography.

Figure 1.50 Initial rates measurements[12]; Reprinted (adapted) with permission from J. Am. Chem. Soc. 2014, 136, 11, 4287–4299. Copyright 2014 American Chemical Society

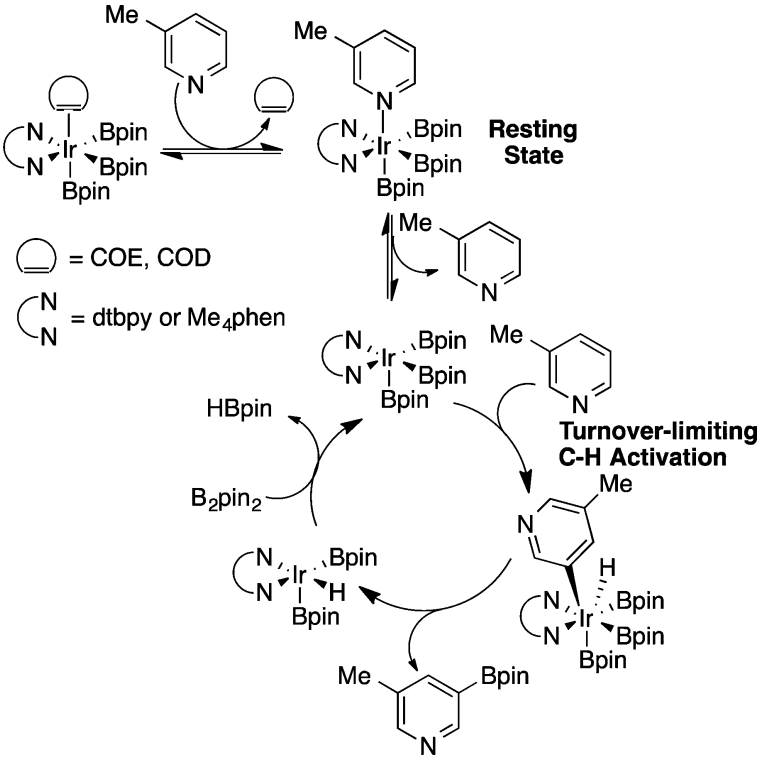

Figure 1.51 Proposed mechanism for the borylation of 3-methylpyridine[12]; Reprinted (adapted) with permission from J. Am. Chem. Soc. 2014, 136, 11, 4287–4299. Copyright 2014 American Chemical Society

Larsen and Hartwig also conducted stoichiometric reactions between 3-methylpyridine and the COE-capped iridium trisboryl complex, demonstrating that 3-methylpyridine binds to iridium as a Lewis base and competes with COE (Figure 1.52).[12]

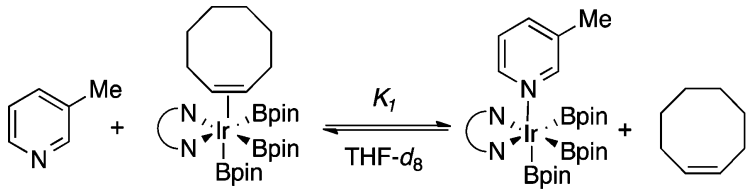

Figure 1.52 K = 1.0; Larsen and Hartwig[12]; Reprinted (adapted) with permission from J. Am. Chem. Soc. 2014, 136, 11, 4287–4299. Copyright 2014 American Chemical Society

Here, stoichiometric reactions between 3-methylpyridine and (COE)(dtbpy)Ir(Bpin)$_3$ were repeated, but in lieu of just initial time points, measurements were taken across an approximate 24-hour time frame (Figures 1.54 & 1.58). Additionally, a comparison between the stoichiometric experiment with and without added COE was conducted (Figures 1.54 & 1.58). While both the stoichiometric experiments with and without added COE revealed full formation of (3-methylpyridine)(dtbpy)Ir(Bpin)$_3$ within the first 5 minutes (as can be seen in the ^{1}H-NMR spectrum, Figure 1.55), the fate of these reactions differed across the 24-hour time frame (Figures 1.54 & 1.58).

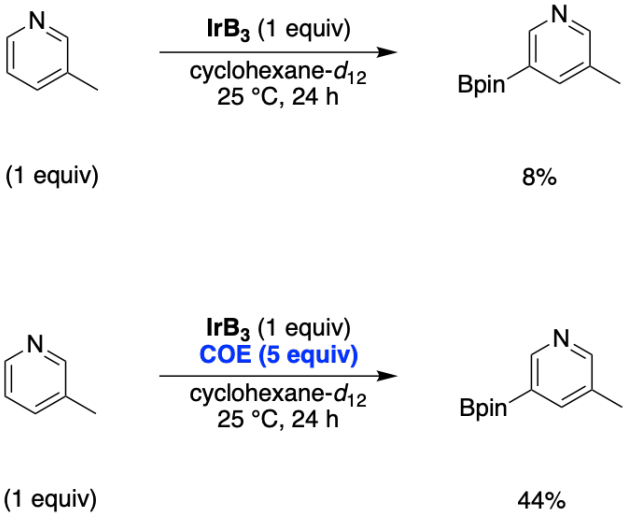

Figure 1.53 Stoichiometric reactions between 3-methylpyridine and IrB$_3$ with and without added COE; IrB$_3$ = (dtbpy)(COE)Ir(Bpin)$_3$

For the stoichiometric reaction conducted without added COE, (3-methylpyridine)(dtbpy)Ir(Bpin)$_3$ is formed within the first 5 minutes (Figures 1.54 & 1.55) and is

stable for 1 hour (Figure 1.54). After 24 hours, however, this complex is completely degraded (Figures 1.54 & 1.56). The ^{1}H-NMR spectrum shows the main reaction components to be general degradation (many peaks in the aryl region, Figure 1.56) and free dtbpy (45%, Figure 1.56, as compared to the 7% observed in the ^{1}H-NMR spectrum taken at 5 minutes, Figure 1.55). Borylated 3-methylpyridine is only present in 8% yield, and free 3-methylpyridine is not observed at all (Figure 1.56). These results suggest that during the course of 24 hours (3-methylpyridine)(dtbpy)Ir(Bpin)$_3$ has degraded to many new unidentified 3-methylpyridine-bound iridium species. The remaining mass balance for dtbpy can likely be accounted for by mono- and bis-borylation of dtbpy (as was reported by Oeschger and Hartwig[10], Figure 1.57, and by Mkhalid and Marder[38]), which in this ^{1}H-NMR spectrum would be challenging to identify since its peaks would overlap with the many decomposition peaks observed in the aryl region (Figure 1.56).

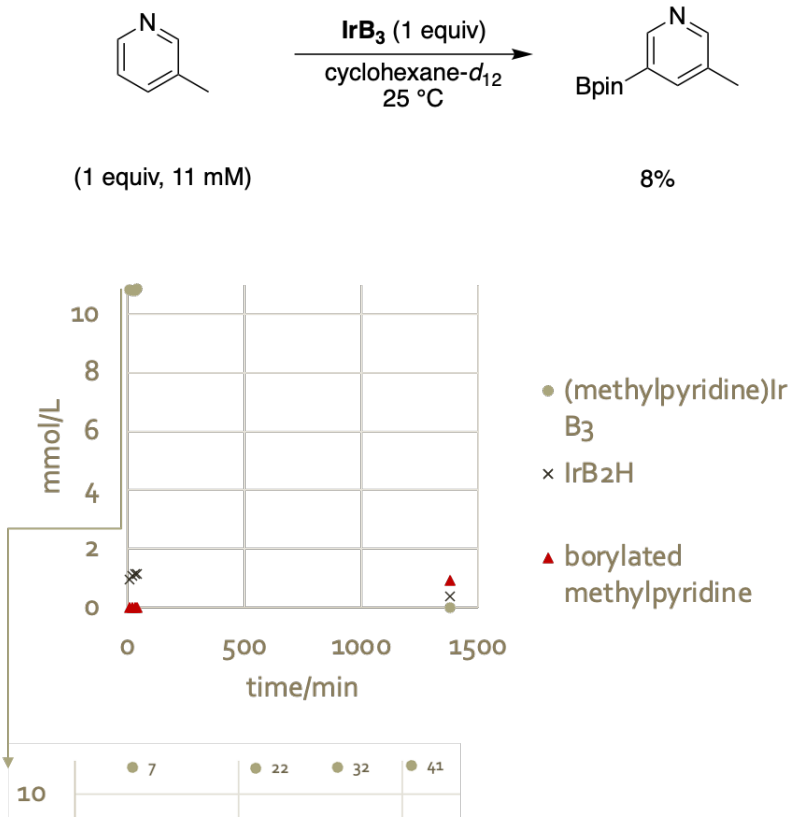

Figure 1.54 Time course for the stoichiometric reaction between 3-methylpyridine (1 equiv) and IrB_3 (1 equiv); IrB_3 = (dtbpy)(COE)Ir(Bpin)$_3$

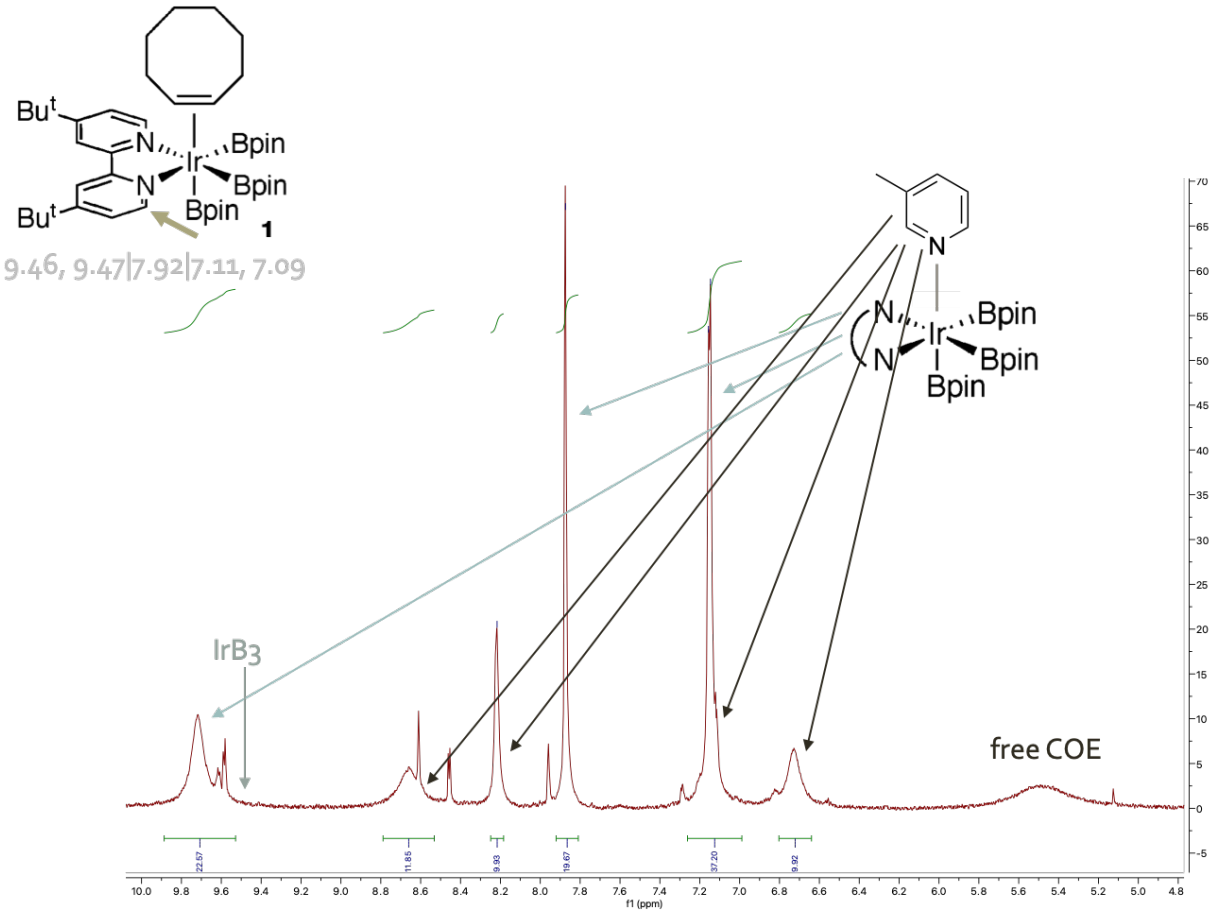

Figure 1.55 ^{1}H-NMR spectrum of the stoichiometric reaction between (COE)(dtbpy)Ir(Bpin)$_3$ (1 equiv) and 3-methylpyridine (1 equiv) at t = 5 min; No free 3-methylpyridine is present (the most obvious absent peak is the original apparent triplet at 6.9 ppm, see Supporting Information for the ^{1}H-NMR spectrum of free 3-methylpyridine) and the Ir-bound 3-methylpyridine peaks can be clearly identified. The dtbpy ligand peaks for the (COE)(dtbpy)Ir(Bpin)$_3$ are likewise absent. Instead, new dtbpy ligand peaks for the (3-methylpyridine)(dtbpy)Ir(Bpin)$_3$ can be clearly identified.

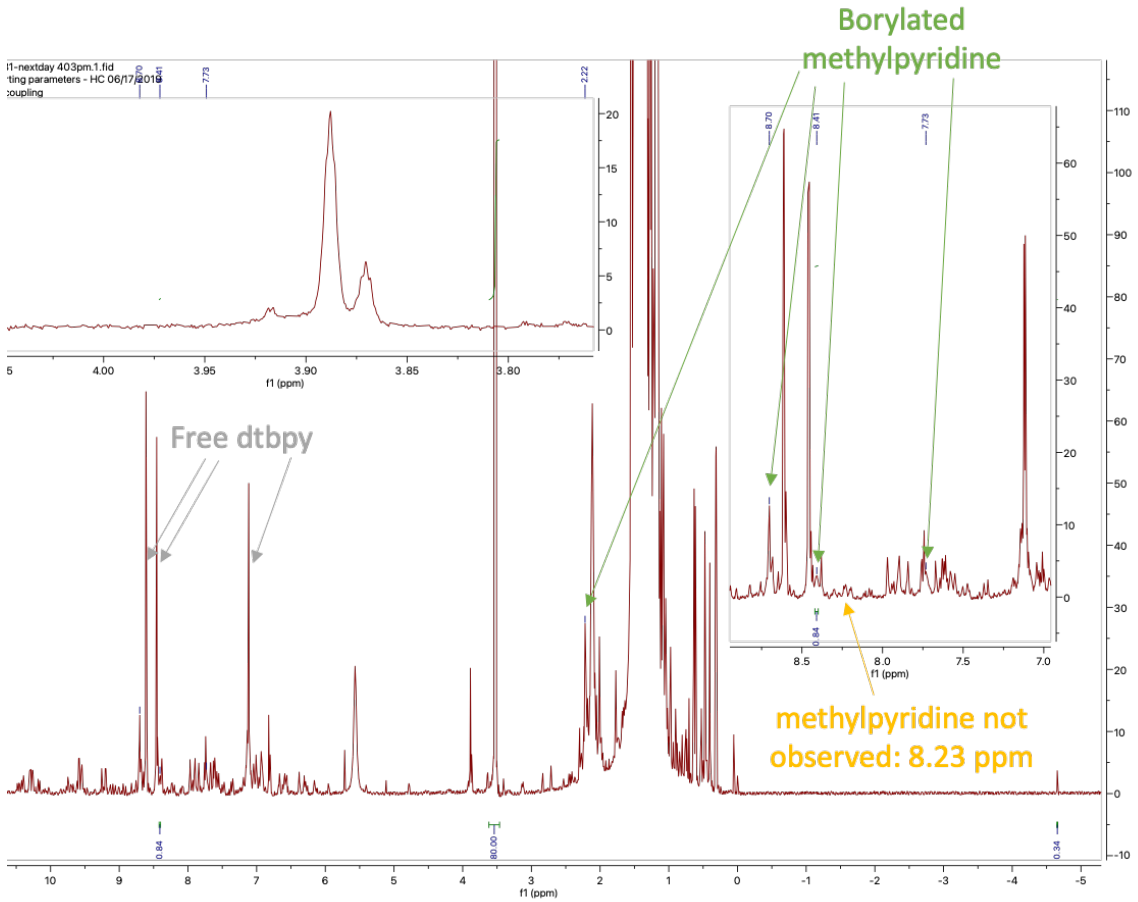

Figure 1.56 ^{1}H-NMR spectrum of the stoichiometric reaction between (COE)(dtbpy)Ir(Bpin)$_3$ (1 equiv) and 3-methylpyridine (1 equiv) at t = 24 h

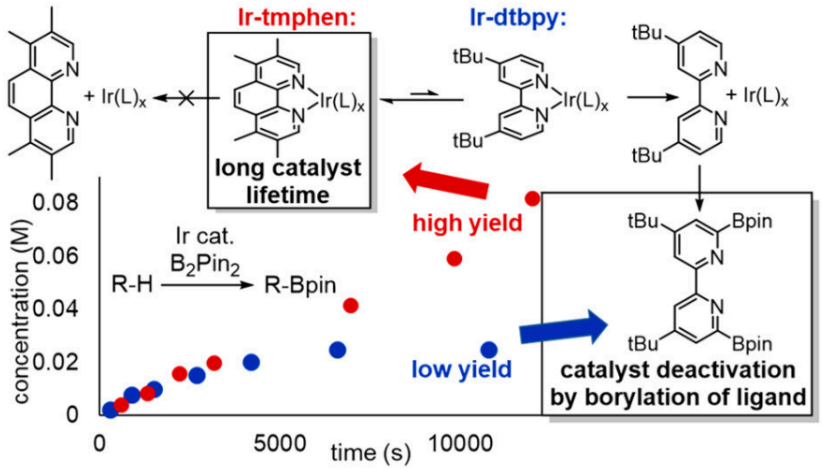

Figure 1.57 Catalyst lifetime: Ir-tmphen versus Ir-dtbpy[10]; Reprinted (adapted) with permission from J. Am. Chem. Soc. 2019, 141, 41, 16479–16485. Copyright 2019 American Chemical Society

For the stoichiometric reaction conducted with added COE, (3-methylpyridine)(dtbpy)Ir(Bpin)$_3$ is formed within the first 5 minutes and is stable for 1 hour

(Figure 1.58). After 24 hours, however, this complex has completely degraded (Figure 1.58). Here, 44% of borylated 3-methylpyridine is formed (Figure 1.58), as compared to the 8% formed in the corresponding reaction without added COE (Figure 1.54). The iridium bisboryl hydride, the byproduct of arene borylation[9] with the iridium trisboryl complex as the borylating agent, is also present in greater proportion (Figure 1.58) than in the corresponding reaction without added COE (Figure 1.54). Added COE facilitates the borylation of 3-methylpyridine.

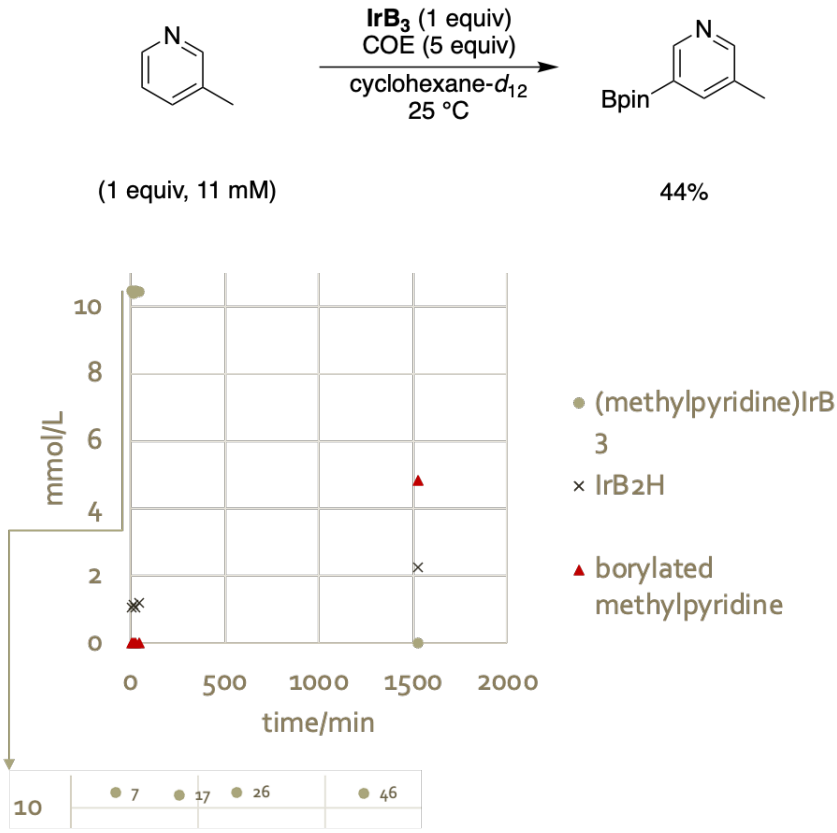

Figure 1.58 Time course for the stoichiometric reaction between 3-methylpyridine (1 equiv) and IrB_3 (1 equiv) in the presence of added COE; IrB_3 = (dtbpy)(COE)Ir(Bpin)$_3$

1.2.5.6 2-Butyne [pKa ~ 43]

Alkynes are another class of compounds that bind to the sixth coordination site of the dtbpy-ligated iridium trisboryl complex. All of the aforementioned Lewis bases displaced COE within the first 5 minutes. By contrast, in the presence of an equimolar amount of 2-butyne, COE is gradually displaced, culminating in a terminal ratio of (2-butyne)(dtbpy)Ir(Bpin)$_3$ to (COE)(dtbpy)Ir(Bpin)$_3$ of 1:5 (Figure 1.59). Furthermore, the alkyne-bound iridium trisboryl complex makes for a complex that is stable to heating to 100 °C for an hour in which time the COE-bound iridium trisboryl complex has entirely degraded. Although it is unsurprising that 2-butyne binds more strongly than does COE and displaces COE, it is surprising that this displacement is so slow. Collectively, (COE)(dtbpy)Ir(Bpin)$_3$ seems kinetically favored whereas (2-butyne)(dtbpy)Ir(Bpin)$_3$ seems thermodynamically favored.

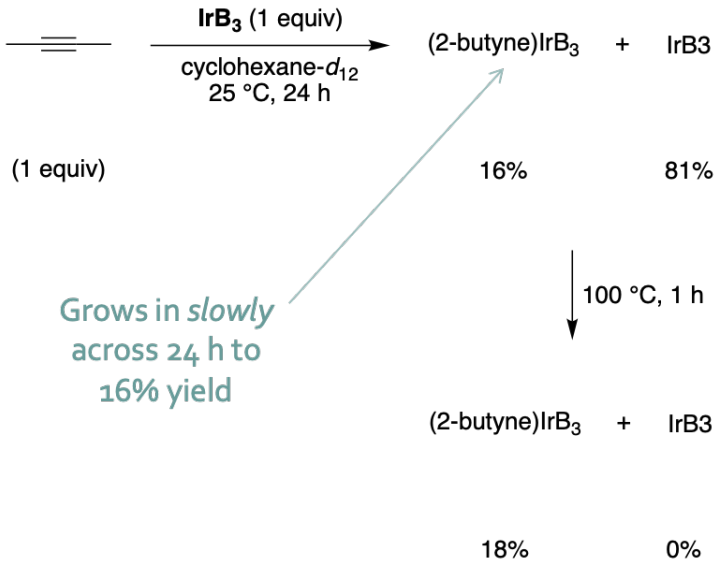

Figure 1.59 Stoichiometric reactions between 2-butyne (1 equiv) and IrB_3 (1 equiv); IrB_3 = (dtbpy)(COE)Ir(Bpin)$_3$. The pKa of 2-butyne is approximated to be 43; it is approximated against the measured value of 44 for propene[20].

(2-butyne)(dtbpy)Ir(Bpin)$_3$ also has a different geometry than does (COE)(dtbpy)Ir(Bpin)$_3$ (Figure 1.60). COE occupies an axial position on the iridium trisboryl complex as evidenced by the symmetric peaks of the two pyridine halves of the bidentate dtbpy ligand (Figure 1.60).[9] By contrast, 2-butyne appears to occupy an equatorial position on the iridium trisboryl complex as evidenced by the desymmetrized peaks of the two pyridine halves of the bidentate dtbpy ligand (Figure 1.60). As the simplest internal alkyne, 2-butyne may be small enough to accommodate this geometry.

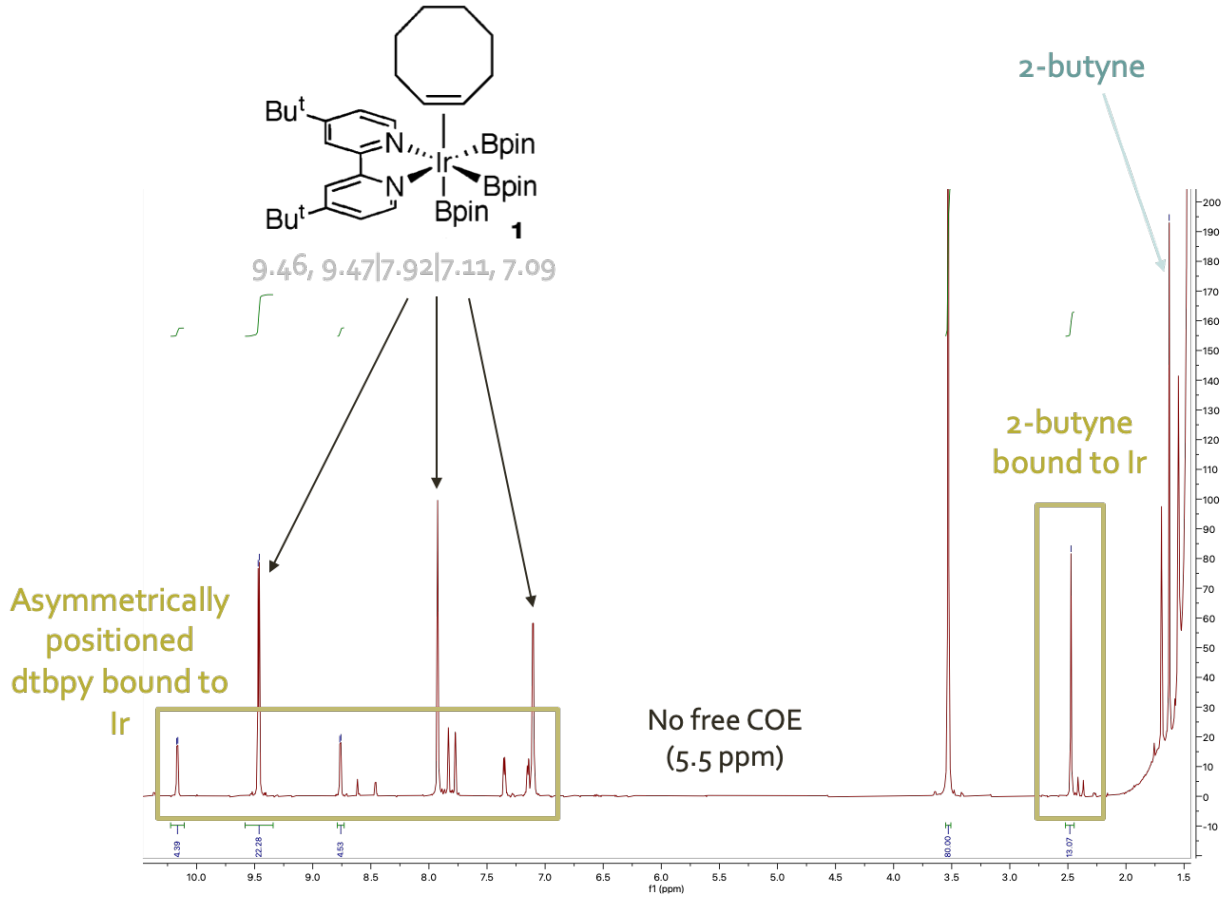

Figure 1.60 ^{1}H-NMR spectrum of the stoichiometric reaction between (dtbpy)Ir(Bpin)$_3$ (1 equiv) and 2-butyne (1 equiv) at t = 24 hours

Repeating the stoichiometric reaction but at an elevated temperature of 50 °C (Figure 1.61) produced a ^{1}H-NMR spectrum showing the same amount of (2-butyne)(dtbpy)Ir(Bpin)$_3$ (16% yield, Figure 1.61) as was formed in the stoichiometric reaction at 25 °C (Figure 1.59). Therefore, it is reestablished that the maximum yield of (2-butyne)(dtbpy)Ir(Bpin)$_3$ is 16%. At 50 °C, (COE)(dtbpy)Ir(Bpin)$_3$ gradually degrades to different unidentified iridium species (Figure 1.61). The elevated temperature only facilitated a trace amount of borylation at the terminal carbon (Figure 1.61).

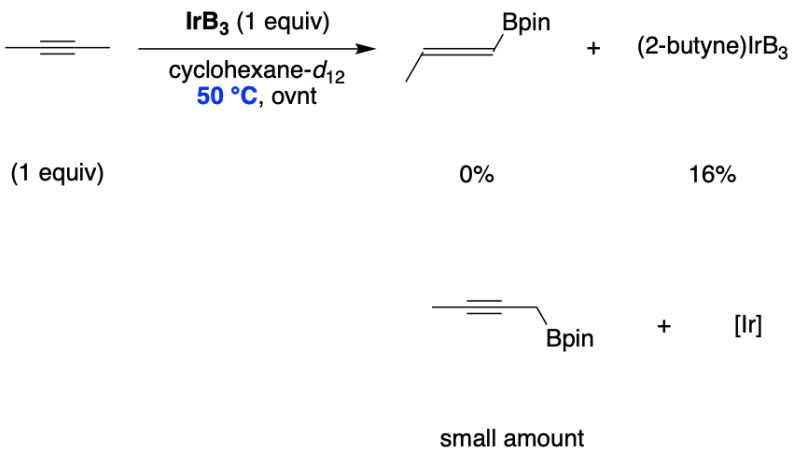

Figure 1.61 Stoichiometric reaction between 2-butyne (1 equiv) and IrB_3 (1 equiv) at 50 °C; IrB_3 = (dtbpy)(COE)Ir(Bpin)$_3$

1.2.5.7 Comparison of Stoichiometric Reactions with and without Added COE as Assay for Mode of Reactivity

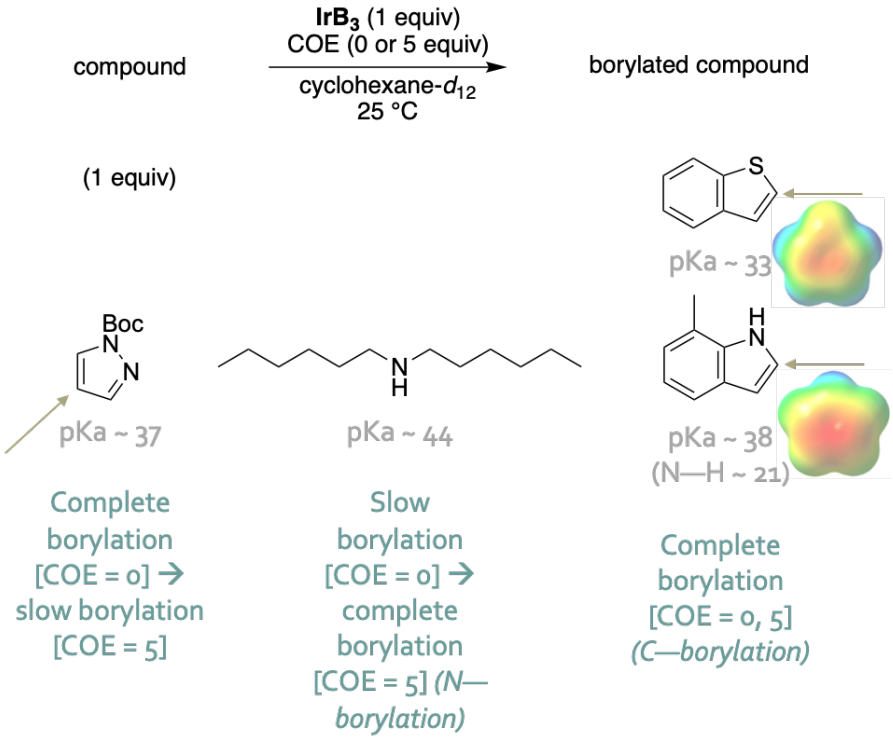

Figure 1.62 Three motifs for the COE assay[20]; IrB_3 = (dtbpy)(COE)Ir(Bpin)$_3$. The approximated pKa of 33 in DMSO for benzothiophene is approximated against the measured pKa value of 33.5 in THF for benzothiophene[39]. The approximated pKa of 38 in DMSO for the C—H bond of 7-methylindole is approximated against the measured pKa value of 38.1 in THF for 1-methylindole[39]. The approximated pKa of 21 in DMSO for the N—H bond of 7-methylindole is approximated against the measured pKa value of 20.95 in DMSO for indole[20].

Thus far, the comparison between stoichiometric reactions with and without added COE has been a useful assay for how a compound reacts with the iridium trisboryl complex. When added COE decreases the rate of borylation, as was seen in the case of boc-pyrazole, the compound is proposed to undergo oxidative addition with the iridium trisboryl complex (Figure 1.21). When added COE has no effect on the rate of borylation, as was seen in the case of 1-hexylamine and N-methylbutyramide, the compound is proposed to coordinate to the Bpin ligand of the iridium trisboryl complex (Figures 1.16, 1.17, 1.20). When added COE increases the rate of borylation, as was seen in the case of dihexylamine, the compound exhibits ambident reactivity (Figure 1.41).

When this assay was applied to benzothiophene and 7-methylindole, it was observed that C—borylation took place within the first 5 minutes regardless of the concentration of COE (Figures 1.63 – 1.66). The collective assessment of Lewis bases suggests that iridium selects for soft Lewis bases. The lone pairs on the nitrogen atom of 7-methylindole as well as one of the lone pairs on the sulfur atom of benzothiophene are delocalized in the extended aromatic system of the biaryl rings. It is proposed that for these compounds of extended aromatic delocalization binding to iridium is facile and complete (COE does not compete with this binding) such that the concentration of COE does not play a role. It is known that benzothiophene can bind to iridium in several ways: κ-S, η^2, η^4, η^5, and η^6 (as was examined by Perez and coworkers in their study of binding modes of thiophene and benzothiophene to N-heterocyclic carbene iridium complexes)[40]. Although it is at present unclear which mode of binding is taking place, it is proposed that once bound, a rearrangement to a C—H σ-complex takes place which then undergoes oxidative addition.

This proposal is further bolstered by the example of 7-methylindole. In every case examined thus far, any X—H bond will borylate at the heteroatom via coordination to the Bpin ligand of the iridium trisboryl complex. 7-methylindole, however, in spite of having an N—H bond, displays selectivity for the C—H bond (Figures 1.65 & 1.66). Sevov and Hartwig, in their 2014 publication on the iridium-catalyzed hydroamination of unactivated alkenes with indoles, also provided an example of selectivity for C—H activation over N—H activation.[41] Here, it is proposed that binding of 7-methylindole to iridium, rearrangement to a C—H σ-complex, and oxidative addition should be much faster than nitrogen coordinating to the Bin ligand of the iridium trisboryl complex.

These compounds are being described as privileged substrates for oxidative addition because they both presumably exhibit facile binding to iridium as well as possess an activated C—H bond for oxidative addition (Figure 1.62). By contrast, boc-pyrazole presumably exhibits competitive binding with COE and has a less activated C—H bond for oxidative addition (one which is not adjacent to a heteroatom) (Figure 1.62).

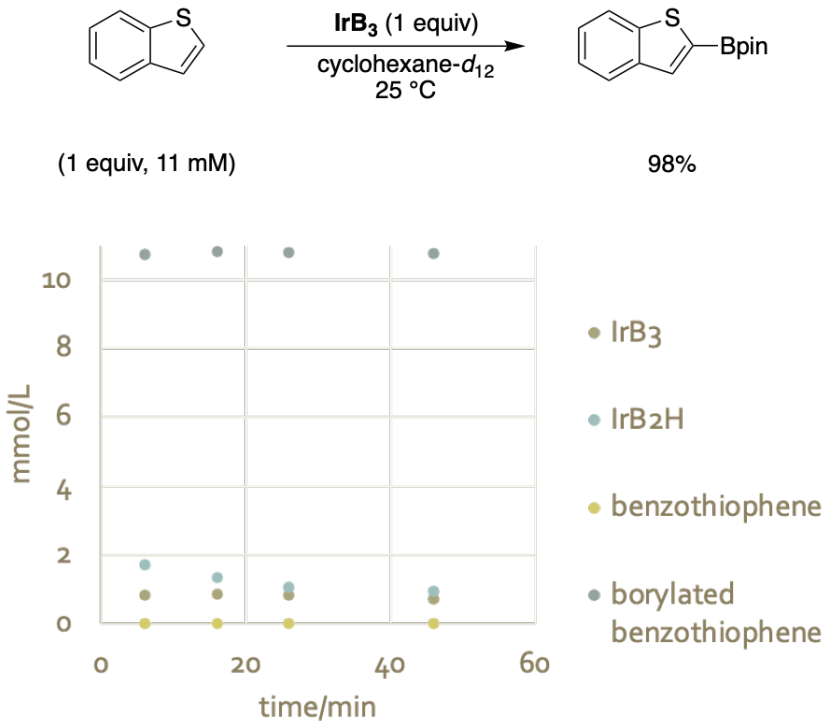

Figure 1.63 Time course for the stoichiometric reaction between benzothiophene (1 equiv) and IrB_3 (1 equiv); IrB_3 = (dtbpy)(COE)Ir(Bpin)$_3$

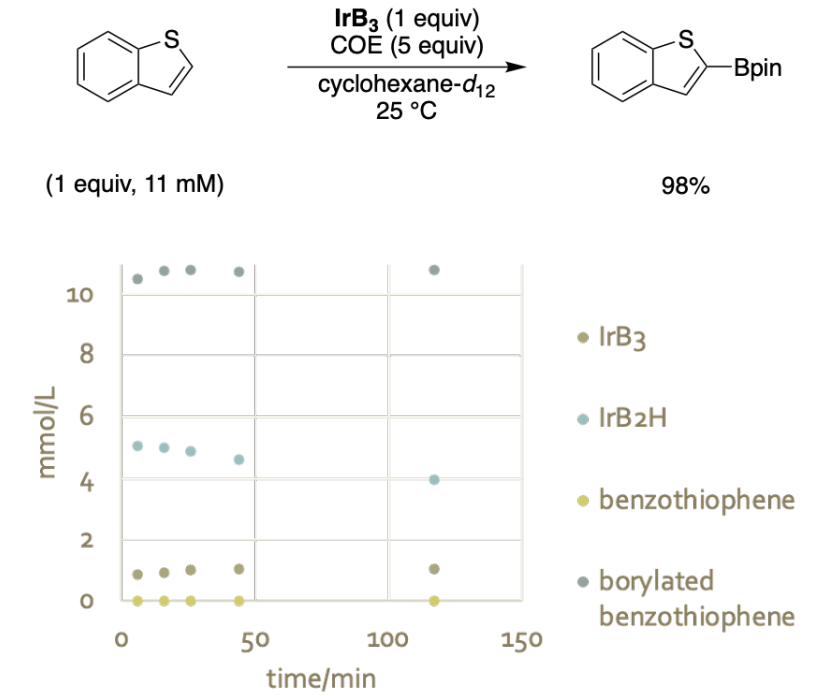

Figure 1.64 Time course for the stoichiometric reaction between benzothiophene (1 equiv) and IrB_3 (1 equiv) with added COE (5 equiv); IrB_3 = (dtbpy)(COE)Ir(Bpin)$_3$

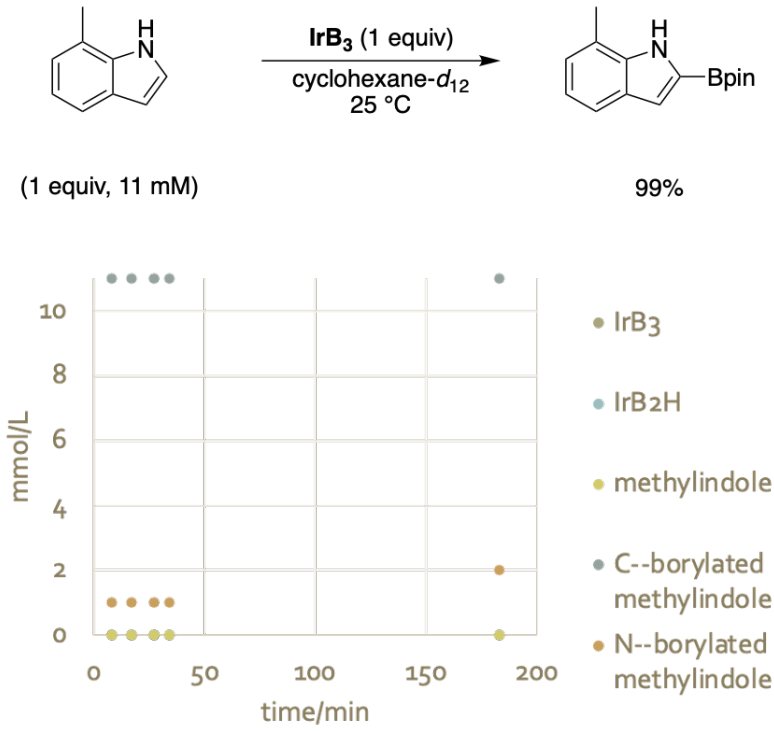

Figure 1.65 Time course for the stoichiometric reaction between 7-methylindole (1 equiv) and IrB_3 (1 equiv); IrB_3 = (dtbpy)(COE)Ir(Bpin)$_3$. The minor amount of N—borylated methylindole (~10%) is proposed to have formed from an error of 1.1 equiv addition of 7-methylindole as opposed to the intended 1 equiv. It is proposed that the iridium bisboryl hydride is the borylating agent for the N—borylation of 7-methylindole.

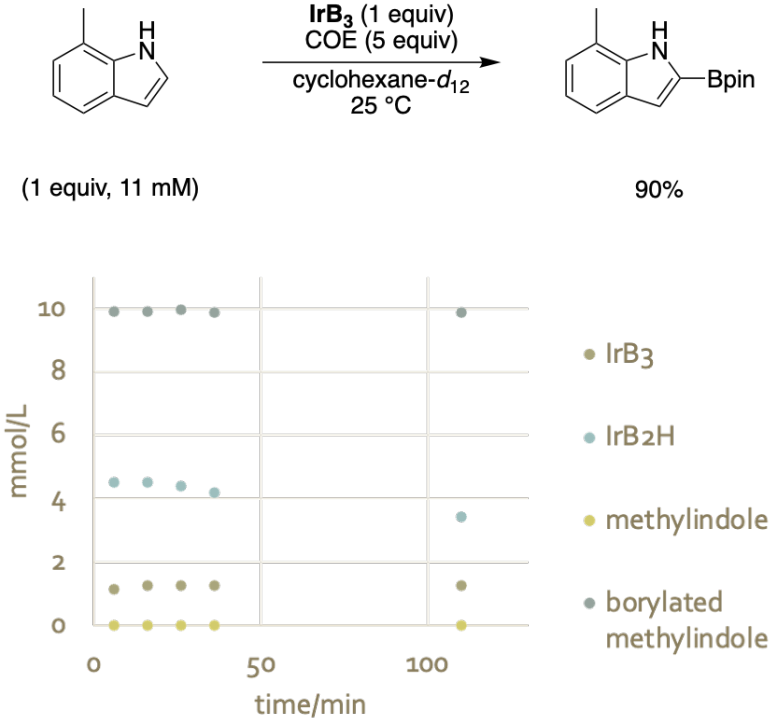

Figure 1.66 Time course for the stoichiometric reaction between 7-methylindole (1 equiv) and IrB_3 (1 equiv) with added COE (5 equiv); IrB_3 = (dtbpy)(COE)Ir(Bpin)$_3$

1.2.5.8 Summary of ^{11}B-NMR Spectroscopy

Throughout this work, ^{11}B-NMR spectroscopy has been an invaluable tool for the characterization of borylated compounds. It has provided distinct ranges for different X—B bonds with clear differentiation based on the electronegativity of the heteroatom (Figure 1.67). Likewise, ^{11}B-NMR spectroscopy has provided distinct ranges for different C(sp^x)—B bonds with clear differentiation based on the electronegativity of the orbital (Figure 1.67).

By contrast, no iridium complex in this study has been observable by ^{11}B-NMR spectroscopy at ambient temperature. The iridium trisboryl complex is reported to exhibit a broad peak in the ^{11}B-NMR spectrum at 34 ppm at ambient temperature.[9] However, in this study, none of the ^{11}B-NMR spectroscopy measurements of the iridium trisboryl complex showed any peak.

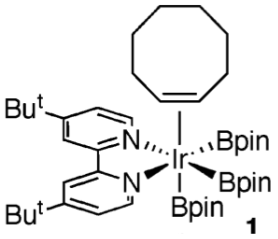

(COE)IrB$_3$
no ^{11}B-NMR resonance

^{11}B-NMR (ppm)					
34	30	29, 28	24	22	21
borylated octanethiol	*borylated arene*	*Hbpin*	*borylated hexylamine*	*borylated hexanol*	*BOB*
S—B	**C(sp²)—B**	**H—B**	**N—B**	**O—B**	**O—B**
Lit example			*borylated phenylacetylene*		
C(sp³)—B			**C(sp)—B**		

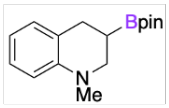

Figure 1.67 Summary of ^{11}B-NMR spectroscopy[42]; IrB_3 = (dtbpy)(COE)Ir(Bpin)$_3$

1.2.6 Solutions for Additives which Impede the Catalytic C—H Borylation Reaction

1.2.6.1 Alkyliodide

The stoichiometric reactions probed the mechanism of reactivity of the iridium trisboryl complex with different classes of organic compounds. These organic compounds mimic

important functional groups of complex molecules used as substrates in the Ir-catalyzed borylation reaction. Understanding the mechanism of reactivity of the iridium trisboryl complex with different organic compounds provides guidance toward solutions to functional groups which hinder the Ir-catalyzed borylation reaction.

Another means of assessing functional group compatibility of complex molecules is to conduct a Glorius robustness screen[13] (Figure 1.68). Hamel and coworkers (unpublished work) adapted the Glorius robustness screen to the Ir-catalyzed borylation reaction (Figures 1.68 & 1.69). The borylation of a variety of arenes was conducted in the presence of different classes of organic compounds (Figure 1.68). A representative screen is shown in Figure 1.69 wherein arenes are borylated in the presence of octyliodide. While the borylation of fast reacting arenes such as 7-methylindole (Ar5) and benzofuran (Ar6) were unaffected by the presence of this additive, the borylation of the other arenes, including 2-chloro-4-fluoro-1-methylbenzene (Ar2), was diminished (Figure 1.69).

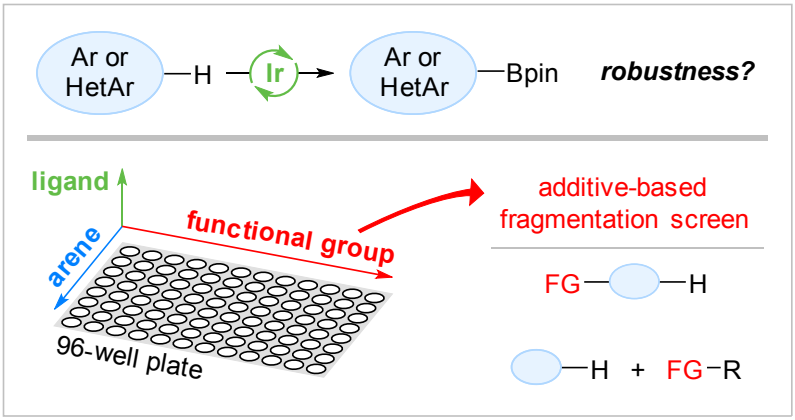

Figure 1.68 Glorius robustness screen for C—H borylation

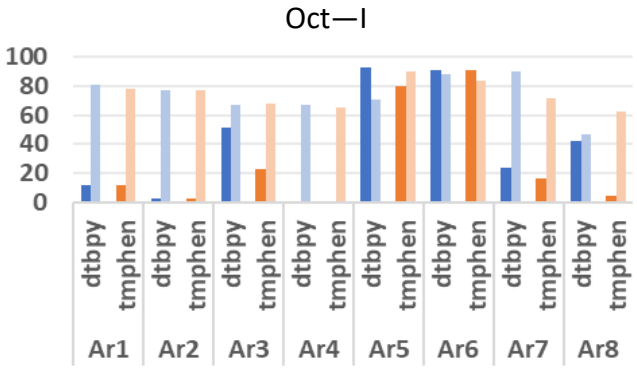

Figure 1.69 Representative Glorius robustness screen result for additive = octyliodide

Alkyliodides in the presence of an organometallic complex can sometimes undergo oxidative addition via an S_N2 pathway. If this happens faster than the oxidative addition of the arene C—H bond, then the presence of an alkyliodide could hinder the borylation of the arene. The S_N2 oxidative addition of an alkyliodide would be facilitated by a polar solvent, such as MeTHF used

in the screens. To test this hypothesis, the borylation of Ar2 in the presence of alkyliodide was conducted in both cyclohexane and THF (Figure 1.70). Reaction in THF gave 44% conversion of Ar2 to its borylated product, whereas reaction in cyclohexane gave 87% conversion of Ar2 to its borylated product. While these results support the hypothesis, corresponding stoichiometric reactions should be conducted to corroborate these results. For the catalytic reaction, however, using a nonpolar solvent enables the borylation of Ar2 in the presence of an alkyliodide.

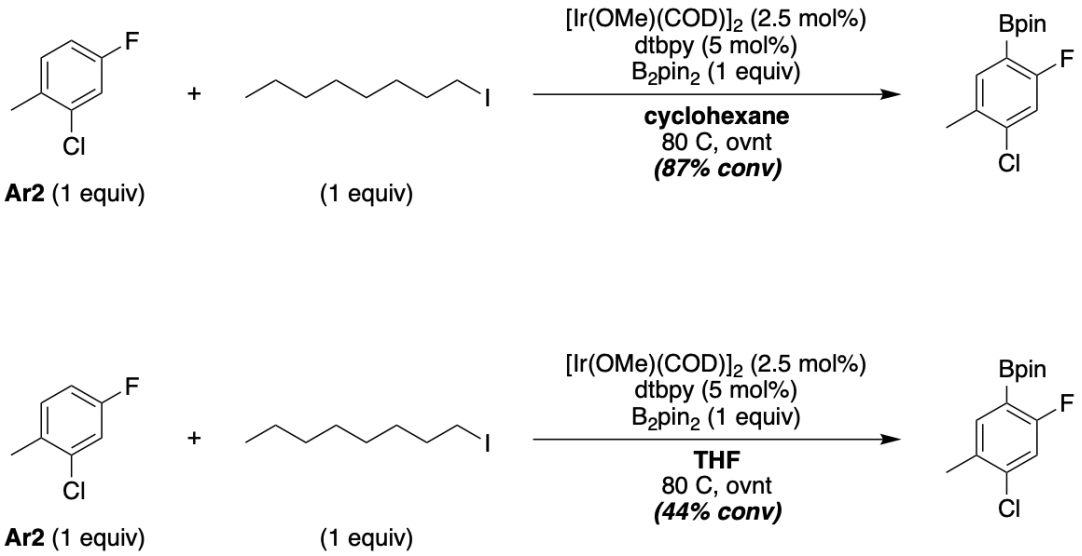

Figure 1.70 Catalytic borylation of Ar2 in the presence of octyliodide in cyclohexane and in THF

1.2.6.2 Primary Thiol

Hamel and coworkers also found practical solutions to protic compounds interfering with the Ir-catalyzed borylation of arenes. One solution is to first protect the protic compound by borylating it with HBpin, then conduct the arene borylation reaction in the presence of the borylated additive, and then deprotect the borylated additive with 2-Py-MeOH (Figure 1.71). This solution, however, was not highly effective for primary thiols. The protection of primary thiols was modestly effective, providing 70 – 80% conversion, but the deprotection did not proceed (Figure 1.71).

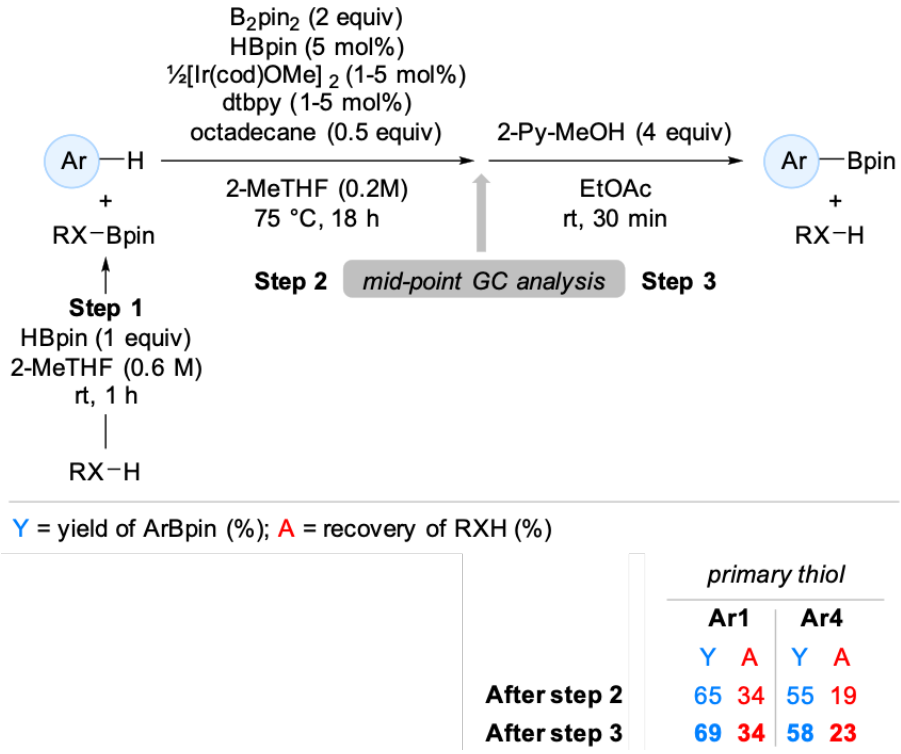

Y = yield of ArBpin (%); A = recovery of RXH (%)

	primary thiol			
	Ar1		**Ar4**	
	Y	A	Y	A
After step 2	65	34	55	19
After step 3	**69**	**34**	**58**	**23**

Figure 1.71 Pre-treatment of protic additive with HBpin

Here, increasing the equivalents of HBpin, as well as the reaction temperature, provided full conversion of the primary thiol (Figure 1.72). Moreover, leveraging the oxophilicity of boron, the borylated primary thiol can be deprotected (90% conversion) with a tertiary alcohol at elevated temperature (Figure 1.72).

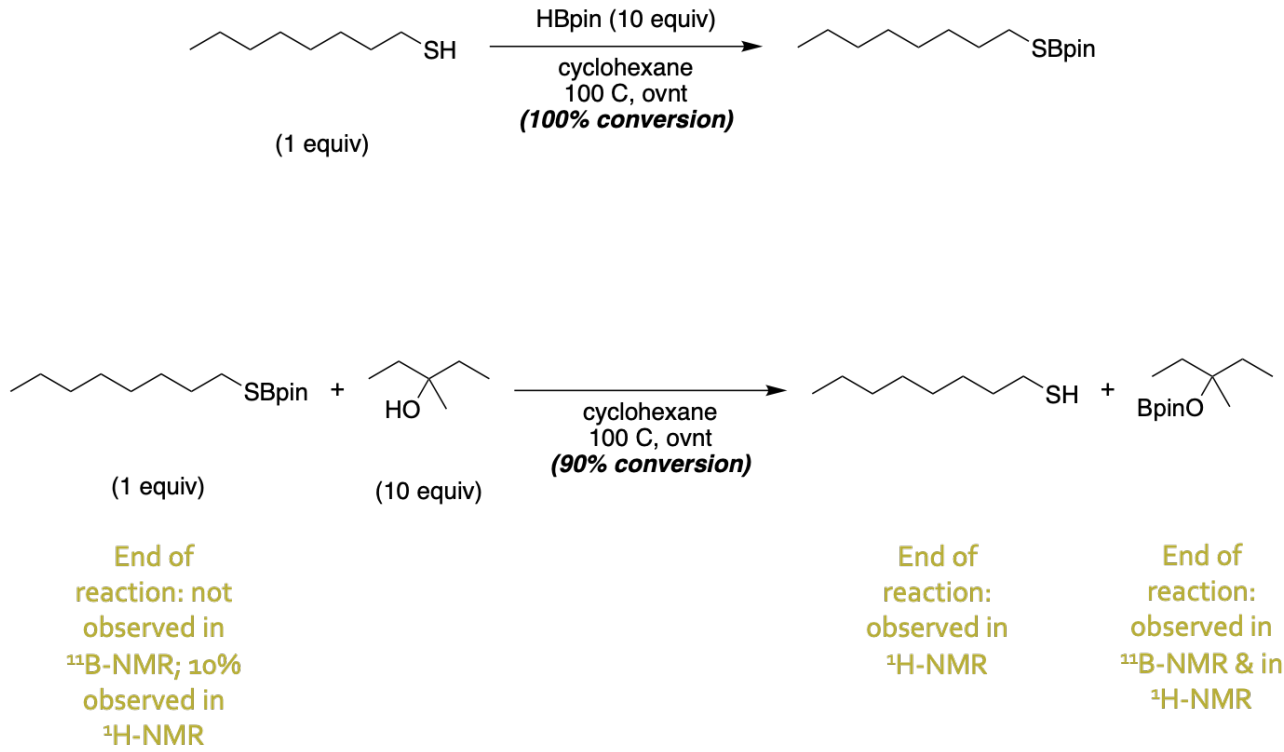

Figure 1.72 Near full deprotection of borylated thiol with hard nucleophile

1.3 Conclusion

The iridium trisboryl complex has two loci of reactivity. The iridium center is the site of oxidative addition of C—H bonds of increased acidity, increased s-character, and decreased steric congestion. It is also a site for the binding of soft Lewis bases of which ones with adjacent activated C—H bonds presumably subsequently undergo oxidative addition. The Bpin ligand is a site for the binding of hard Lewis bases of which those with protic X—H bonds subsequently undergo borylation. Lewis bases intermediate in the hard-soft spectrum display ambident reactivity, binding at both the iridium center and the Bpin ligand. The fundamental principles of acidity, s-character, sterics, and Lewis basicity are elaborated upon with the many examples of classes of compounds to give delineation to specific ranges and structures. Better predictive power is now in place for the borylation of a new compound as well as for the borylation of a complex molecule with many sites of functionality.

1.4 Experimental

1.4.1 Background & Control Experiments

(dtbpy)(COE)Ir(Bpin)$_3$ [IrB$_3$] Characterization[9]

[Synthesis]

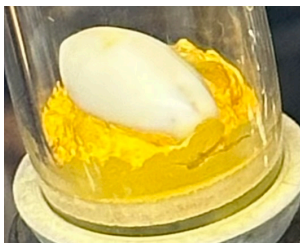

In a glovebox, under an inert atmosphere of nitrogen, to a 100-mL round bottom flask equipped with a stir bar was added bis(1,5-cyclooctadiene)di-μ-methoxydiiridium(I) (838 mg, 1.3 mmol). Cyclohexane (80 mL) and cis-cyclooctene (2.2 mL, 16.9 mmol) were added, and the mixture was stirred for a minimum of 20 minutes until full dissolution of contents to make for a homogeneous solution. Then, dropwise, HBpin (2.2 mL, 15.2 mmol) was added to the stirred solution which was further stirred at ambient temperature for an additional hour. 4,4’-di-tert-butyl-2,2’-dipyridyl (663 mg, 2.5 mmol) was added, and the mixture was stirred inside the glovebox overnight.

Inside the glovebox, the solution was concentrated as thoroughly as possible. Then, the opened flask was allowed to sit inside the glovebox overnight to ensure full dryness of the crude material. Tetramethylsilane was used to suspend the crude which was then poured atop a fritted funnel. The mixture was vacuum filtered (still inside the glovebox) and rinsed with tetramethylsilane. In the event that all the material seeps through the frit (the pure compound can only be well separated from the impurities when it is in high enough yield; impurities increase the solubility of the pure compound in tetramethylsilane) the crude solution in tetramethylsilane was allowed to settle inside the glovebox fridge overnight. Then, using a pipette, the top black solution was removed from the bottom loose bed of yellow solids. The wet solids were spread around the vial to increase the surface area of this crude material. Then, tetramethylsilane was used to rinse the solids and the rinse was decanted. This process was repeated iteratively. In total, 100-mL of tetramethylsilane is needed for purification. The title compound was isolated as a bright yellow powder (75%).

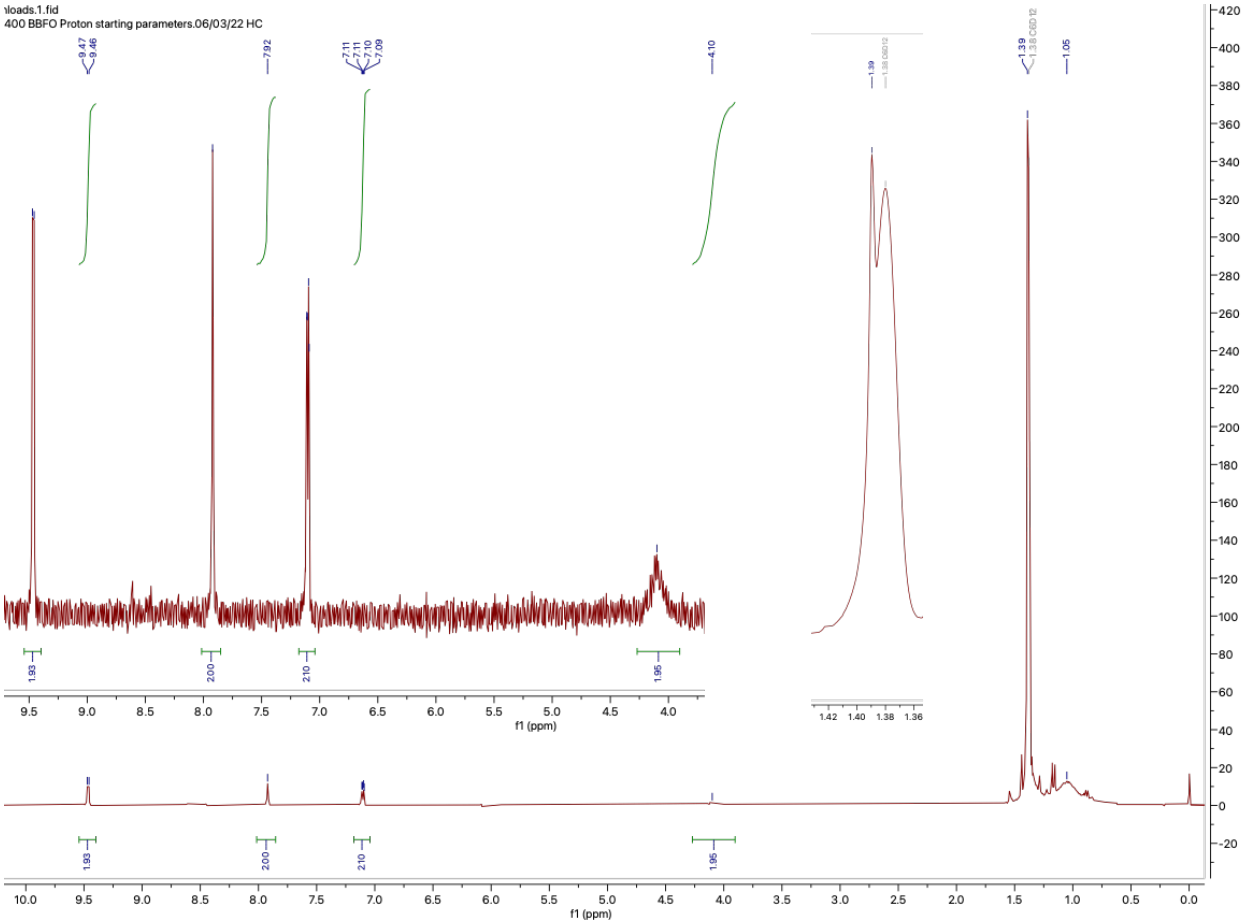

^{1}H-NMR:

9.47, 9.46 (2H); 7.92 (2H); 7.11, 7.11, 7.10, 7.09 (2H), 1.39 (18H) [dtbpy ligand]

4.10 (2H) [vinyl C—H of COE ligand]

1.05 (36H) [Bpin ligand]

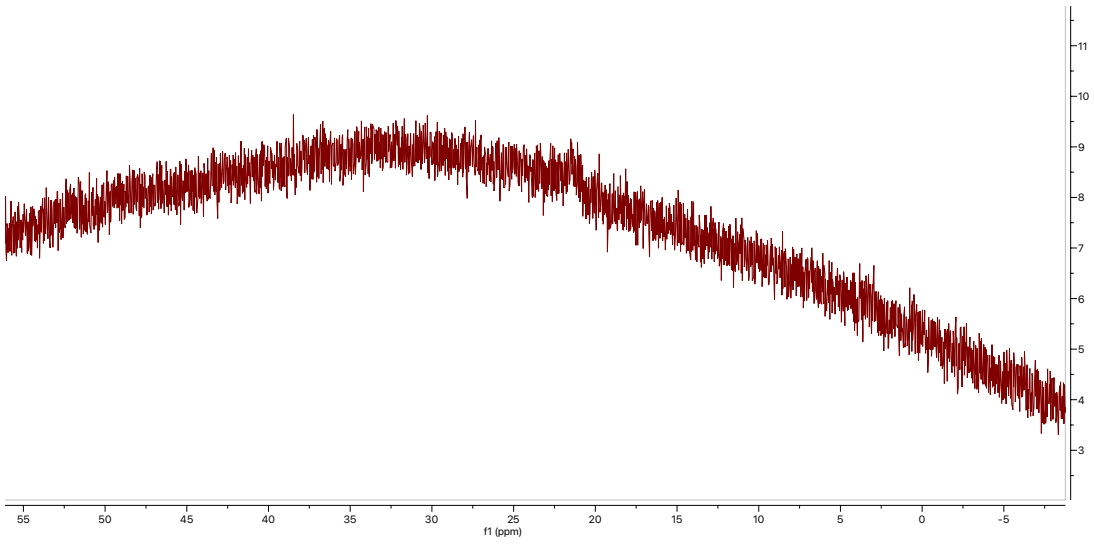

^{11}B-NMR

(dtbpy)Ir(Bpin)$_2$H Characterization[9]

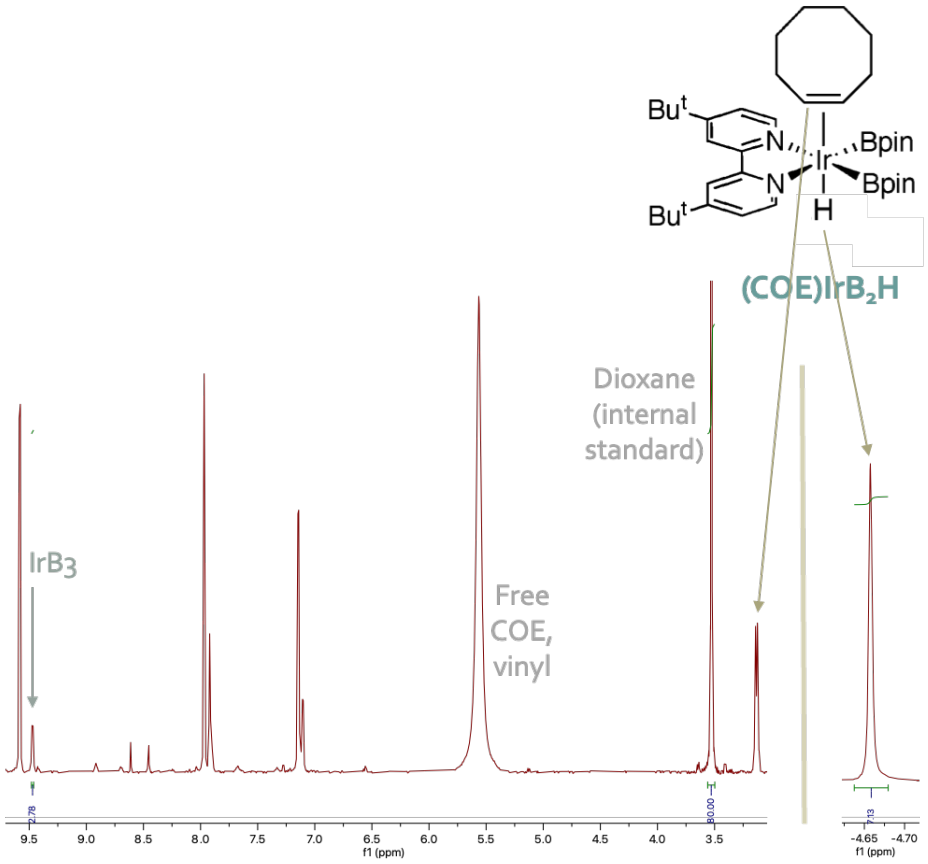

(dtbpy)Ir(Bpin)H$_2$ Characterization[9]

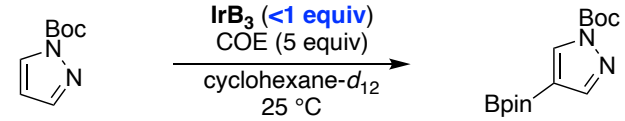

(1 equiv)

54%

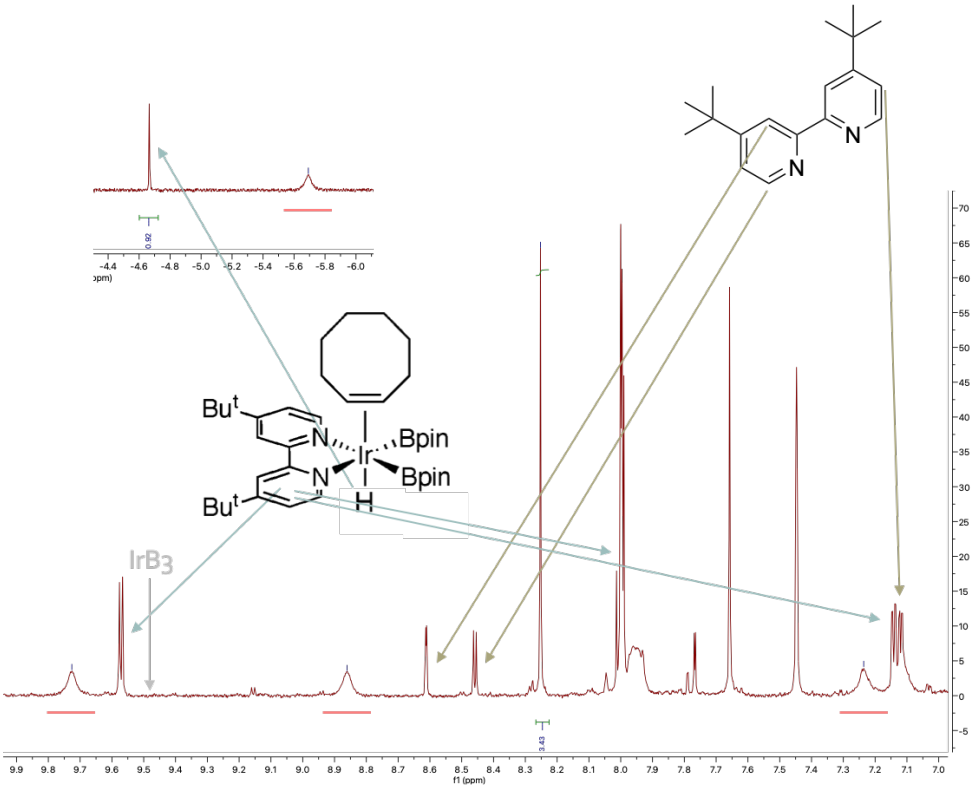

^{1}H-NMR spectrum of (dtbpy)Ir(Bpin)H$_2$ (peaks underlined in red), t = 40 min

Dioxane (Internal Standard) Characterization

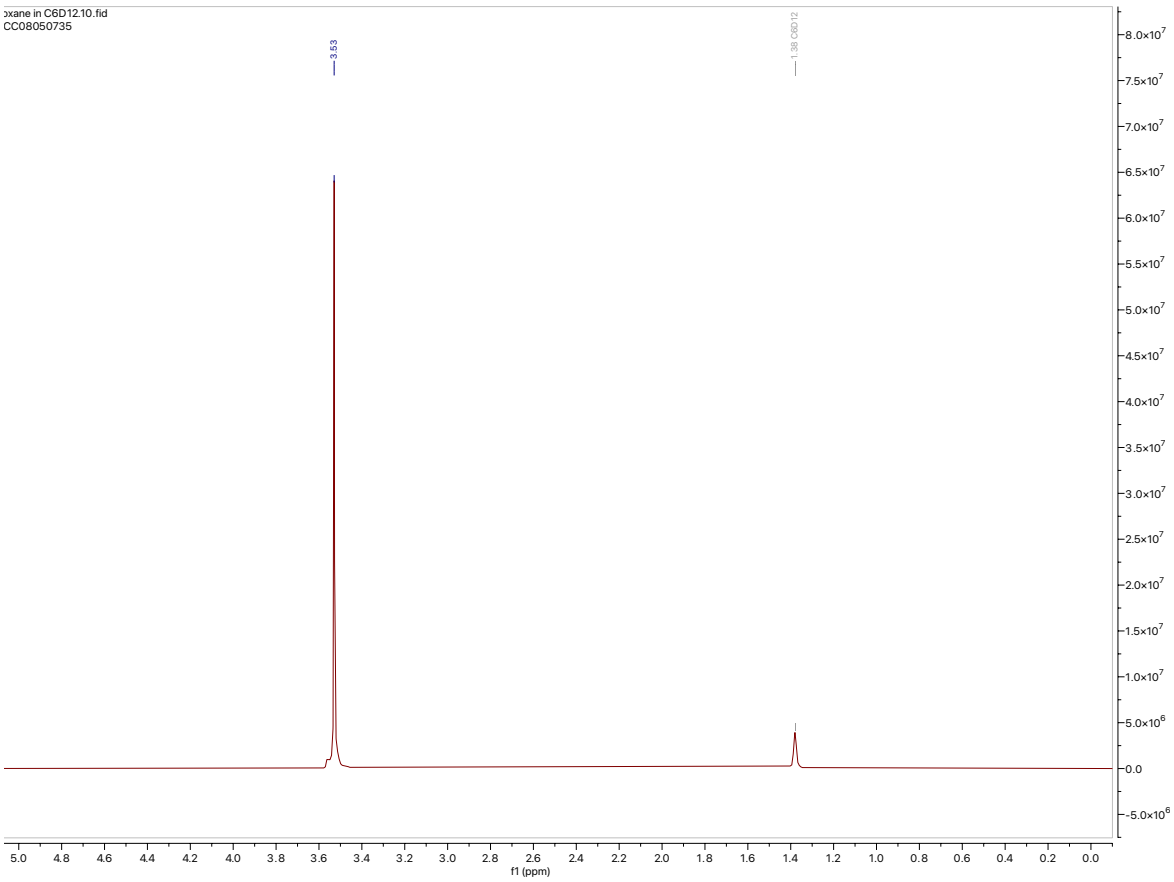

^{1}H-NMR

Dtbpy Characterization

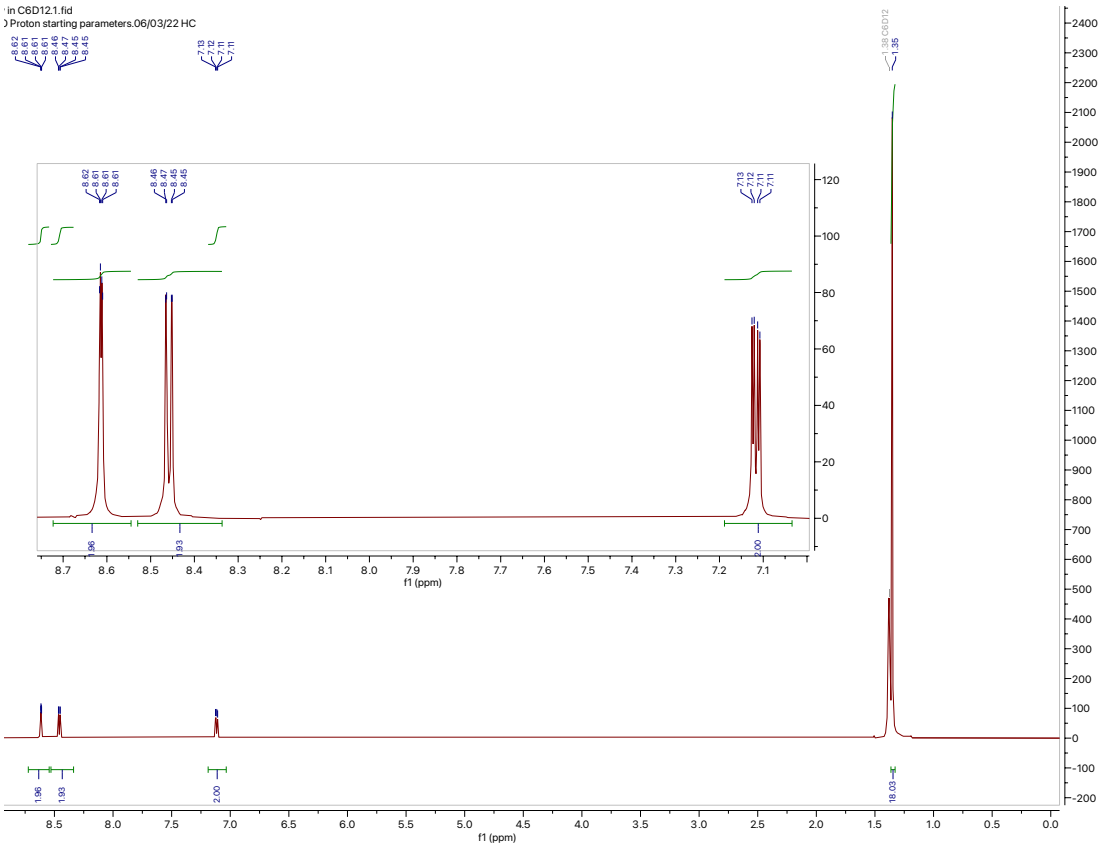

^{1}H-NMR

HBpin Characterization

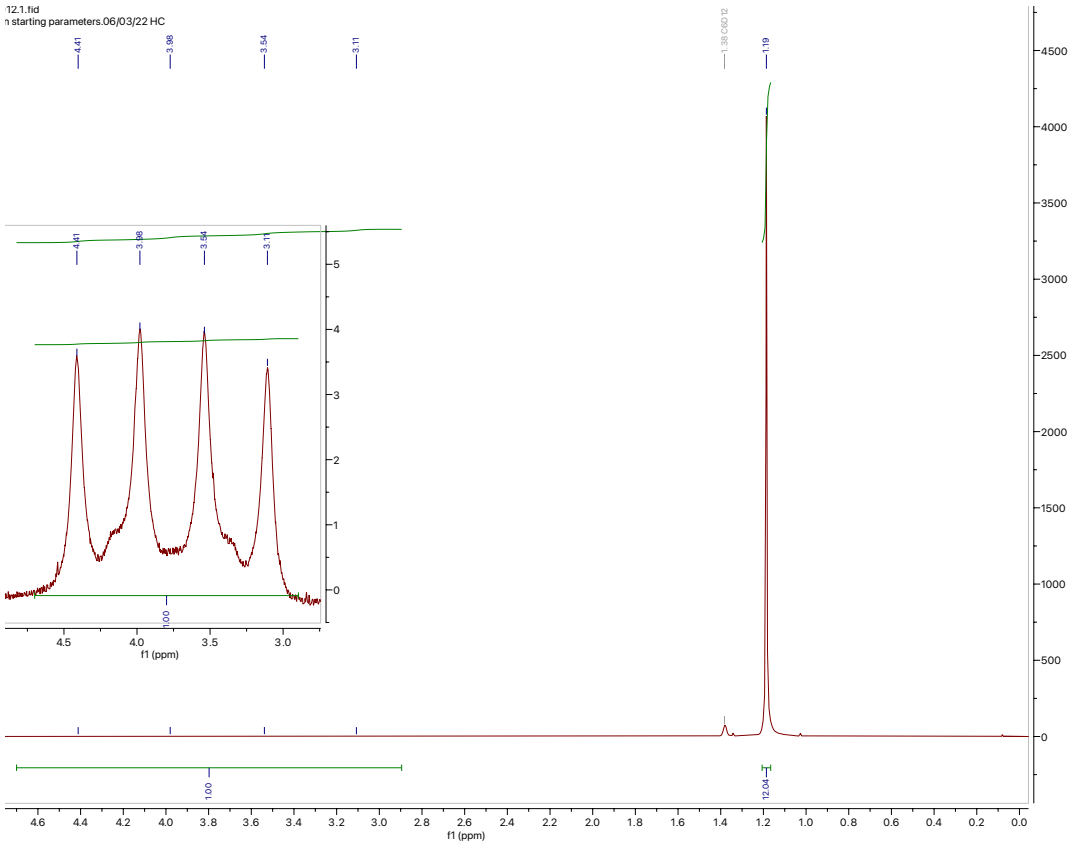
12.1.fid
n starting parameters.06/03/22 HC
4.41
3.98
3.54
3.11
1.38
1.19
1.00
12.04
f1 (ppm)

^{1}H-NMR

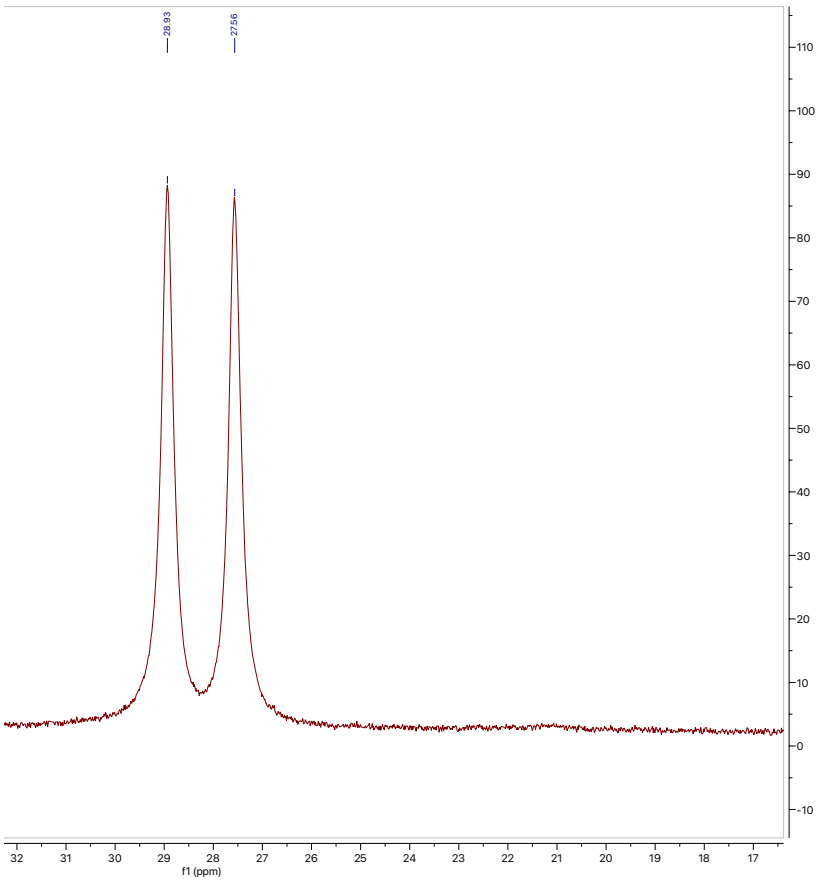

^{11}B-NMR

Bpin—O—Bpin [BOB] Characterization

[Synthesis]

In a glovebox, under an inert atmosphere of nitrogen, to a 4-mL vial equipped with a stir bar was added HBpin (400 mg, 3 mmol) which was diluted with cyclohexane (650 uL). The vial was sealed and allowed to stir at 100 °C for 18 h. The vial was allowed to cool to room temperature. An aliquot of the reaction mixture was taken and diluted with C_6D_{12} for ^{1}H-NMR, ^{11}B-NMR, ^{13}C-NMR spectroscopy and GCMS analysis.

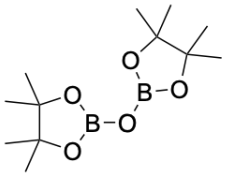

Exact Mass: 270.18

retention time (min)	m/z
5.9	270.2, 255.2

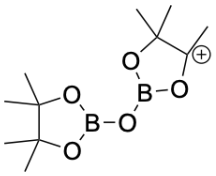

Exact Mass: 255.16

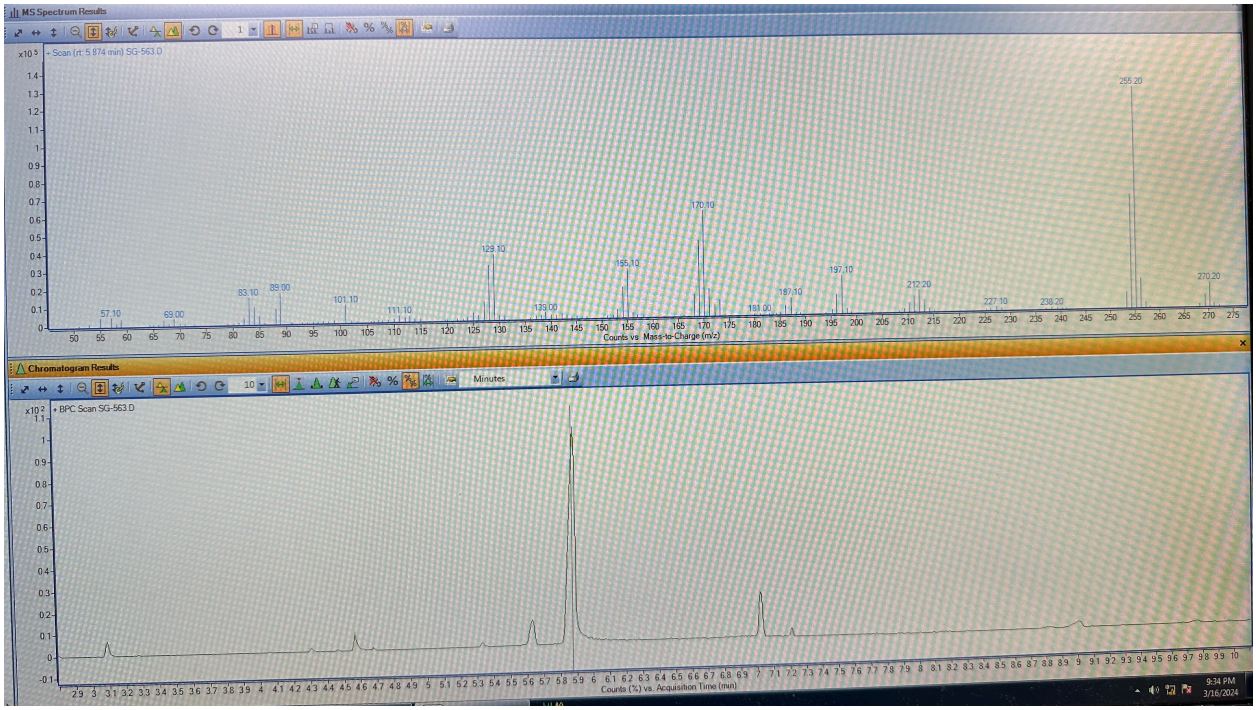

GCMS

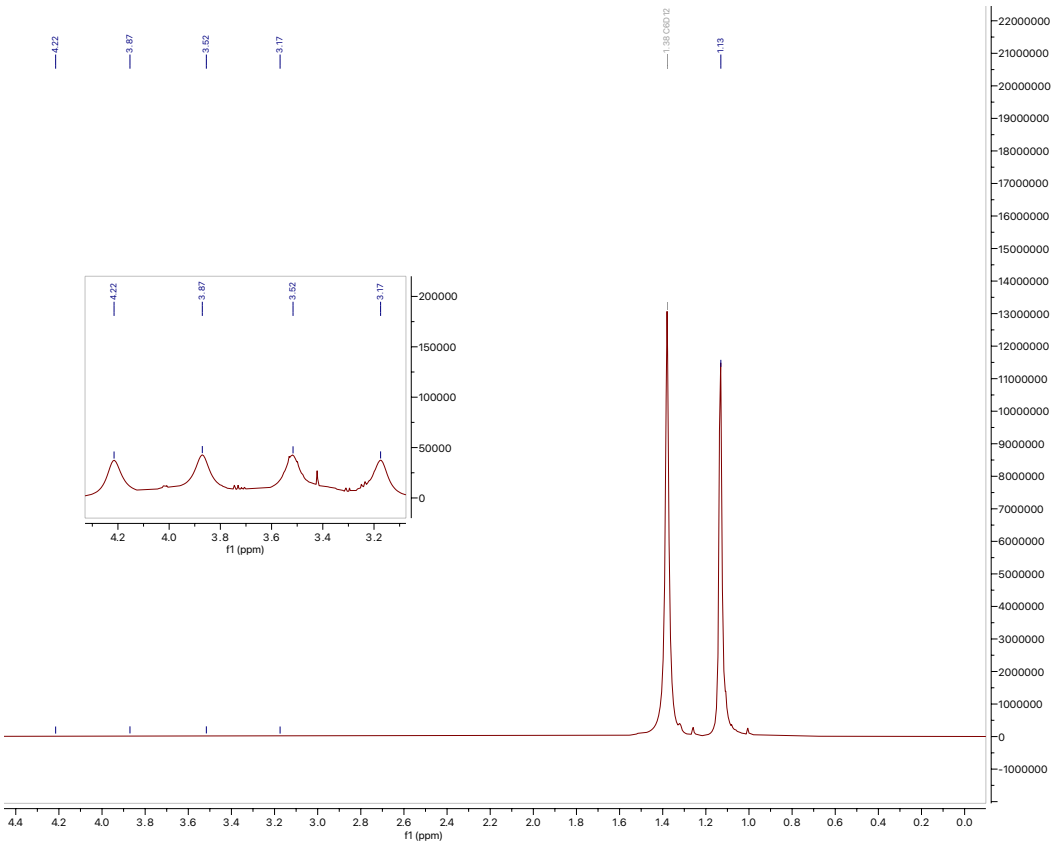

^{1}H-NMR

Note: The methyl peaks of BOB and HBpin overlap; BOB and HBpin cannot be distinguished by ^{1}H-NMR spectroscopy

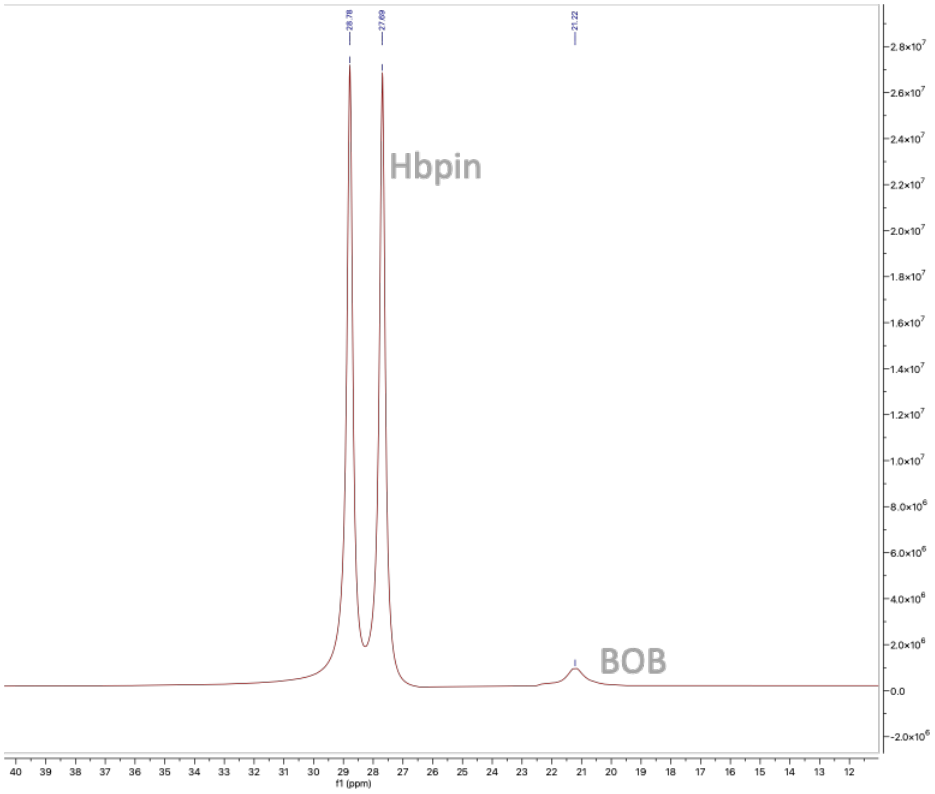
28.78
27.69
21.22
Hbpin
BOB
f1 (ppm)

^{11}B-NMR

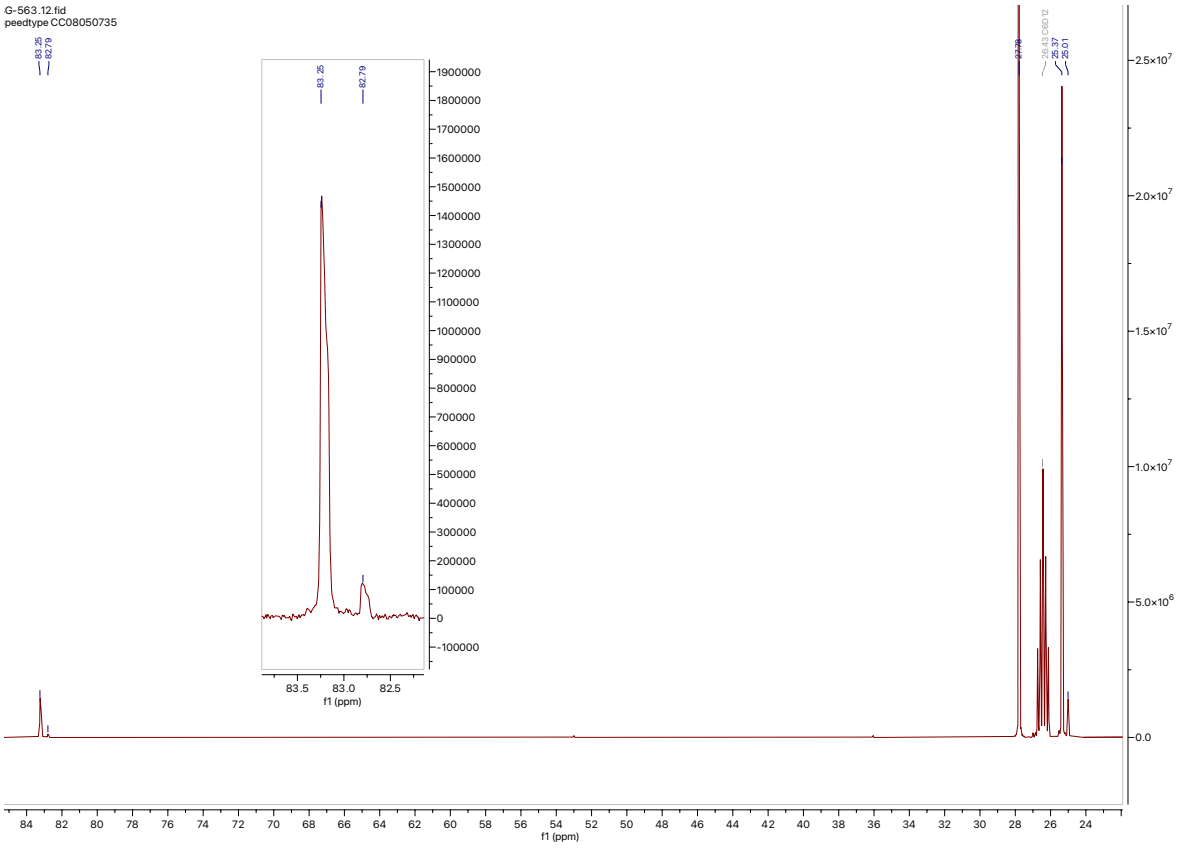
G-563.12.fid
peedtype CC08050735
83.25
82.79
27.78
25.37
25.01
f1 (ppm)

^{13}C-NMR

Note: BOB (82.79, 25.01 ppm) can be distinguished from HBpin (83.25, 25.37 ppm) by ^{13}C-NMR spectroscopy. 27.78 ppm belongs to cyclohexane-h_{12}

B_2pin_2 Characterization

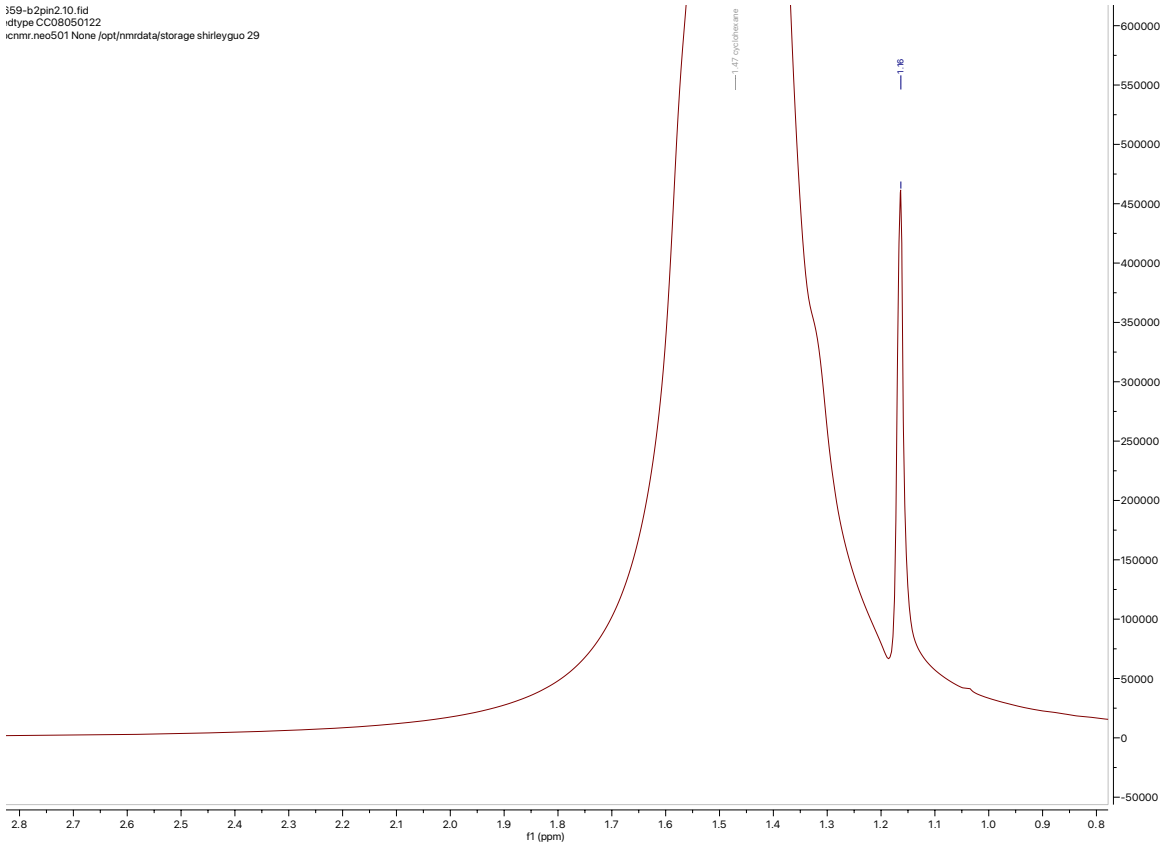

^{1}H-NMR (cyclohexane)

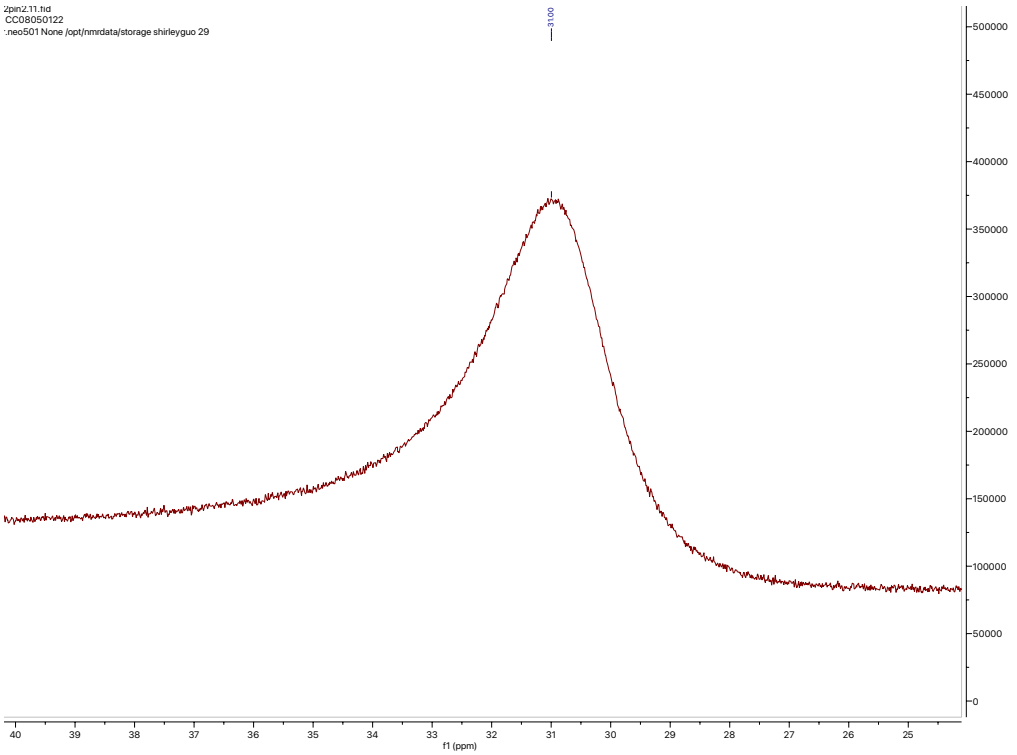

^{11}B-NMR (cyclohexane)

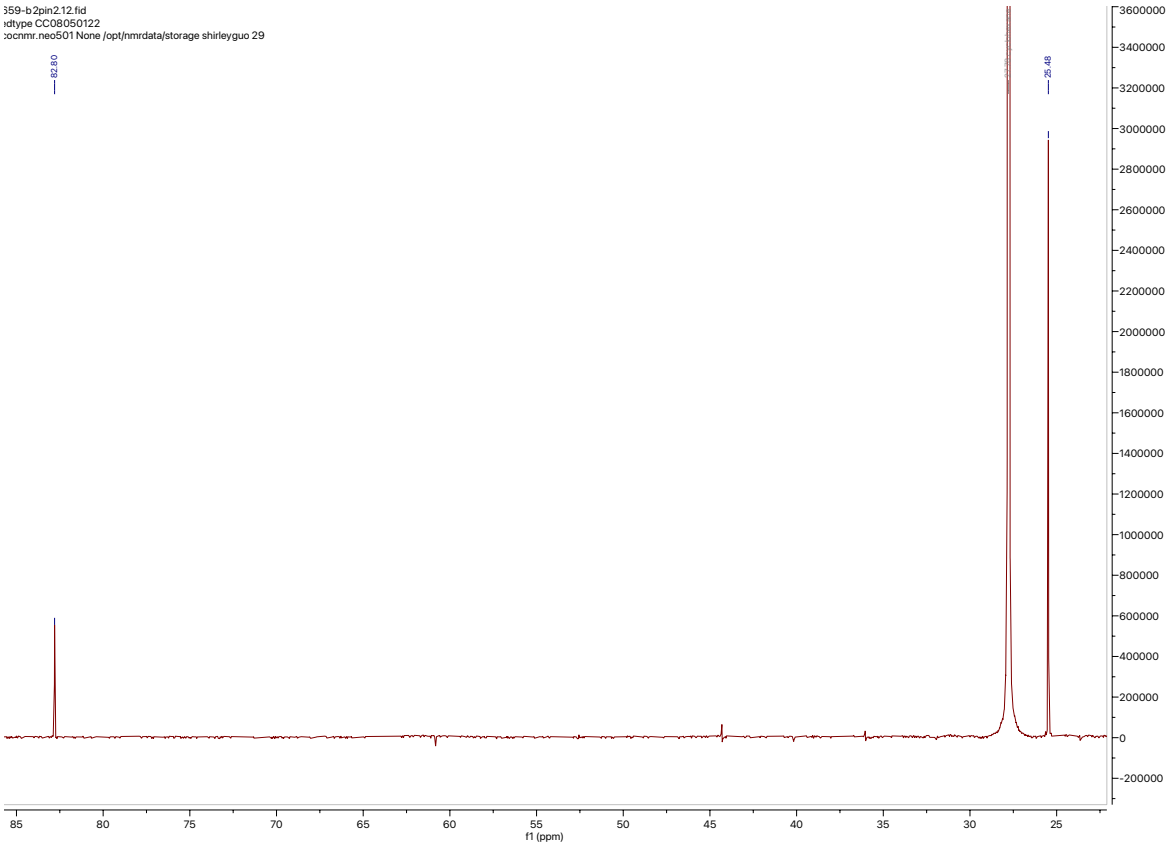

^{13}C-NMR (cyclohexane)

1.4.2 Stoichiometric Experiments: Time Course Analysis & Select Spectra

Procedure

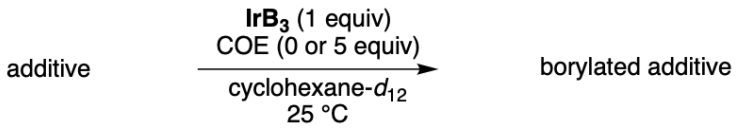

(1 equiv)

In a glovebox, under an inert atmosphere of nitrogen, to a 4-mL vial equipped with a stir bar was added (dtbpy)Ir(Bpin)$_3$ (10 mg, 11 umol) and 2 drops of dioxane stock [46.5 mg (0.5 mmol) dioxane diluted to 1-mL with a volumetric with cyclohexane] (internal standard; recorded weight of added stock). Immediately, diluted contents of vial with C_6D_{12} (500 uL). Immediately capped vial and let stir gently to make for a homogeneous solution.

To a separate 4-mL vial was added C_6D_{12} (500 uL) into which the additive stock (in cyclohexane) (10 uL of stock, 11 umol of additive) was directly injected. This second solution was then transferred to the first 4-mL vial. The vial was stirred for a few seconds and then its contents were transferred to a J-Young NMR tube which was subsequently sealed with a septum lined screw cap at which point the time was recorded and designated as t0. ^{1}H-NMR and ^{11}B-NMR spectra were acquired throughout time.

Reactivity at Bpin Ligand

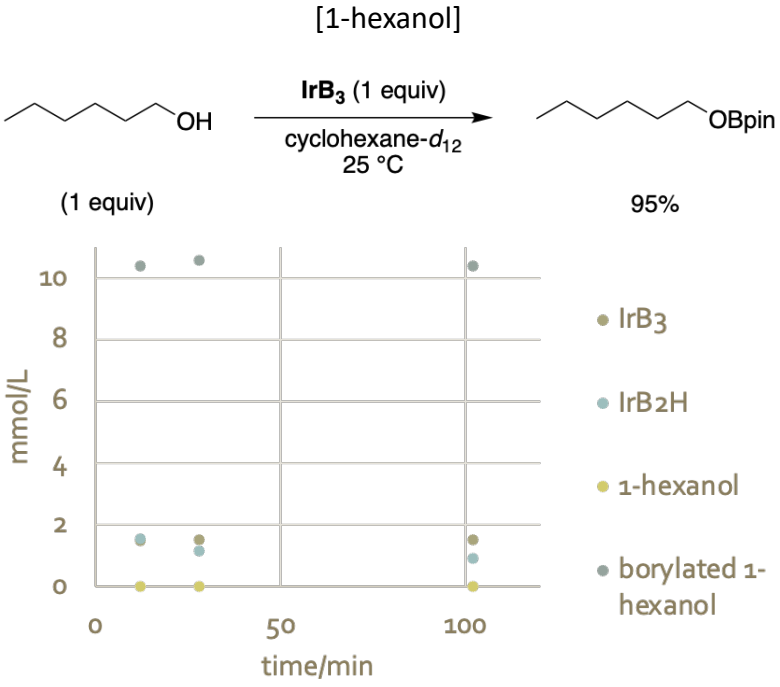

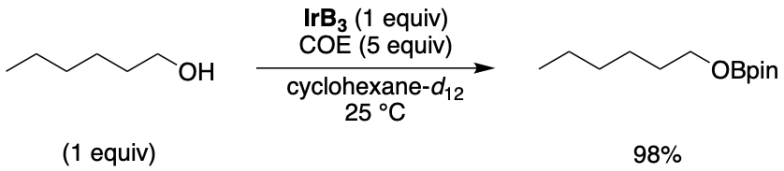

(1 equiv)

98%

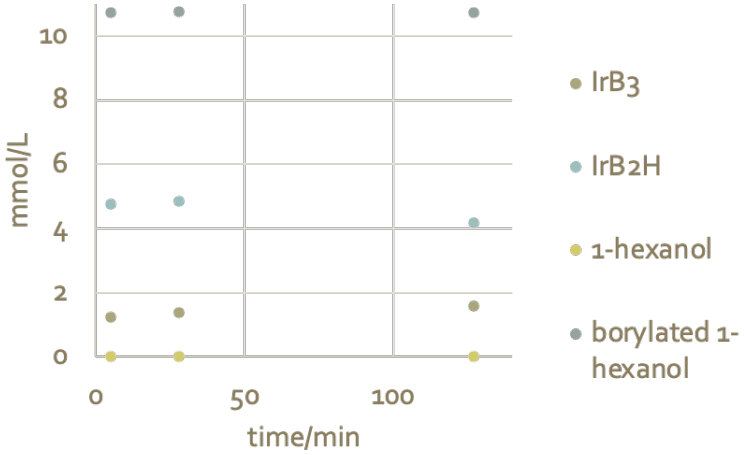

[dodecylamine]

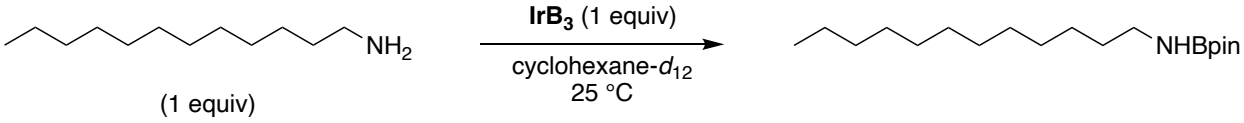

(1 equiv)

93%

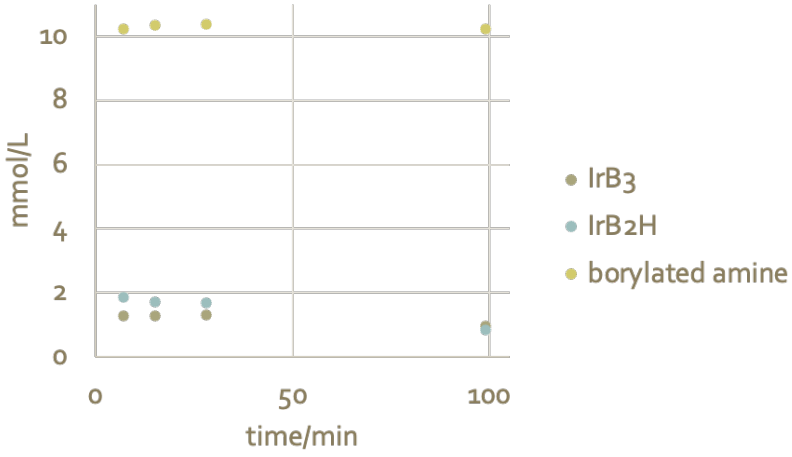

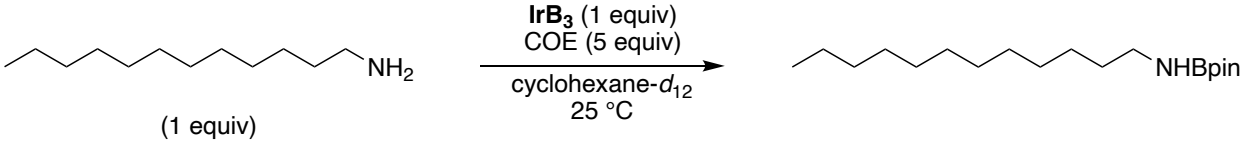

(1 equiv)

98%

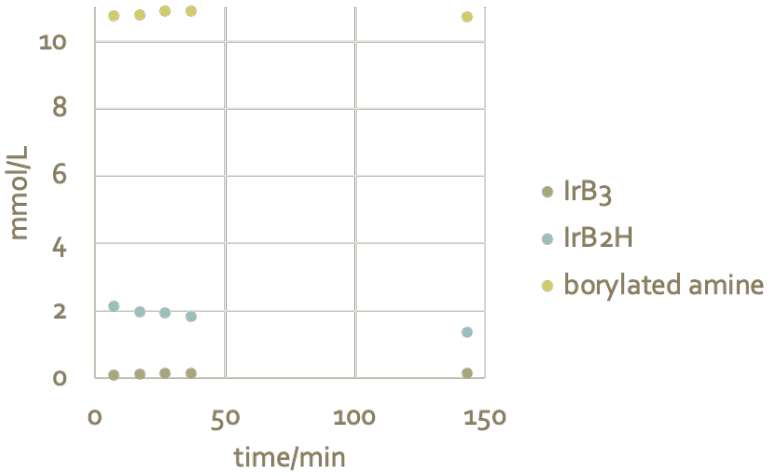

[octanethiol]

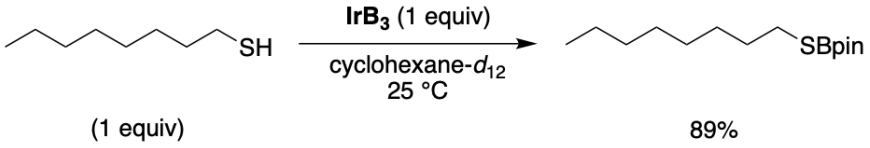

(1 equiv) 89%

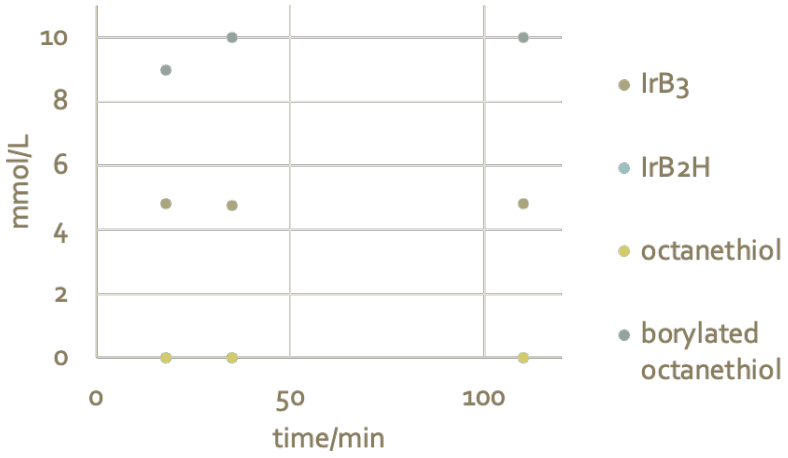

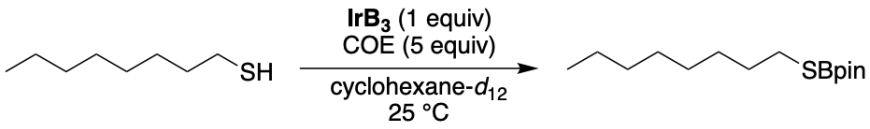

(1 equiv) 89%

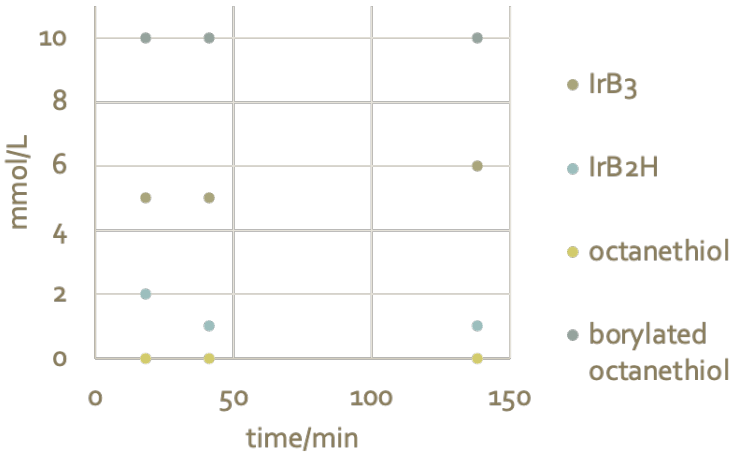

[N-methylbutyramide]

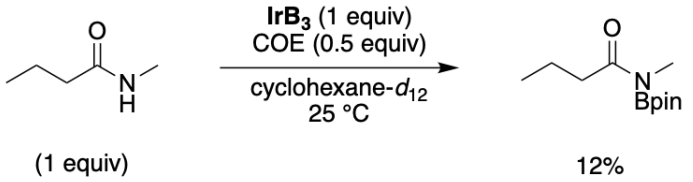

(1 equiv) 12%

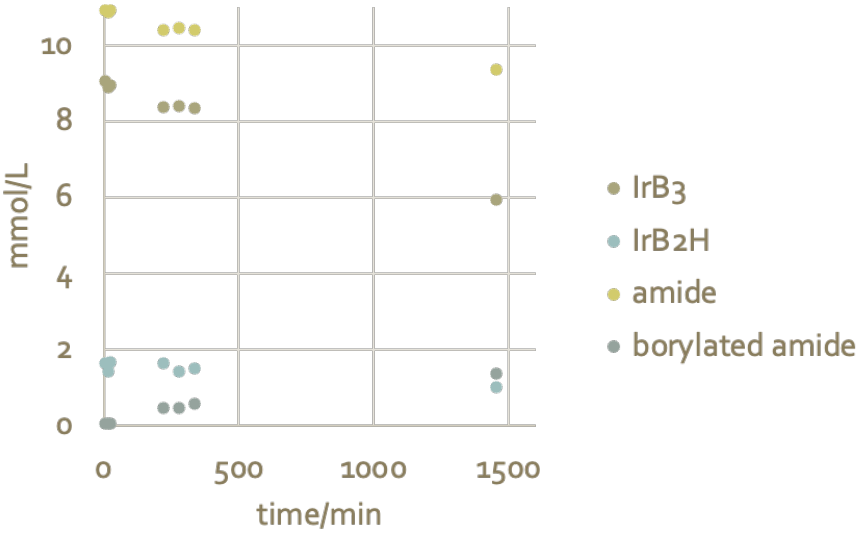

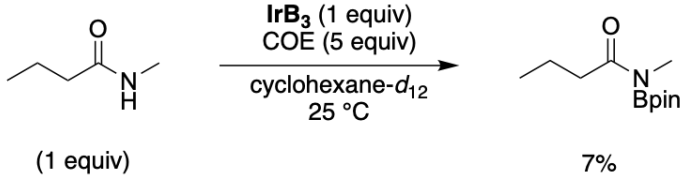

(1 equiv) 7%

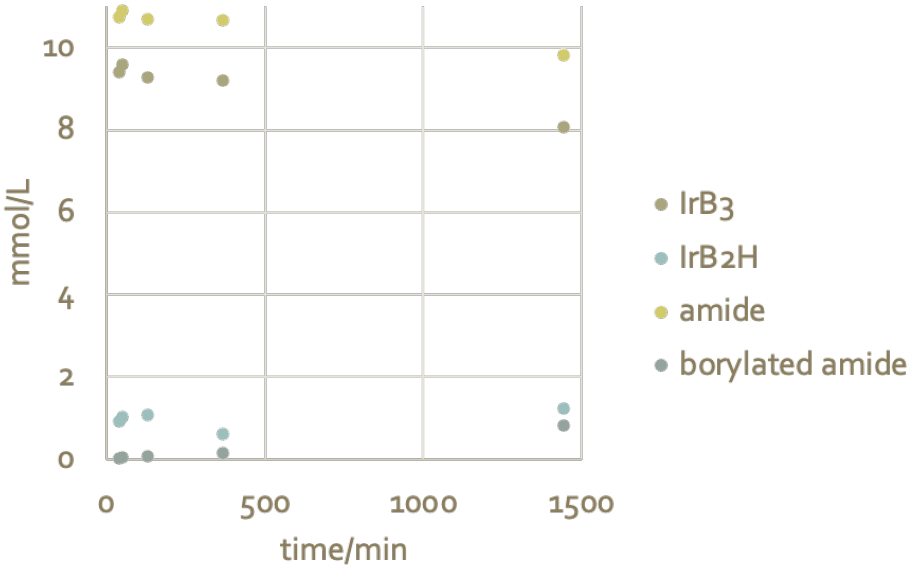

Reactivity at Ir

[m-xylene]

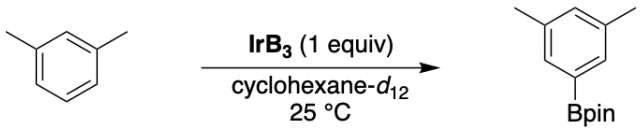

(1 equiv) 0%

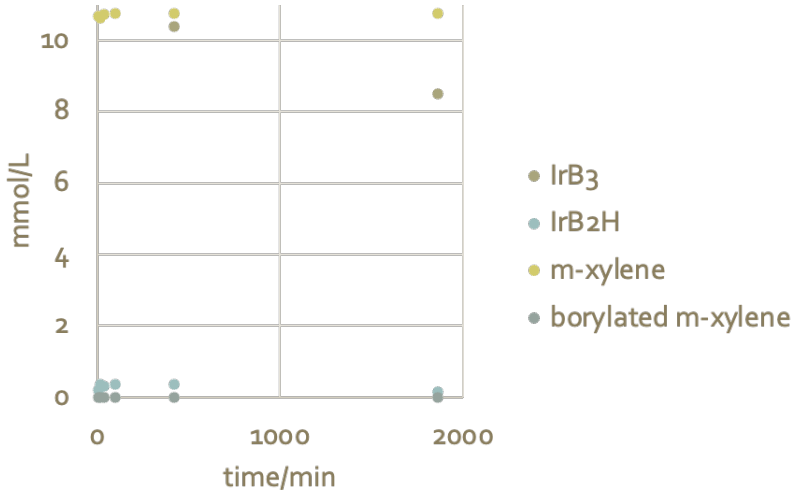

[2-methylheptan-3-one]

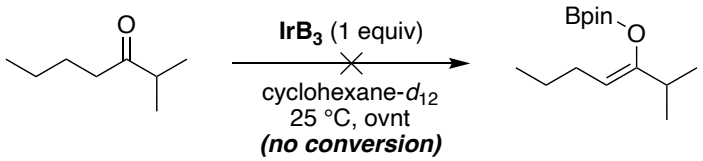

(1 equiv)

[cyclooctanone]

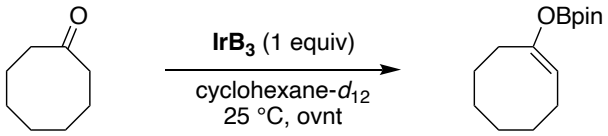

(1 equiv) 19%

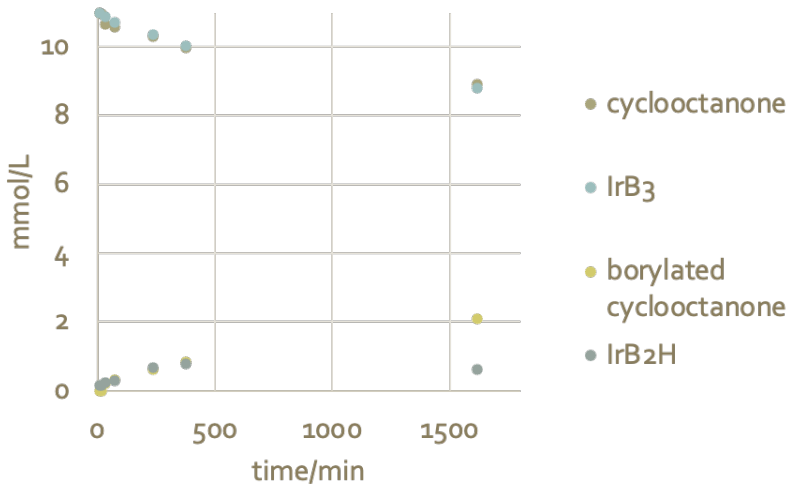

Note: Subsequent heating at 100 °C for 1 hour provided a terminal yield of 32% (0% IrB_3).

[methyl propionate]

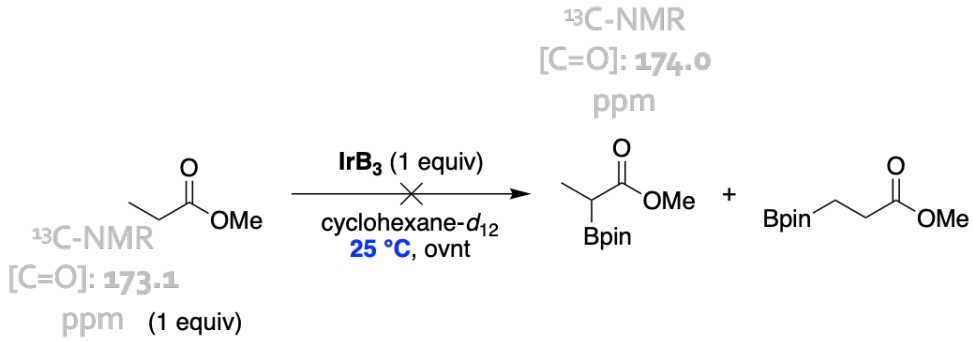

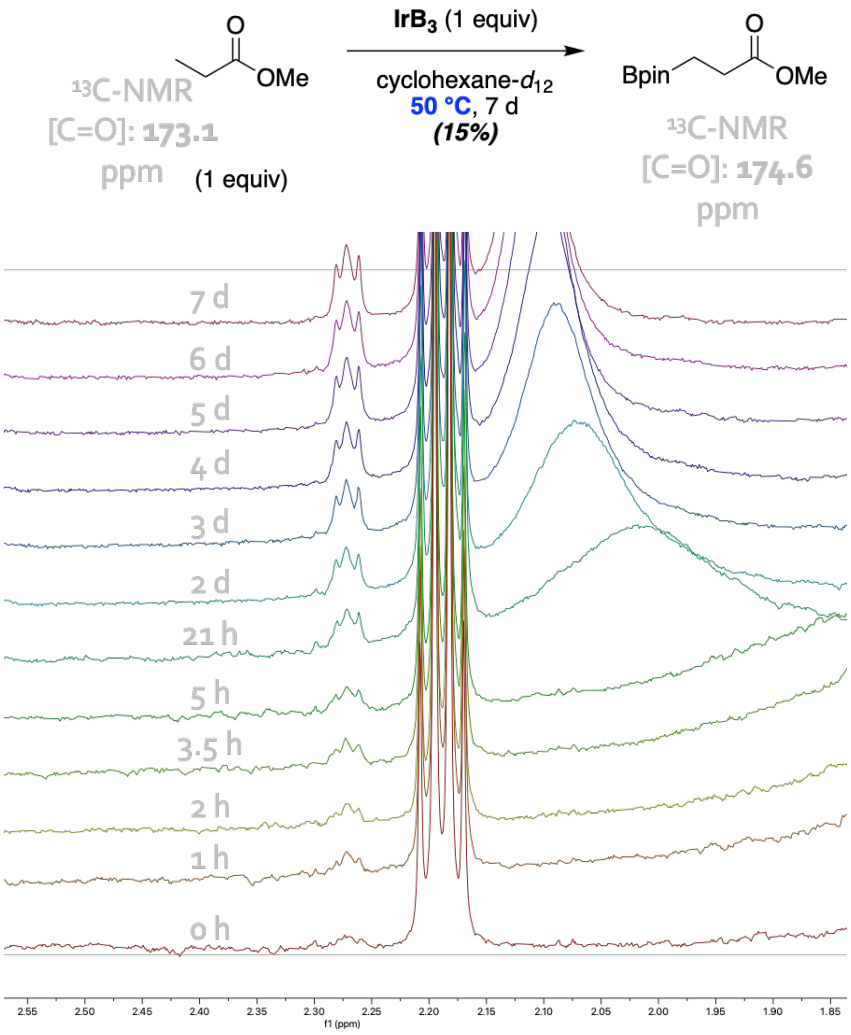
IrB3 (1 equiv)
cyclohexane-d12
50 °C, 7 d
(15%)
13C-NMR
[C=O]: 173.1
ppm
(1 equiv)
Bpin
OMe
13C-NMR
[C=O]: 174.6
ppm
7 d
6 d
5 d
4 d
3 d
2 d
21 h
5 h
3.5 h
2 h
1 h
0 h
2.55 2.50 2.45 2.40 2.35 2.30 2.25 2.20 2.15 2.10 2.05 2.00 1.95 1.90 1.85
f1 (ppm)

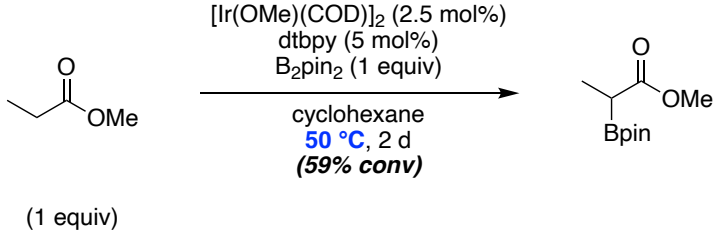
[Ir(OMe)(COD)]2 (2.5 mol%)
dtbpy (5 mol%)
B2pin2 (1 equiv)
cyclohexane
50 °C, 2 d
(59% conv)
OMe
OMe
Bpin

(1 equiv)

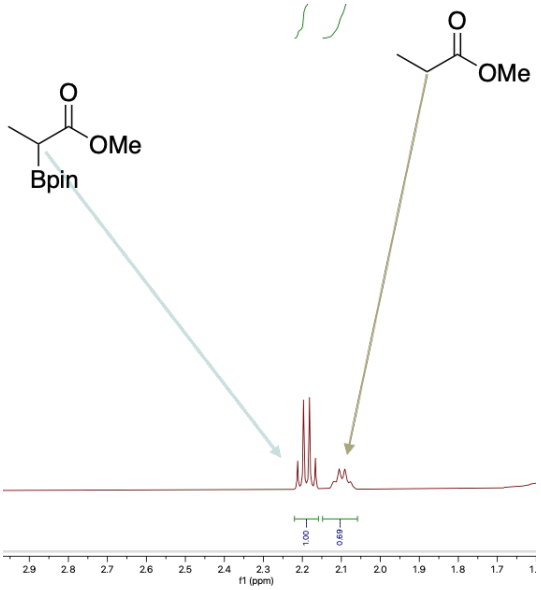

^{1}H-NMR spectrum of the terminal profile of the catalytic reaction (in-situ)

Note: catalytic reactions are conducted with catalyst pre-activation whereby $[Ir(OMe)(COD)]_2$, dtbpy, and B_2pin_2 are stirred together in cyclohexane at 80 °C for 1 h and then cooled to 25 °C before addition of the substrate (all conducted inside a glovebox) and subsequent reaction at the designated temperature.

[N,N-dimethylpropionamide]

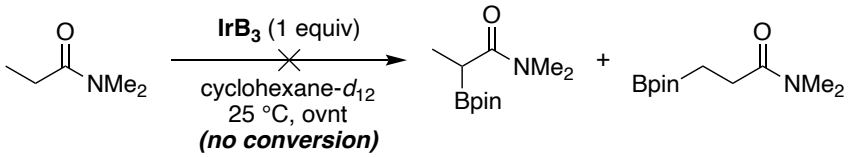

(1 equiv)

Note: Subsequent heating at 100 °C for 1 hour provided a terminal yield of 0% (0% IrB_3).

[bromocyclopropane]

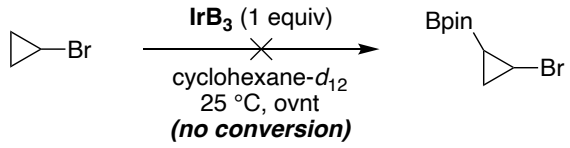

(1 equiv)

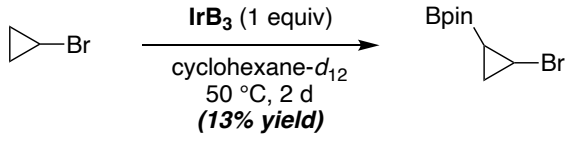

(1 equiv)

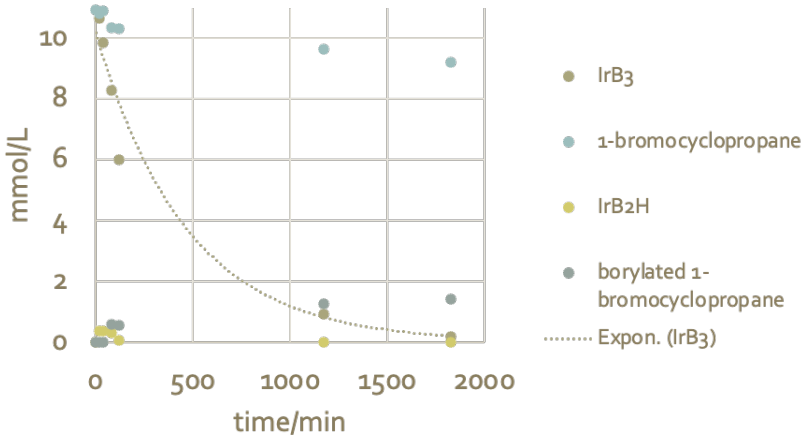

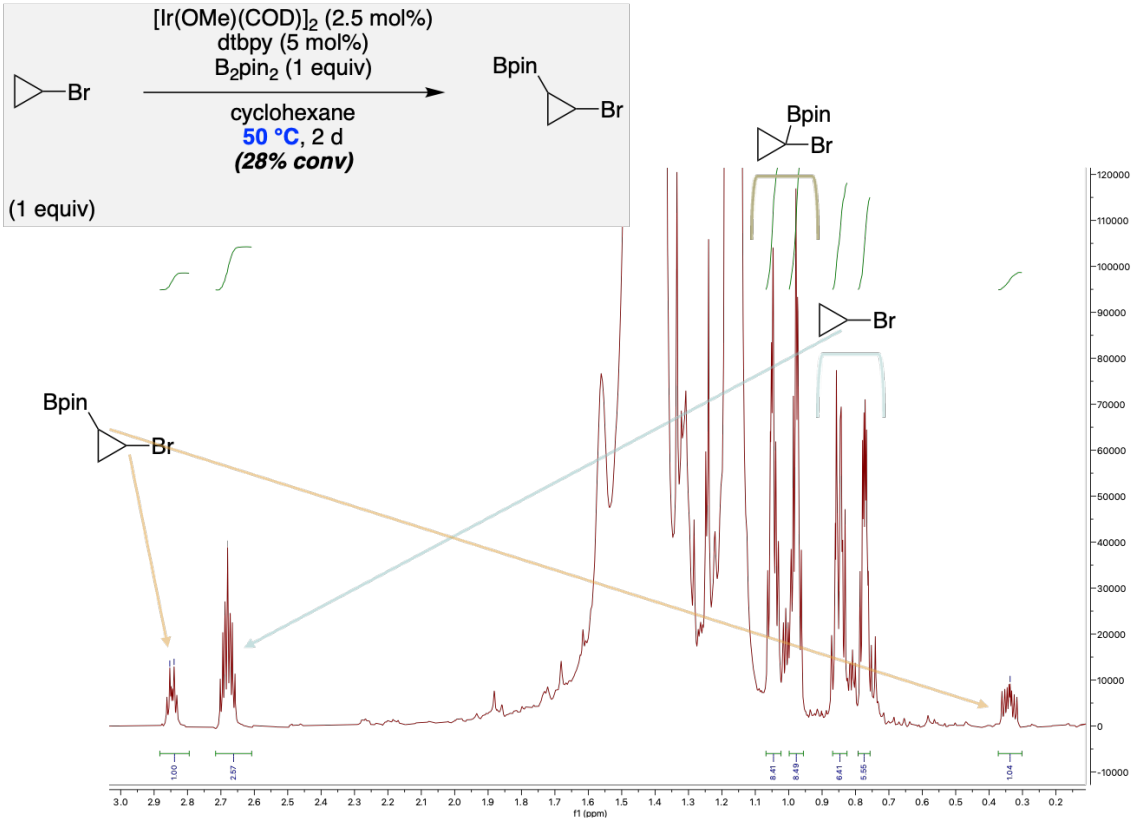

Alpha-borylation > SM > beta-borylation

^{1}H-NMR spectrum of in-situ profile of catalytic reaction [50 °C, 2 d]

Note: catalytic reactions are conducted with catalyst pre-activation whereby $[Ir(OMe)(COD)]_2$, dtbpy, and B_2pin_2 are stirred together in cyclohexane at 80 °C for 1 h and then cooled to 25 °C before addition of the substrate (all conducted inside a glovebox) and subsequent reaction at the designated temperature.

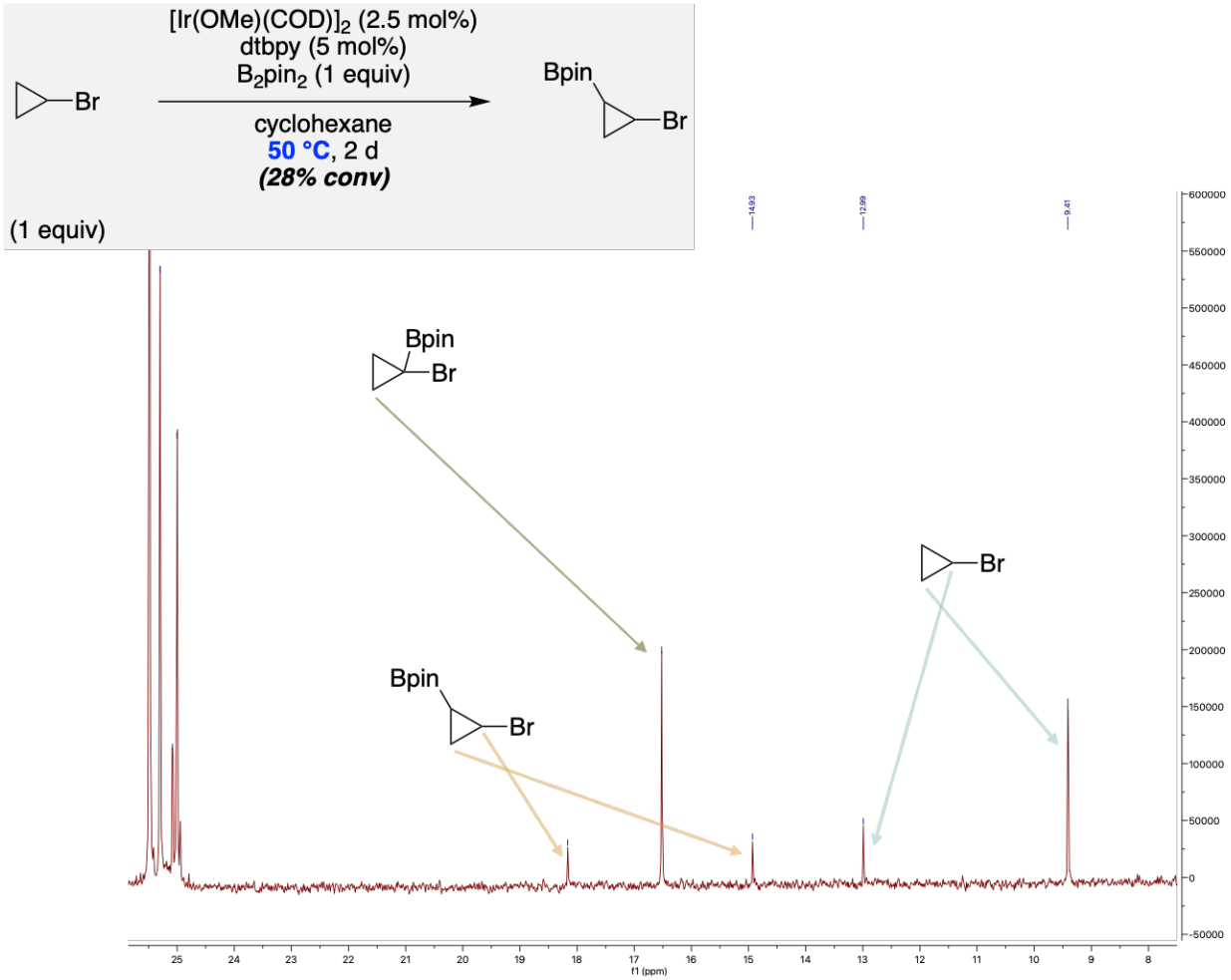

^{13}C-NMR spectrum of the in-situ profile of catalytic reaction [50 °C, 2 d]

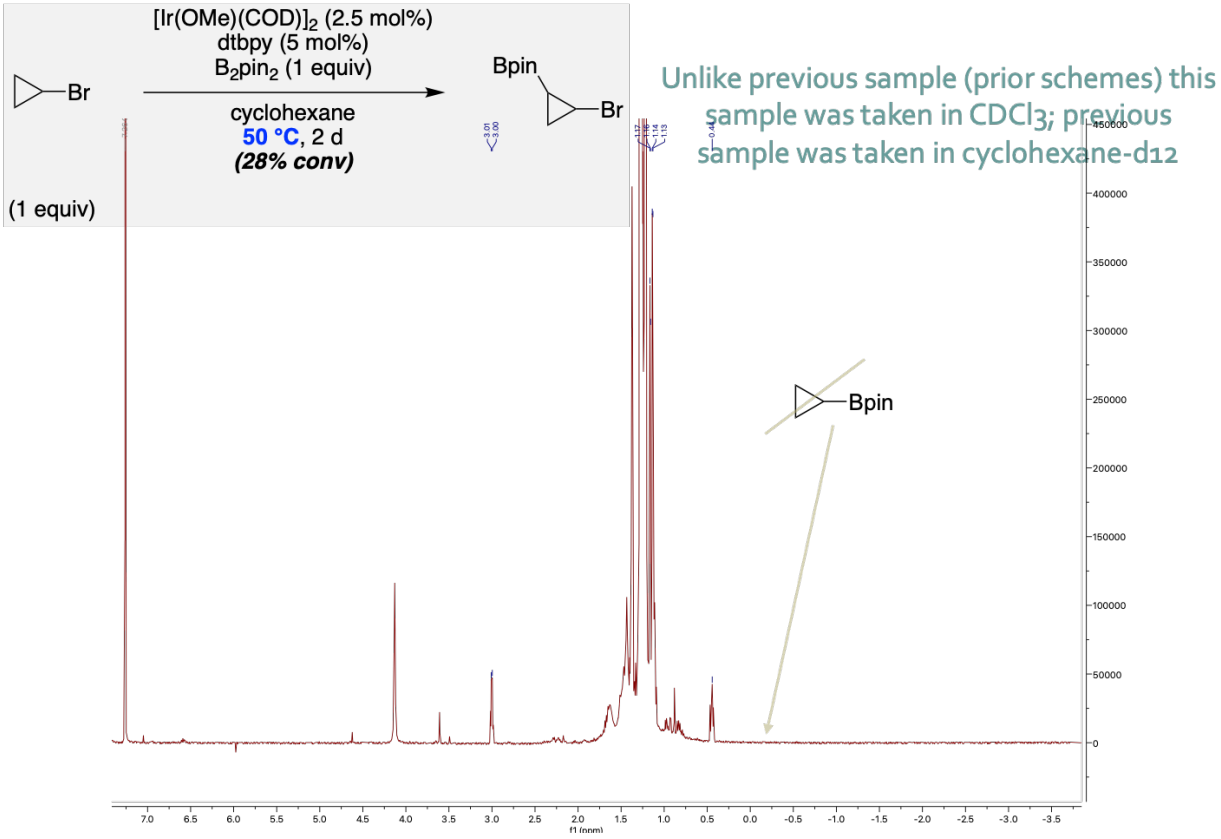

¹H-NMR of reaction days later showed disappearance of SM; alpha- & beta-borylated compounds remain

^{1}H-NMR spectrum of the in-situ profile of catalytic reaction [50 °C, >2 d]
Note: full spectrum shows no formation of 2-cyclopropyl-4,4,5,5-tetramethyl-1,3,2-dioxaborolane (see literature reference for compound below)

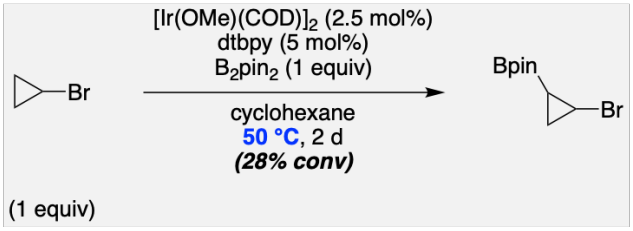

Unlike previous sample (prior schemes) this sample was taken in $CDCl_3$; previous sample was taken in cyclohexane-d12

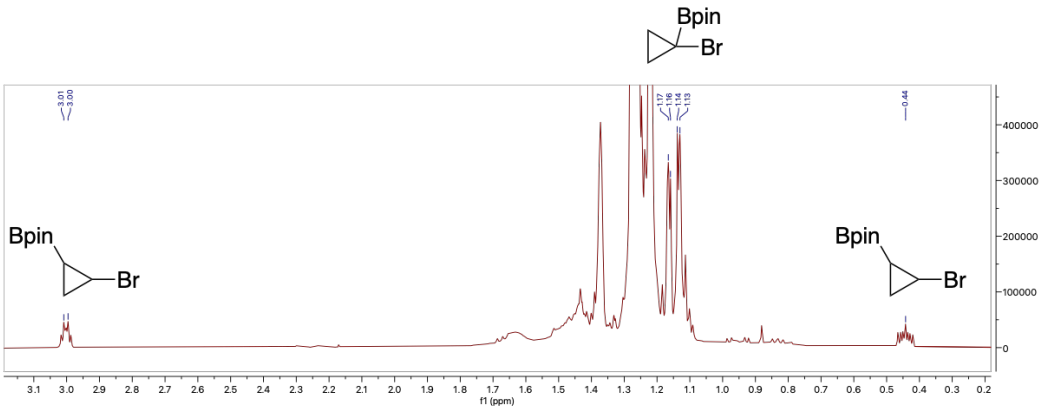

^{1}H-NMR of reaction days later showed disappearance of SM; alpha- & beta-borylated compounds remain

^{1}H-NMR spectrum of the in-situ profile of catalytic reaction [50 °C, >2 d]
Note: abbreviated spectrum shows alpha and beta borylated compounds

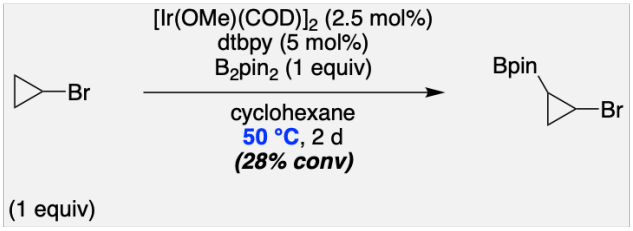

Unlike previous sample (prior schemes) this sample was taken in $CDCl_3$; previous sample was taken in cyclohexane-d12

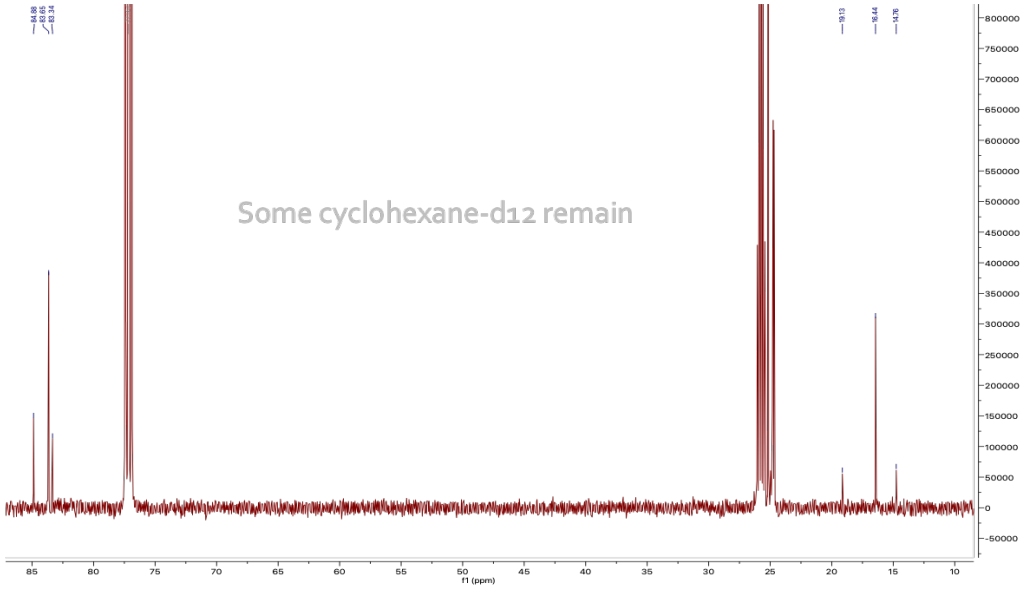

^{13}C-NMR of reaction days later showed disappearance of SM; alpha- & beta-borylated compounds remain

^{13}C-NMR spectrum of the in-situ profile of catalytic reaction [50 °C, >2 d]

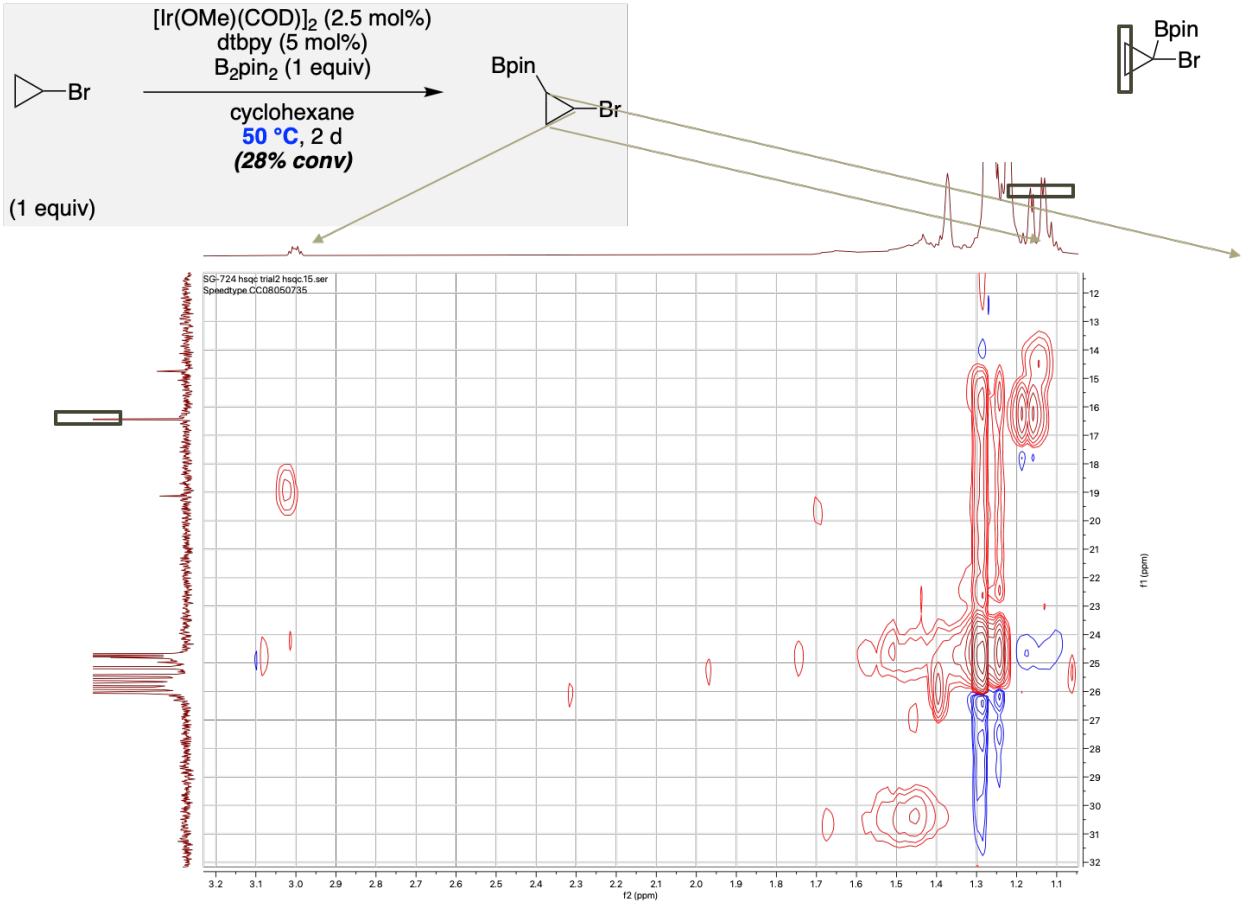

HSQC spectrum of the in-situ profile of catalytic reaction [50 °C, >2 d]

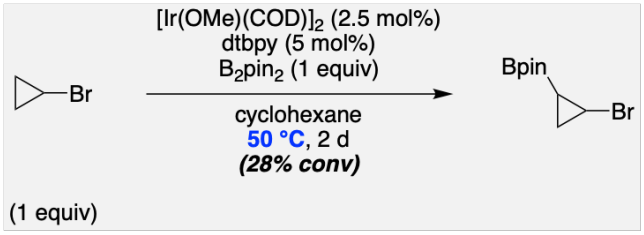

COSY not useful for identifying alpha borylation (peaks are too close together)

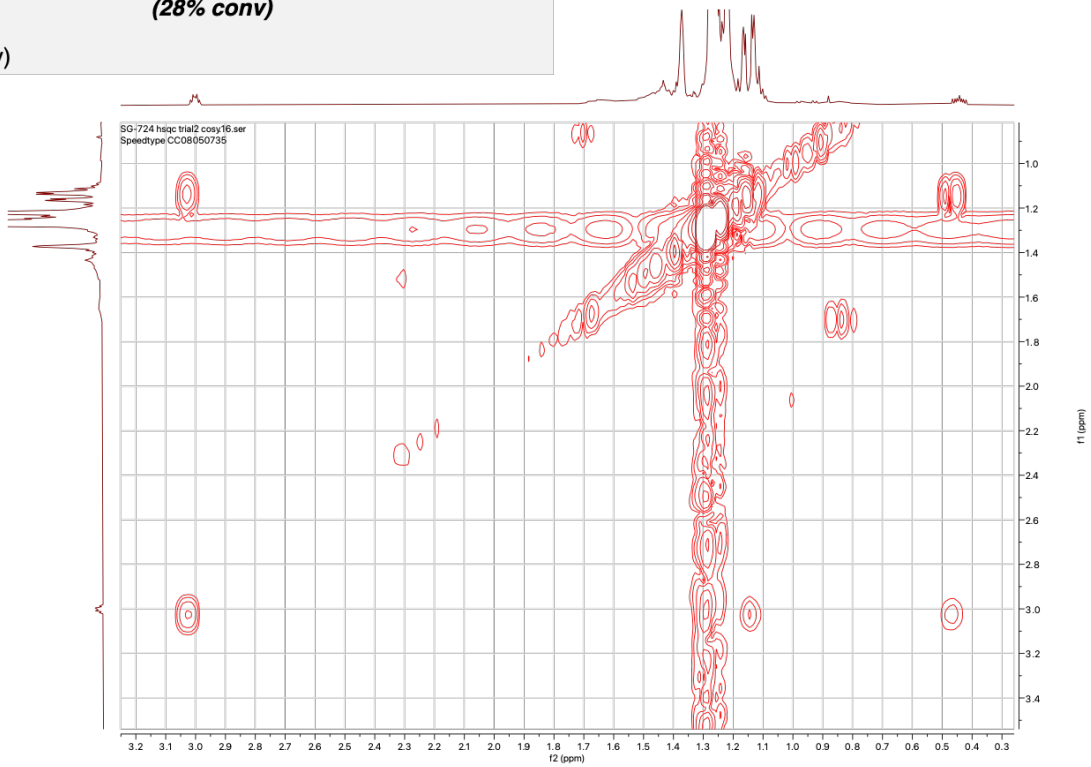

COSY spectrum of the in-situ profile of catalytic reaction [50 °C, >2 d]

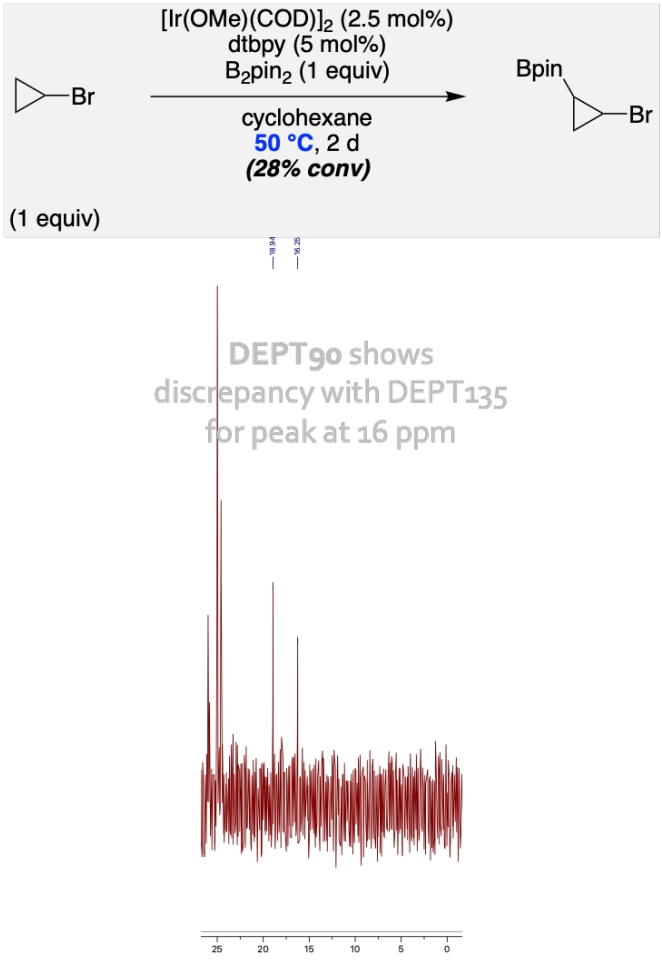

DEPT spectrum of the in-situ profile of catalytic reaction [50 °C, >2 d]

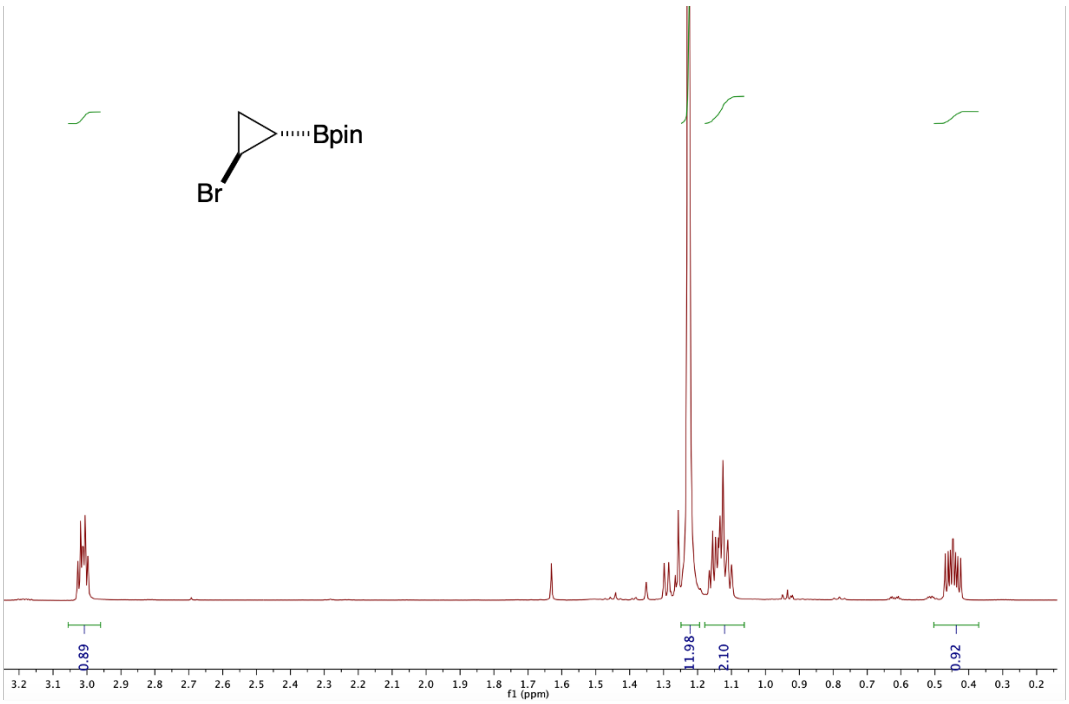

Liskey/Hartwig, 10.1021/ja400103p

^{1}H-NMR spectrum of literature reference

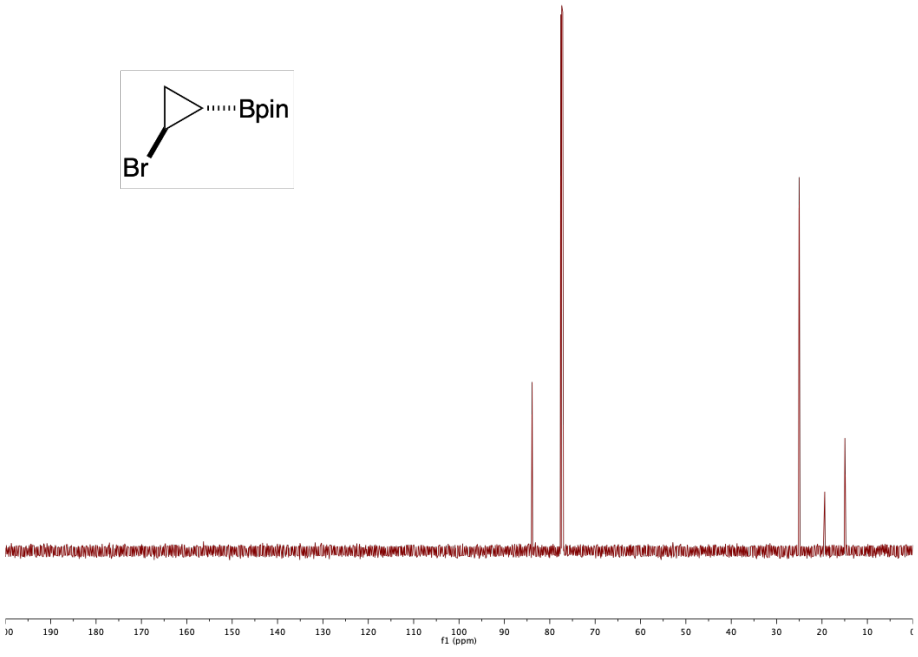

Liskey/Hartwig, 10.1021/ja400103p

^{13}C-NMR spectrum of literature reference

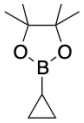

J. Am. Chem. Soc. 2011, 133, 42, 16794–16797

16g

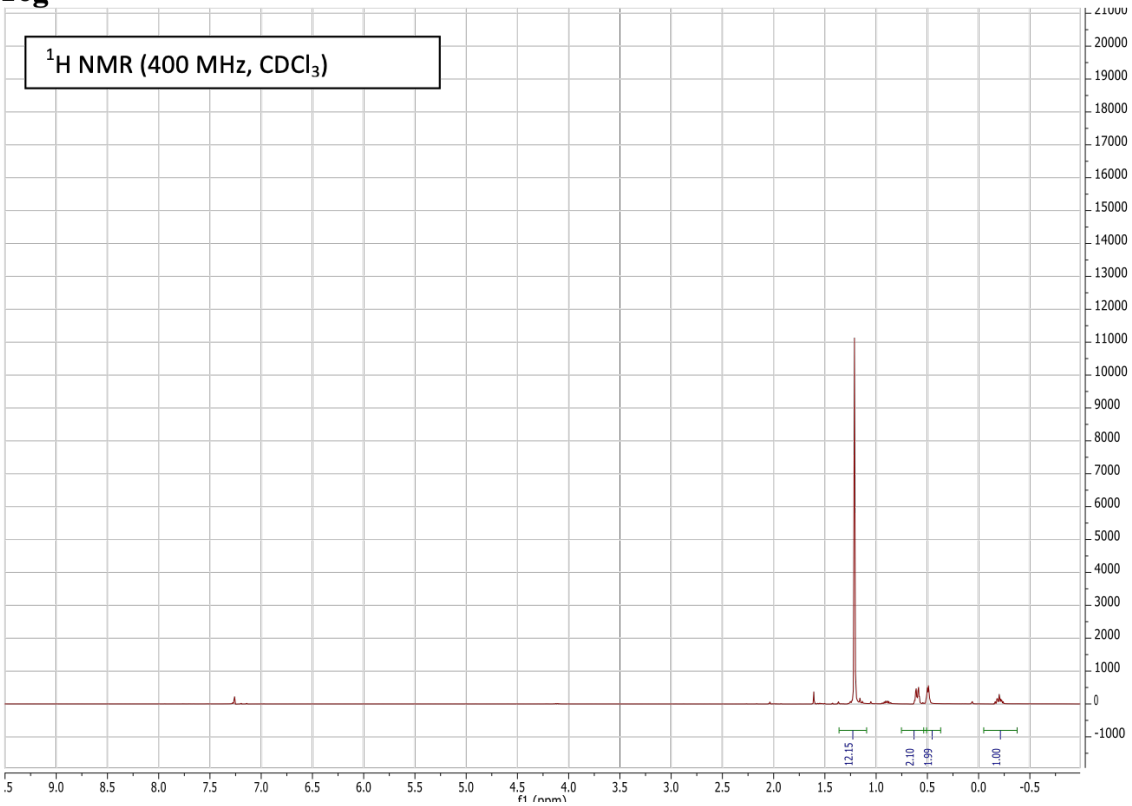

^{1}H-NMR spectrum of literature reference

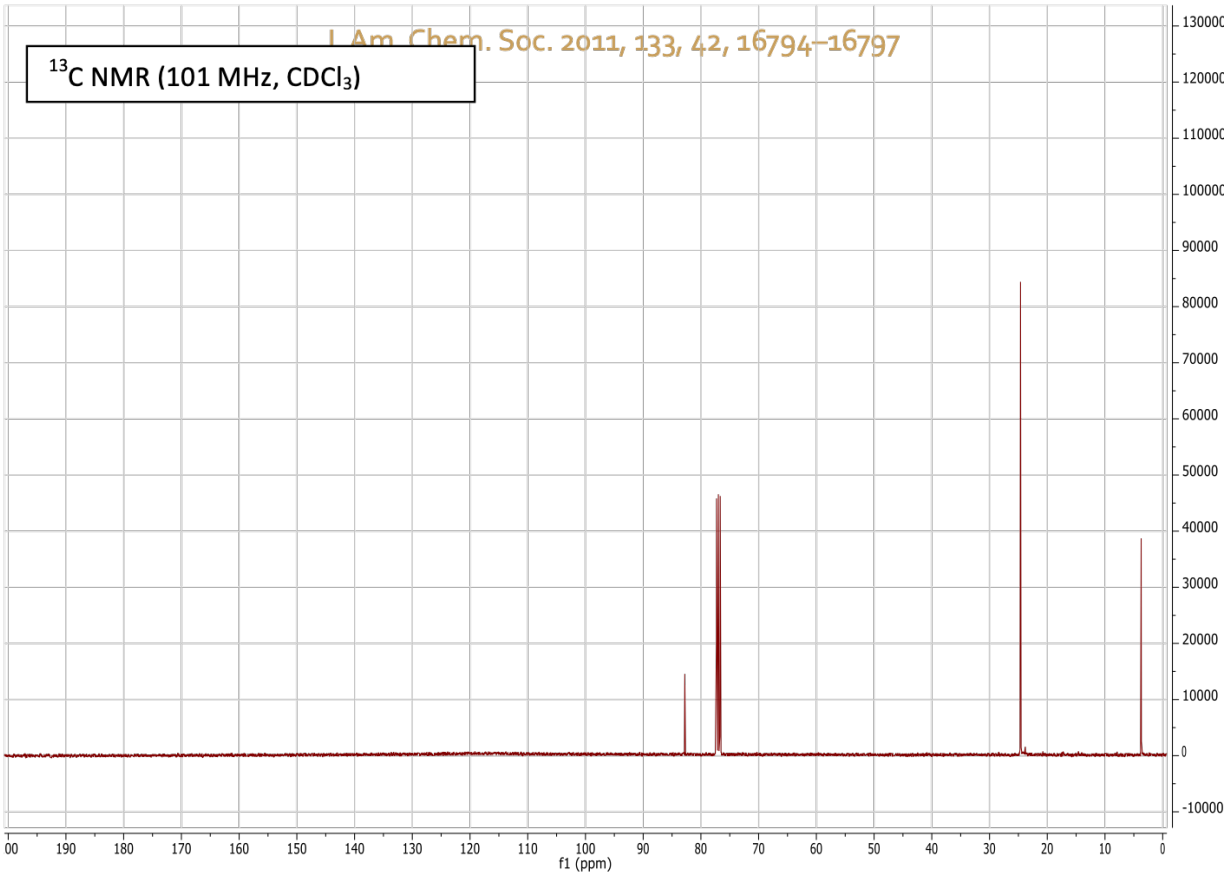

^{13}C-NMR spectrum of literature reference

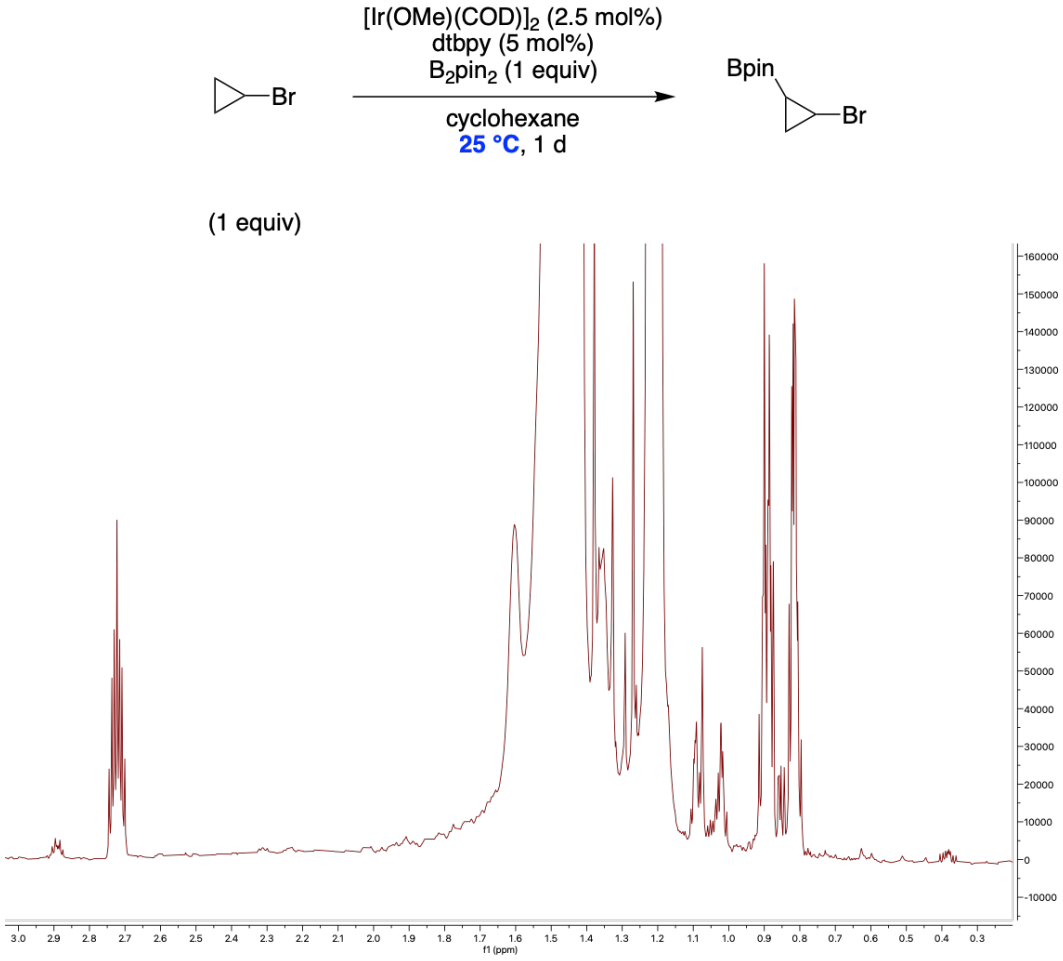

^{1}H-NMR spectrum of in-situ terminal profile of catalytic reaction [25 °C, 1 d]

Note: this reaction of milder conditions and lower conversion to borylated compounds also demonstrates alpha-borylation > beta-borylation

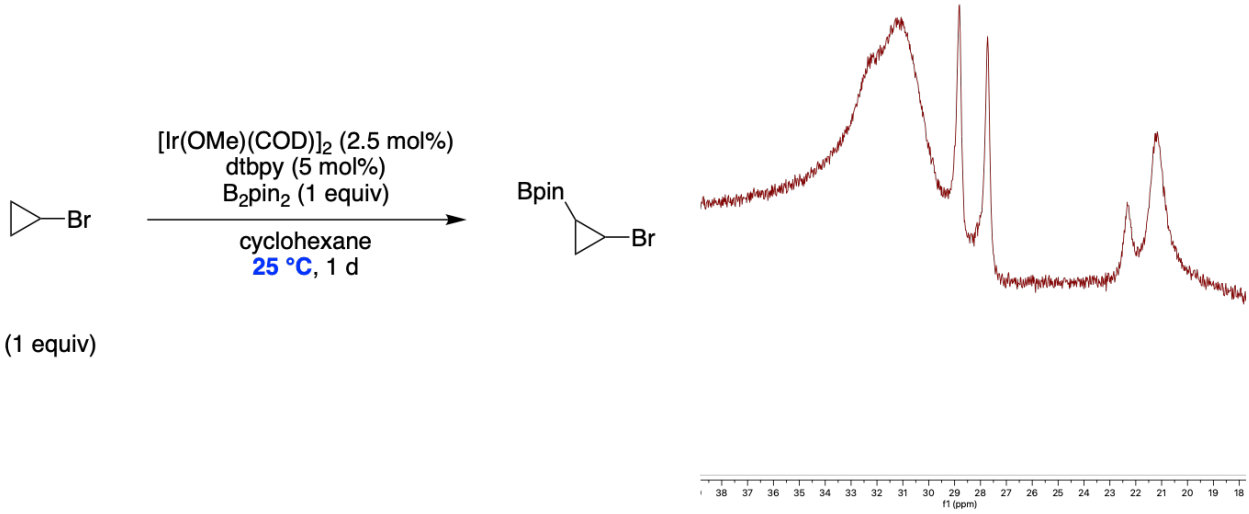

^{11}B-NMR spectrum of in-situ terminal profile of catalytic reaction [25 °C, 1 d]

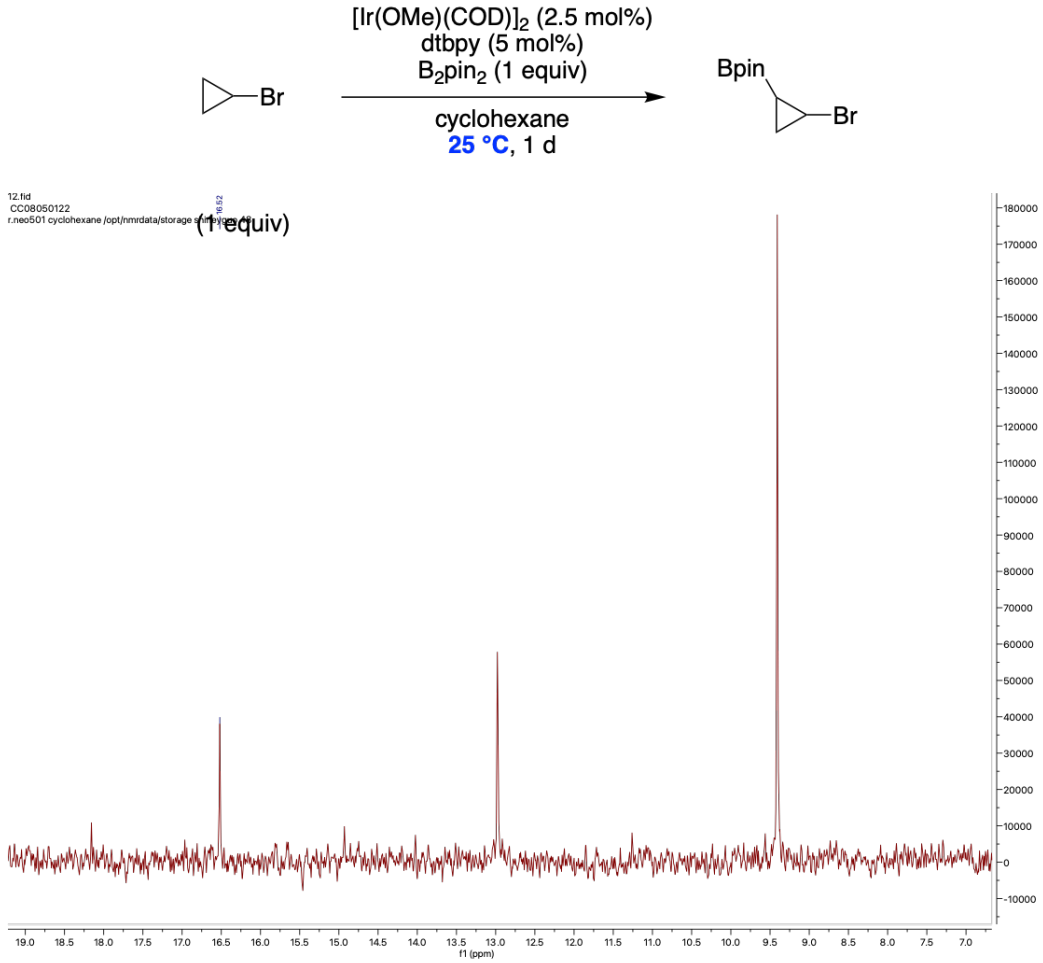

^{13}C-NMR spectrum of in-situ terminal profile of catalytic reaction [25 °C, 1 d]

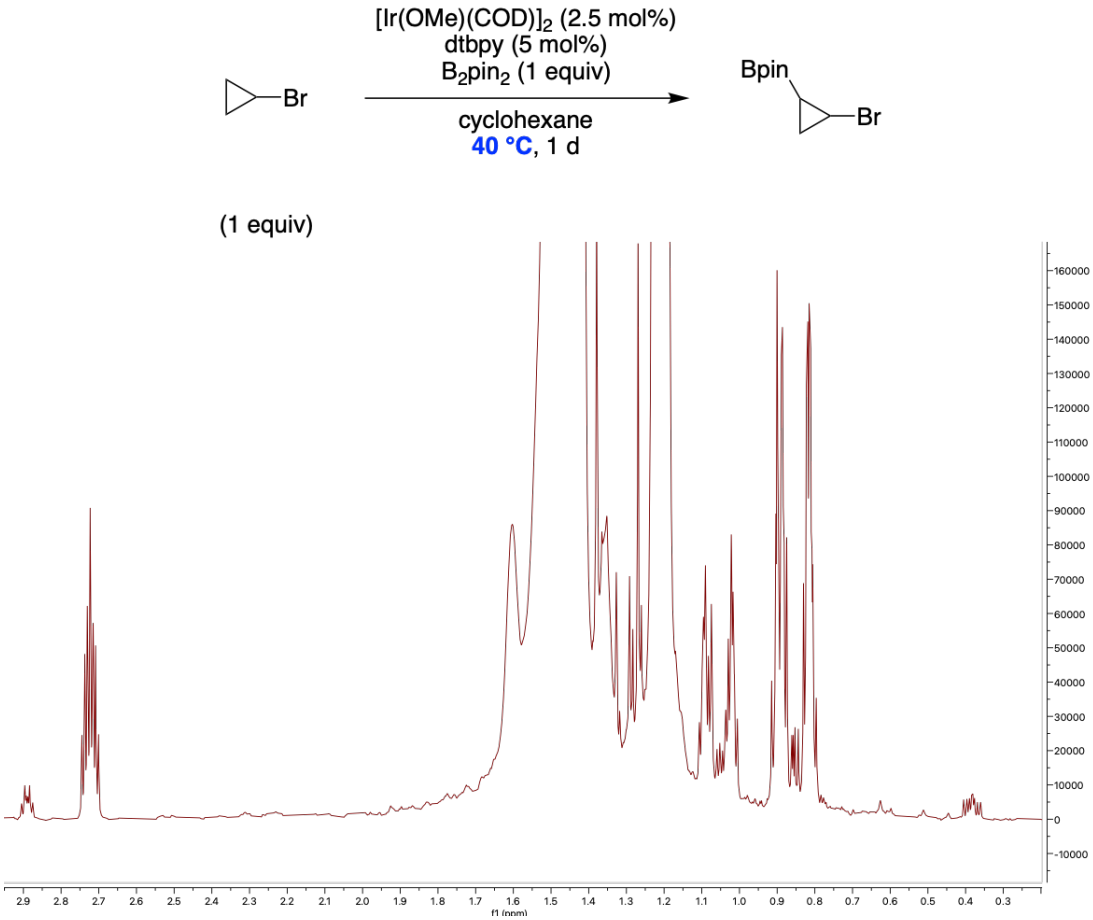

^{1}H-NMR spectrum of in-situ terminal profile of catalytic reaction [40 °C, 1 d]

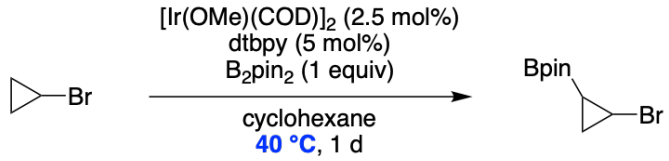

(1 equiv)

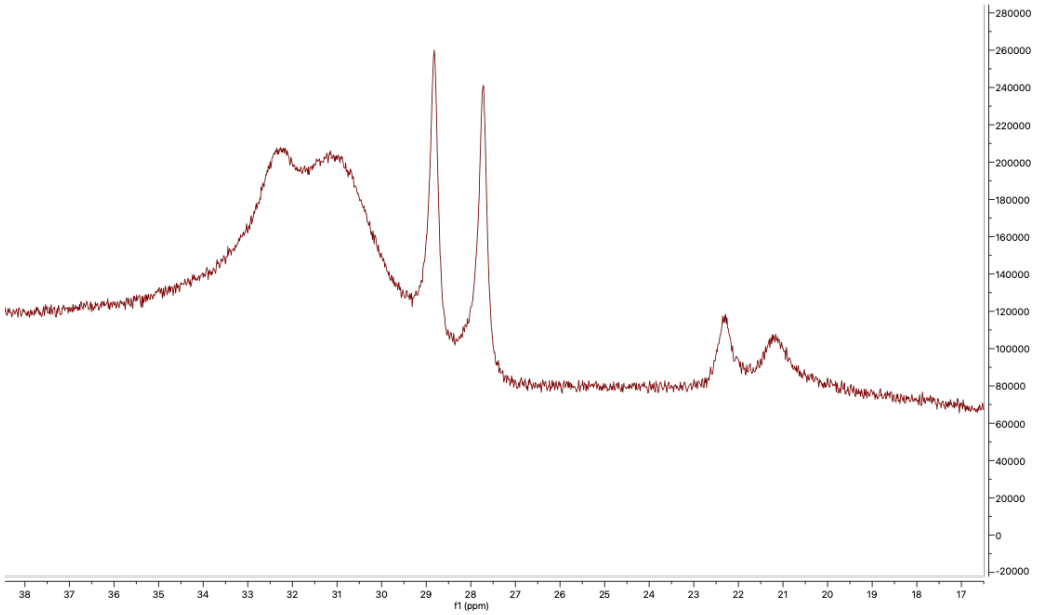

^{11}B-NMR spectrum of in-situ terminal profile of catalytic reaction [40 °C, 1 d]

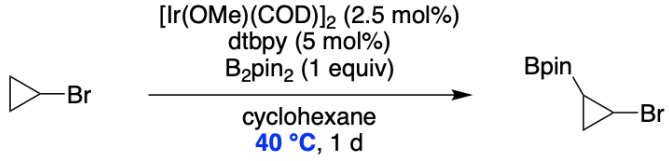

(1 equiv)

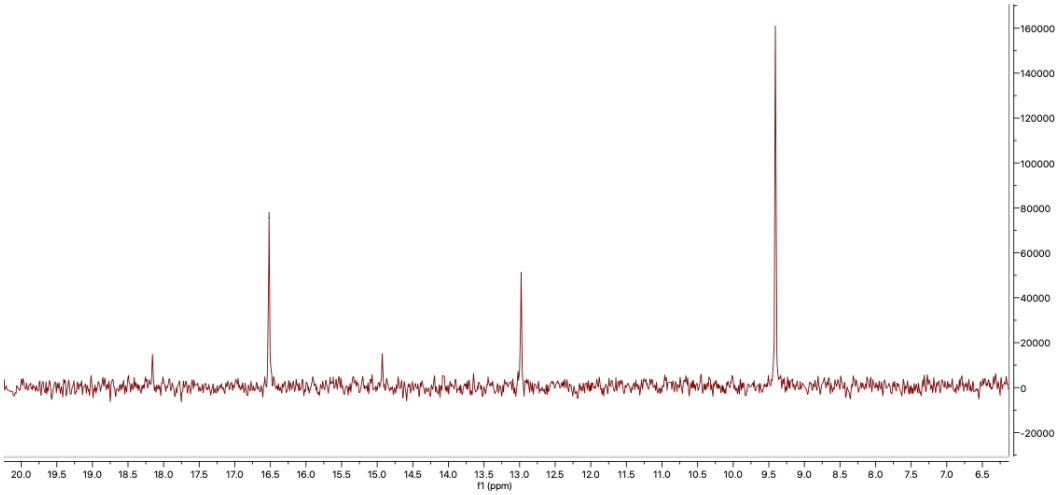

^{13}C-NMR spectrum of in-situ terminal profile of catalytic reaction [40 °C, 1 d]

[1-bromopropane]

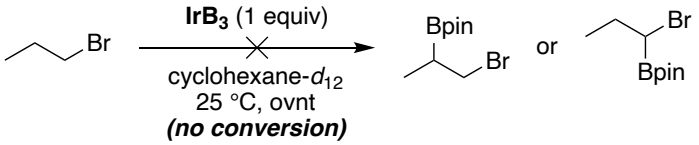

(1 equiv)

Note: Subsequent heating at 100 °C for 1 hour provided a terminal yield of 0% (9% IrB_3).

[phenylacetylene]

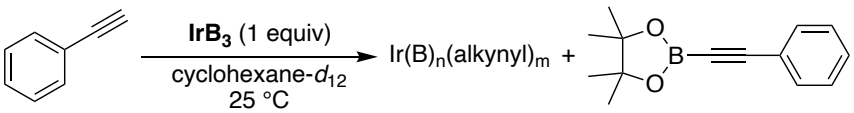

(1 equiv)

major, 54%
minor, 21%

11%

Ambident Reactivity

[dithiane]

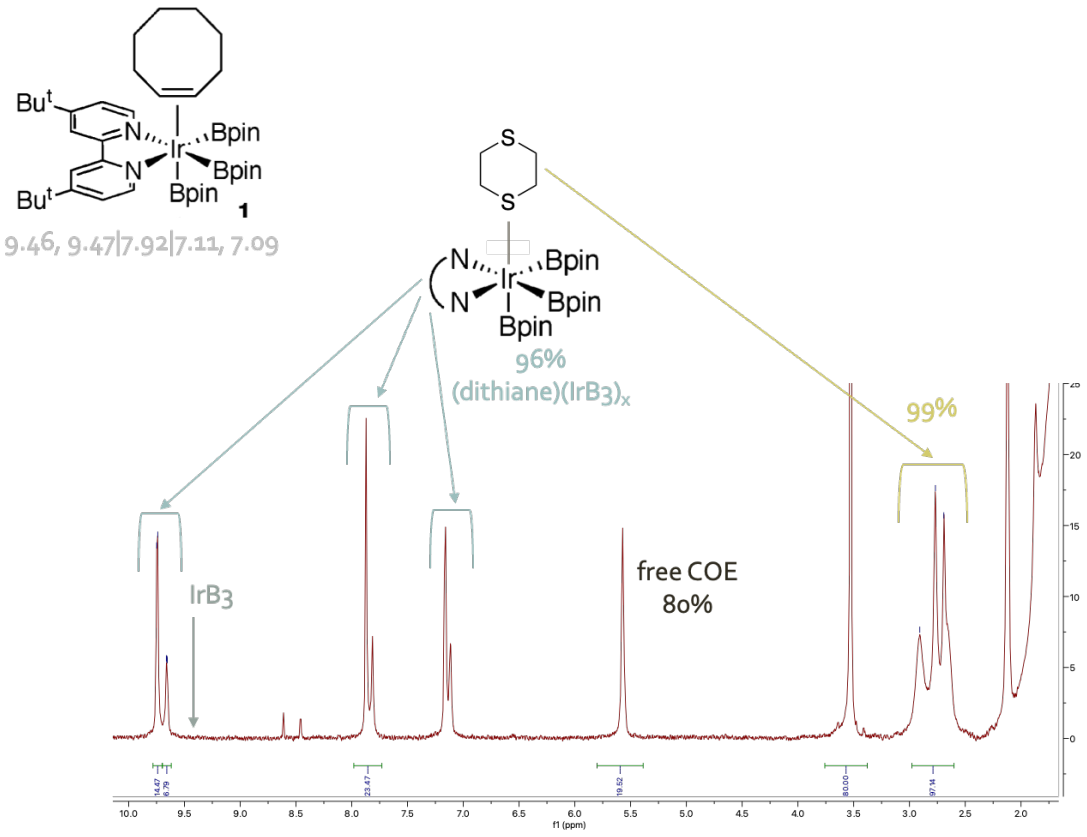

1:1 dithiane:IrB3 → **(dithiane)IrB3** [major] & (dithiane)$(IrB_3)_2$ [minor]

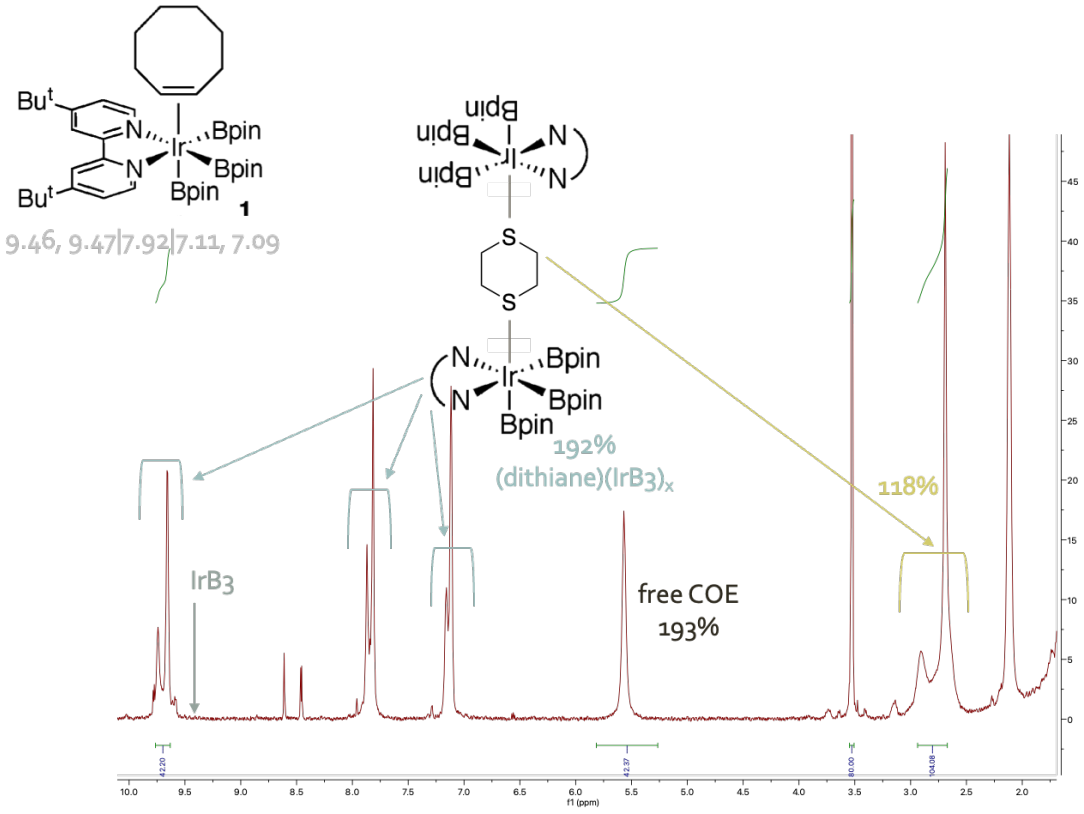

1:2 dithiane:IrB3 → (dithiane)IrB3 [minor] & **(dithiane)(IrB3)$_2$** [major]

[dihexylamine]

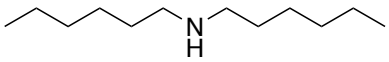

(1 equiv)

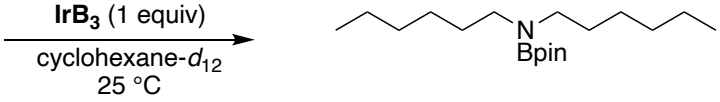

93%

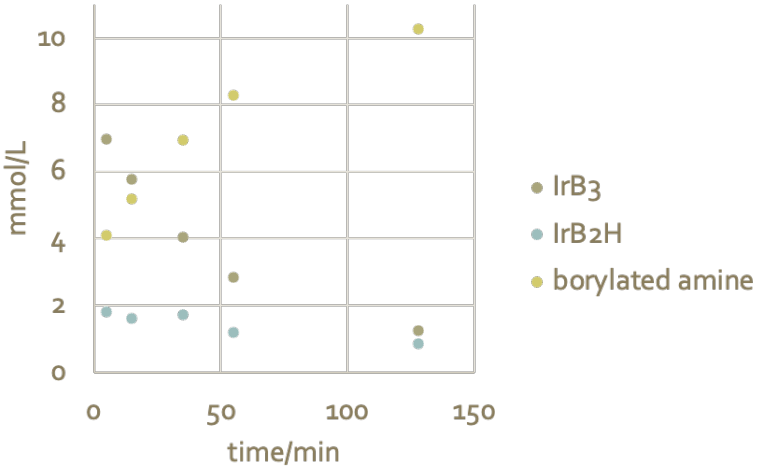
10
8
6
4
2
0
mmol/L
0
50
100
150
time/min
IrB3
IrB2H
borylated amine

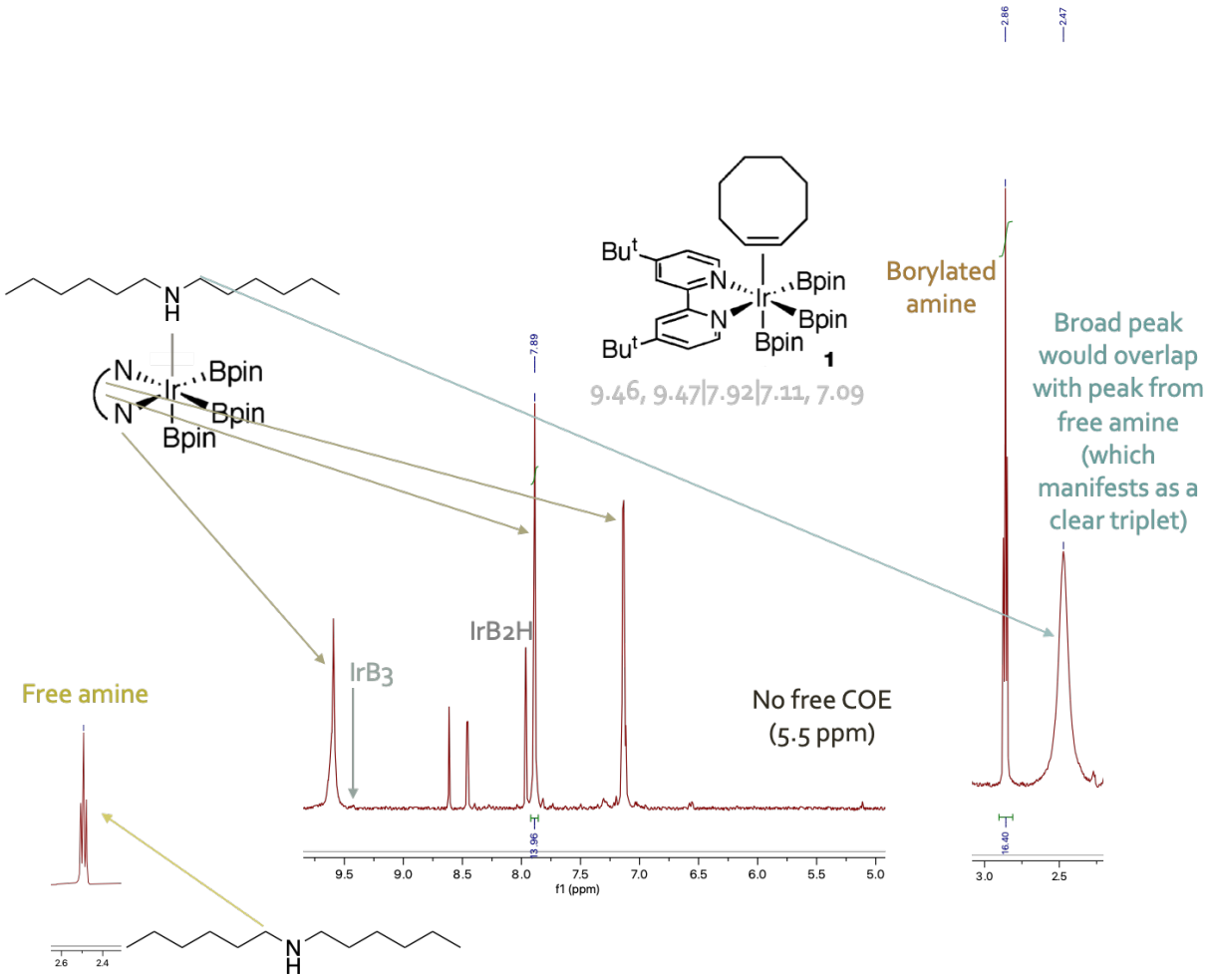
Bu^t
Bpin
Ir
N
Bpin
Bpin
Bu^t
1
9.46, 9.47|7.92|7.11, 7.09
N
H
N
Ir
Bpin
Bpin
Bpin
Borylated amine
Broad peak would overlap with peak from free amine (which manifests as a clear triplet)
IrB2H
IrB3
Free amine
No free COE (5.5 ppm)
f1 (ppm)

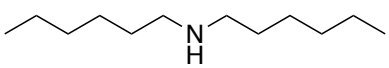

(1 equiv)

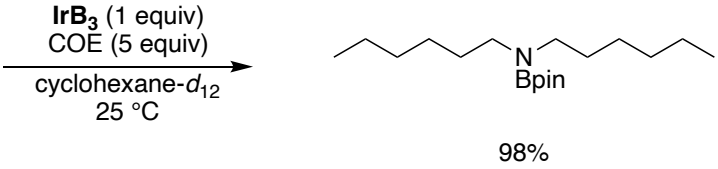

98%

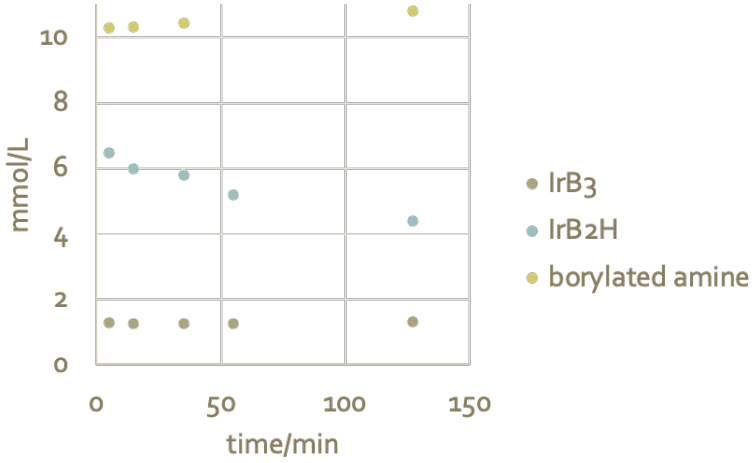

[phenol]

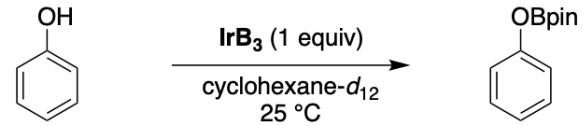

(1 equiv)

95%

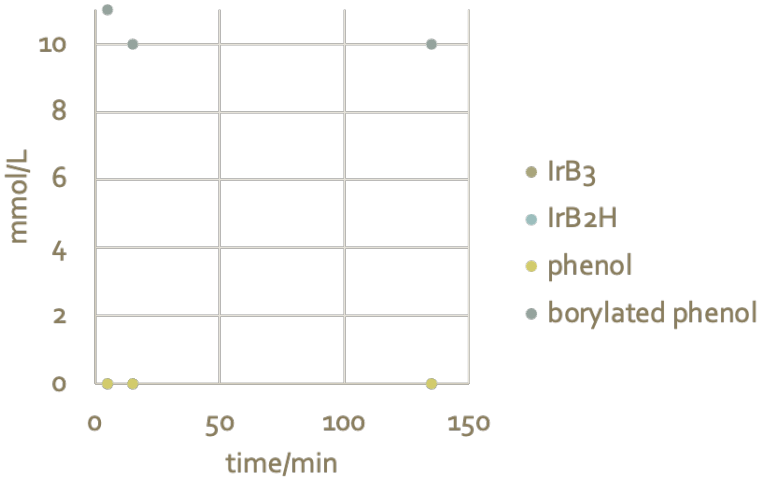

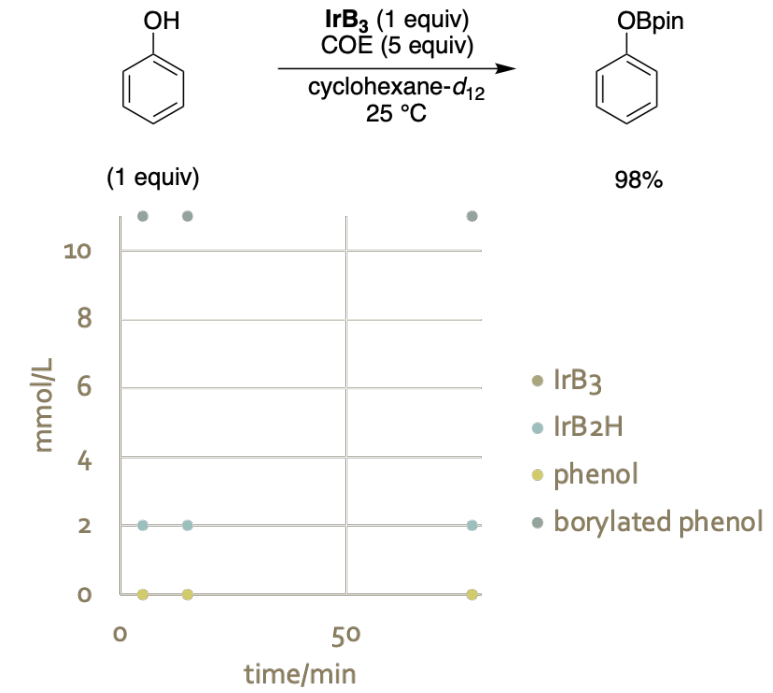
OH
IrB3 (1 equiv)
COE (5 equiv)
cyclohexane-d12
25 °C
OBpin
(1 equiv)
98%
10
8
6
4
2
0
mmol/L
0
50
time/min
IrB3
IrB2H
phenol
borylated phenol

[aniline]

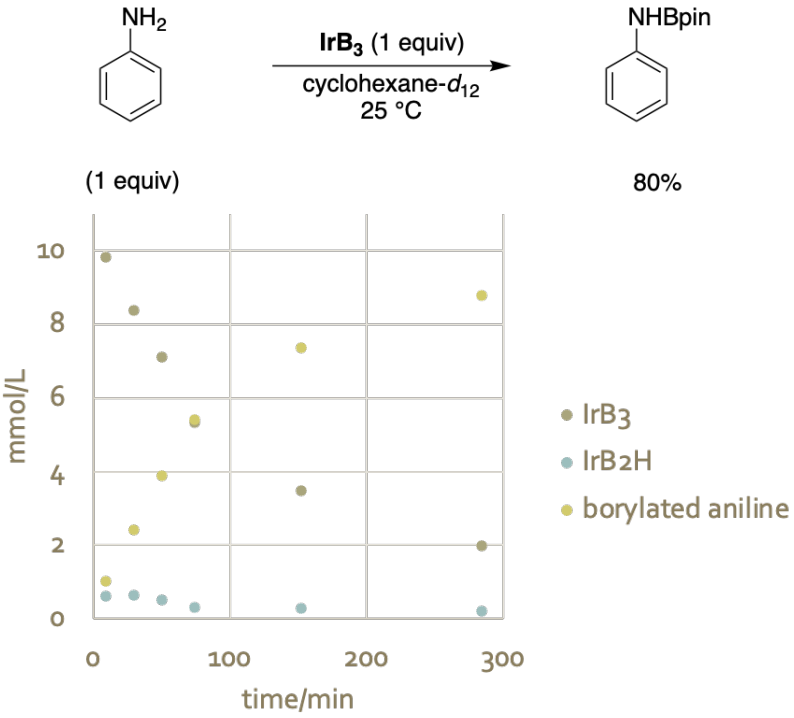
NH2
IrB3 (1 equiv)
cyclohexane-d12
25 °C
NHBpin
(1 equiv)
80%
10
8
6
4
2
0
mmol/L
0
100
200
300
time/min
IrB3
IrB2H
borylated aniline

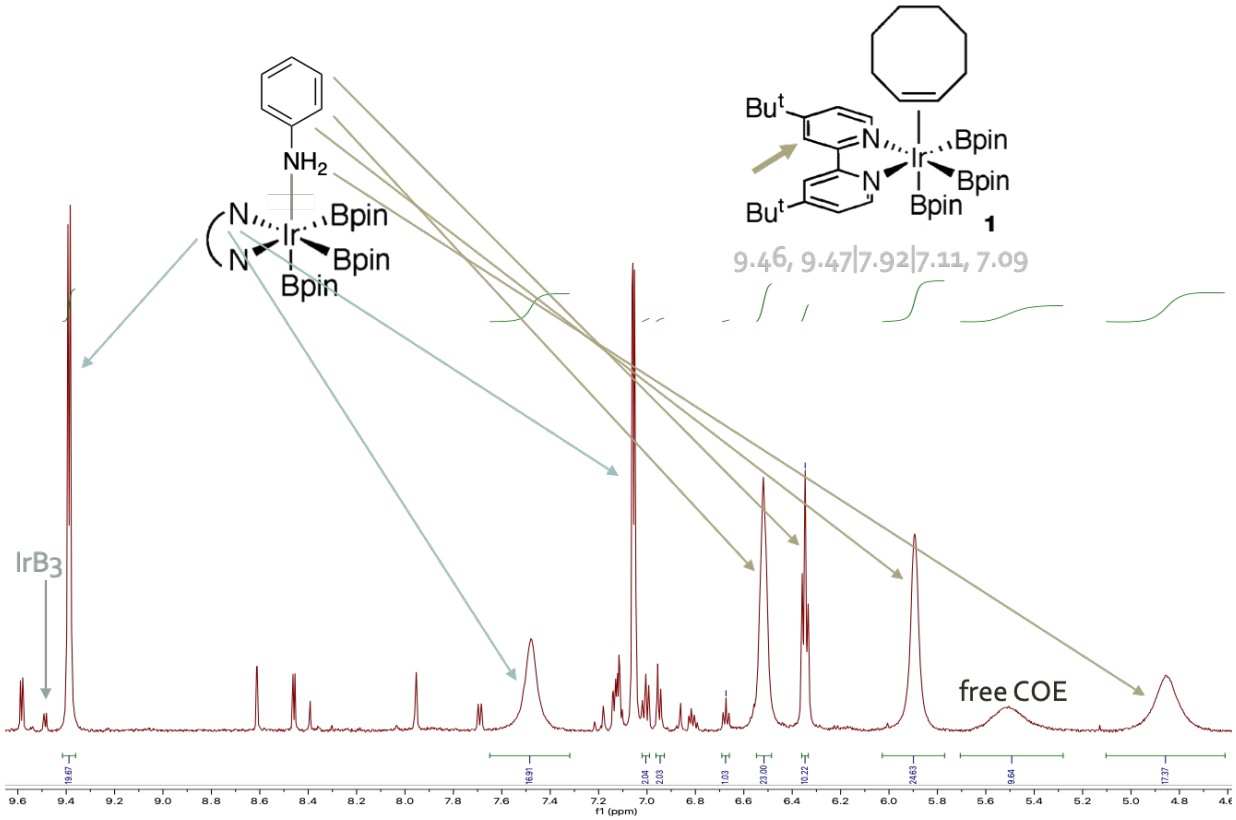

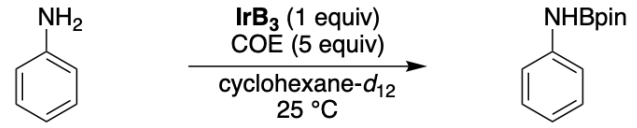

(1 equiv) 76%

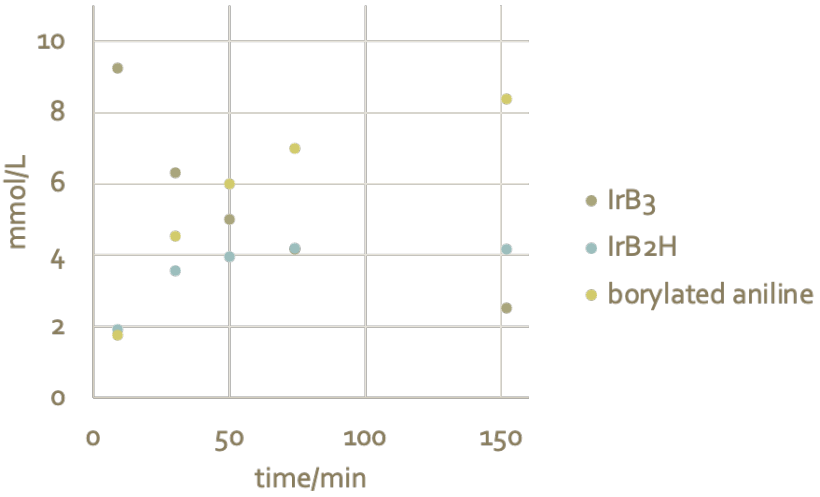

[thiophenol]

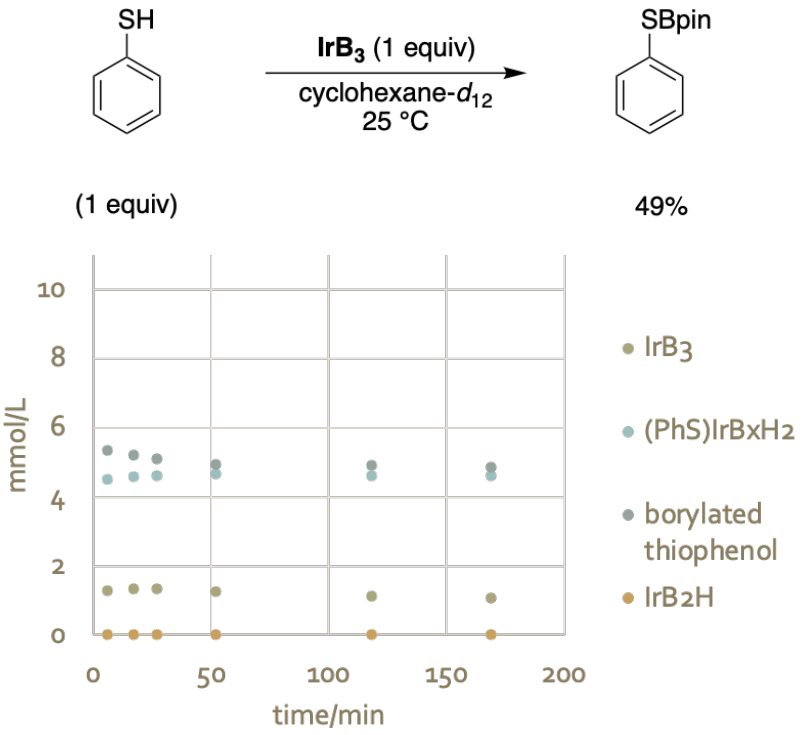

Note: Subsequent analysis overnight revealed no change.

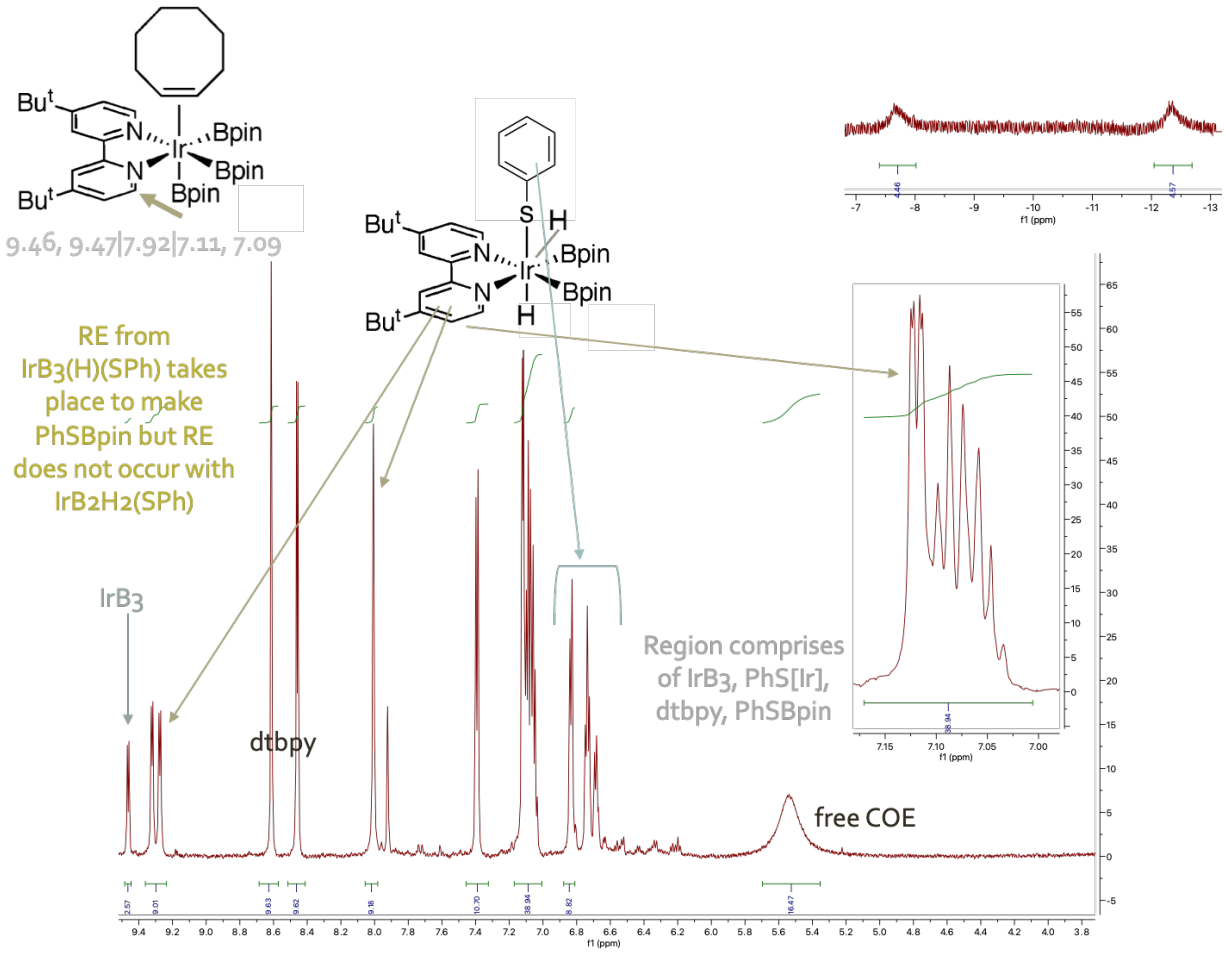
9.46, 9.47|7.92|7.11, 7.09
RE from IrB3(H)(SPh) takes place to make PhSBpin but RE does not occur with IrB2H2(SPh)
IrB3
dtbpy
Region comprises of IrB3, PhS[Ir], dtbpy, PhSBpin
free COE

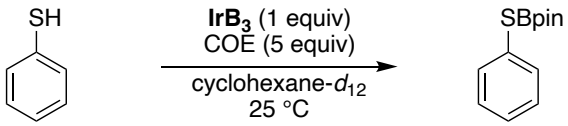
SH
IrB3 (1 equiv)
COE (5 equiv)
cyclohexane-d12
25 °C
SBpin
(1 equiv)
55%

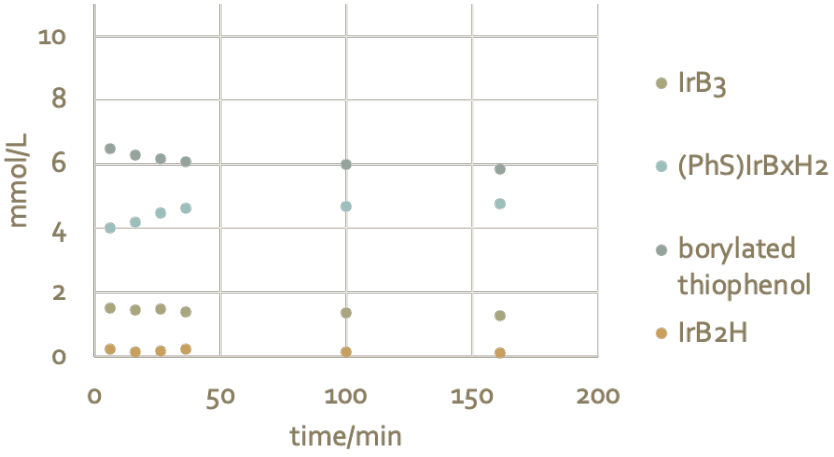
mmol/L
time/min
IrB3
(PhS)IrBxH2
borylated thiophenol
IrB2H

Note: Subsequent analysis overnight revealed no change.

[3-methylpyridine]

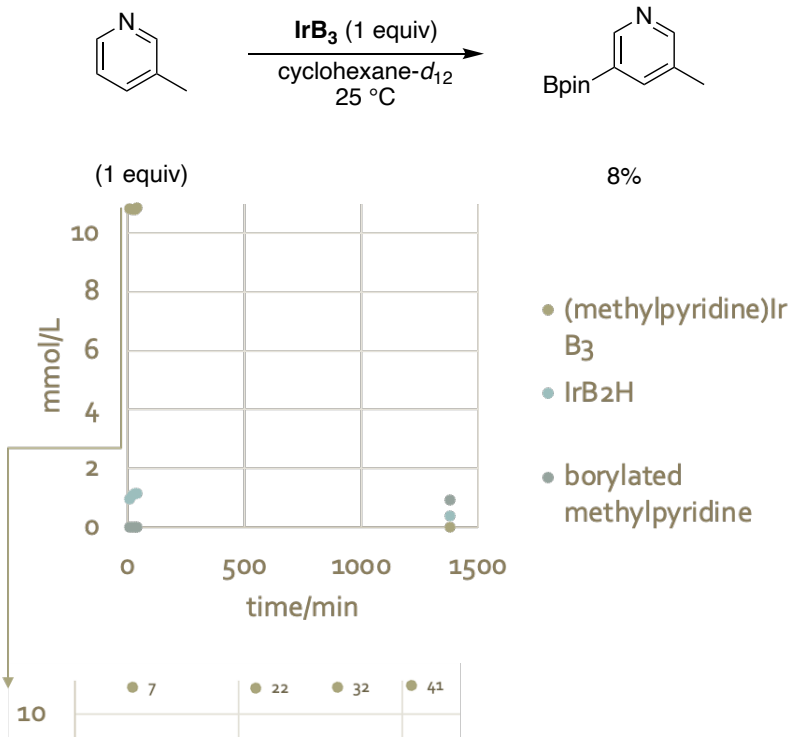

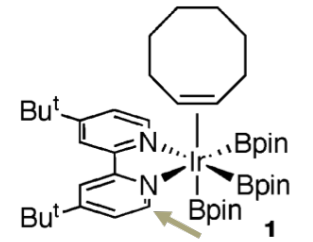

9.46, 9.47|7.92|7.11, 7.09

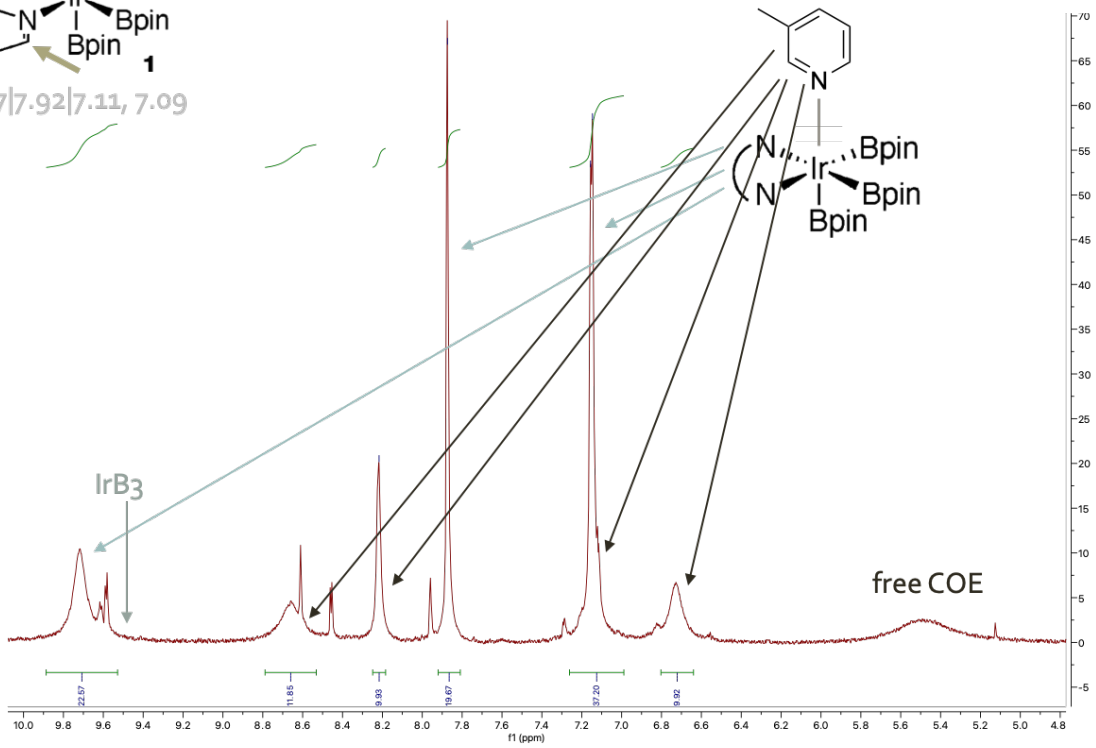

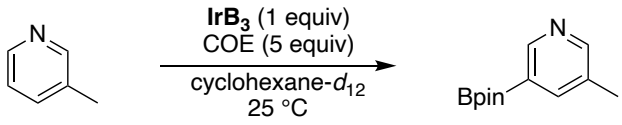

(1 equiv) 44%

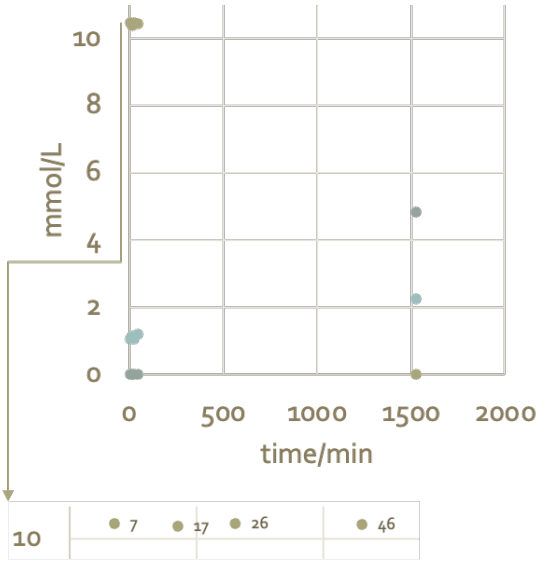

[2-butyne]

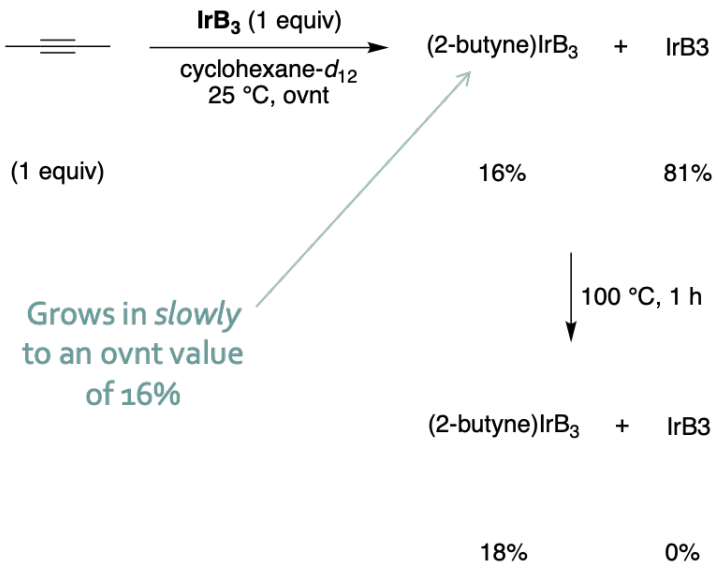

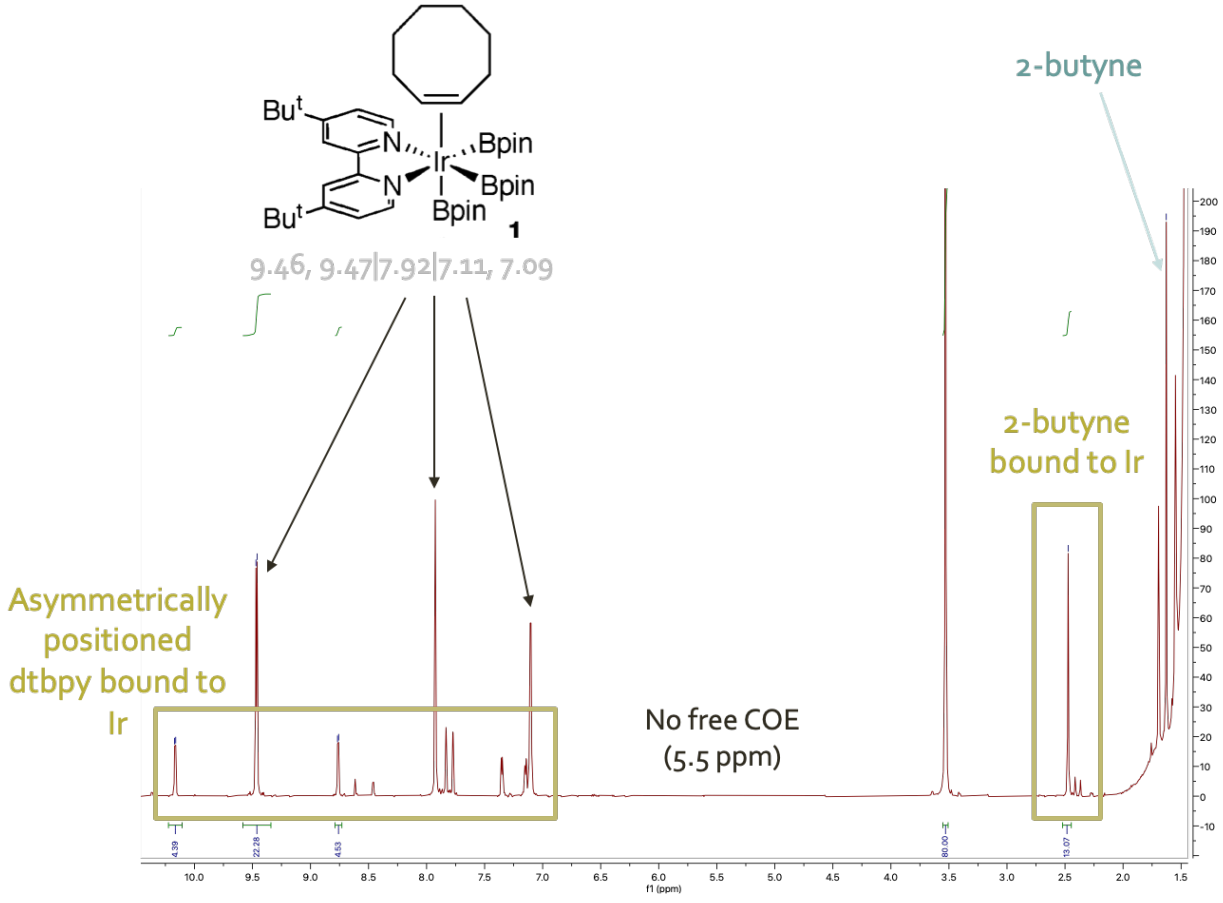

[benzothiophene]

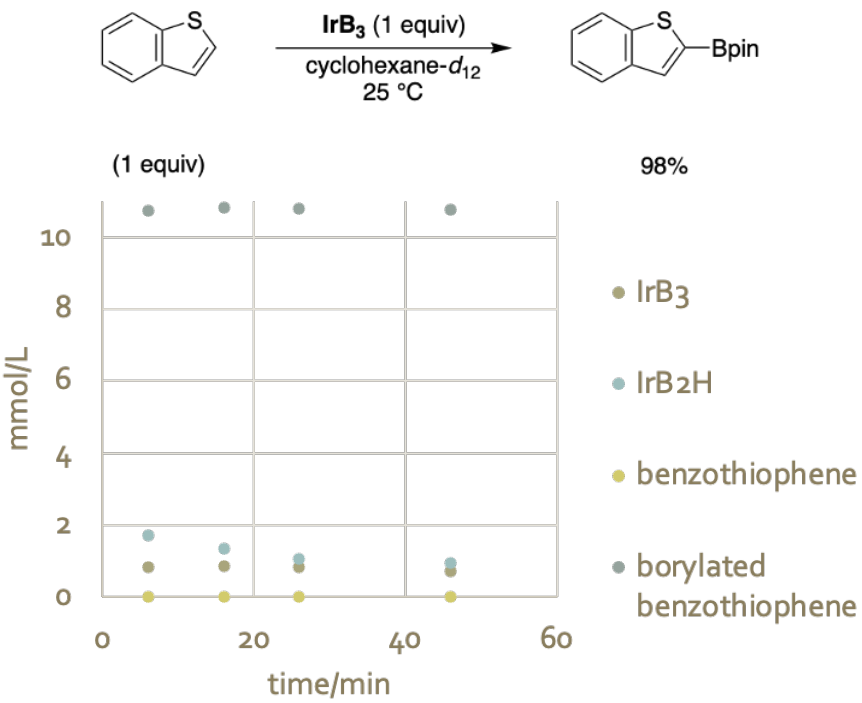

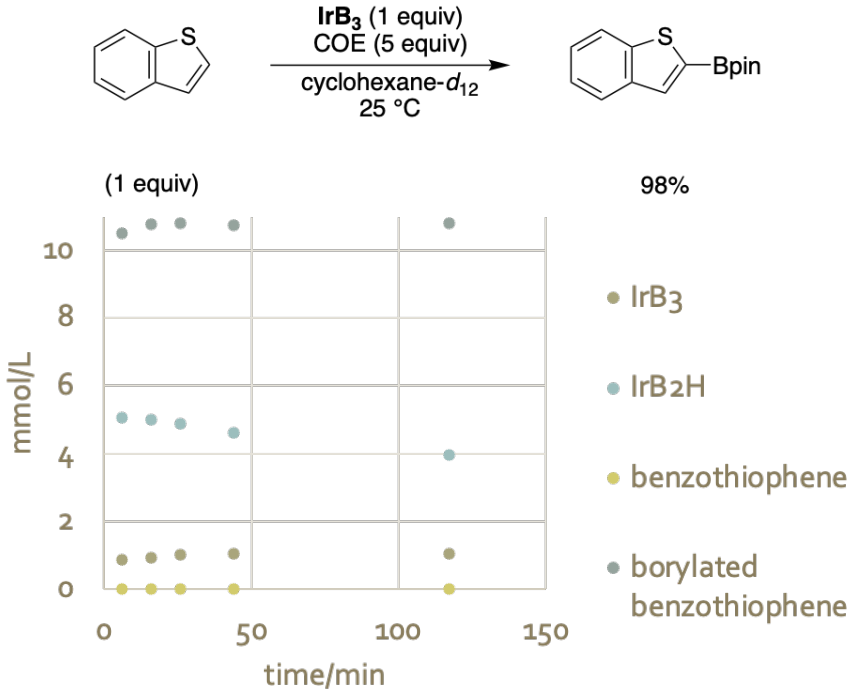

[methylindole]

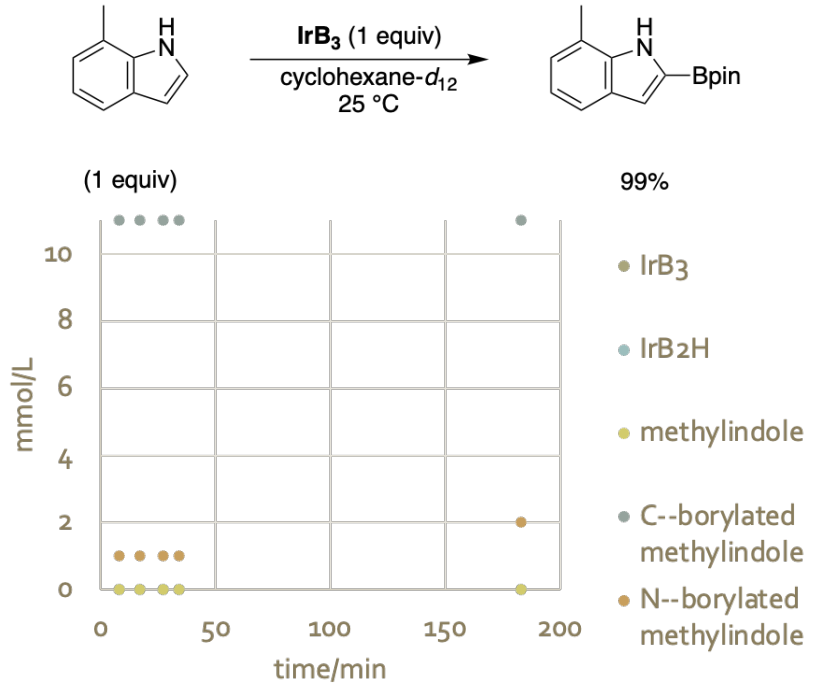

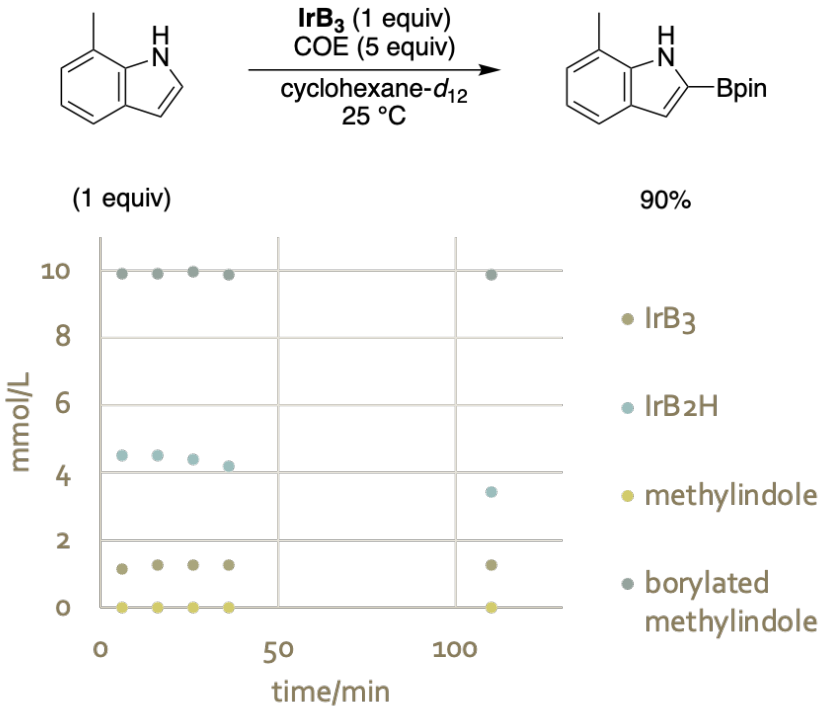

1.4.3 Stoichiometric Experiments: NMR Analysis of Terminal Time Point (as well as Initial Time Point for Additives that Bind to Ir)

Reactivity at Bpin Ligand

[1-hexanol]

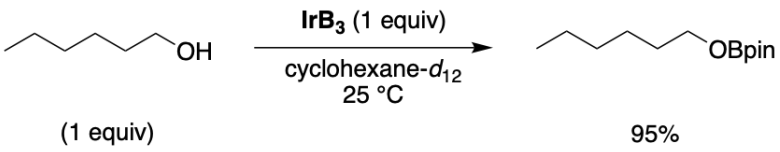

(1 equiv) 95%

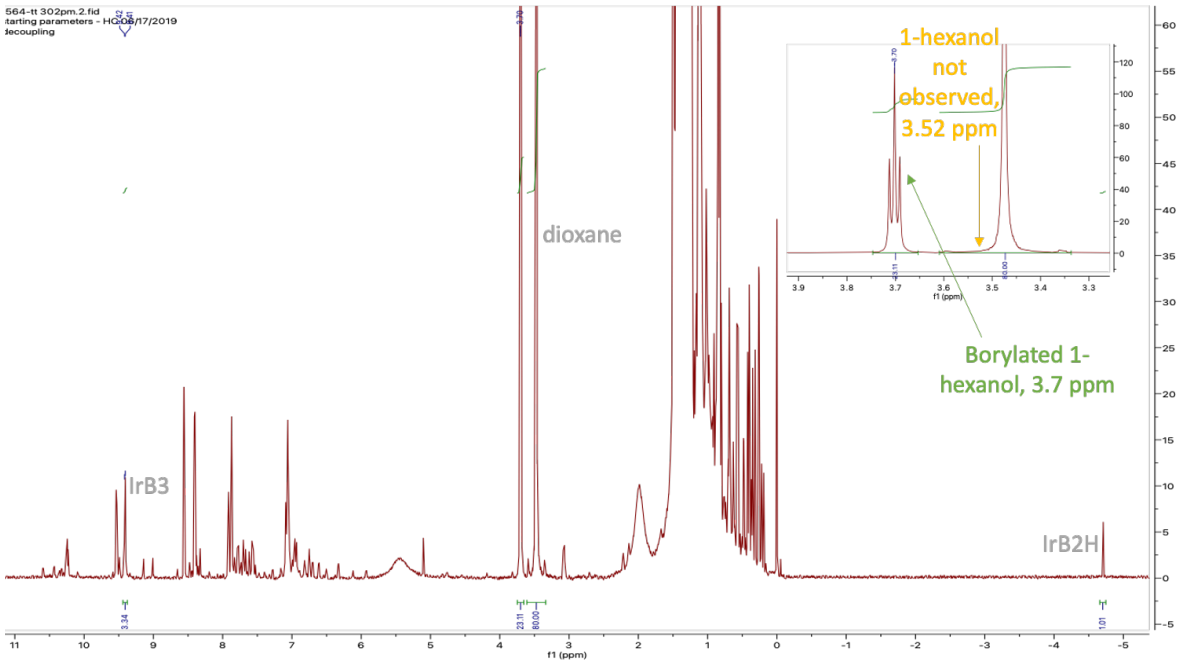

^{1}H-NMR

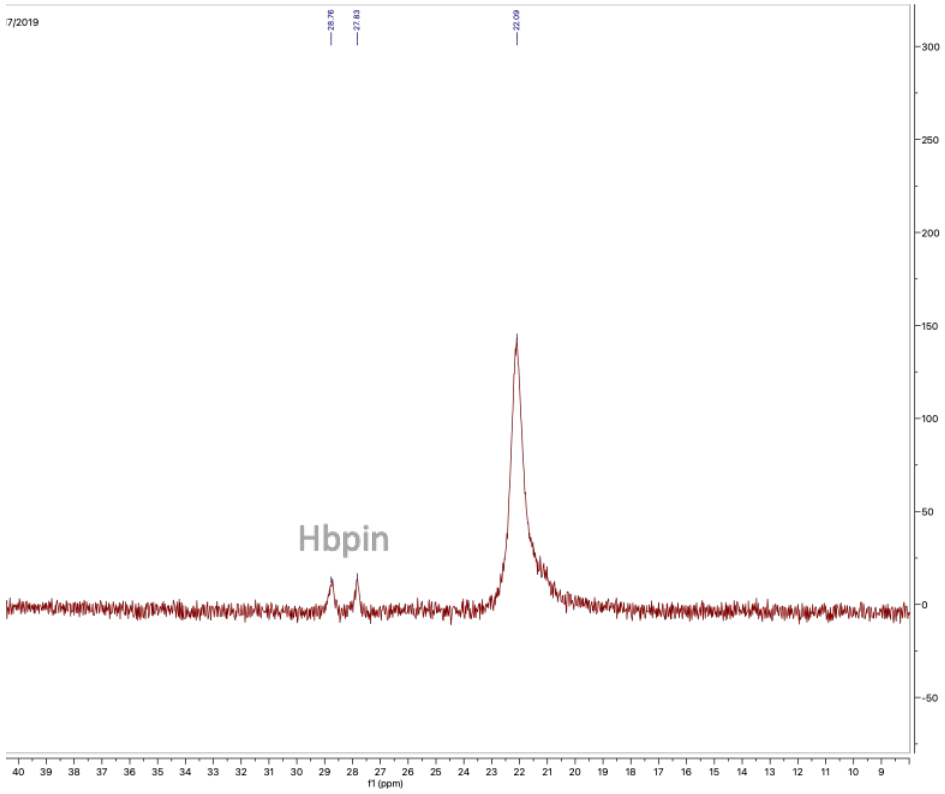
7/2019
28.76
27.83
22.09
Hbpin
f1 (ppm)

^{11}B-NMR

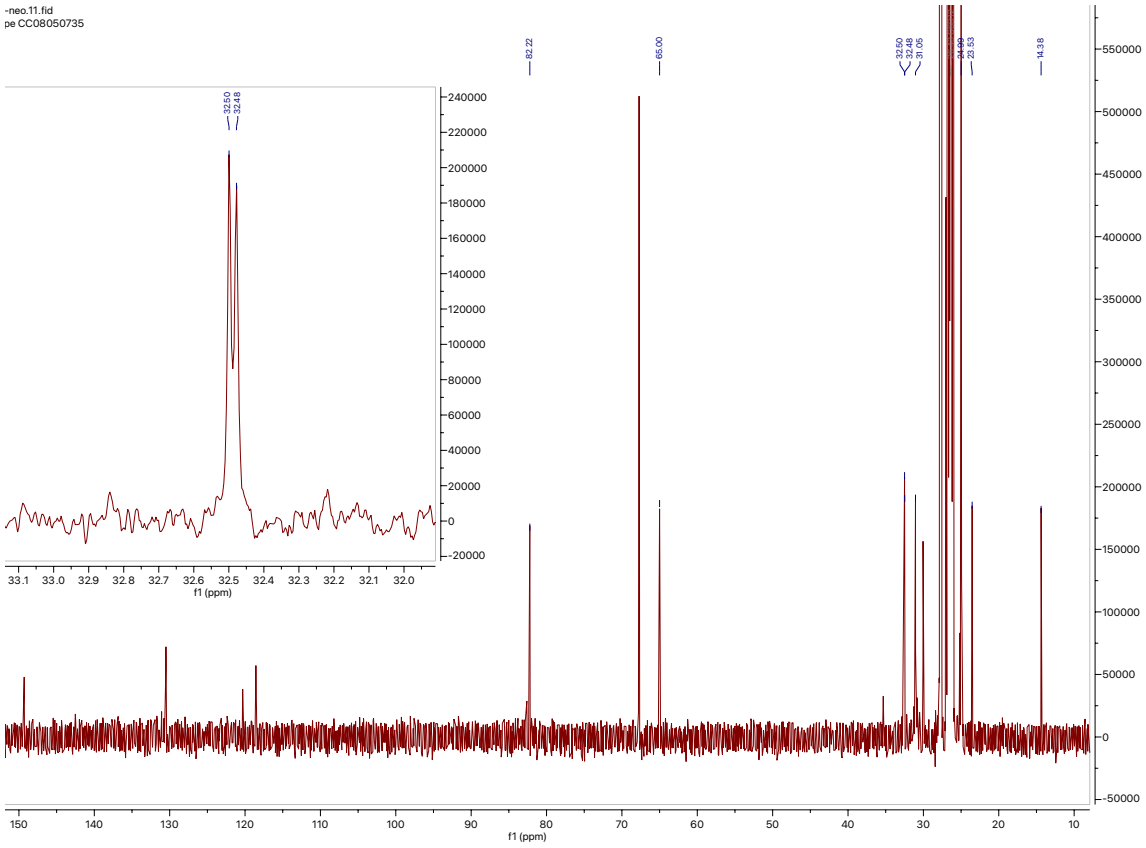
-neo.11.fid
pe CC08050735
82.22
65.00
32.50
32.48
31.05
24.89
23.53
14.38
32.50
32.48
f1 (ppm)

^{13}C-NMR

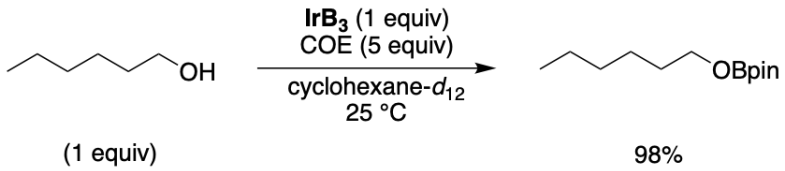

(1 equiv) 98%

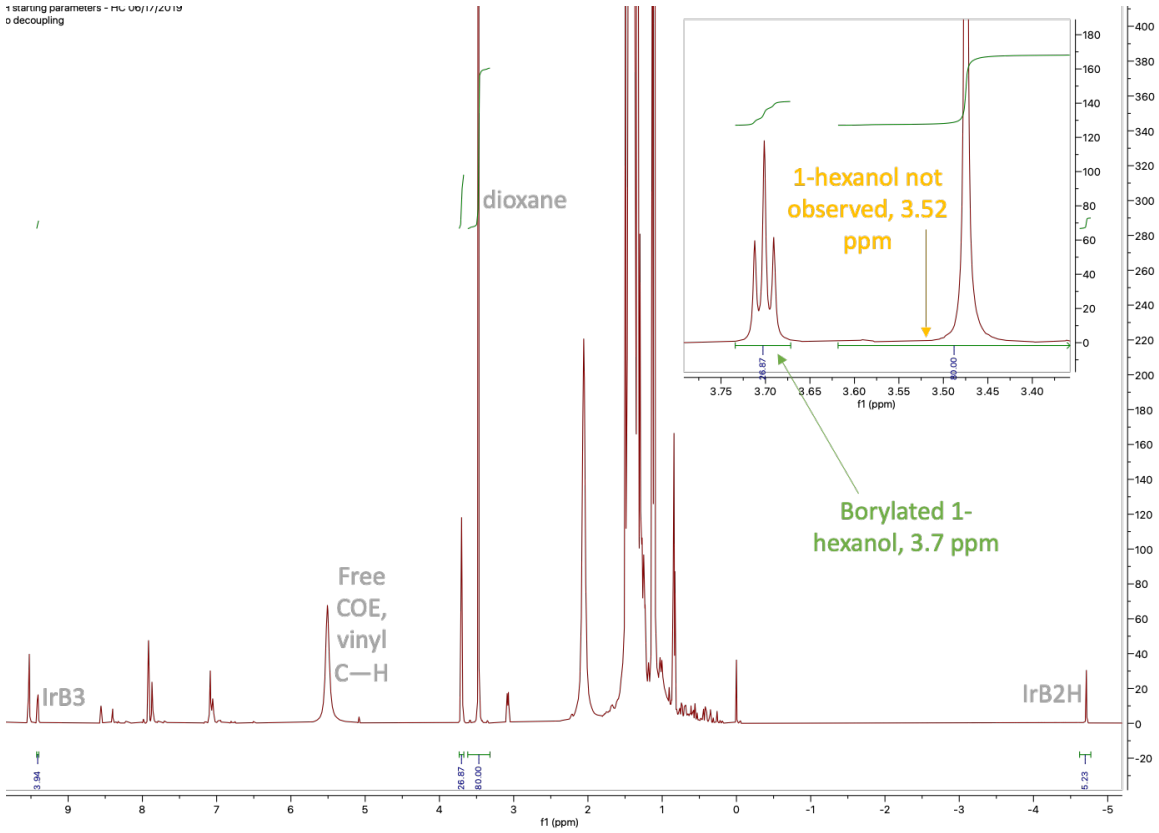

^{1}H-NMR

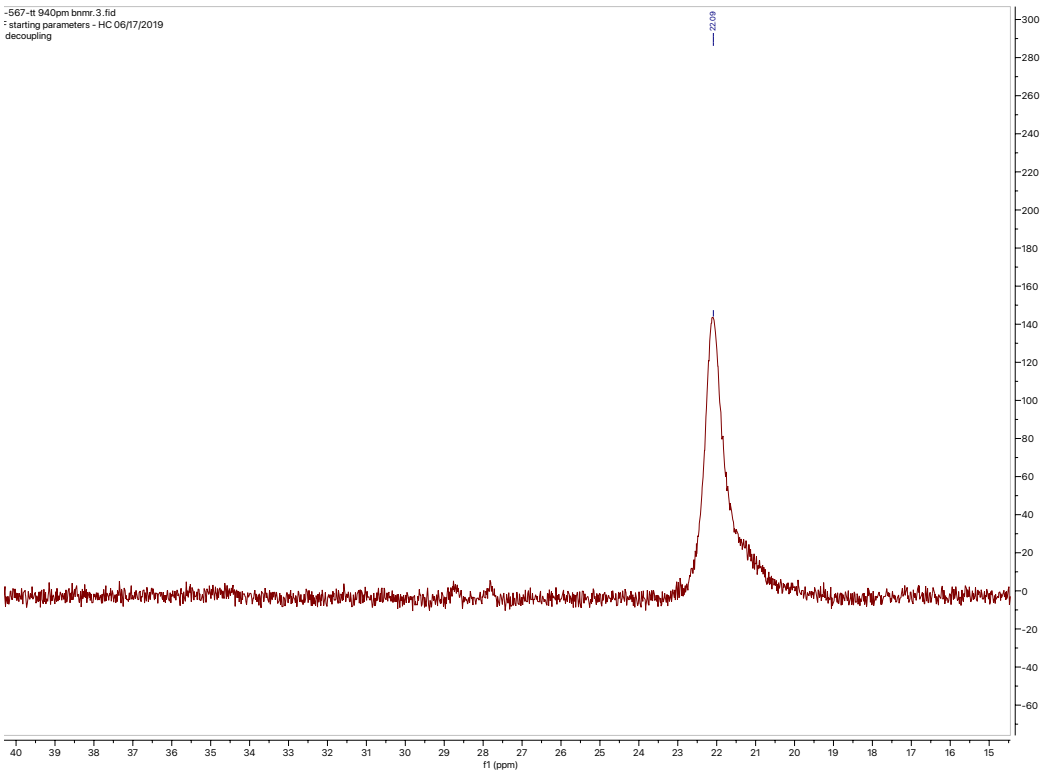

^{11}B-NMR

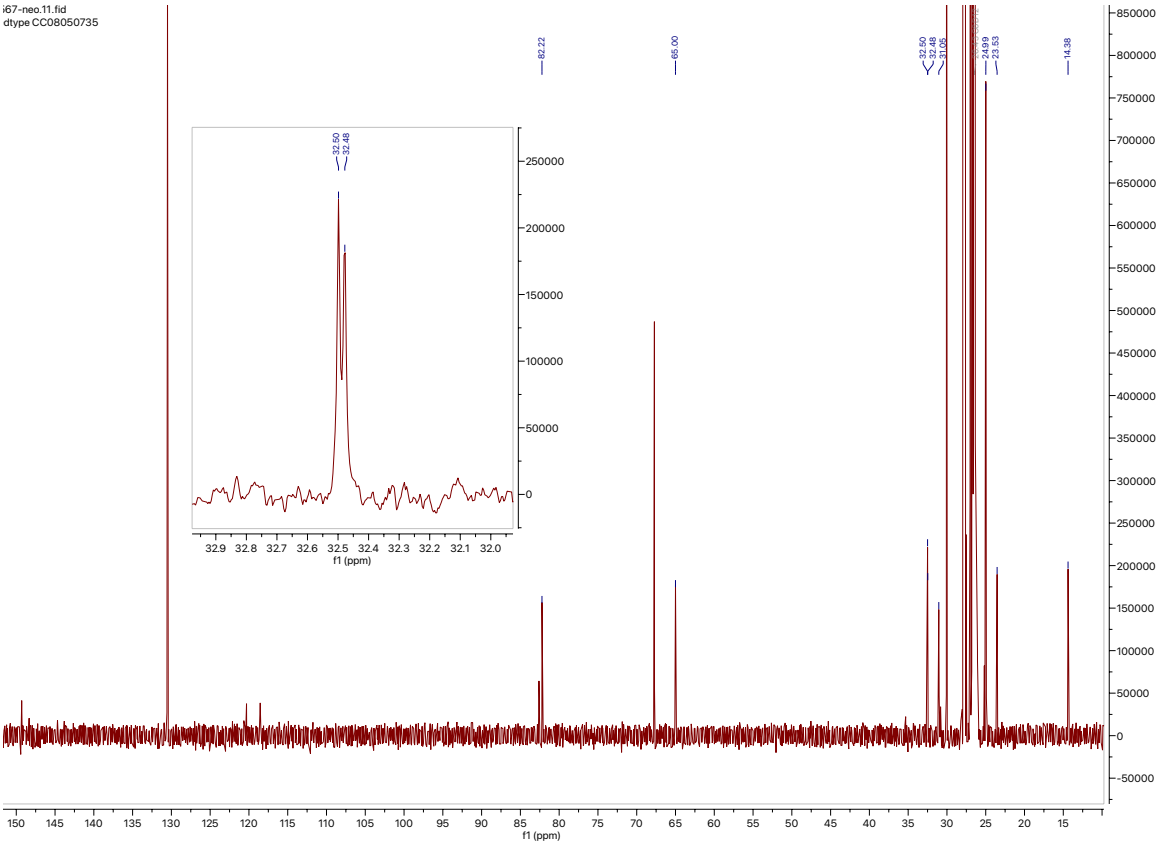

^{13}C-NMR

[dodecylamine]

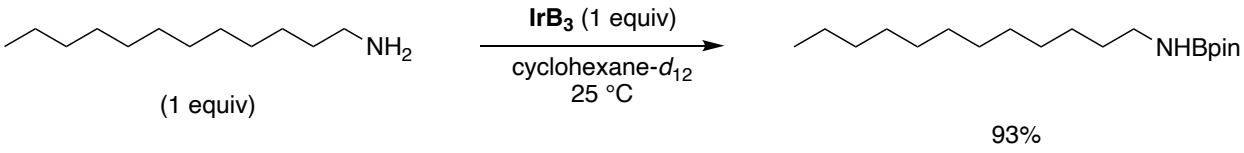

(1 equiv)

93%

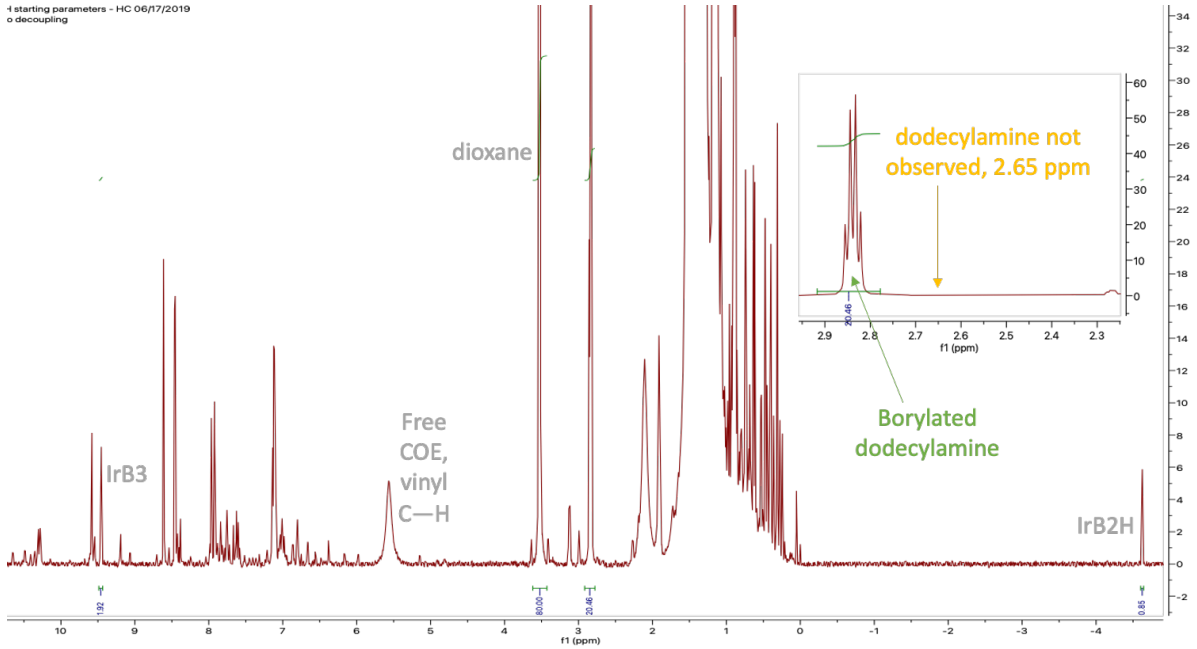

^{1}H-NMR

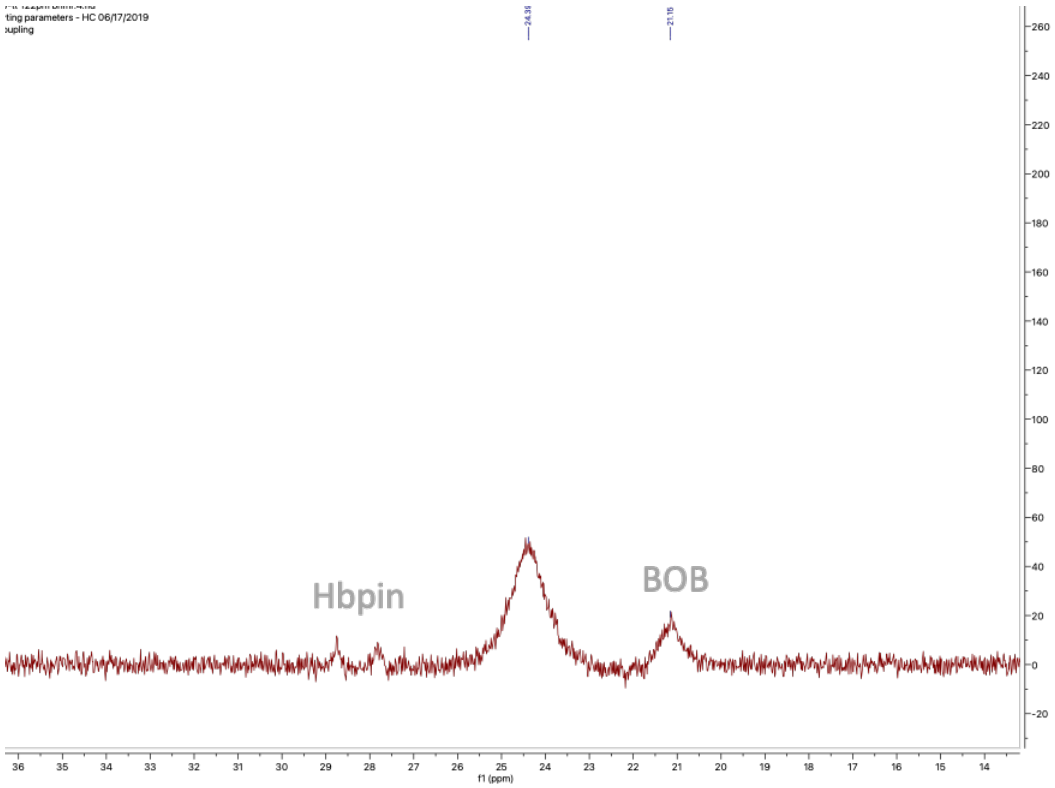

^{11}B-NMR

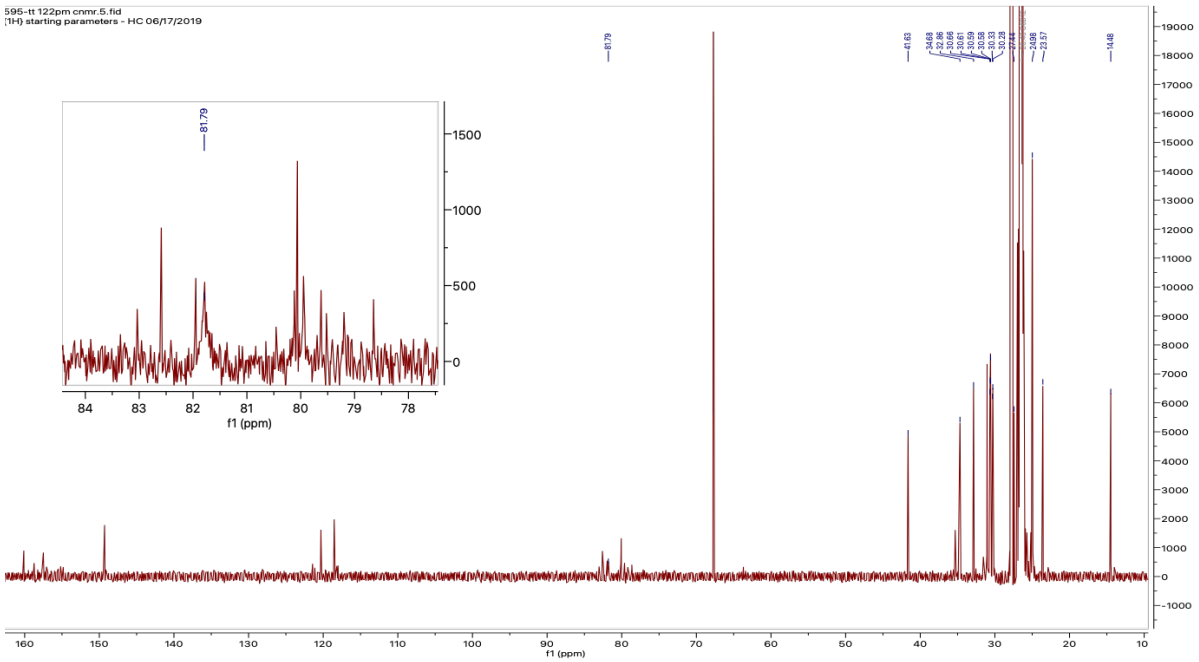

^{13}C-NMR

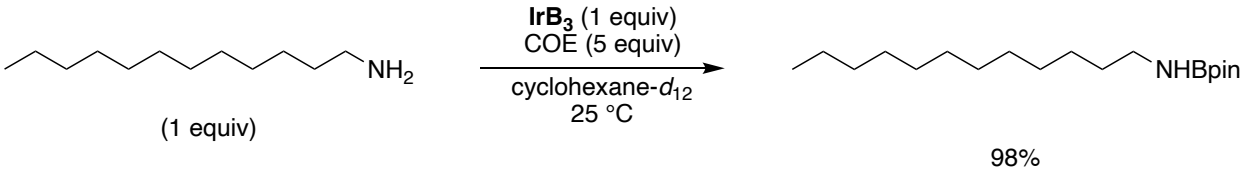

(1 equiv)

98%

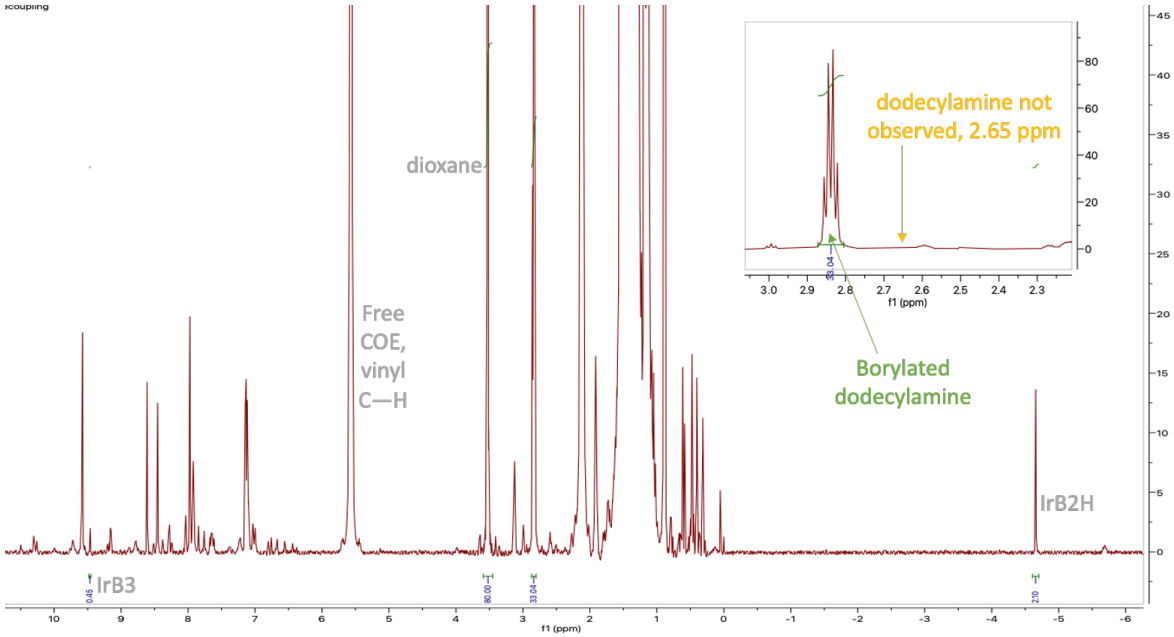

^{1}H-NMR

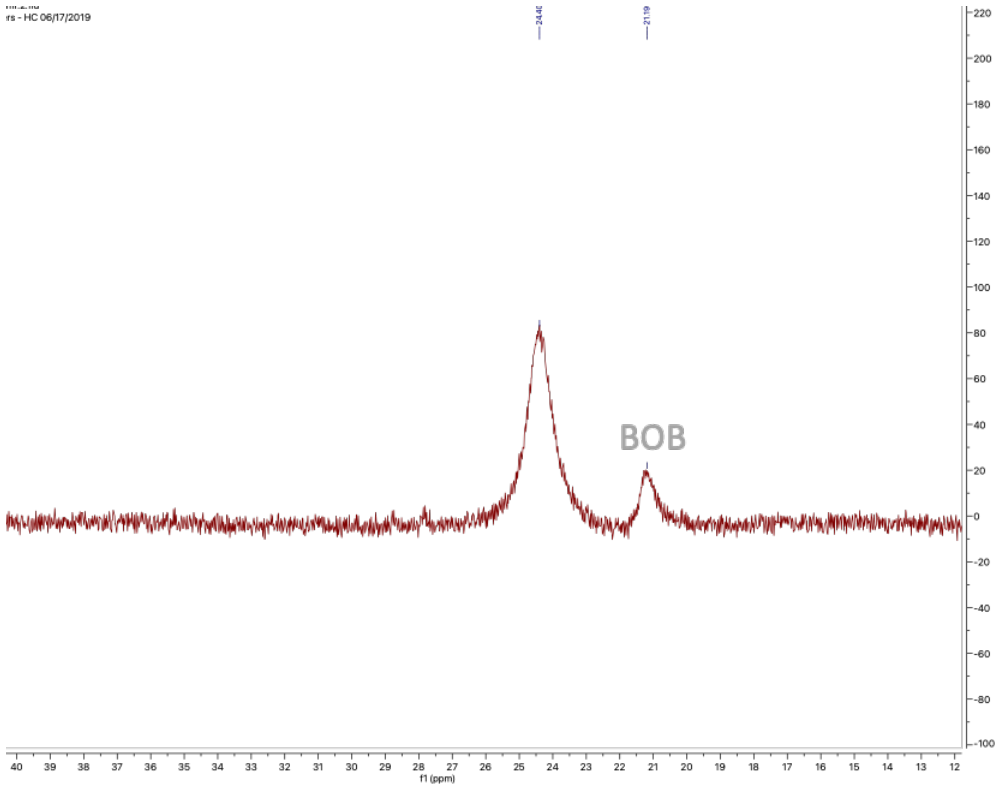

^{11}B-NMR

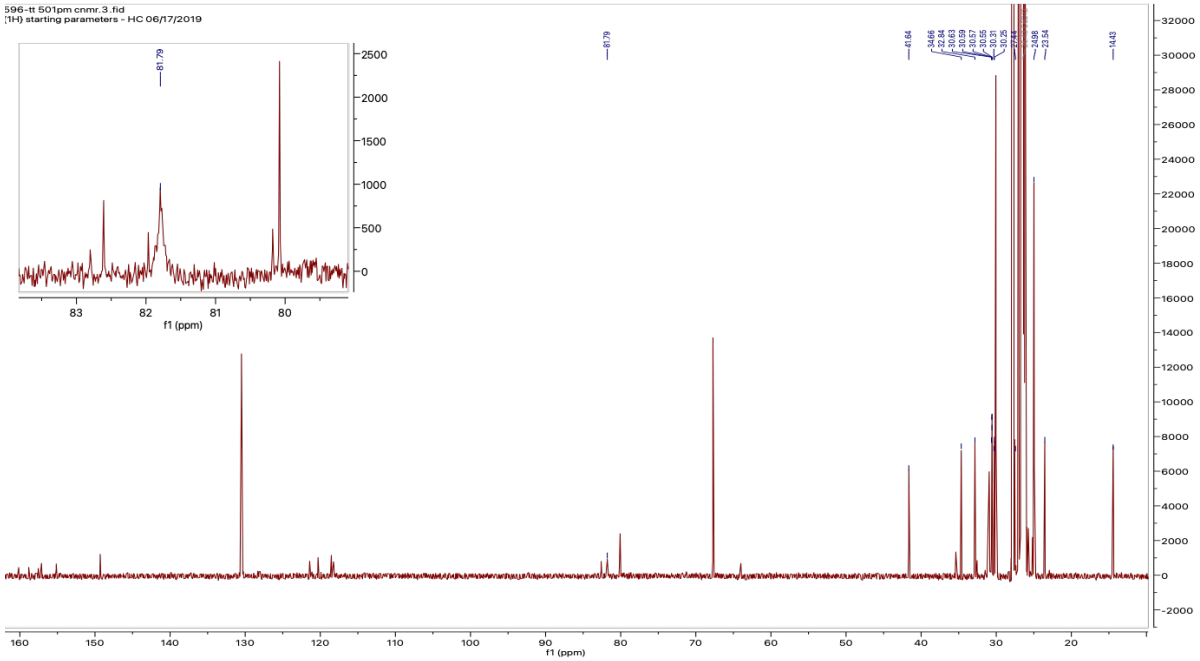

^{13}C-NMR

[octanethiol]

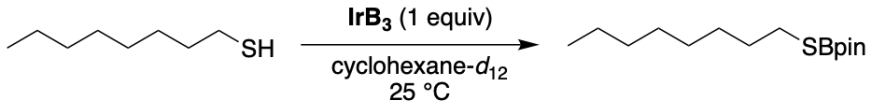

(1 equiv) 89%

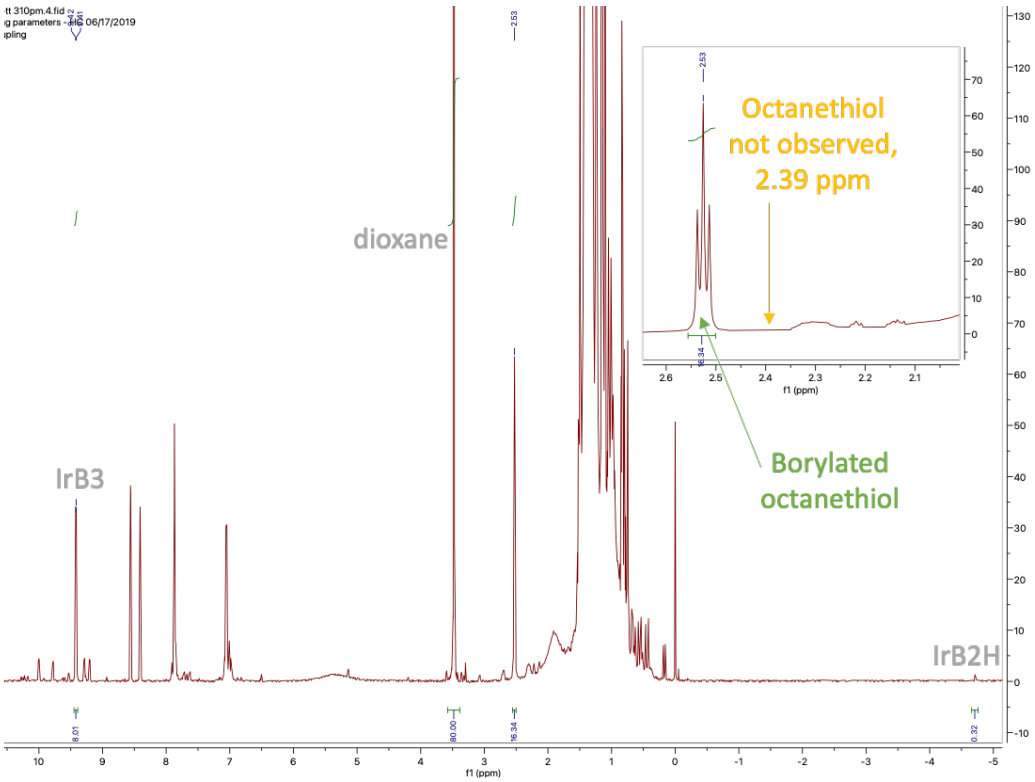

^{1}H-NMR

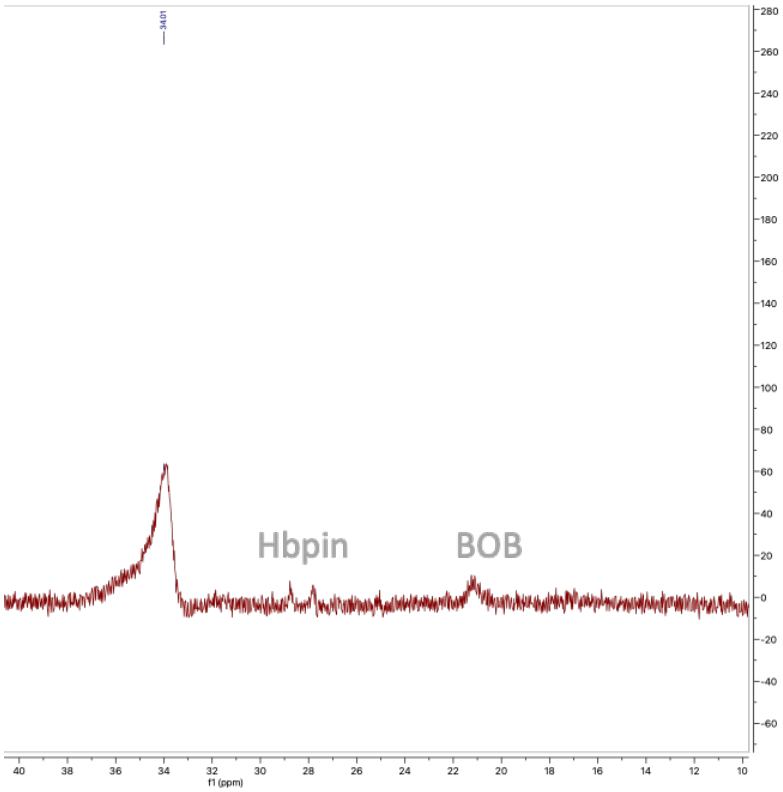

^{11}B-NMR

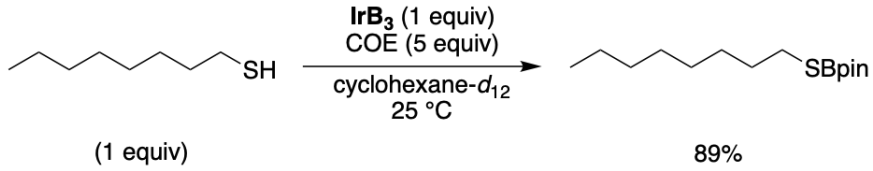
IrB3 (1 equiv)
COE (5 equiv)
cyclohexane-d12
25 °C
SH
SBpin
(1 equiv)
89%

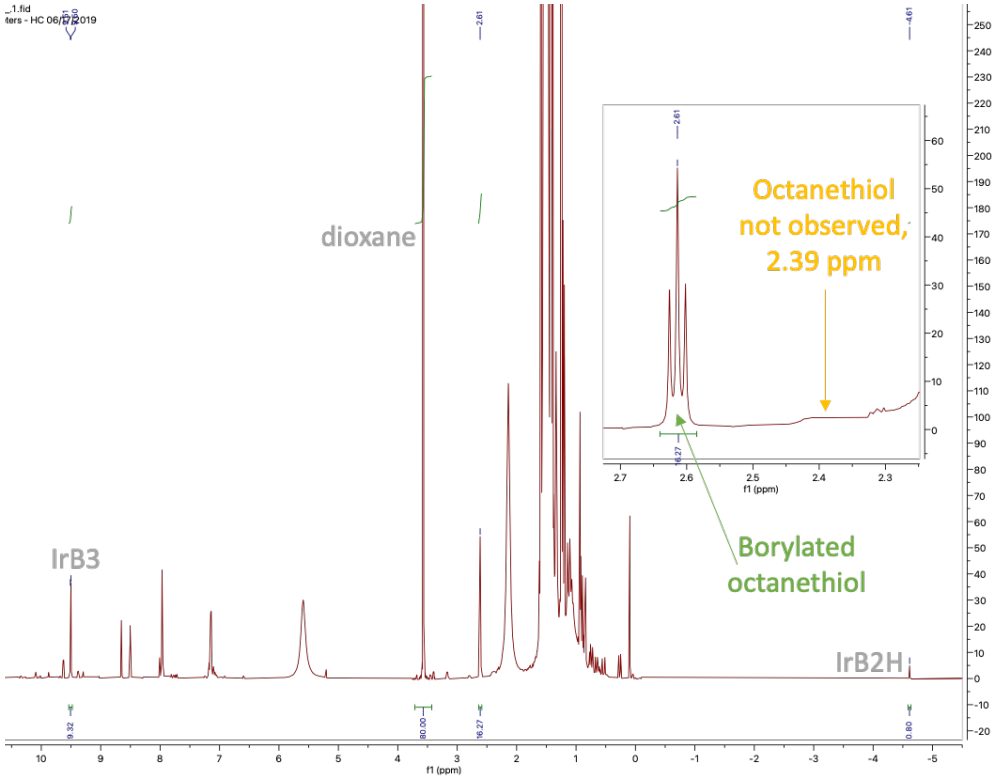
dioxane
IrB3
IrB2H
Octanethiol
not observed,
2.39 ppm
Borylated
octanethiol
f1 (ppm)

^{1}H-NMR

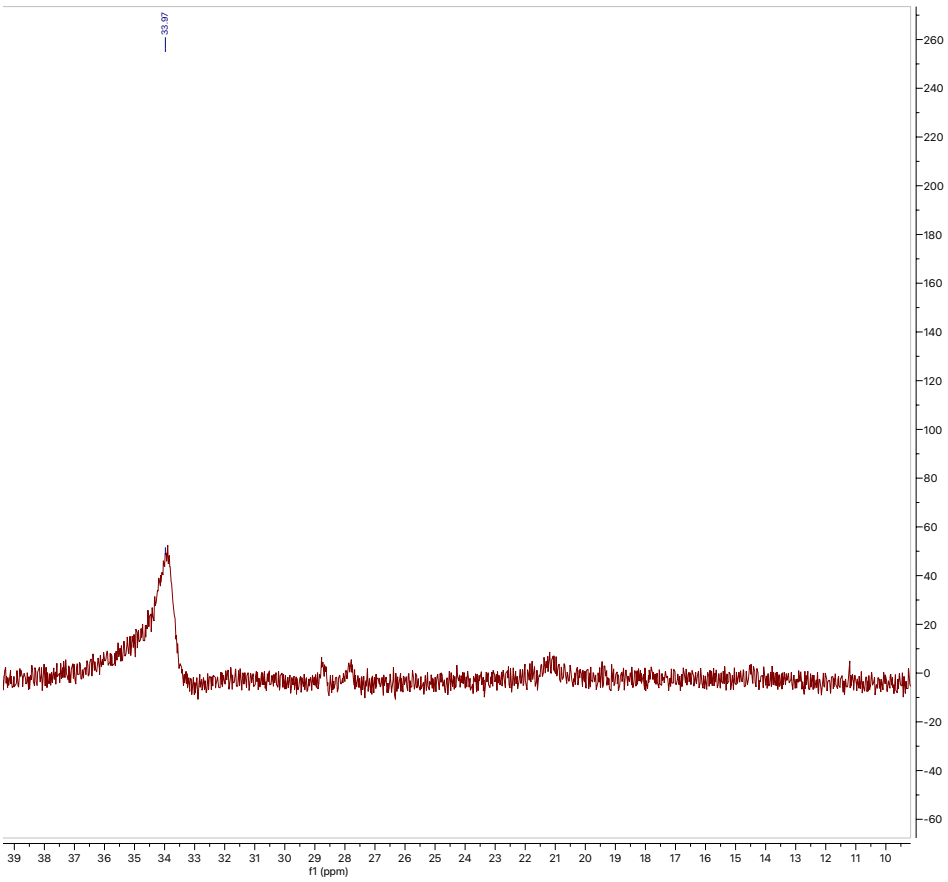

^{11}B-NMR

[N-methylbutyramide]

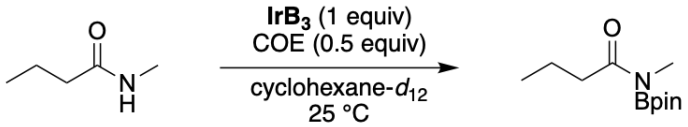

(1 equiv) 12%

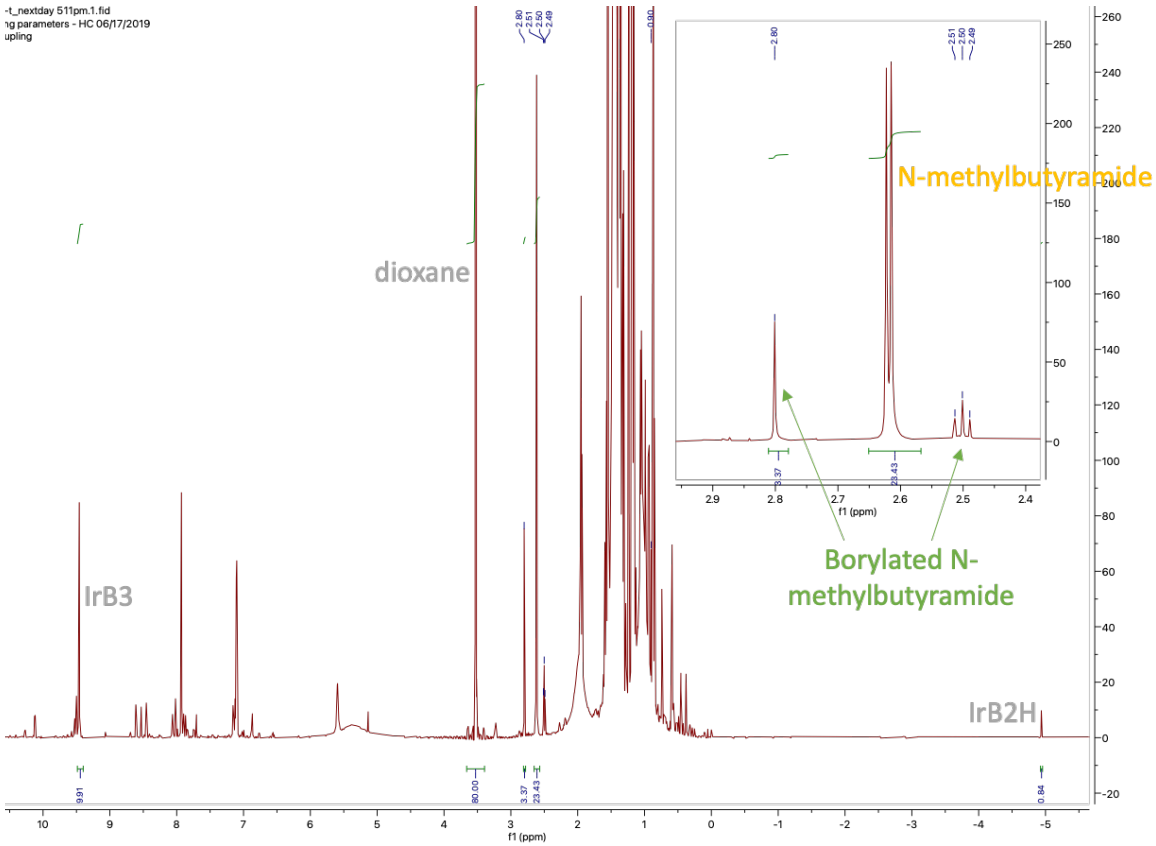

^{1}H-NMR

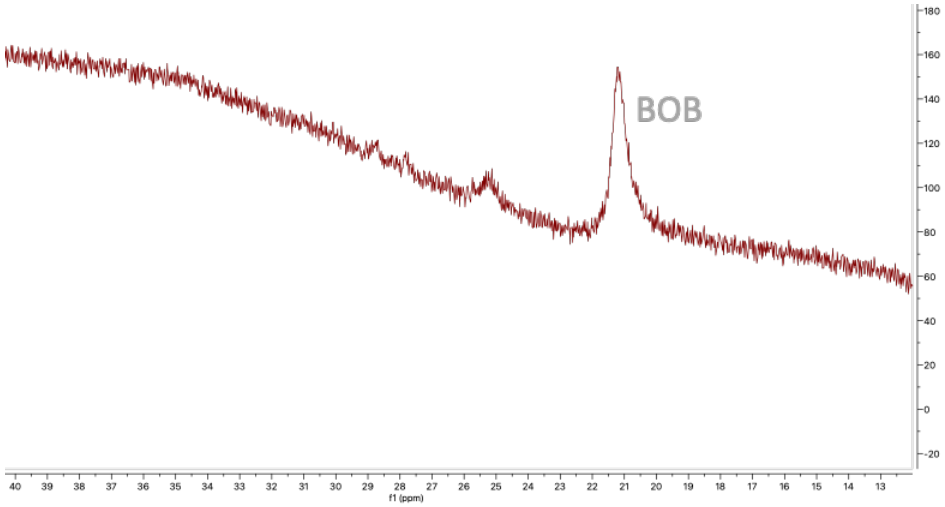

^{11}B-NMR

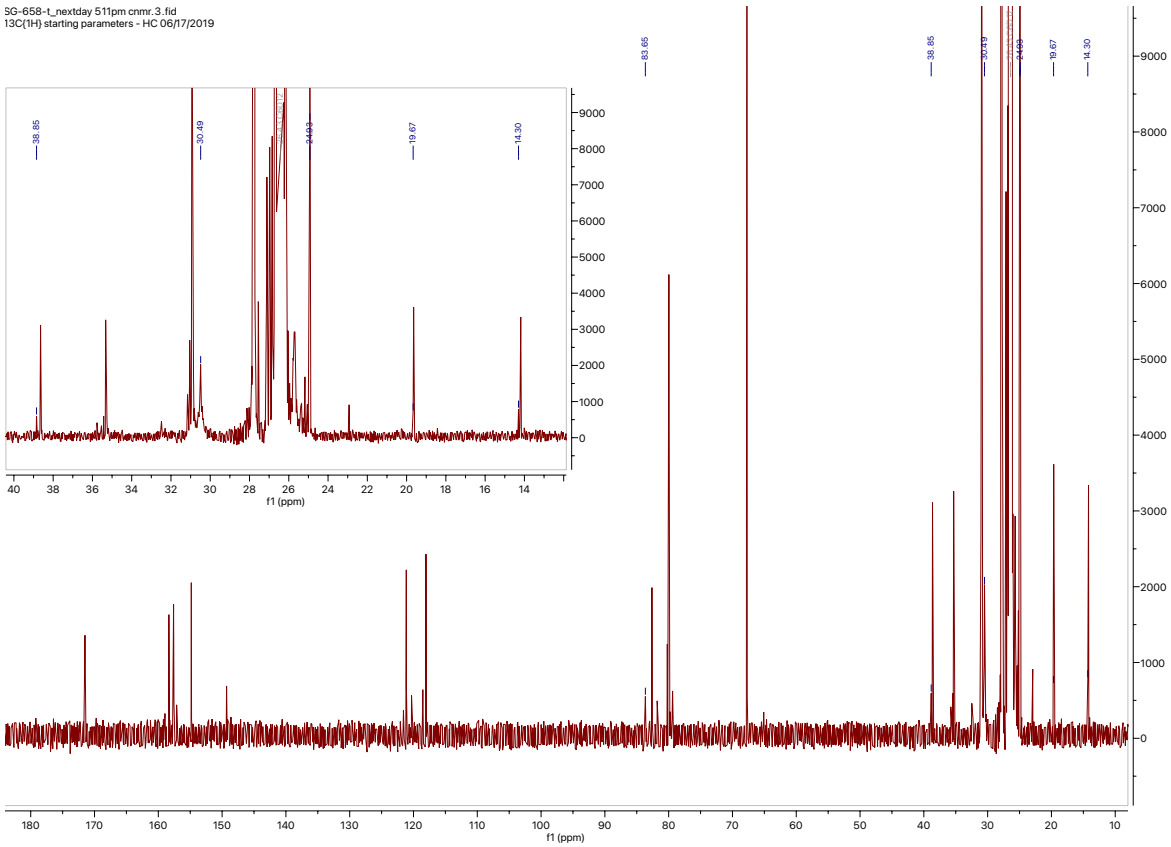

^{13}C-NMR

Note: **C**=O (177.1 ppm) too small to be observed in this reaction of low conversion

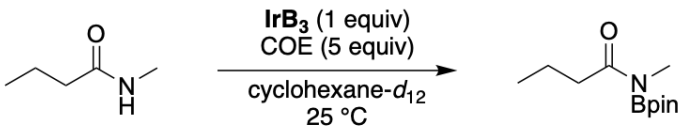

(1 equiv) 7%

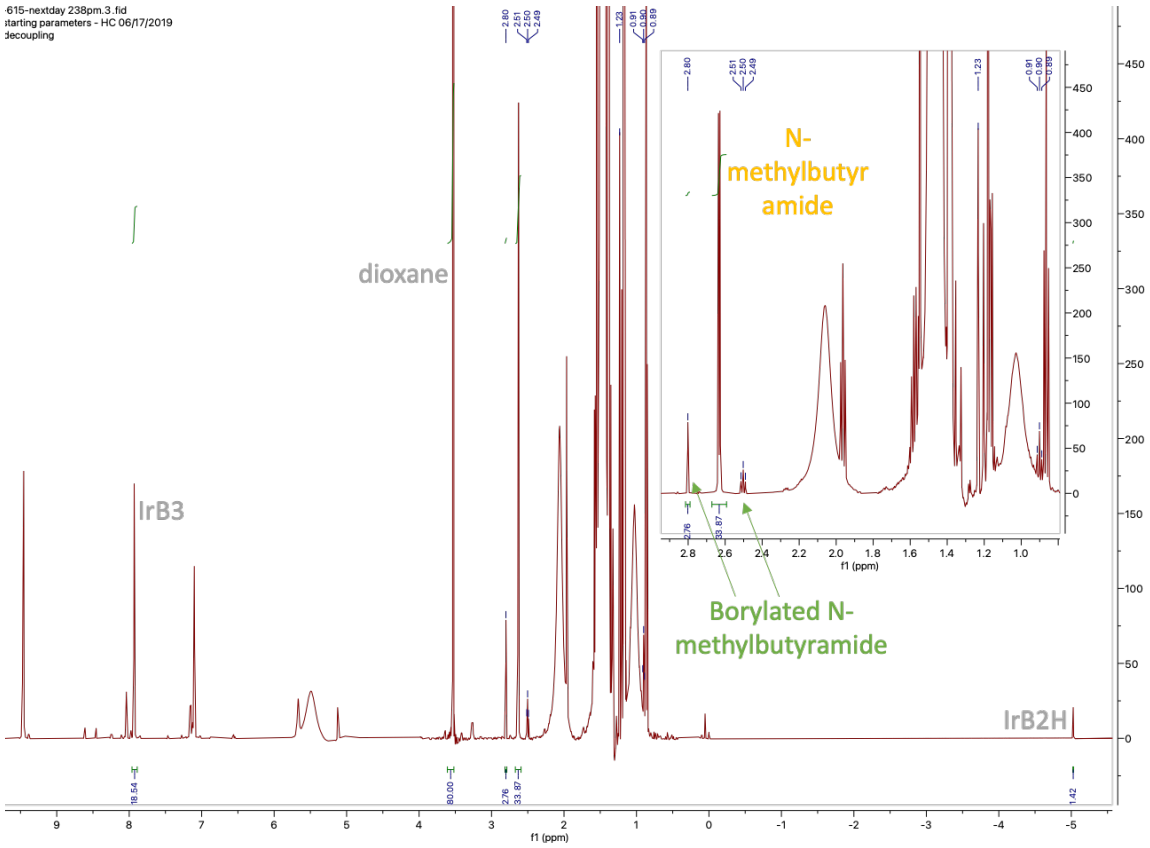

^{1}H-NMR

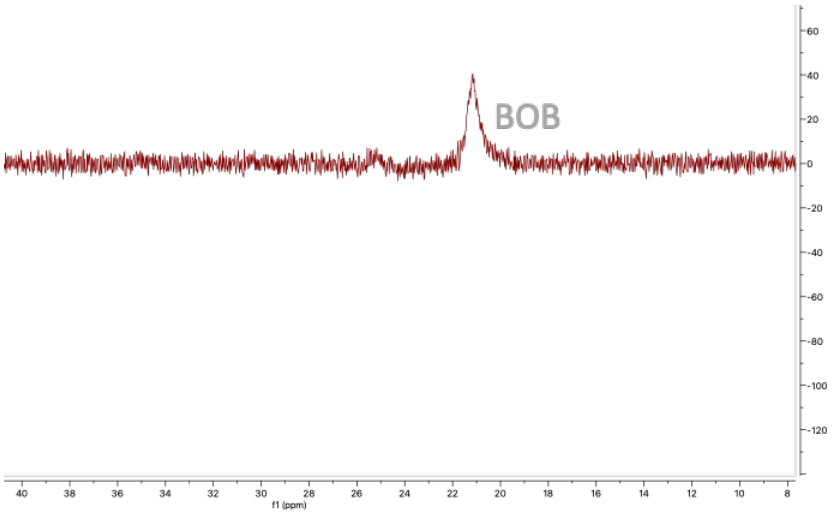

^{11}B-NMR

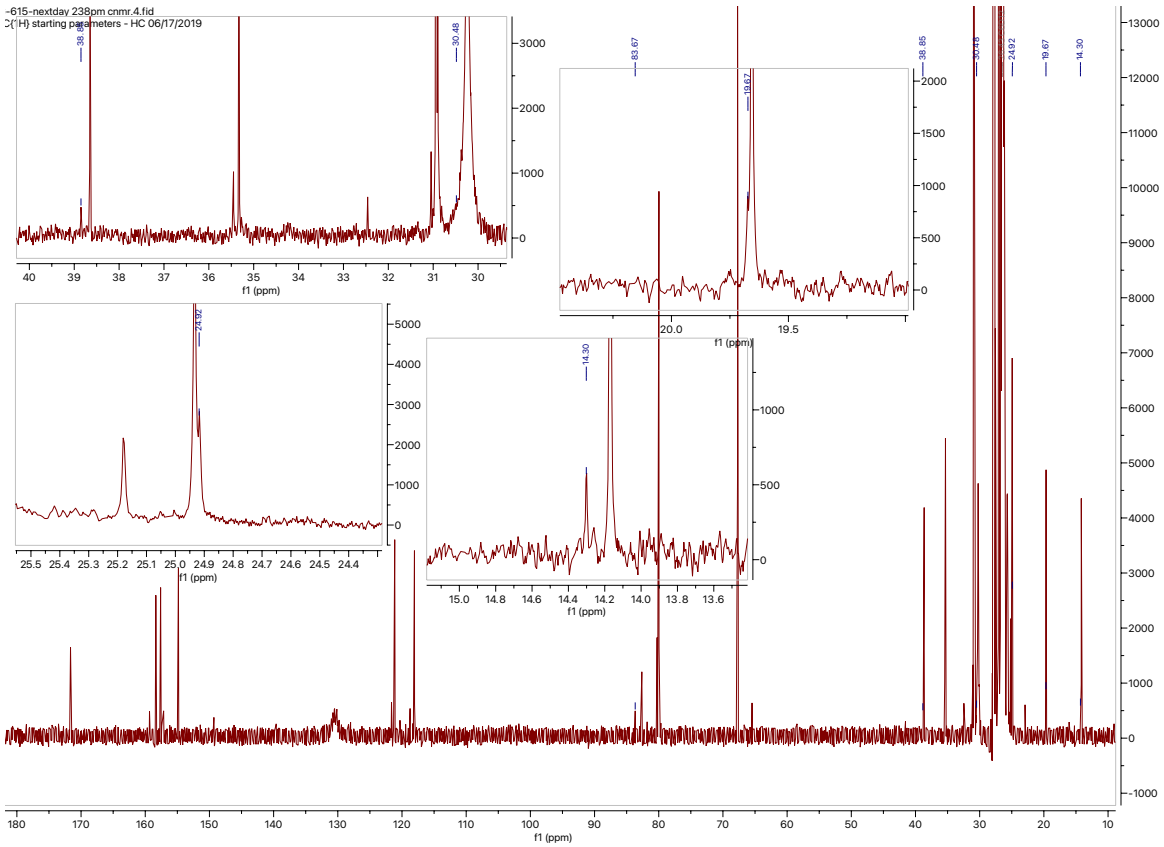

^{13}C-NMR

Note: **C**=O (177.1 ppm) too small to be observed in this reaction of low conversion

[m-xylene]

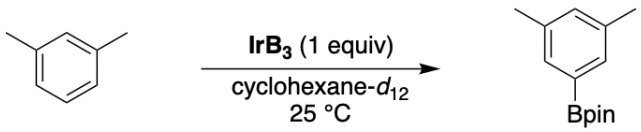

(1 equiv) 0%

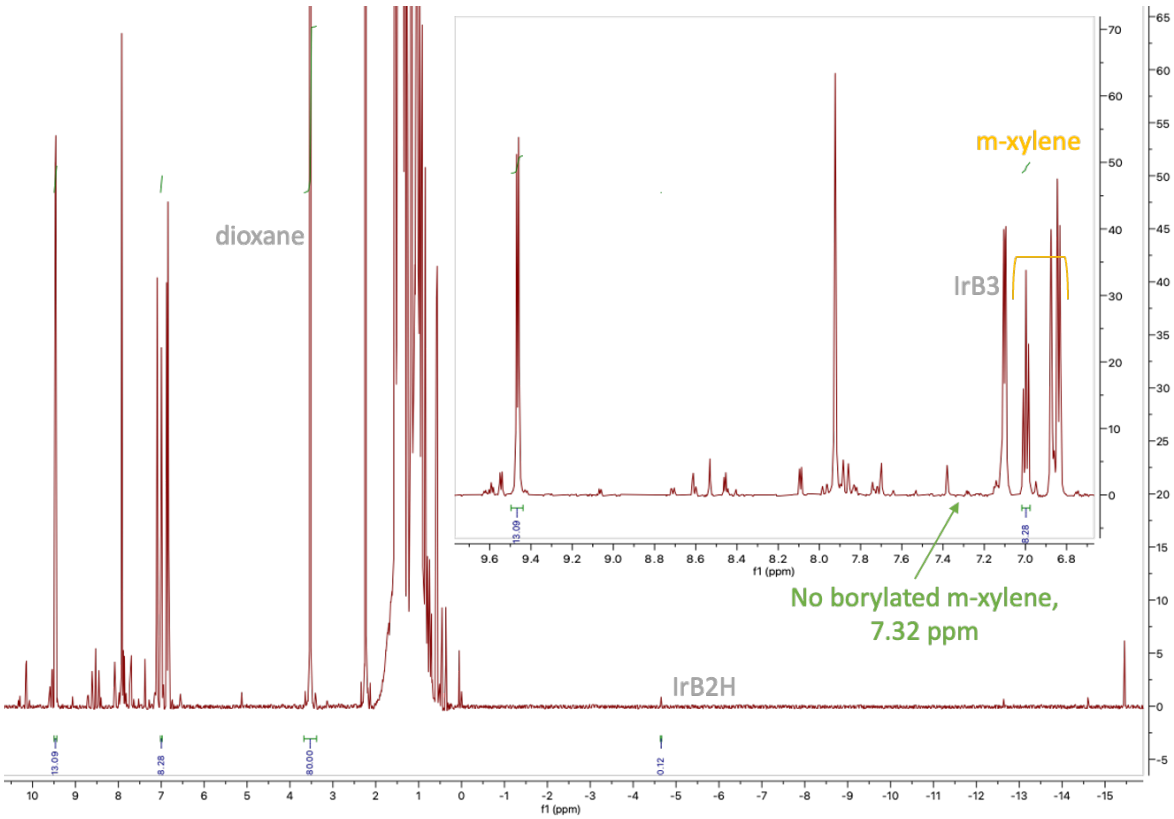

^{1}H-NMR

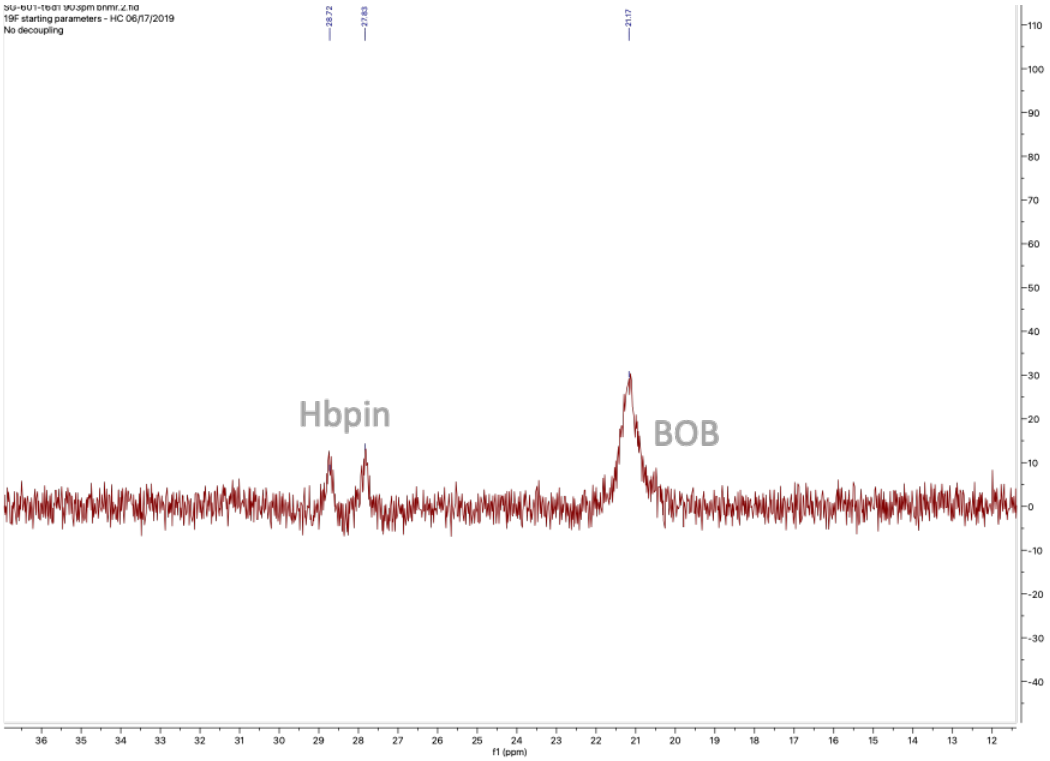

^{11}B-NMR

[2-methylheptan-3-one]

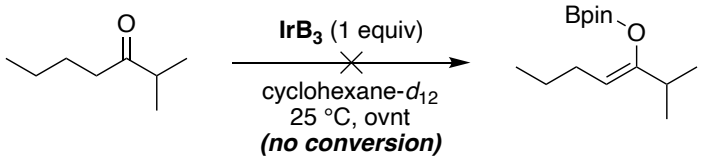

(1 equiv)

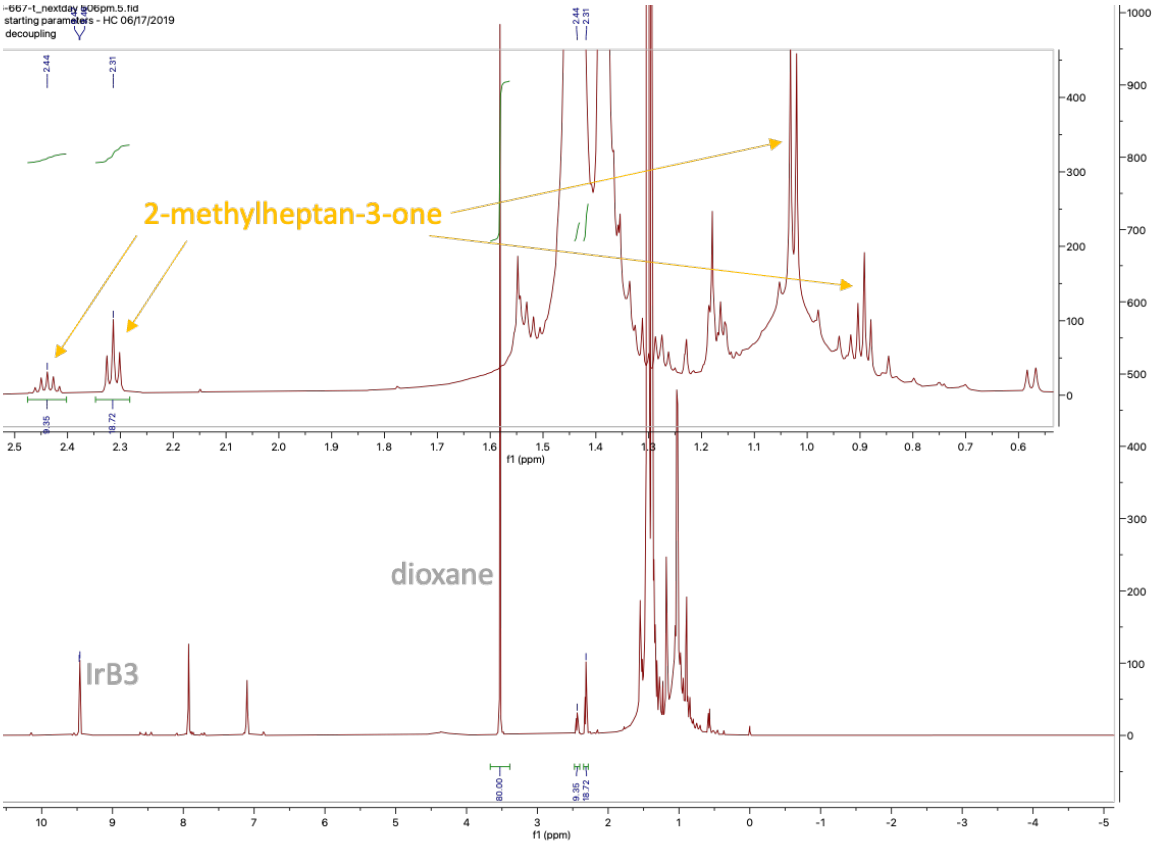

^{1}H-NMR

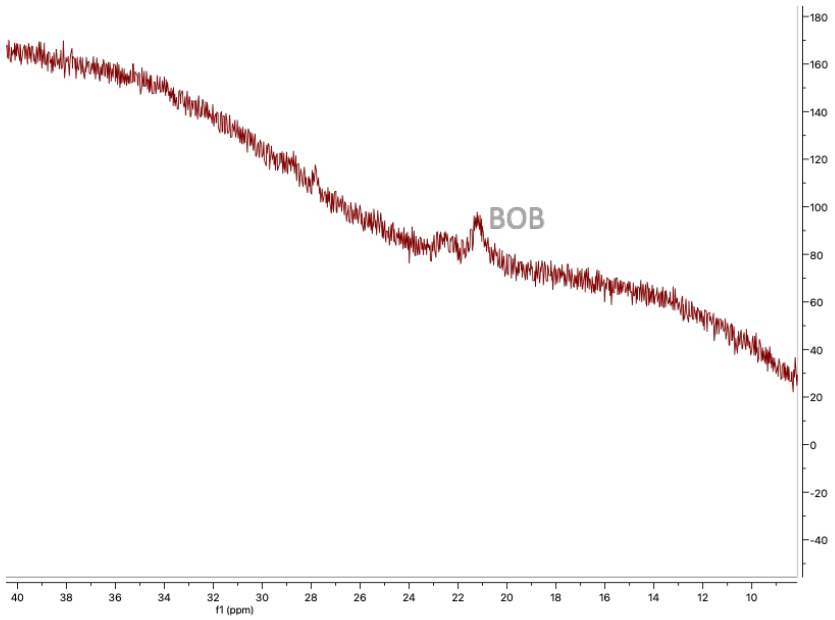

^{11}B-NMR

Note: The miniature peak around 22 ppm does not correspond to the O—borylated compound which would also show a ^{1}H-NMR resonance in the vinyl region (absent)

[cyclooctanone]

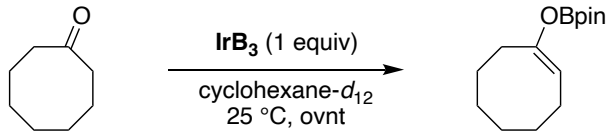

(1 equiv) 19%

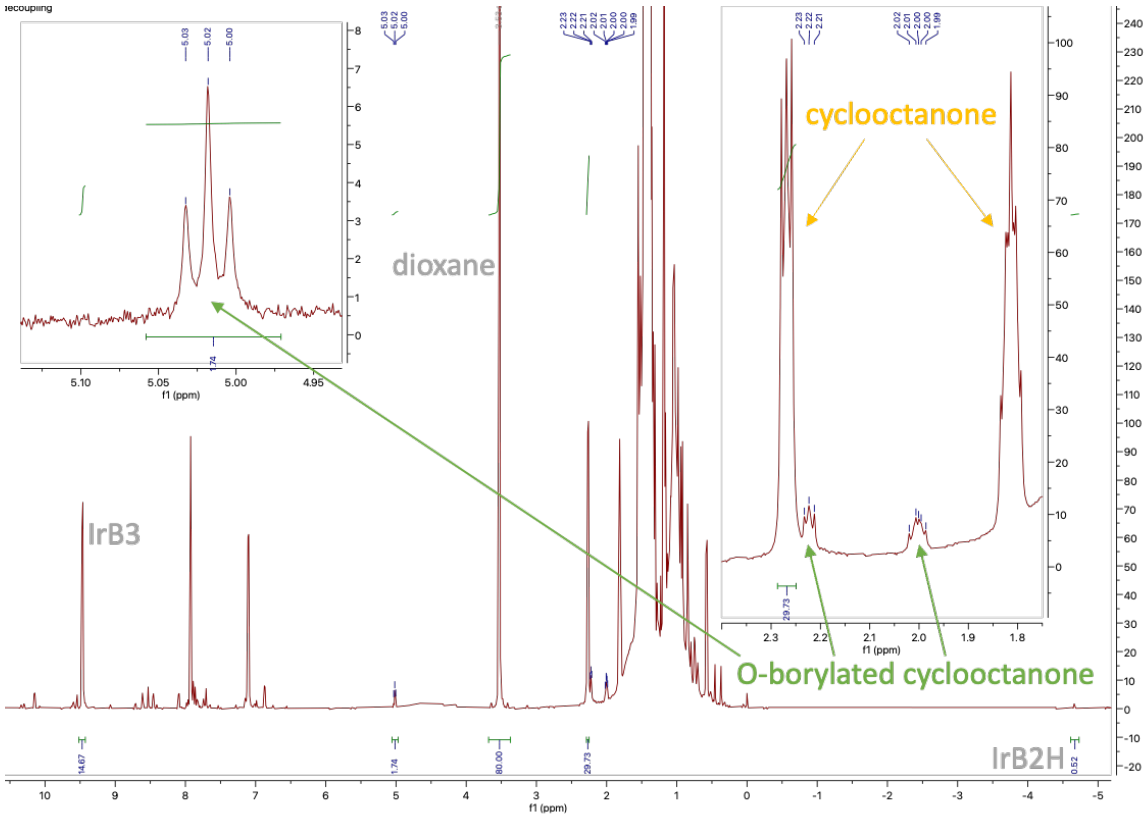

^{1}H-NMR

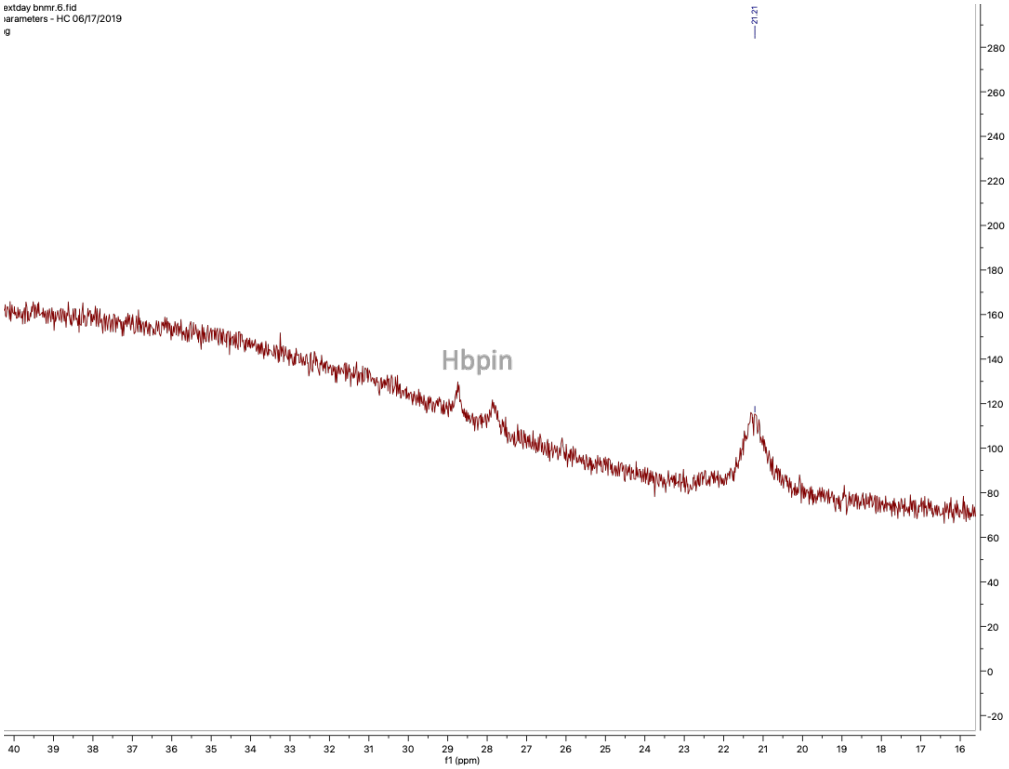

^{11}B-NMR

Note: O—borylated cyclooctanone overlaps with BOB impurity

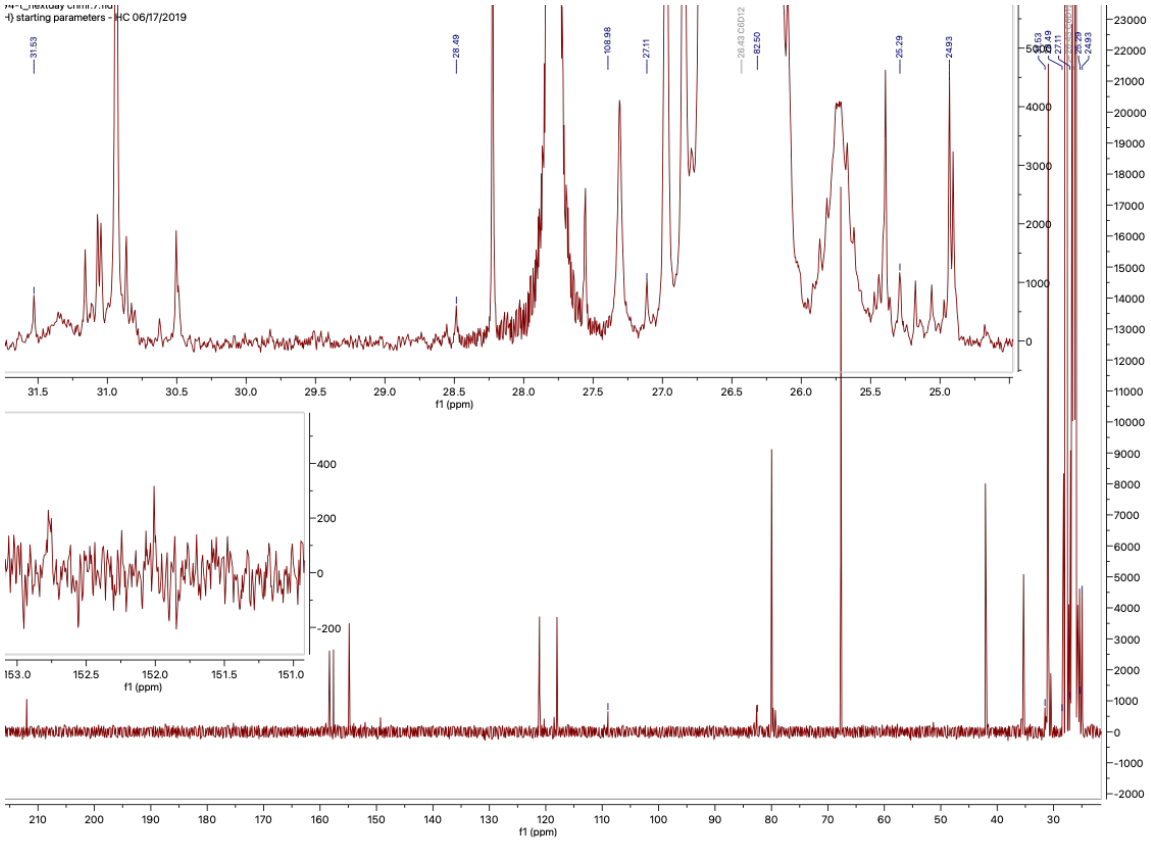

^{13}C-NMR

Note: 152.00, 30.48, 26.99 ppm peaks also present

{Subsequent heating at 100 °C for 1 hour provided a terminal yield of 32% (0% IrB_3)}

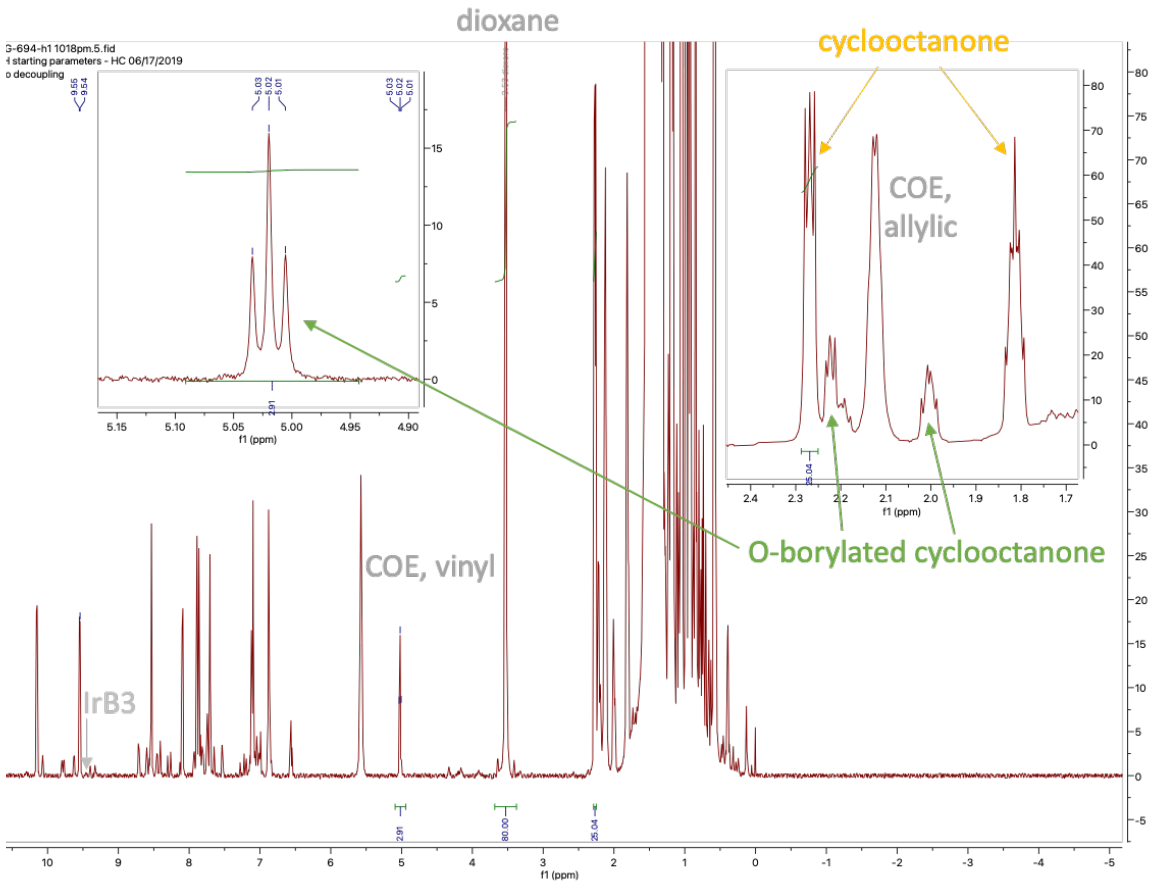

^{1}H-NMR

Note: doublet at 9.55, 9.54 ppm does not belong to (dtbpy)Ir(Bpin)$_3$ (9.47, 9.46 ppm)

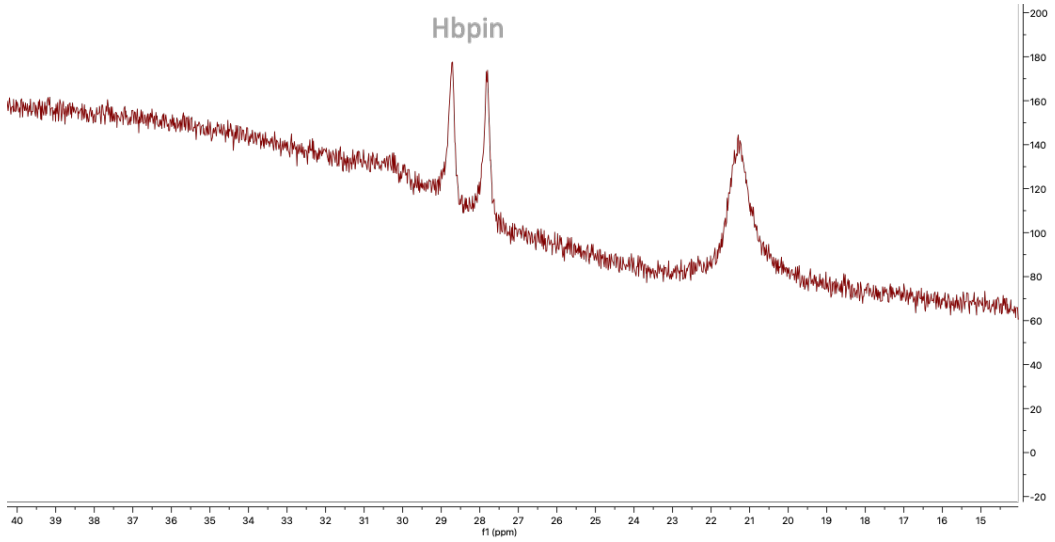

^{11}B-NMR

Note: O—borylated cyclooctanone overlaps with BOB impurity

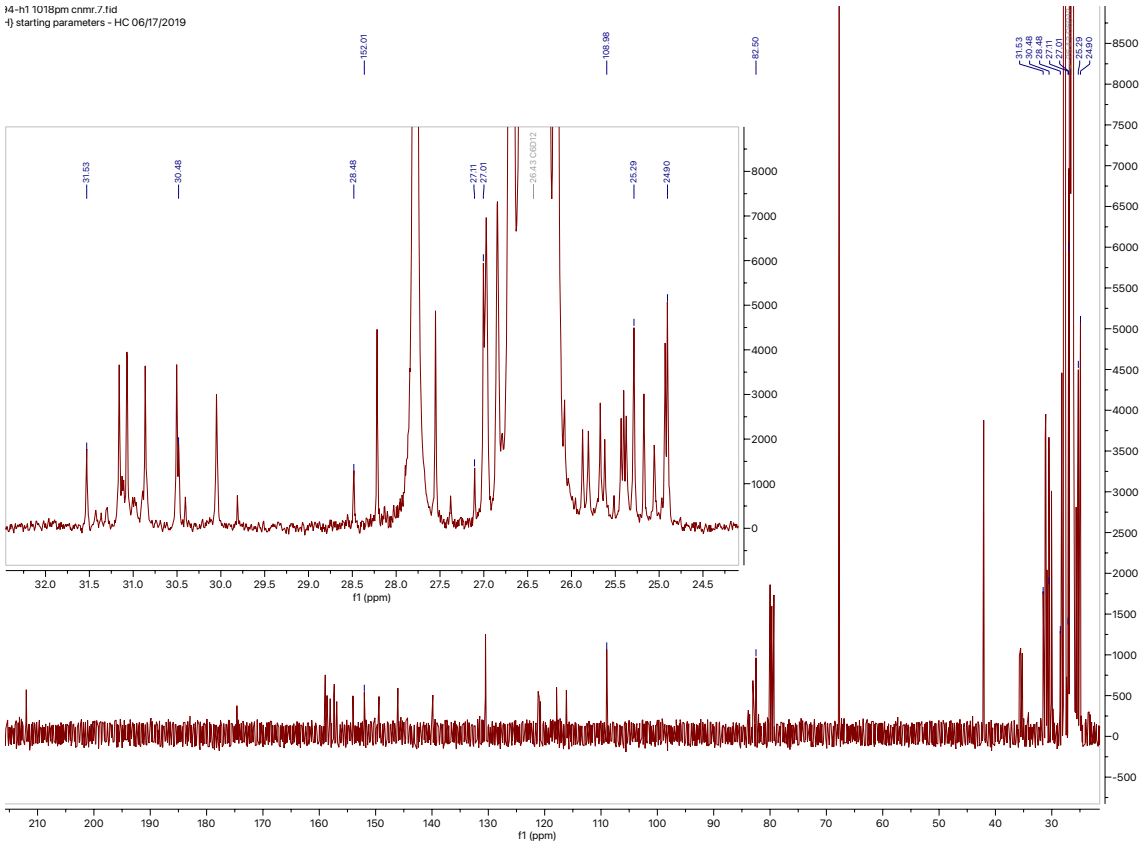

^{13}C-NMR

[methyl propionate]

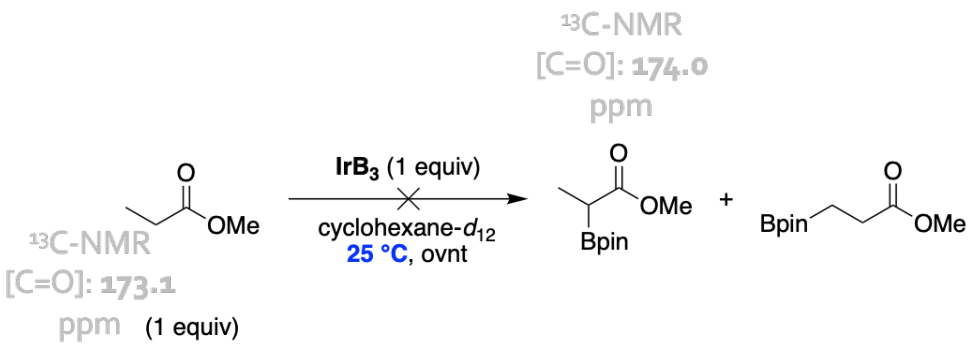

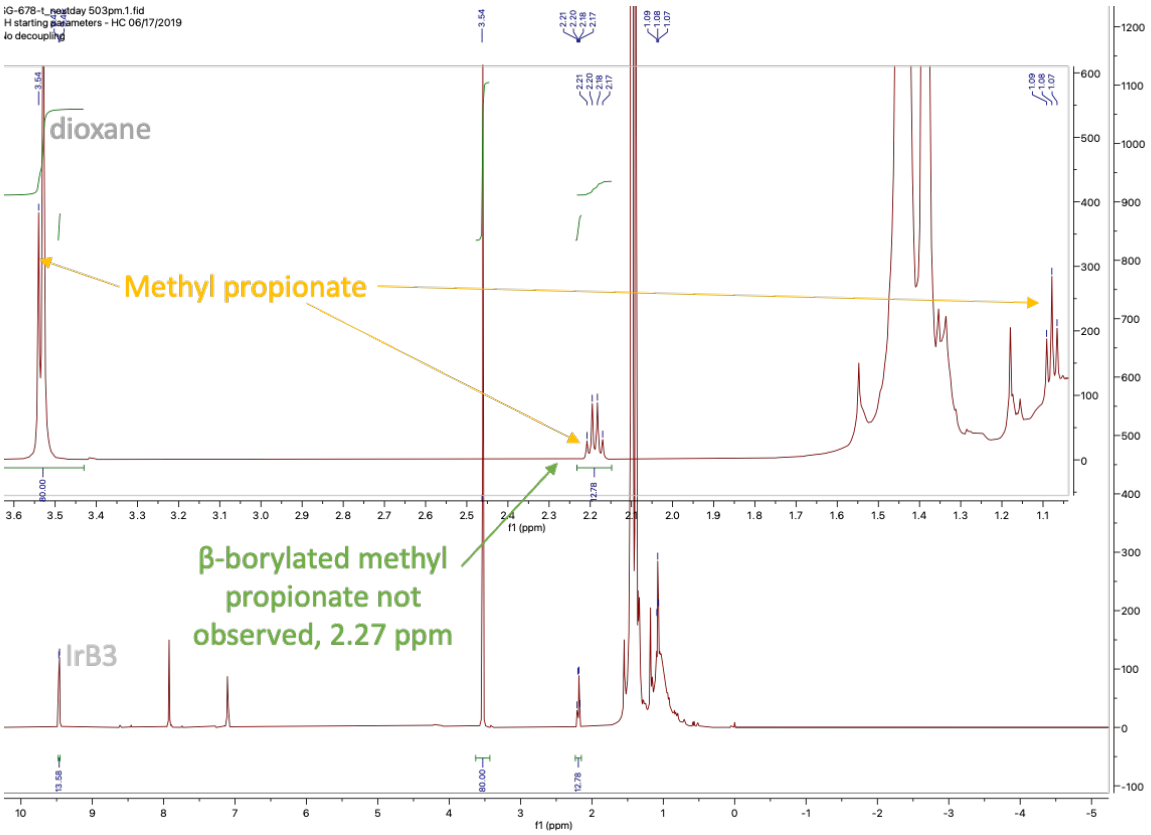

^{1}H-NMR

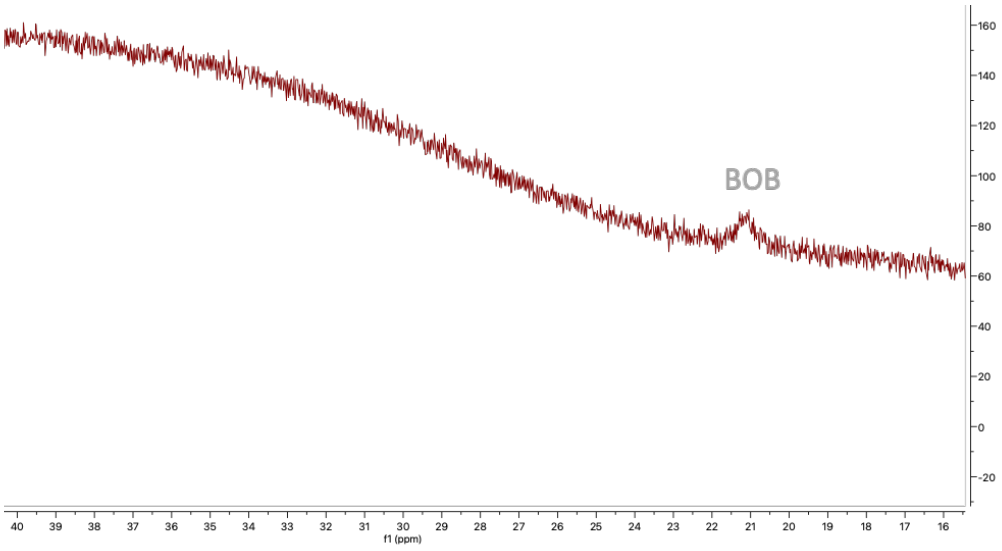

^{11}B-NMR

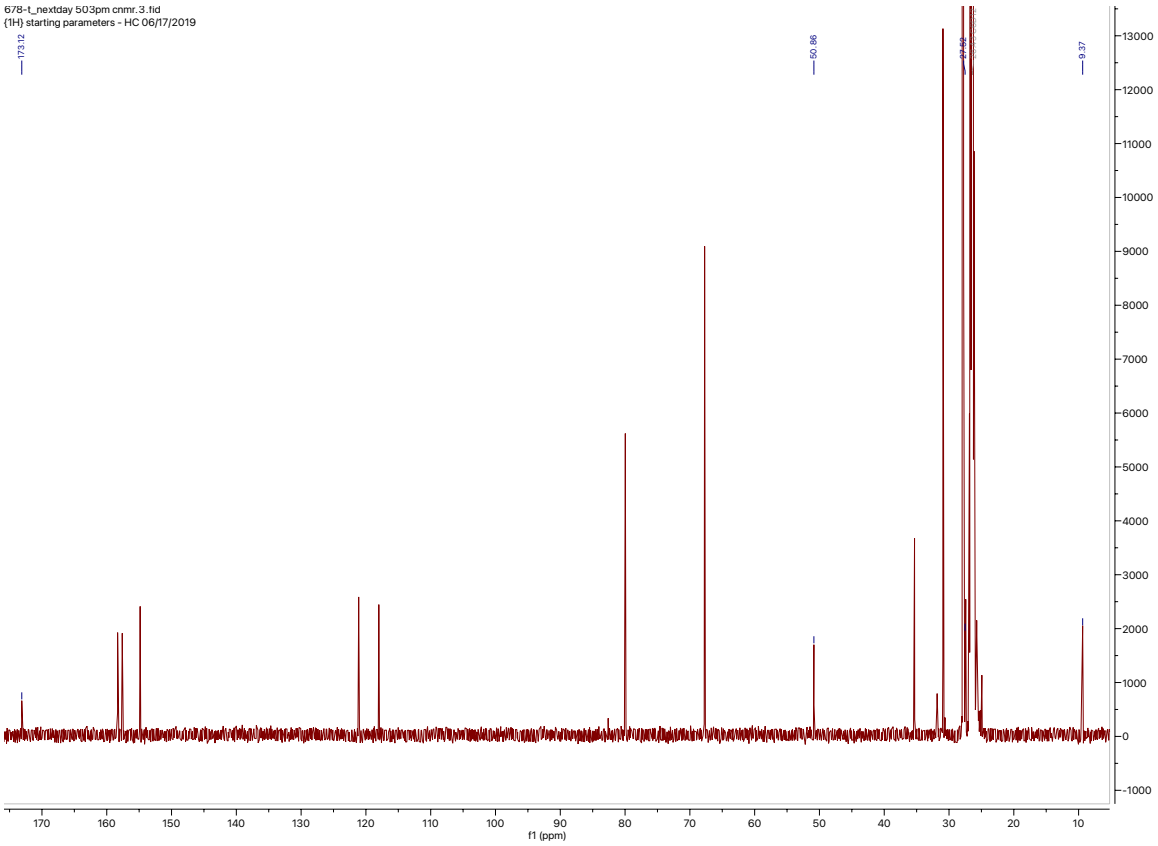

^{13}C-NMR

Note: designated peaks are for methyl propionate

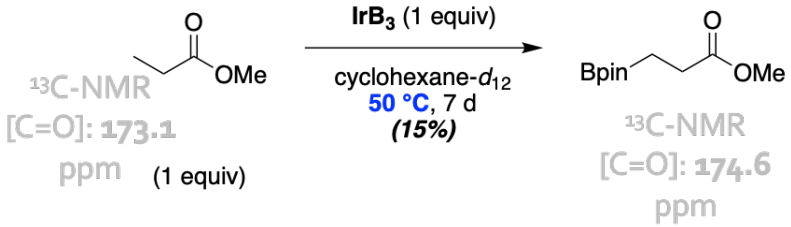

^{13}C-NMR
[C=O]: 173.1
ppm

(1 equiv)

^{13}C-NMR
[C=O]: 174.6
ppm

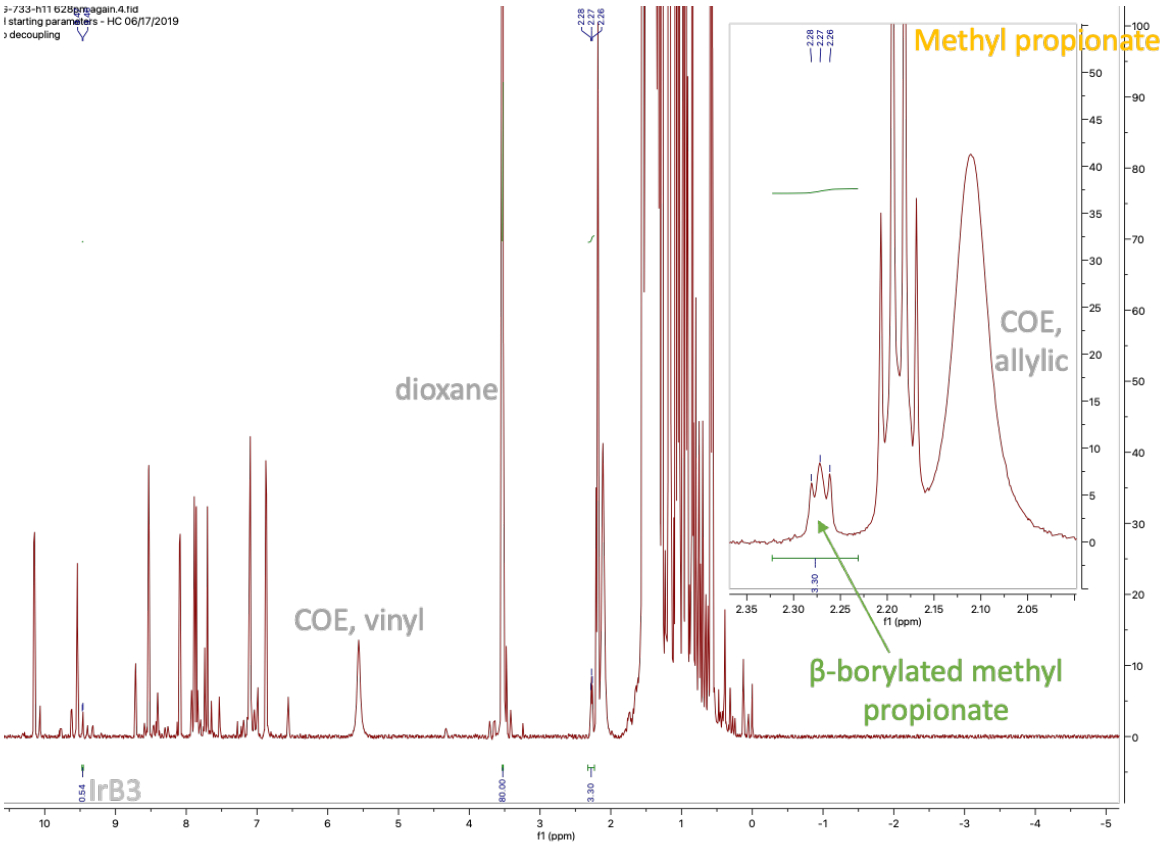

^{1}H-NMR

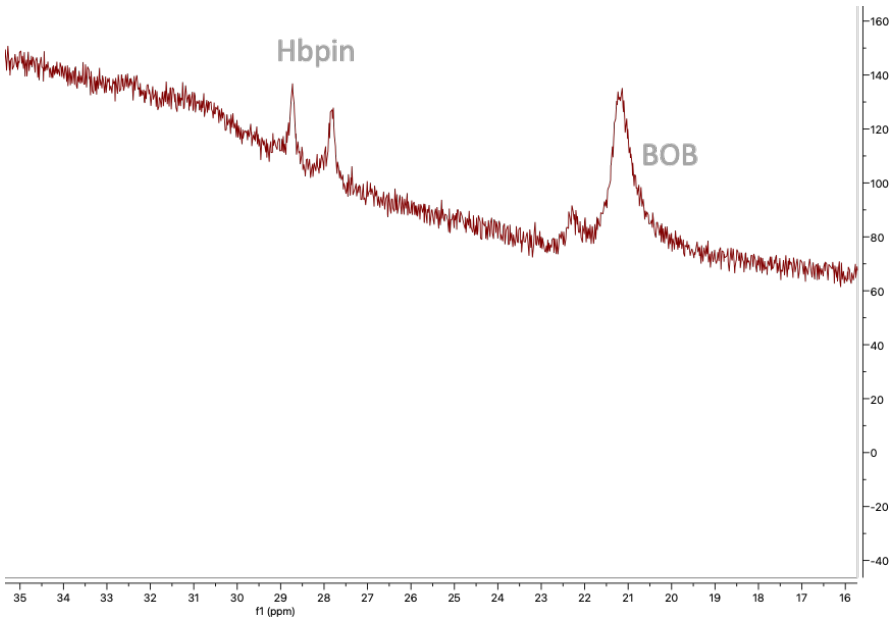

^{11}B-NMR

Note: The C—borylated compound is of too small conversion to give an appreciable peak in ^{11}B-NMR. It is also not reported in: JACS (2017), 139(8), 3153-3160. The miniature peak around 22 ppm does not correspond to the O—borylated compound which would also show a ^{1}H-NMR resonance in the vinyl region (absent).

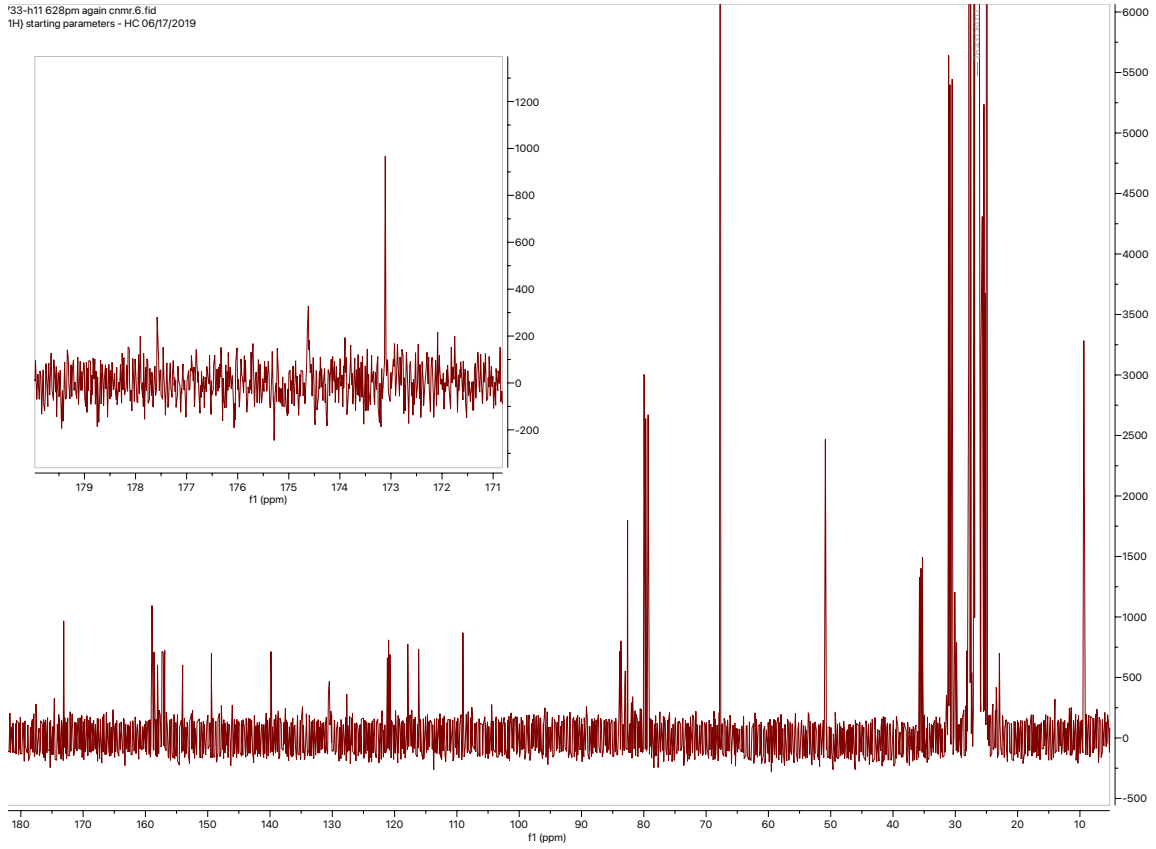

^{13}C-NMR

Note: beta-borylated compound exists in too small yield to be able to be well observed by ^{13}C-NMR spectroscopy. However, the diagnostic carbonyl C at 174.6 ppm is present and is matched by literature precedence: JACS (2017), 139(8), 3153-3160 [which does not observe **C**—Bpin]

[N,N-dimethylpropionamide]

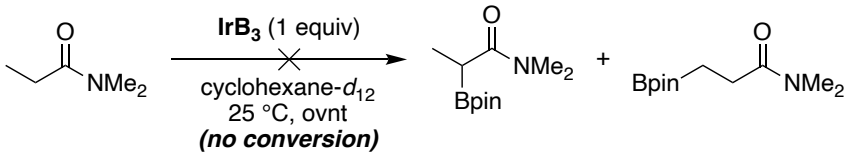

(1 equiv)

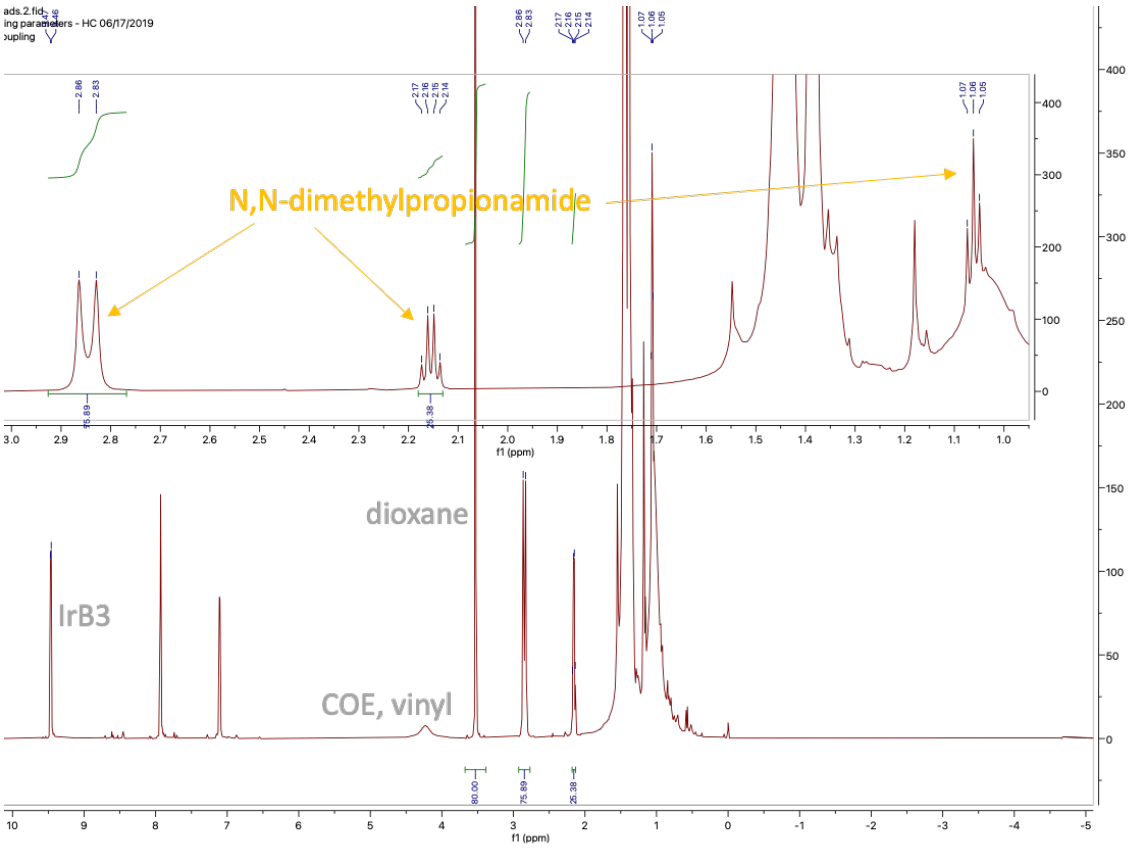

^{1}H-NMR

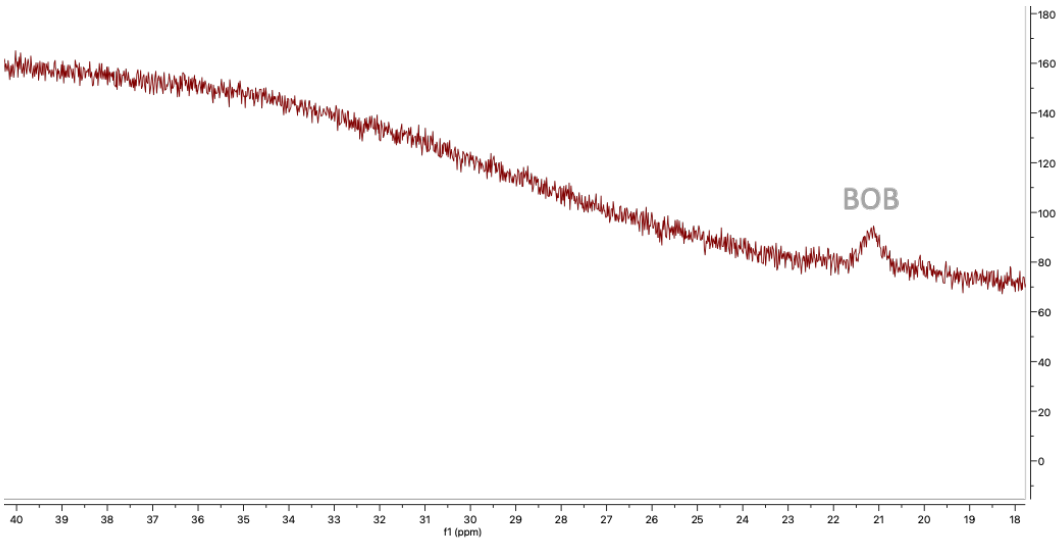

^{11}B-NMR

[bromocyclopropane]

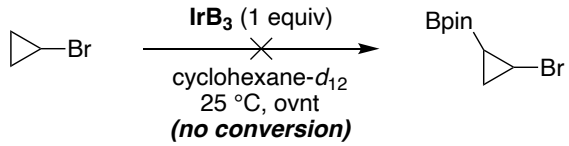

(1 equiv)

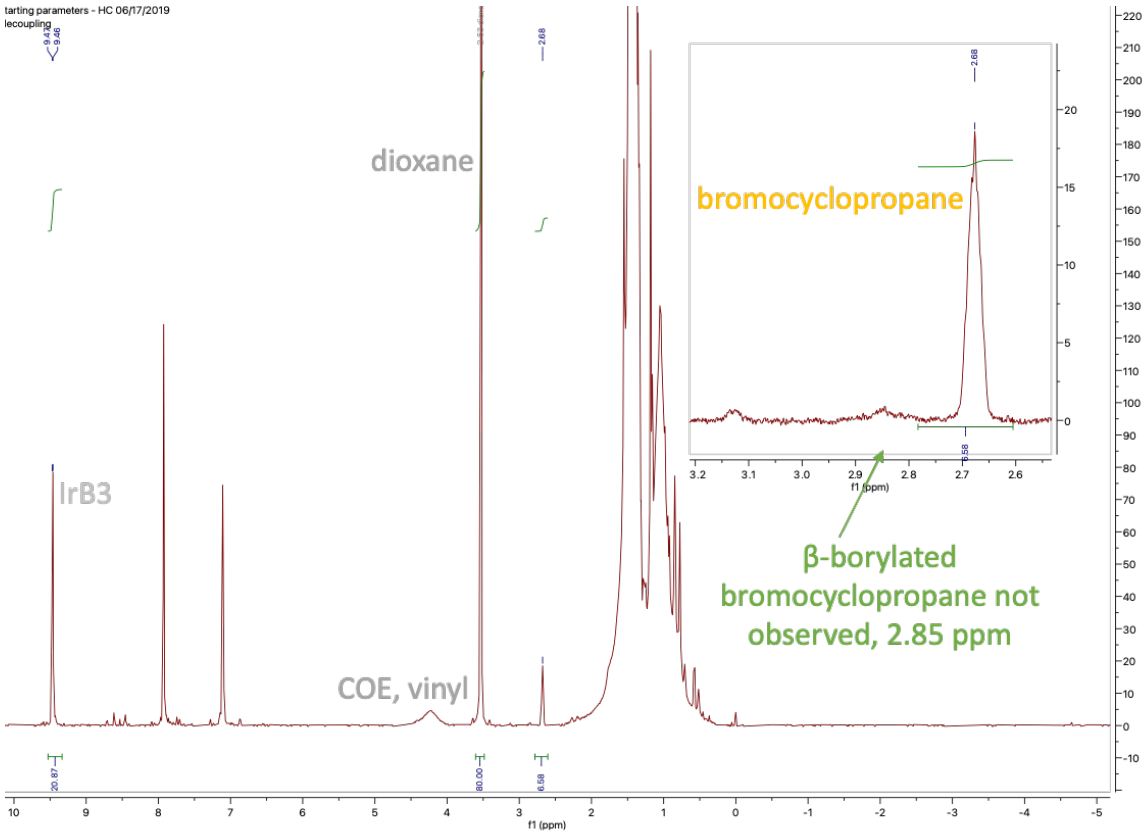

^{1}H-NMR

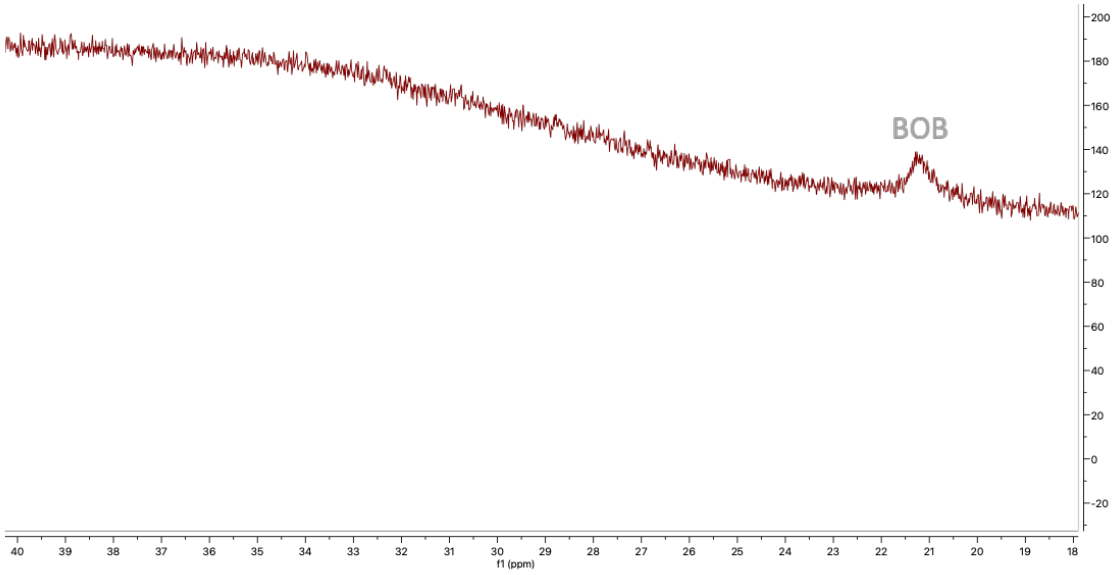

^{11}B-NMR

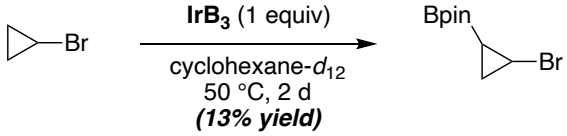

(1 equiv)

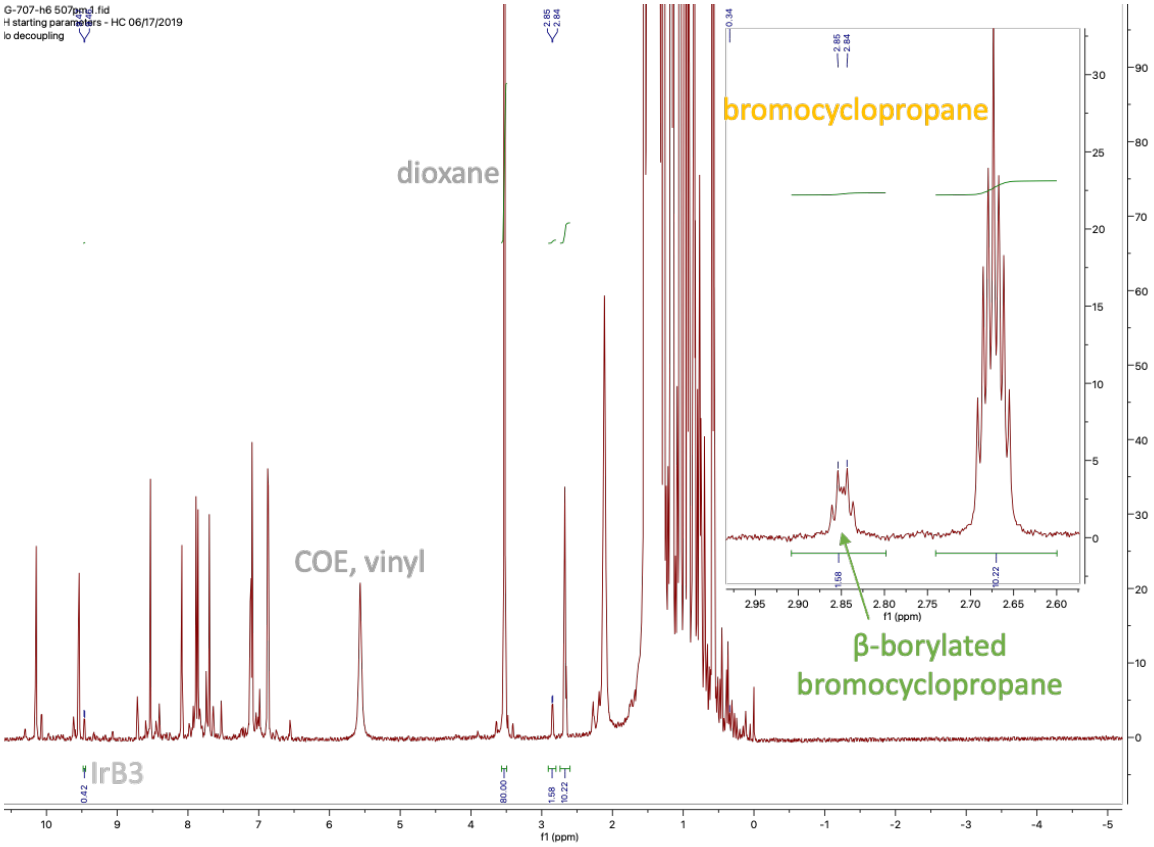

^{1}H-NMR

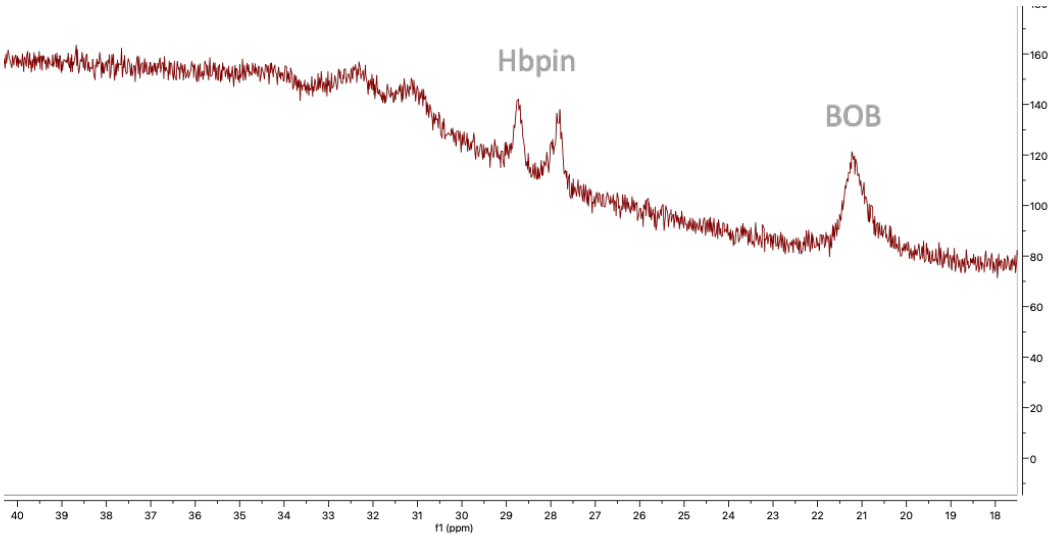

^{11}B-NMR

[1-bromopropane]

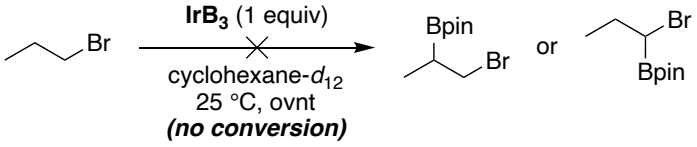

(1 equiv)

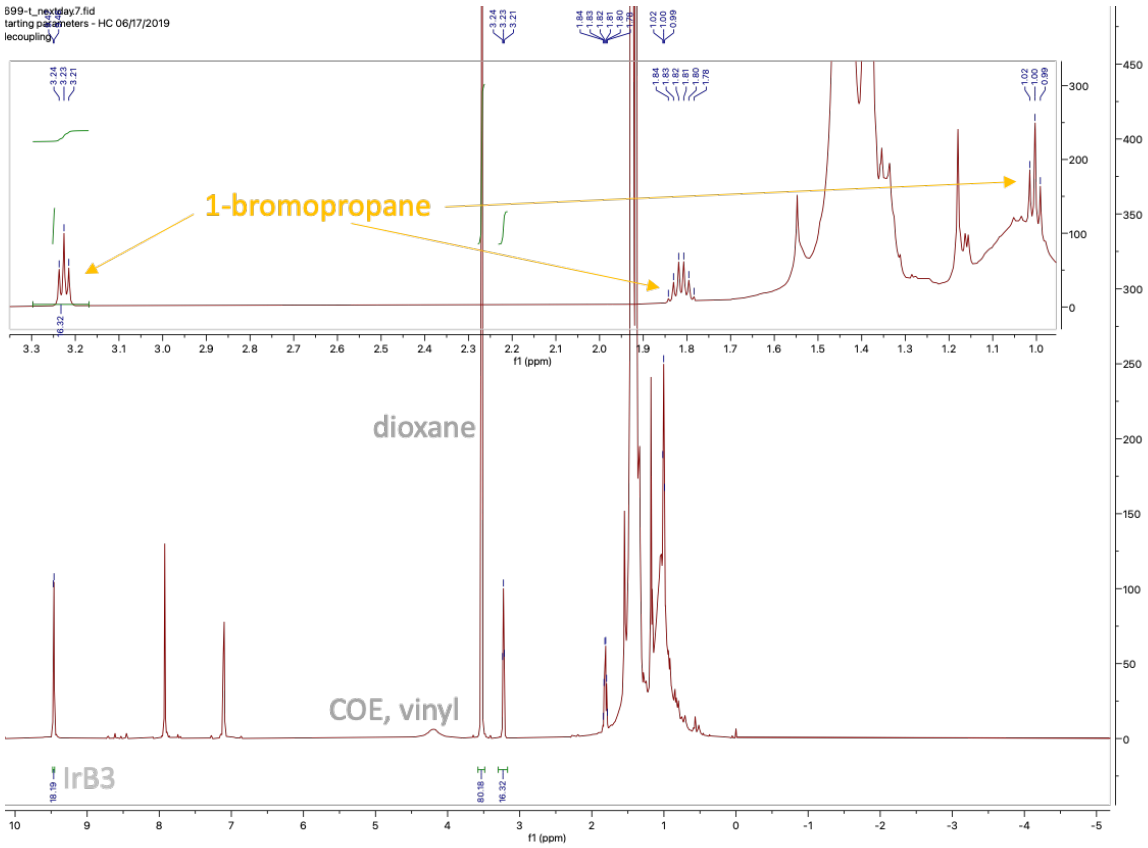

^{1}H-NMR

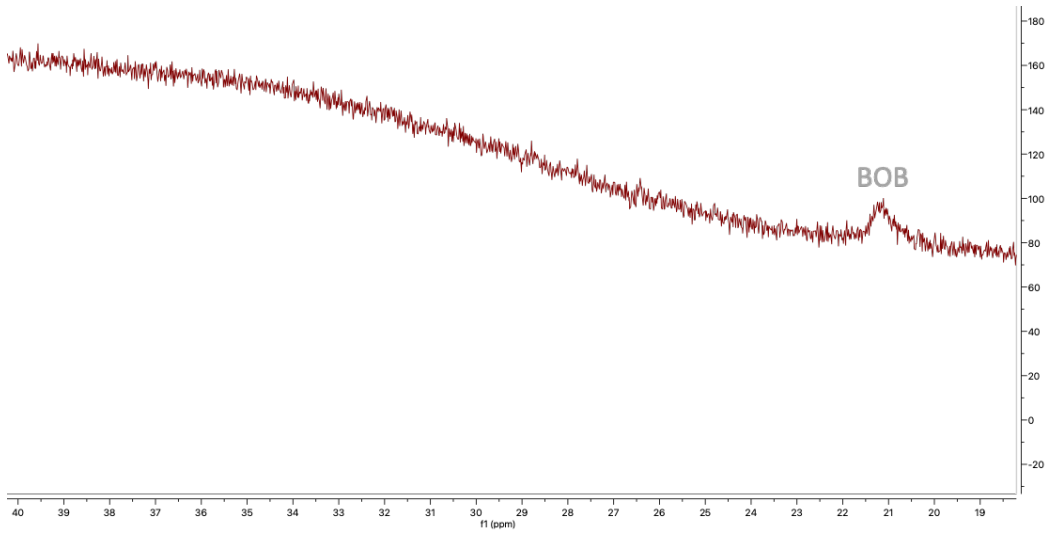

^{11}B-NMR

{Subsequent heating at 100 °C for 1 hour provided a terminal yield of 0% (9% IrB_3)}

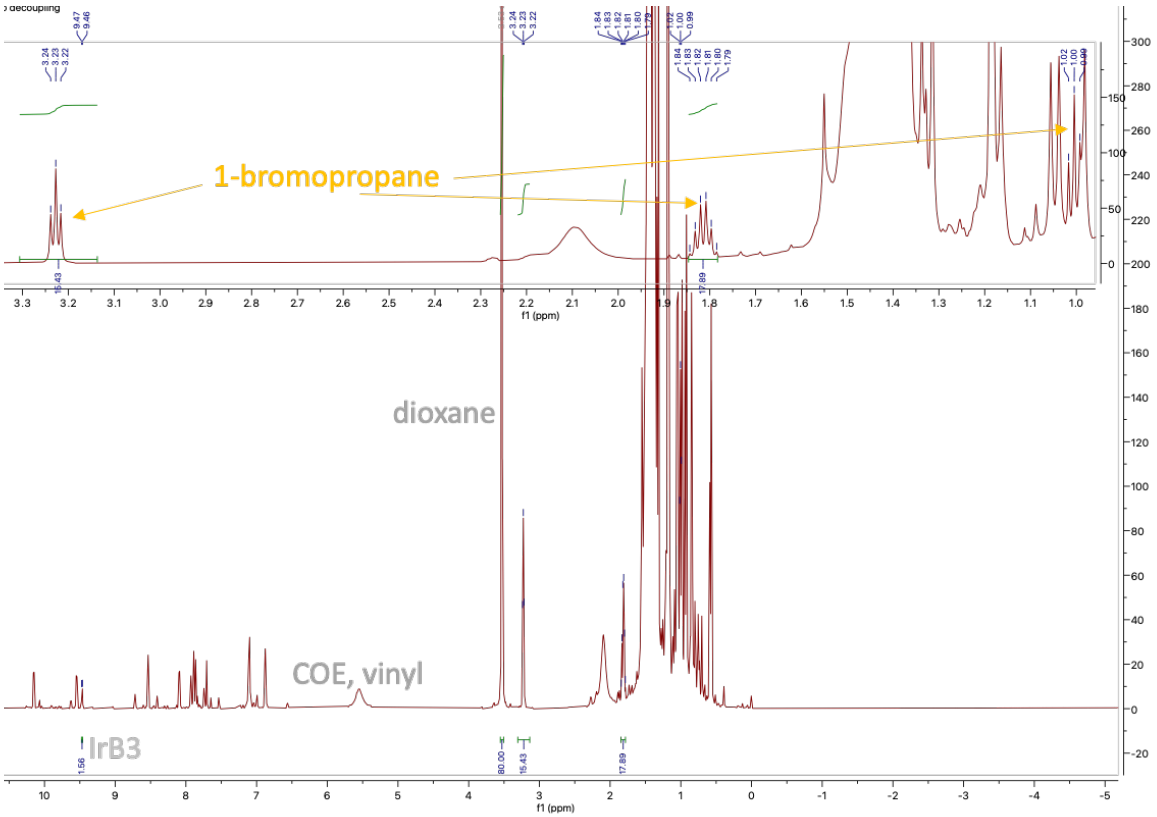

^{1}H-NMR

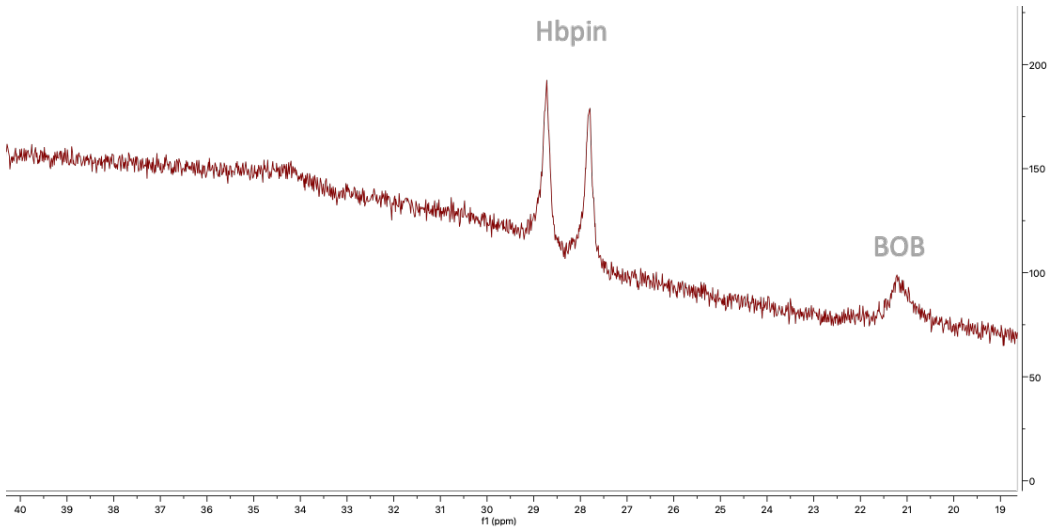

^{11}B-NMR

[phenylacetylene]

Note: in the case of phenylacetylene, NMR spectra of t_5 min (first/initial) are provided

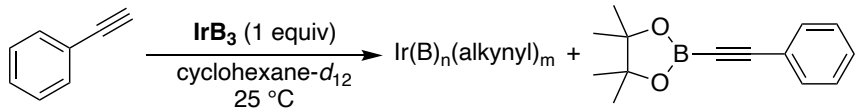

(1 equiv) major, 54% minor, 21% 11%

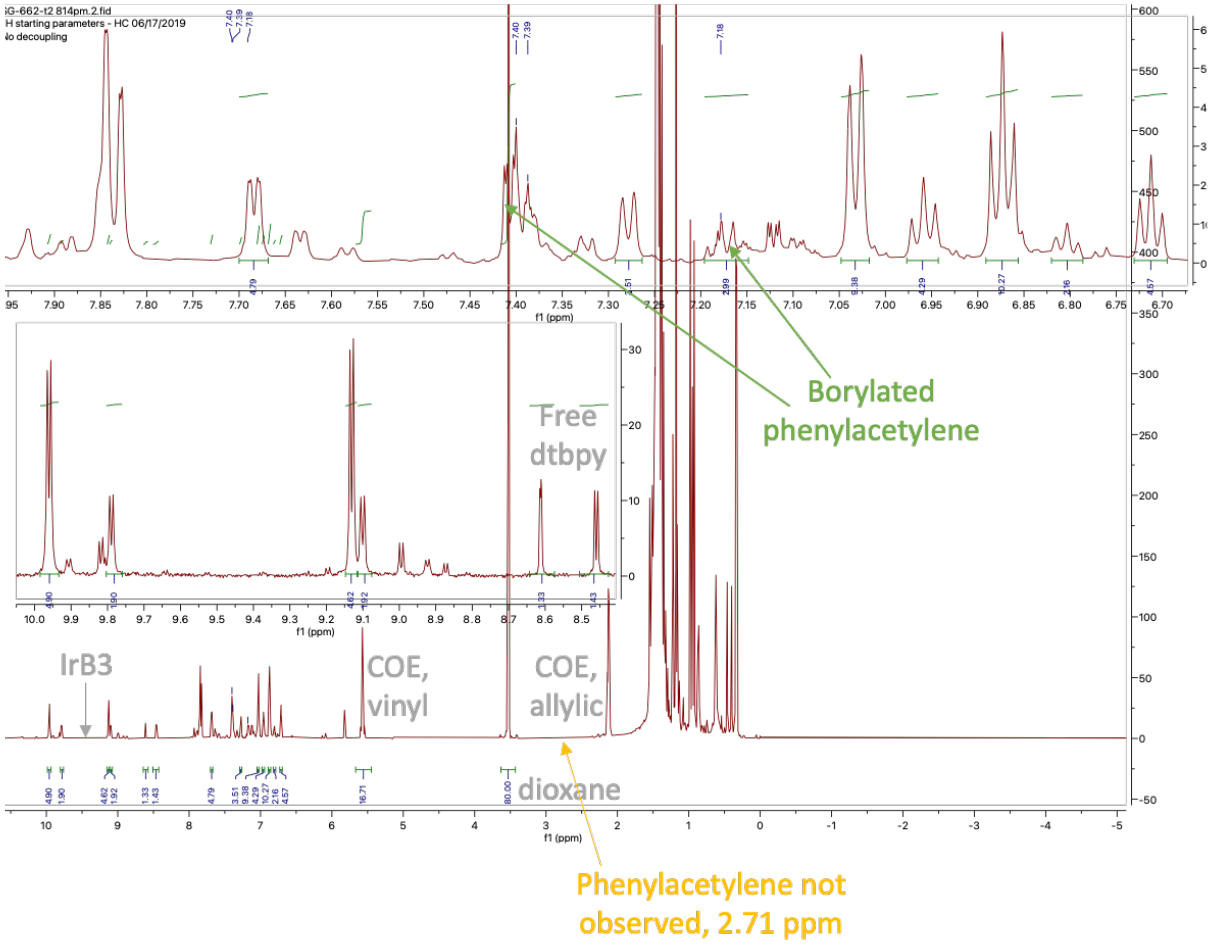

^{1}H-NMR

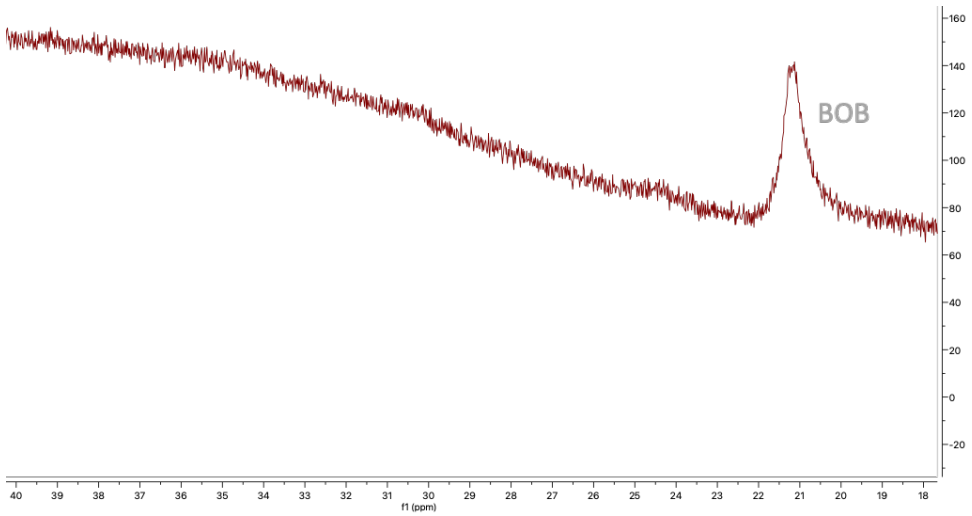

^{11}B-NMR

Note: authentic standard of borylated phenylacetylene shows an ^{11}B-NMR peak at 24.33 ppm which, although faint, can be observed in this spectrum of 11% yield

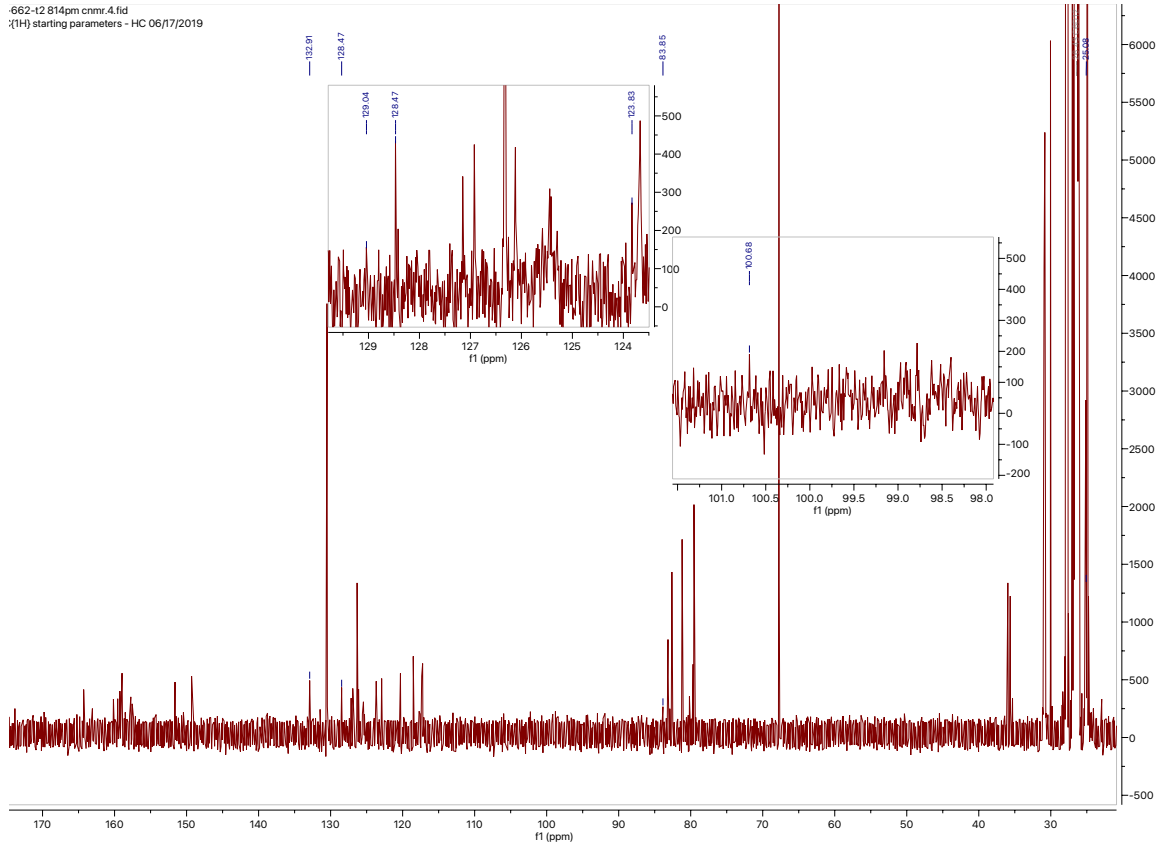

^{13}C-NMR

Note: the low 11% yield of borylated phenylacetylene makes select carbon peaks challenging to observe including that of **C**—Bpin (82.66 ppm). However, most of the carbon peaks can be observed and well match that of the authentic standard

Ambident Reactivity

[dithiane]

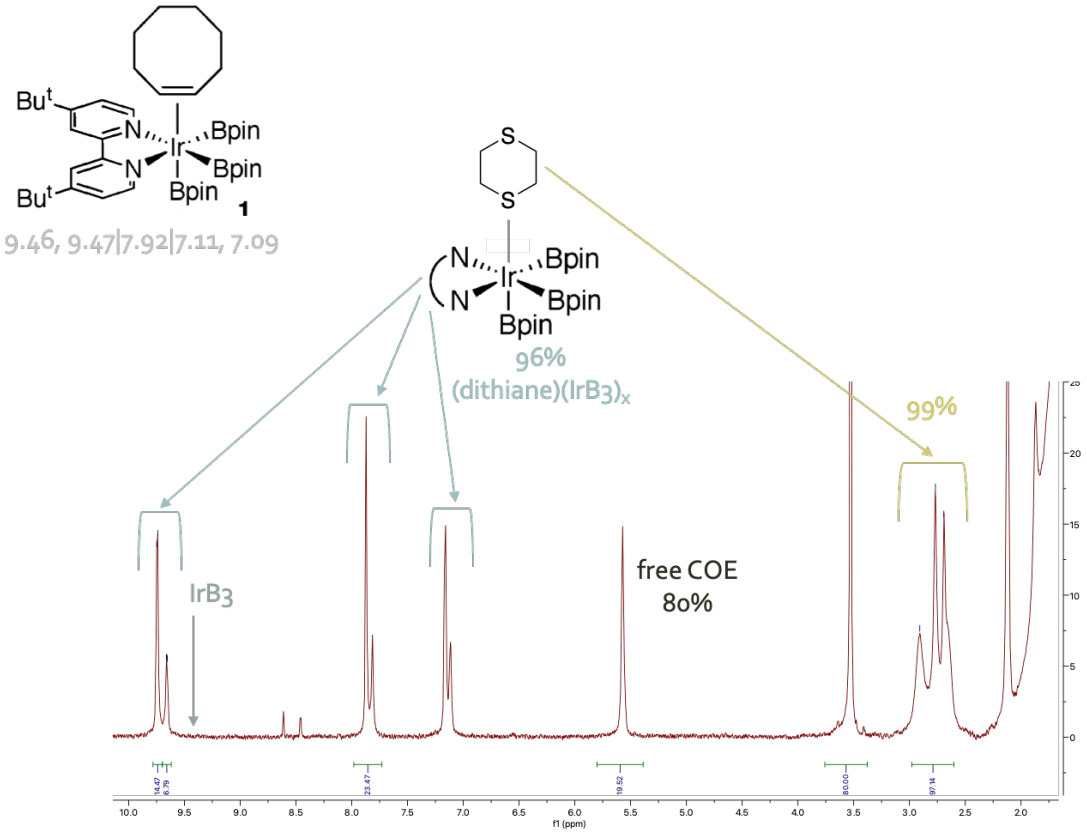

1:1 dithiane:IrB3 → **(dithiane)IrB3** [major] & (dithiane)$(IrB_3)_2$ [minor]

t_24 h

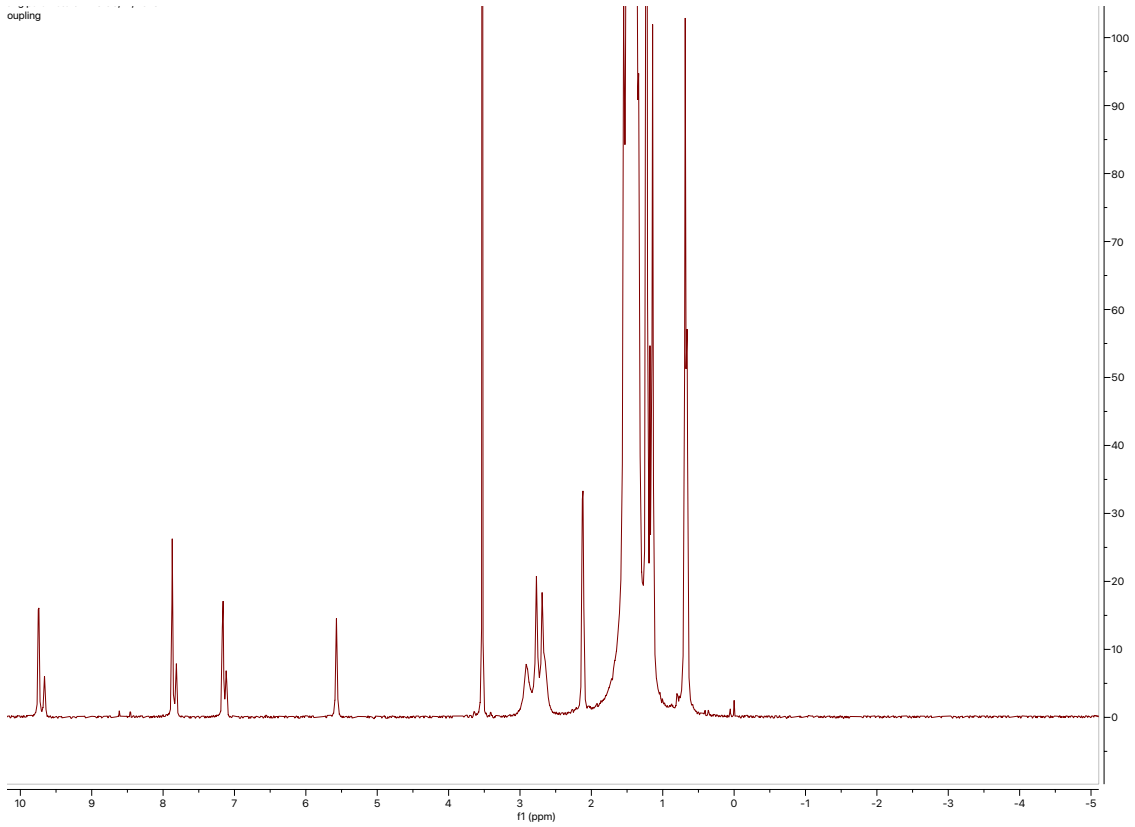

^{1}H-NMR (t_5 min)

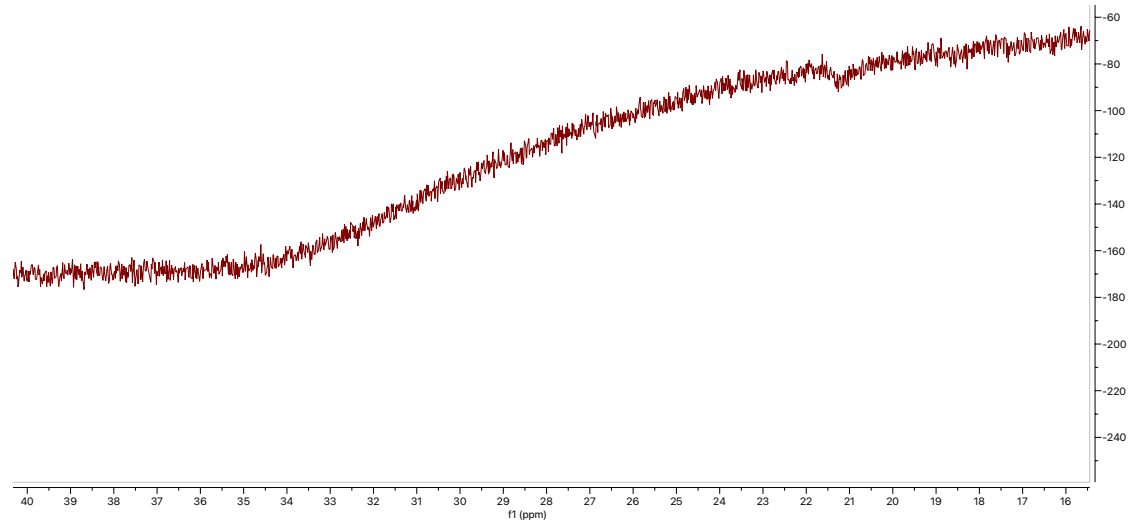

^{11}B-NMR (t_5 min)

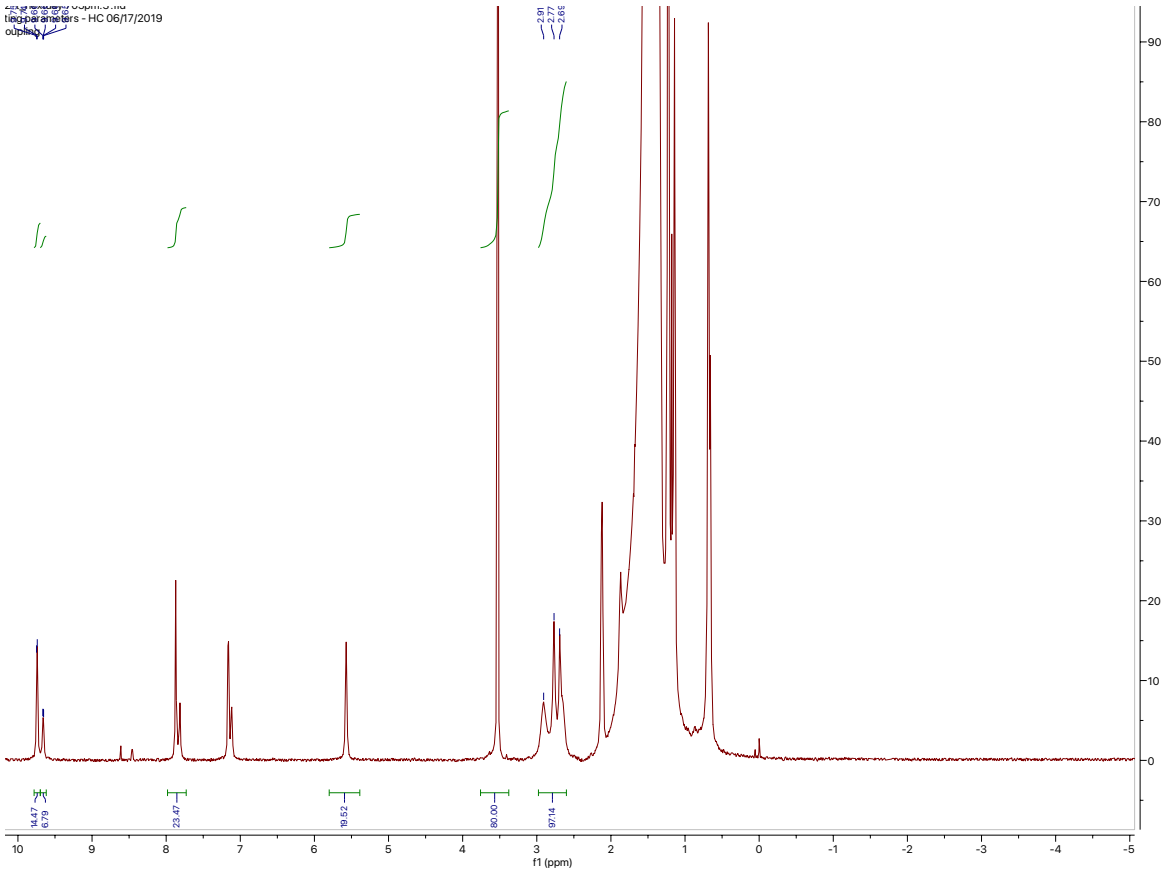

^{1}H-NMR (t_24 h)

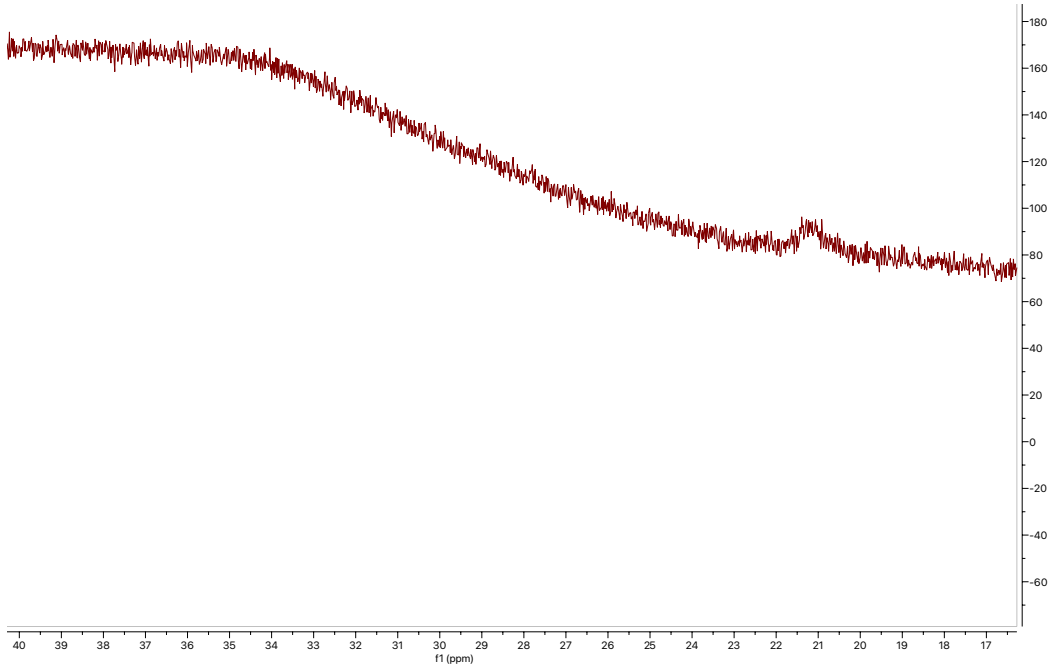

^{11}B-NMR (t_24 h)

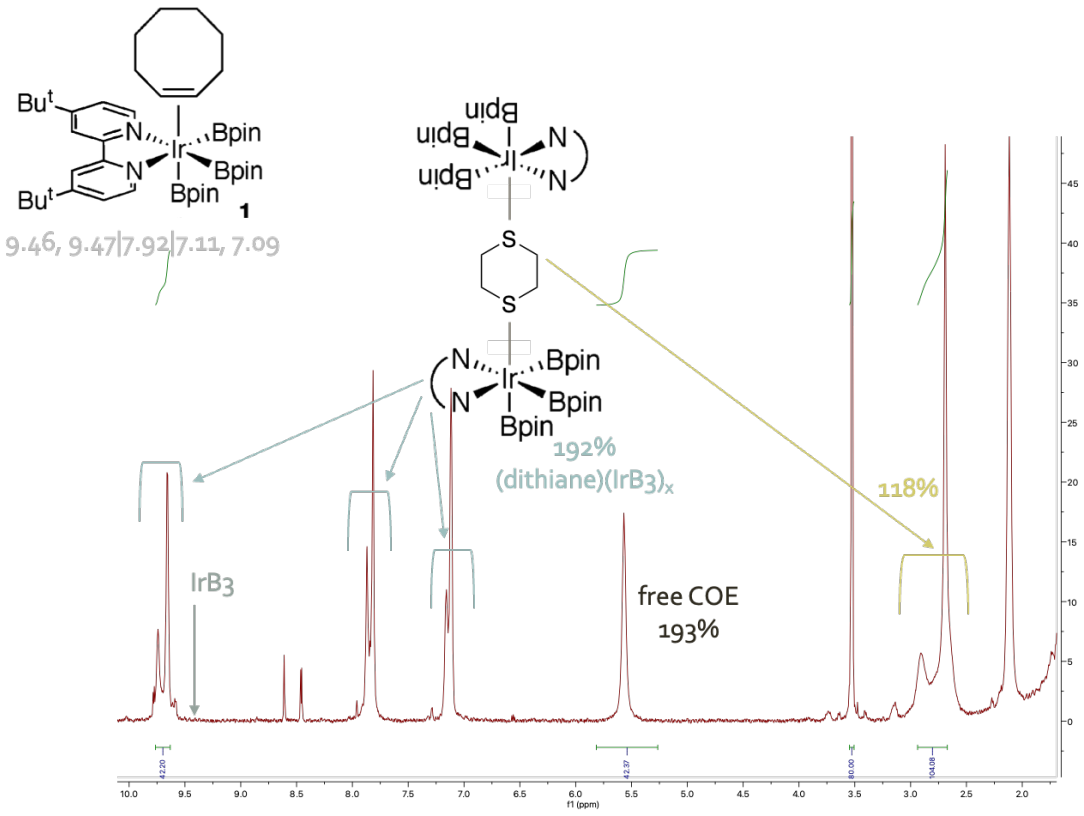

1:2 dithiane:IrB3 → (dithiane)IrB3 [minor] & **(dithiane)(IrB3)$_2$** [major]

t_5 min

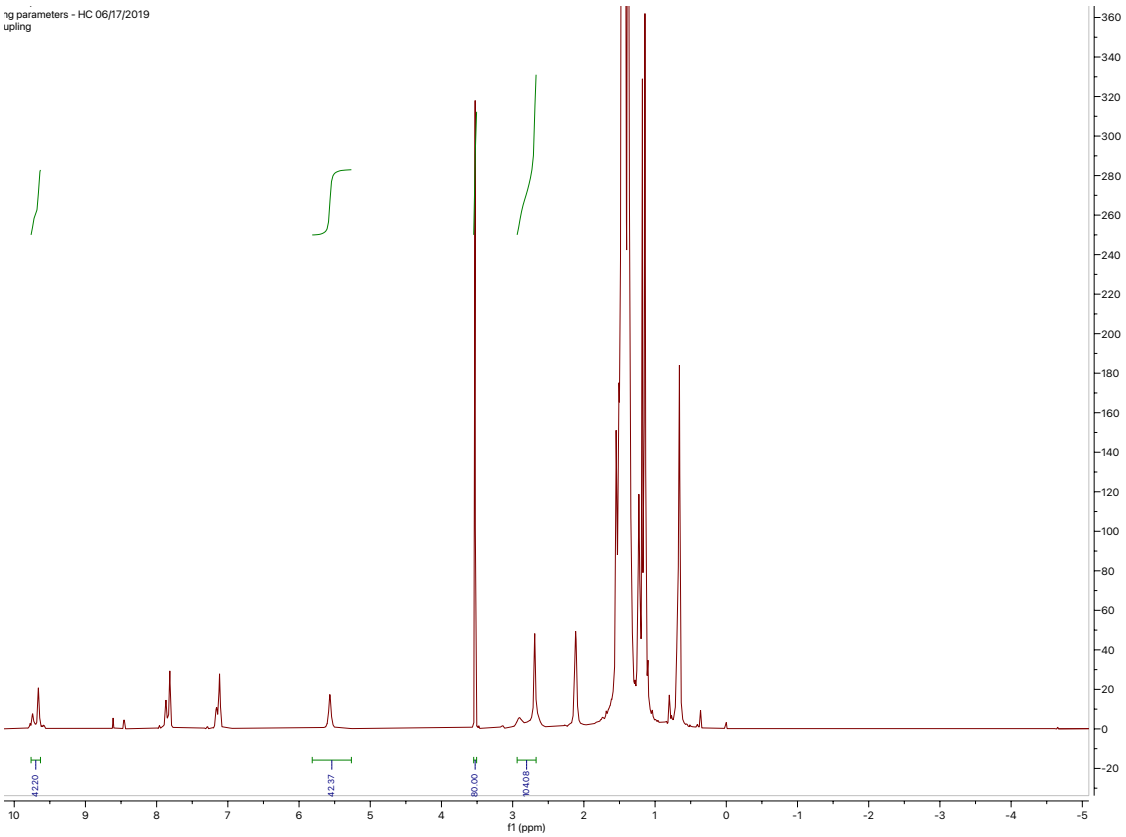

^{1}H-NMR (t_5 min)

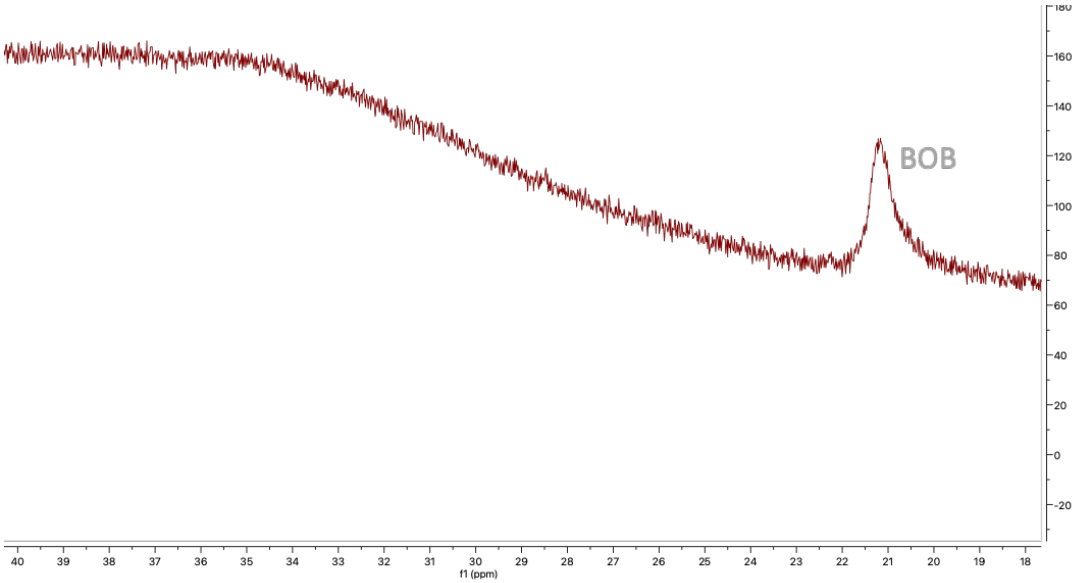

^{11}B-NMR (t_5 min)

[dihexylamine]

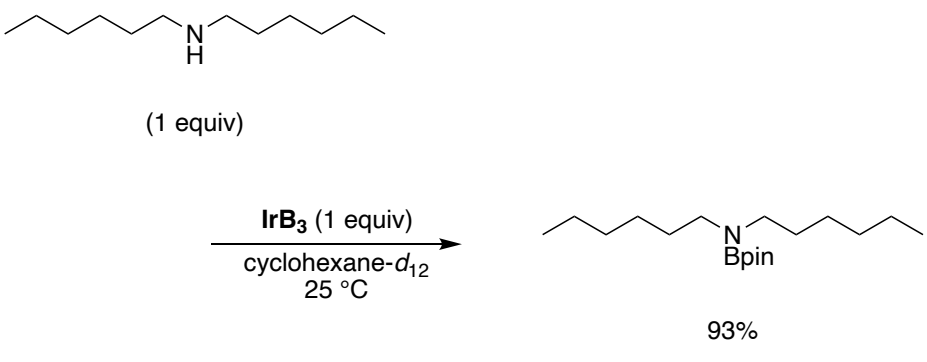
(1 equiv)
IrB3 (1 equiv)
cyclohexane-d12
25 °C
Bpin
93%

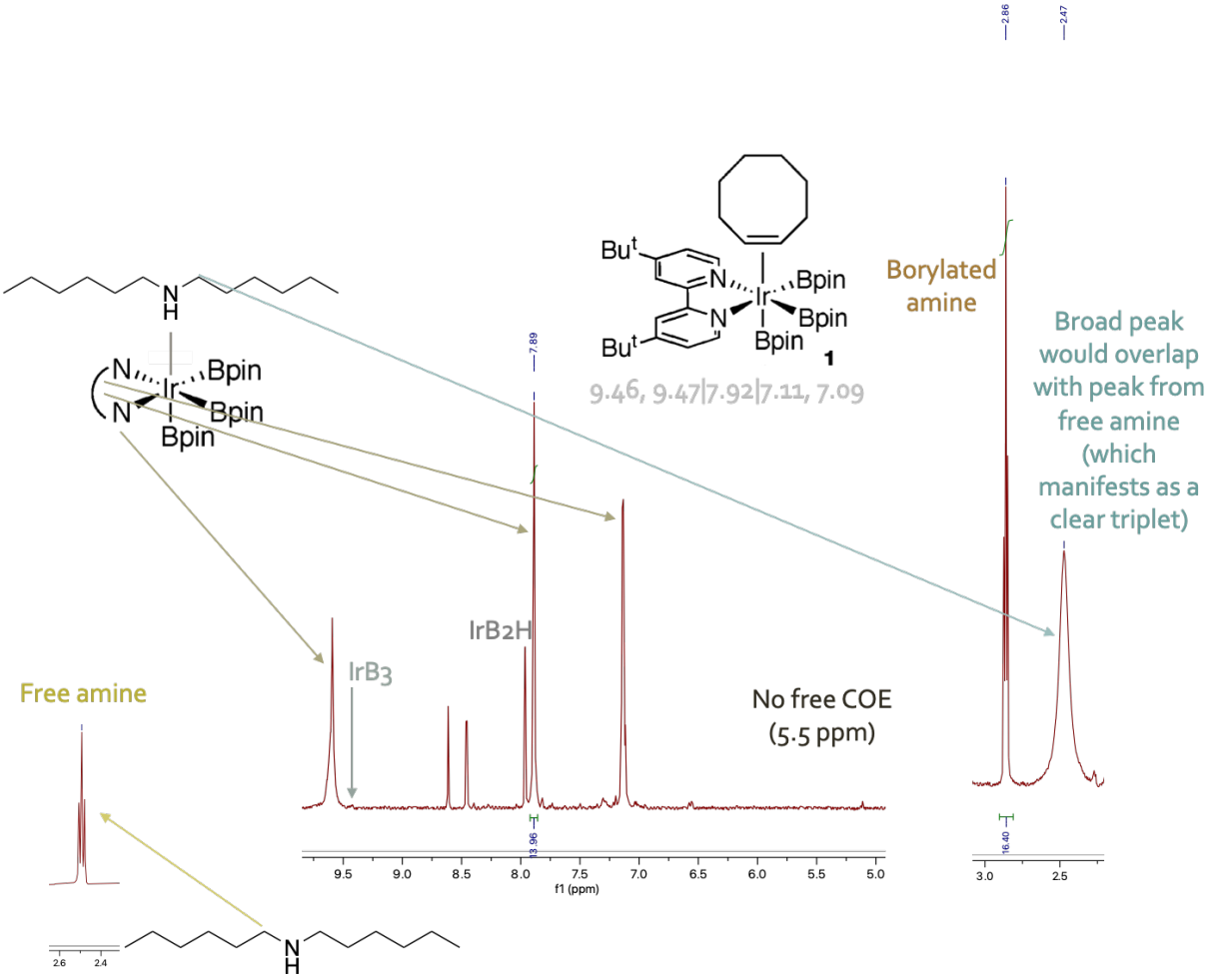
Bpin
Bpin
Bpin
Bu
Bu
Bpin
Bpin
Bpin
1
9.46, 9.47|7.92|7.11, 7.09
Borylated amine
Broad peak would overlap with peak from free amine (which manifests as a clear triplet)
IrB2H
IrB3
Free amine
No free COE (5.5 ppm)
f1 (ppm)

^{1}H-NMR (t_5 min)

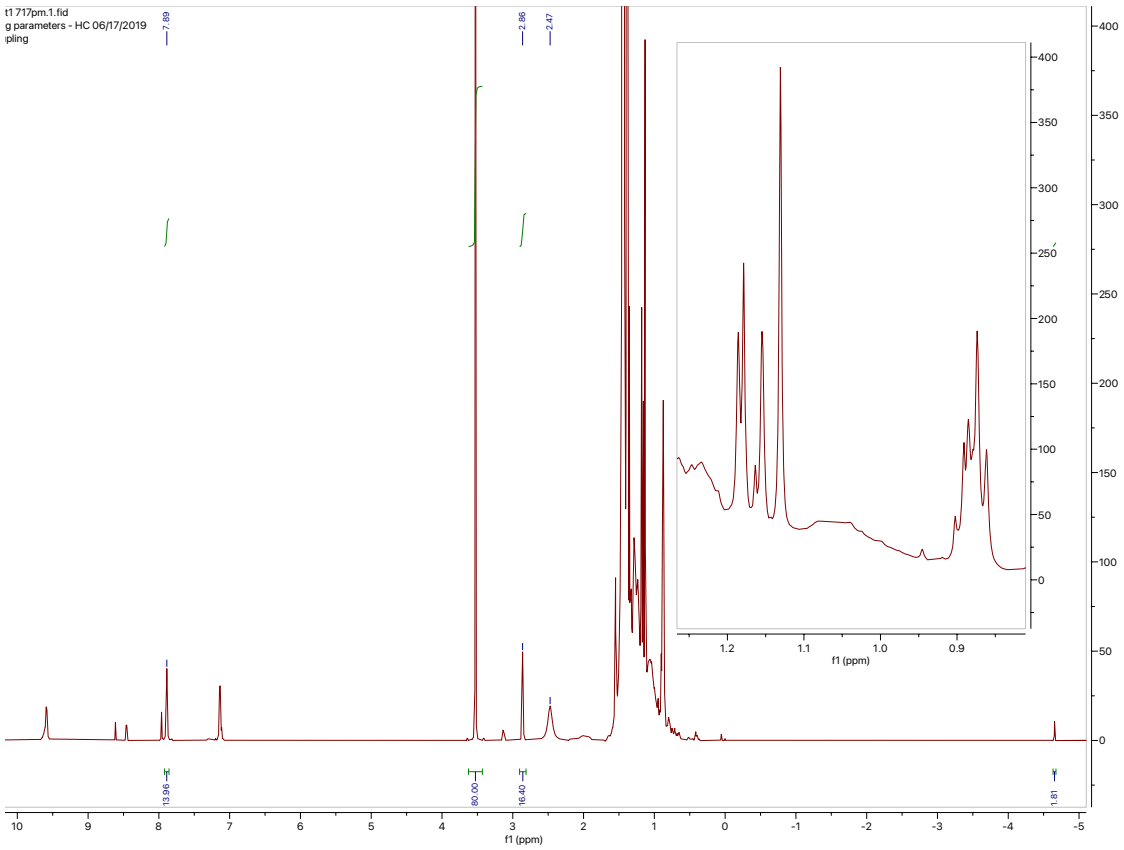

^{1}H-NMR (t_5 min)

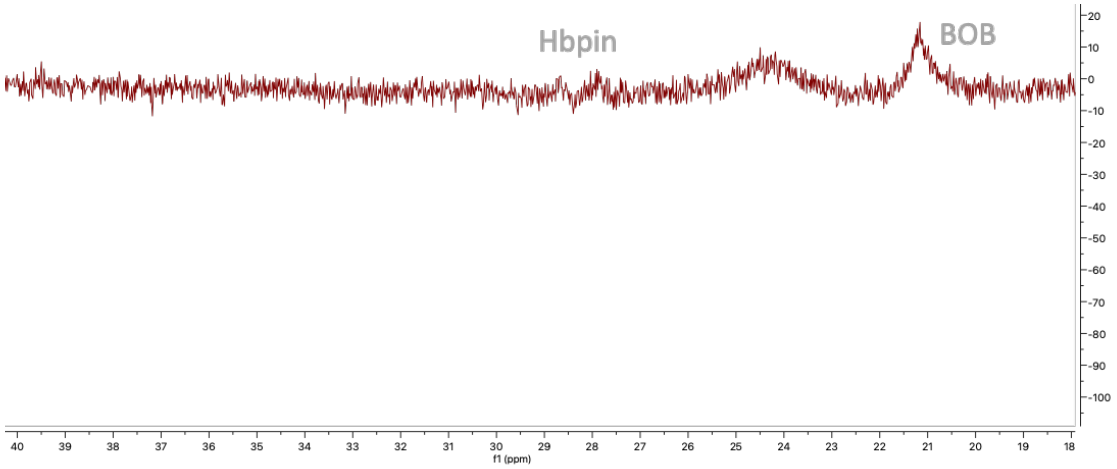

^{11}B-NMR (t_5 min)

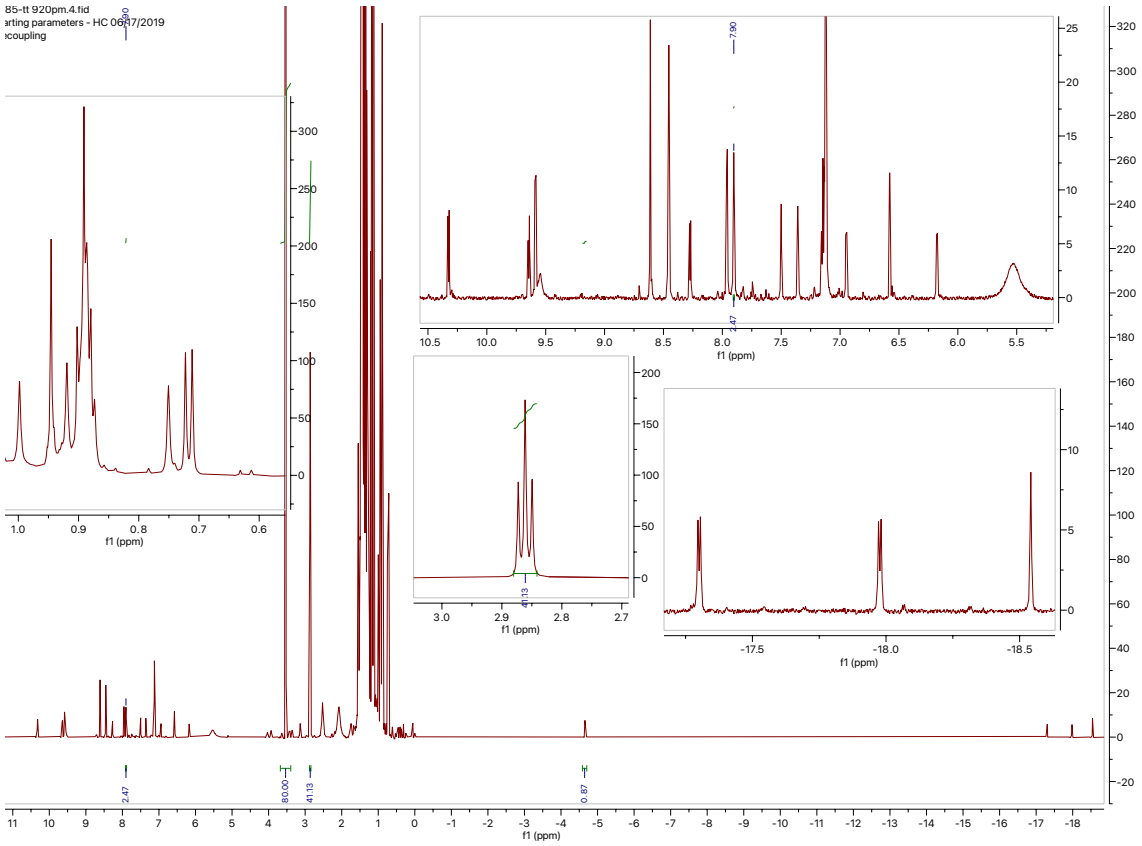

^{1}H-NMR (t_24 h)

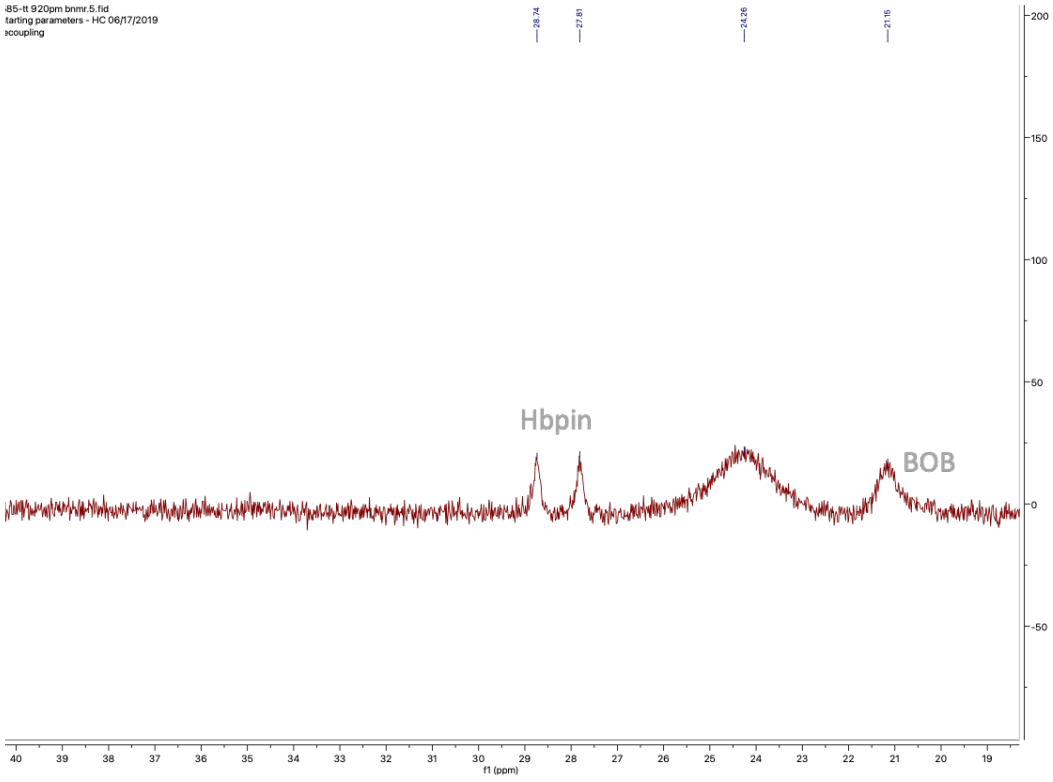

^{11}B-NMR (t_24 h)

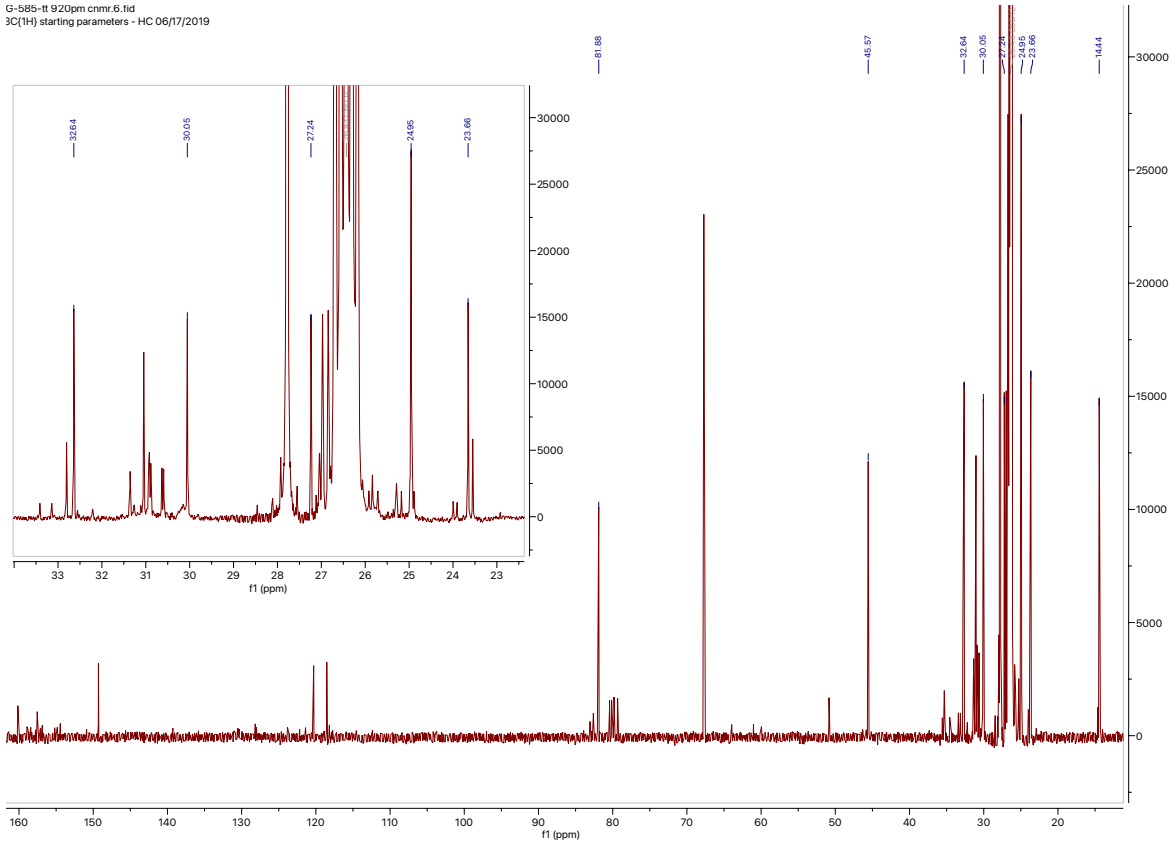

^{13}C-NMR (t_24 h)

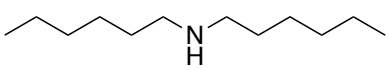

(1 equiv)

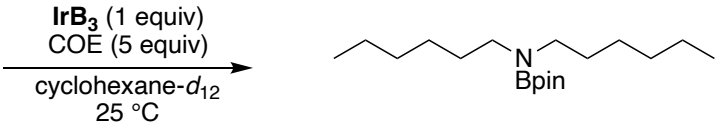

98%

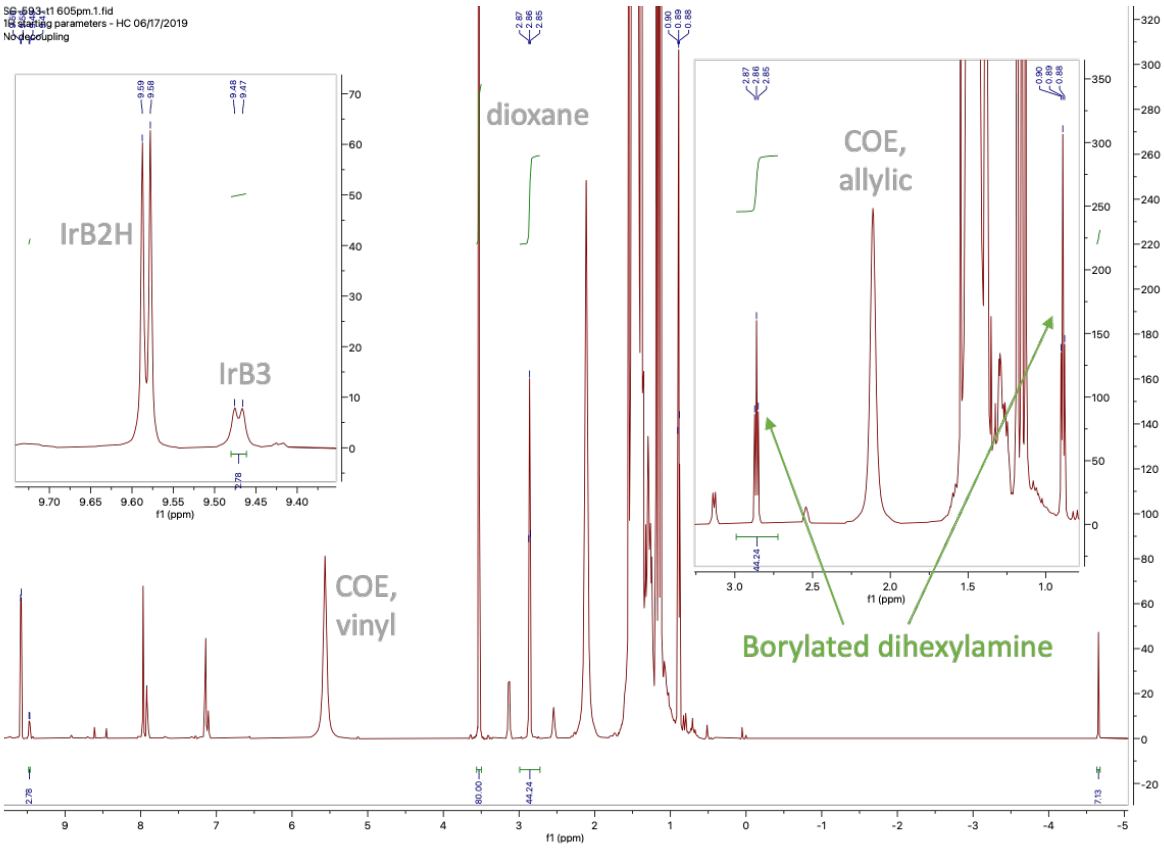

^{1}H-NMR (t_5 min)

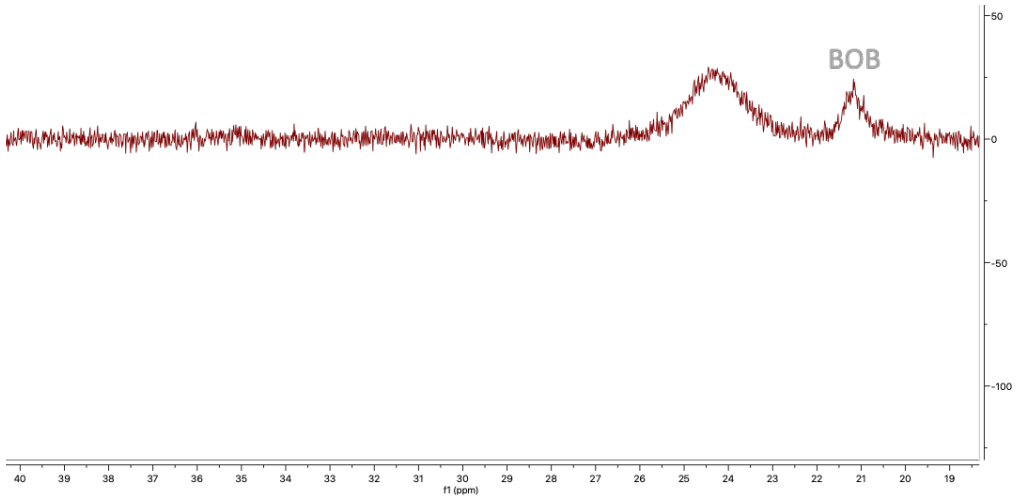

^{11}B-NMR (t_5 min)

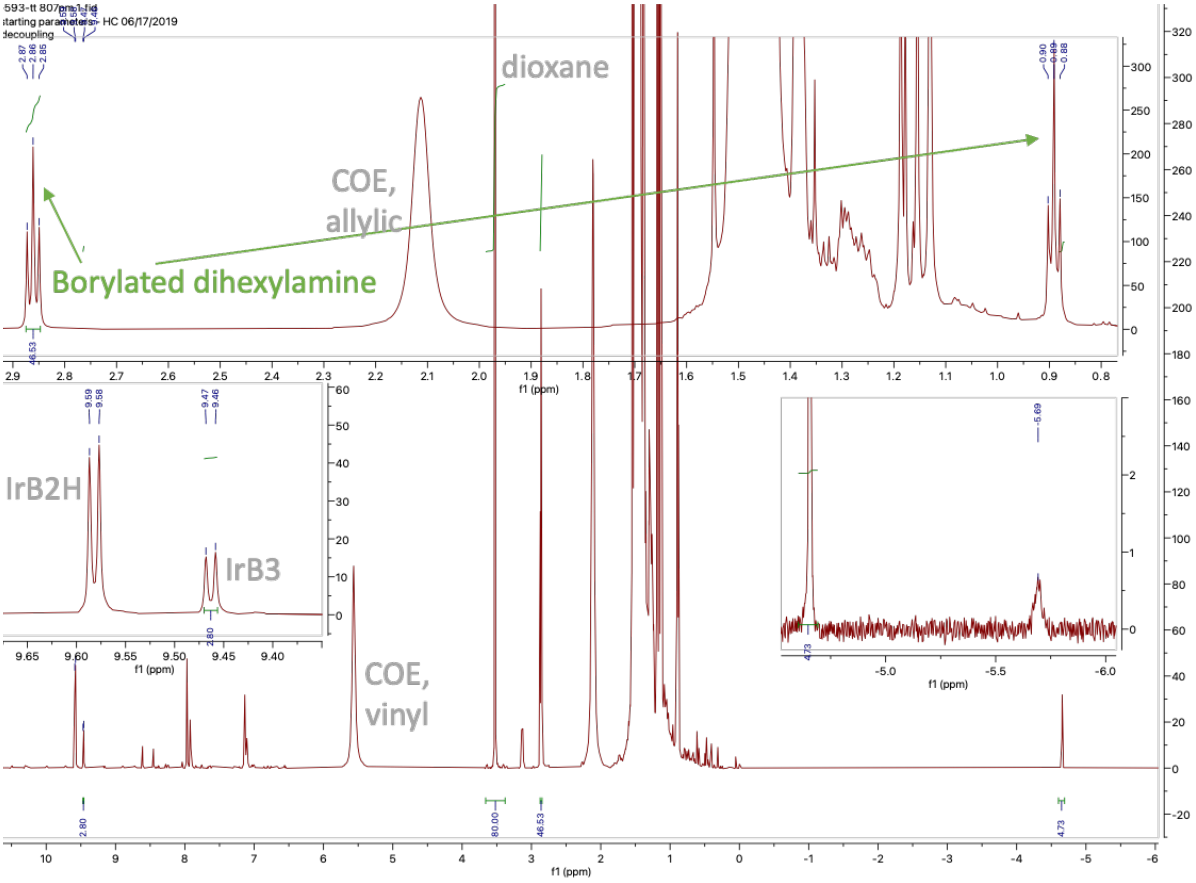
dioxane
COE,
allylic
Borylated dihexylamine
IrB2H
IrB3
COE,
vinyl
f1 (ppm)

^{1}H-NMR (t_24 h)

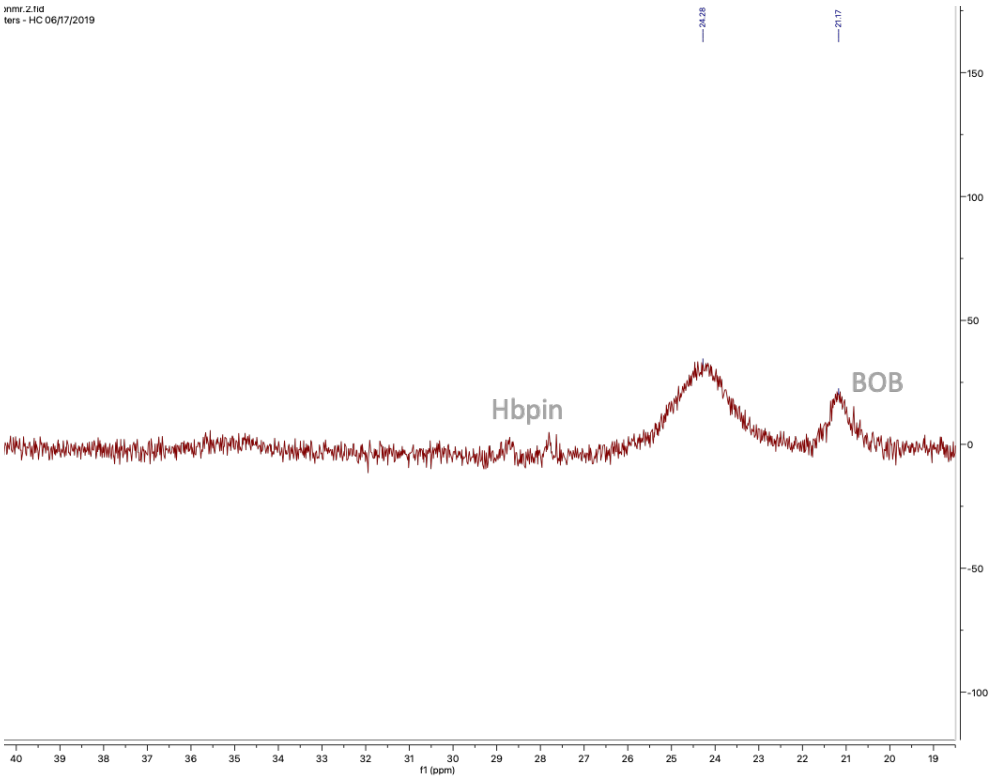

^{11}B-NMR (t_24 h)

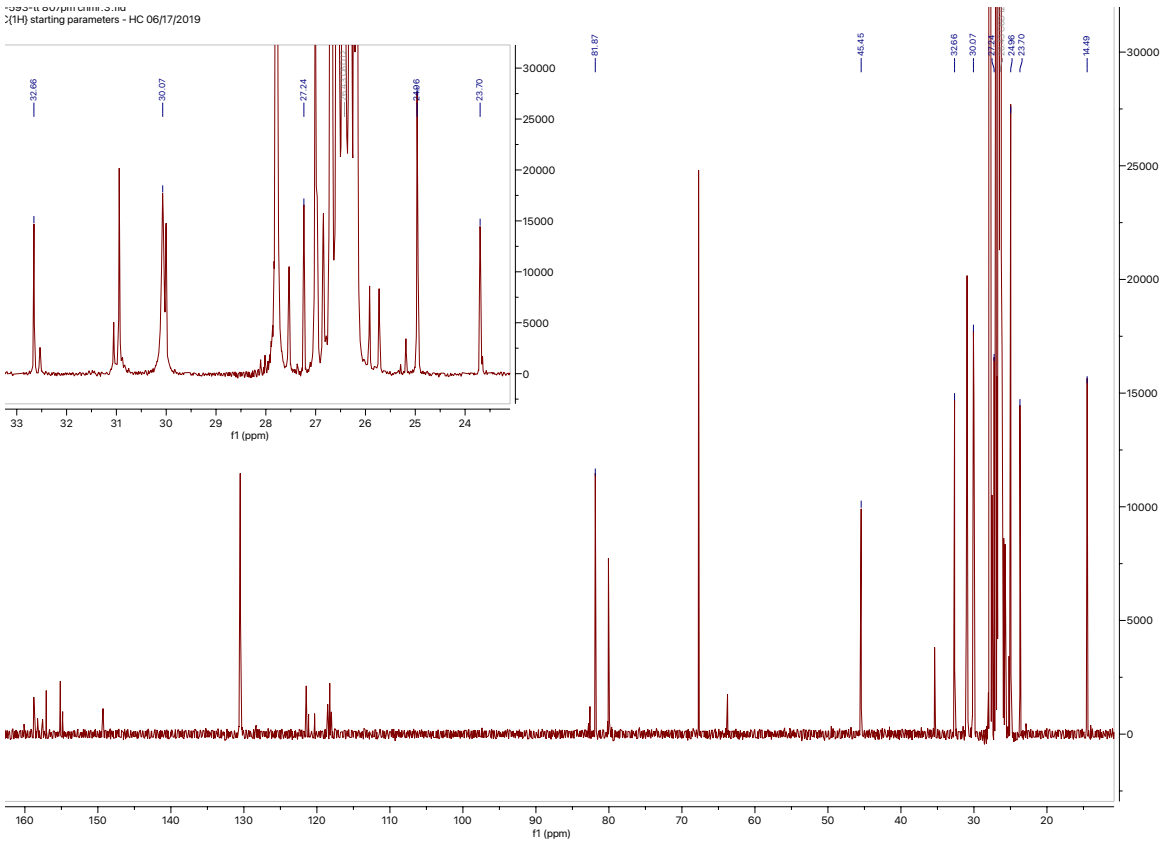

^{13}C-NMR (t_24 h)

[phenol]

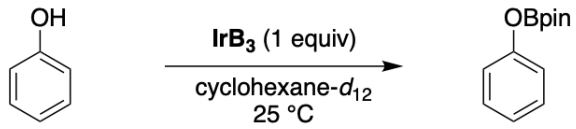

(1 equiv) 95%

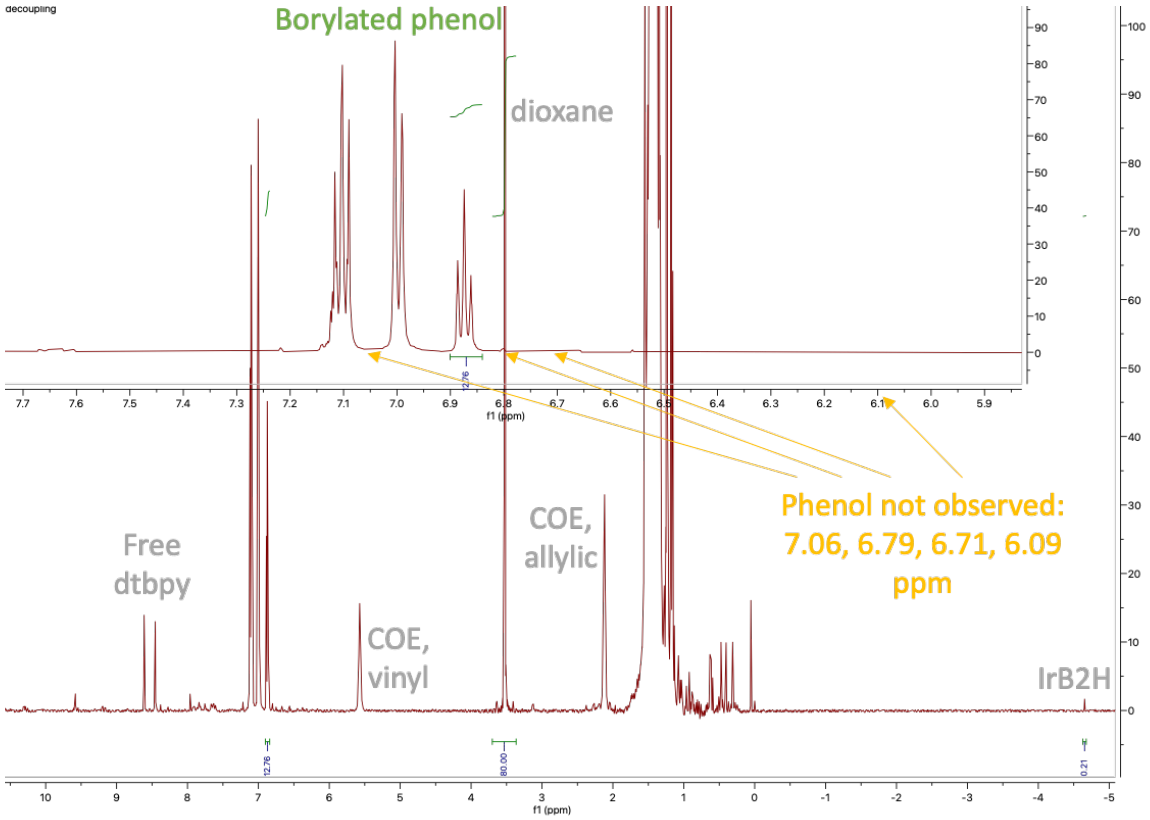

^{1}H-NMR (t_5 min)

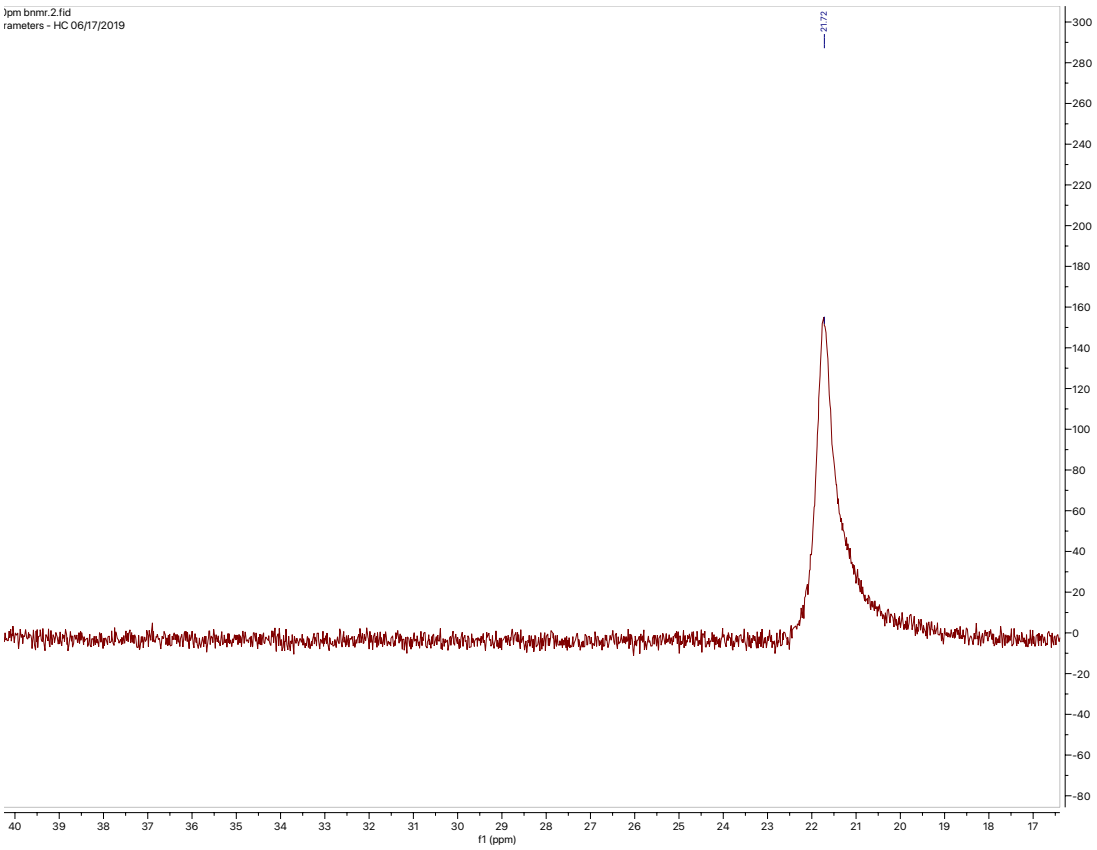

^{11}B-NMR (t_5 min)

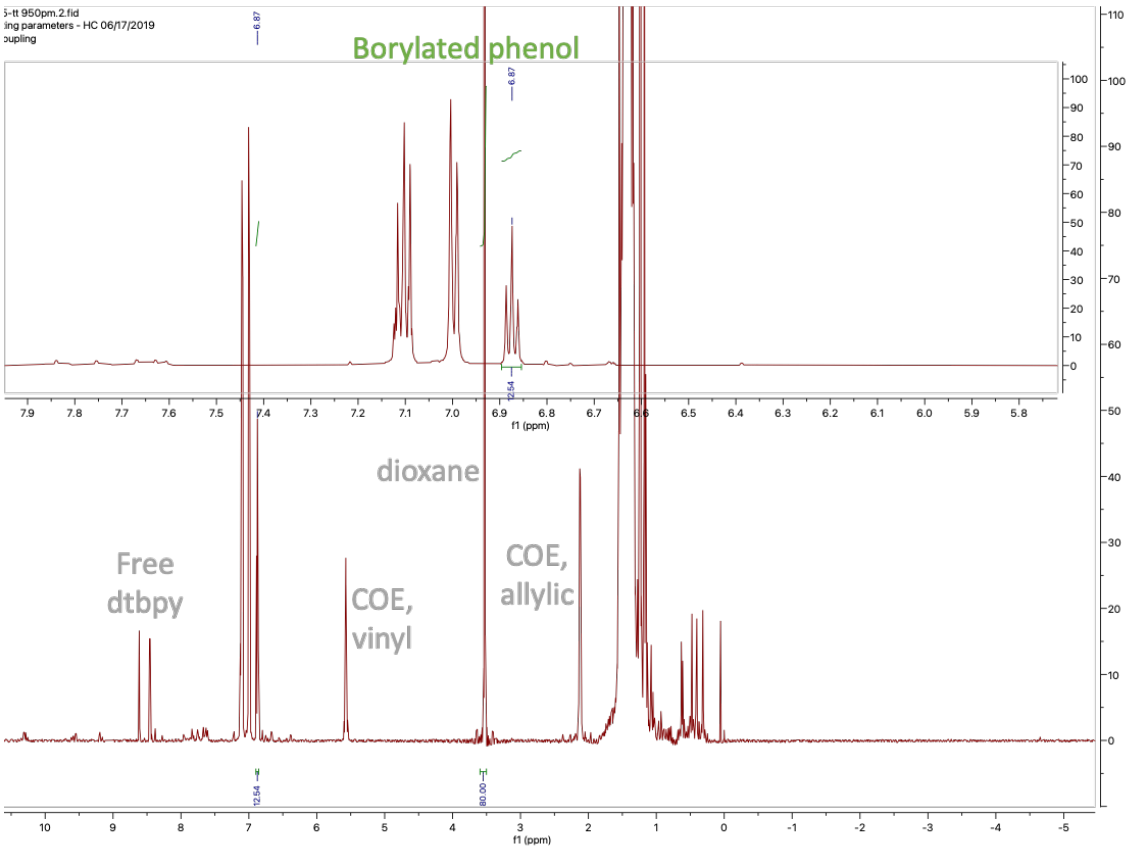
Borylated phenol
dioxane
Free
dtbpy
COE,
vinyl
COE,
allylic
f1 (ppm)

^{1}H-NMR (t_24 h)

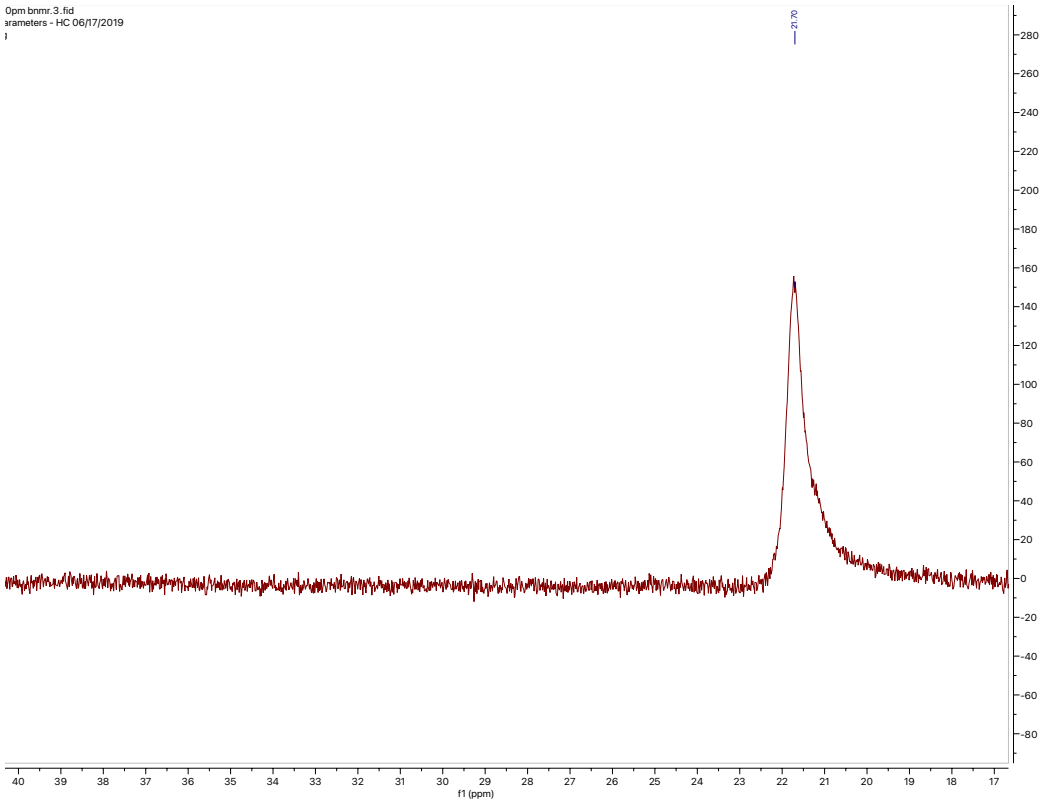
f1 (ppm)

^{11}B-NMR (t_24 h)

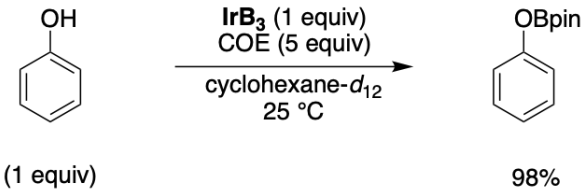

(1 equiv) 98%

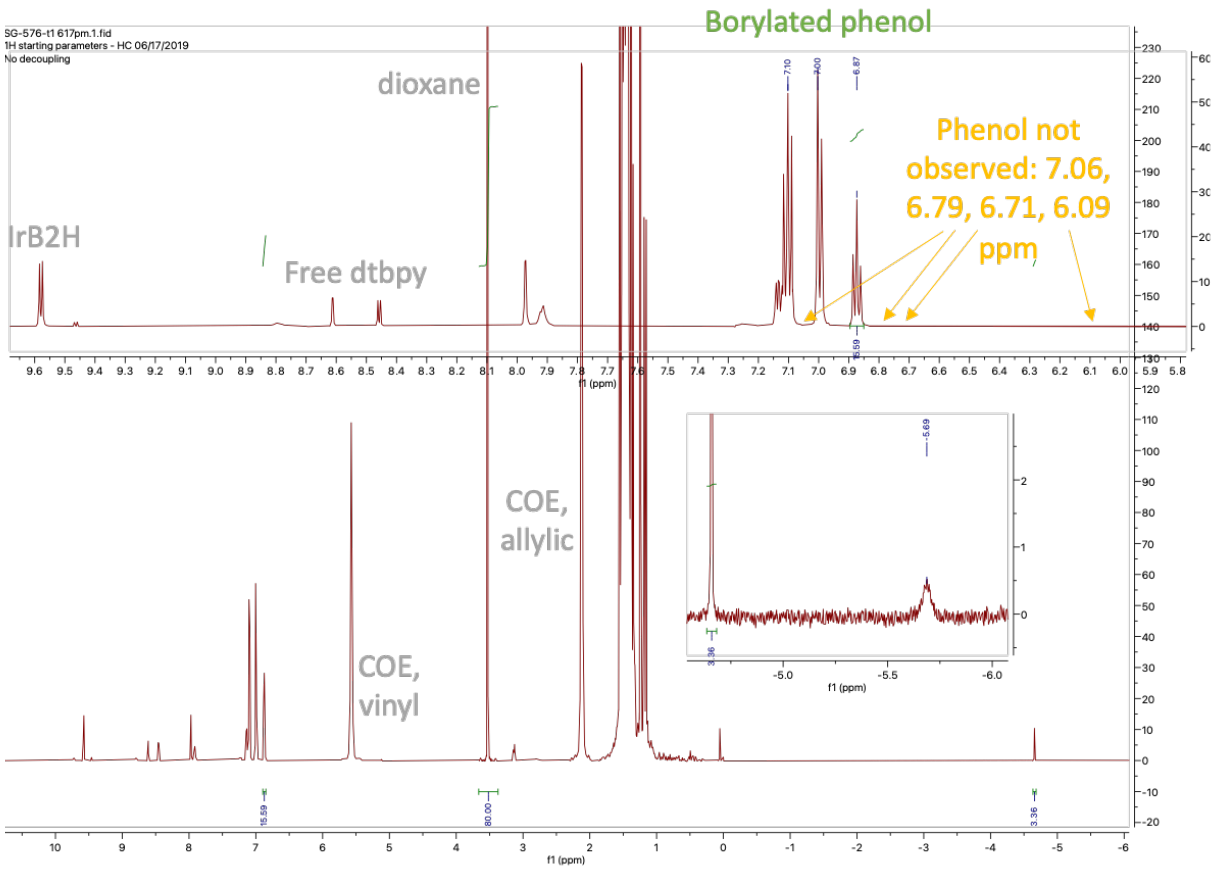

^{1}H-NMR (t_5 min)

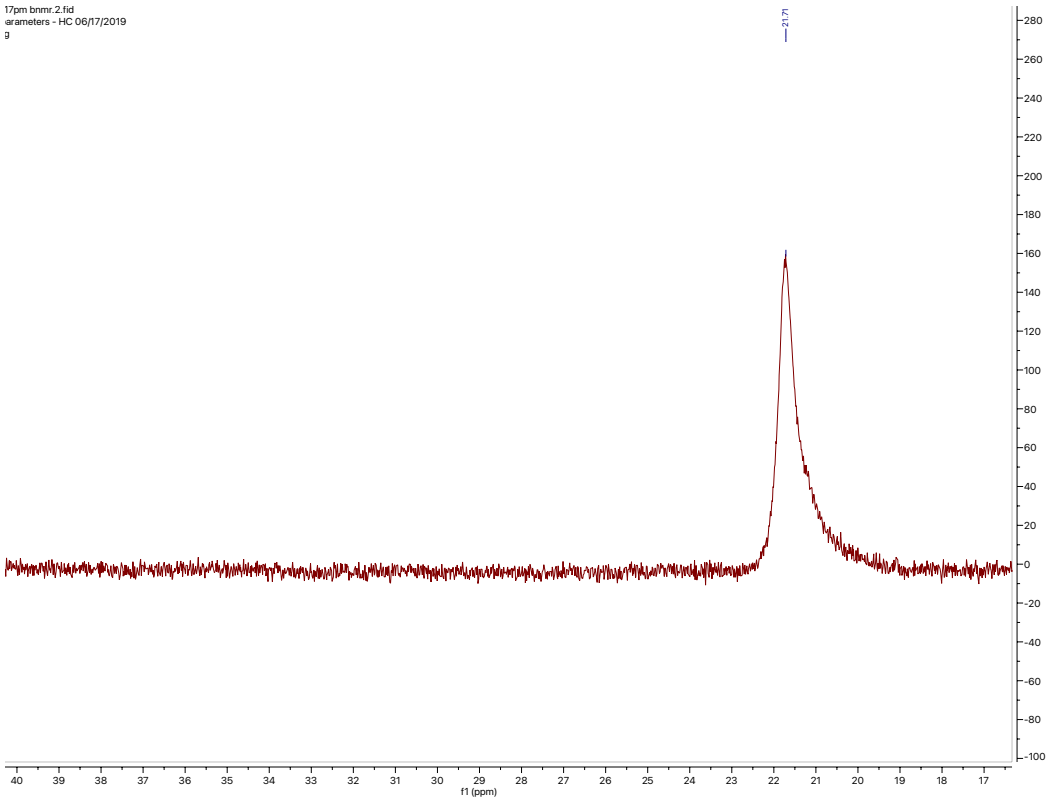

^{11}B-NMR (t_5 min)

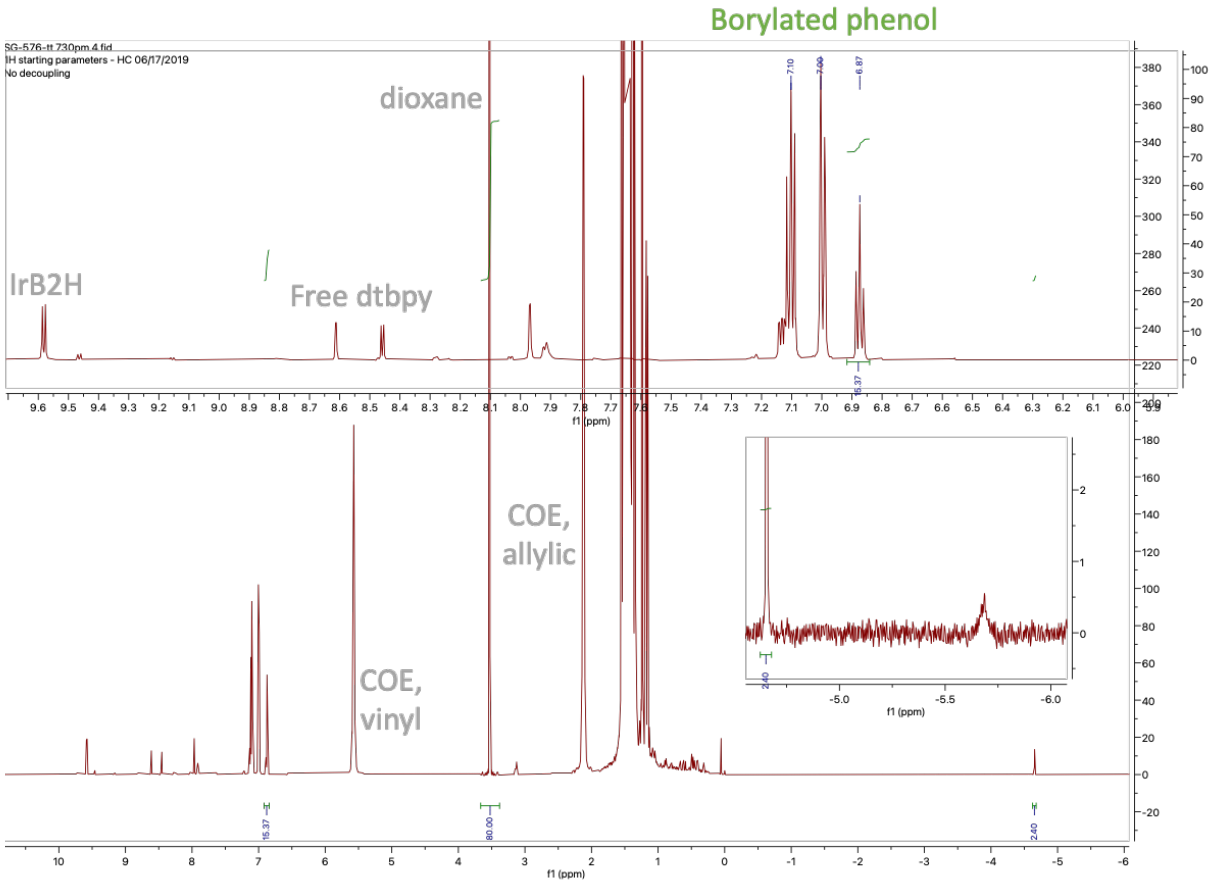
Borylated phenol
dioxane
IrB2H
Free dtbpy
COE,
allylic
COE,
vinyl
f1 (ppm)

^{1}H-NMR (t_24 h)

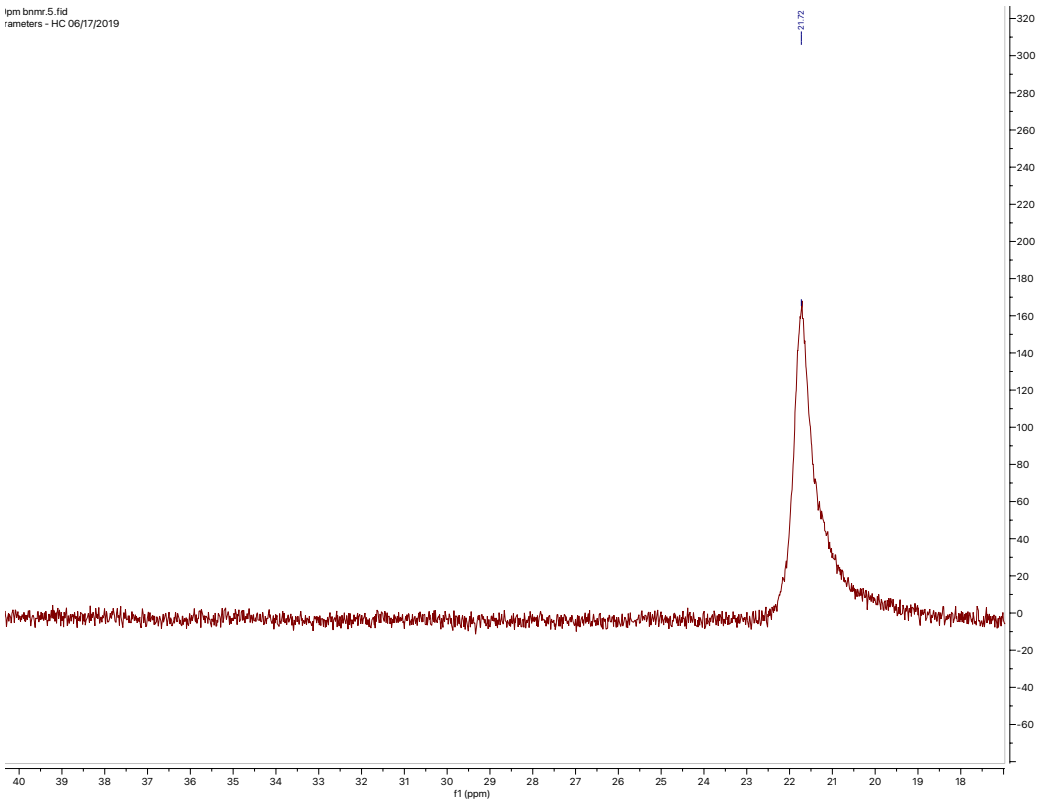

^{11}B-NMR (t_24 h)

[aniline]

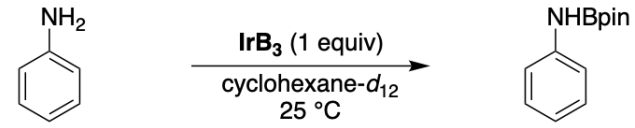

(1 equiv)

80%

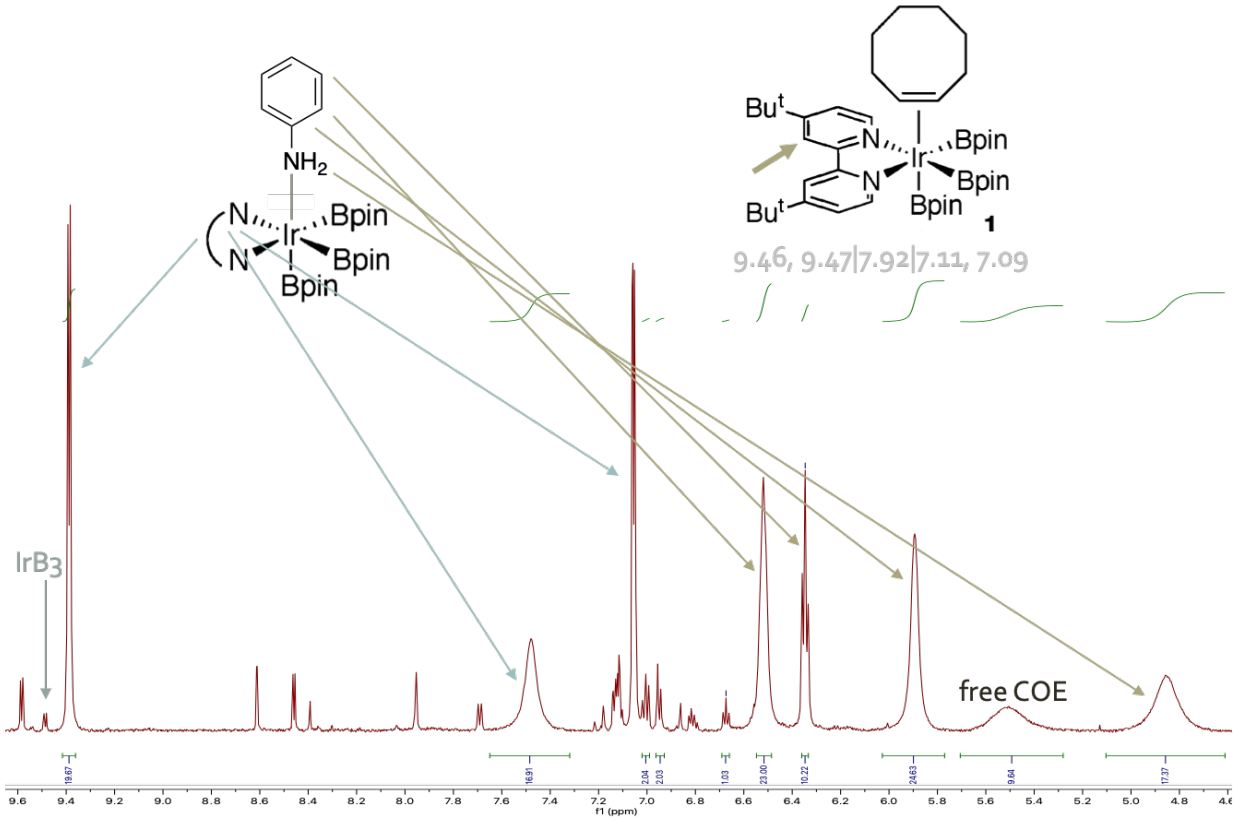
NH2
N
Ir
Bpin
Bpin
Bpin
N
Bu^t
N
Ir
Bpin
Bpin
Bpin
Bu^t
1
9.46, 9.47|7.92|7.11, 7.09
IrB3
free COE
19.67
16.91
2.04
2.03
1.03
23.00
10.22
24.63
9.64
17.37
9.6
9.4
9.2
9.0
8.8
8.6
8.4
8.2
8.0
7.8
7.6
7.4
7.2
7.0
6.8
6.6
6.4
6.2
6.0
5.8
5.6
5.4
5.2
5.0
4.8
f1 (ppm)

^{1}H-NMR (t_5 min)

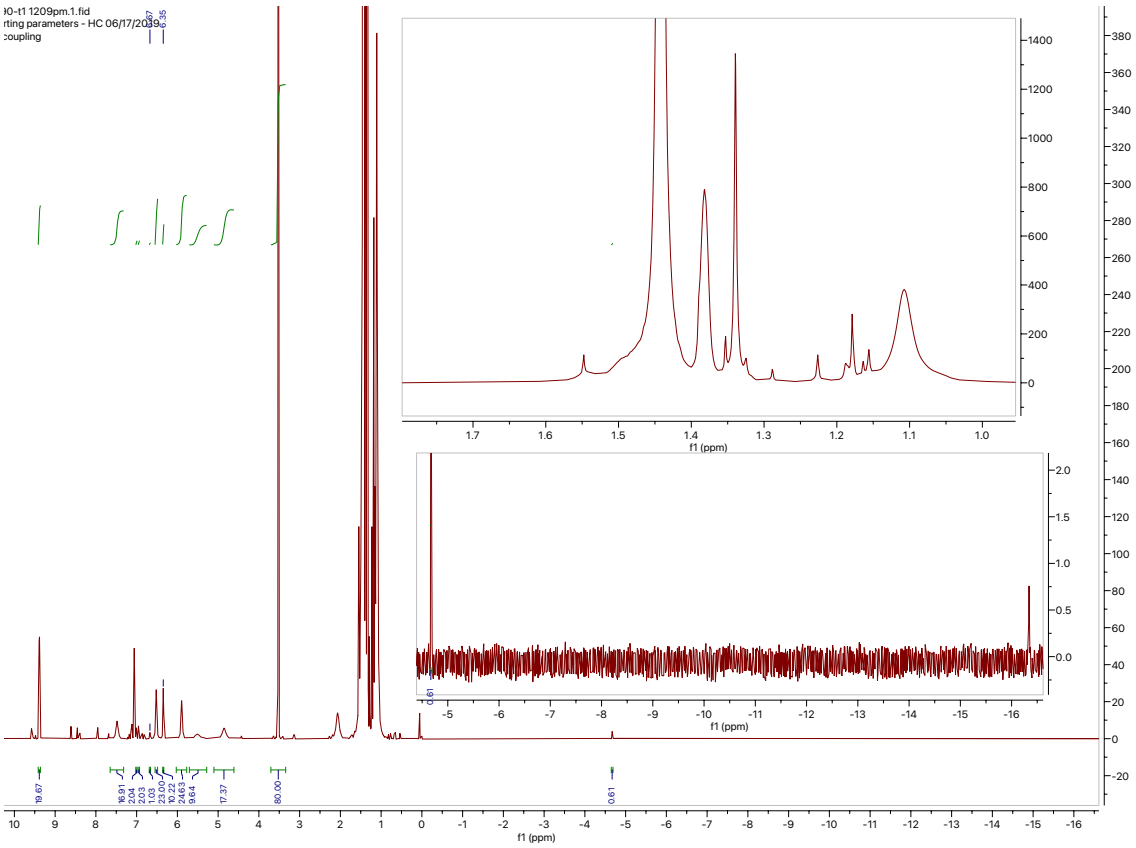

^{1}H-NMR (t_5 min)

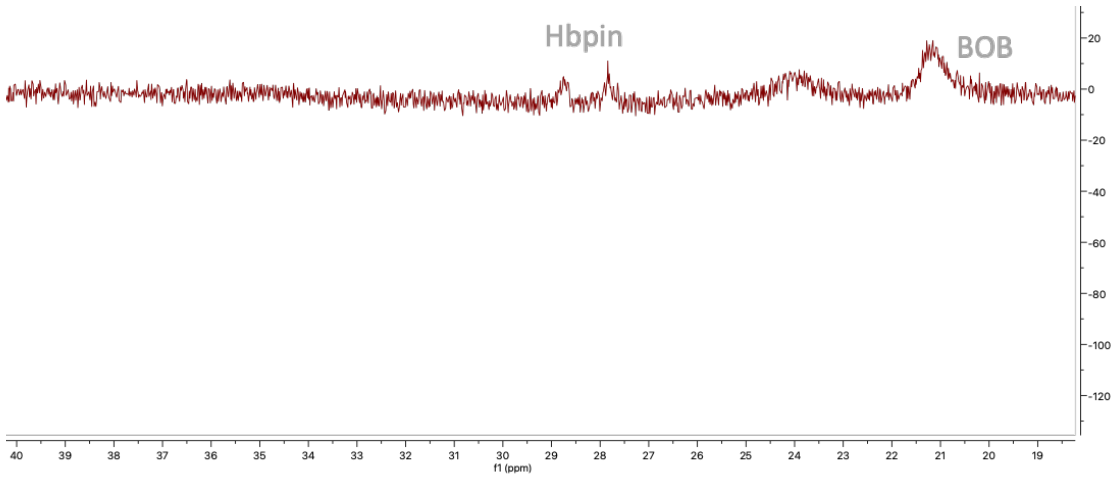

^{11}B-NMR (t_5 min)

Borylated aniline

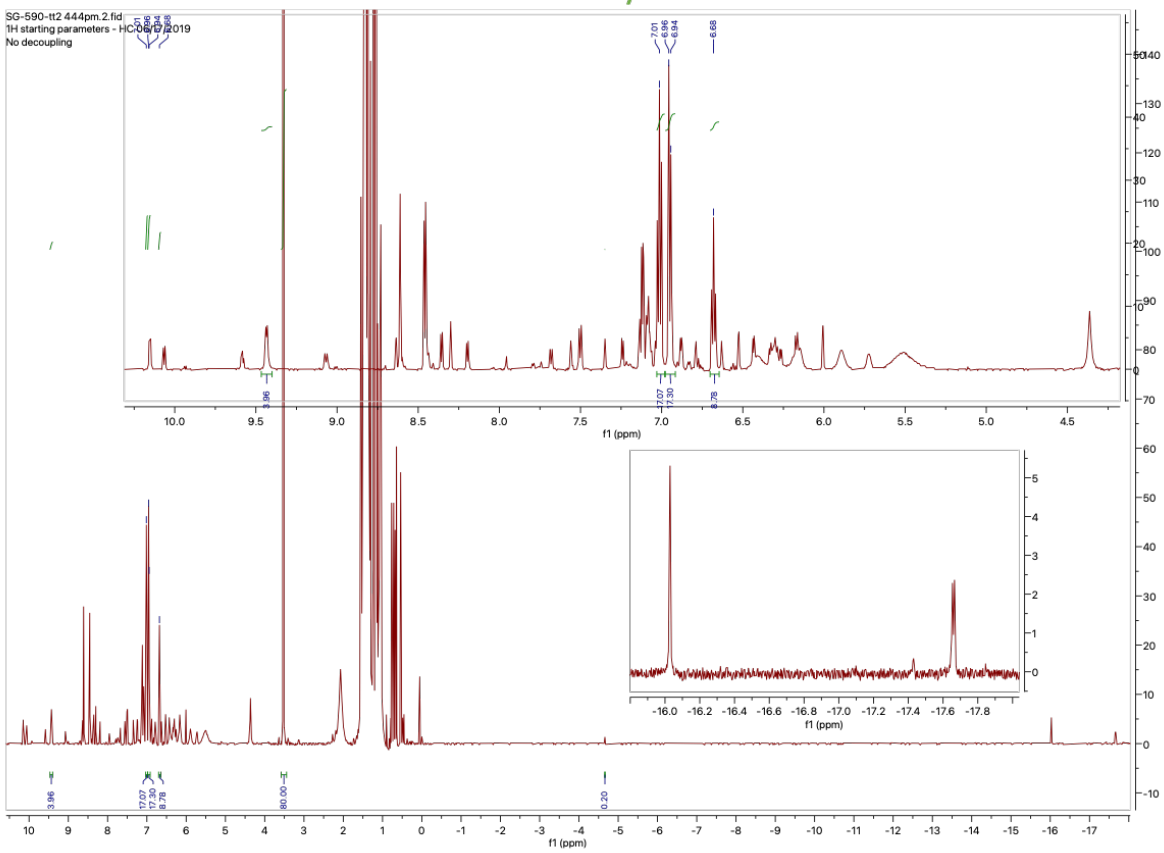

^{1}H-NMR (t_24 h)

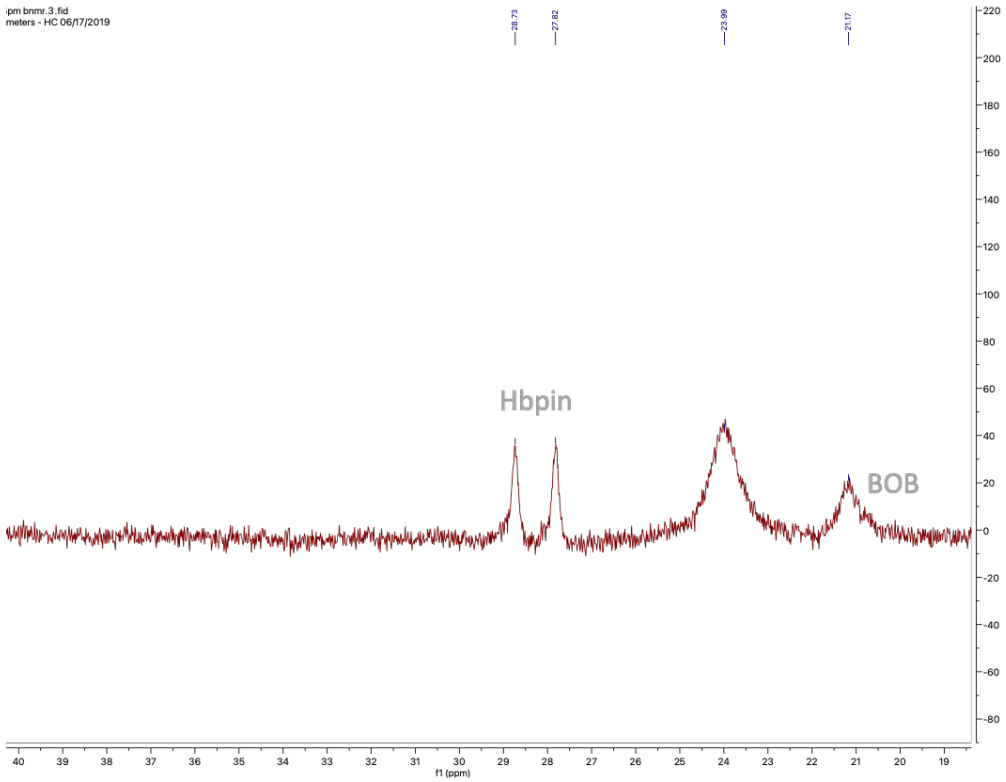

^{11}B-NMR (t_24 h)

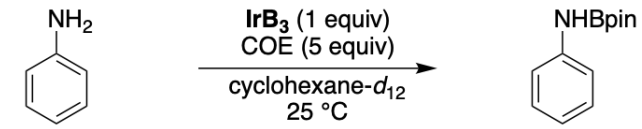

(1 equiv) 76%

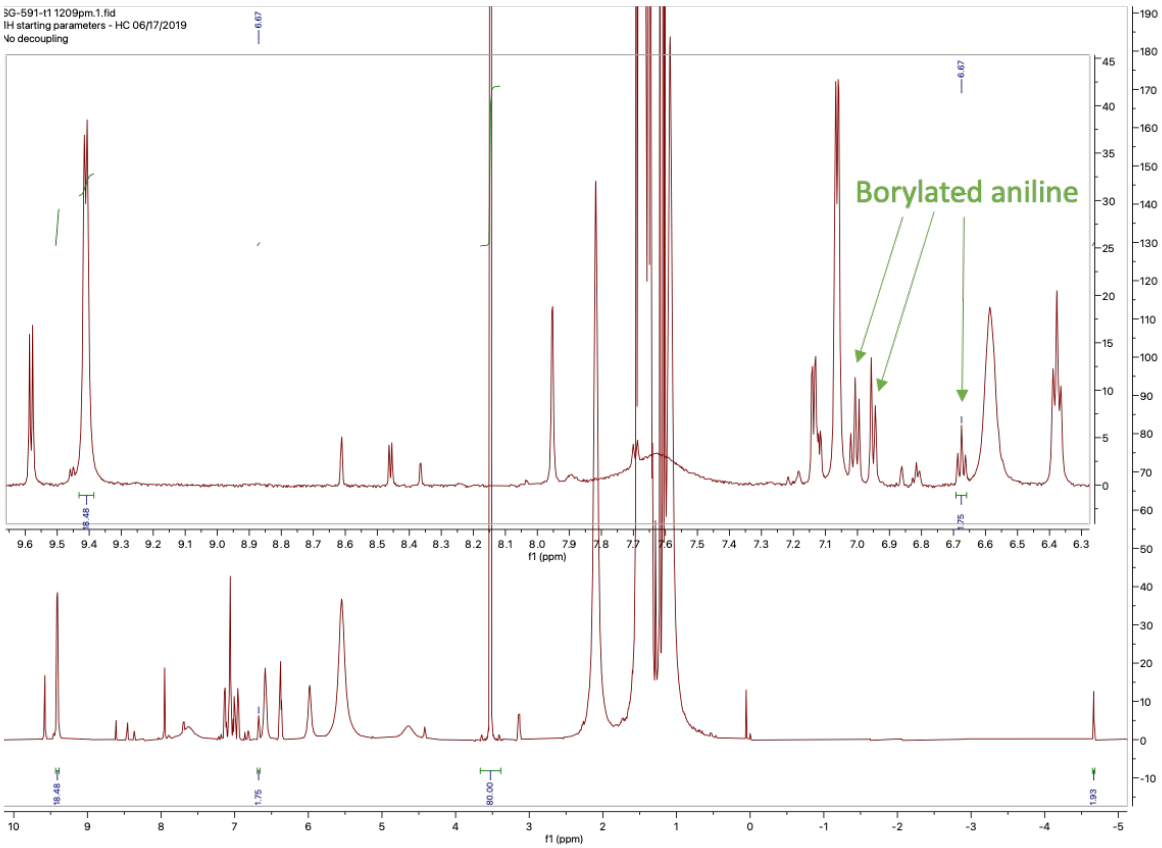

^{1}H-NMR (t_5 min)

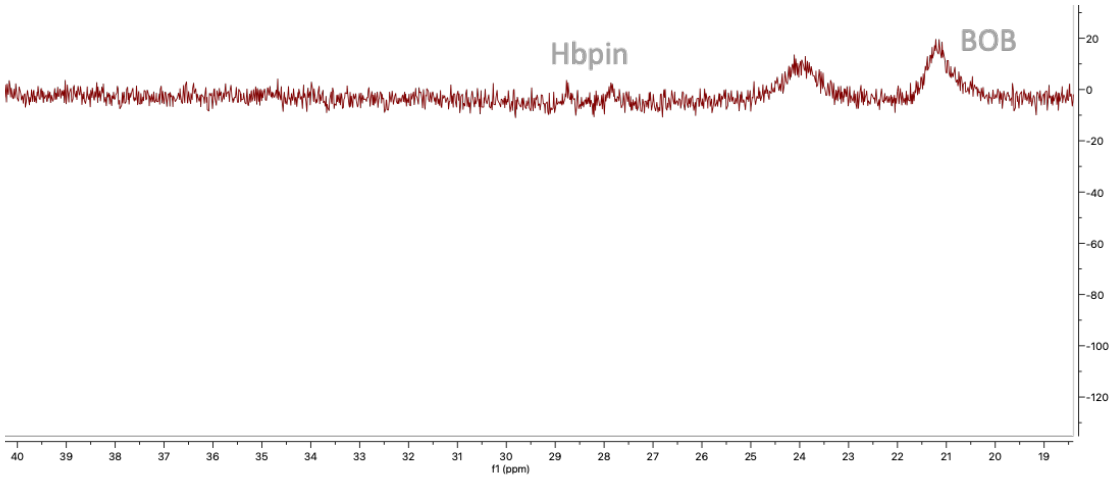

^{11}B-NMR (t_5 min)

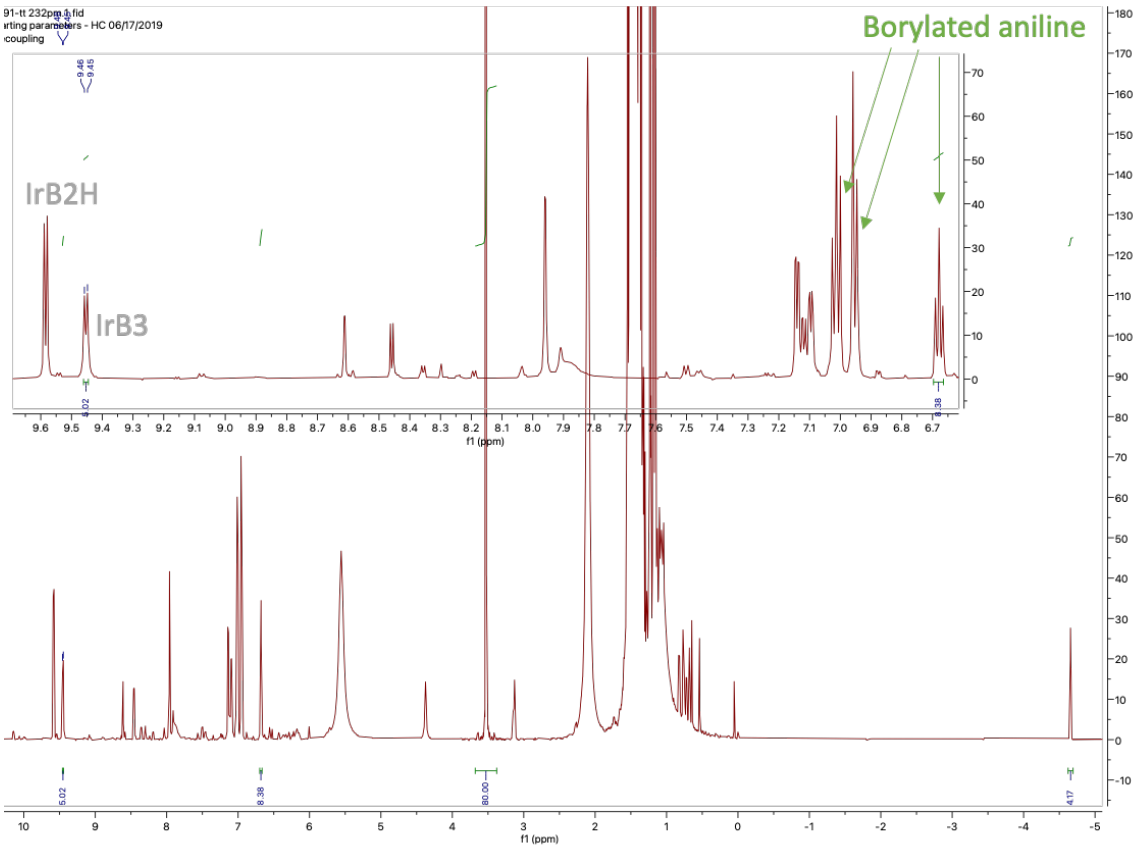

^{1}H-NMR (t_24 h)

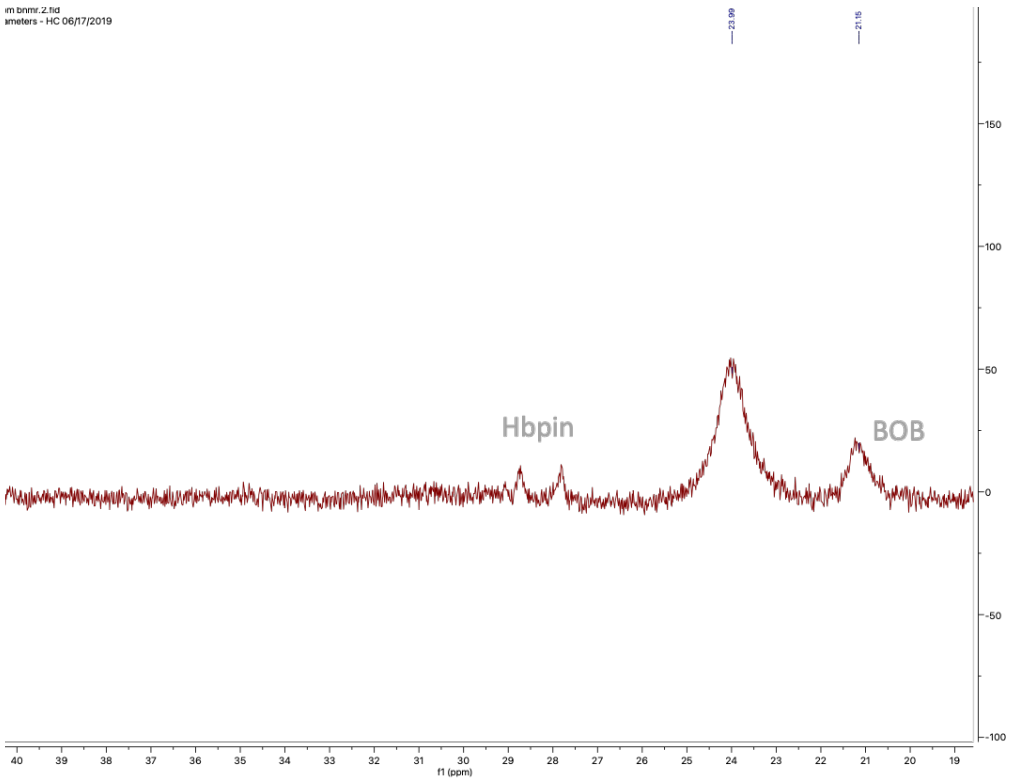

^{11}B-NMR (t_24 h)

[thiophenol]

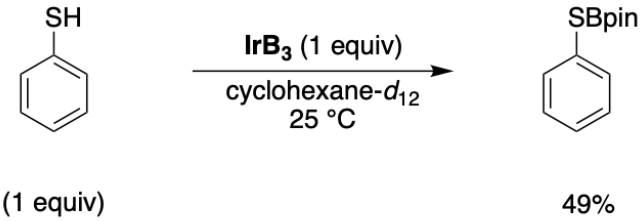

(1 equiv) 49%

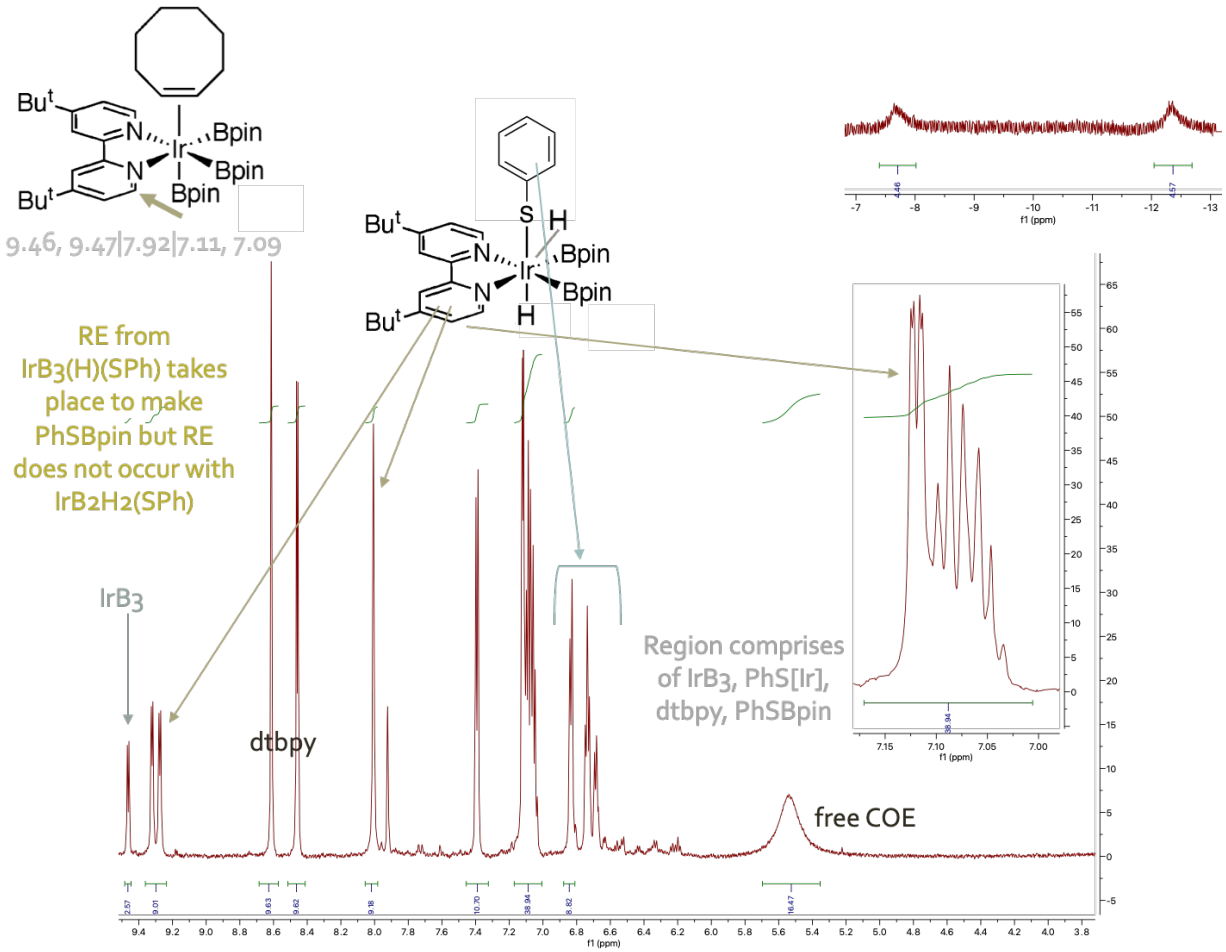

^{1}H-NMR (t_5 min)

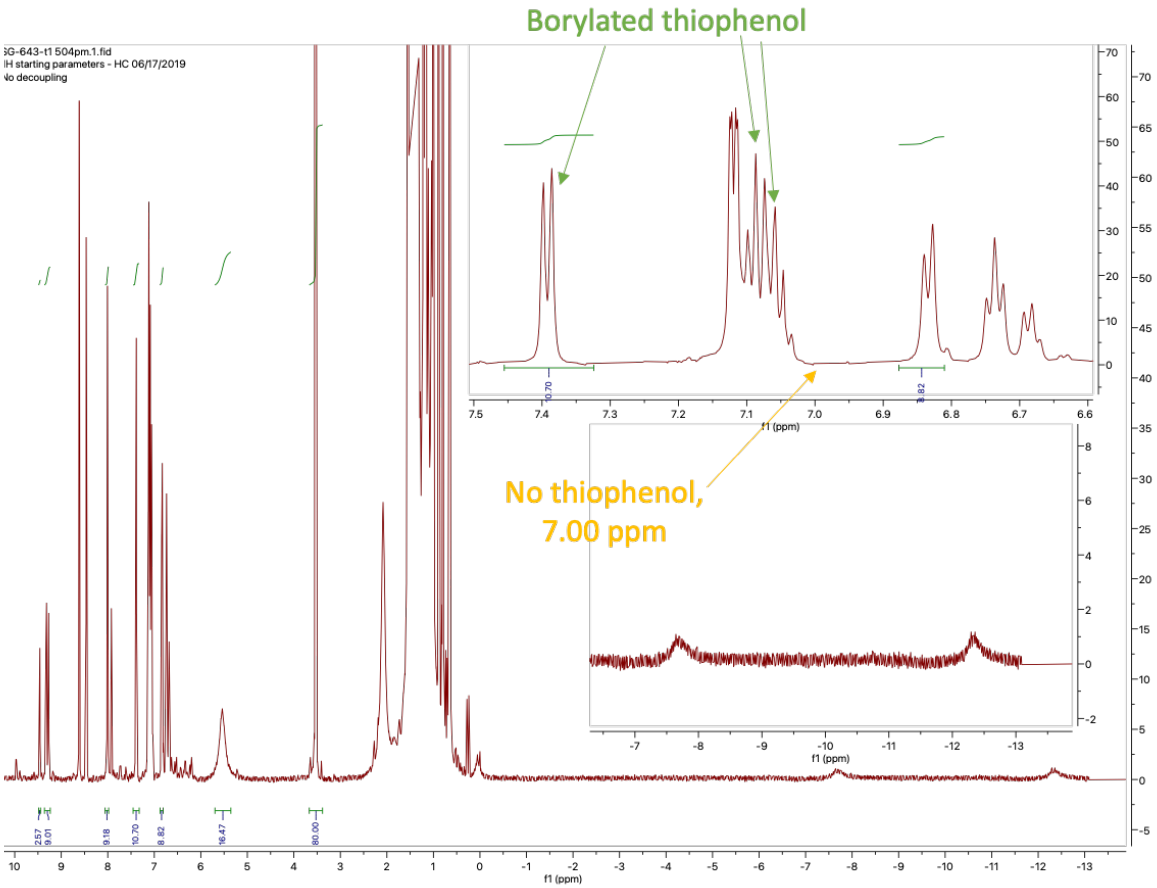

^{1}H-NMR (t_5 min)

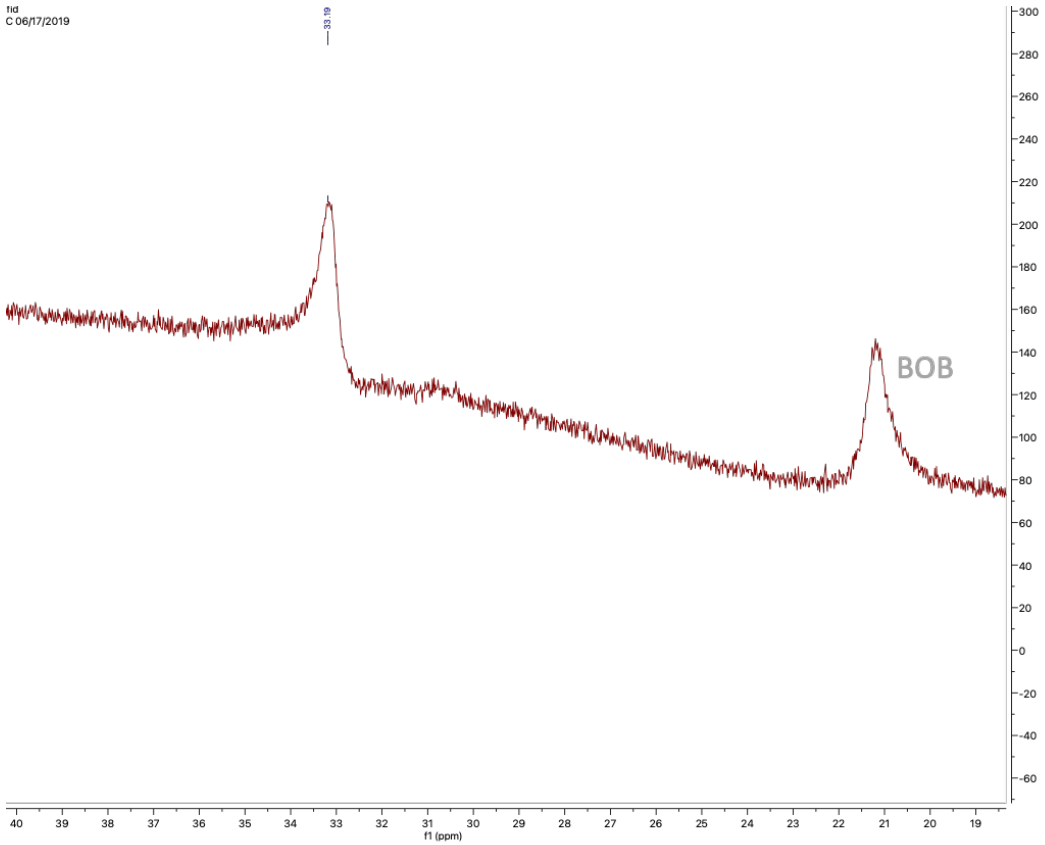

^{11}B-NMR (t_5 min)

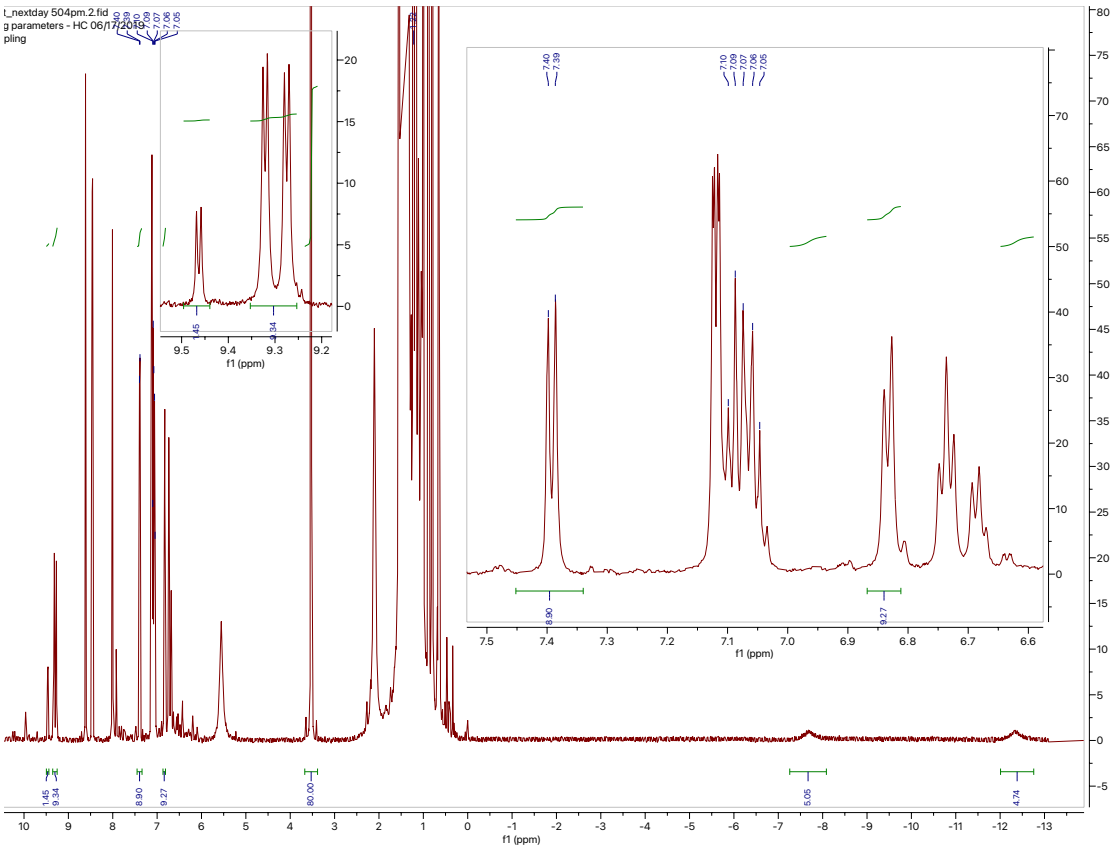

^{1}H-NMR (t_24 h)

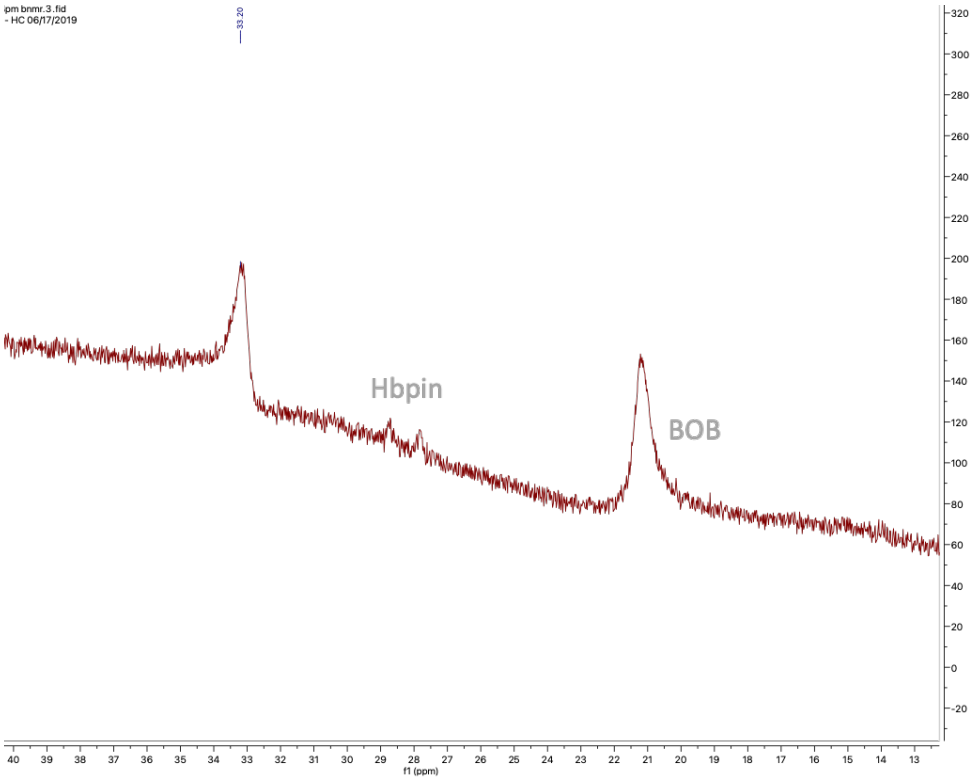

^{11}B-NMR (t_24 h)

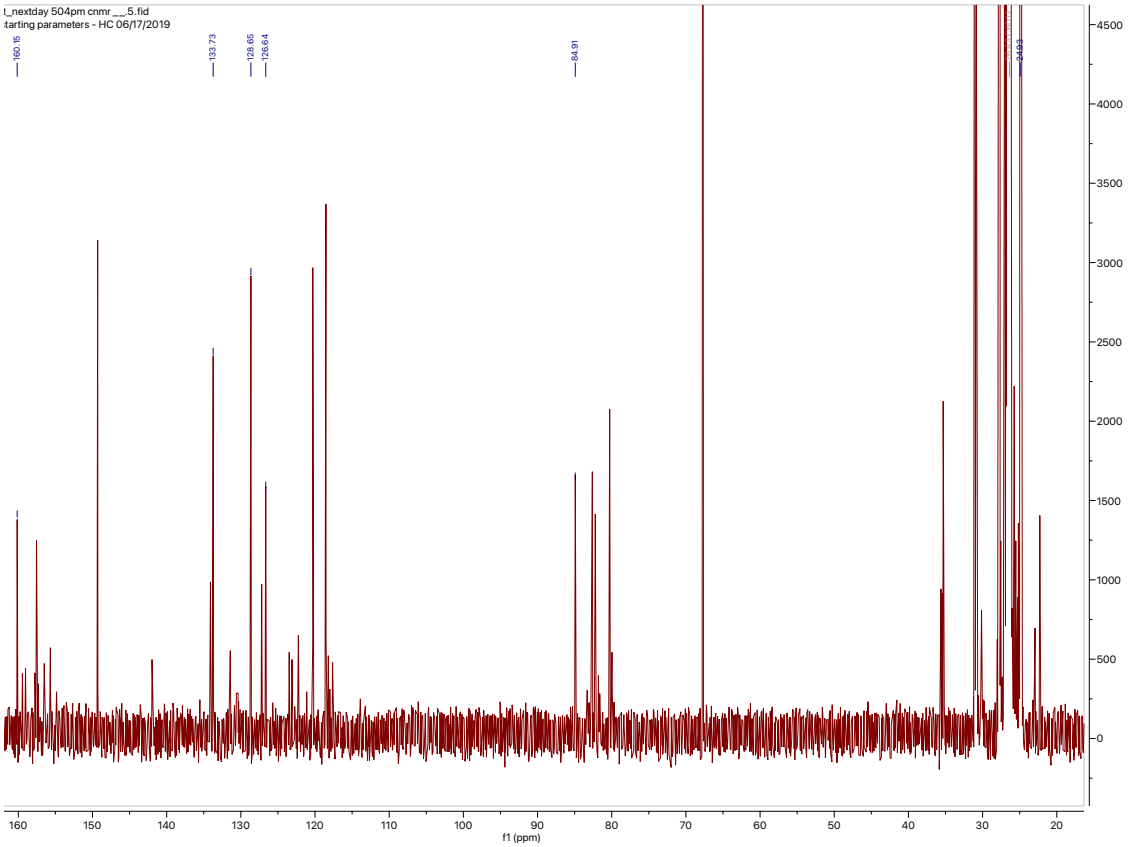

^{13}C-NMR (t_24 h)

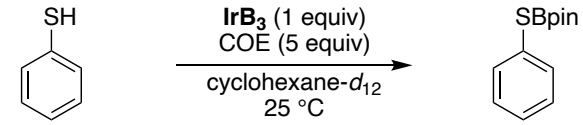

(1 equiv) 55%

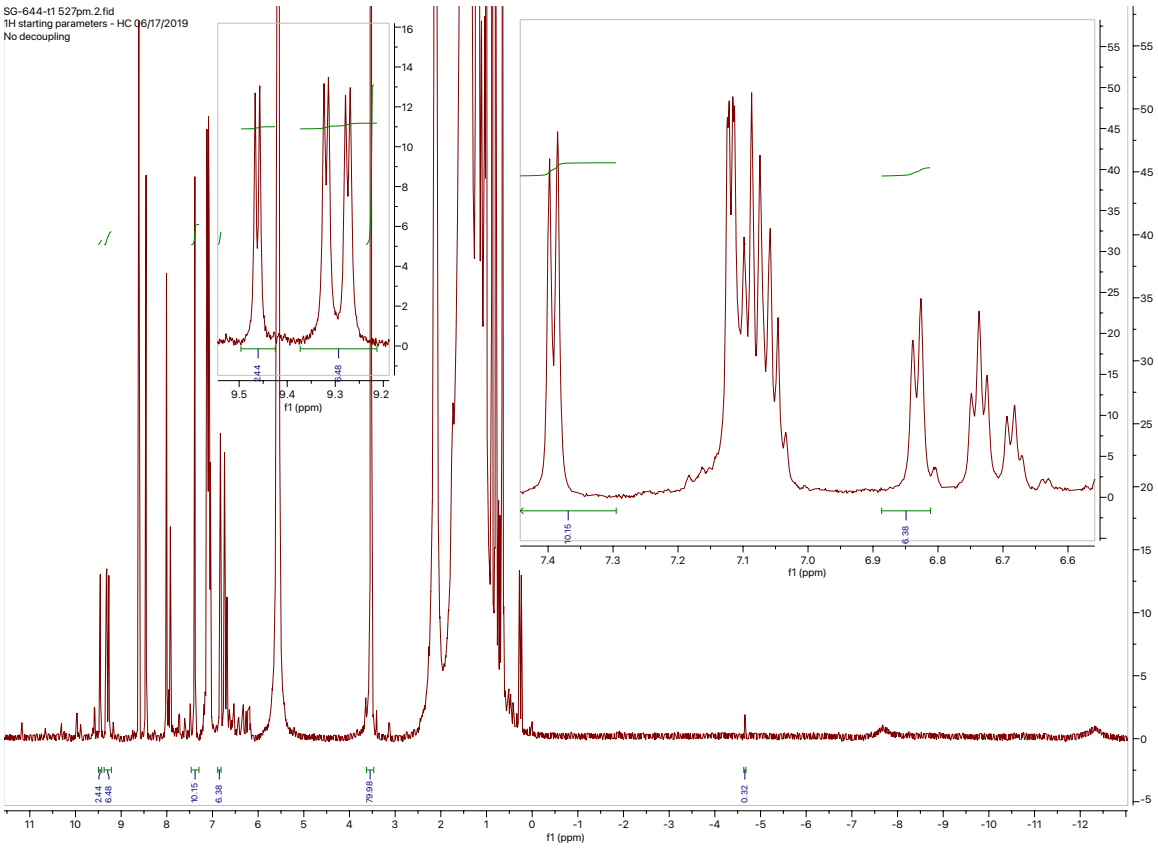

^{1}H-NMR (t_5 min)

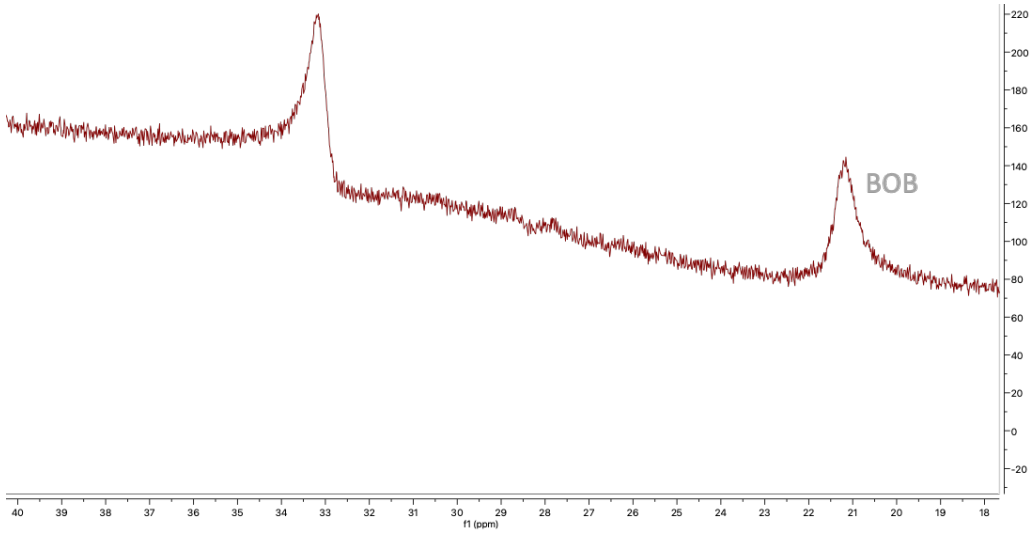

^{11}B-NMR (t_5 min)

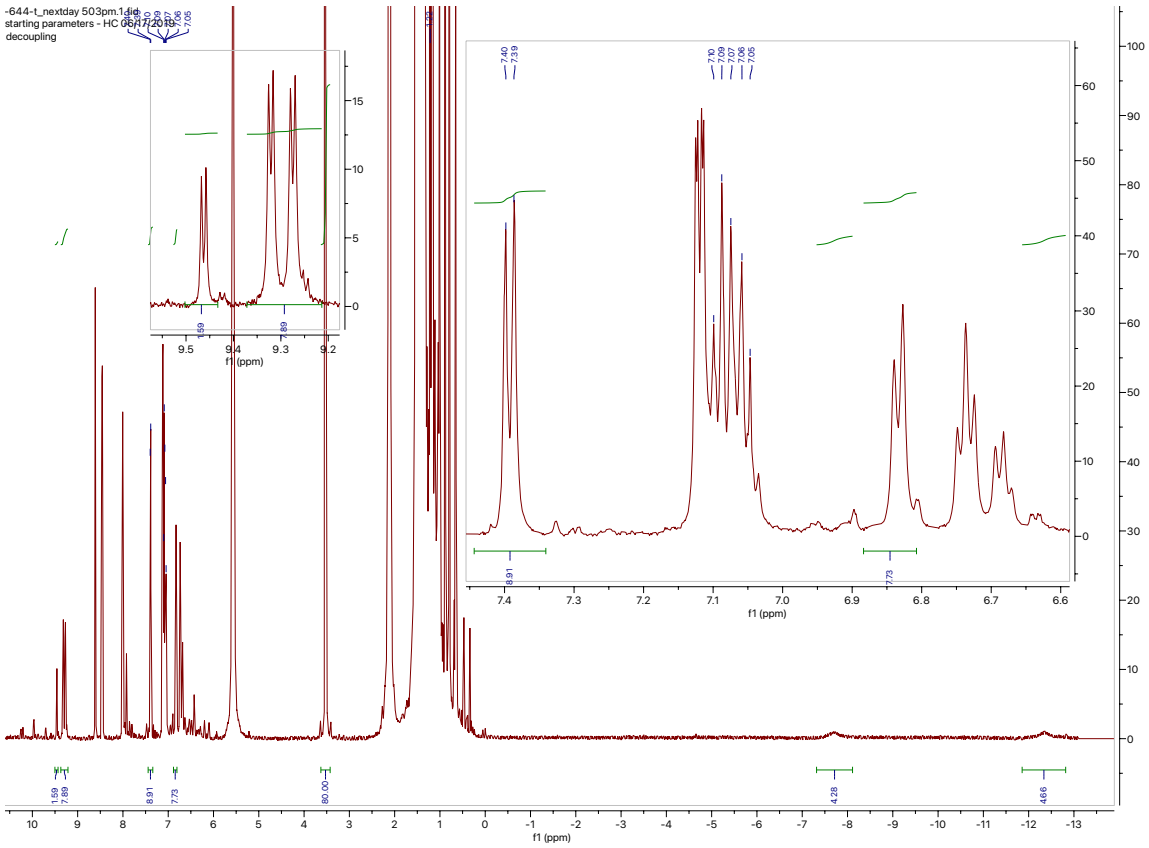
-644-t_nextday 503pm.1.fid
starting parameters - HC 06/17/2019
decoupling
f1 (ppm)

^{1}H-NMR (t_24 h)

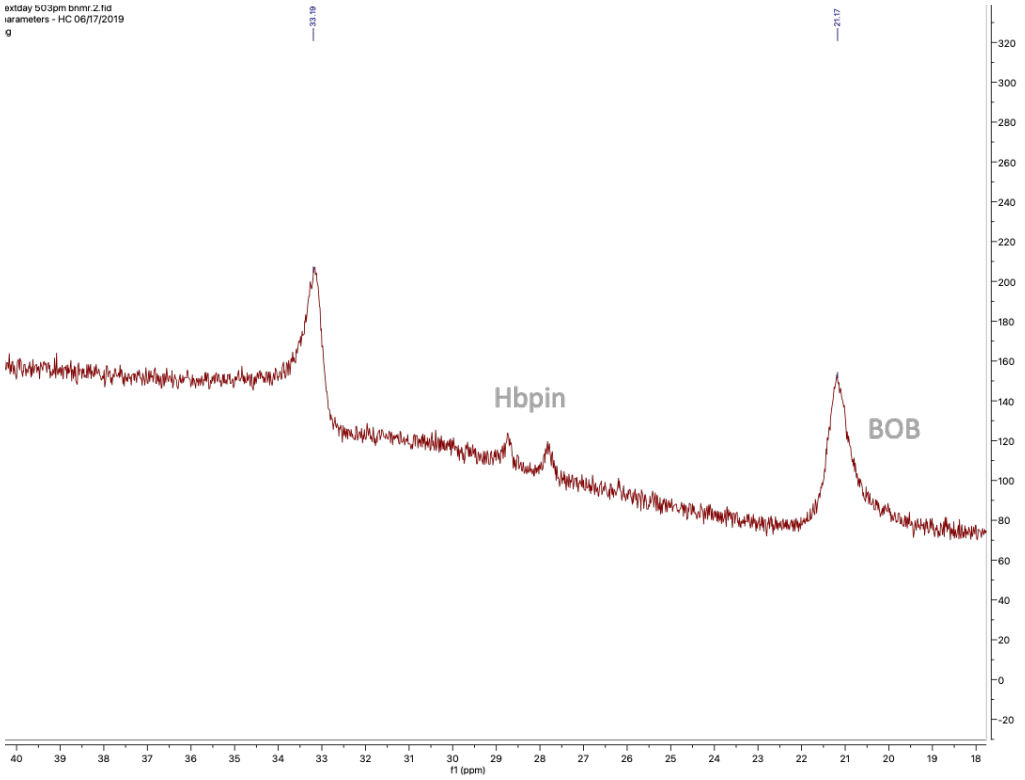
extday 503pm bnmr.2.fid
arameters - HC 06/17/2019
g
33.19
21.17
Hbpin
BOB
f1 (ppm)

^{11}B-NMR (t_24 h)

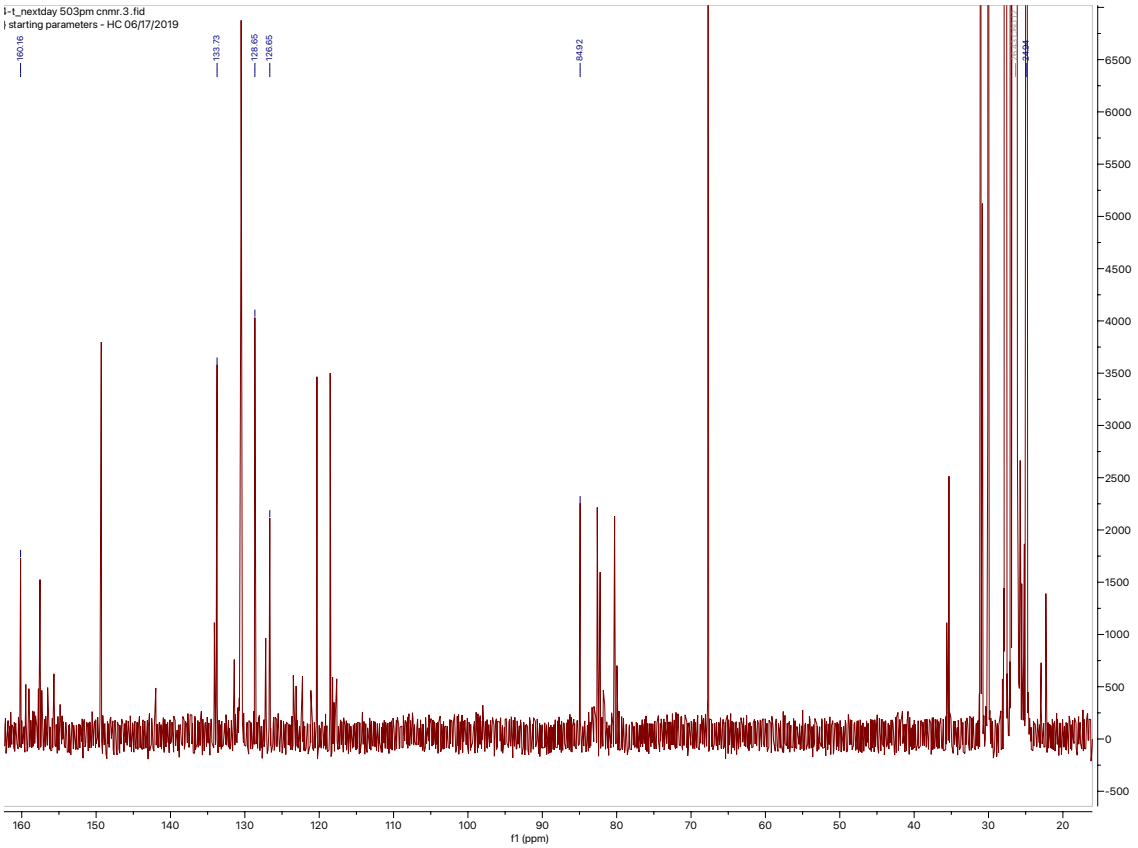

^{13}C-NMR (t_24 h)

[3-methylpyridine]

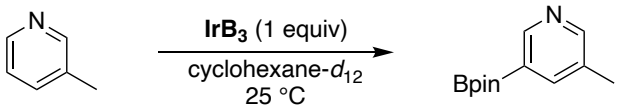

(1 equiv) 8%

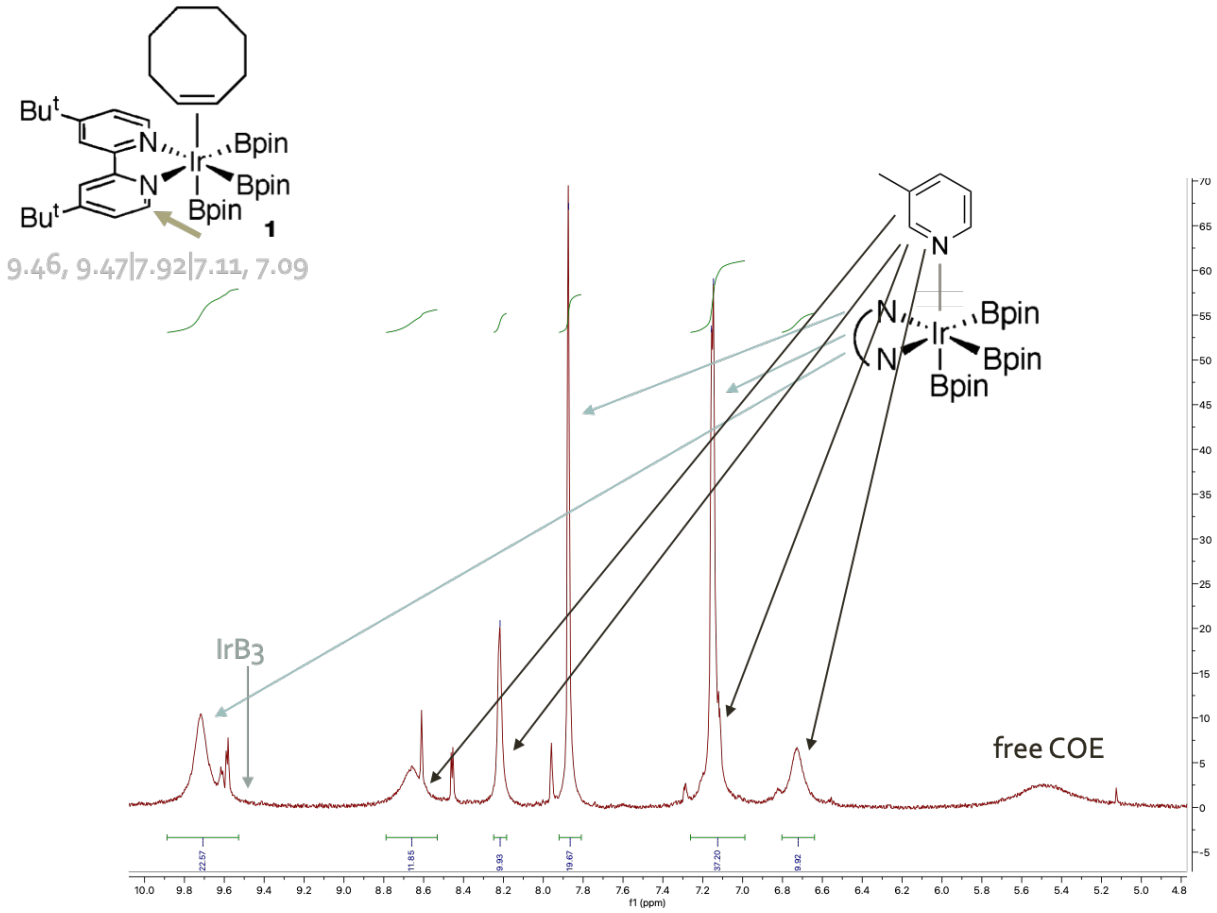
Bu^t
N
Ir
Bpin
Bpin
Bu^t
N
Bpin
1
9.46, 9.47|7.92|7.11, 7.09
IrB3
free COE
f1 (ppm)

^{1}H-NMR (t_5 min)

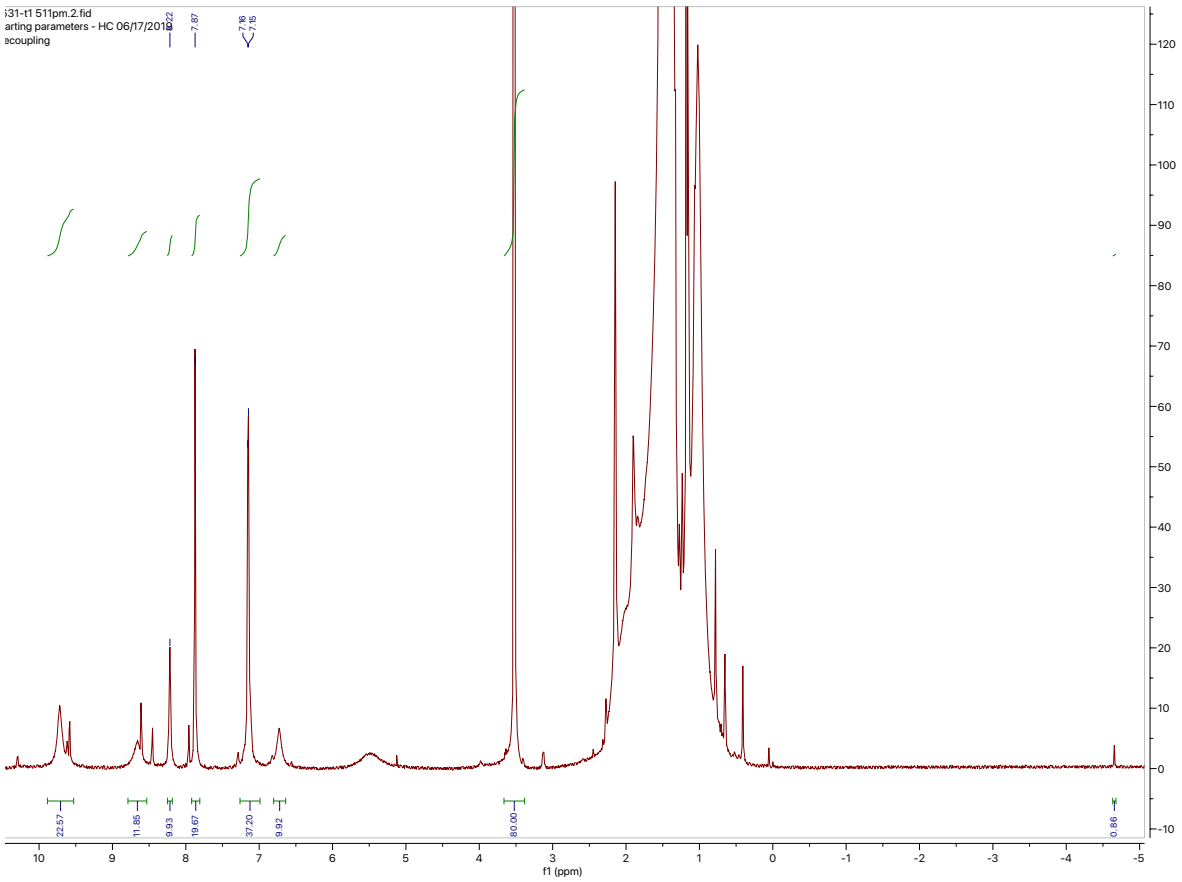

^{1}H-NMR (t_5 min)

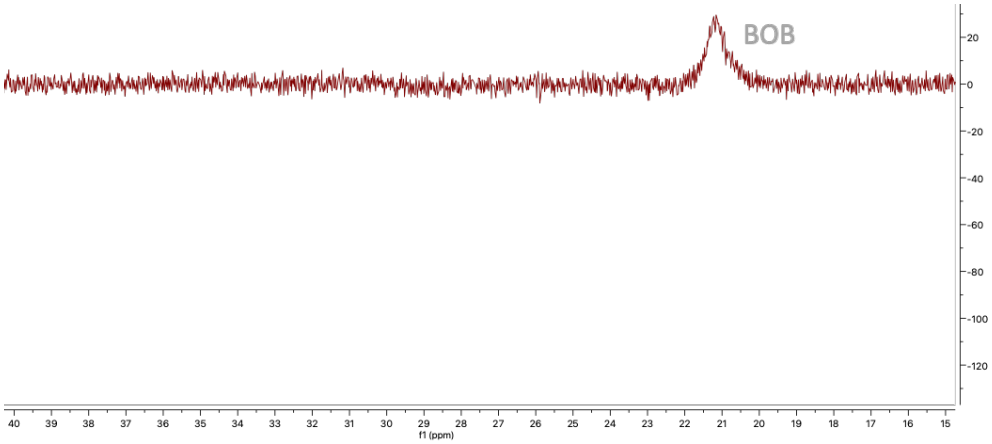

^{11}B-NMR (t_5 min)

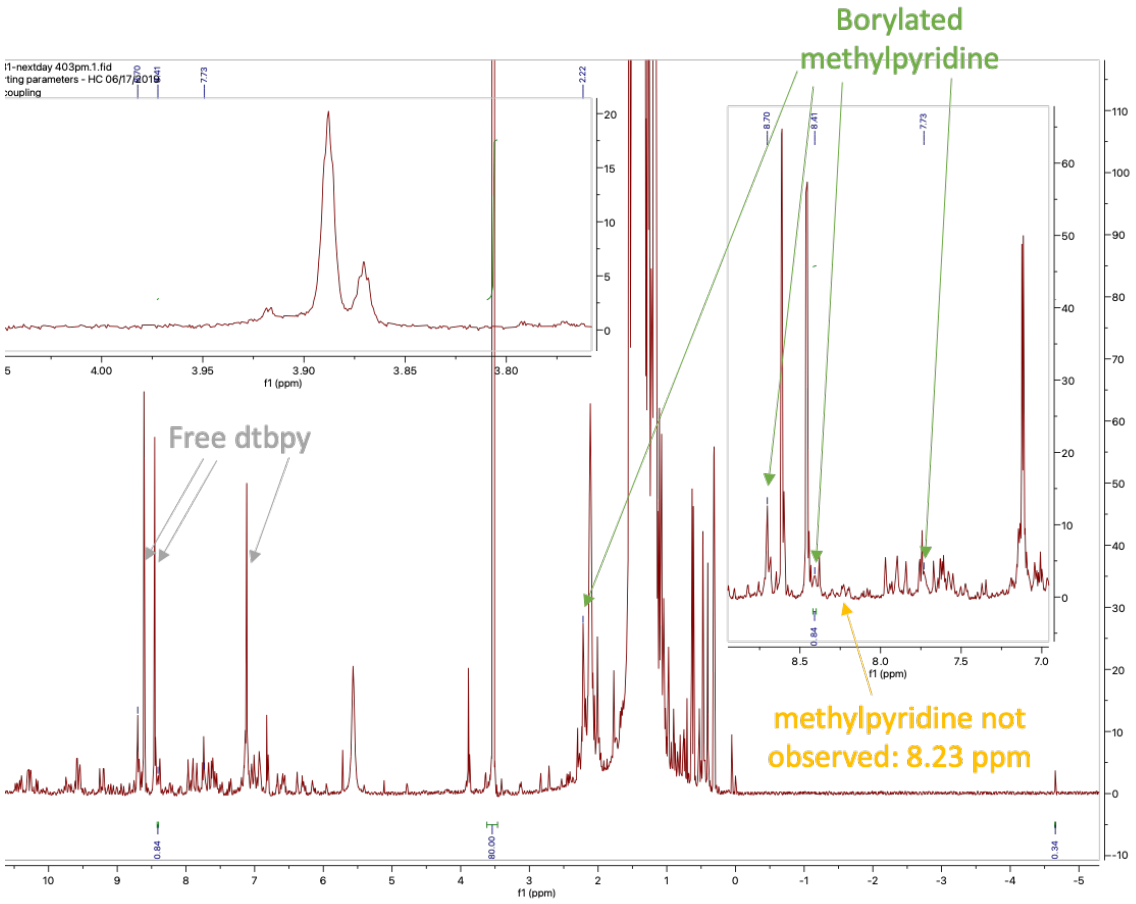

^{1}H-NMR (t_24 h)

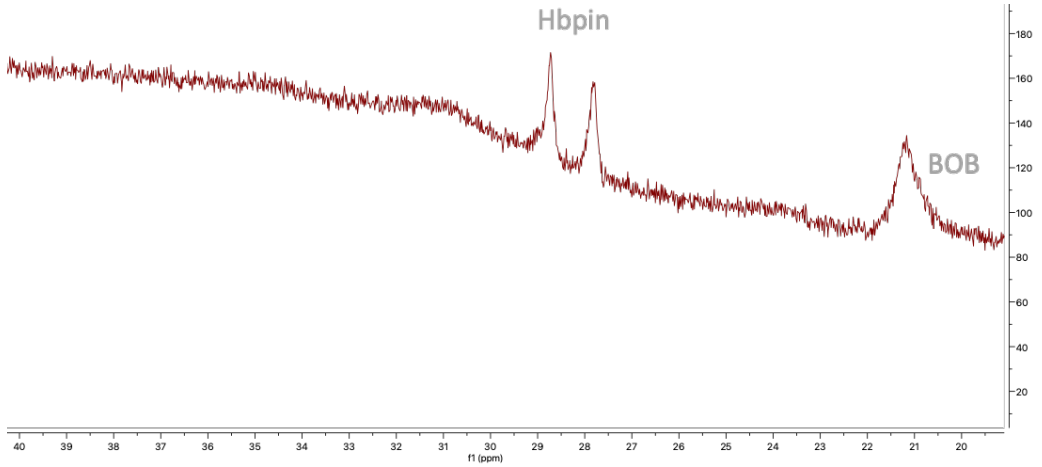

^{11}B-NMR (t_24 h)

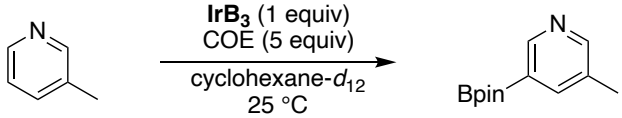

(1 equiv) 44%

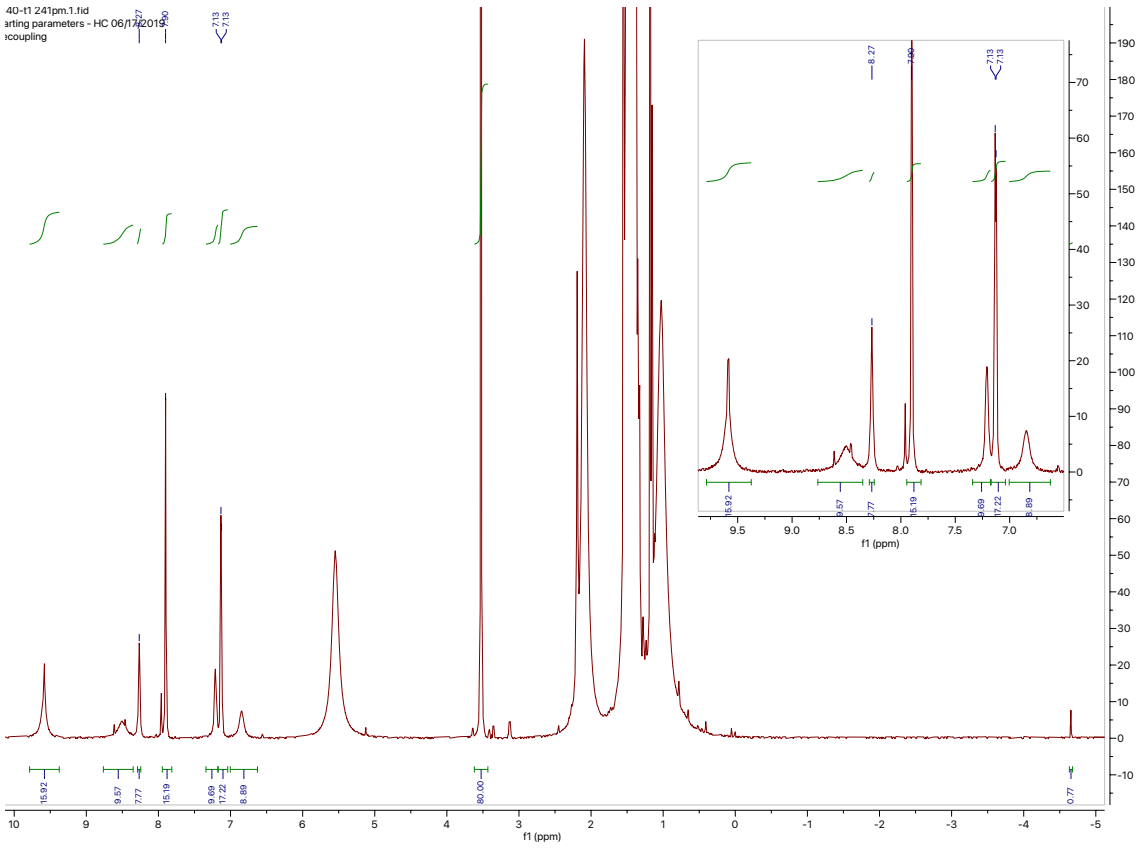

^{1}H-NMR (t_5 min)

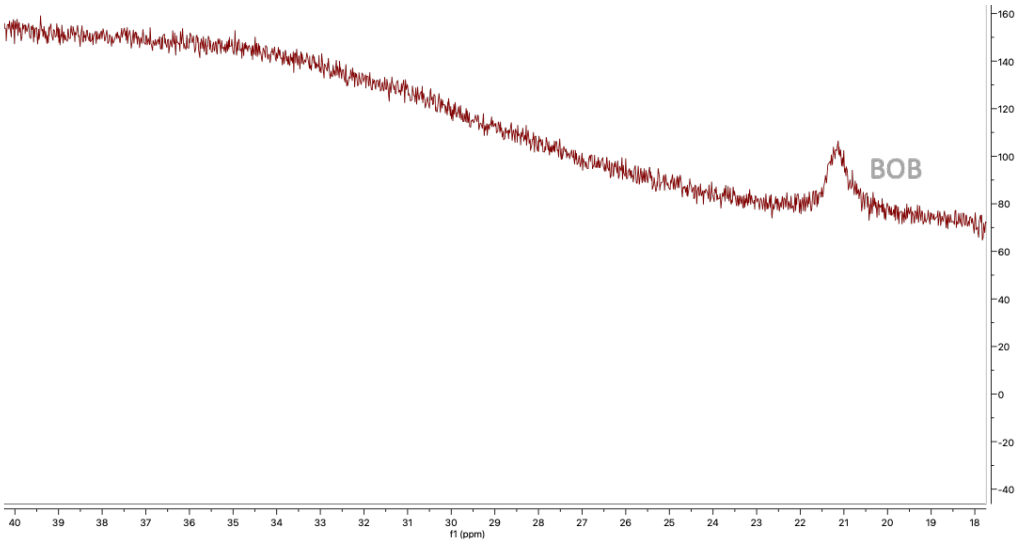

^{11}B-NMR (t_5 min)

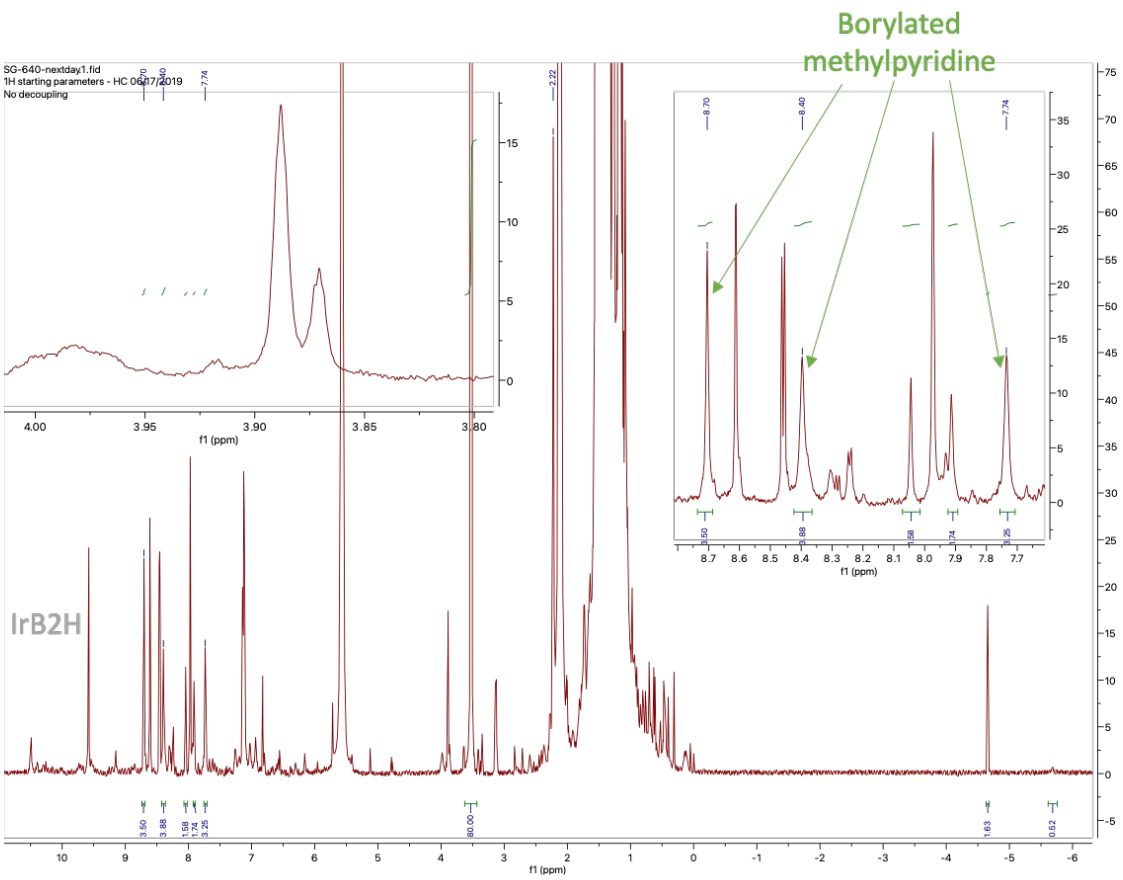

^{1}H-NMR (t_24 h)

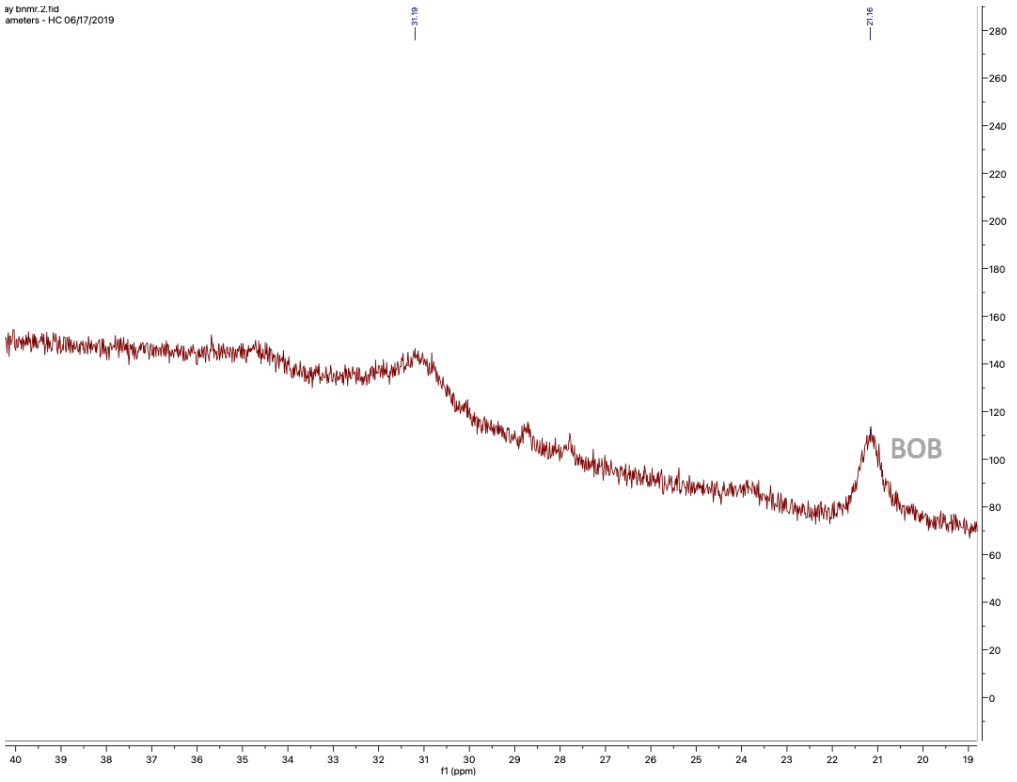

^{11}B-NMR (t_24 h)

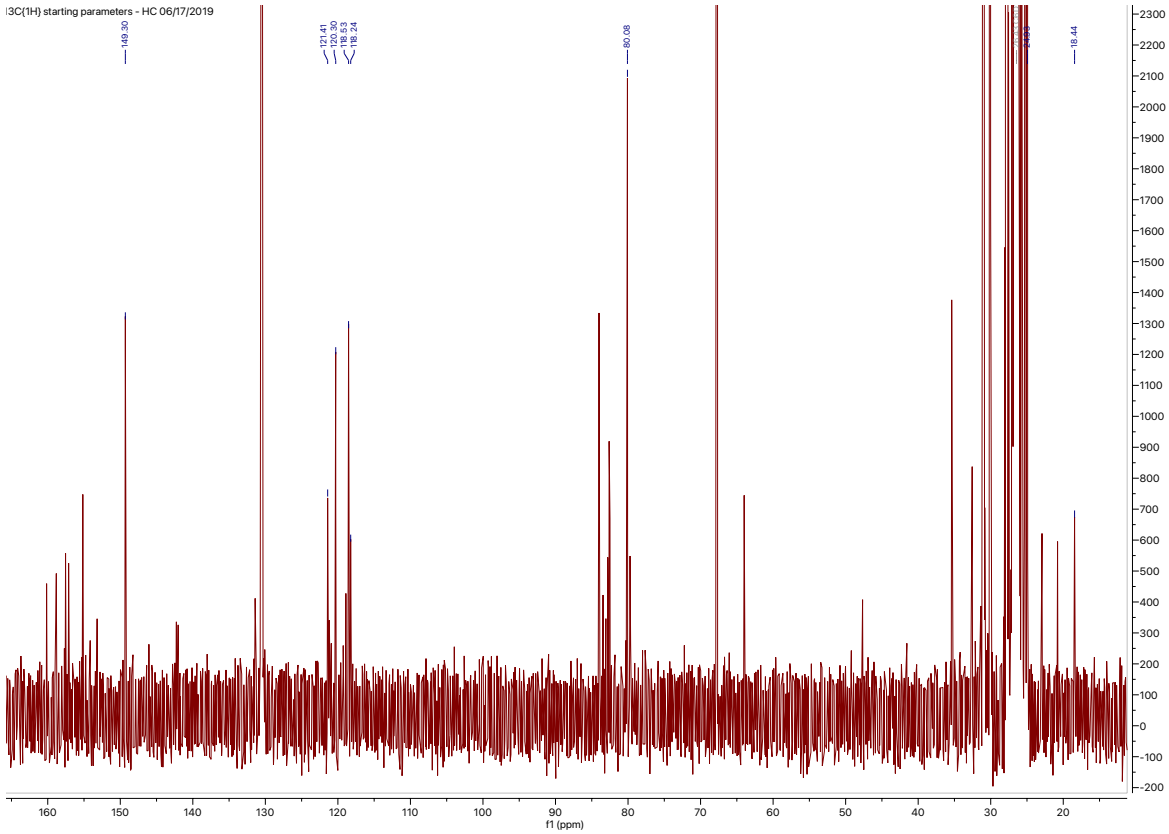

^{13}C-NMR (t_24 h)

[2-butyne]

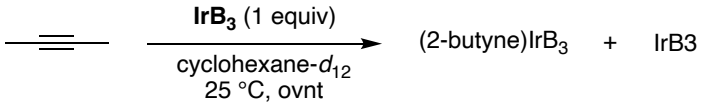

(1 equiv) 16% 81%

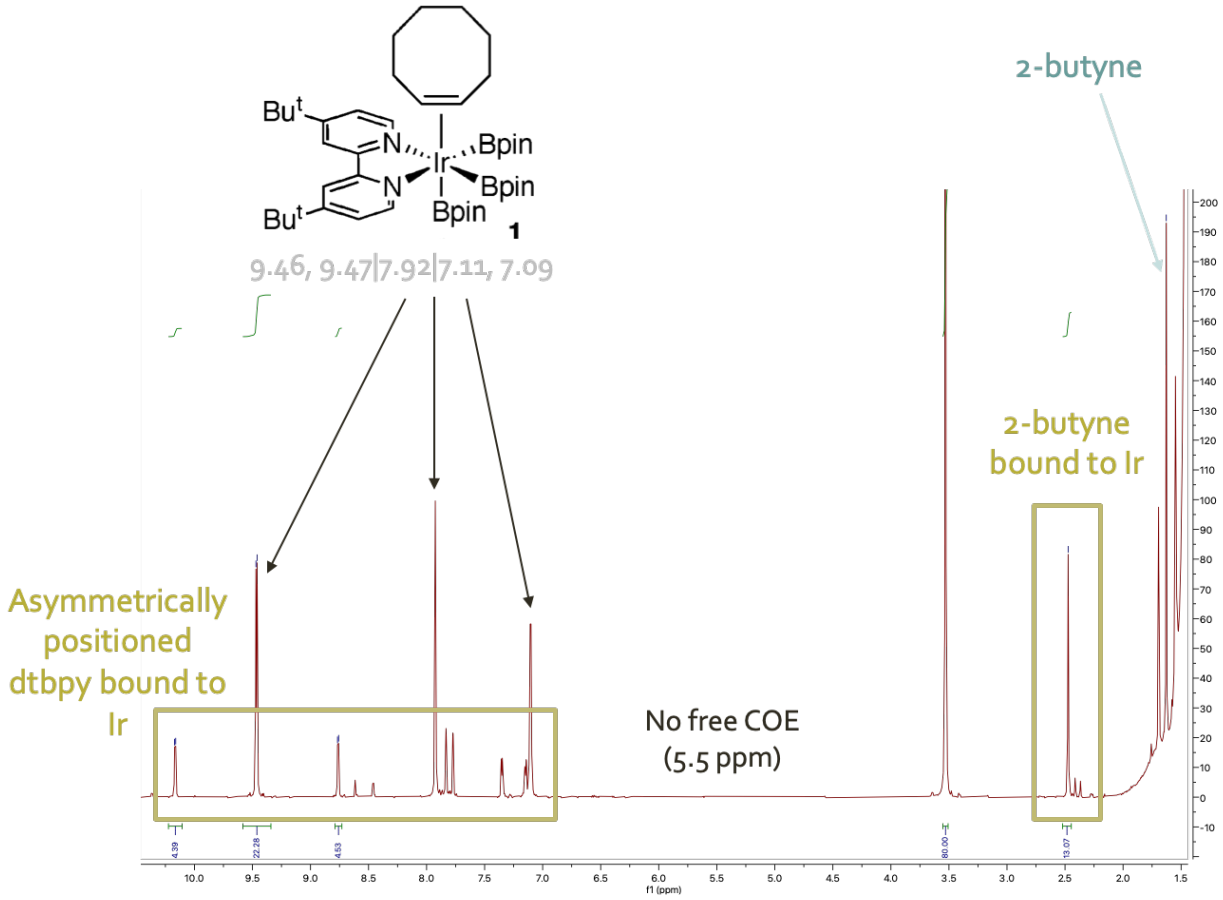
Bu^t
N
Ir
Bpin
Bpin
Bpin
Bu^t
1
9.46, 9.47|7.92|7.11, 7.09
2-butyne
2-butyne bound to Ir
Asymmetrically positioned dtbpy bound to Ir
No free COE (5.5 ppm)
f1 (ppm)

^{1}H-NMR (t_24 h)

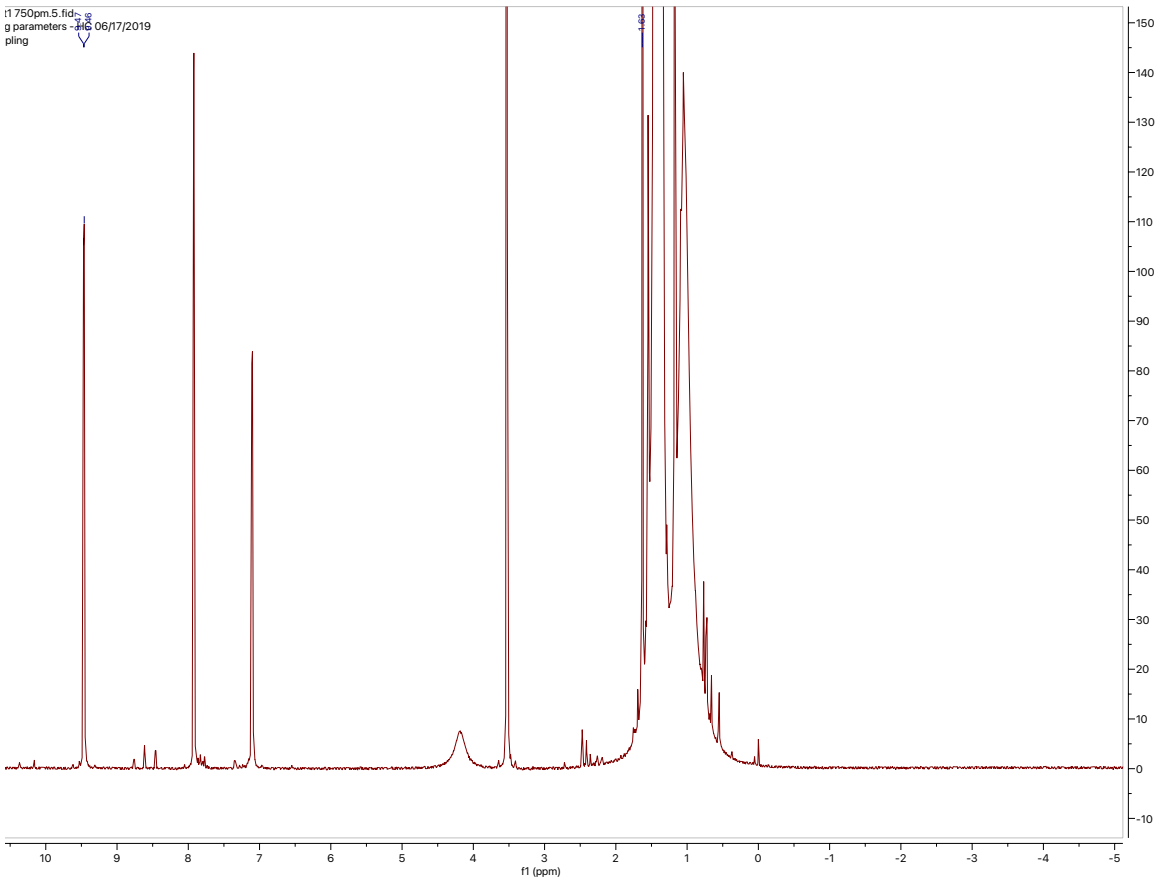

^{1}H-NMR (t_5 min)

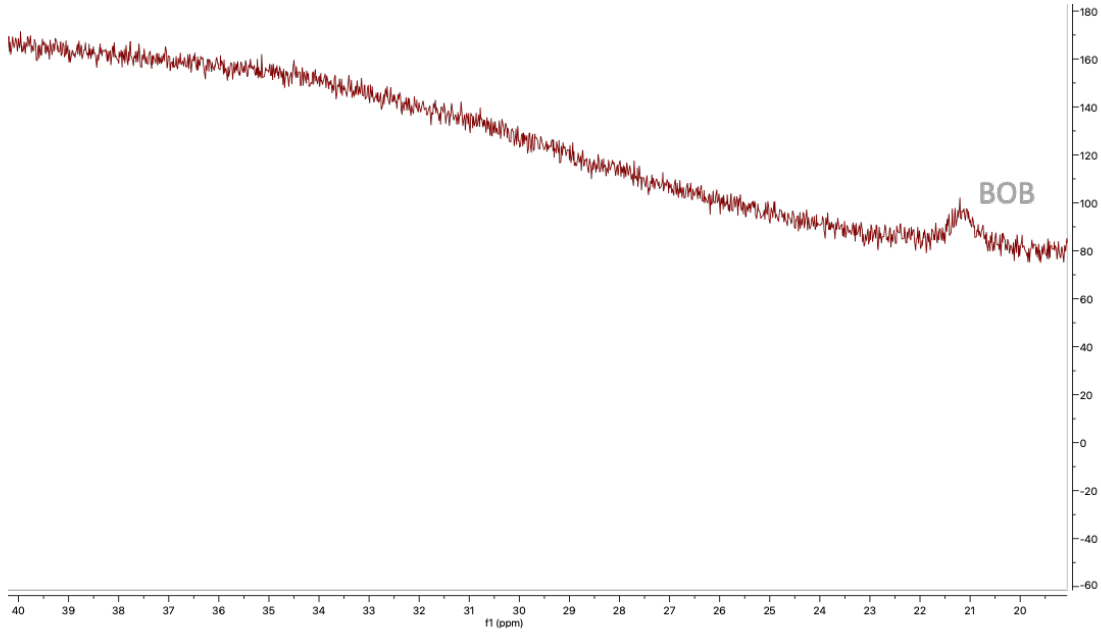

^{11}B-NMR (t_5 min)

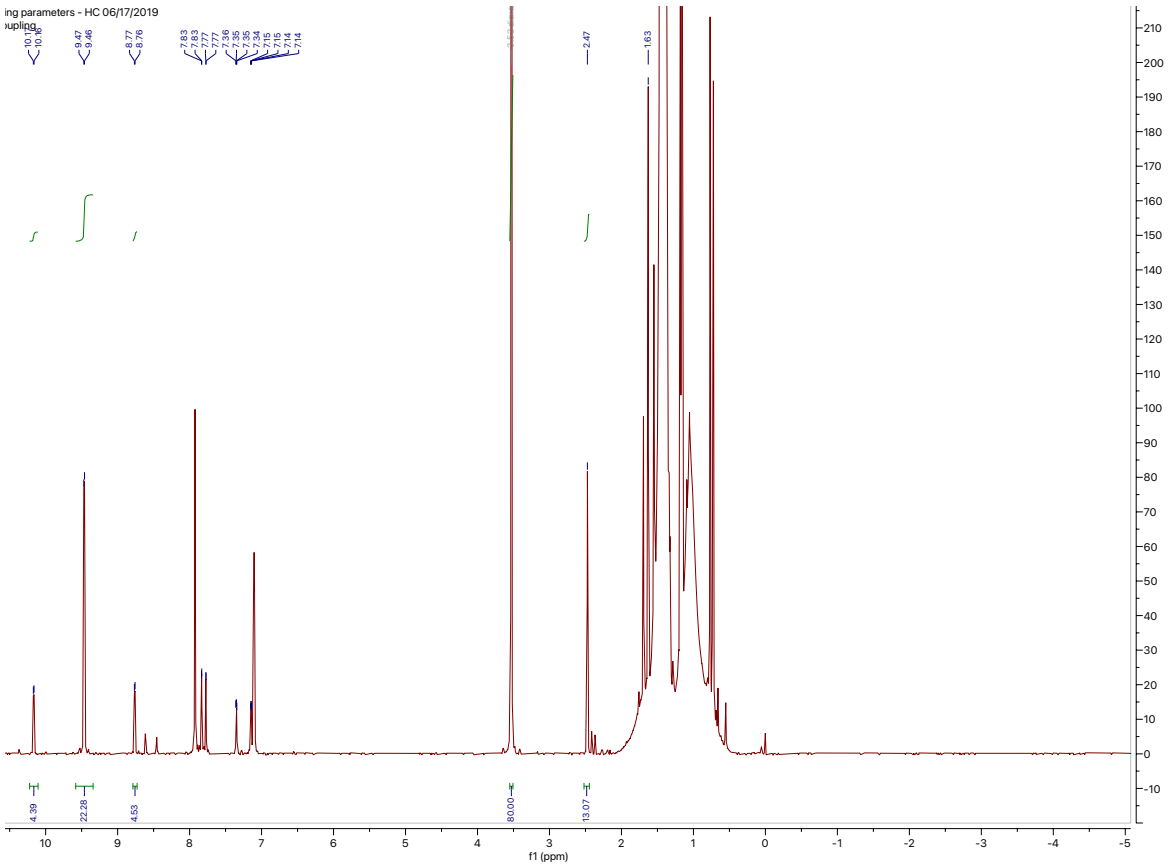

^{1}H-NMR (t_24 h)

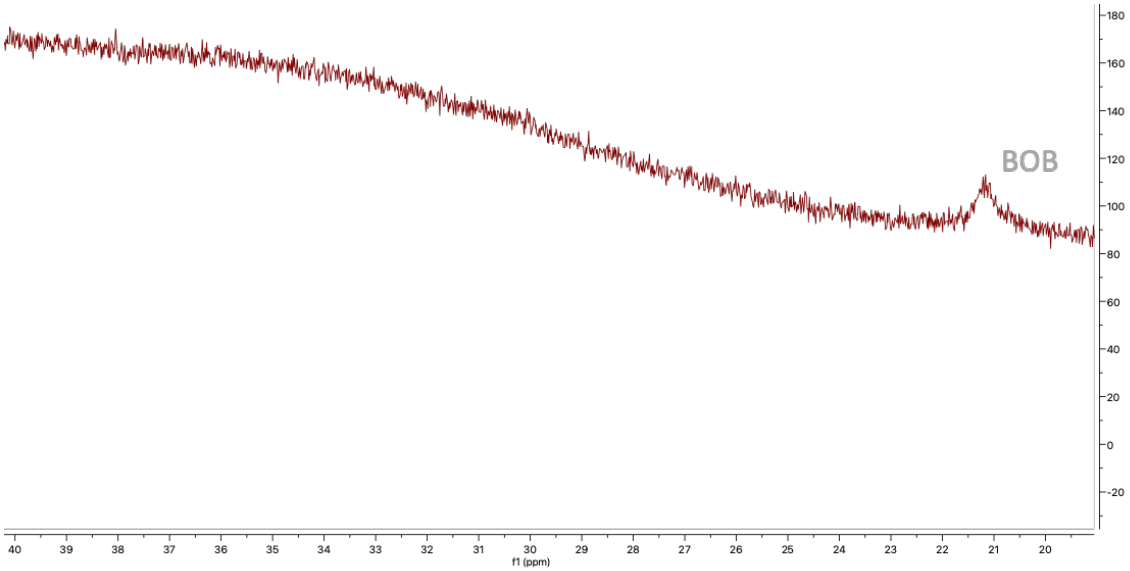

^{11}B-NMR (t_24 h)

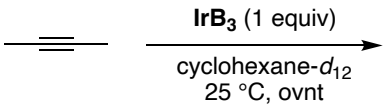

	(2-butyne)IrB_3	+	IrB3
(1 equiv)	16%		81%
	100 °C, 1 h		
	(2-butyne)IrB_3	+	IrB3
	18%		0%

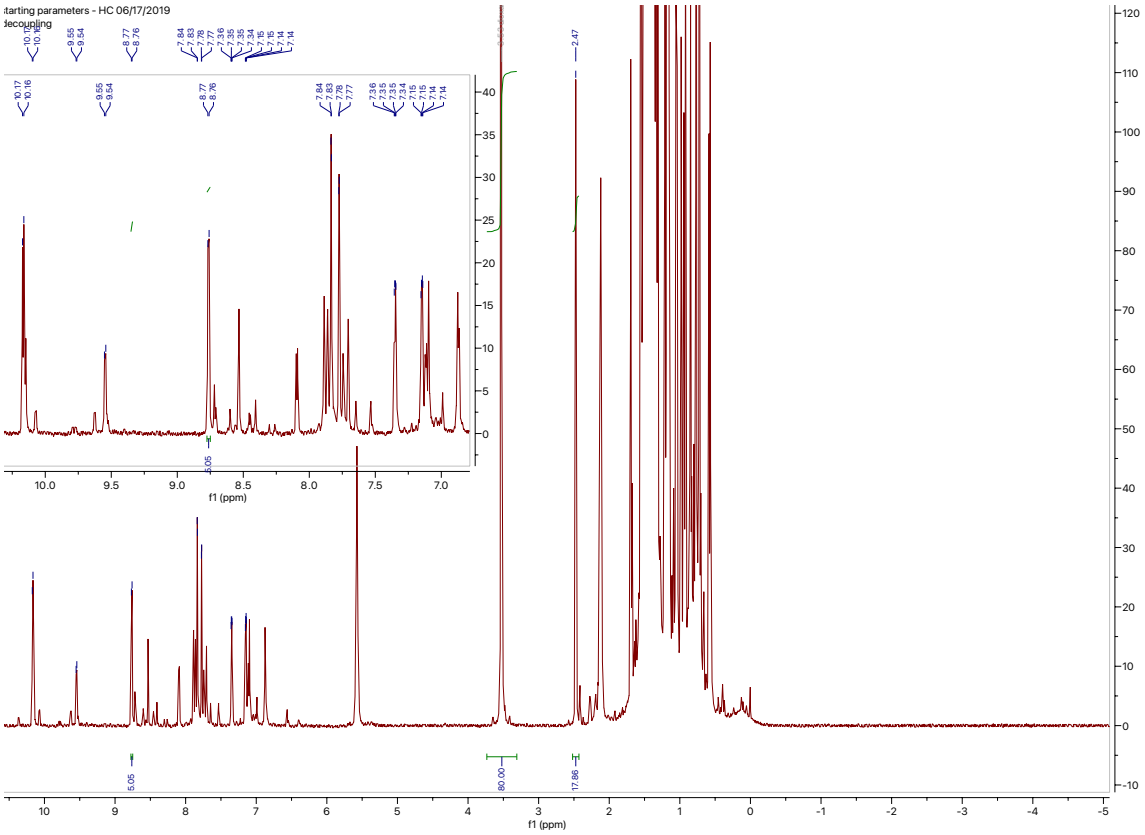

^{1}H-NMR (100 °C, 1 h)

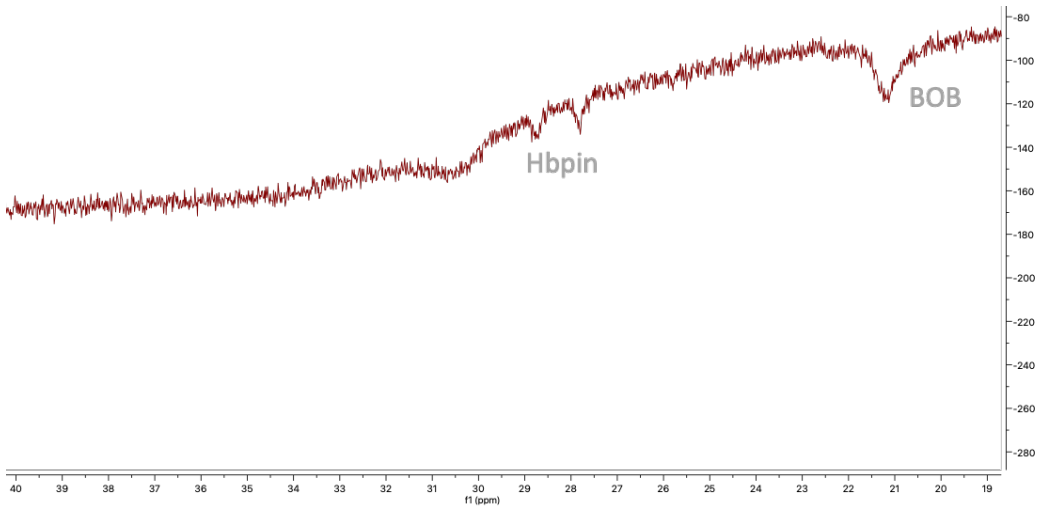

^{11}B-NMR (100 °C, 1 h)

[benzothiophene]

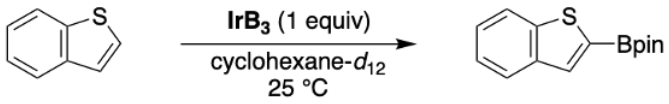

(1 equiv) 98%

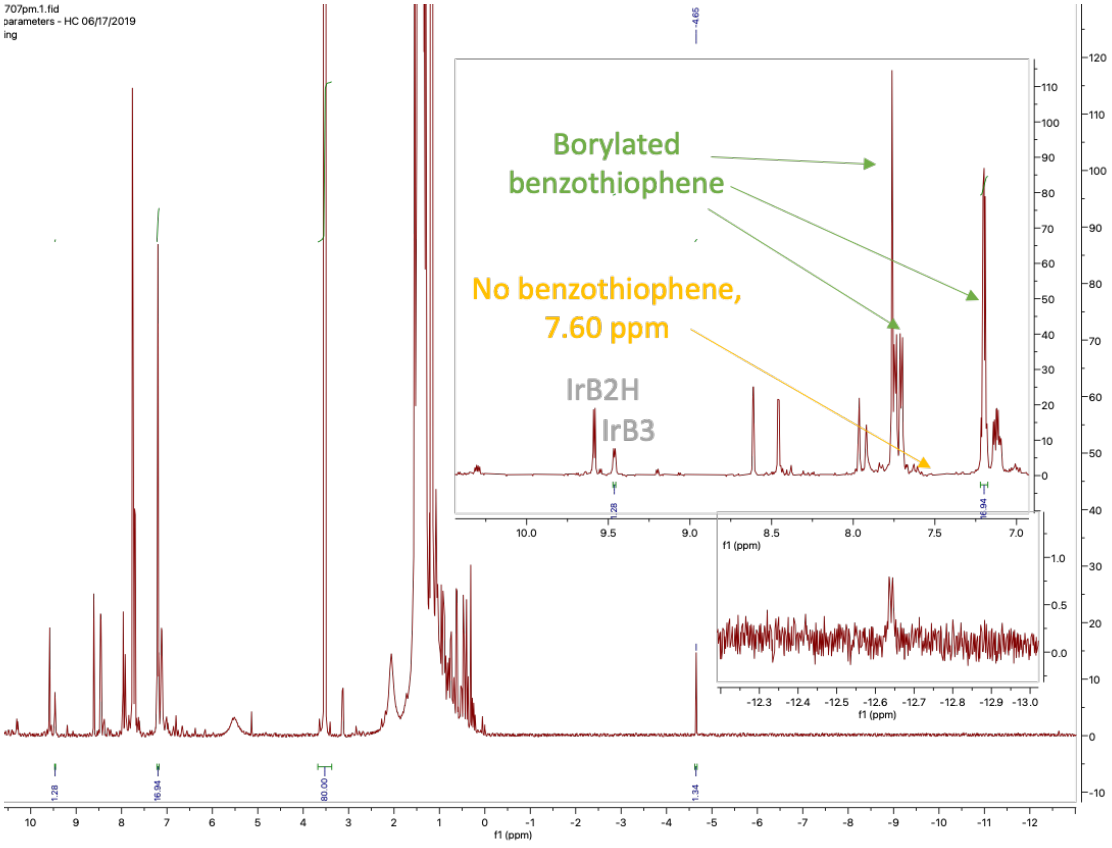

^{1}H-NMR (t_5 min)

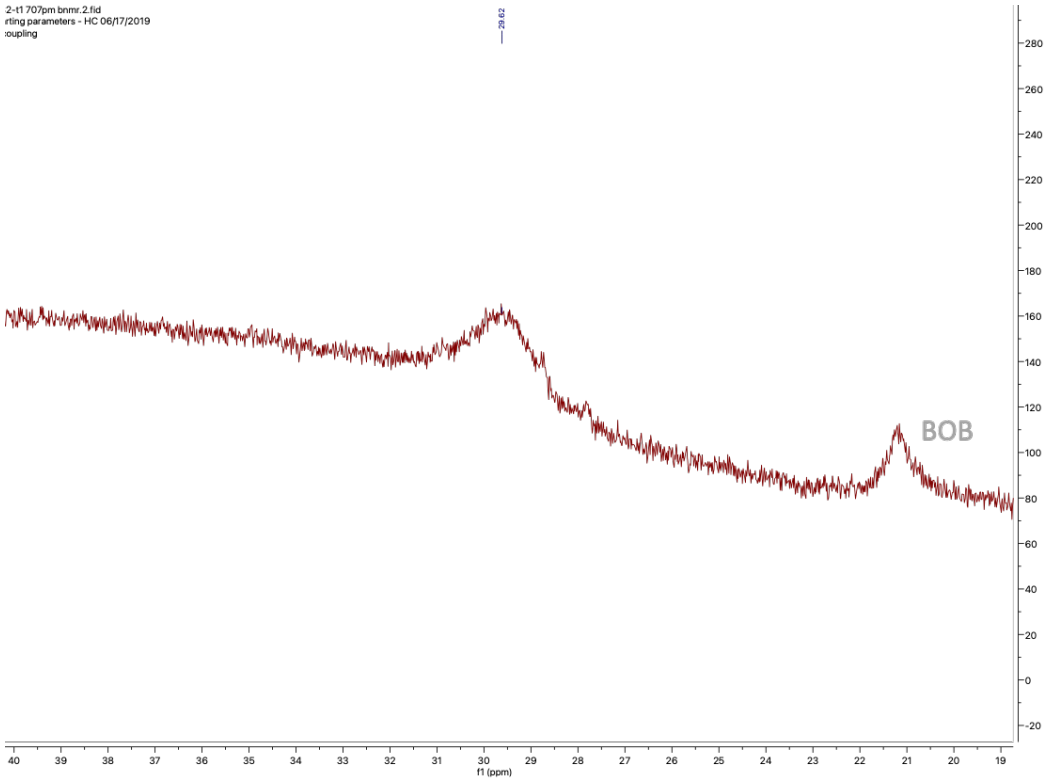

^{11}B-NMR (t_5 min)

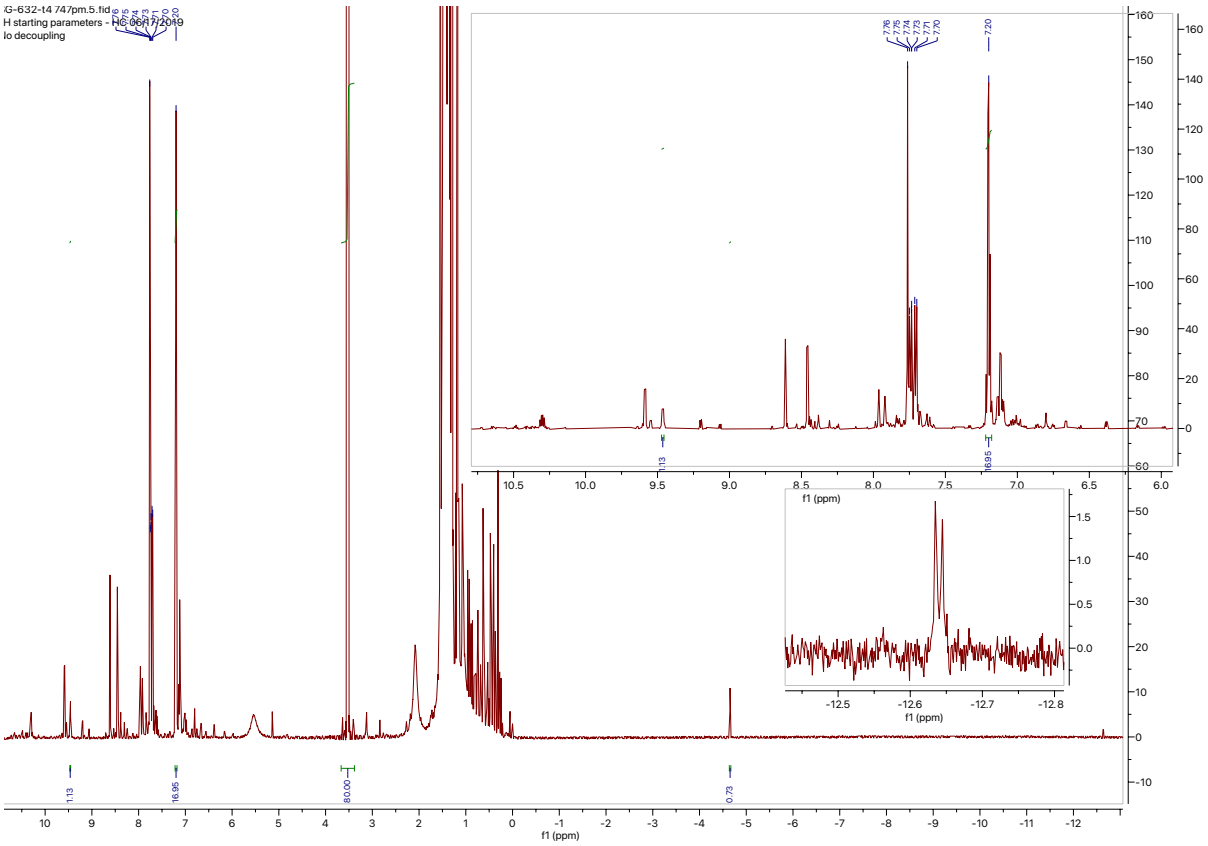

^{1}H-NMR (t_24 h)

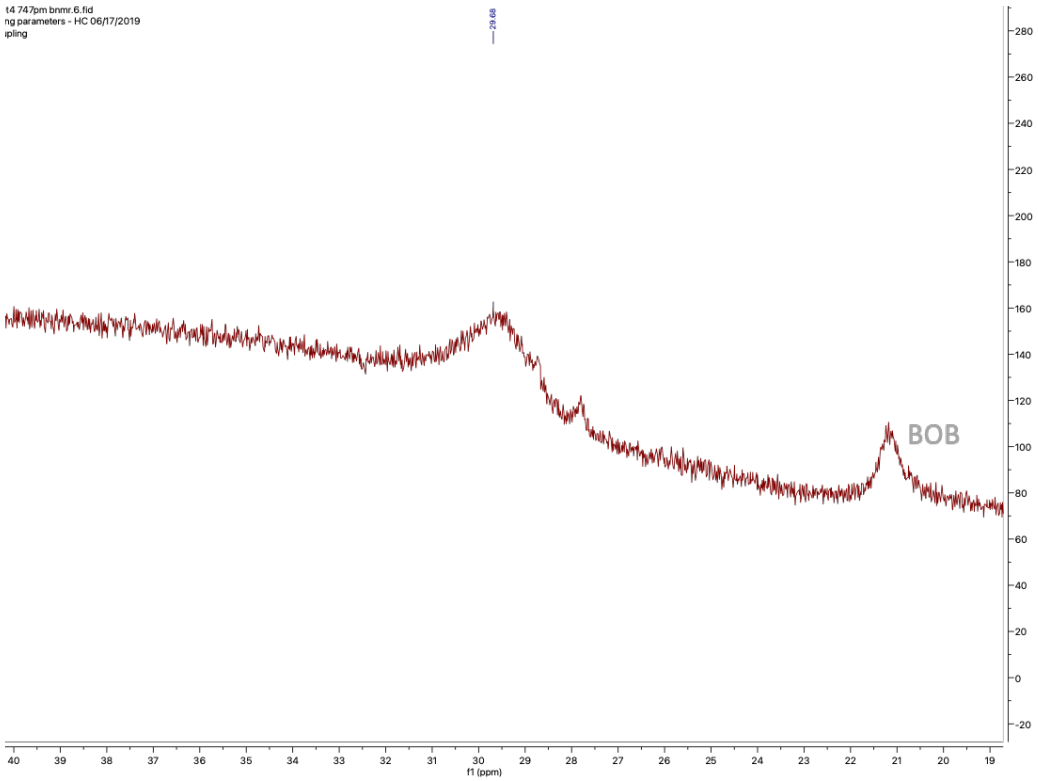

^{11}B-NMR (t_24 h)

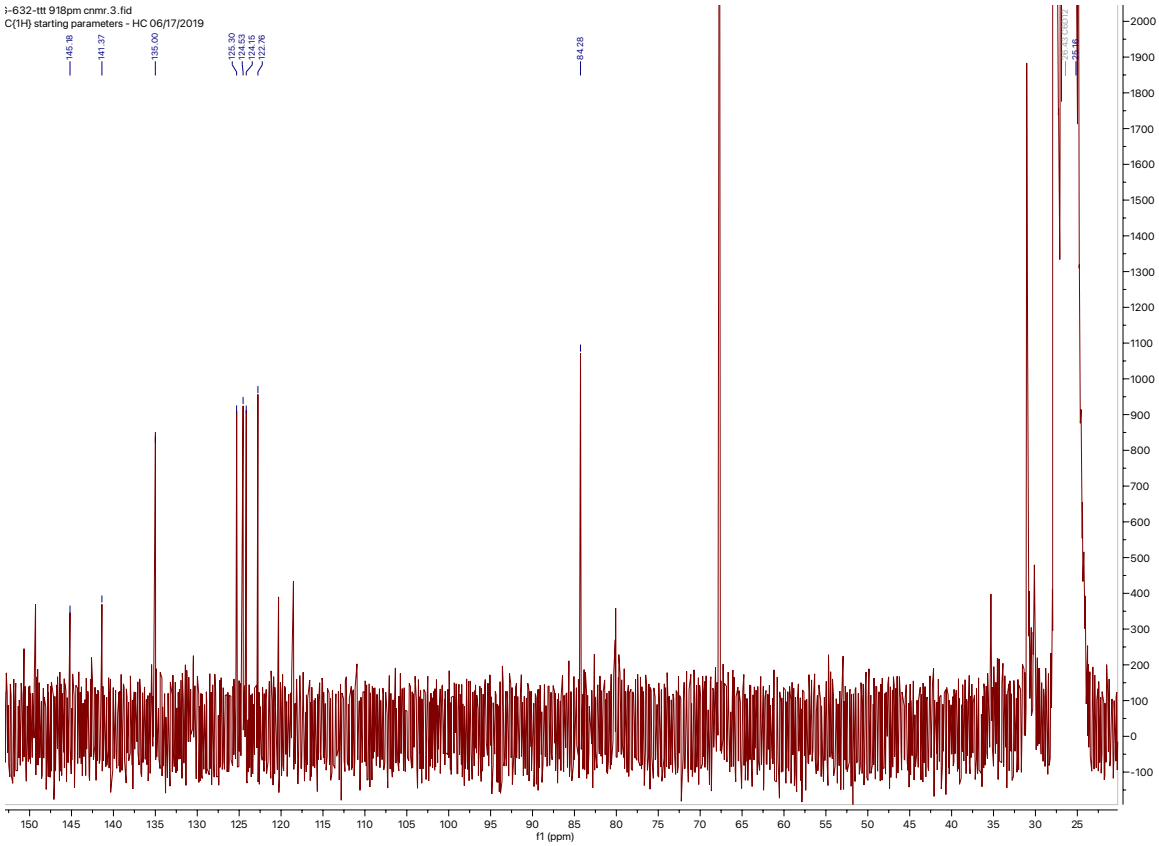

^{13}C-NMR (t_24 h)

Note: **C**—Bpin not observable in this sample or in that of the authentic standard

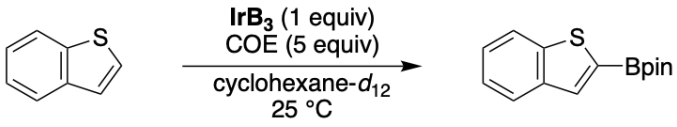

(1 equiv) 98%

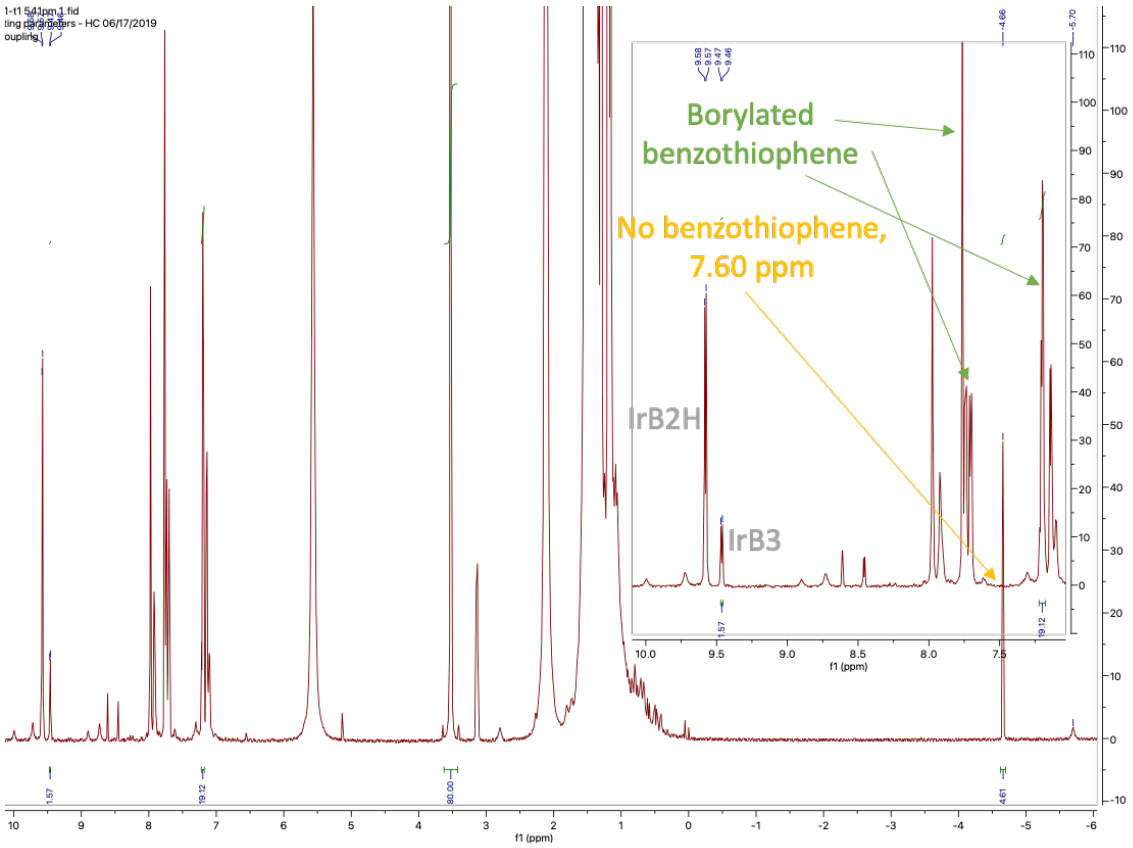
Borylated
benzothiophene
No benzothiophene,
7.60 ppm
IrB2H
IrB3
f1 (ppm)

^{1}H-NMR (t_5 min)

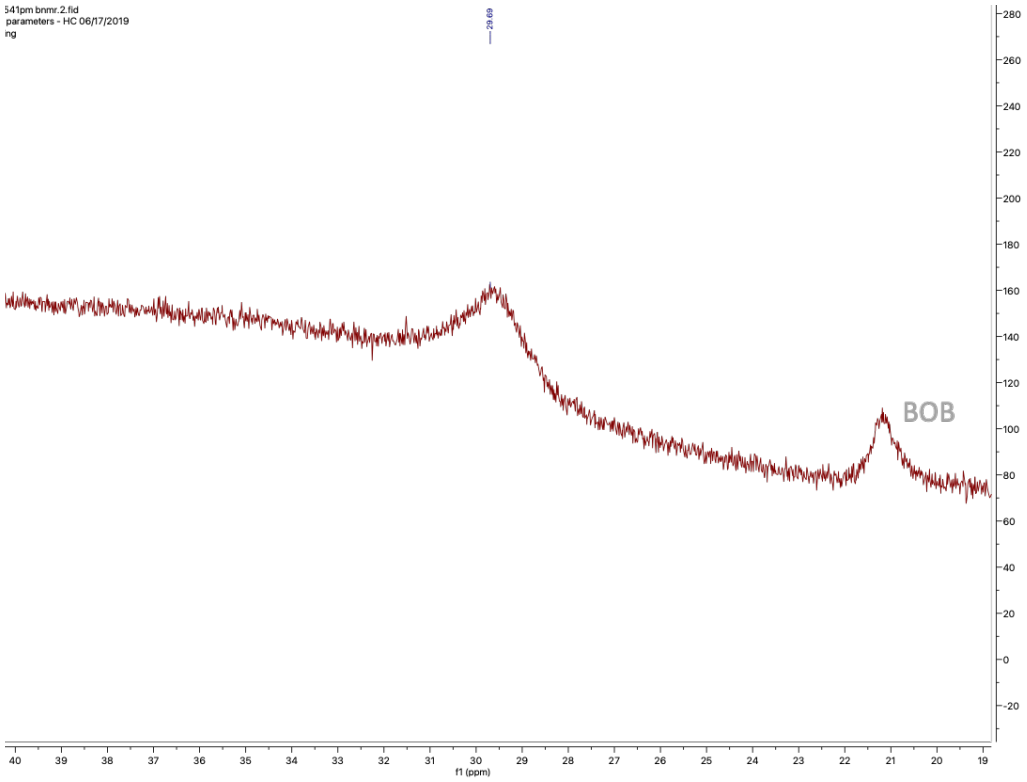
BOB
f1 (ppm)

^{11}B-NMR (t_5 min)

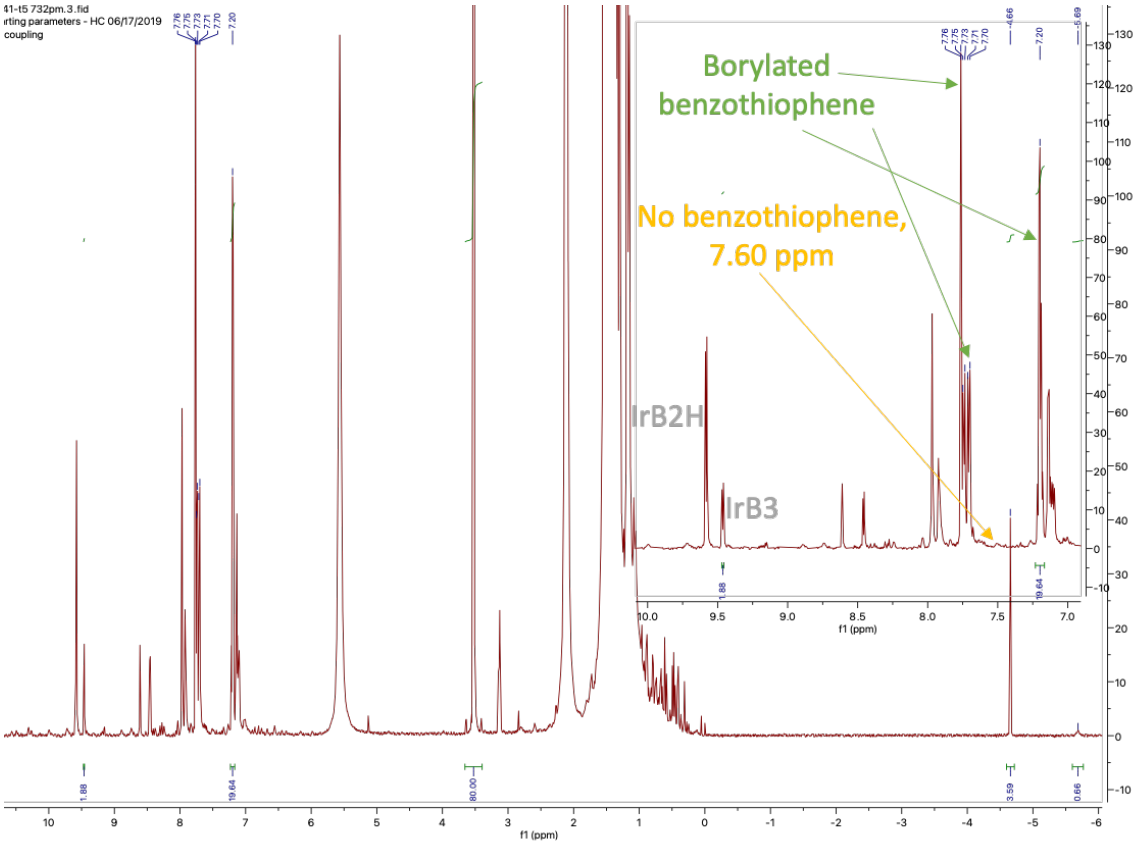

^{1}H-NMR (t_24 h)

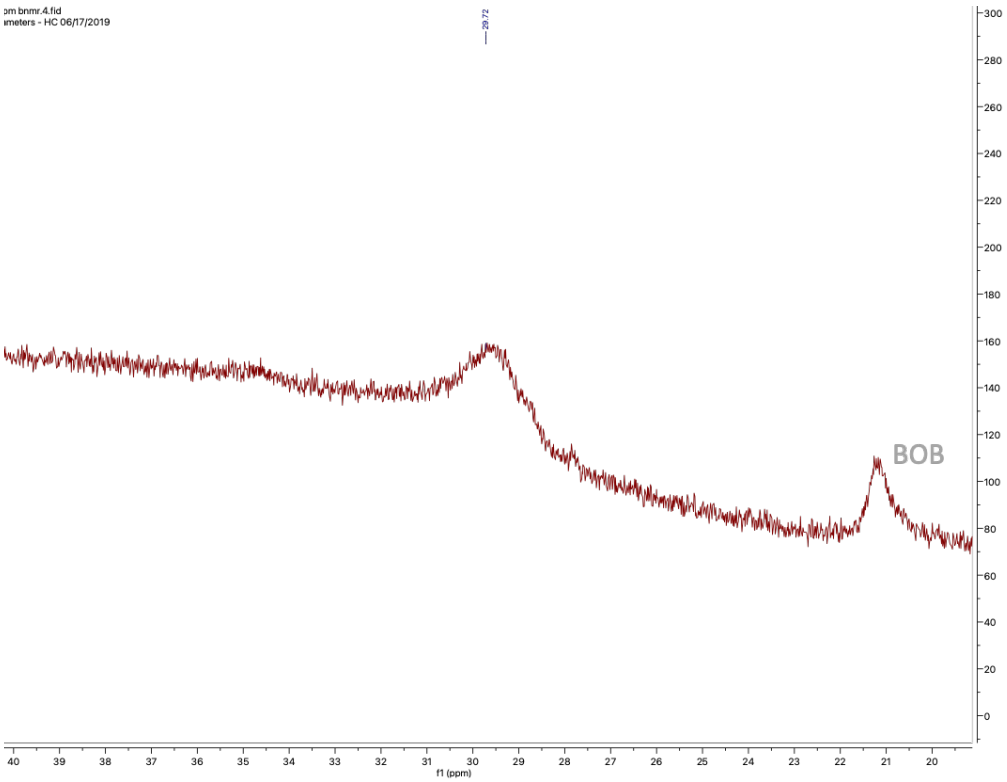

^{11}B-NMR (t_24 h)

[methylindole]

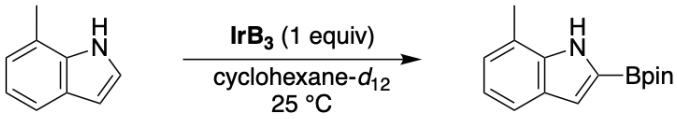

(1 equiv) 99%

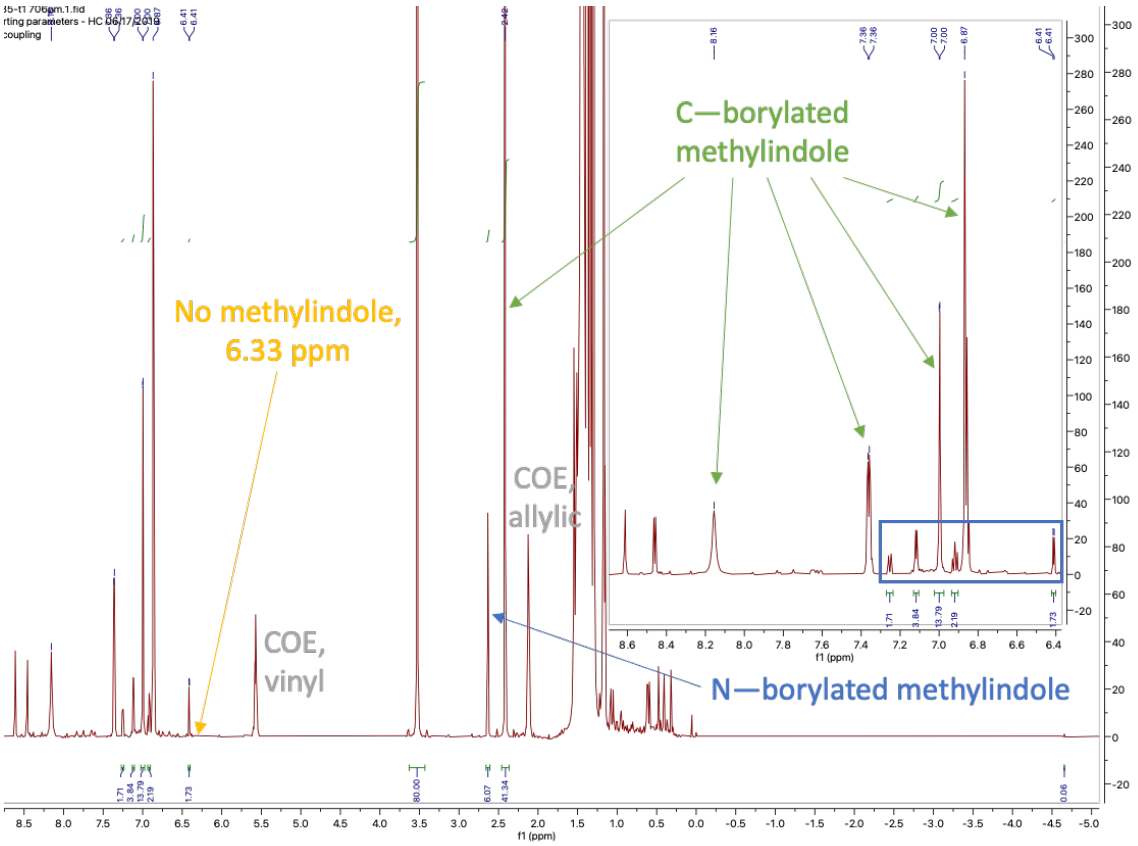

^{1}H-NMR (t_5 min)

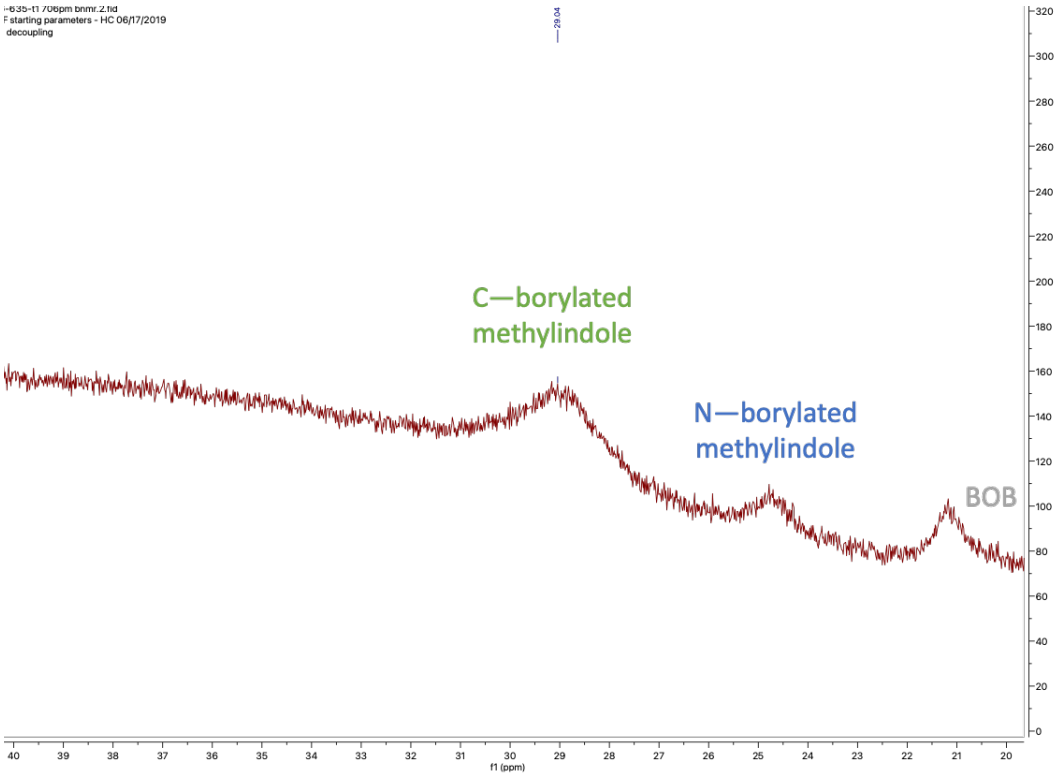

^{11}B-NMR (t_5 min)

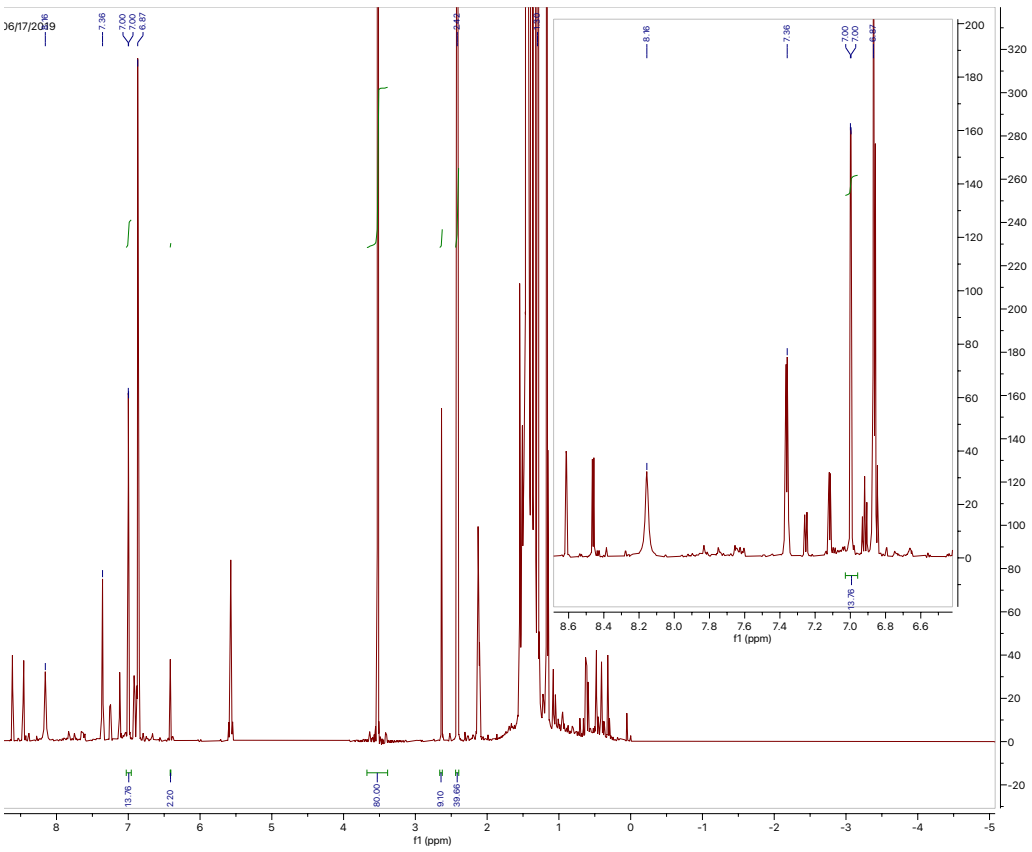

^{1}H-NMR (t_24 h)

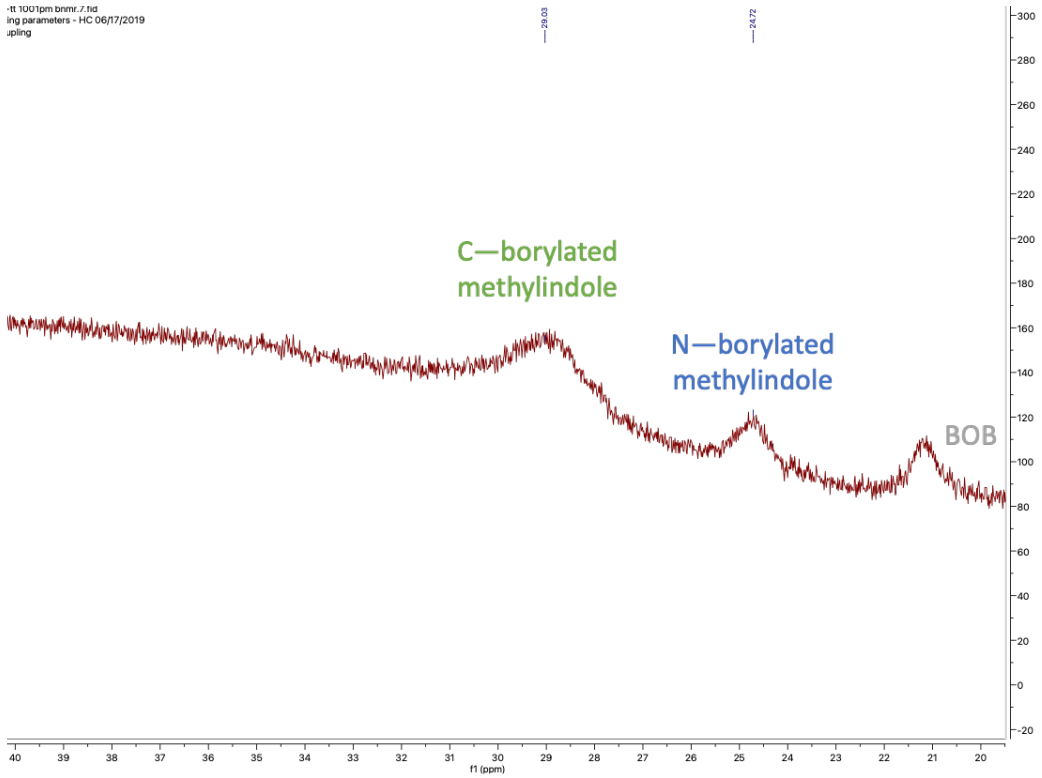

^{11}B-NMR (t_24 h)

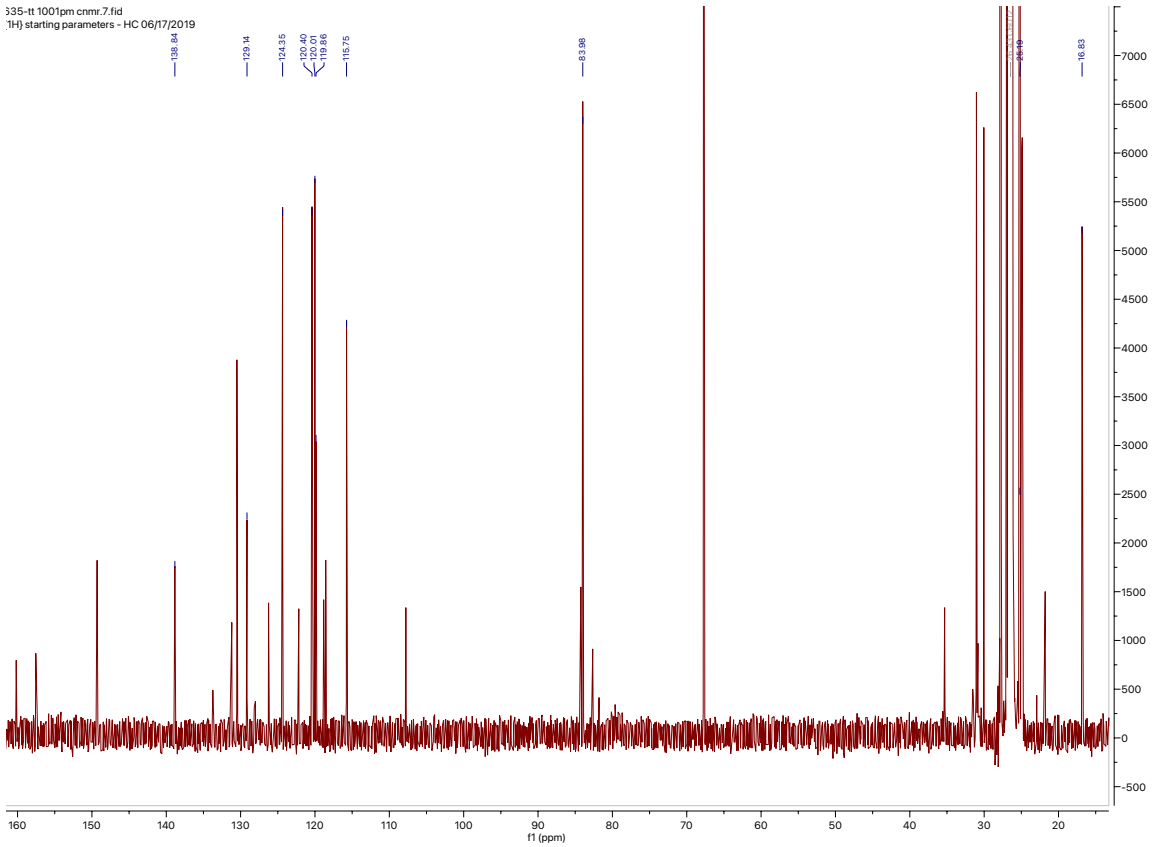

^{13}C-NMR (t_24 h)

Note: **C**—Bpin challenging to observe (104.14 ppm)

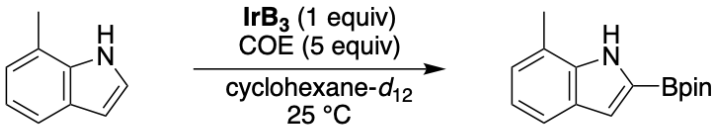

(1 equiv) 90%

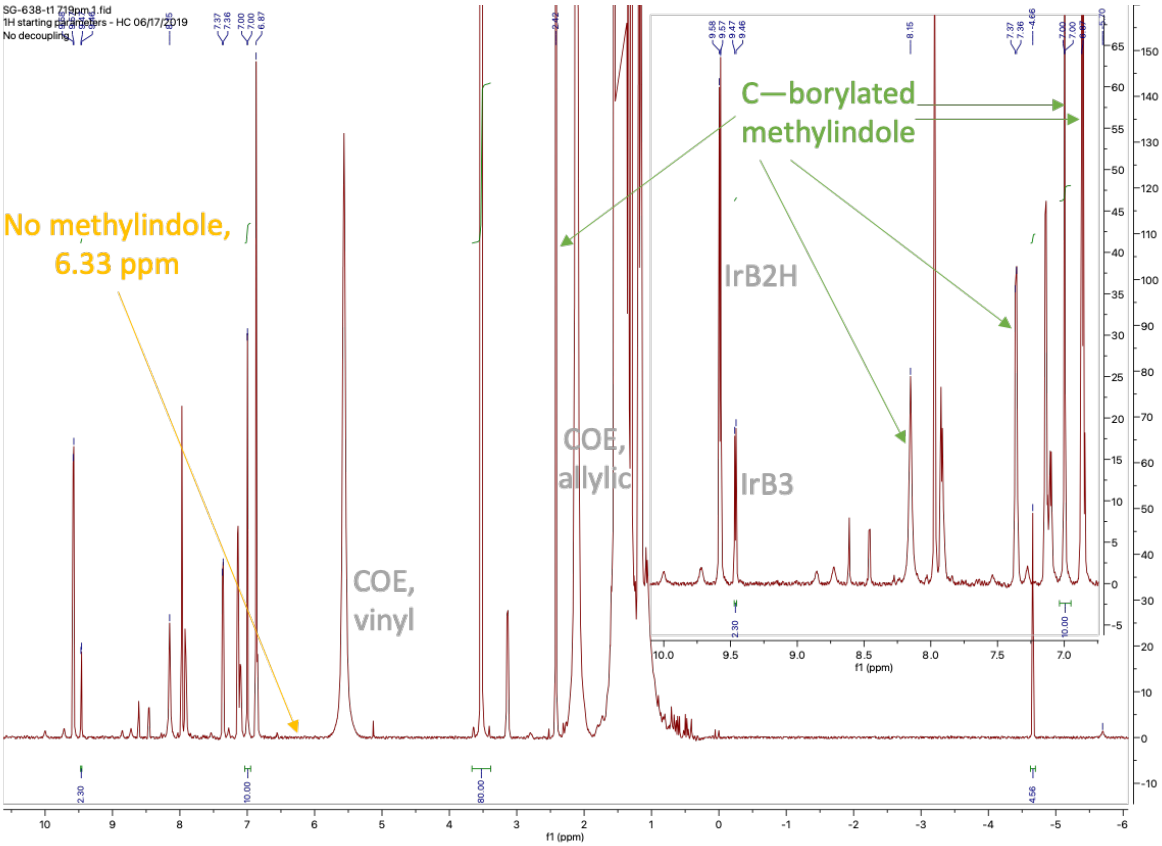

^{1}H-NMR (t_5 min)

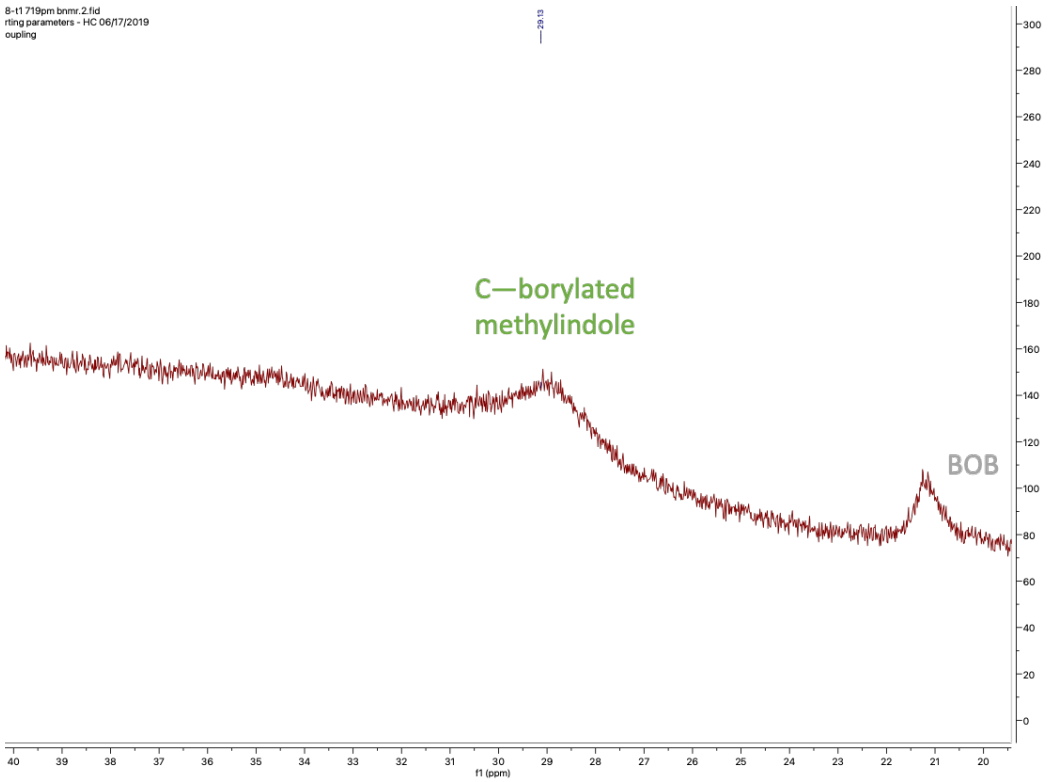

^{11}B-NMR (t_5 min)

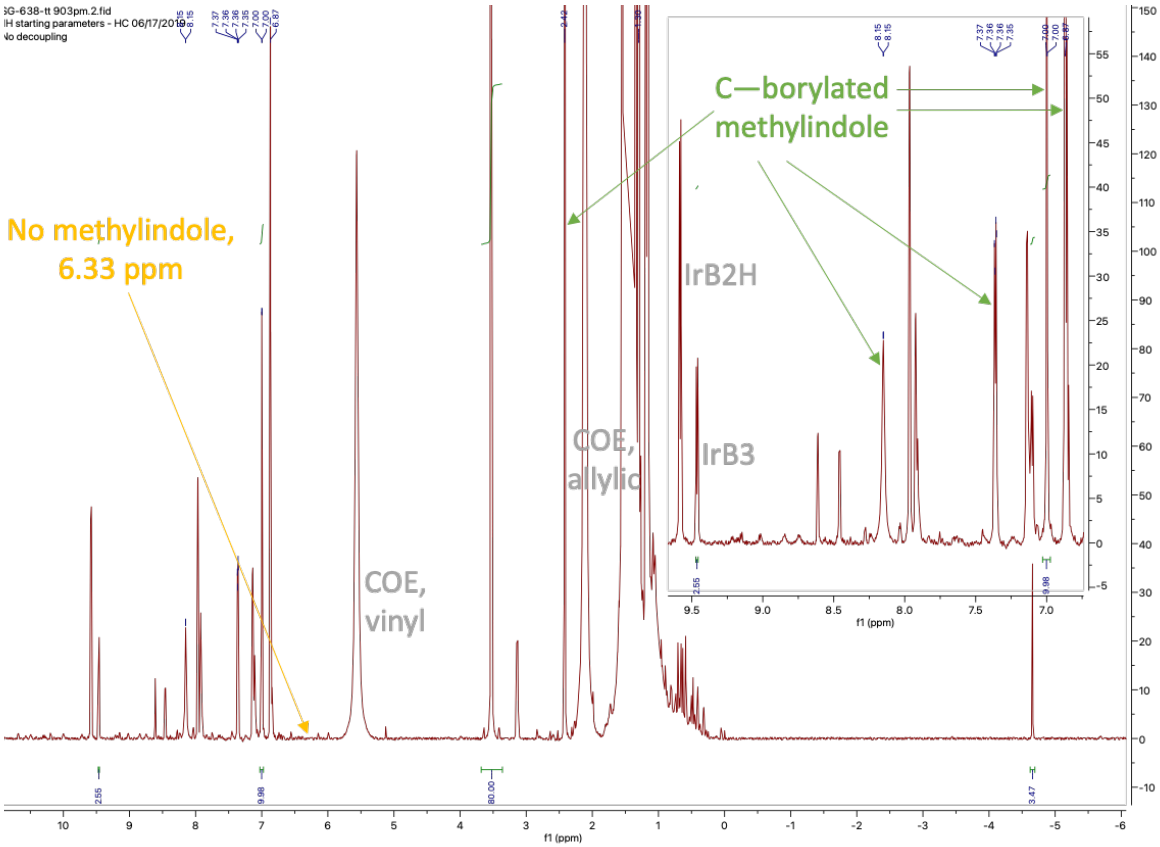

^{1}H-NMR (t_24 h)

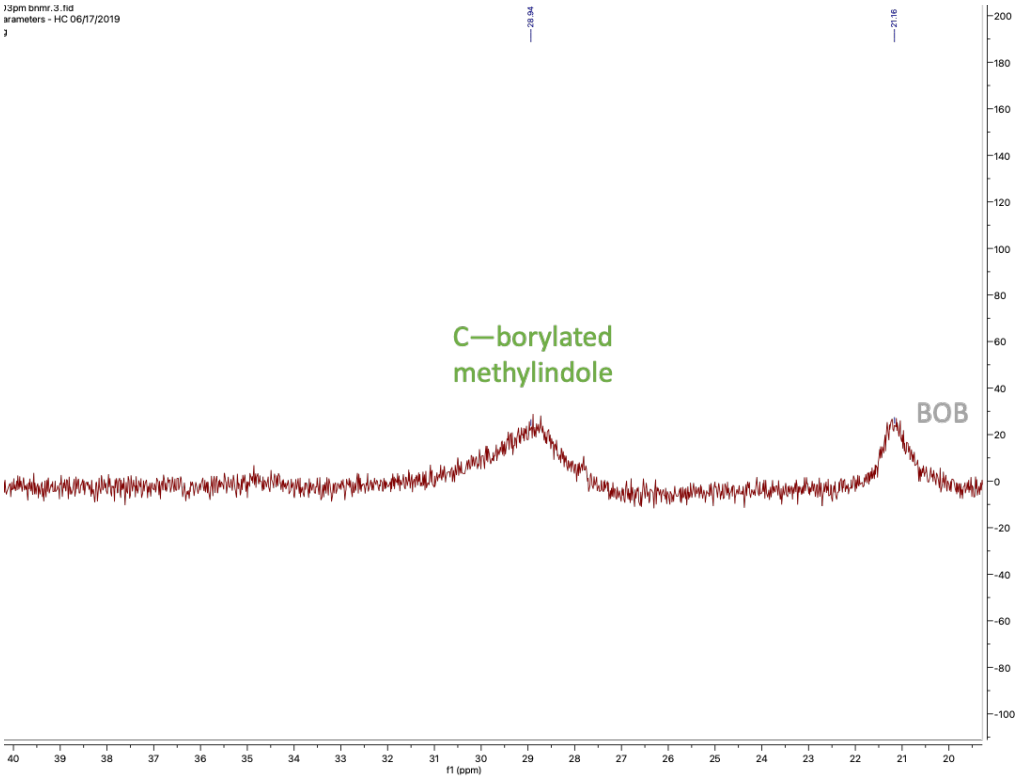

^{11}B-NMR (t_24 h)

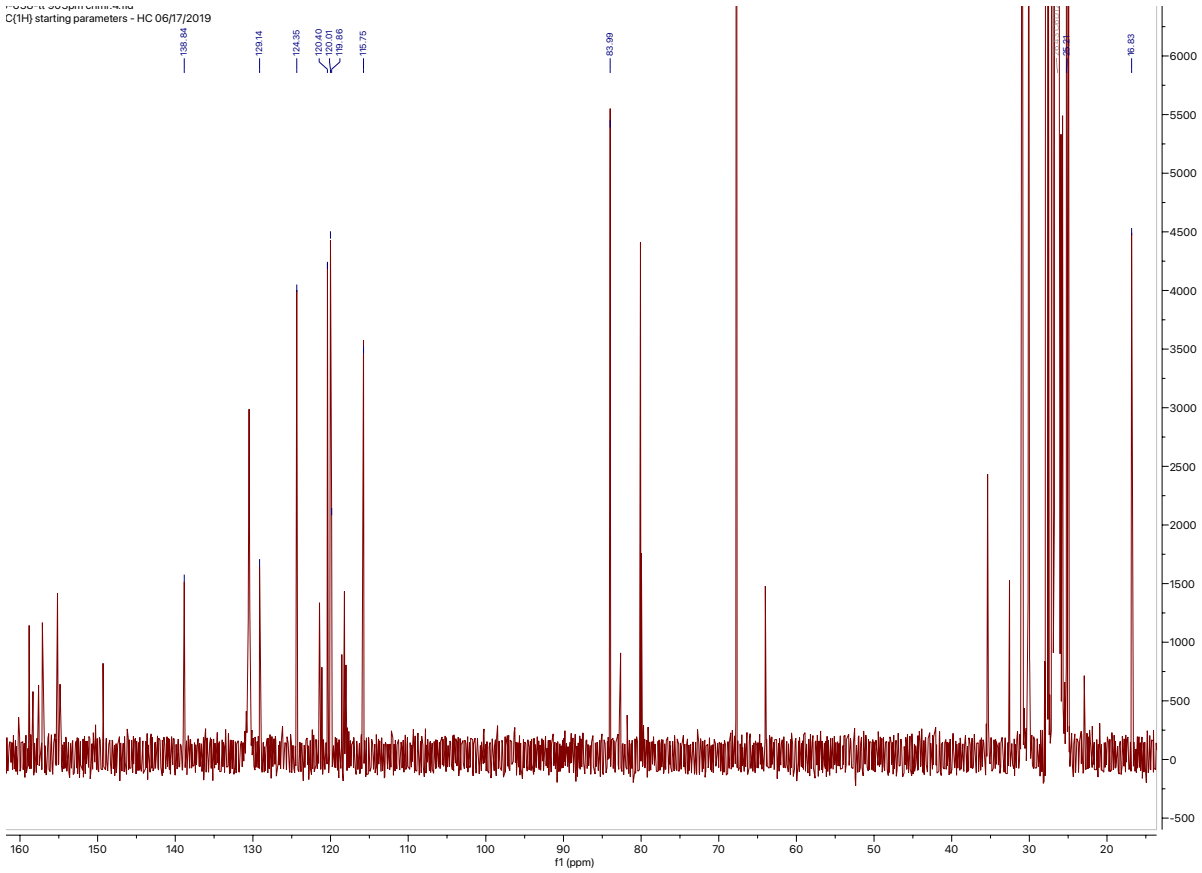

^{13}C-NMR (t_24 h)

Note: **C**—Bpin challenging to observe (104.14 ppm)

1.4.4 Synthesis of Borylated Additives

General Procedure 1

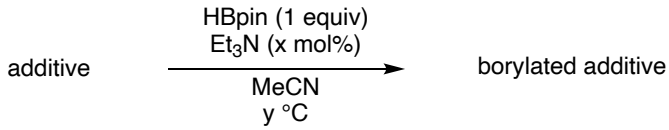

(1 equiv)

In a glovebox, under an inert atmosphere of nitrogen, to a 4-mL vial equipped with a stir bar was added the additive (in this case, dodecylamine) (140 mg, 0.75 mmol) which was diluted with an excess of acetonitrile (approximately 1 mL). HBpin (91 mg, 0.75 mmol) was added and the solution was stirred for 18 h.

General Procedure 2

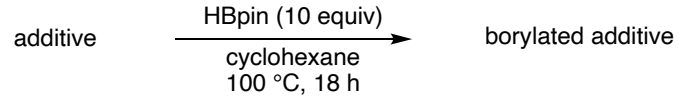

(1 equiv)

In a glovebox, under an inert atmosphere of nitrogen, to a 4-mL vial equipped with a stir bar was added the additive (in this case, 1-hexanol) (30 mg, 0.3 mmol) which was diluted with cyclohexane (650 uL). HBpin (0.4 mL, 3 mmol) was added. The vial was sealed and allowed to stir at 100 °C for 18 h. The vial was allowed to cool to room temperature. The borylated compound was diluted with C_6D_{12} for ^{1}H-NMR, ^{11}B-NMR and ^{13}C-NMR spectroscopy.

General Procedure 3

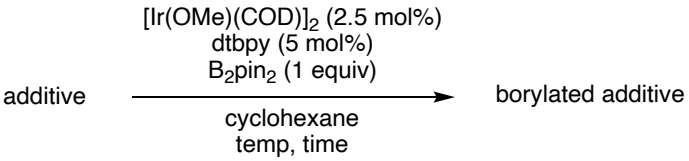

(1 equiv)

In a glovebox, under an inert atmosphere of nitrogen, to a 4-mL vial equipped with a stir bar was added $[Ir(OMe)(COD)]_2$ (10 mg, 0.02 mmol), dtbpy (10 mg, 0.04 mmol) and B_2pin_2 (200 mg, 0.8 mmol). The contents were diluted with cyclohexane (1 mL) and then heated to 80 °C for 1 h to make for a homogeneous dark red solution. This catalyst solution was cooled to 25 °C inside the glovebox. Then, to this solution was added the additive (in this case, cyclooctanone) (100 mg, 0.8 mmol). The vial was sealed and then heated at the designated temperature for the designated amount of time.

Reactivity at Bpin Ligand

[2-(hexyloxy)-4,4,5,5-tetramethyl-1,3,2-dioxaborolane][43]

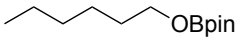

CAS_2047809-94-7

General Procedure 2

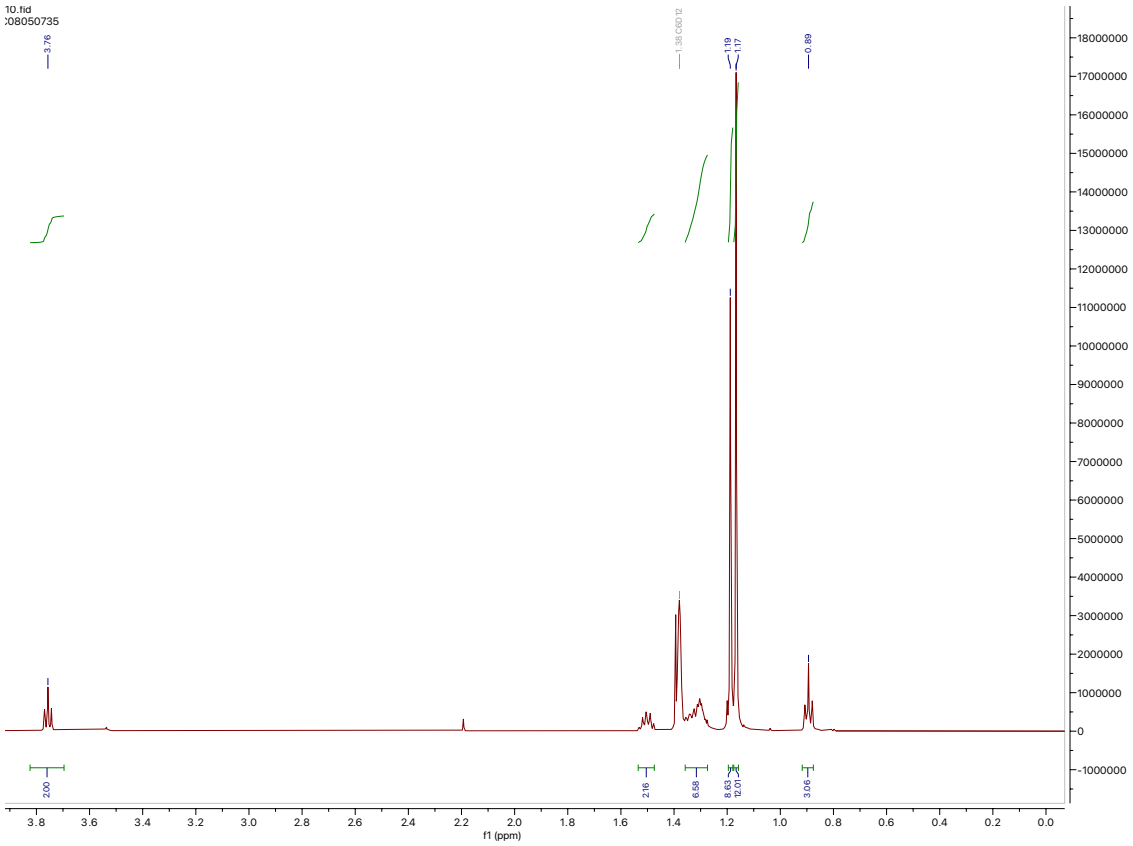

^{1}H-NMR

Note: 1.19 ppm singlet belongs to BOB impurity and is distinct from the methyls of Bpin on the product as the singlet at 1.17 ppm

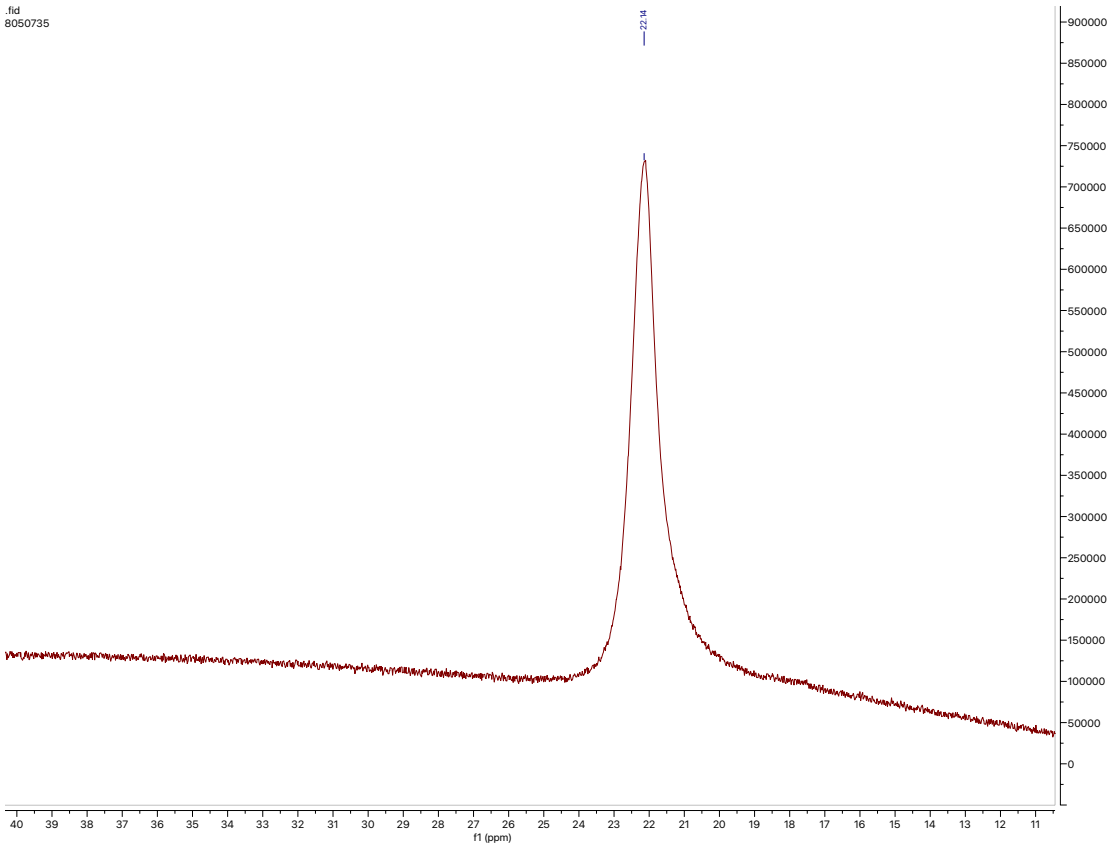

^{11}B-NMR

Note: BOB impurity and product are indistinguishable by ^{11}B-NMR spectroscopy

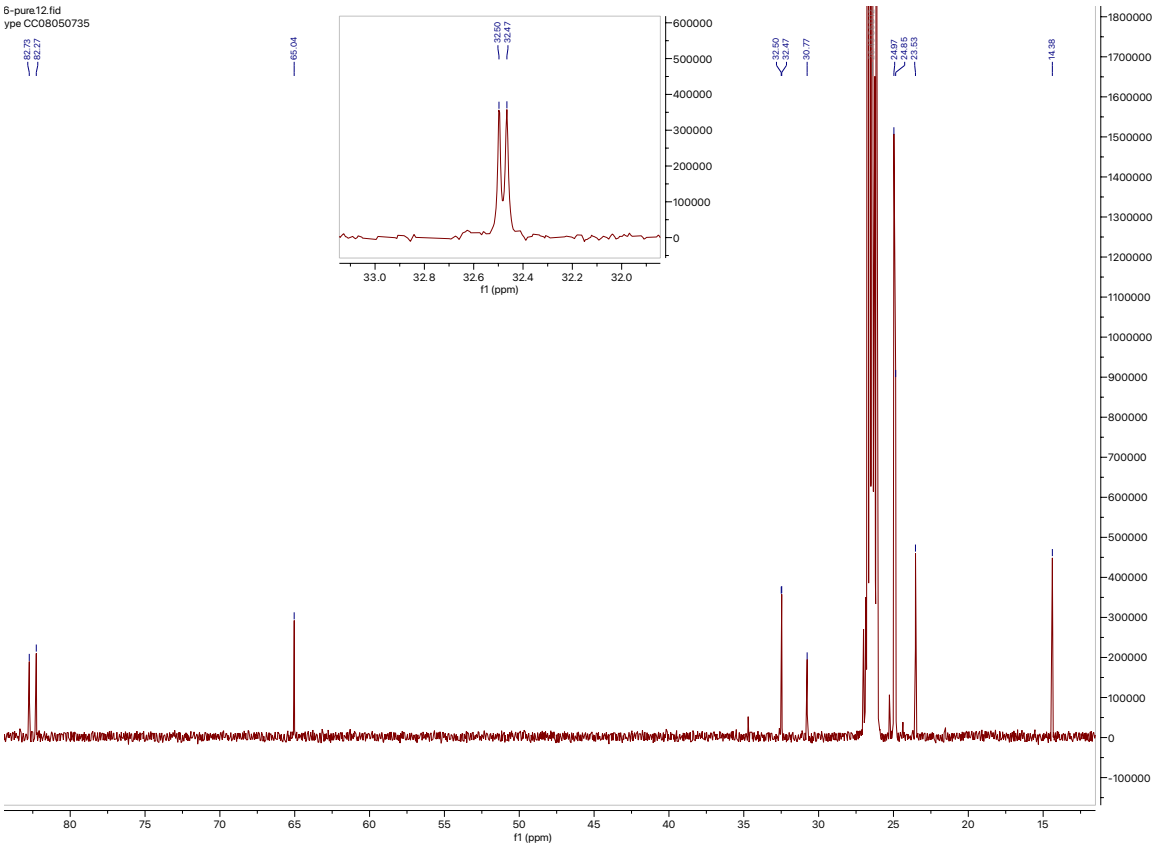

^{13}C-NMR

Note: Based on authentic sample of BOB impurity 82.73 ppm and 24.97 ppm belong to BOB impurity, and 82.27 ppm and 24.85 ppm belong to product

[2-(hexan-3-yloxy)-4,4,5,5-tetramethyl-1,3,2-dioxaborolane]

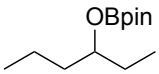

Unknown

<u>General Procedure 2</u> but with 0.5 equiv HBpin and C_6D_{12} as solvent

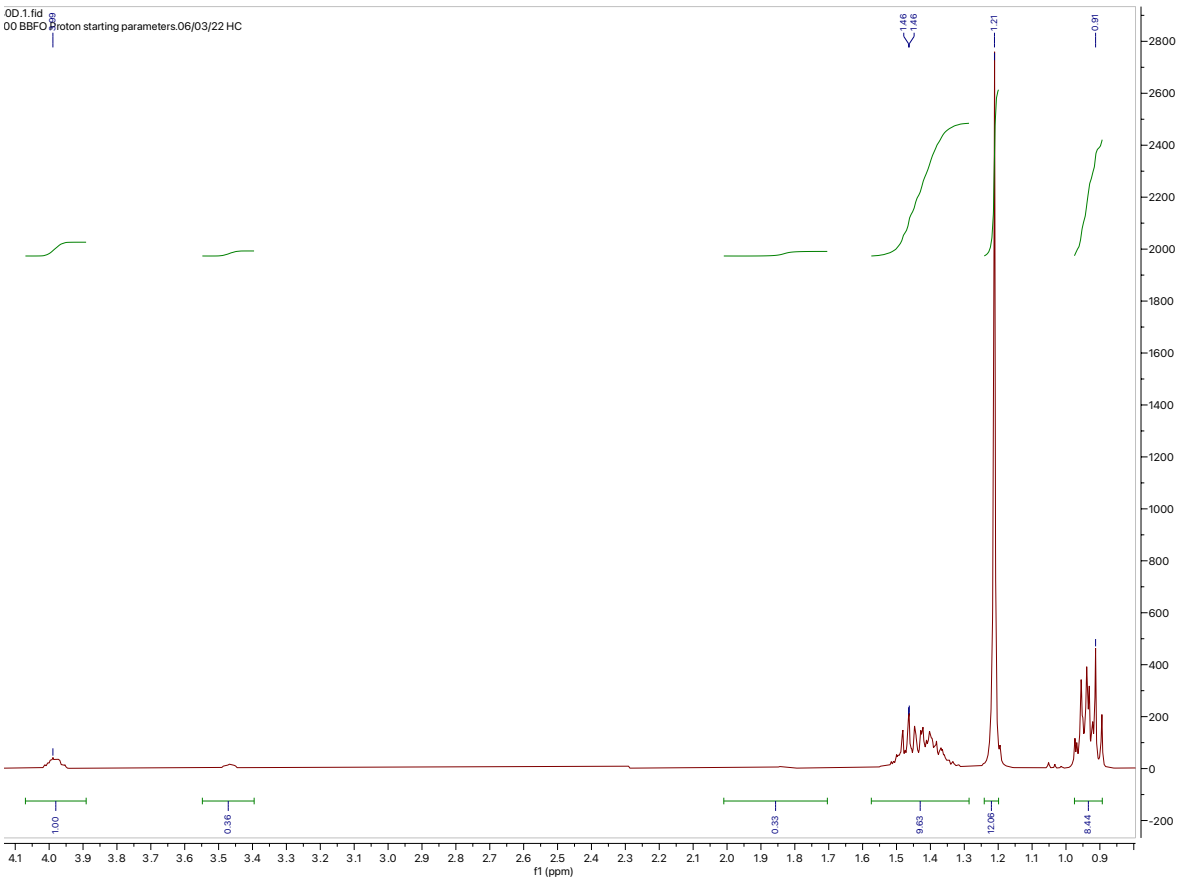

^{1}H-NMR

Note: the labeled peaks belong to the borylated alcohol. Unlabeled integrated peaks belong to residual alcohol (characteristic alpha proton around 3.5 ppm shows good separation from that of the borylated alcohol around 4 ppm). Peaks for residual alcohol and borylated alcohol overlap around 1.4 ppm, along with residual peaks for C_6D_{12}. Peaks for residual alcohol and borylated alcohol overlap around 0.9 ppm.

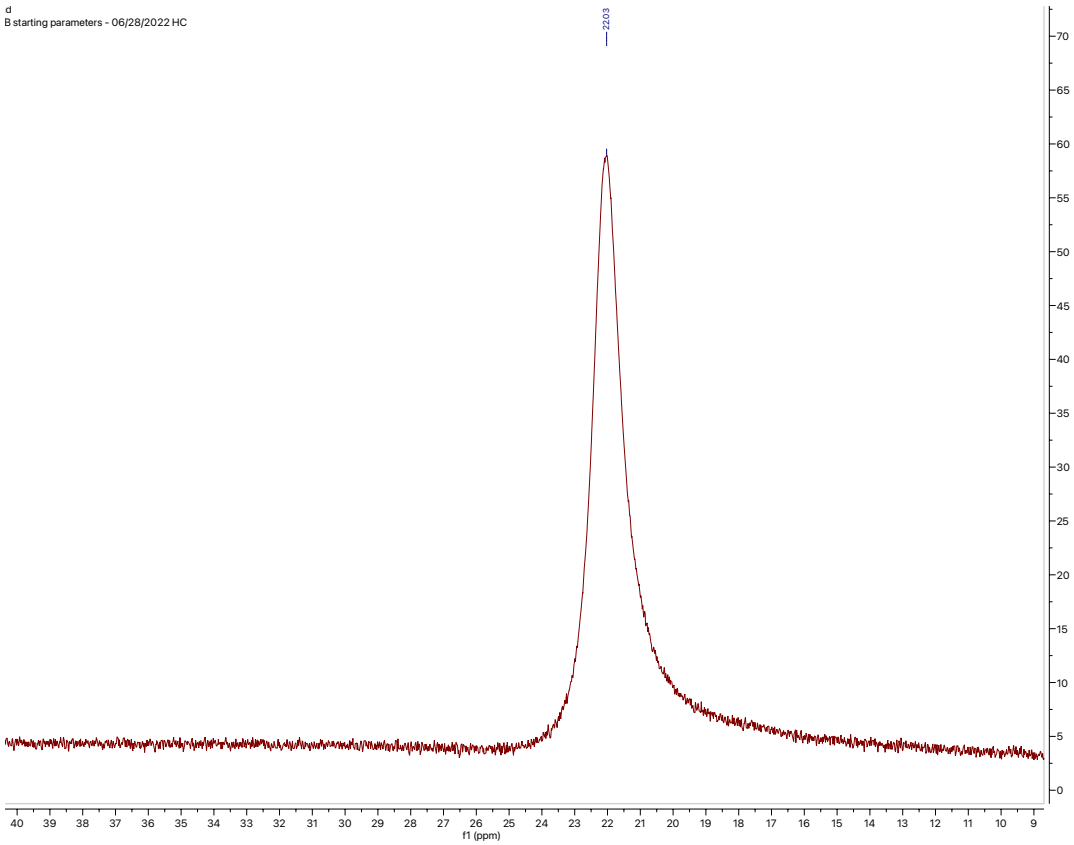

^{11}B-NMR

[4,4,5,5-tetramethyl-2-((3-methylpentan-3-yl)oxy)-1,3,2-dioxaborolane]

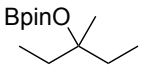

Unknown

General Procedure 2 but with 0.5 equiv HBpin and C_6D_{12} as solvent

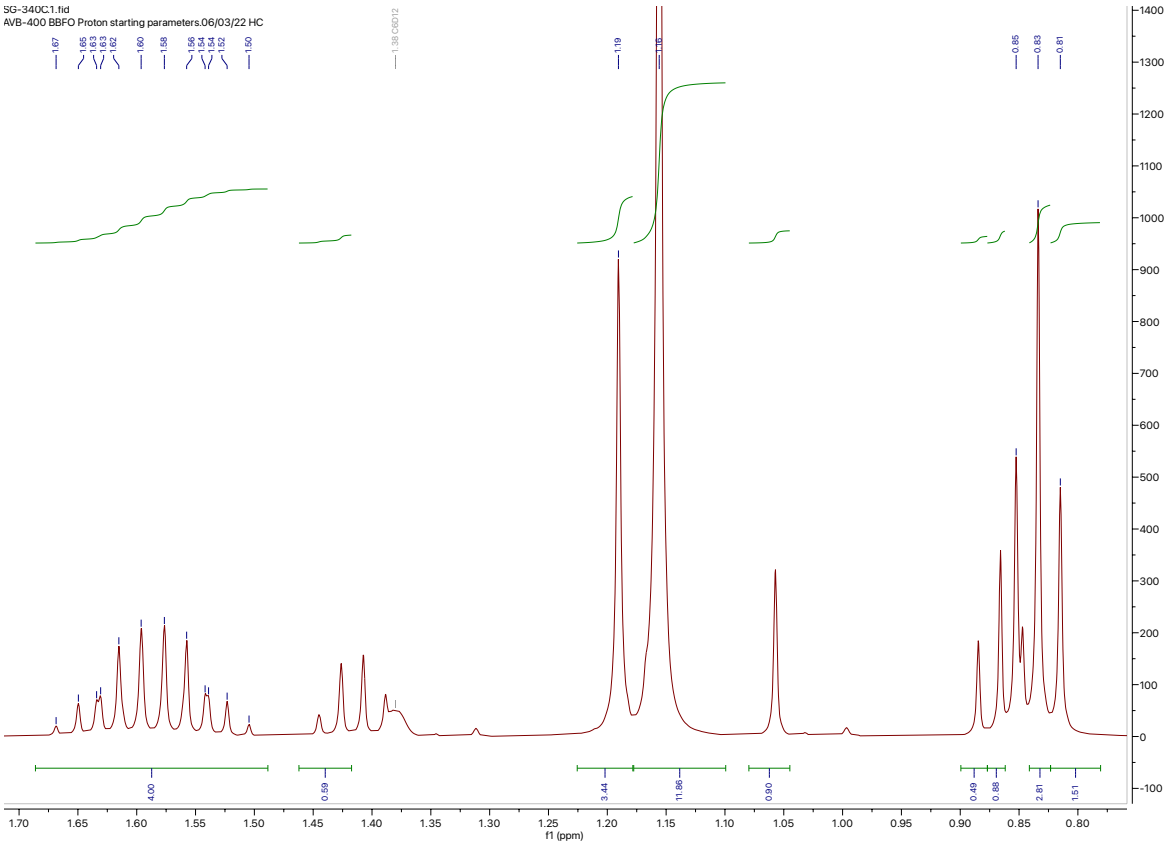

^{1}H-NMR

Note: the labeled peaks belong to the borylated alcohol. Unlabeled integrated peaks belong to residual alcohol

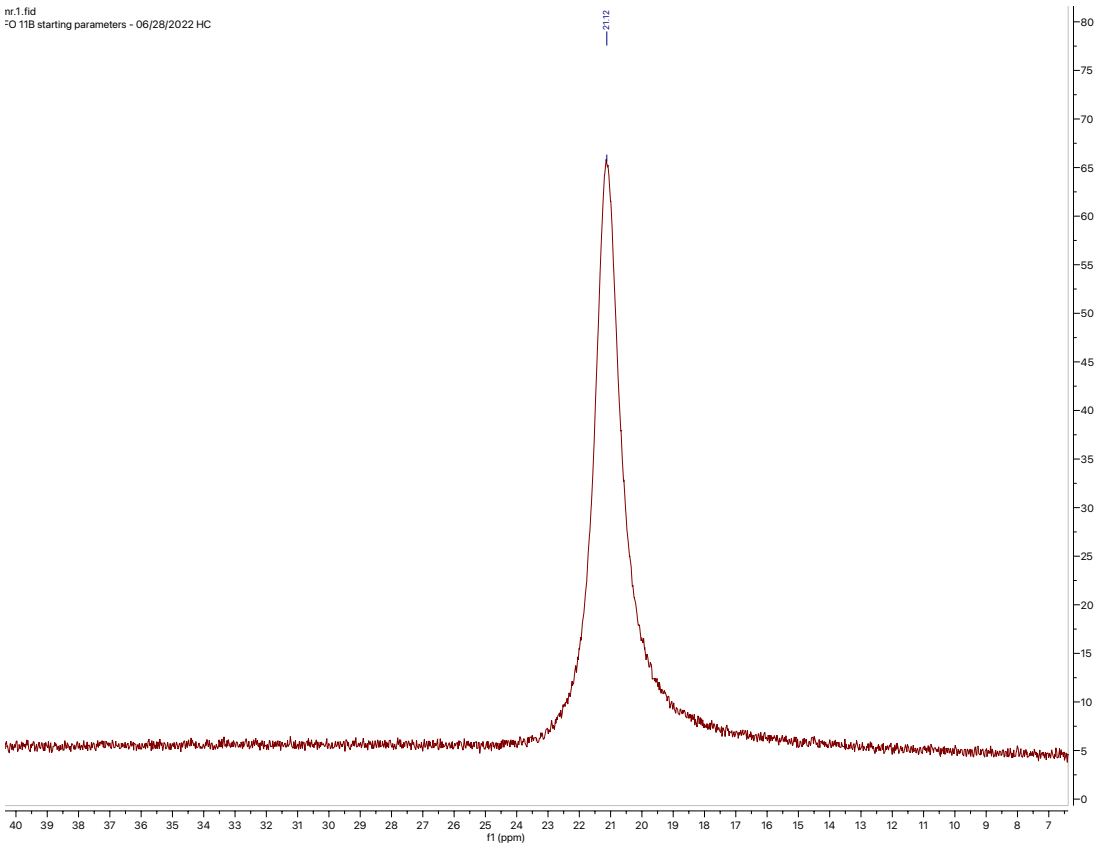

^{11}B-NMR

[N-dodecyl-4,4,5,5-tetramethyl-1,3,2-dioxaborolan-2-amine]

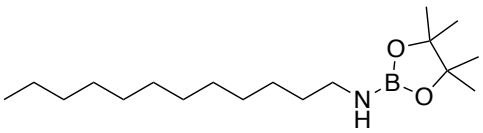

Unknown

General Procedure 1 at 25 °C. Reaction starts out as a slurry but upon stirring overnight clears out to a homogeneous solution. An aliquot was taken and diluted with C_6D_{12}

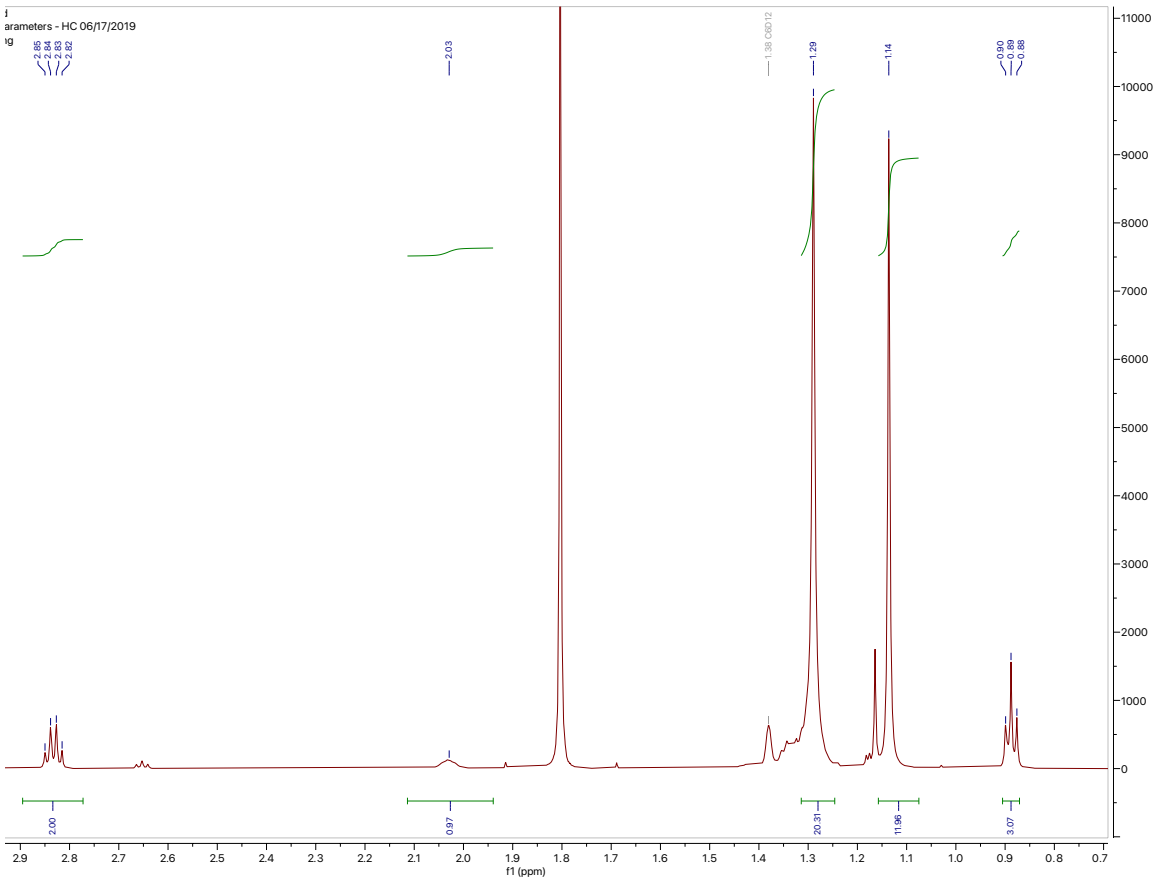

^{1}H-NMR

Note: the singlet around 1.8 ppm belongs to MeCN solvent. A minor amount of starting material can be observed

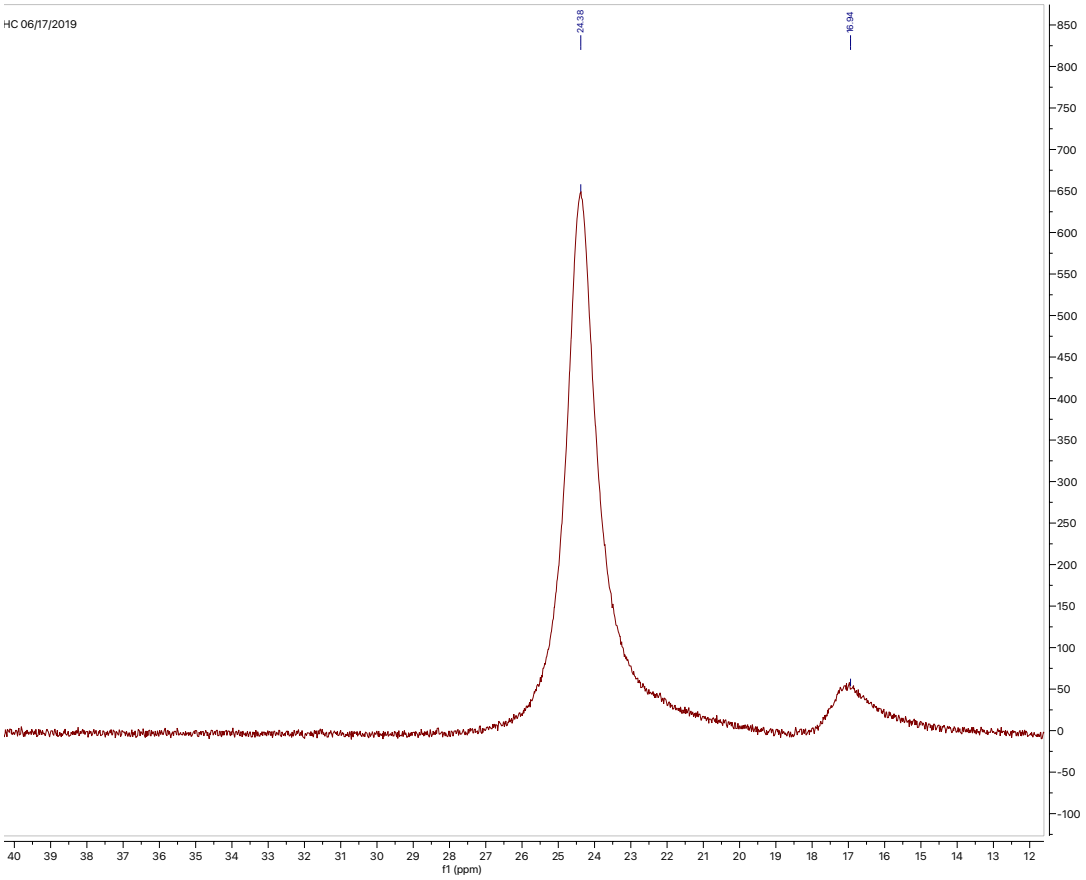
HC 06/17/2019
24.38
16.94
850
800
750
700
650
600
550
500
450
400
350
300
250
200
150
100
50
0
-50
-100
40 39 38 37 36 35 34 33 32 31 30 29 28 27 26 25 24 23 22 21 20 19 18 17 16 15 14 13 12
f1 (ppm)

^{11}B-NMR

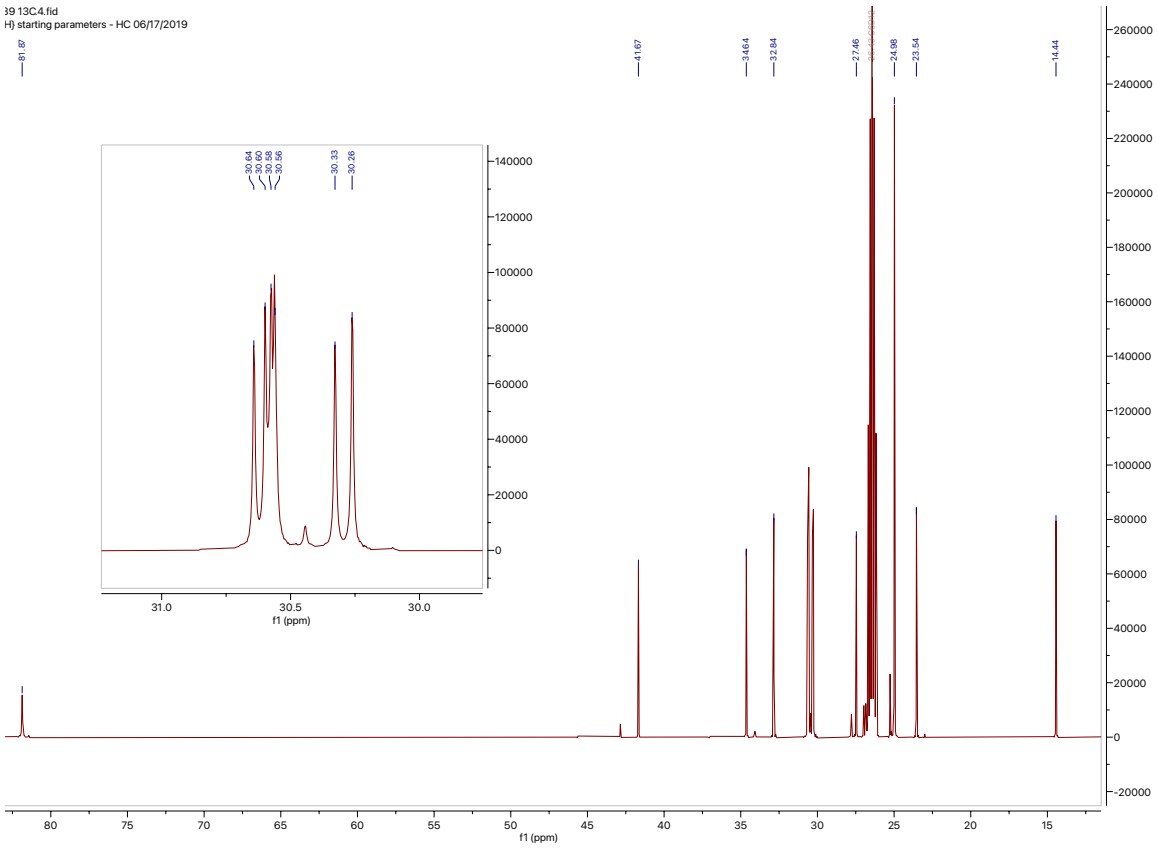

^{13}C-NMR

[4,4,5,5-tetramethyl-2-(octylthio)-1,3,2-dioxaborolane]

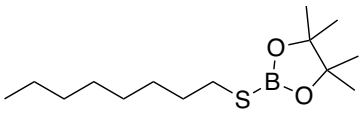

Unknown

General Procedure 2. Due to instability of product upon concentration instead an aliquot of the non-concentrated reaction mixture was taken and diluted with C_6D_{12}.

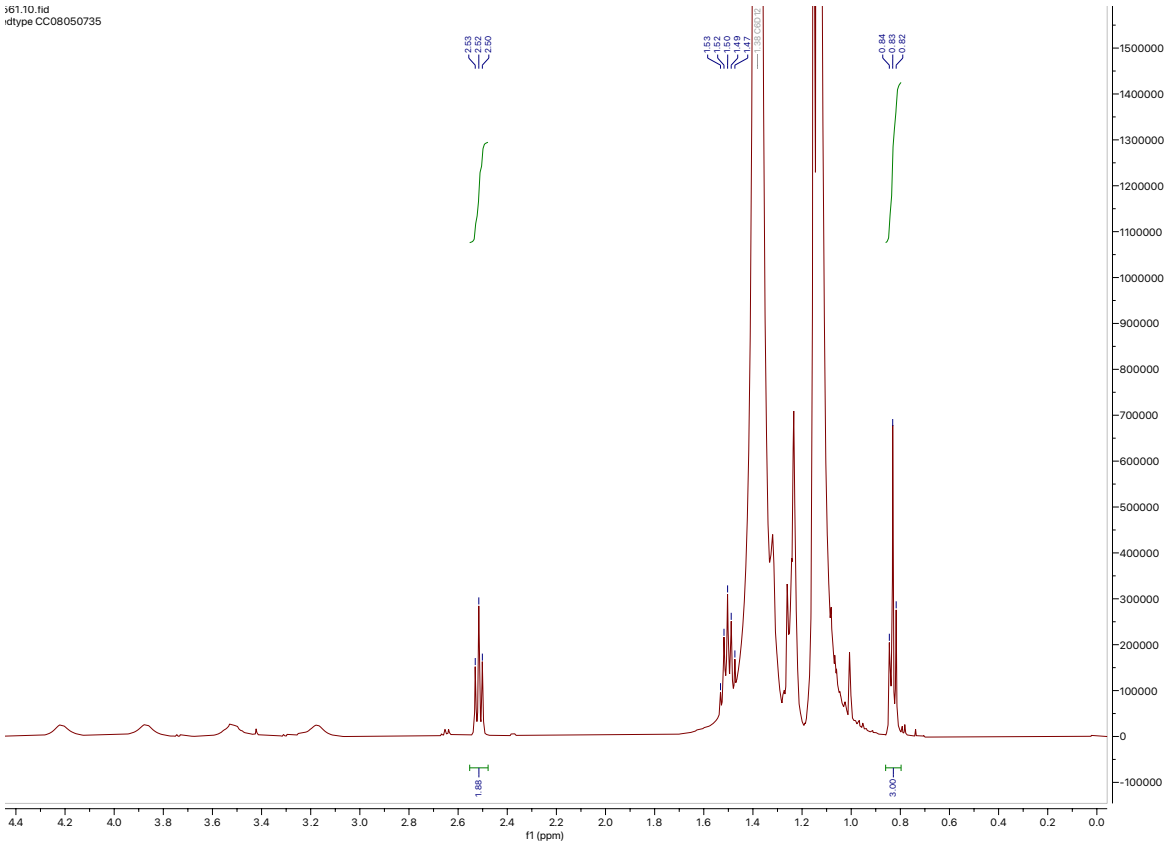

^{1}H-NMR

Note: the large peaks around 1.1 ppm are the overlapping Bpin methyls of the product, HBpin and BOB impurity

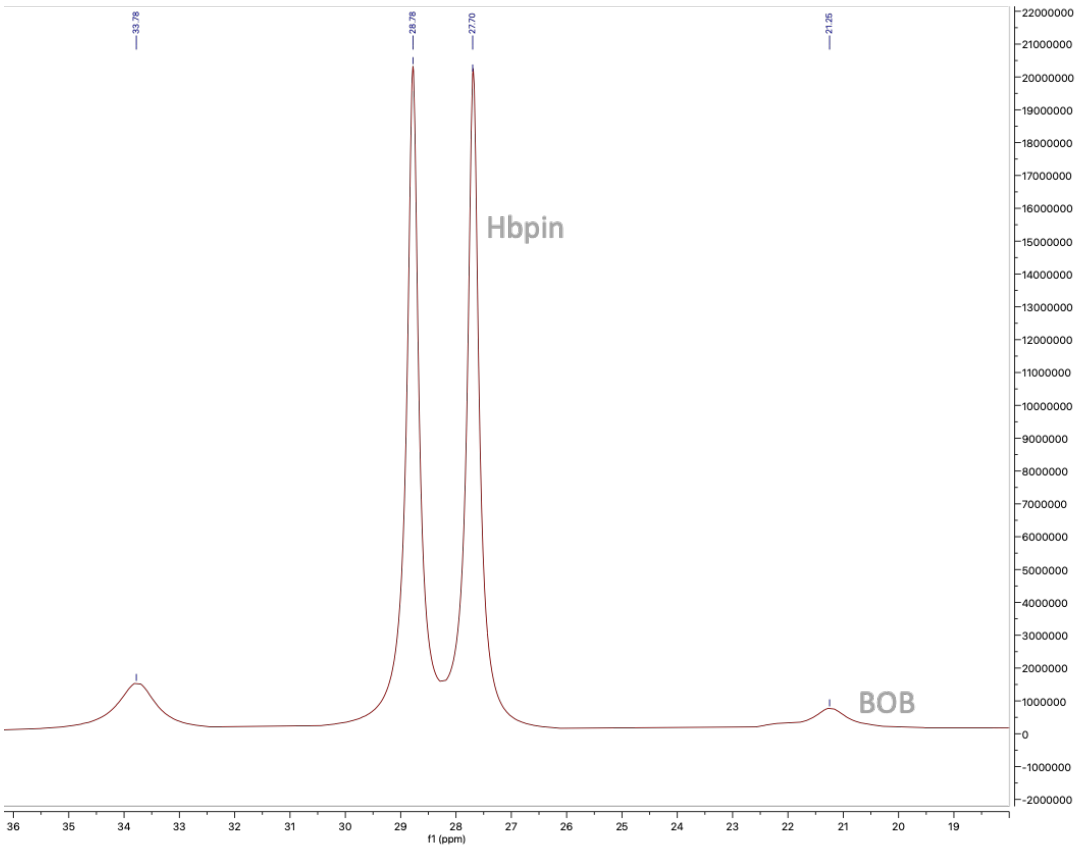

^{11}B-NMR

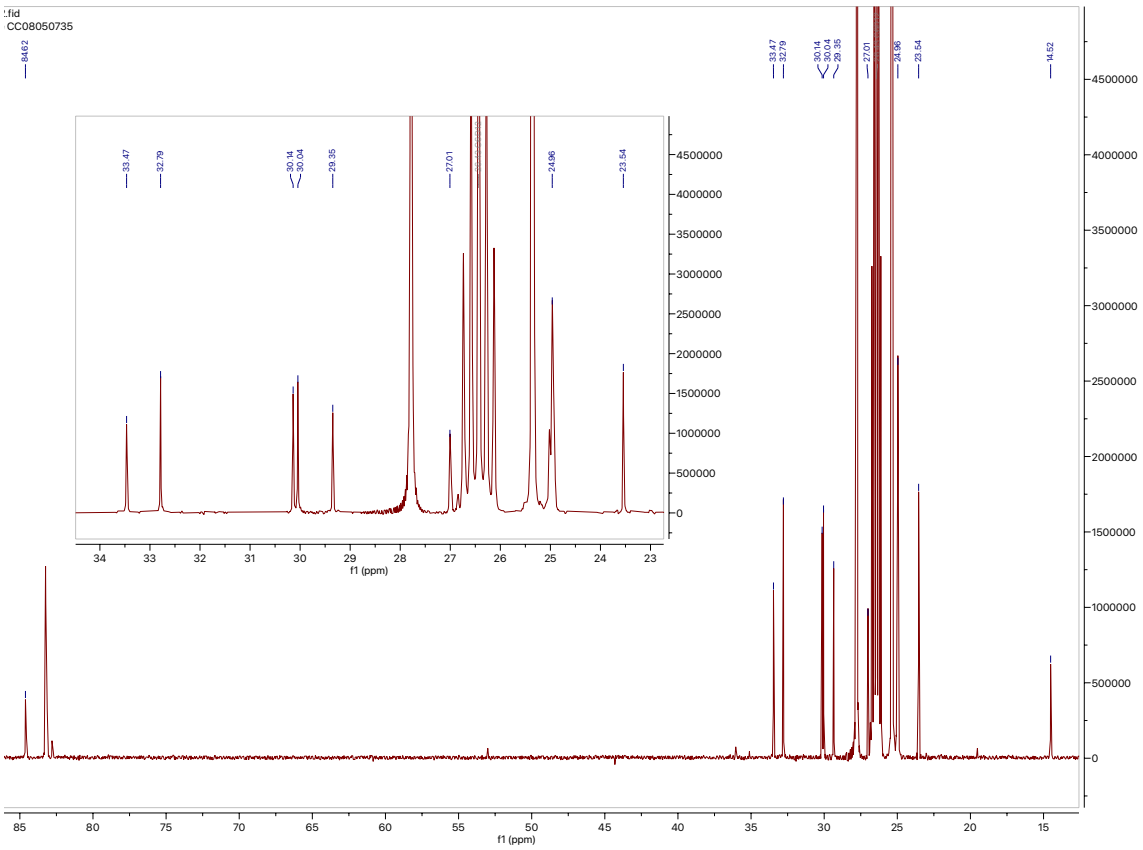

^{13}C-NMR

Note: the unlabeled peaks around 83 ppm belong to the quaternary carbons of residual HBpin and BOB impurity. The unlabeled peaks around 25 ppm belong to the methyl peaks of residual HBpin and BOB impurity

[N-methyl-N-(4,4,5,5-tetramethyl-1,3,2-dioxaborolan-2-yl)butyramide]

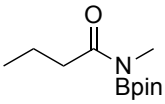

Unknown

General Procedure 1 with added 1 mol% Et_3N and an elevated temp of 120 °C. Aliquot of reaction mixture was diluted in C_6D_{12} for NMR spectroscopic analysis

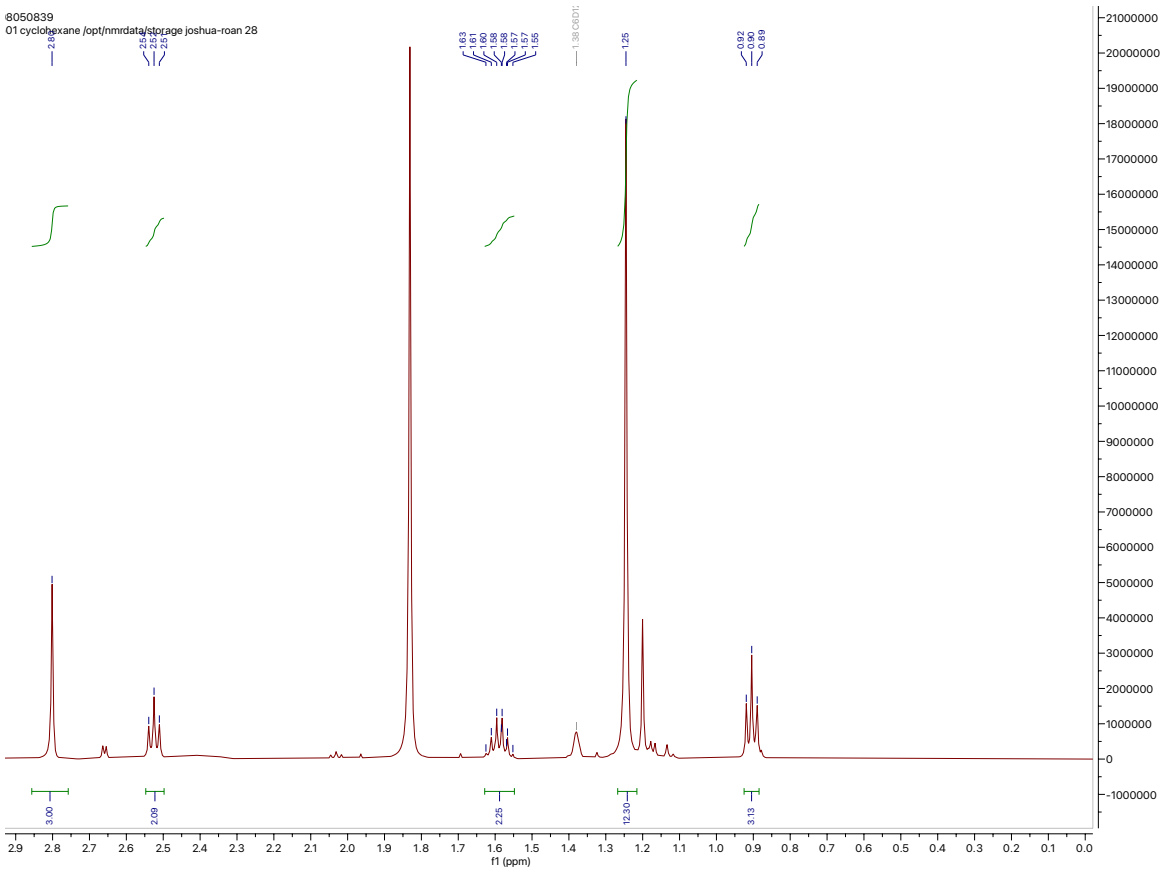

^{1}H-NMR

Note: singlet around 1.8 ppm is MeCN solvent. Unlabeled peak around 1.2 ppm belongs to the methyls of BOB impurity. Minor residual starting material can be seen

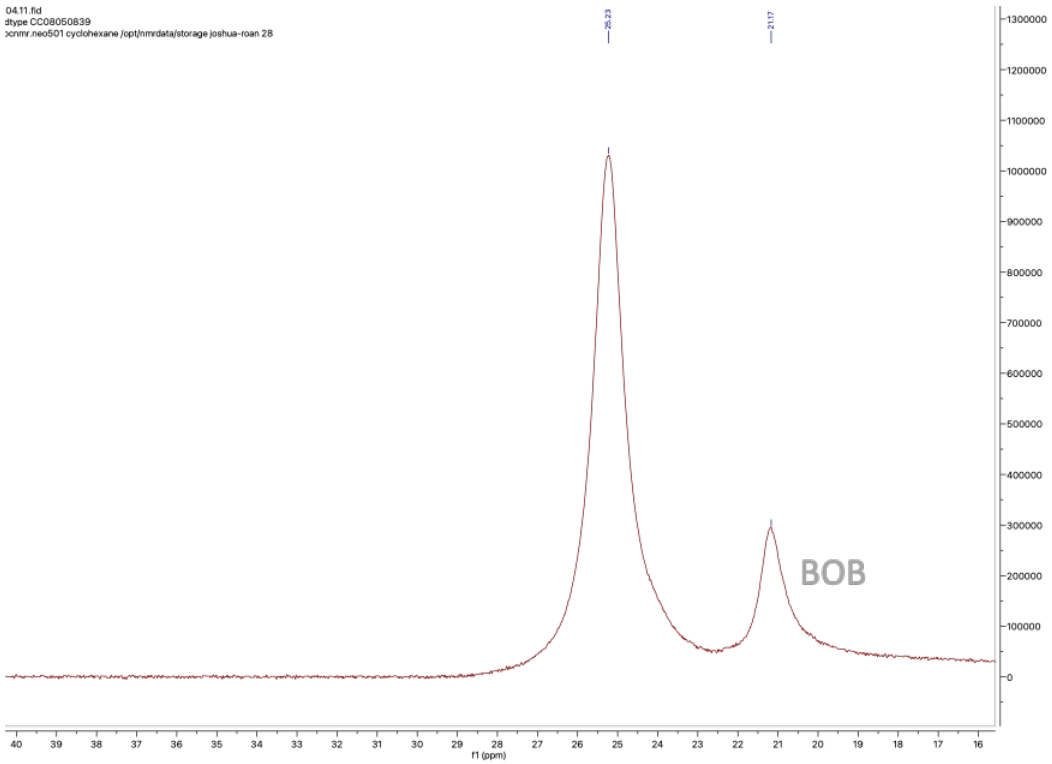
04.11.fid
dtype CC08050839
ocnmr.neo501 cyclohexane /opt/nmrdata/storage joshua-roan 28
25.23
21.17
BOB
f1 (ppm)

^{11}B-NMR

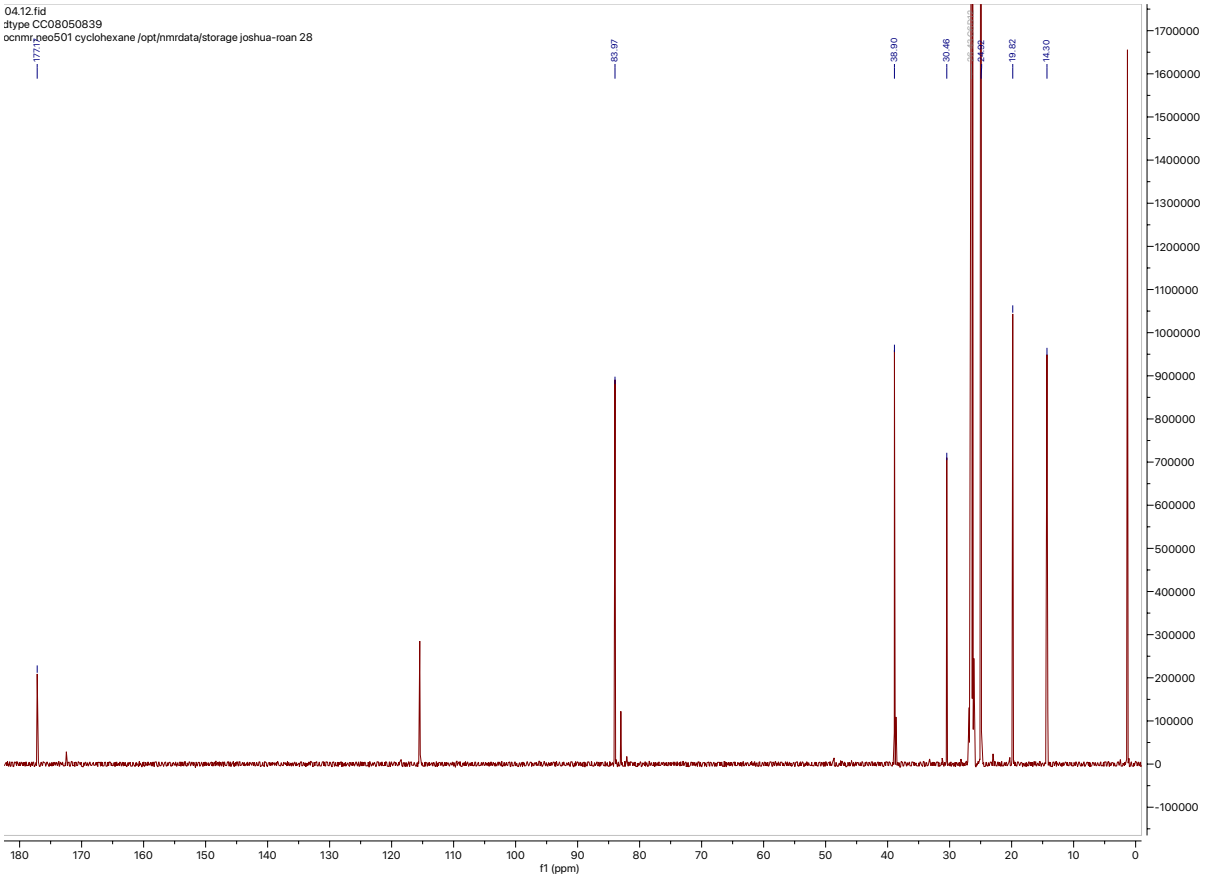
04.12.fid
dtype CC08050839
ocnmr.neo501 cyclohexane /opt/nmrdata/storage joshua-roan 28
83.97
38.90
30.46
24.66
19.82
14.30
f1 (ppm)

^{13}C-NMR

Note: the unlabeled peaks around 115 and 1 ppm belong to MeCN solvent. The unlabeled peak around 83 ppm belongs to the quaternary carbons of BOB impurity. The methyls of BOB impurity overlap with those of the product

Reactivity at Ir

[1*H*-Pyrazole-1-carboxylic acid, 4-(4,4,5,5-tetramethyl-1,3,2-dioxaborolan-2-yl)-, 1,1-dimethylethyl ester][44]

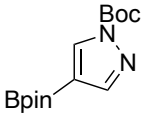

CAS_552846-17-0

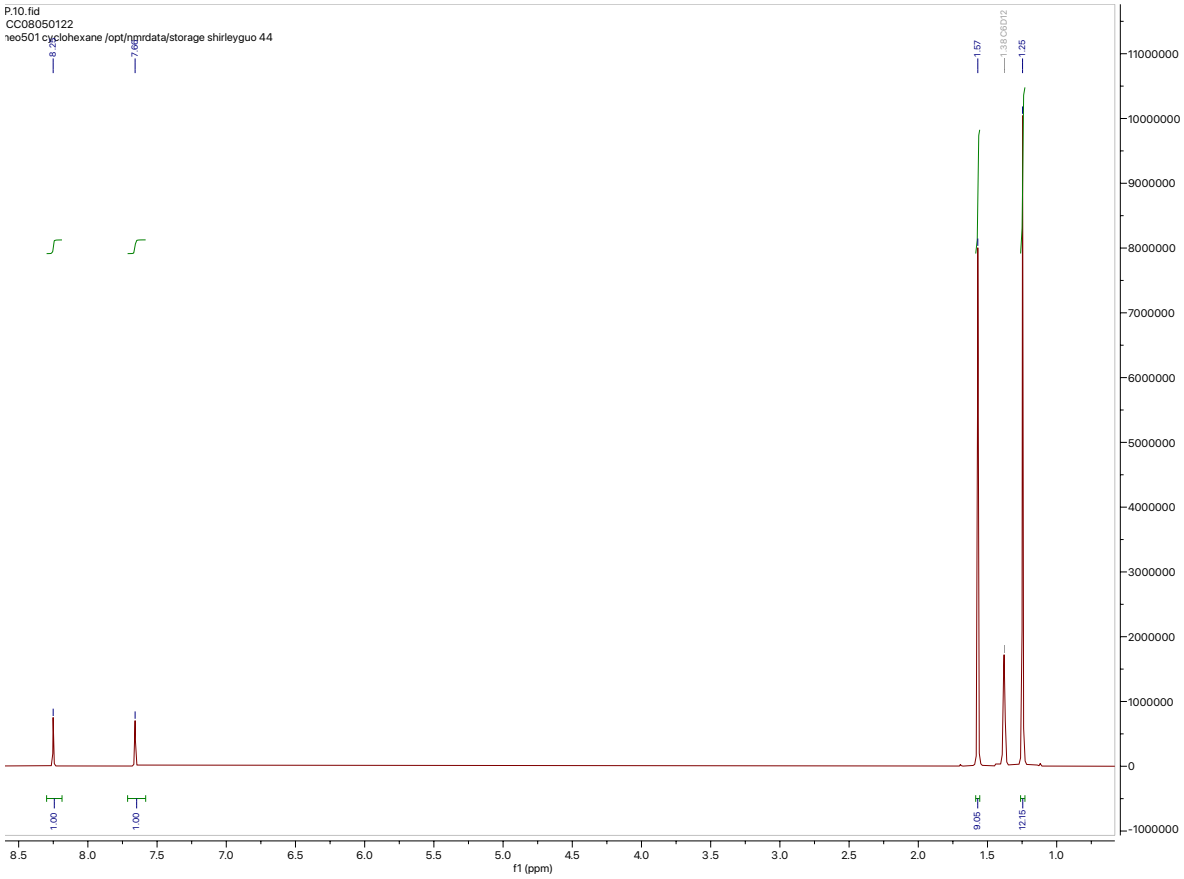

^{1}H-NMR

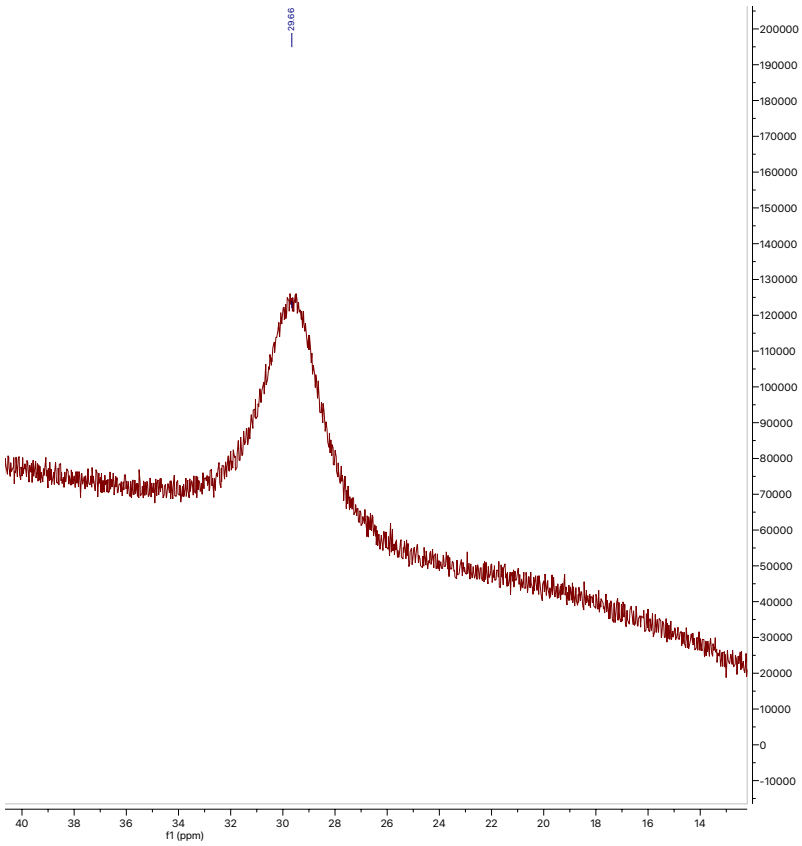
29.66
200000
190000
180000
170000
160000
150000
140000
130000
120000
110000
100000
90000
80000
70000
60000
50000
40000
30000
20000
10000
0
-10000
40
38
36
34
32
30
28
26
24
22
20
18
16
14
f1 (ppm)

^{11}B-NMR

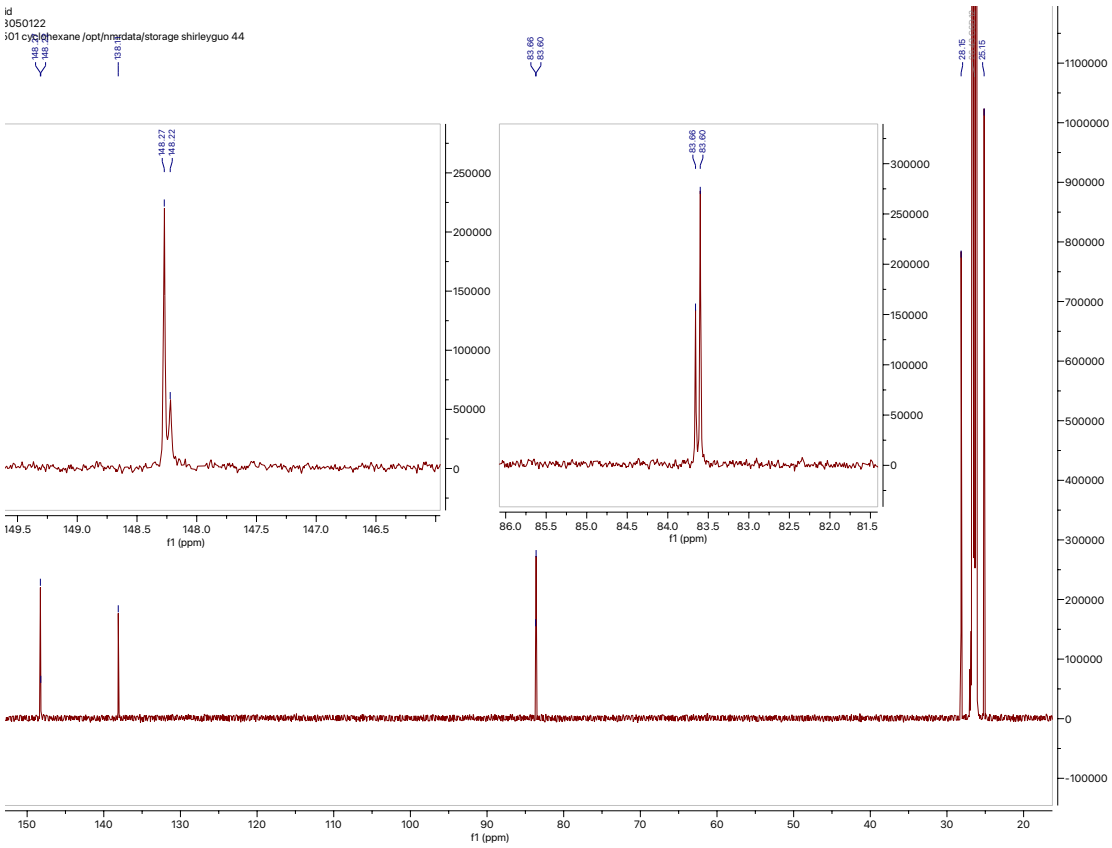

^{13}C-NMR

[2-(4-chloro-2-fluoro-5-methylphenyl)-4,4,5,5-tetramethyl-1,3,2-dioxaborolane][45]

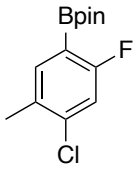

CAS_1126320-27-1

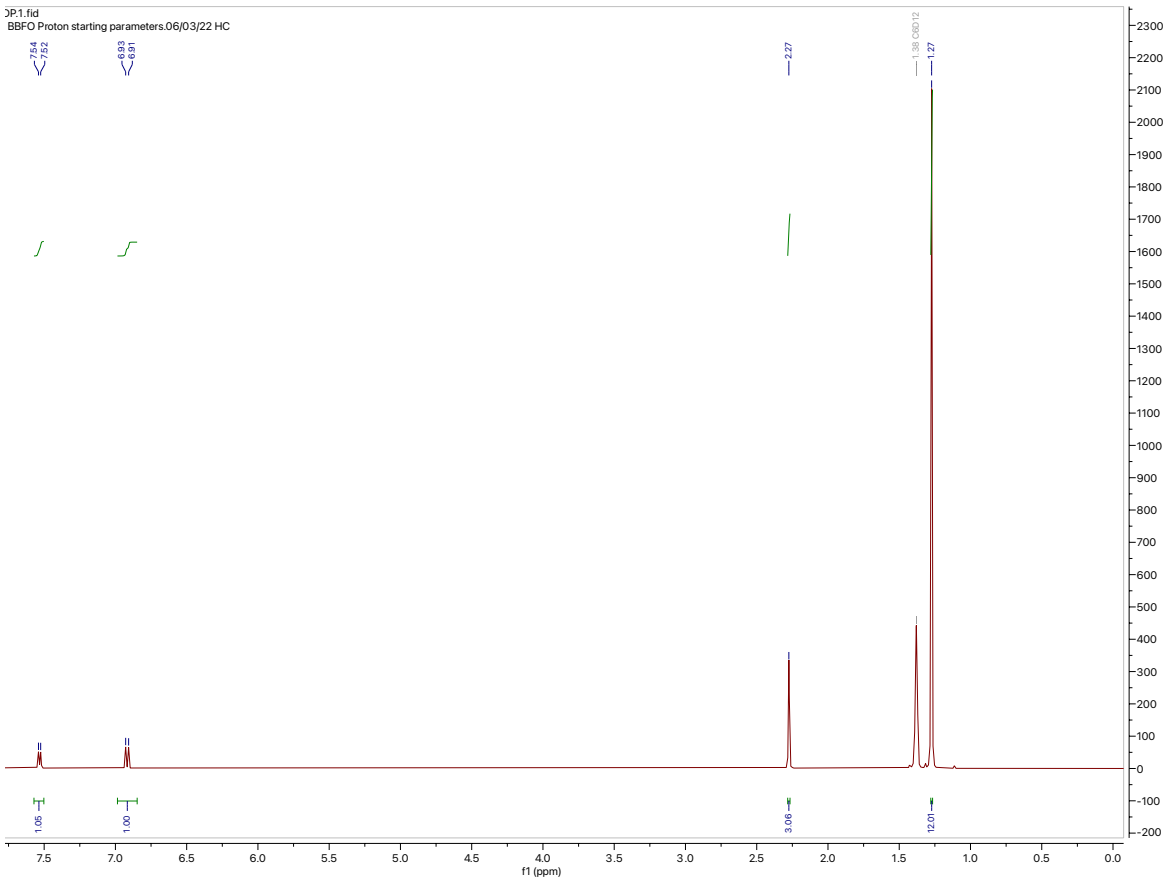
DP.1.fid
BBFO Proton starting parameters.06/03/22 HC
7.54
7.52
6.93
6.91
2.27
1.38
1.27
1.05
1.00
3.06
12.01
f1 (ppm)

^{1}H-NMR

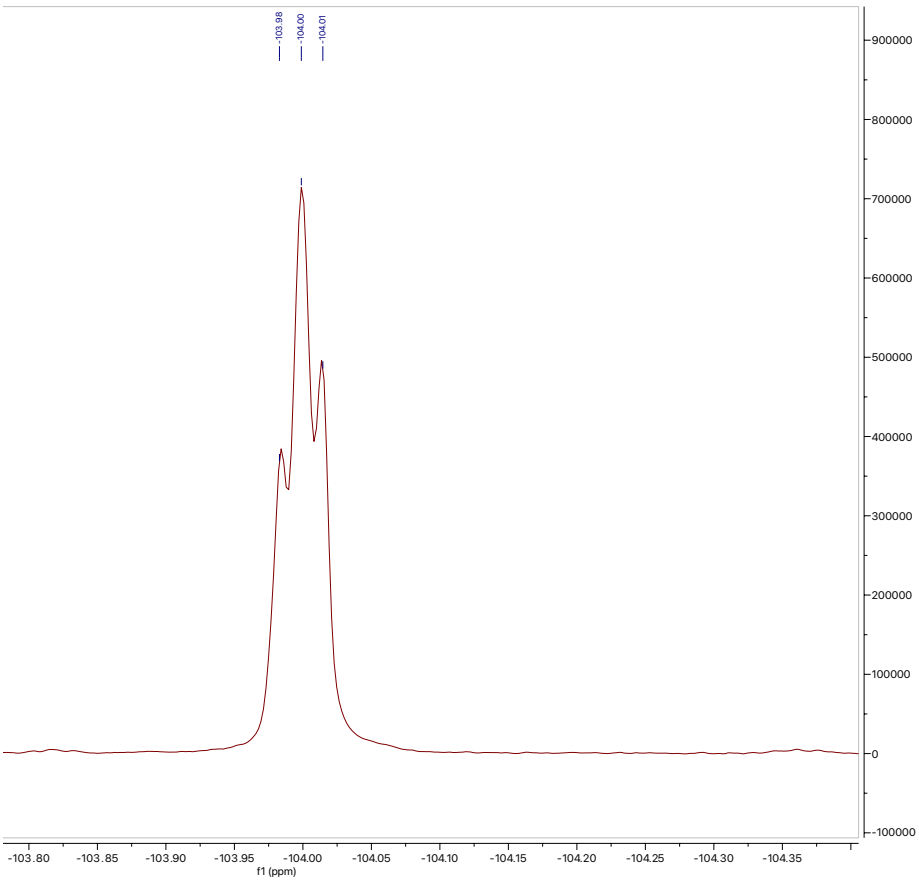
-103.98
-104.00
-104.01
900000
800000
700000
600000
500000
400000
300000
200000
100000
0
-100000
-103.80
-103.85
-103.90
-103.95
-104.00
-104.05
-104.10
-104.15
-104.20
-104.25
-104.30
-104.35
f1 (ppm)

^{19}F-NMR

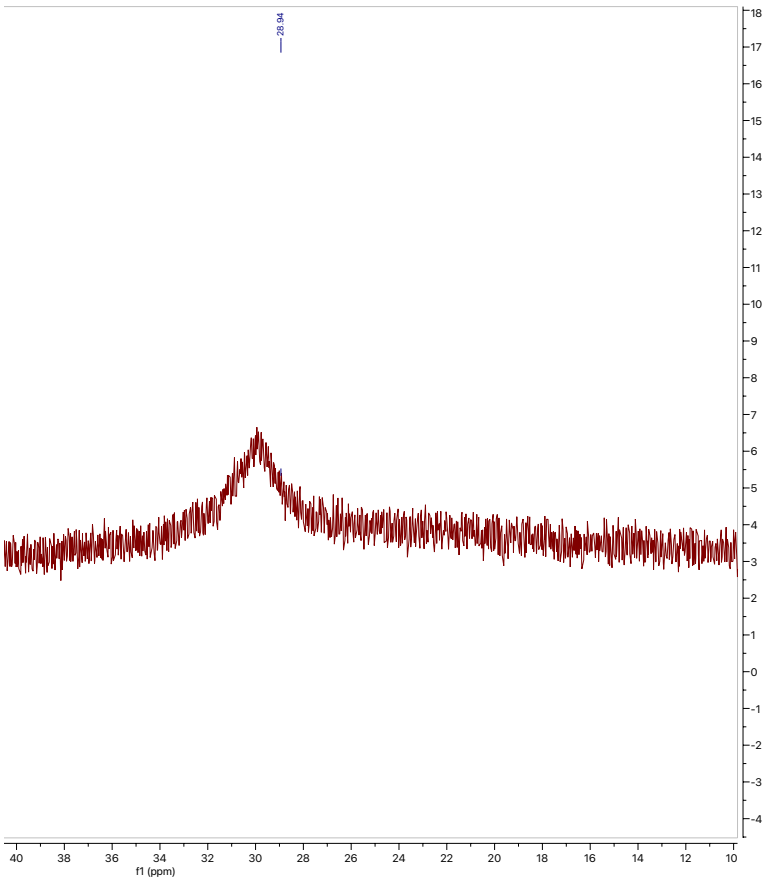

^{11}B-NMR

[2-(3,5-Dimethylphenyl)-4,4,5,5-tetramethyl-1,3,2-dioxaborolane][46]

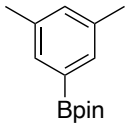

CAS_325142-93-6

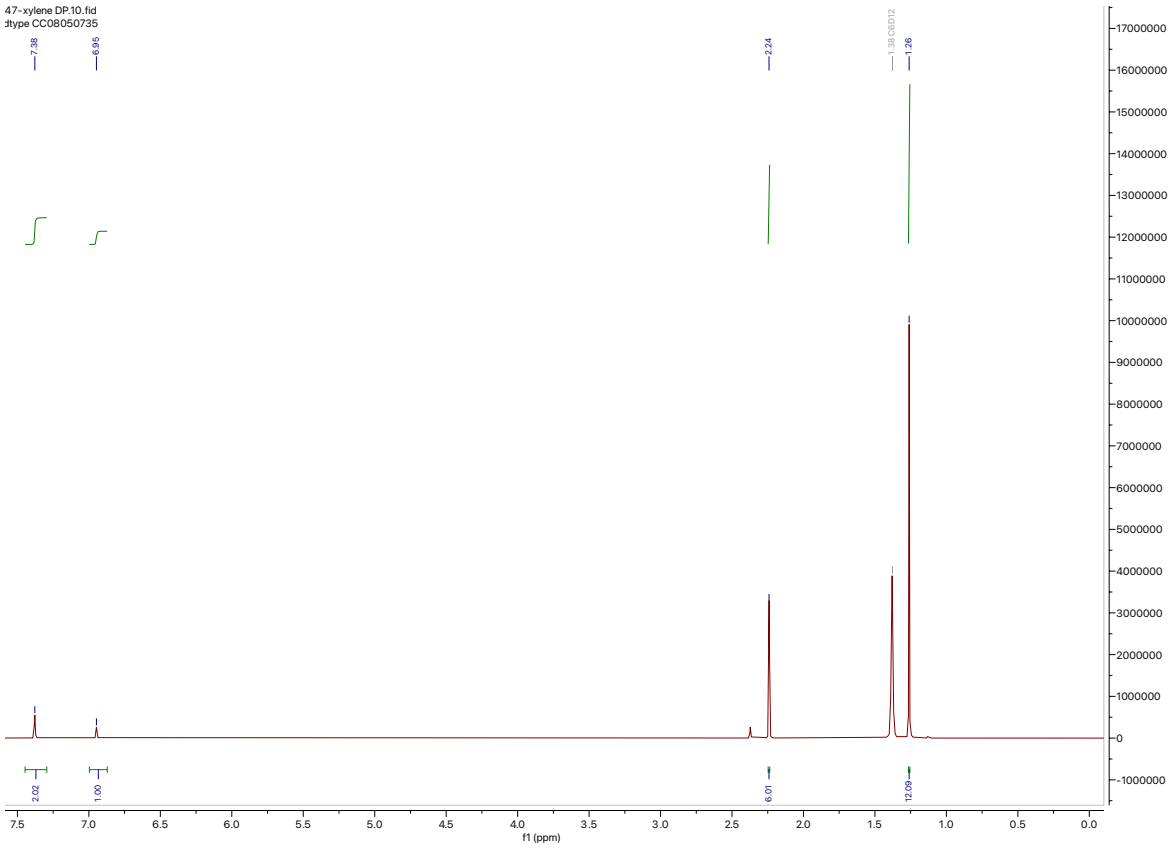
47-xylene DP.10.fid
dtype CC08050735
7.38
6.95
2.24
1.38 C6D12
1.26
2.02
1.00
6.01
12.09
f1 (ppm)

^{1}H-NMR

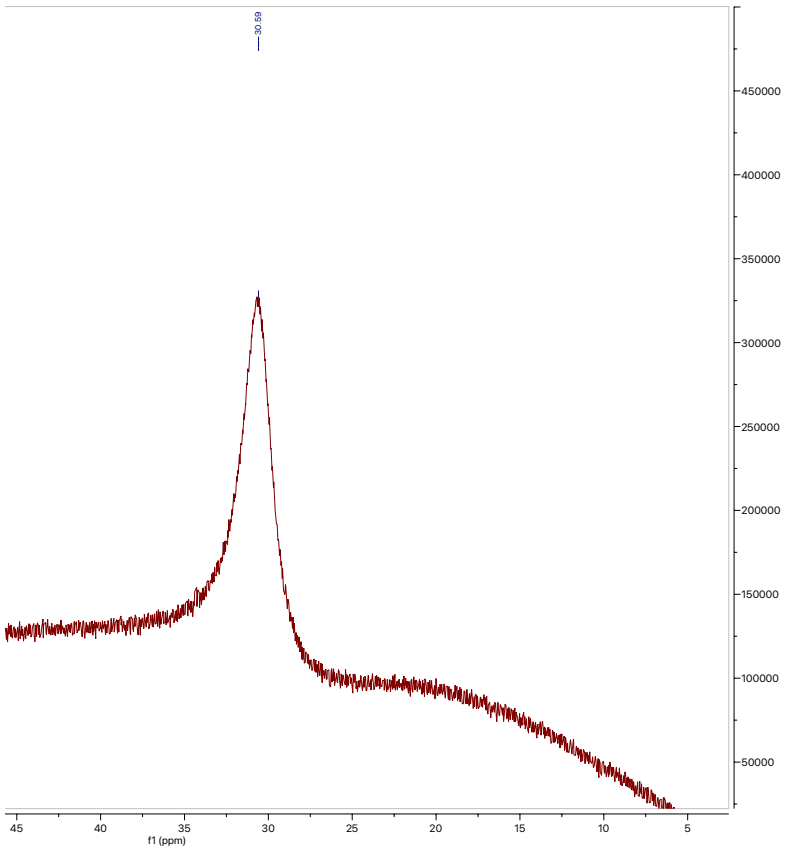
30.59
450000
400000
350000
300000
250000
200000
150000
100000
50000
45
40
35
30
25
20
15
10
5
f1 (ppm)

^{11}B-NMR

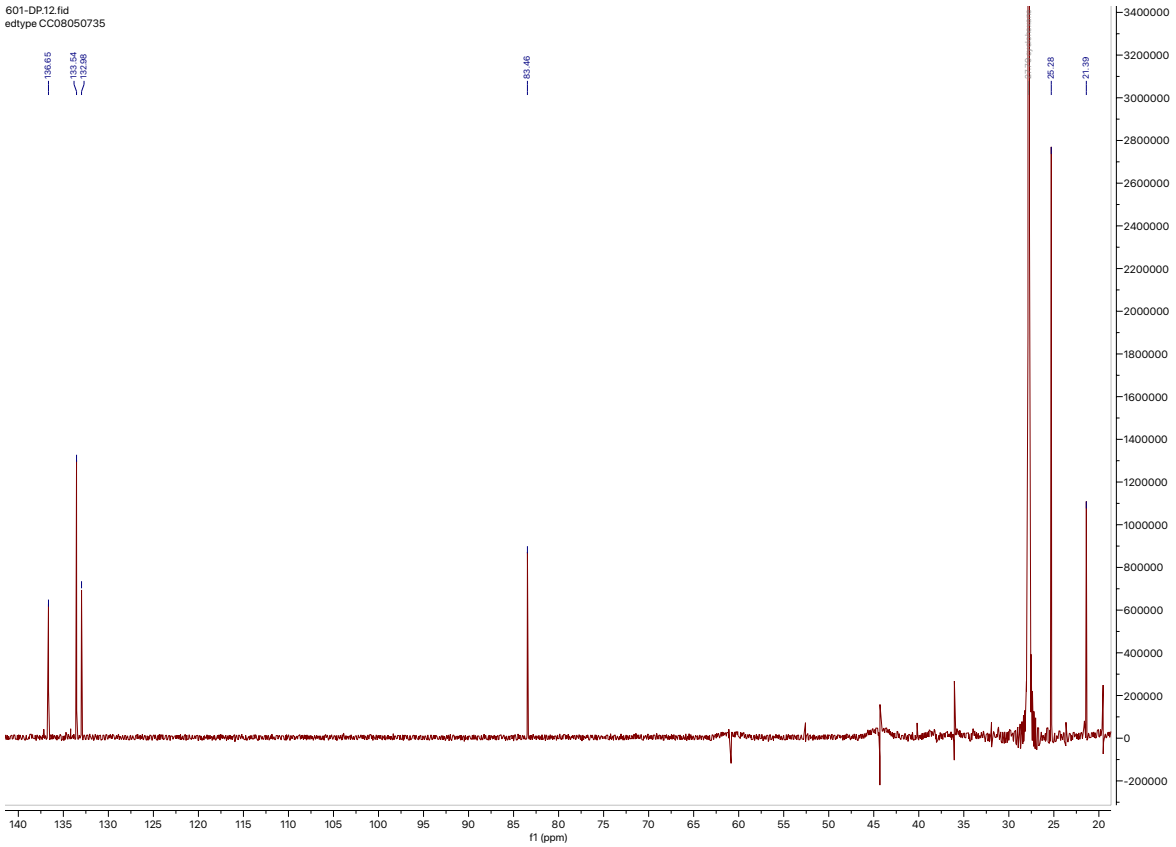

^{13}C-NMR

Note: **C**—Bpin is not observable

[(E)-2-(cyclooct-1-en-1-yloxy)-4,4,5,5-tetramethyl-1,3,2-dioxaborolane]

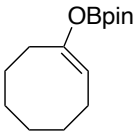

Unknown

General Procedure 3 conducted at 50 °C

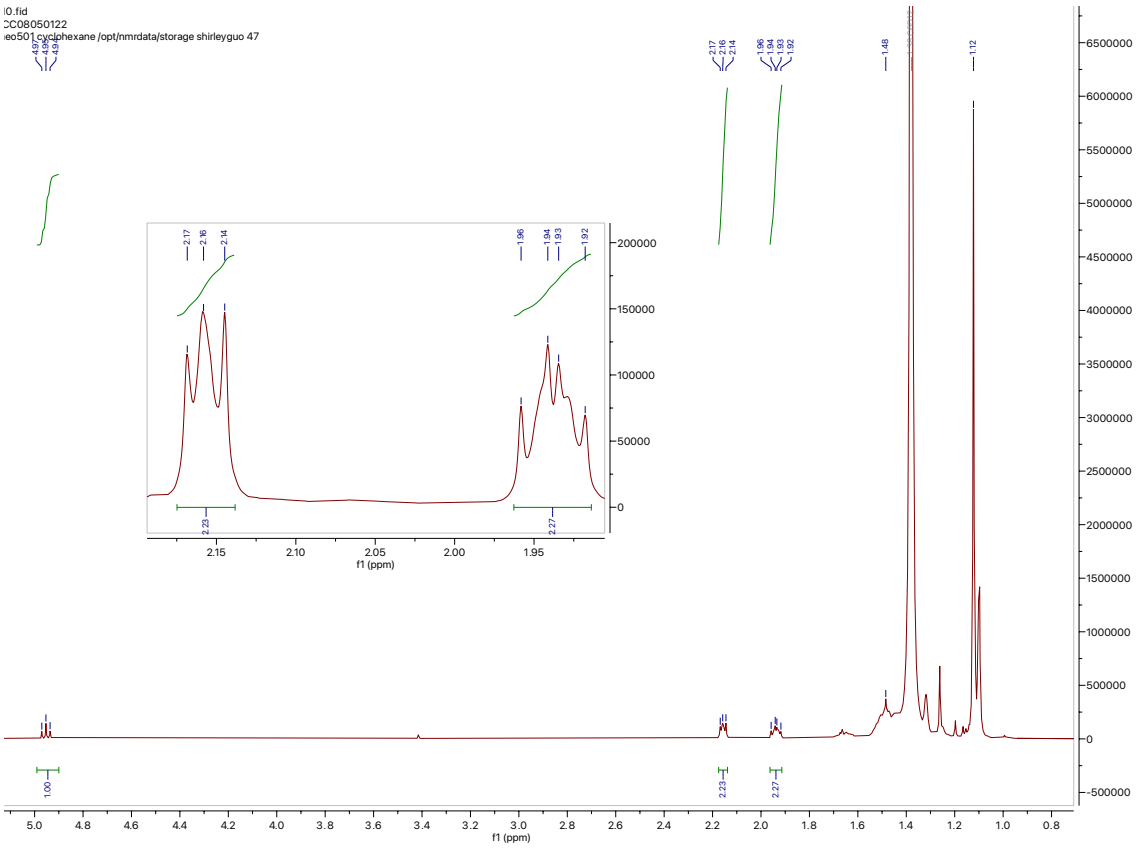
10.fid
DC08050122
eo501 cyclohexane /opt/nmrdata/storage shirleyguo 47
2.17
2.16
2.14
1.96
1.94
1.93
1.92
1.48
1.12
1.00
2.23
2.27
f1 (ppm)

^{1}H-NMR

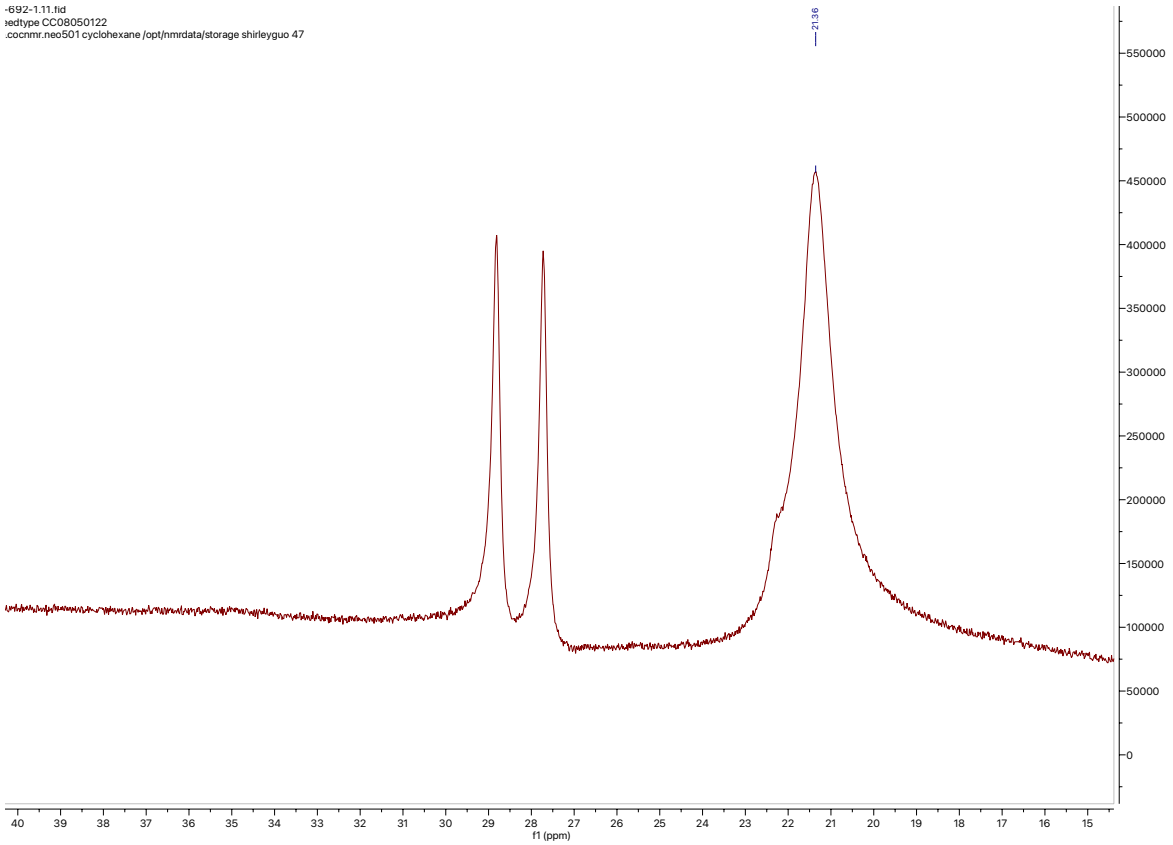

^{11}B-NMR

Note: confirms only O—borylation took place (no C—borylation peak observed). Borylated compound overlaps with BOB impurity. HBpin impurity observed

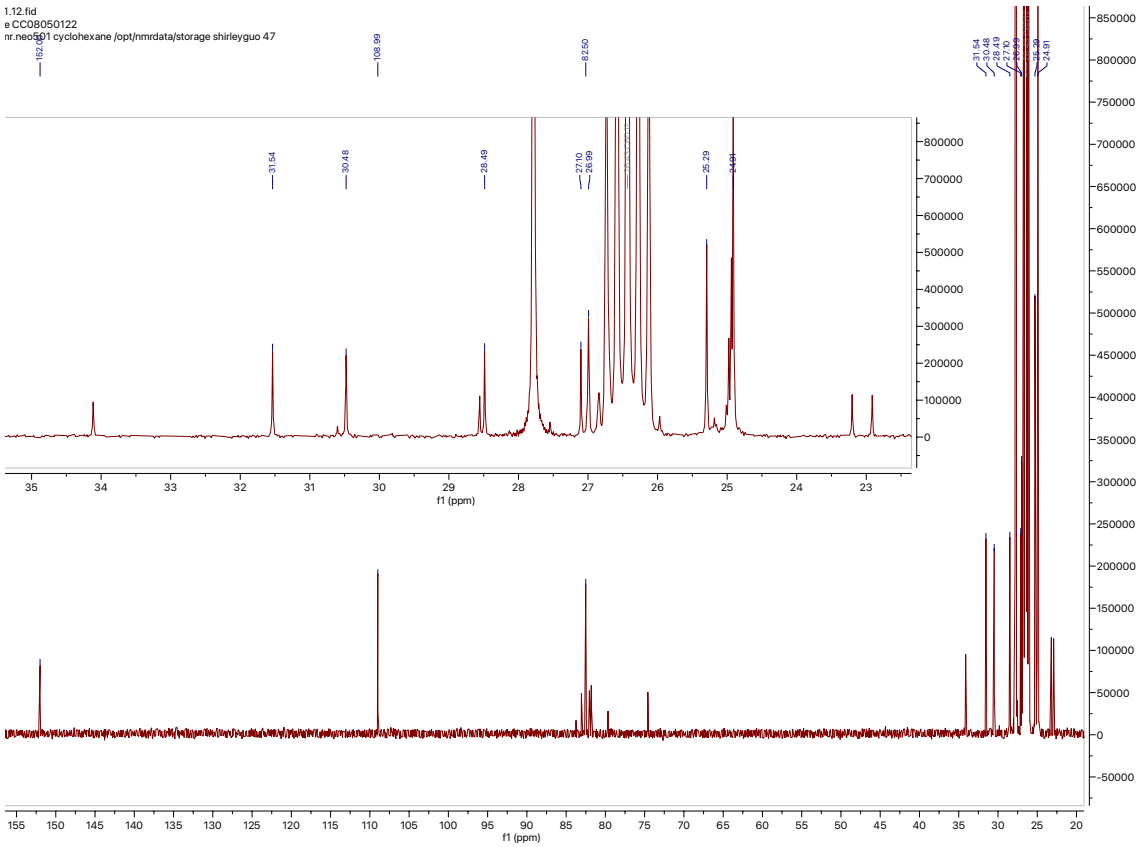

^{13}C-NMR

Note: confirms no residual cyclooctanone starting material

[methyl 3-(4,4,5,5-tetramethyl-1,3,2-dioxaborolan-2-yl)propanoate][47]

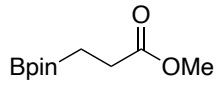

CAS_1150561-77-5

[N,N-dimethyl-3-(4,4,5,5-tetramethyl-1,3,2-dioxaborolan-2-yl)propanamide][47]

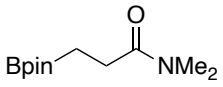

CAS_134892-18-5

[*rel*-2-[(1*R*,2*S*)-2-Bromocyclopropyl]-4,4,5,5-tetramethyl-1,3,2-dioxaborolane][48]

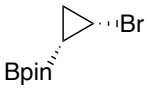

CAS_1396215-92-1

[*rel*-2-[(1*R*,2*R*)-2-Bromocyclopropyl]-4,4,5,5-tetramethyl-1,3,2-dioxaborolane][48]

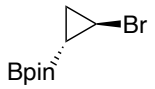

CAS_1396216-45-7

[(-)-2-(1-Bromopropyl)-4,4,5,5-tetramethyl-1,3,2-dioxaborolane][49]

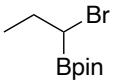

CAS_1584694-33-6
Note: (+) CAS_1584694-34-7

[2-(2-Bromo-1-methylethyl)-4,4,5,5-tetramethyl-1,3,2-dioxaborolane][50]

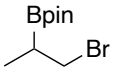

CAS_2176497-16-6

[4,4,5,5-Tetramethyl-2-(phenylethynyl)-1,3,2-dioxaborolane][51]

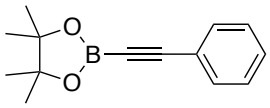

CAS_159087-45-3

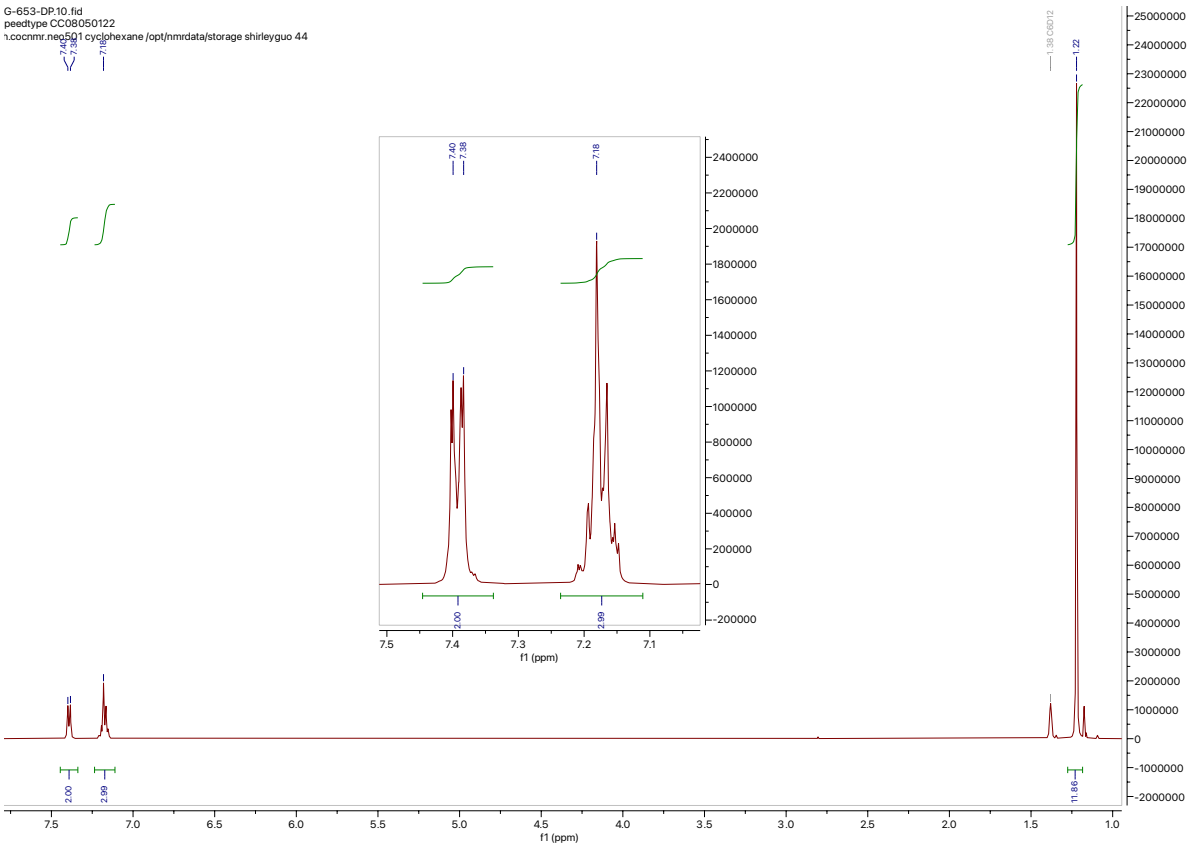
G-653-DP.10.fid
peedtype CC08050122
1.cocnmr.neo501 cyclohexane /opt/nmrdata/storage shirleyguo 44
7.40
7.38
7.18
1.22
2.00
2.99
11.86
f1 (ppm)

^{1}H-NMR

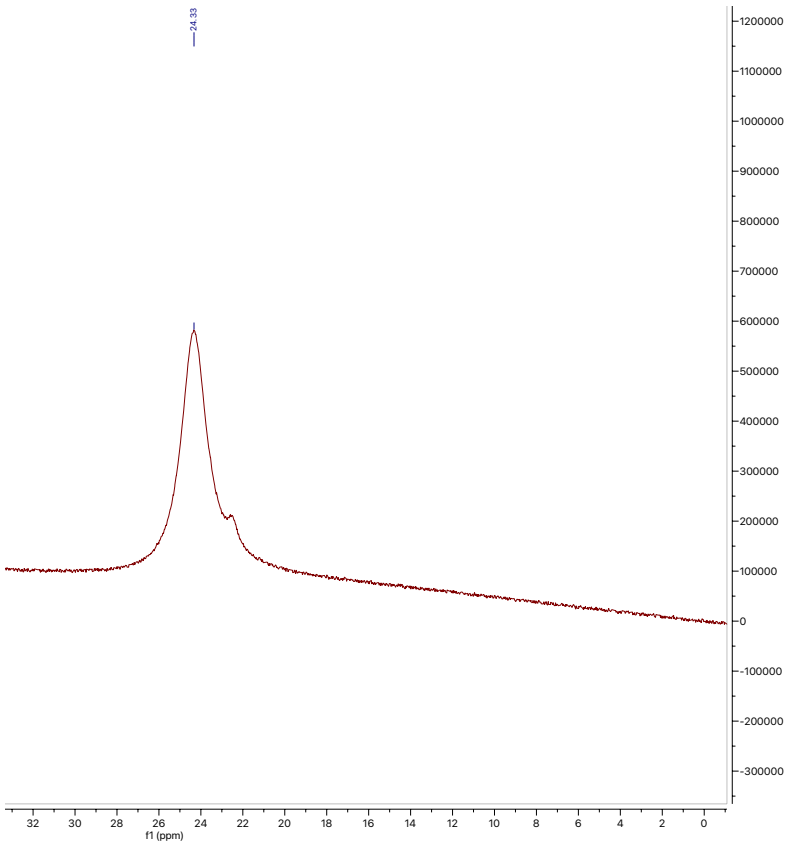

^{11}B-NMR

Note: a minor amount of BOB impurity can be seen as a shoulder peak overlapping with the main peak

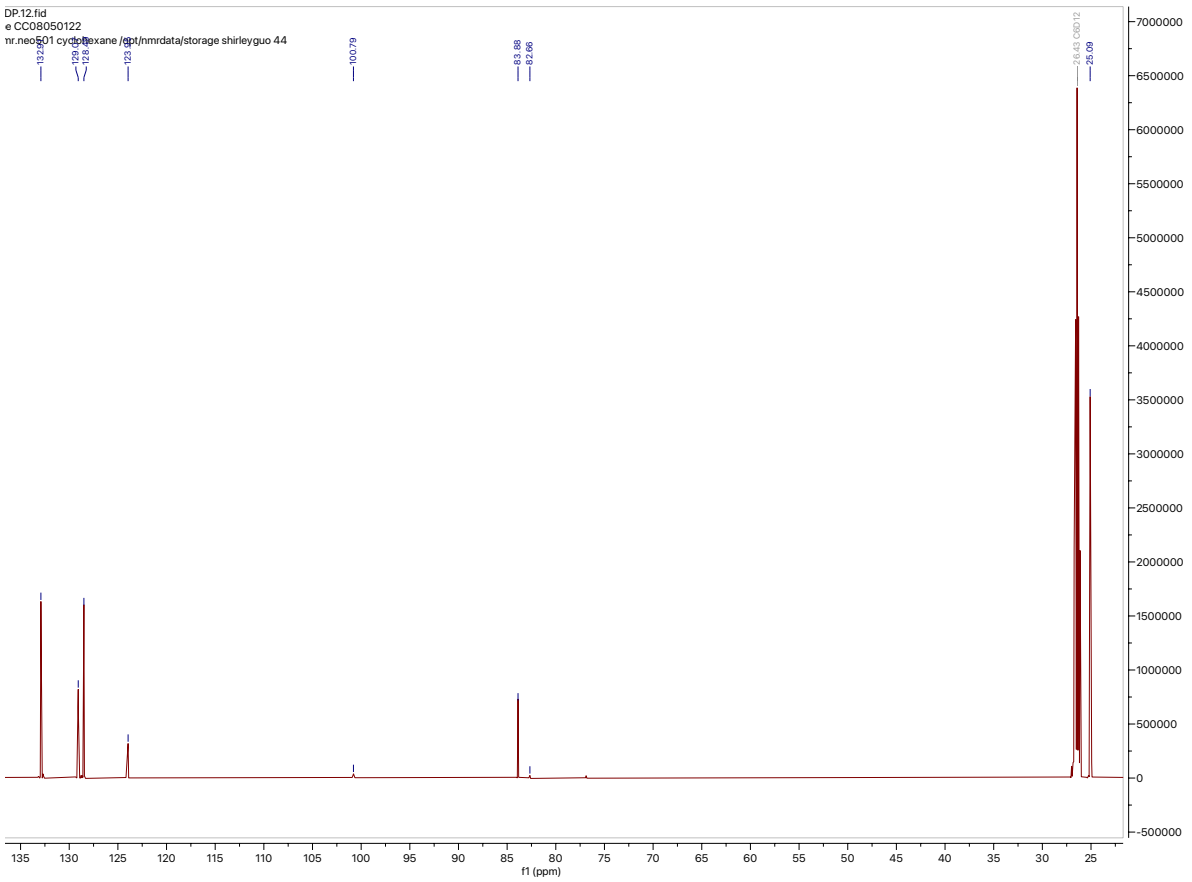

^{13}C-NMR

Ambident Reactivity

[N,N-dihexyl-4,4,5,5-tetramethyl-1,3,2-dioxaborolan-2-amine]

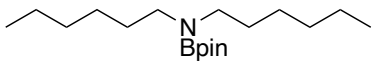

Unknown

General Procedure 1 conducted at 25 °C. An aliquot of the terminal reaction mixture was taken to which a drop of dihexylamine starting material was added. The mixture was diluted with C_6D_{12}

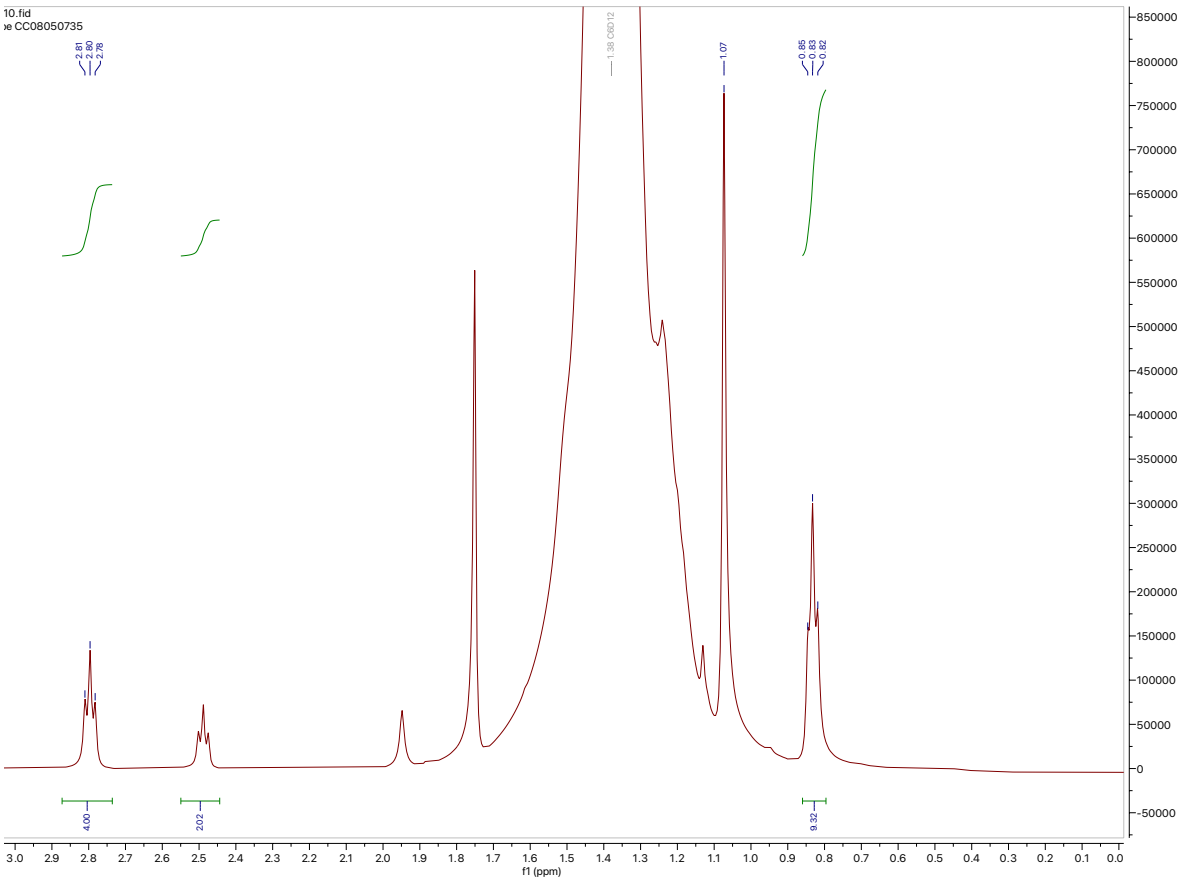

^{1}H-NMR

Note: the triplet around 2.5 ppm belongs to the alpha protons of added dihexylamine to show its resolution with those of borylated dihexylamine. The methyl protons of both dihexylamine and borylated dihexylamine overlap at 0.83 ppm. Residual MeCN can be seen at around 1.75 ppm

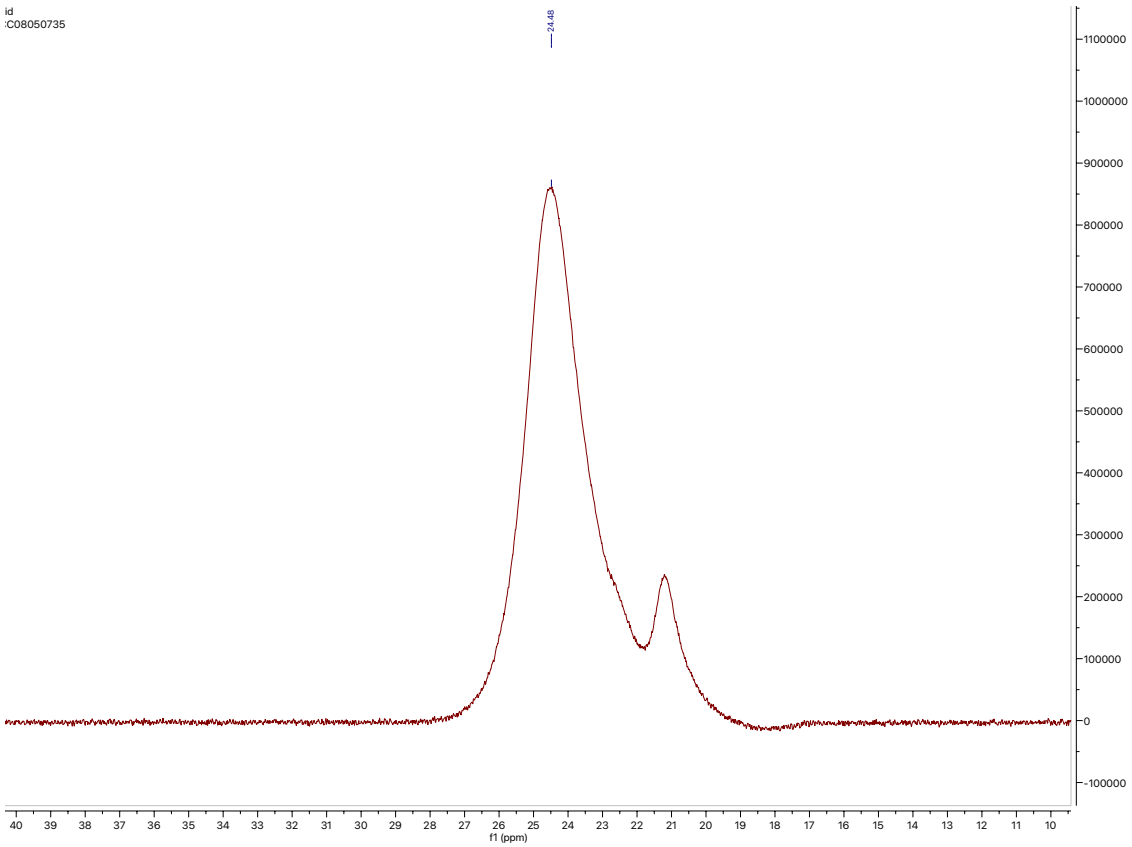

^{11}B-NMR

Note: the unlabeled peak around 21 ppm belongs to BOB impurity

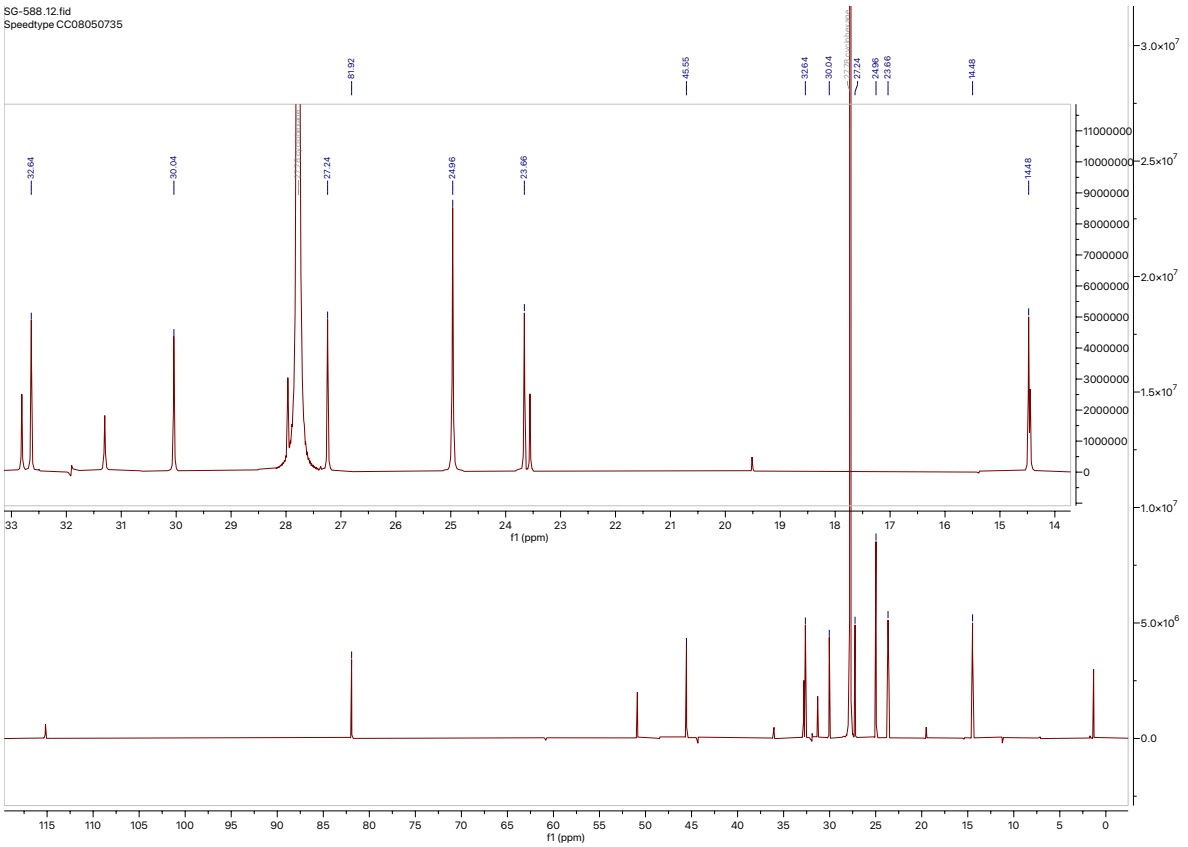

^{13}C-NMR

Note: the unlabeled peaks around 1 ppm & 115 ppm belong to residual MeCN. The remaining unlabeled peaks belong to the added dihexylamine and demonstrate its resolution with the borylated dihexylamine (labeled peaks)

[4,4,5,5-Tetramethyl-2-phenoxy-1,3,2-dioxaborolane][52]

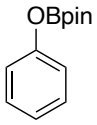

CAS_95770-20-0

General Procedure 2. Due to instability of product upon concentration instead an aliquot of the non-concentrated reaction mixture was taken and diluted with C_6D_{12}

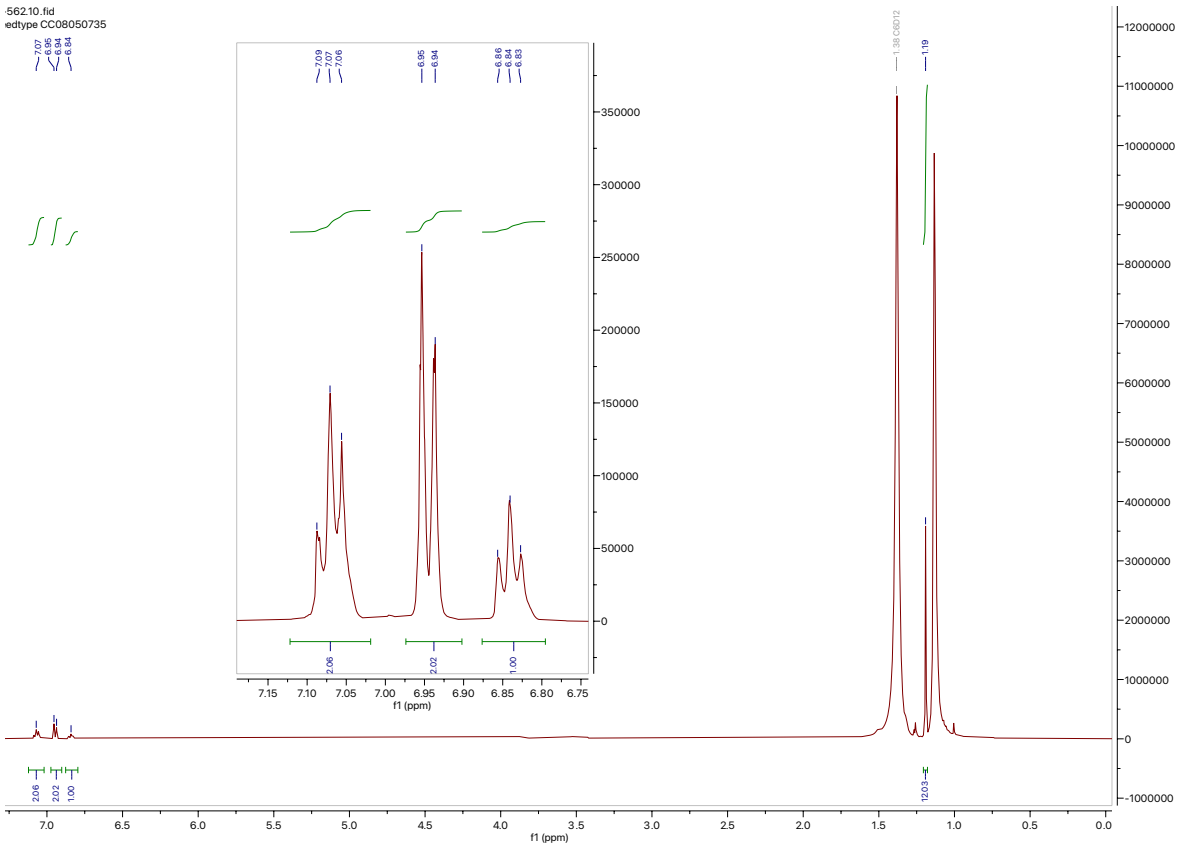

^{1}H-NMR

Note: the unlabeled peak around 1.1 ppm belongs to the methyls of residual HBpin

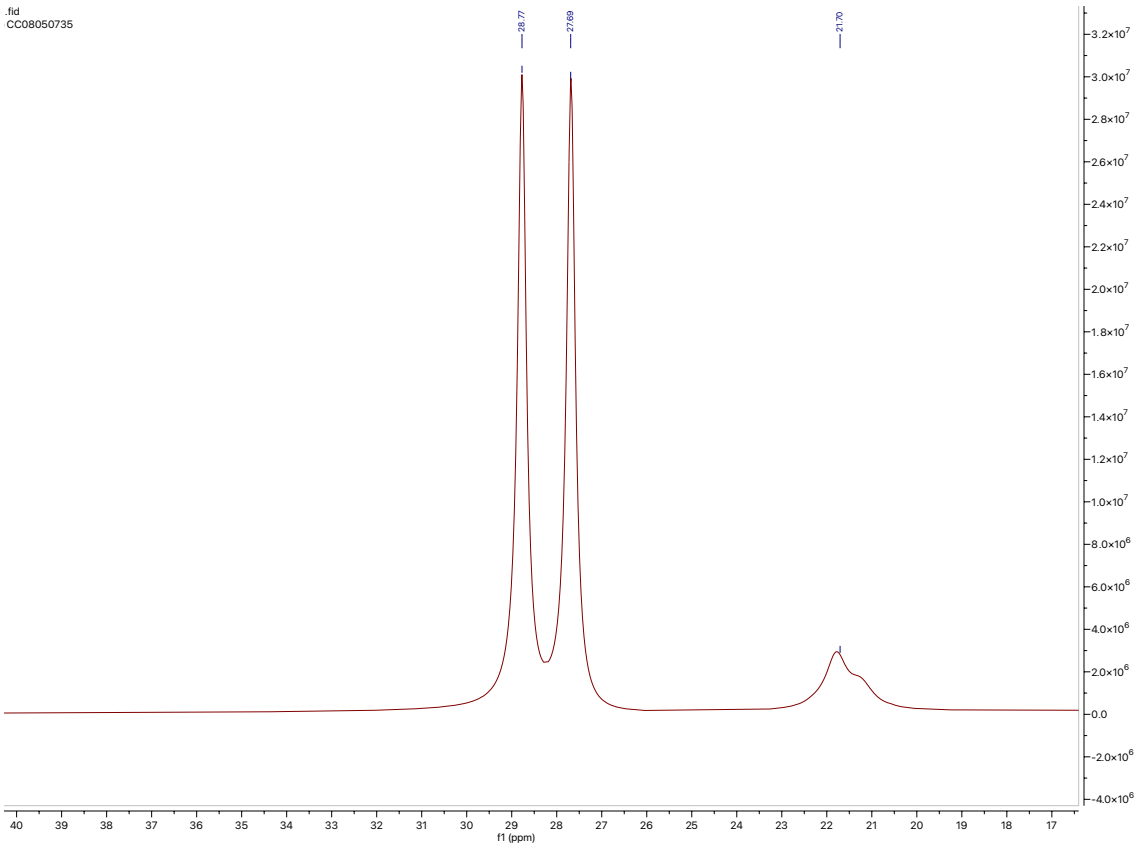

^{11}B-NMR

Note: the unlabeled shoulder peak around 21 ppm belongs to BOB impurity

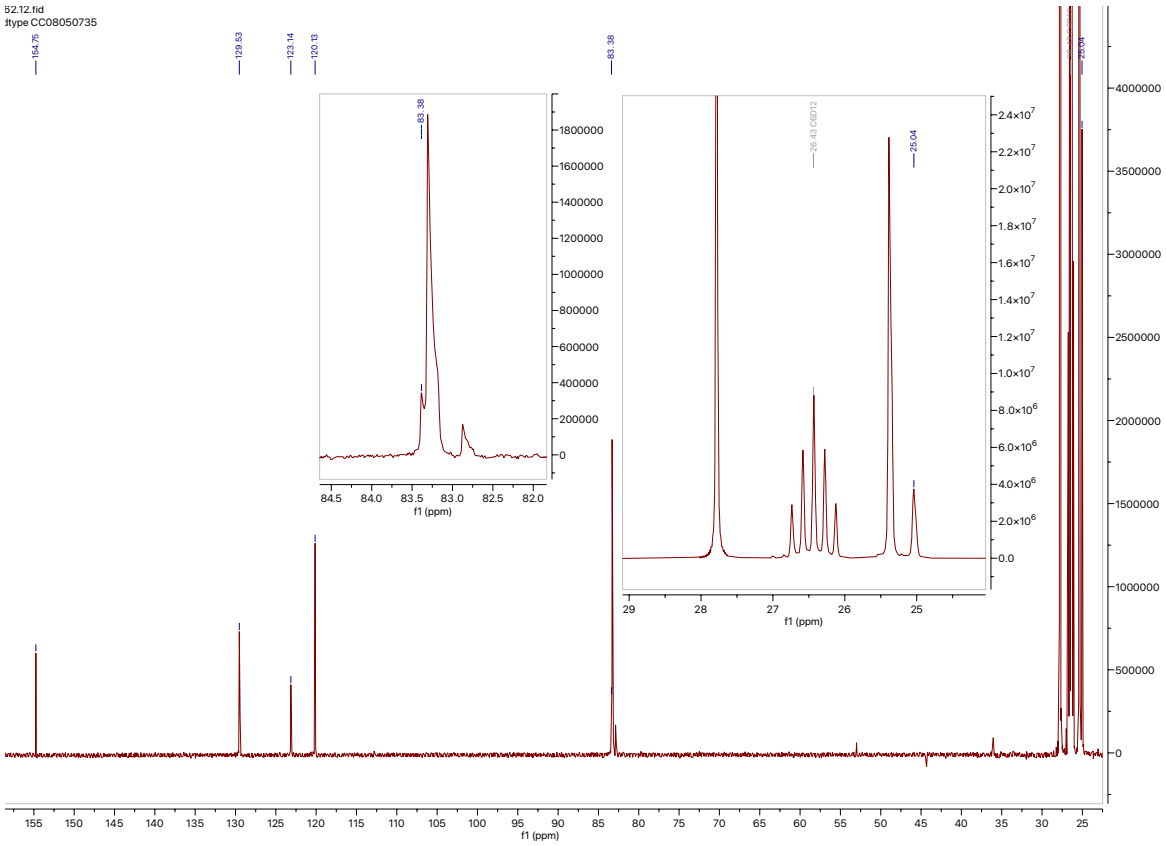

^{13}C-NMR

Note: the unlabeled peaks around 83 ppm belong to the quaternary carbons of residual HBpin and BOB impurity. The unlabeled peak at 27.78 ppm is cyclohexane solvent. The unlabeled peak around 25.4 ppm belongs to the methyls of residual HBpin. The methyls of residual BOB impurity overlap with those of the product at 25.04 ppm

[4,4,5,5-Tetramethyl-*N*-phenyl-1,3,2-dioxaborolan-2-amine][53]

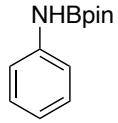

CAS_857402-61-0

General Procedure 1 but with an added 1 mol% Et_3N and an elevated temperature of 120 °C. Residual solvent was evaporated. To the crude was added a minimal amount of acetonitrile. The mixture was stirred briefly and then the filtrate decanted. This purification method was repeated twice more. A sample of the purified crystal was diluted in C_6D_{12}.

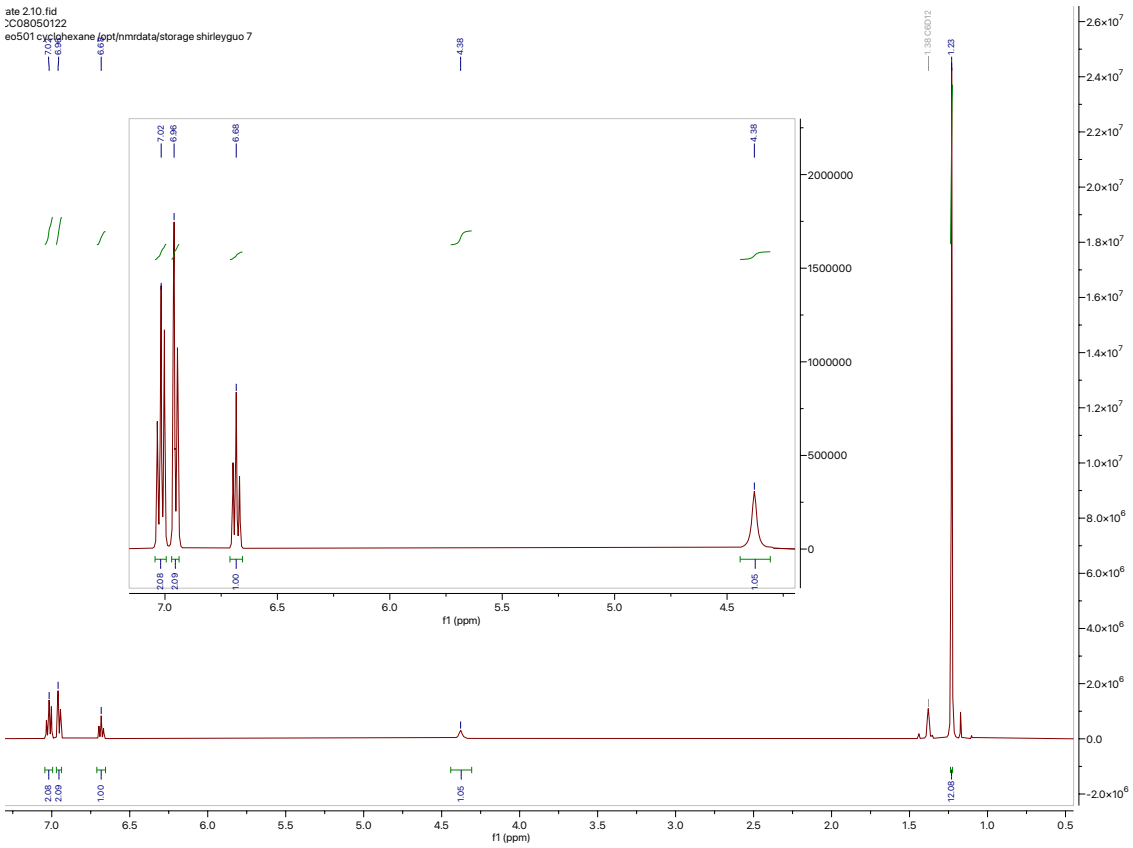
ate 2.10.fid
C08050122
eo501 cyclohexane /opt/nmrdata/storage shirleyguo 7
7.02
6.96
6.68
4.38
1.38 C6D12
1.23
2.08
2.09
1.00
1.05
12.08
f1 (ppm)

^{1}H-NMR

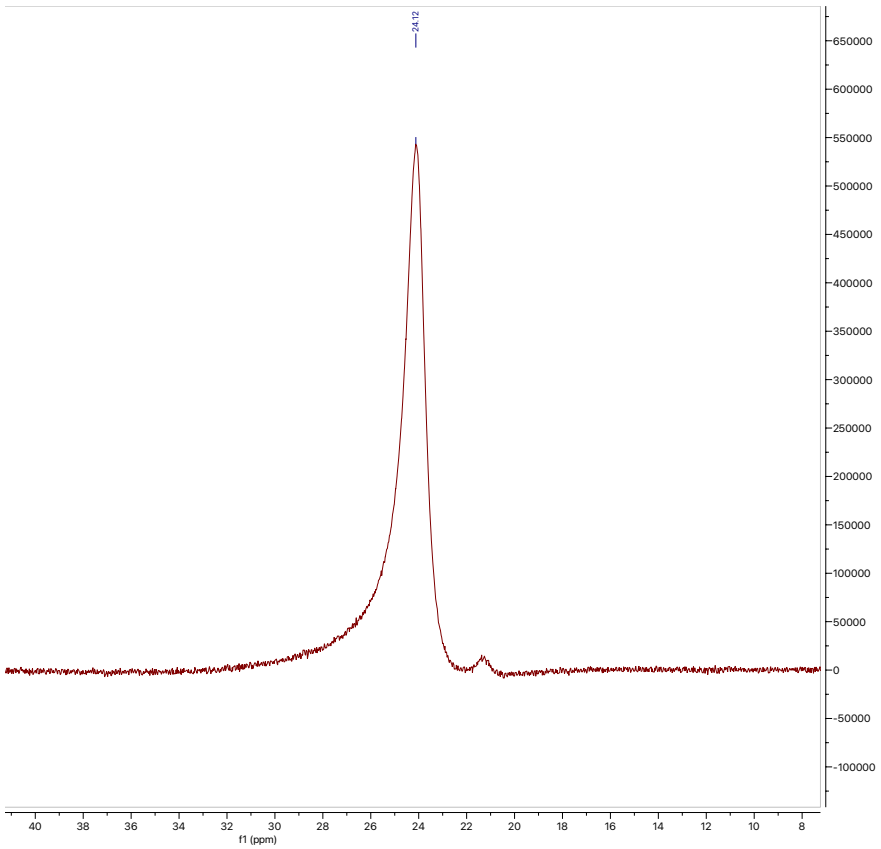
24.12
650000
600000
550000
500000
450000
400000
350000
300000
250000
200000
150000
100000
50000
0
-50000
-100000
40
38
36
34
32
30
28
26
24
22
20
18
16
14
12
10
8
f1 (ppm)

^{11}B-NMR

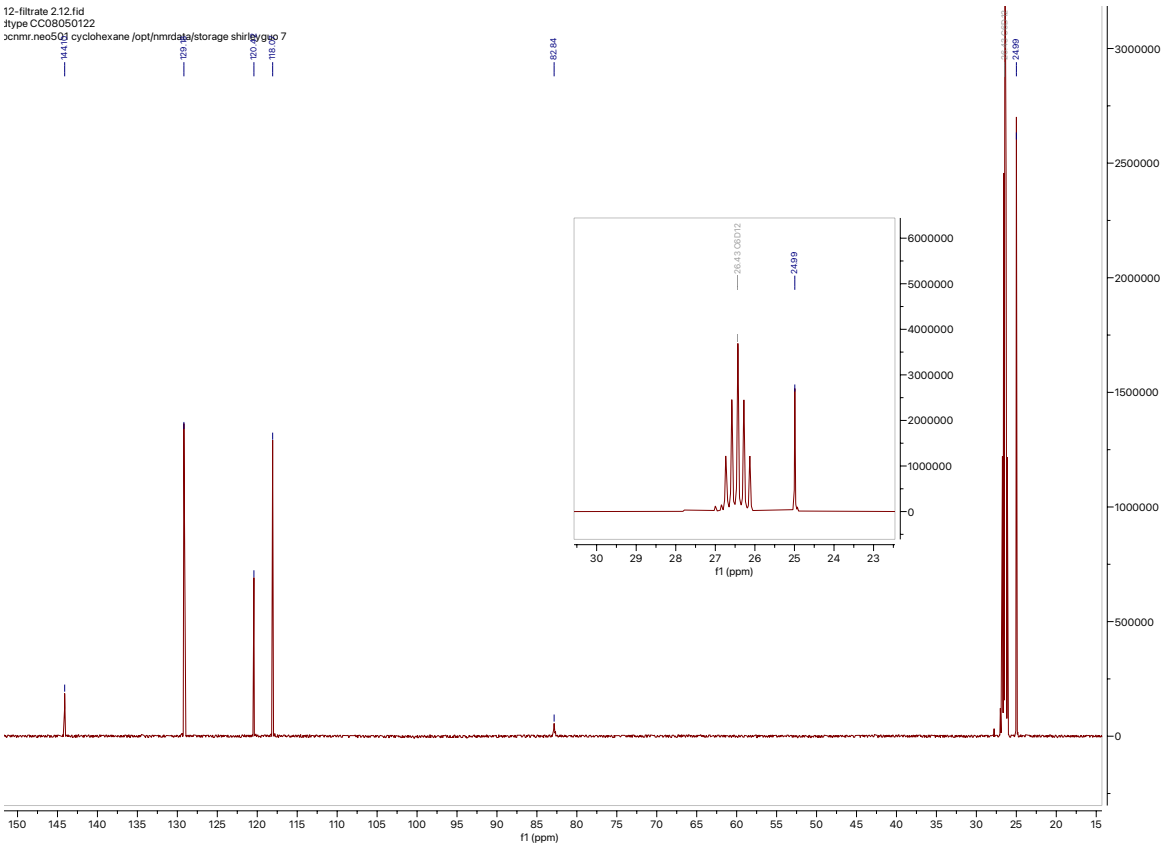

^{13}C-NMR

[4,4,5,5-Tetramethyl-2-(phenylthio)-1,3,2-dioxaborolane][54]

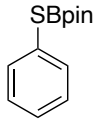

CAS_1443045-55-3

[3-Methyl-5-(4,4,5,5-tetramethyl-1,3,2-dioxaborolan-2-yl)pyridine][12]

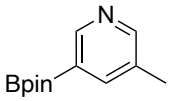

CAS_1171891-42-1

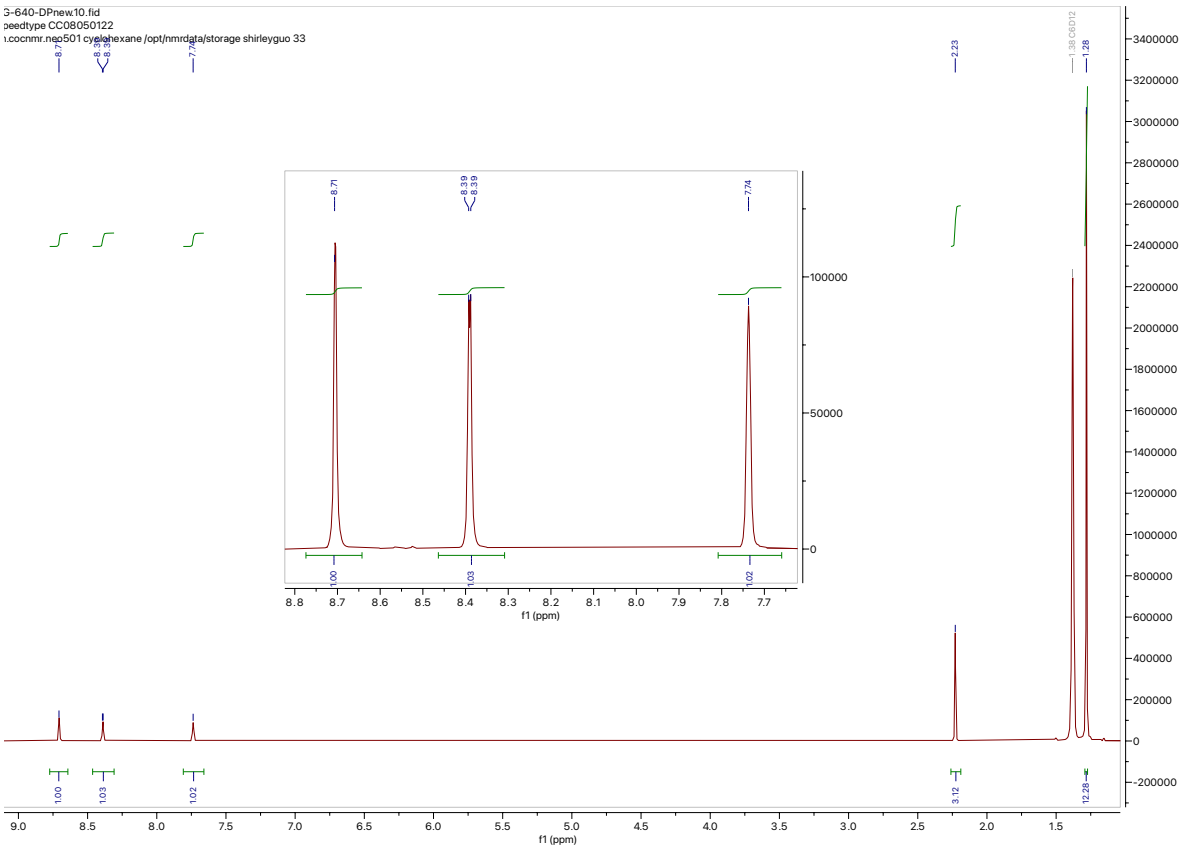

^{1}H-NMR

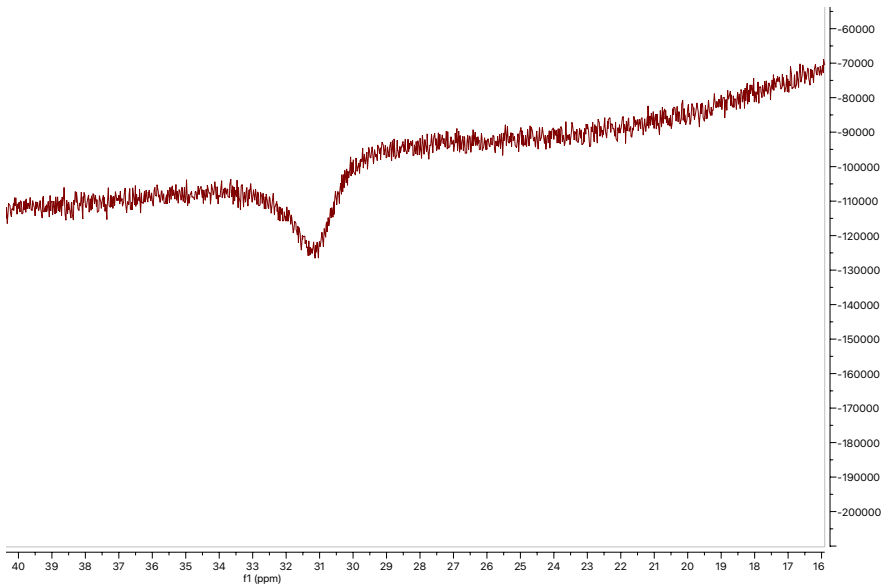

^{11}B-NMR

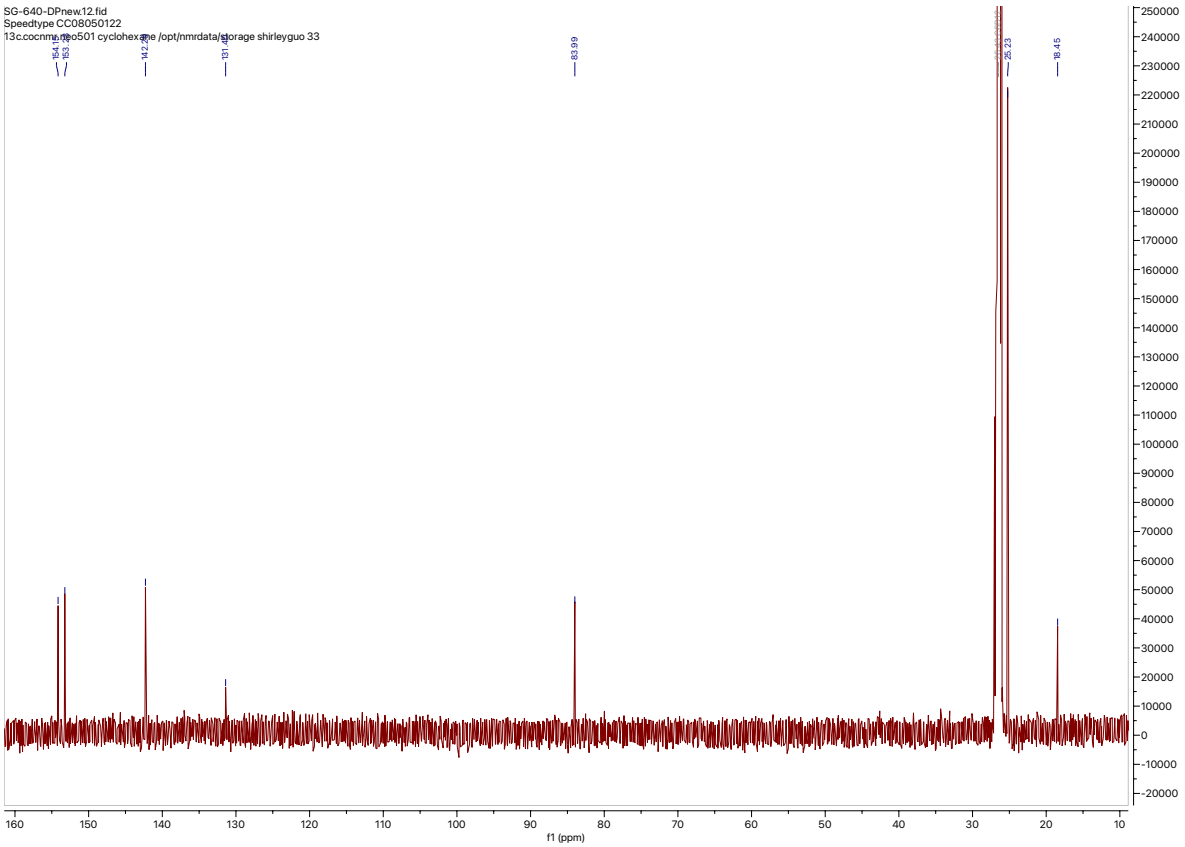

^{13}C-NMR

Note: **C**—Bpin not observed

[2-(2-Butyn-1-yl)-4,4,5,5-tetramethyl-1,3,2-dioxaborolane][55]

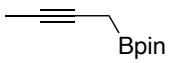

CAS_2249756-26-9

[2-(1,2-Butadien-1-yl)-4,4,5,5-tetramethyl-1,3,2-dioxaborolane][56]

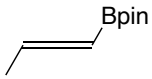

CAS_1427165-74-9

[(Benzothiophen-2-yl)boronic acid pinacol ester][57]

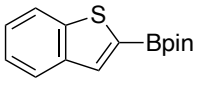

CAS_376584-76-8

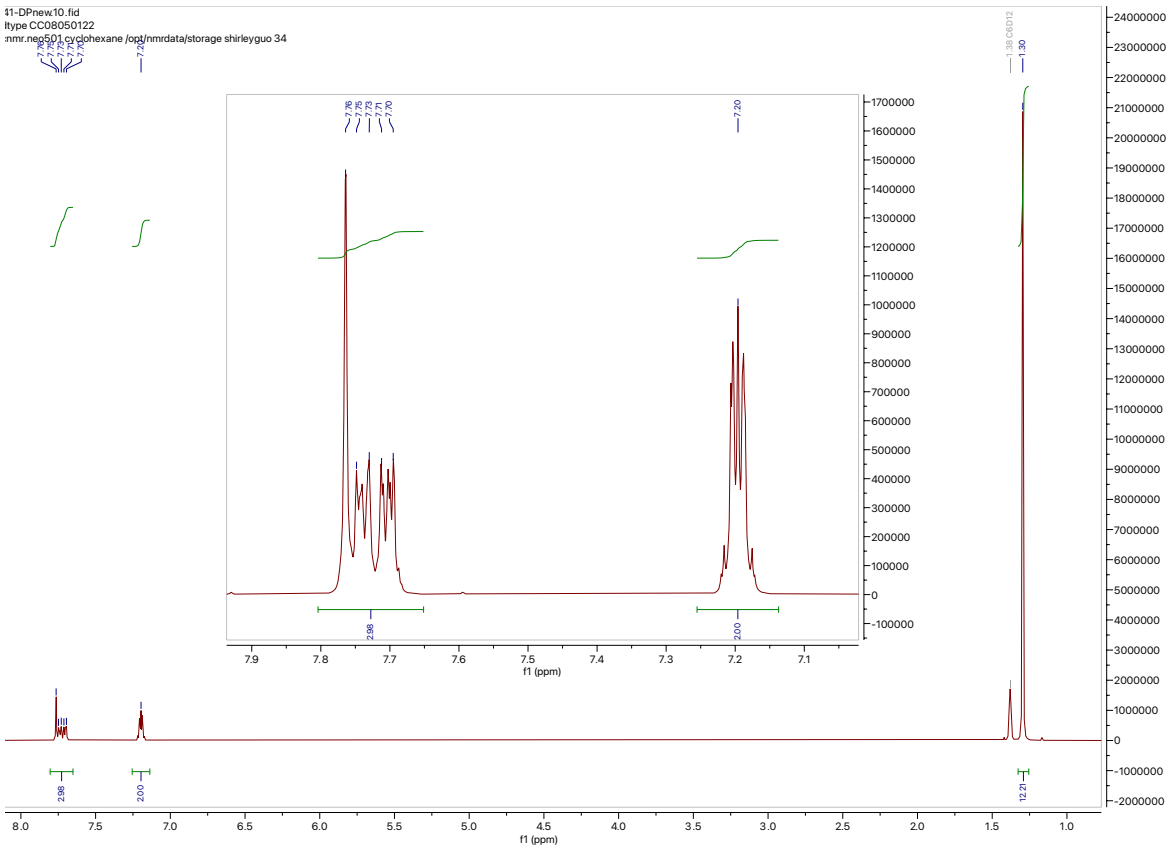

^{1}H-NMR

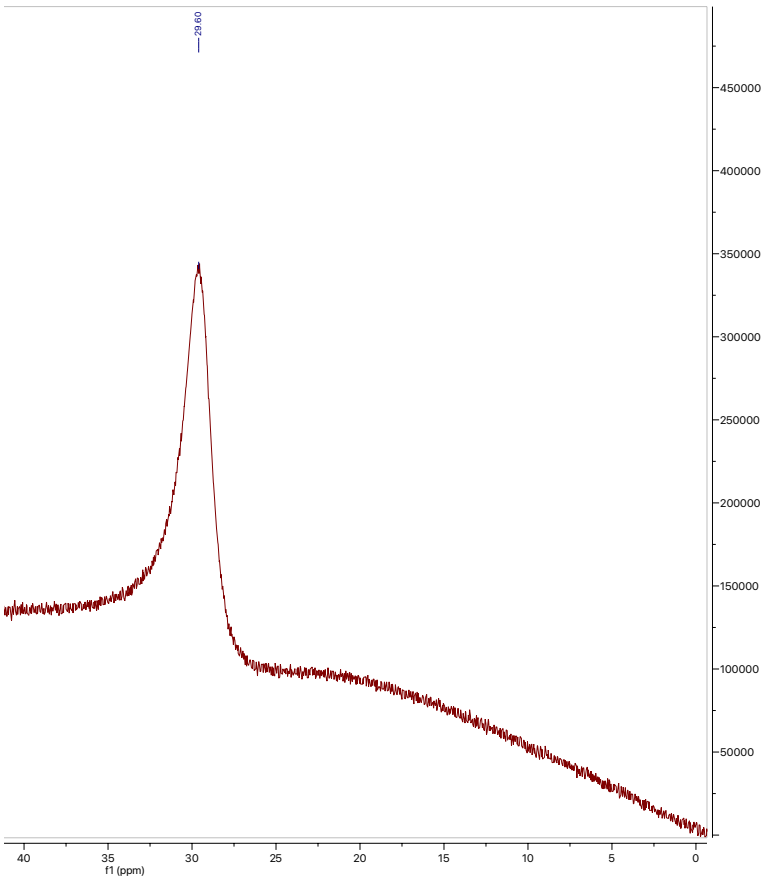
29.60
450000
400000
350000
300000
250000
200000
150000
100000
50000
40
35
30
25
20
15
10
5
0
f1 (ppm)

^{11}B-NMR

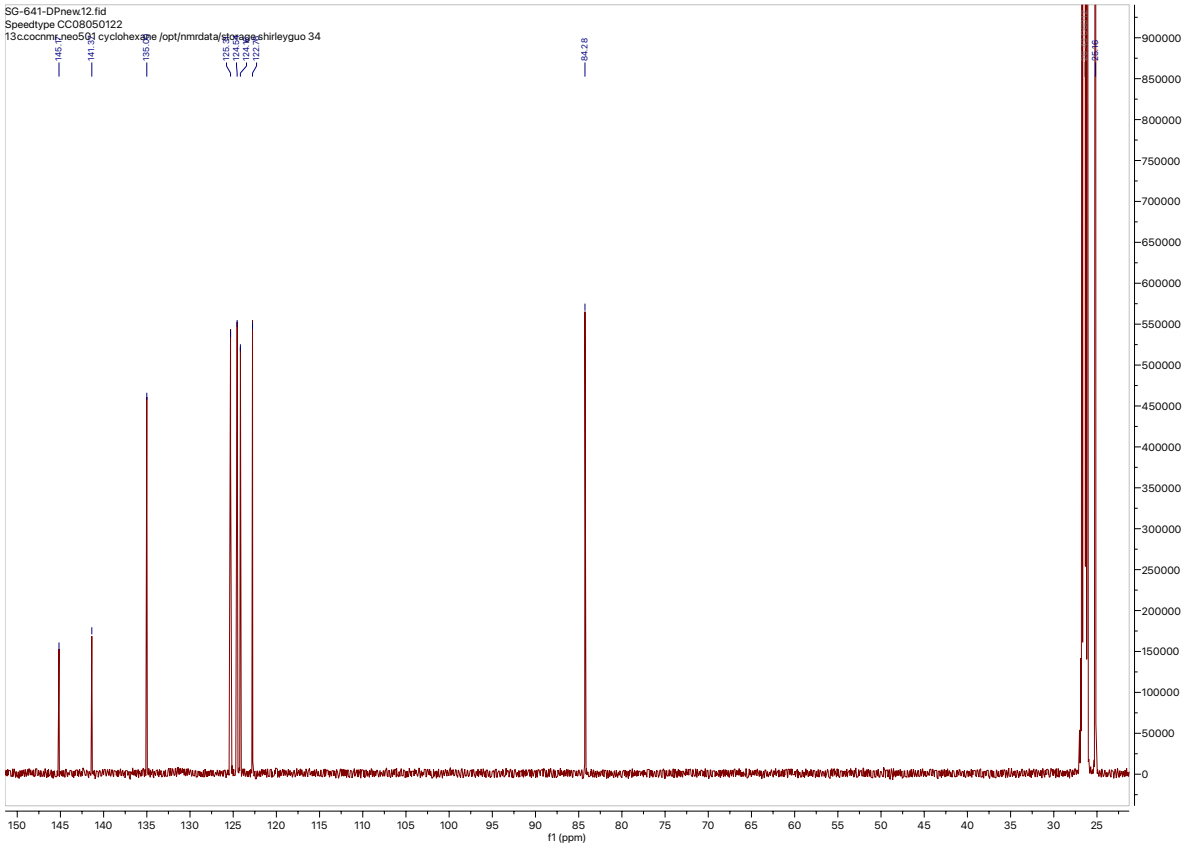

^{13}C-NMR

Note: **C**—Bpin not observed

[7-Methyl-2-(4,4,5,5-tetramethyl-1,3,2-dioxaborolan-2-yl)-1*H*-indole][58]

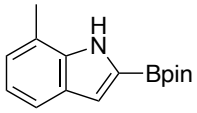

CAS_912331-68-1

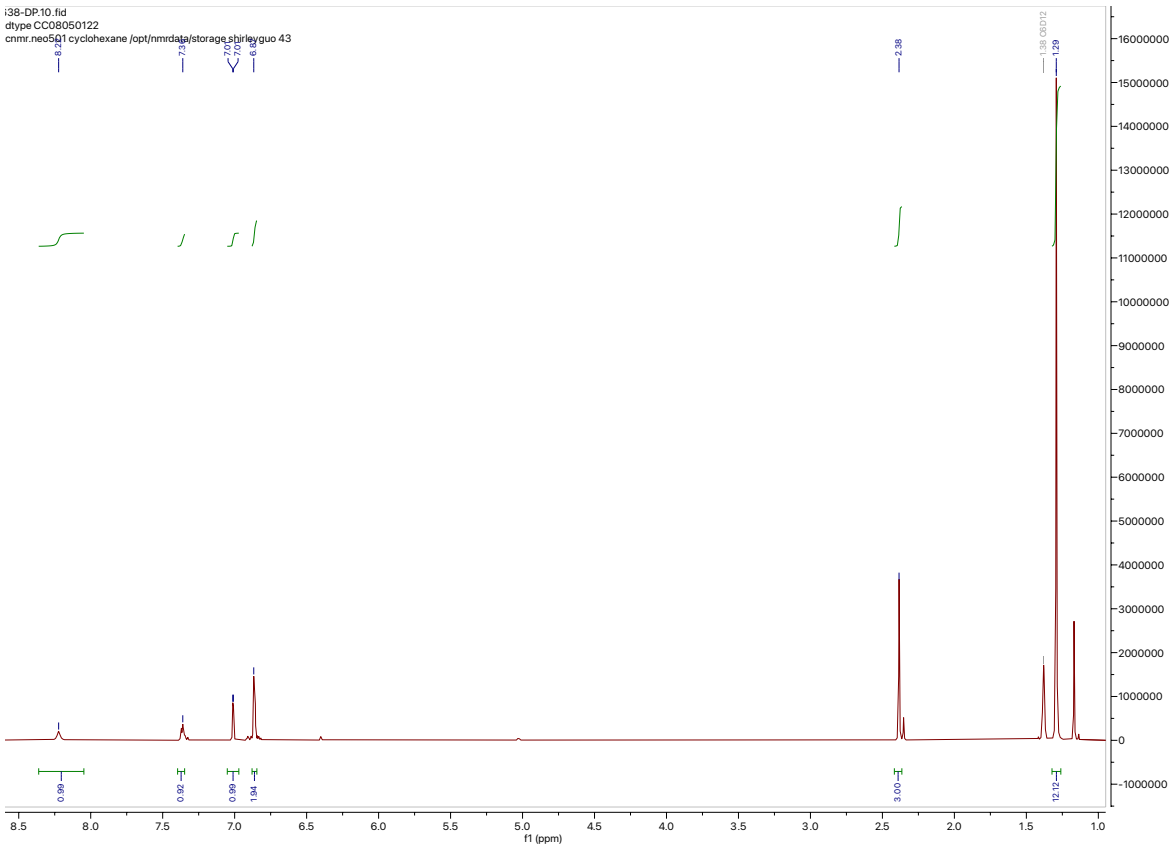

^{1}H-NMR

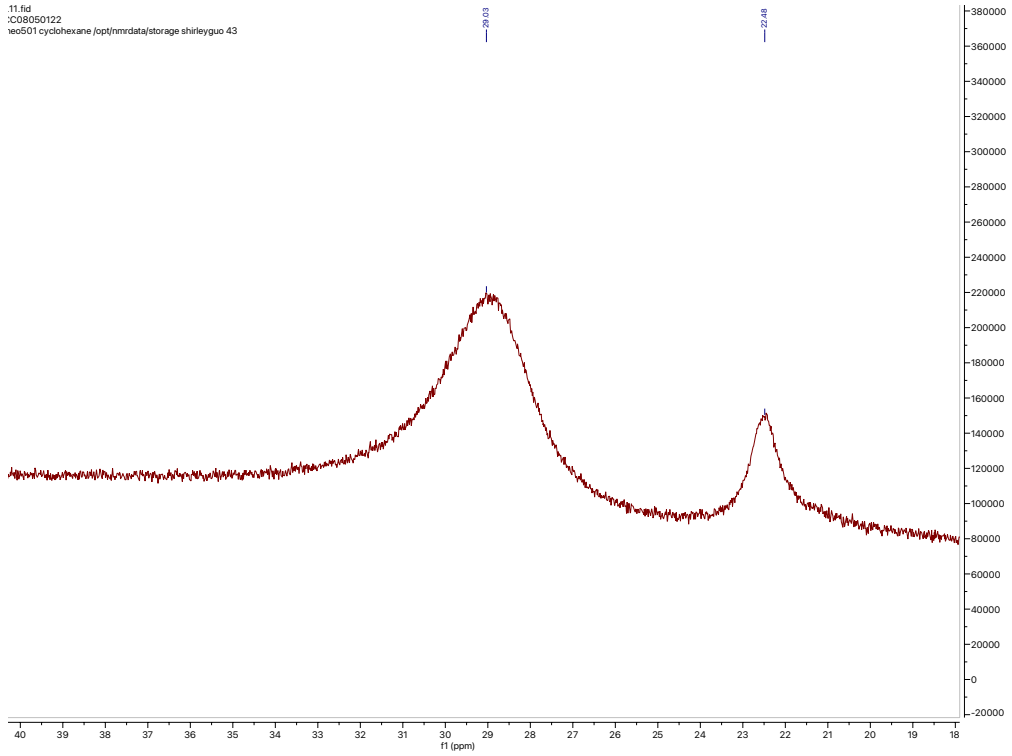

^{11}B-NMR

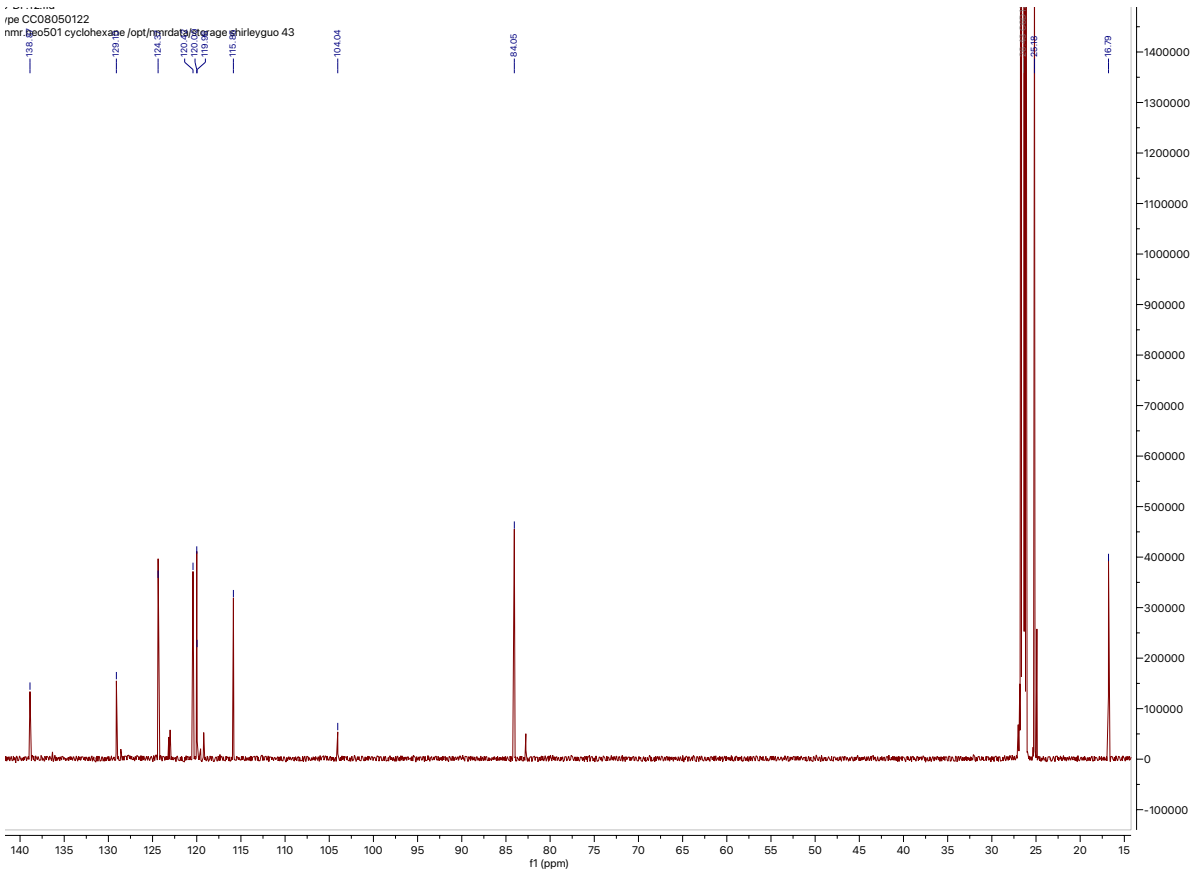

^{13}C-NMR

1.4.5 NMR Spectroscopy of Additives in Cyclohexane-d_{12}

Reactivity at Bpin Ligand

[1-hexanol]

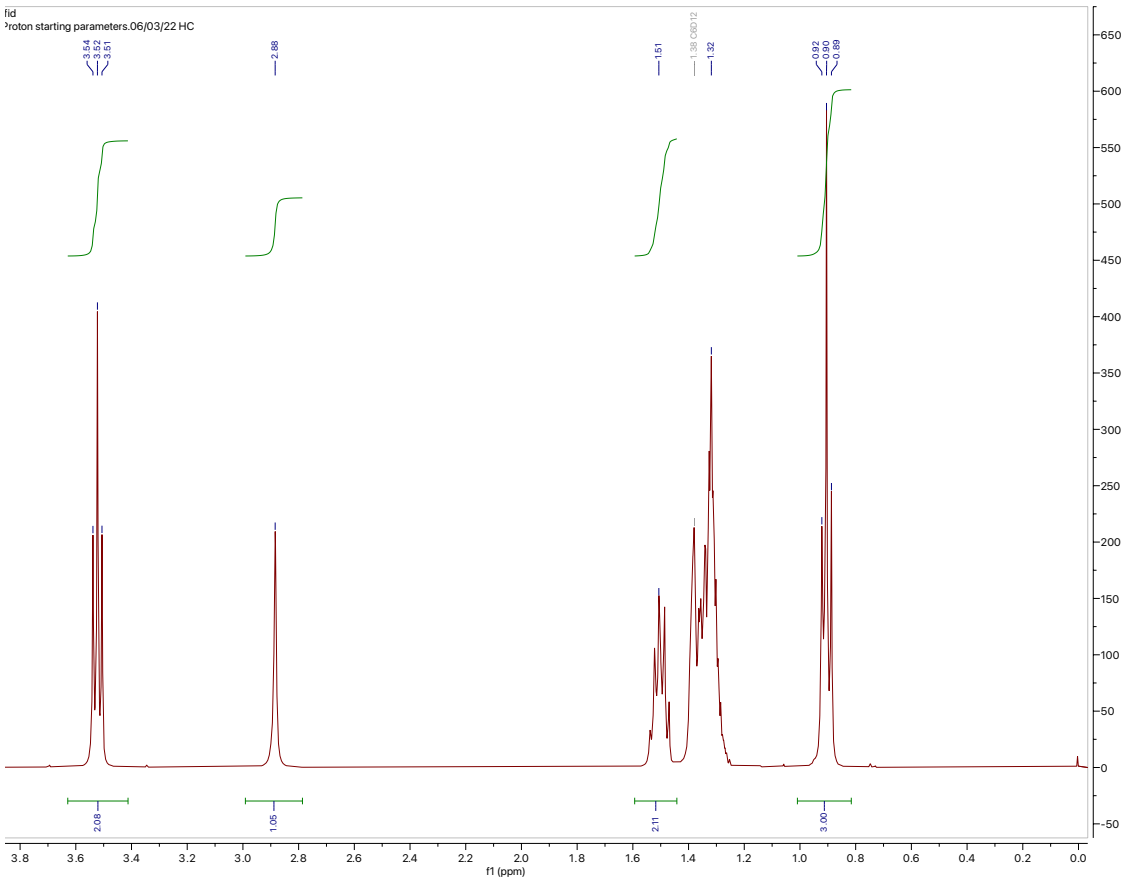

^{1}H-NMR

Note: compound overlaps with cyclohexane-d_{12}

[3-hexanol]

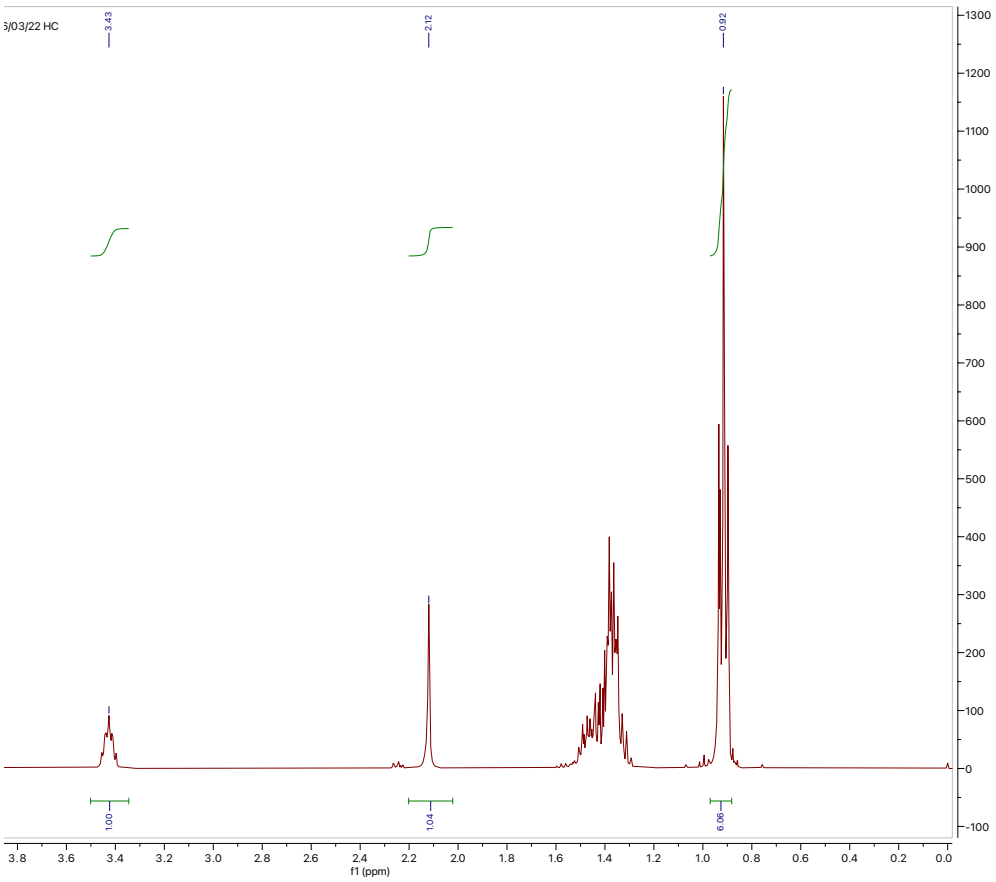

^{1}H-NMR

Note: compound overlaps with cyclohexane-d_{12}

[3-methyl-3-pentanol]

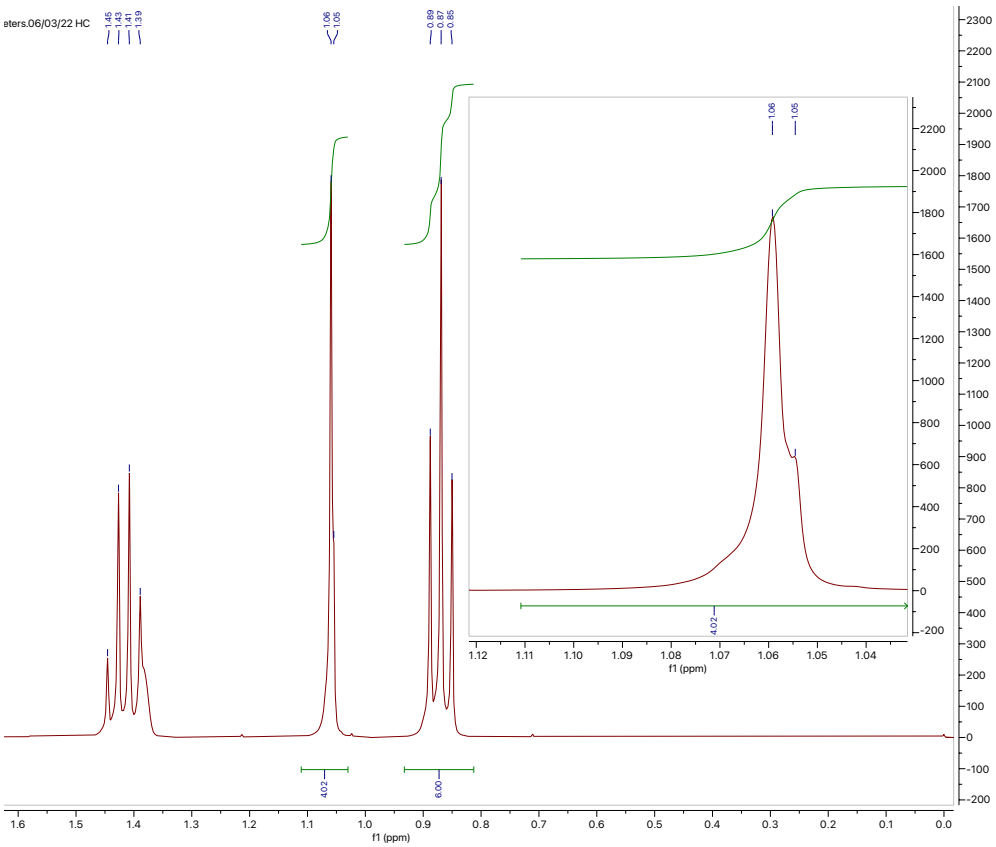

^{1}H-NMR

Note: compound overlaps with cyclohexane-d_{12}

[dodecylamine]

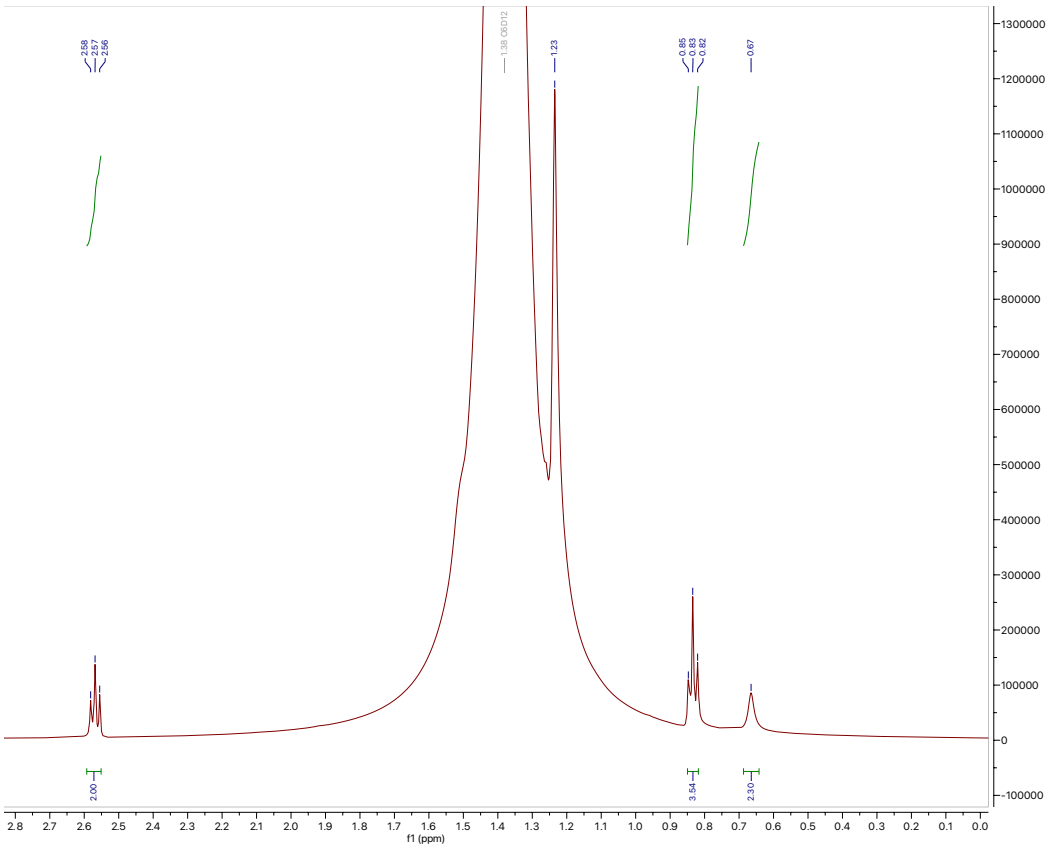

^{1}H-NMR (in cyclohexane)

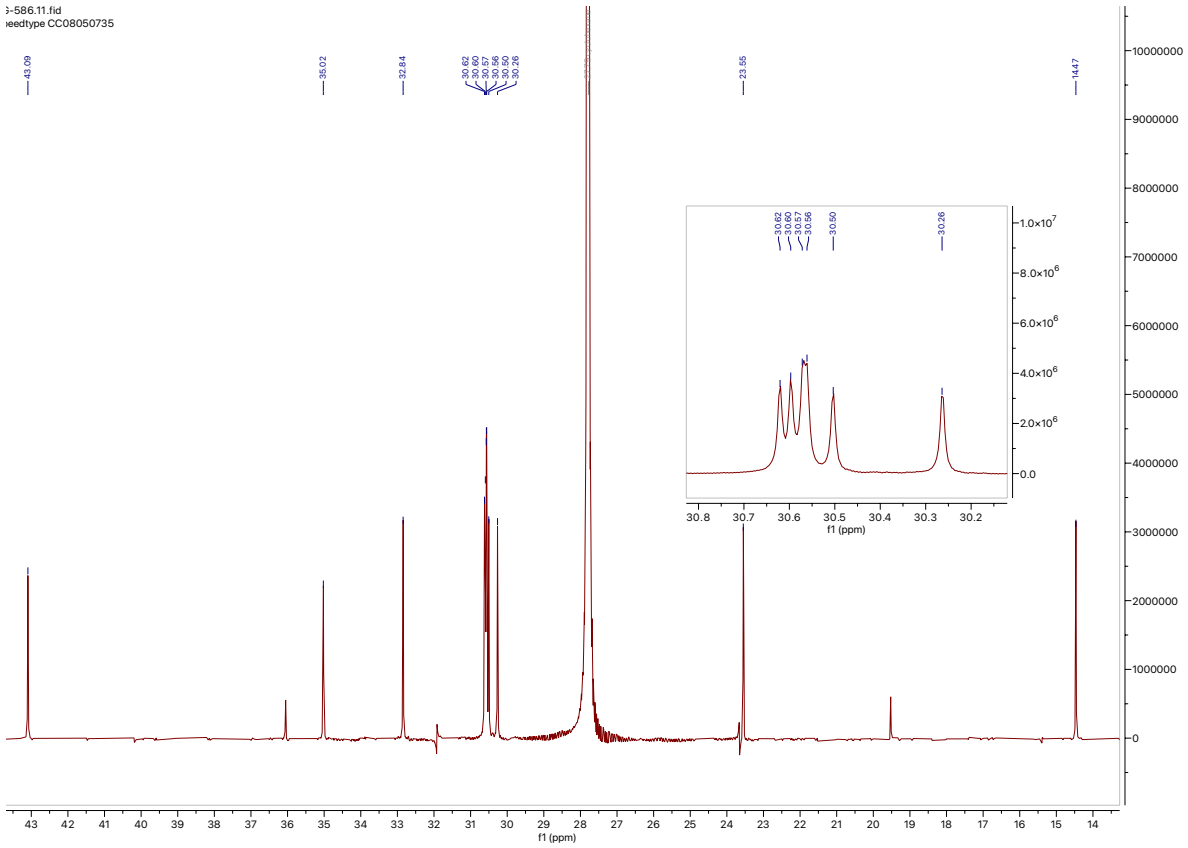

^{13}C-NMR (in cyclohexane)

Note: for a long aliphatic chain compound some C peaks will overlap

[octanethiol]

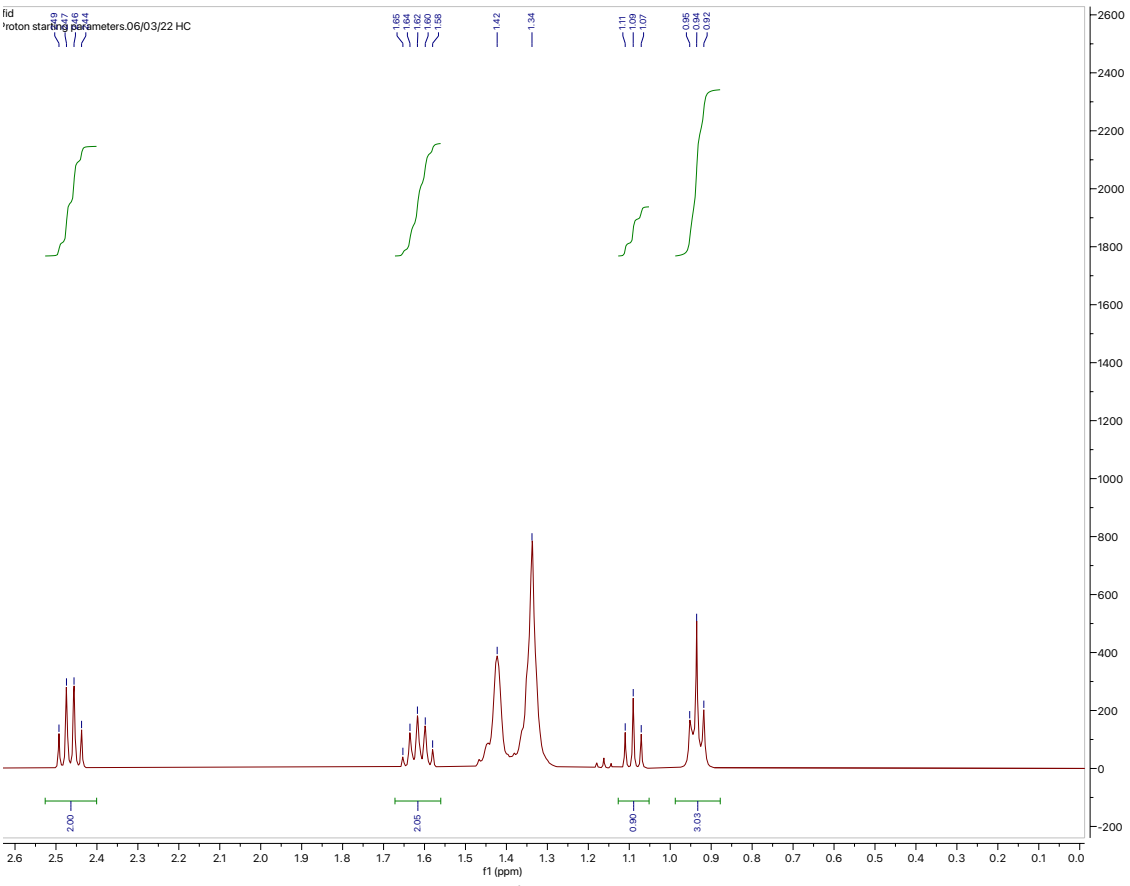

^{1}H-NMR

Note: compound peaks overlap with C_6D_{12}

[N-methylbutyramide]

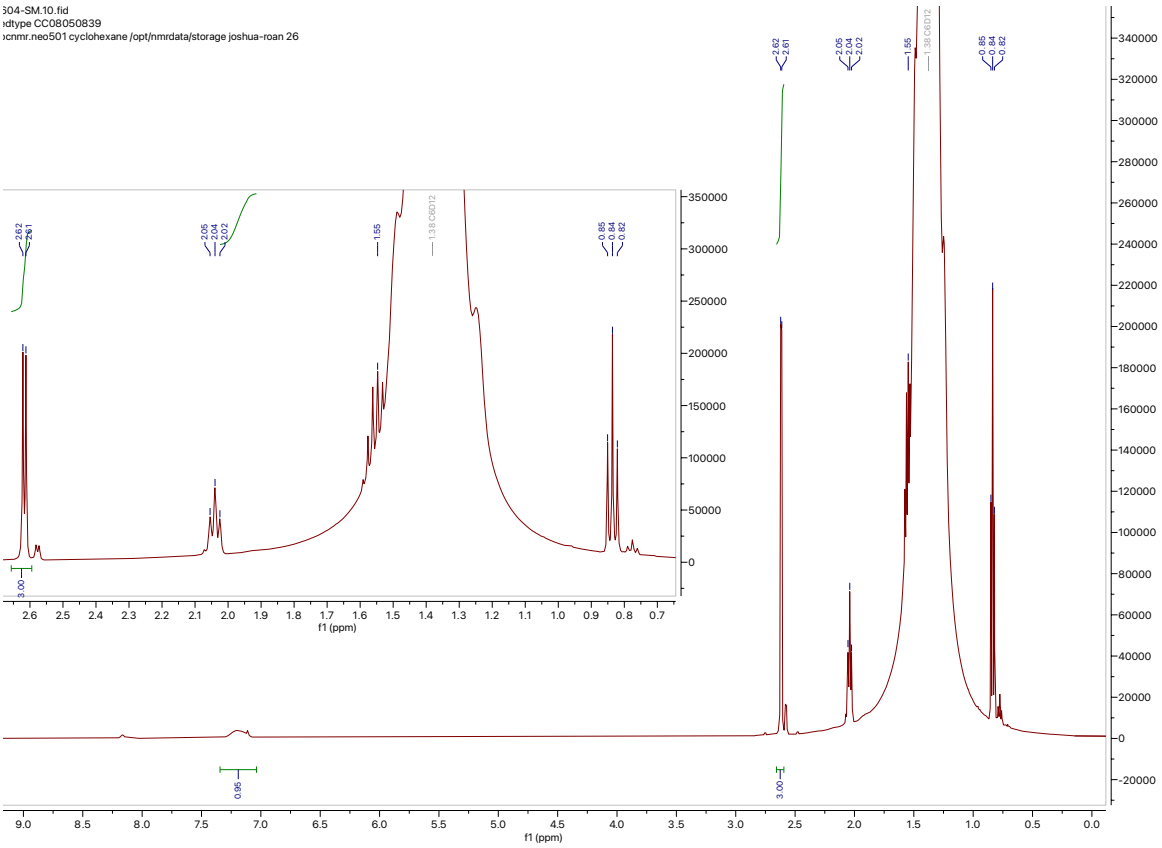

^{1}H-NMR (in cyclohexane-h_{12}/d_{12})

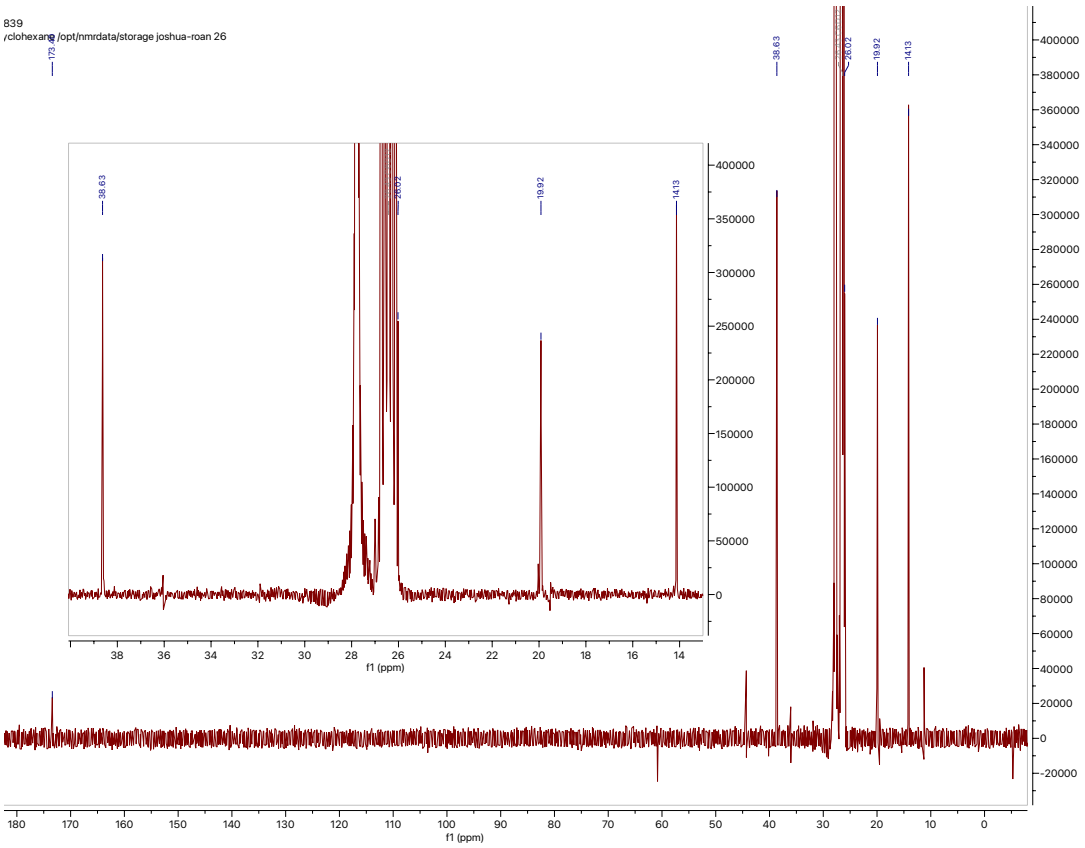

^{13}C-NMR (in cyclohexane-h_{12}/d_{12})

Reactivity at Ir

[boc-pyrazole]

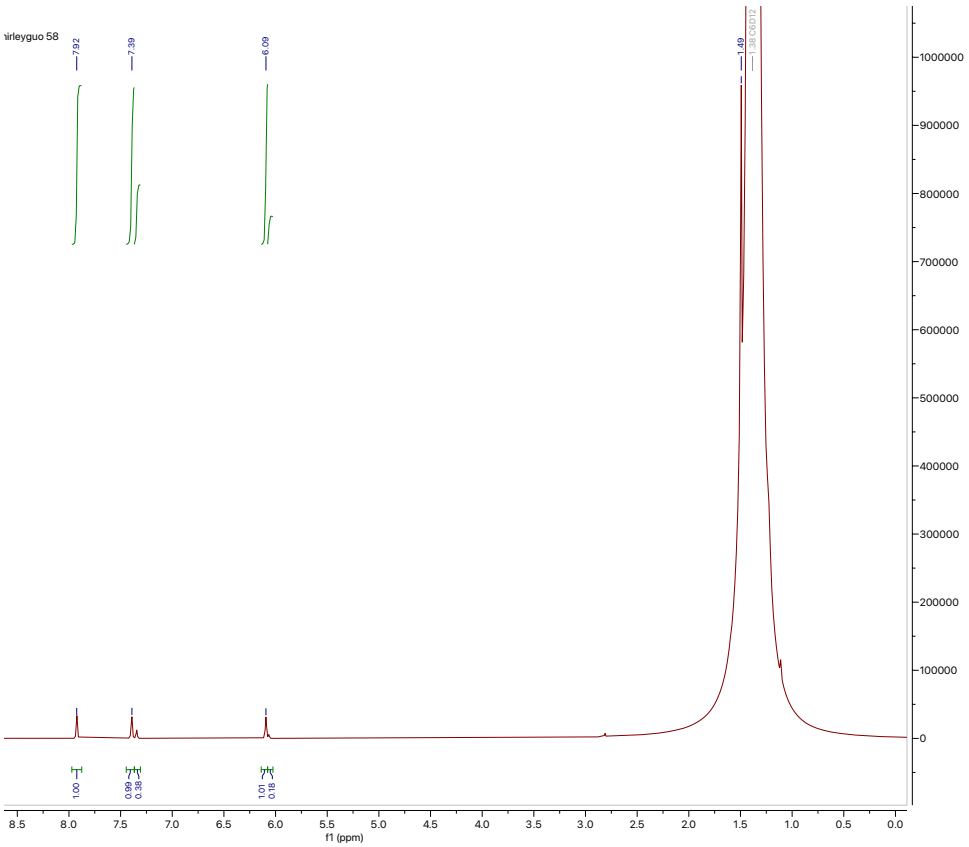

^{1}H-NMR (in cyclohexane)

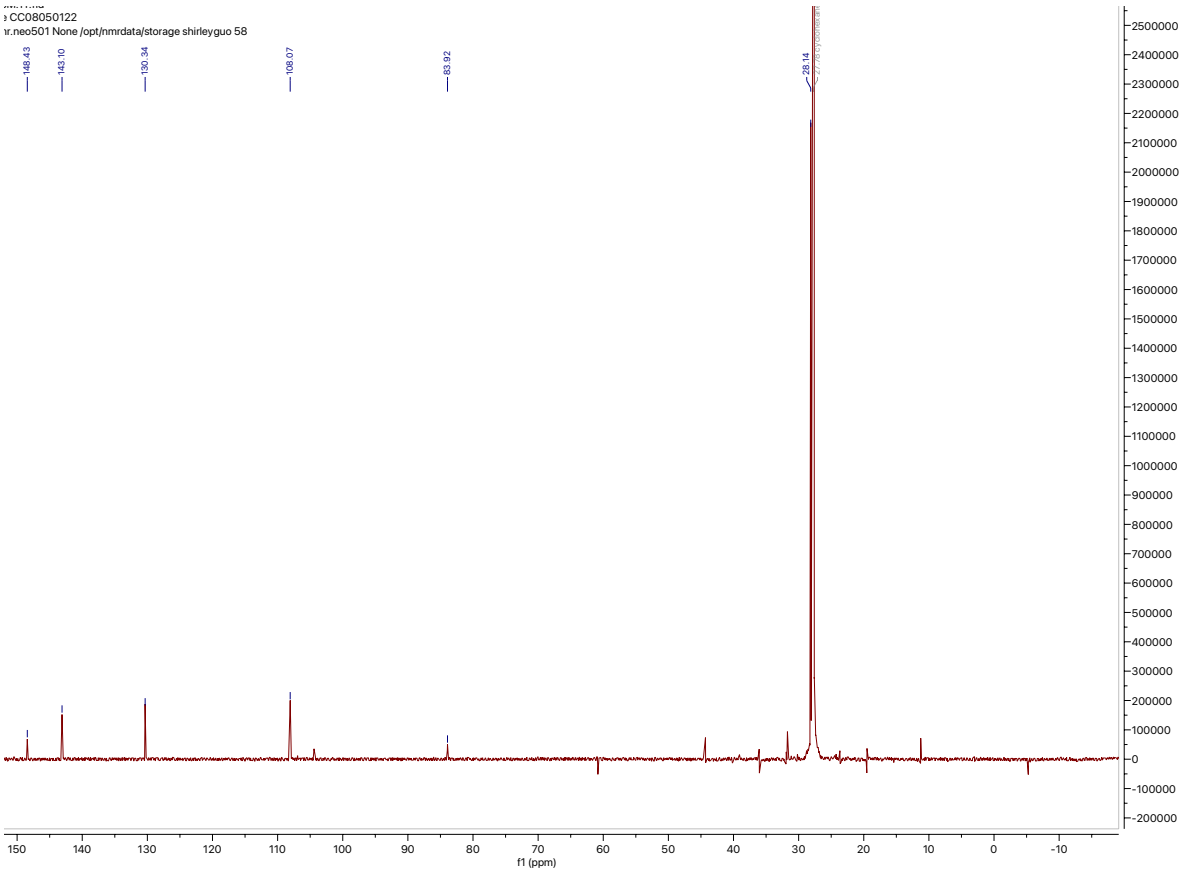

^{13}C-NMR (in cyclohexane)

[2-chloro-4-fluoro-1-methylbenzene]

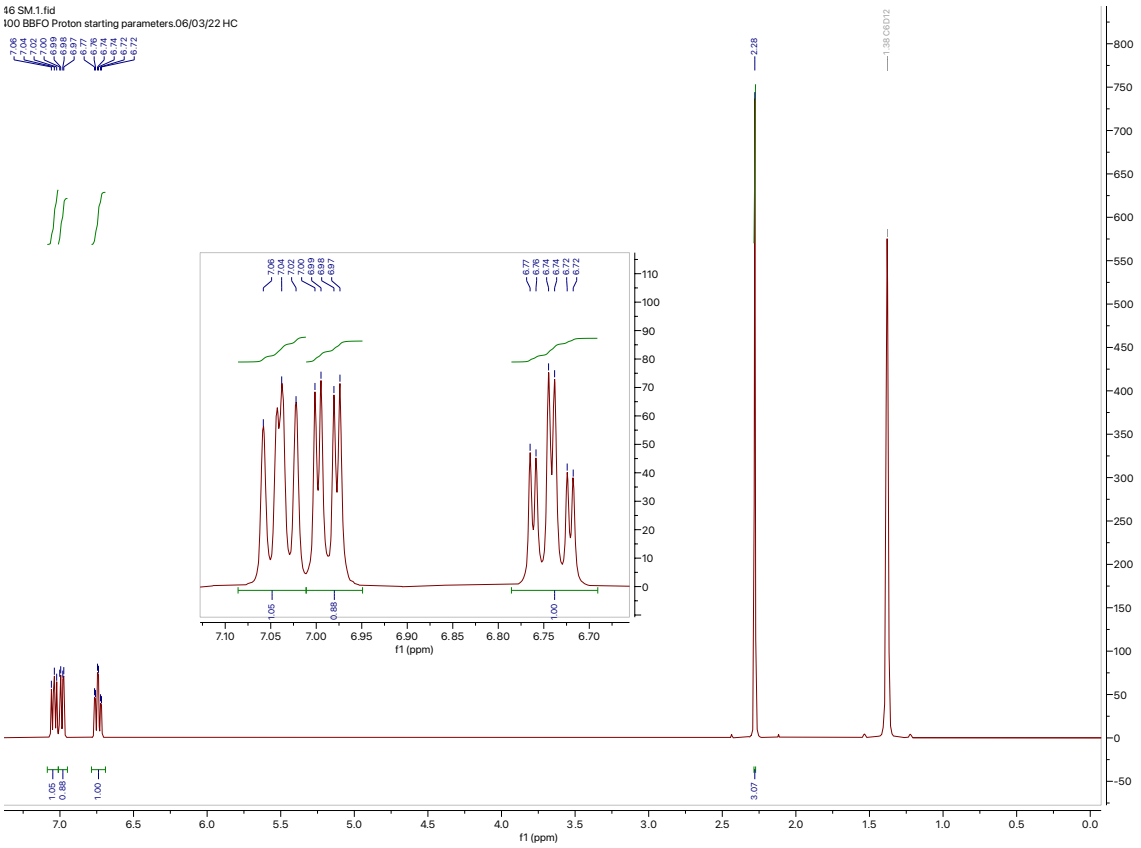
46 SM.1.fid
400 BBFO Proton starting parameters.06/03/22 HC
7.06
7.04
7.02
7.00
6.99
6.98
6.97
6.77
6.76
6.74
6.74
6.72
6.72
2.28
1.38
1.05
0.88
1.00
3.07
f1 (ppm)

^{1}H-NMR

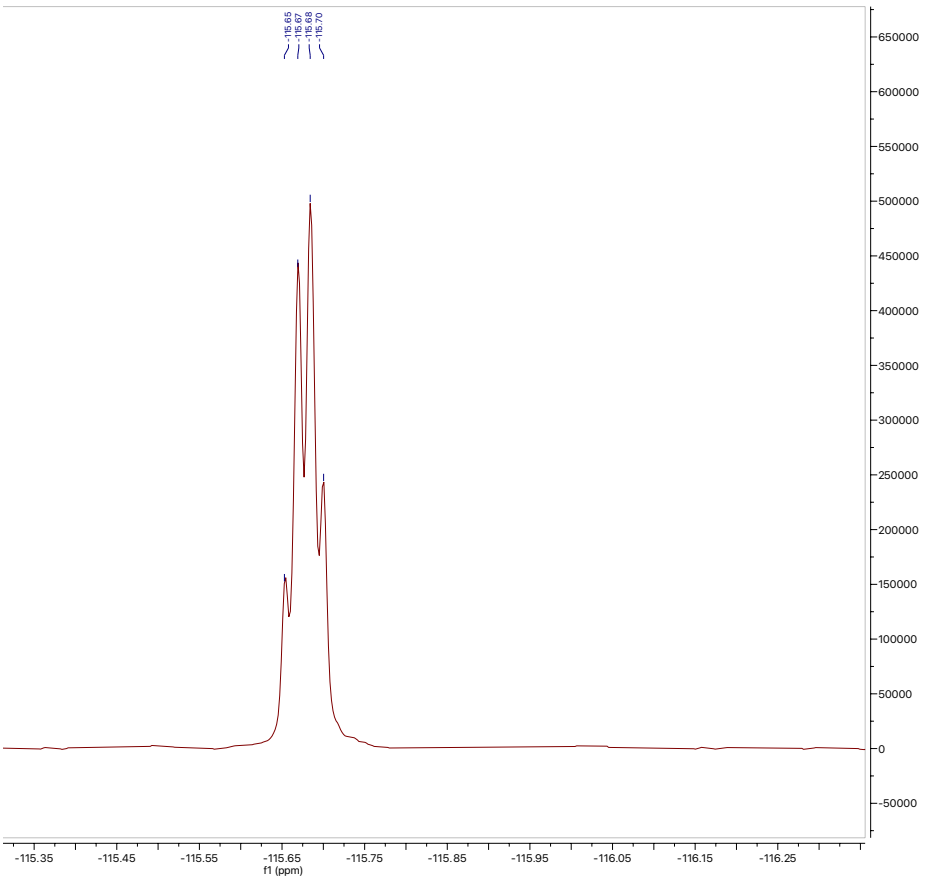
-115.65
-115.67
-115.68
-115.70
650000
600000
550000
500000
450000
400000
350000
300000
250000
200000
150000
100000
50000
0
-50000
-115.35
-115.45
-115.55
-115.65
-115.75
-115.85
-115.95
-116.05
-116.15
-116.25
f1 (ppm)

^{19}F-NMR

[m-xylene]

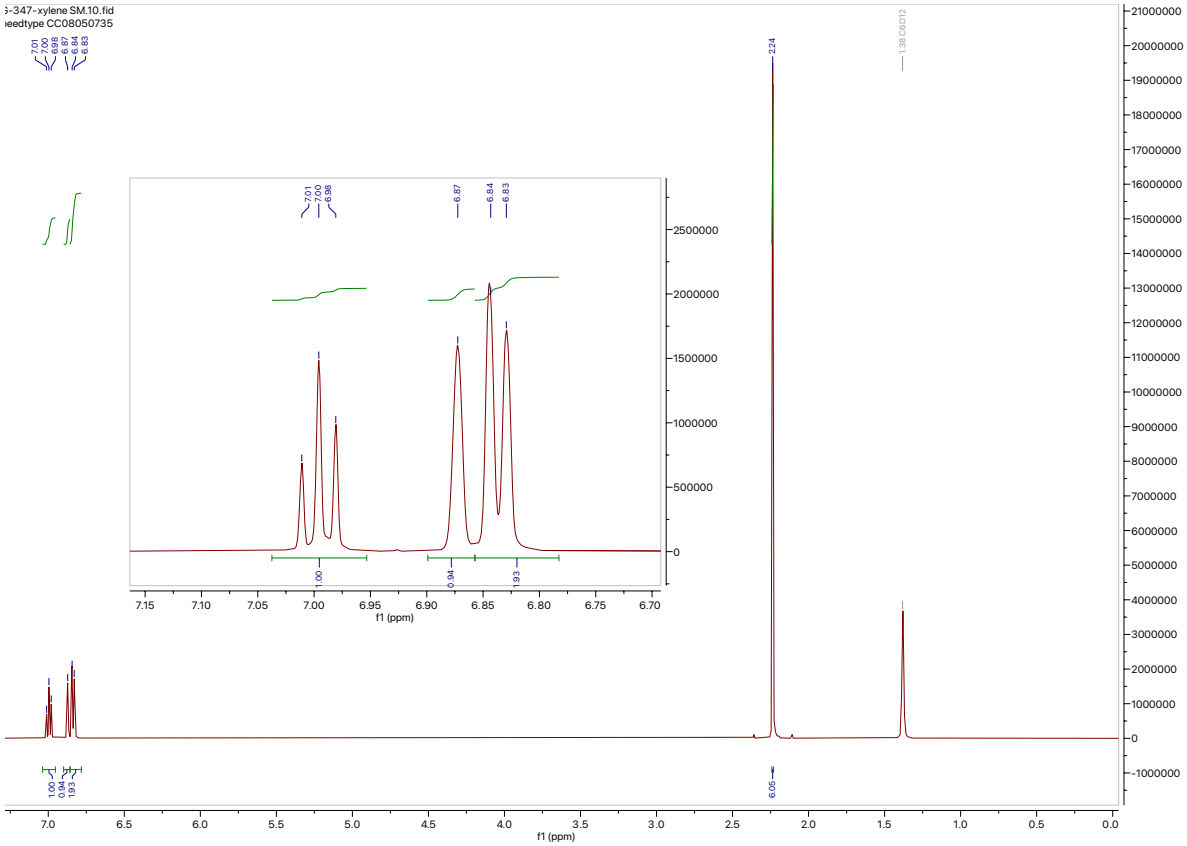

^{1}H-NMR

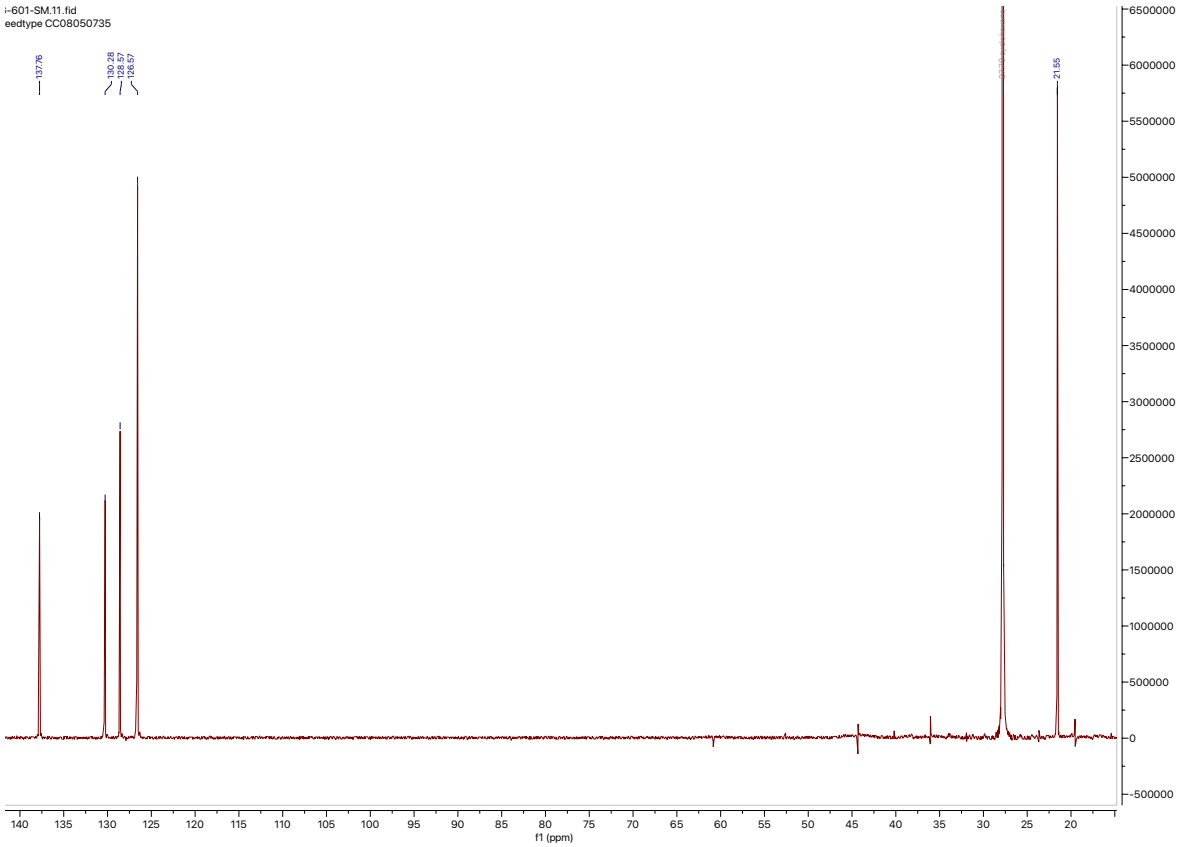

^{13}C-NMR (in cyclohexane)

[2-methylheptan-3-one]

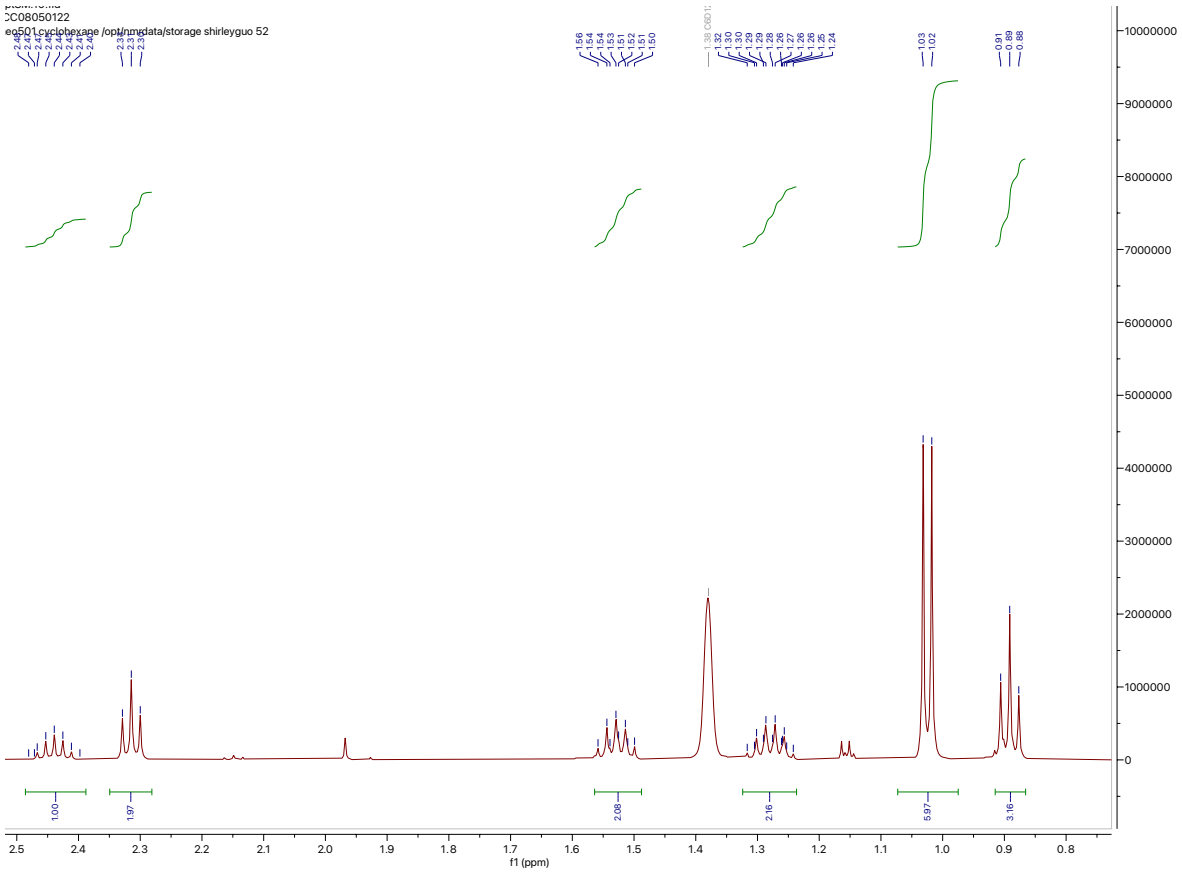
CC08050122
eq501.cyclobexane /opt/nmrdata/storage shirleyguo 52
1.00
1.97
2.08
2.16
5.97
3.16
f1 (ppm)

^{1}H-NMR

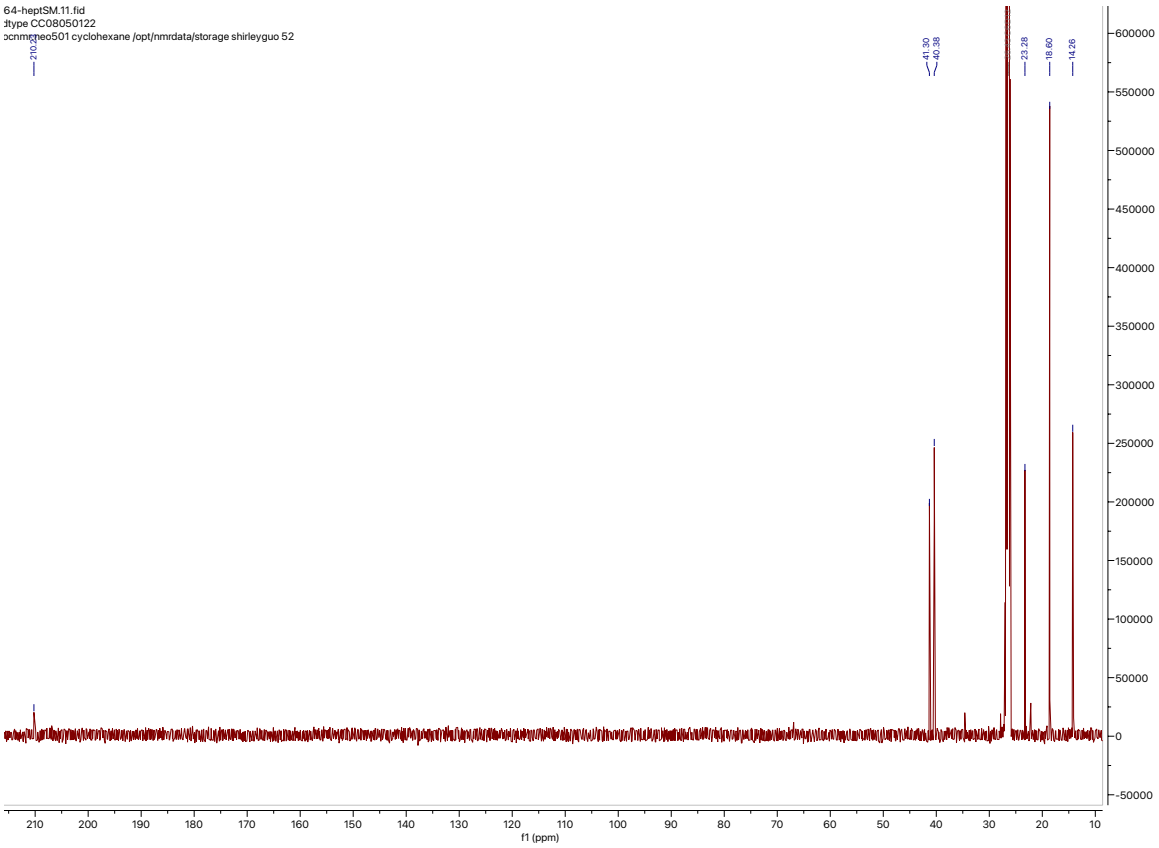

^{13}C-NMR

Note: one C peak should be overlapping with the peaks for C_6D_{12}

[cyclooctanone]

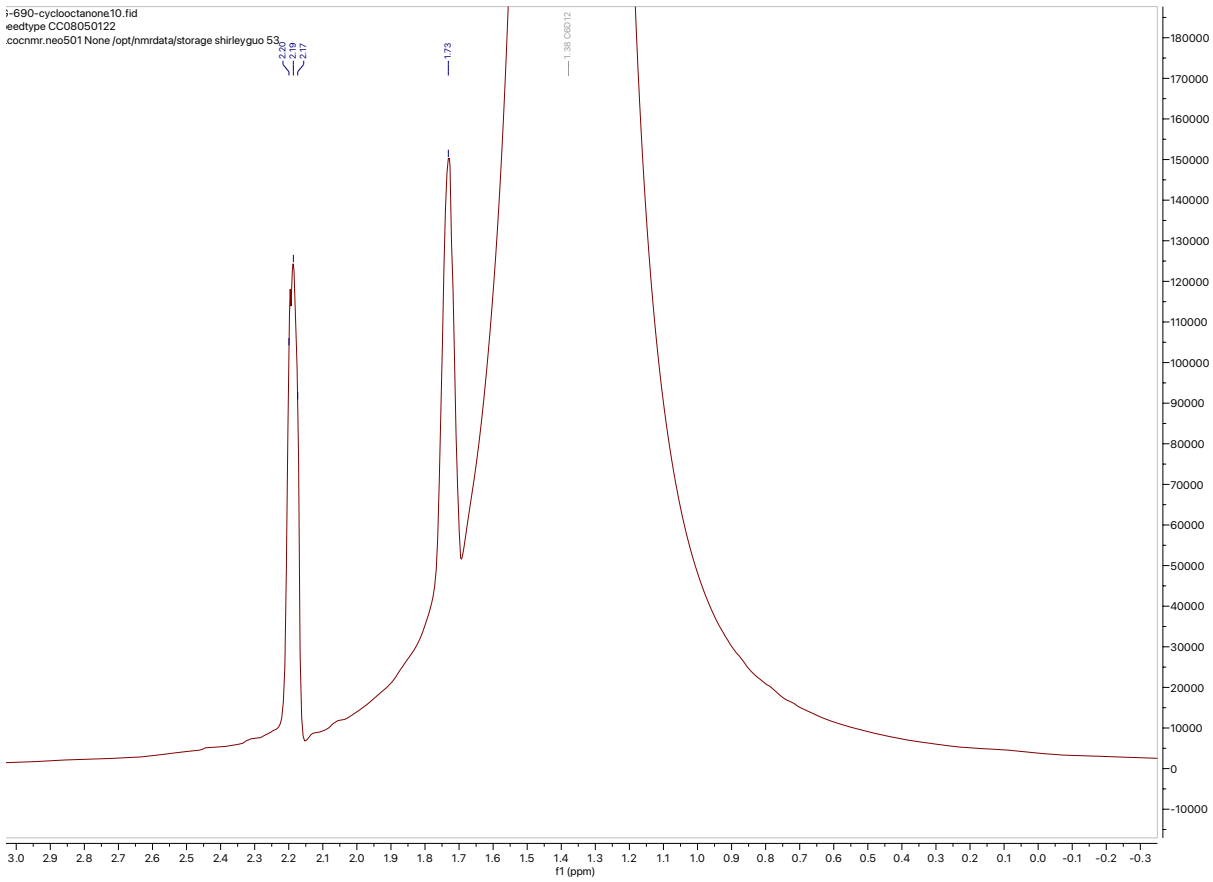

^{1}H-NMR (in cyclohexane)

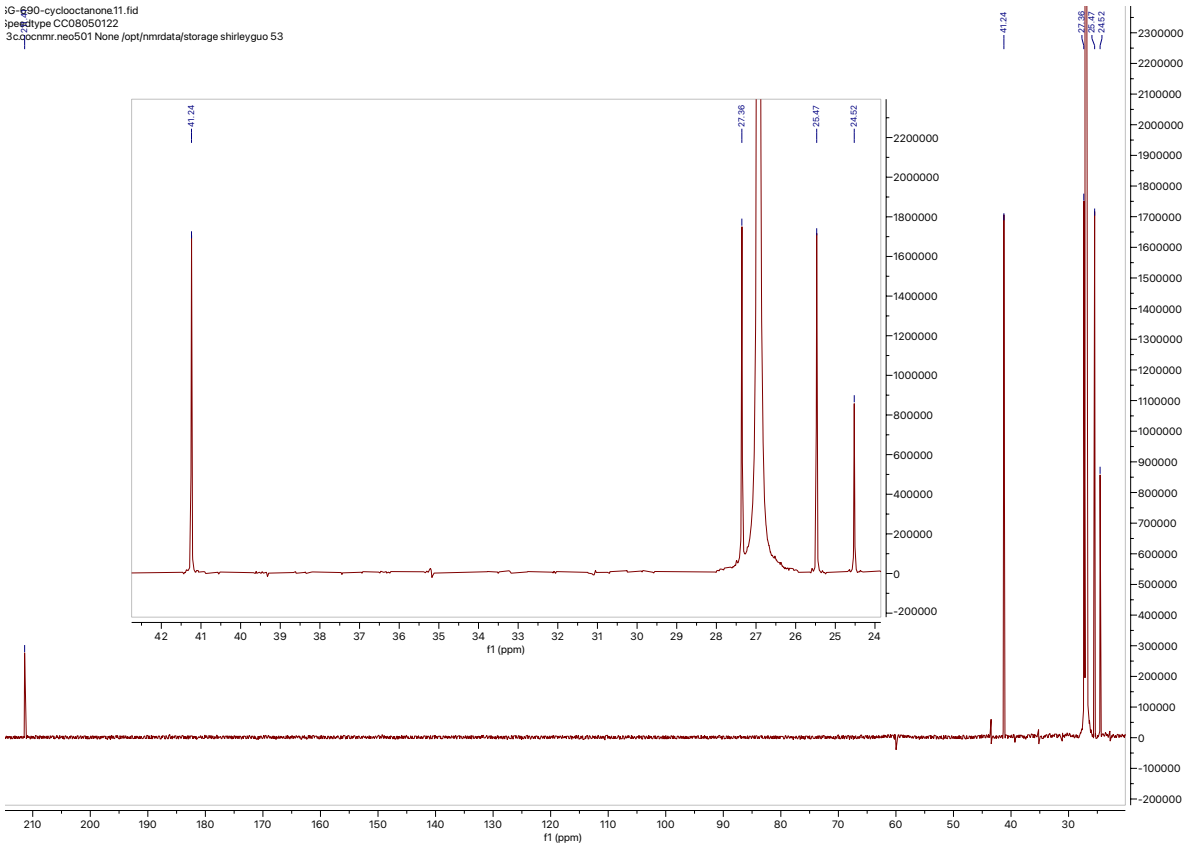

^{13}C-NMR (in cyclohexane)

[methyl propionate]

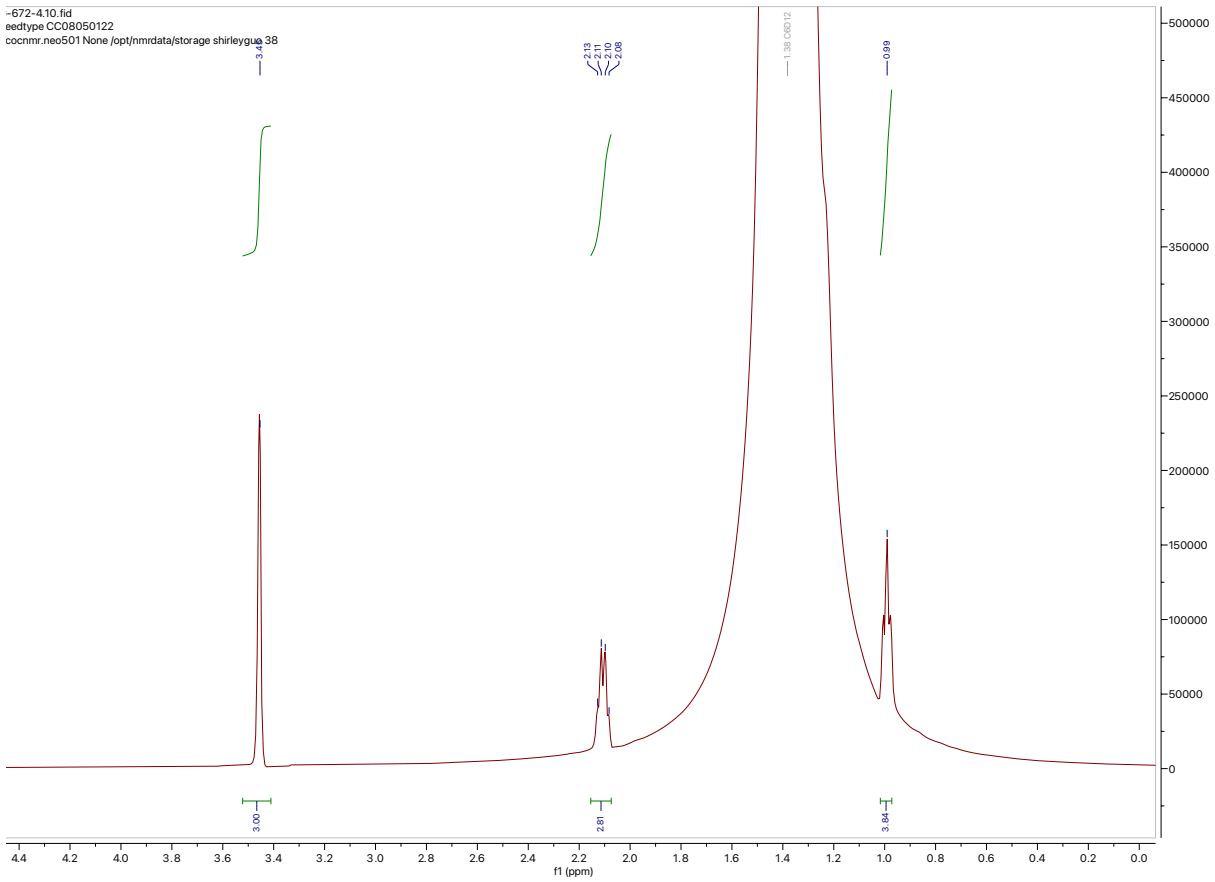

^{1}H-NMR (in cyclohexane)

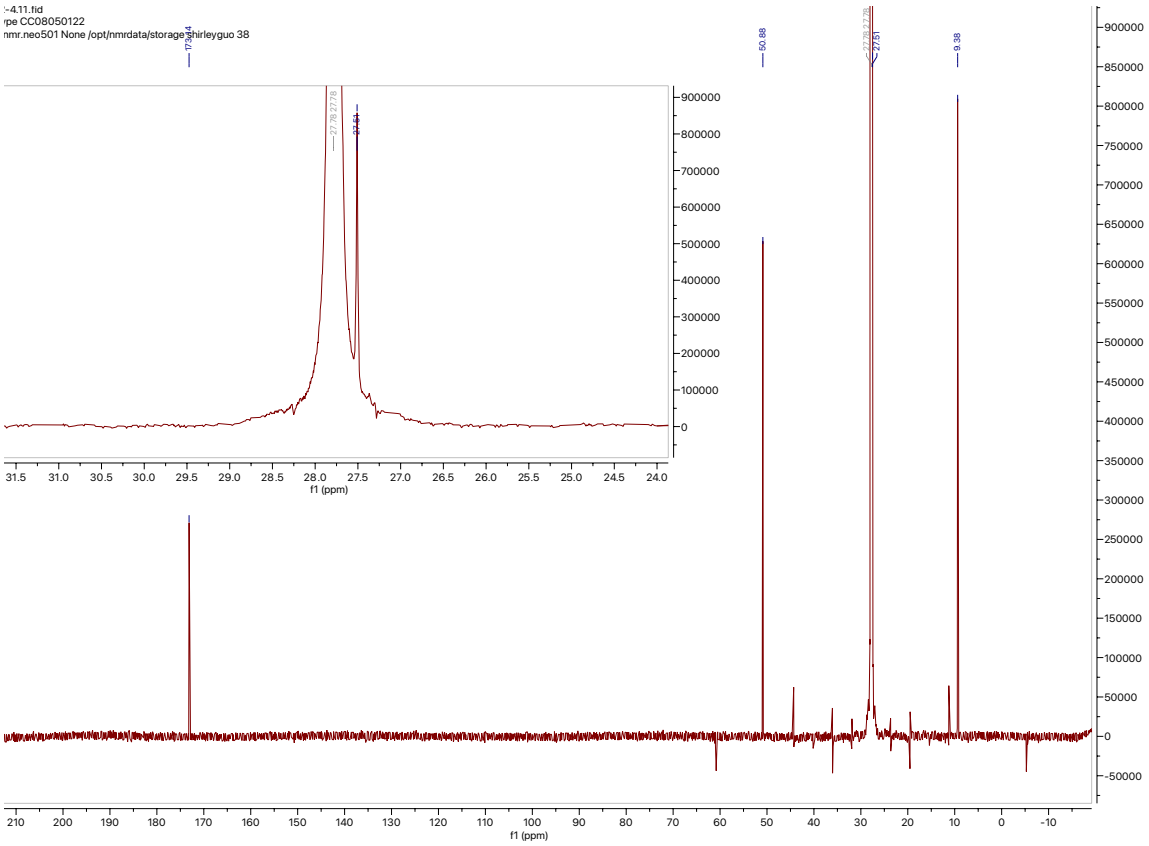

^{13}C-NMR (in cyclohexane)

[N,N-dimethylpropionamide]

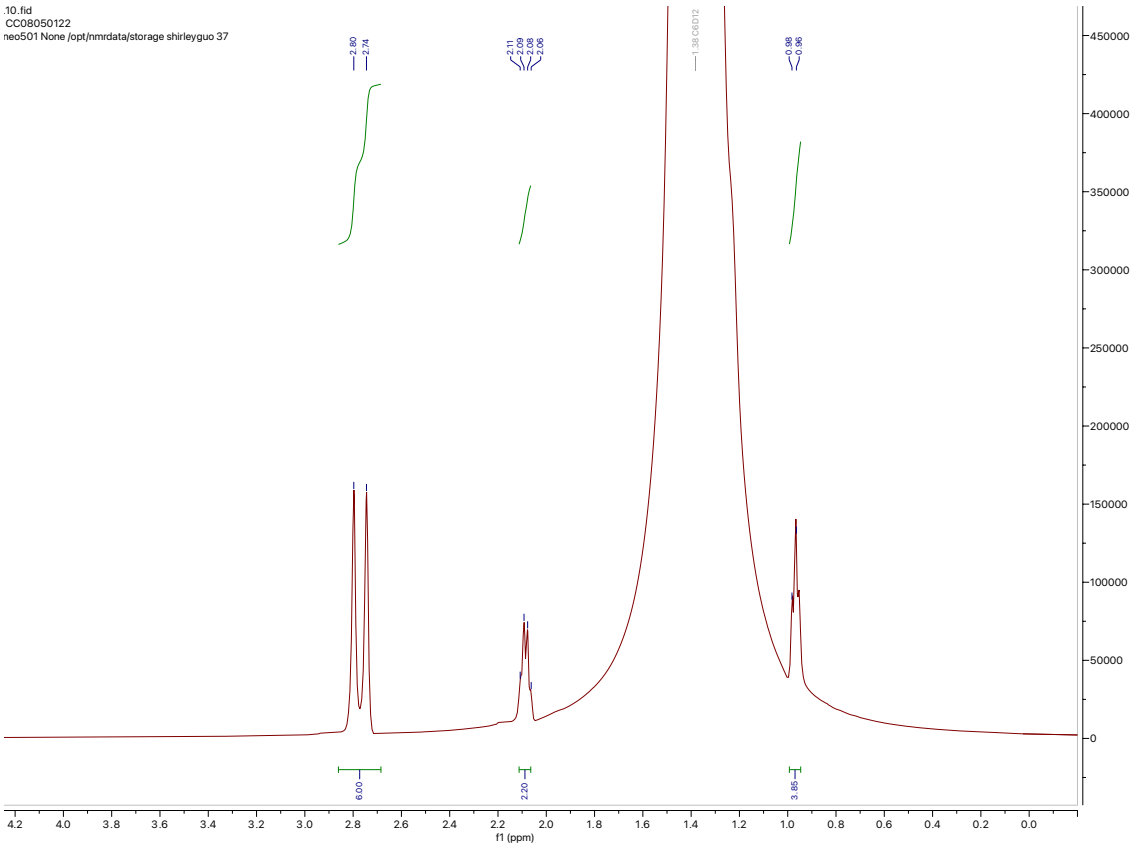

^{1}H-NMR (in cyclohexane)

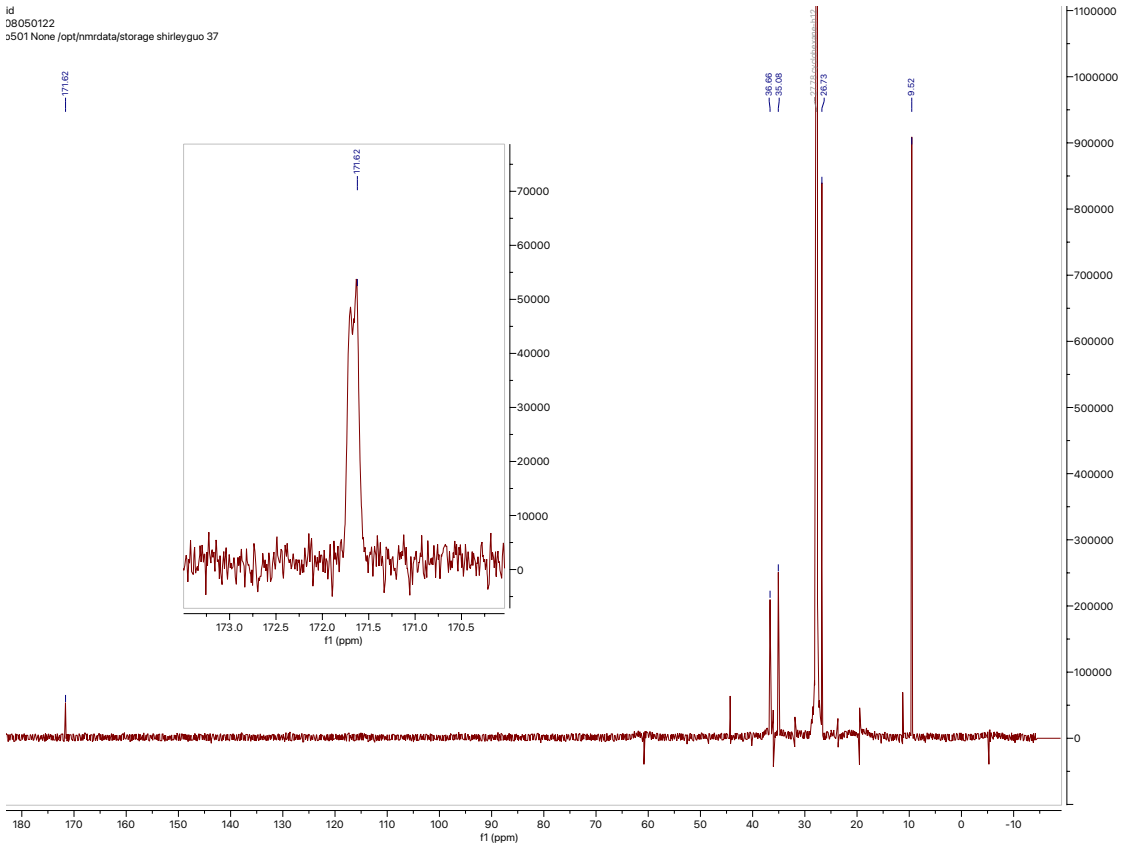

^{13}C-NMR (in cyclohexane)

[bromocyclopropane]

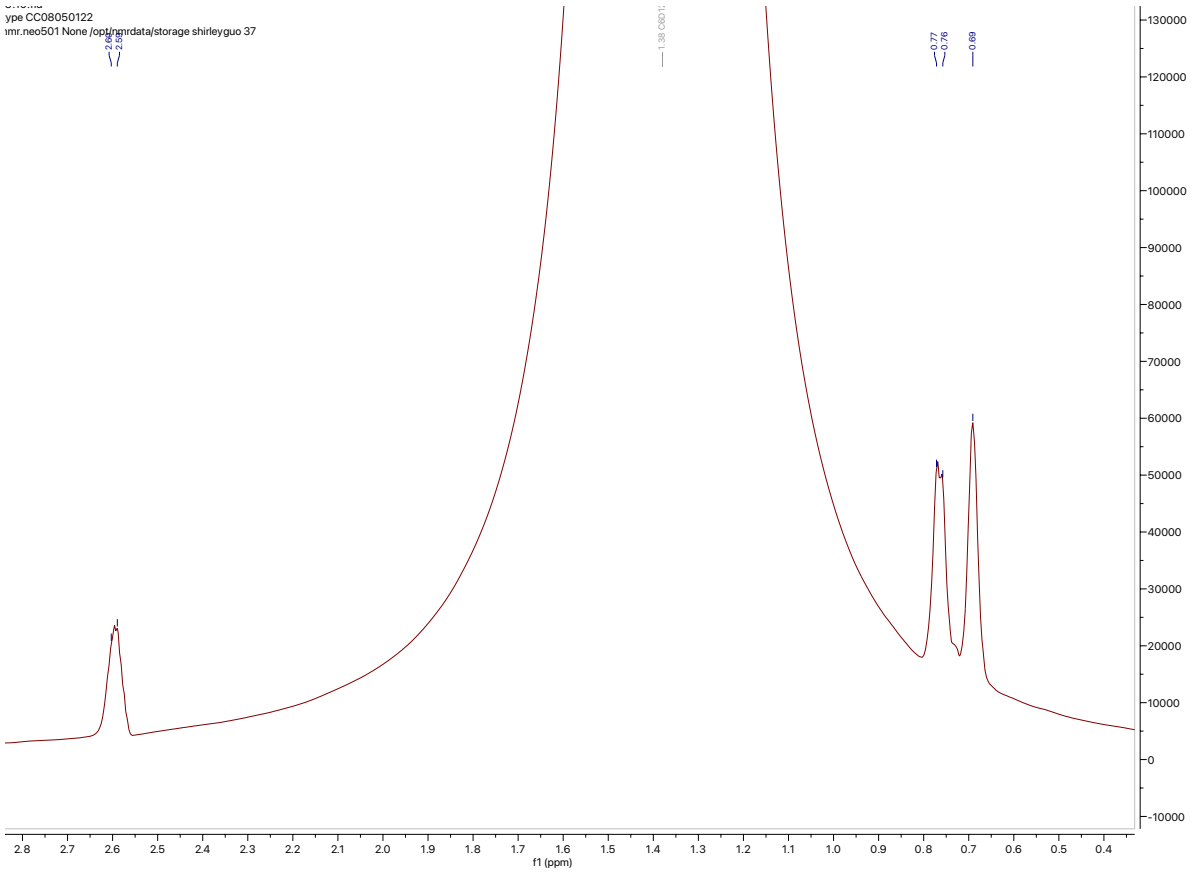

^{1}H-NMR (in cyclohexane)

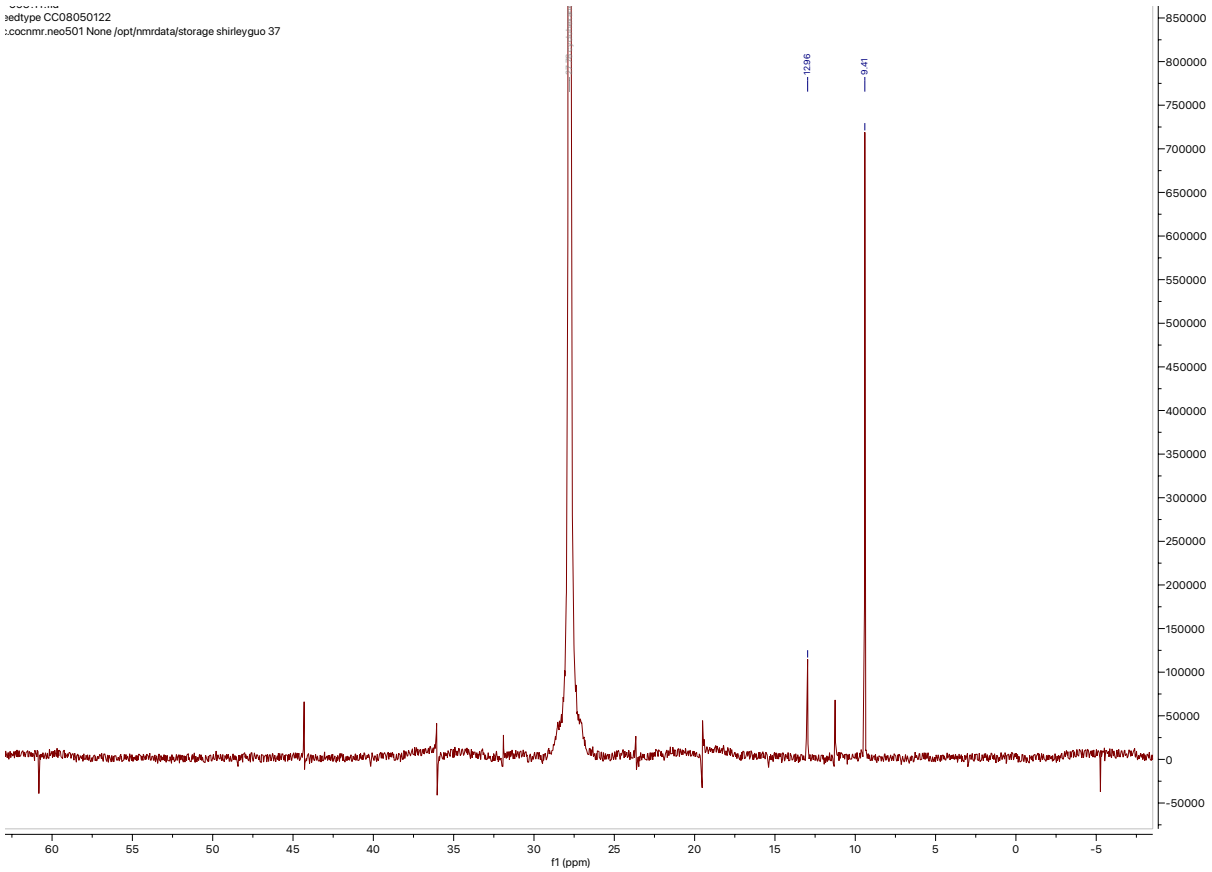

^{13}C-NMR (in cyclohexane)

[1-bromopropane]

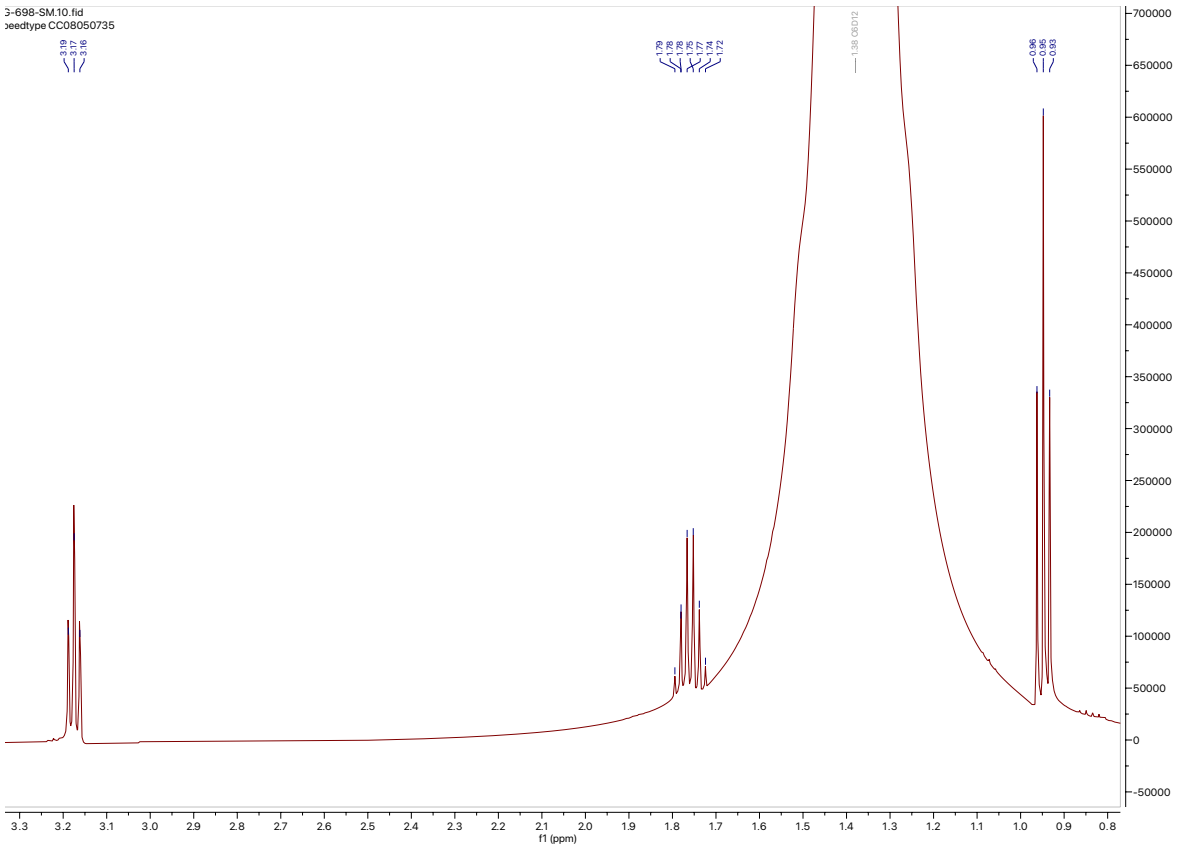

^{1}H-NMR (in cyclohexane)

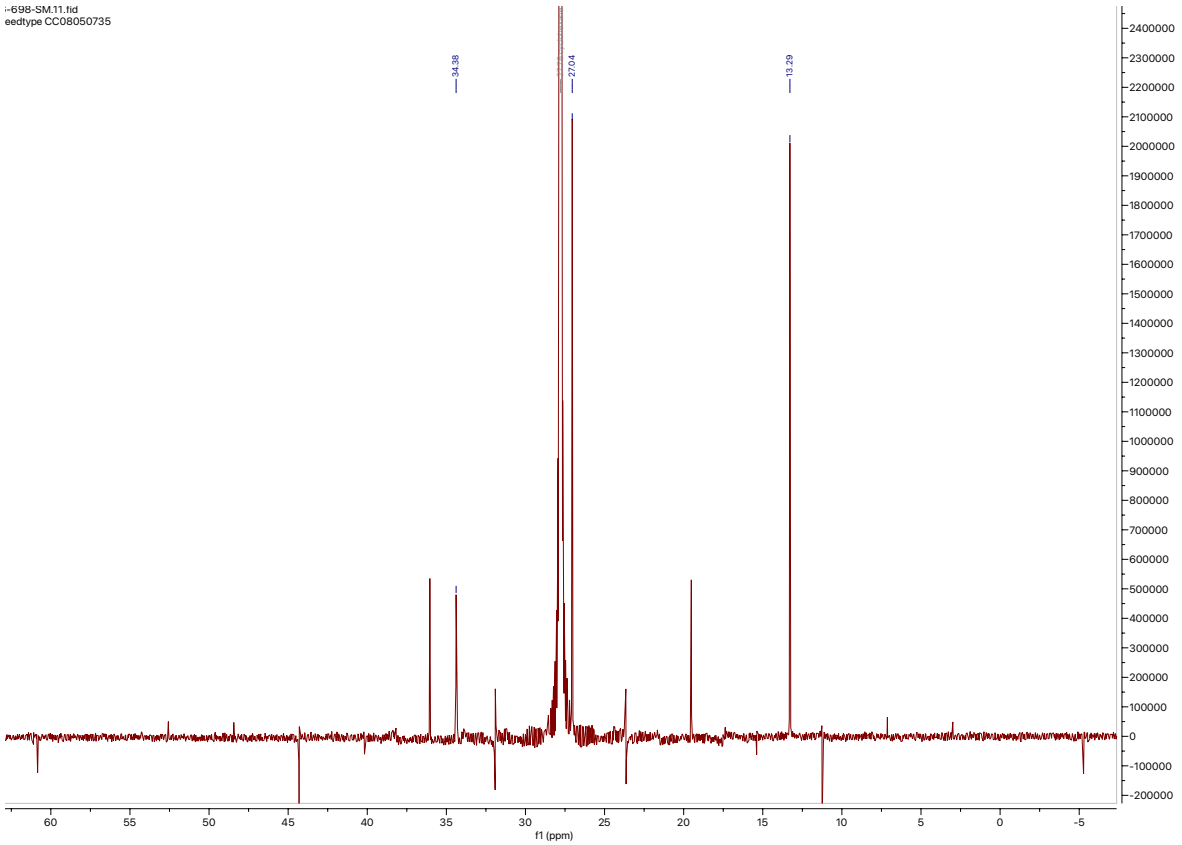

^{13}C-NMR (in cyclohexane)

[phenylacetylene]

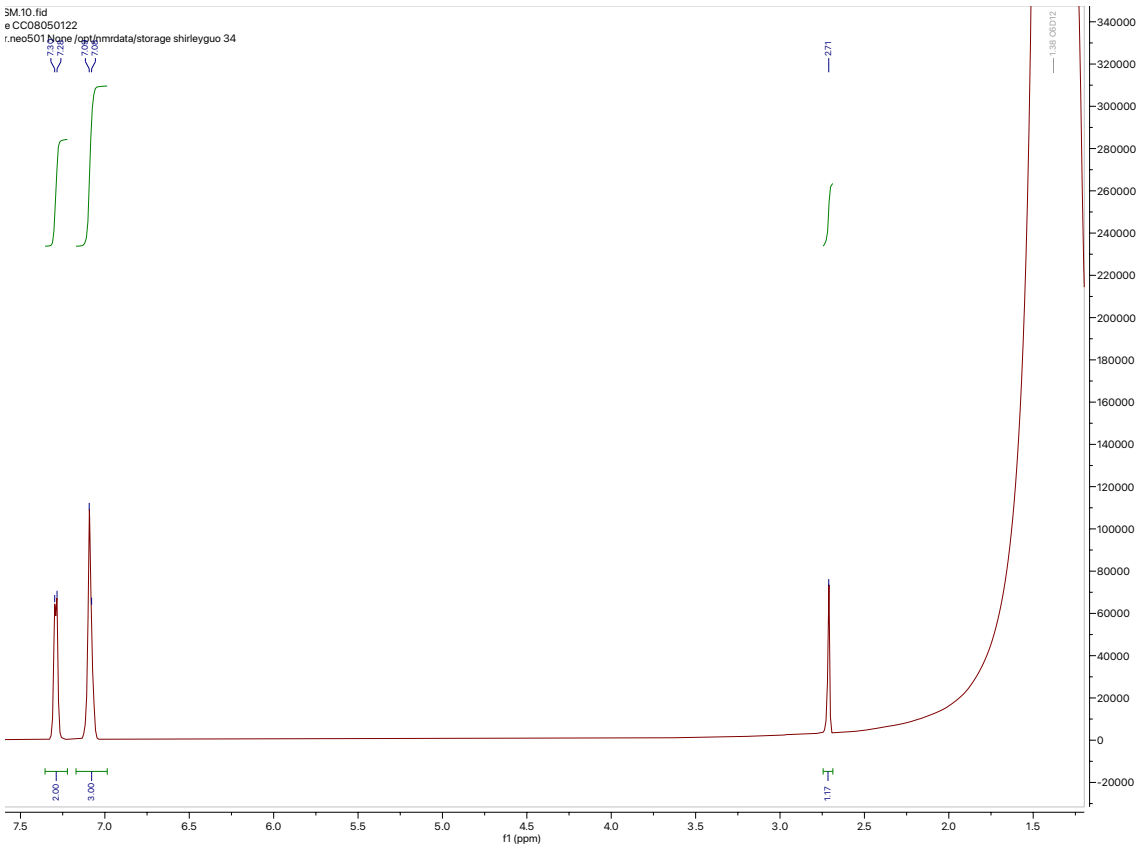

^{1}H-NMR (in cyclohexane)

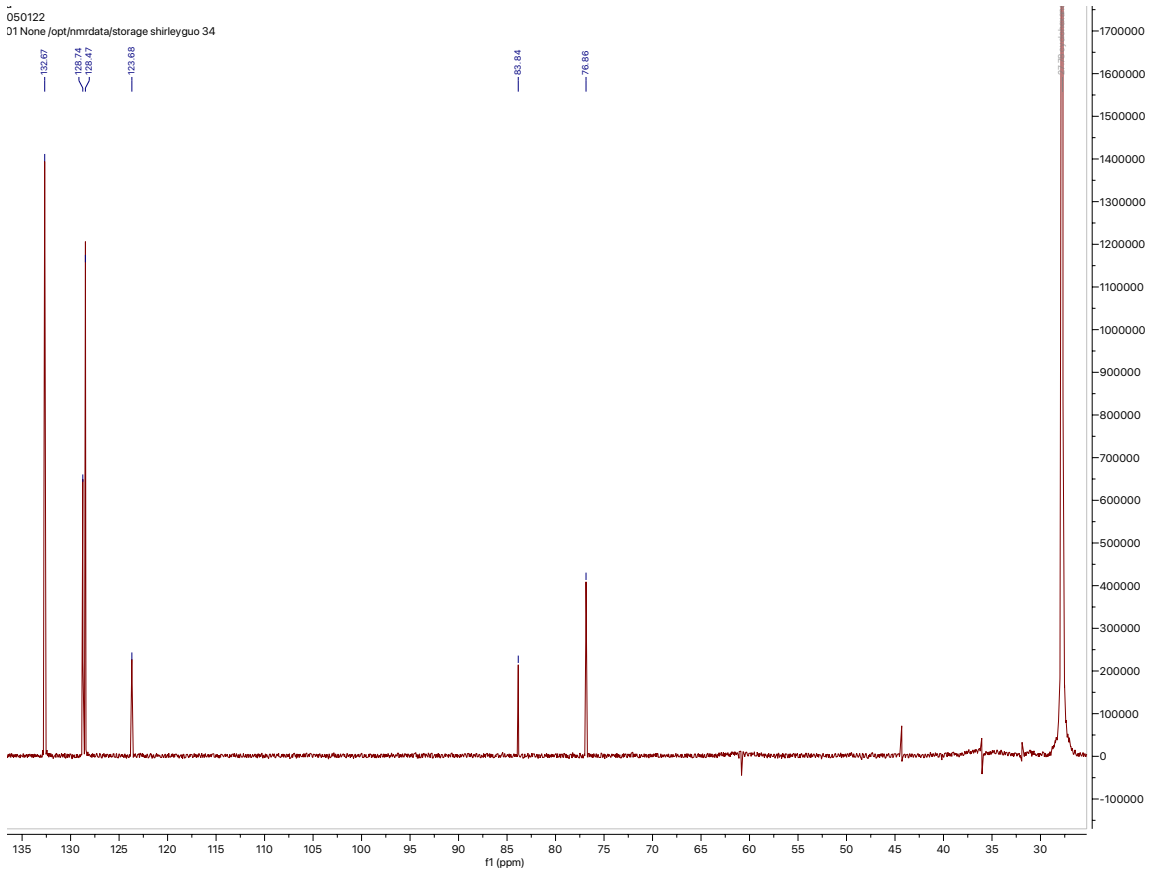

^{13}C-NMR (in cyclohexane)

Ambident Reactivity

[dithiane]

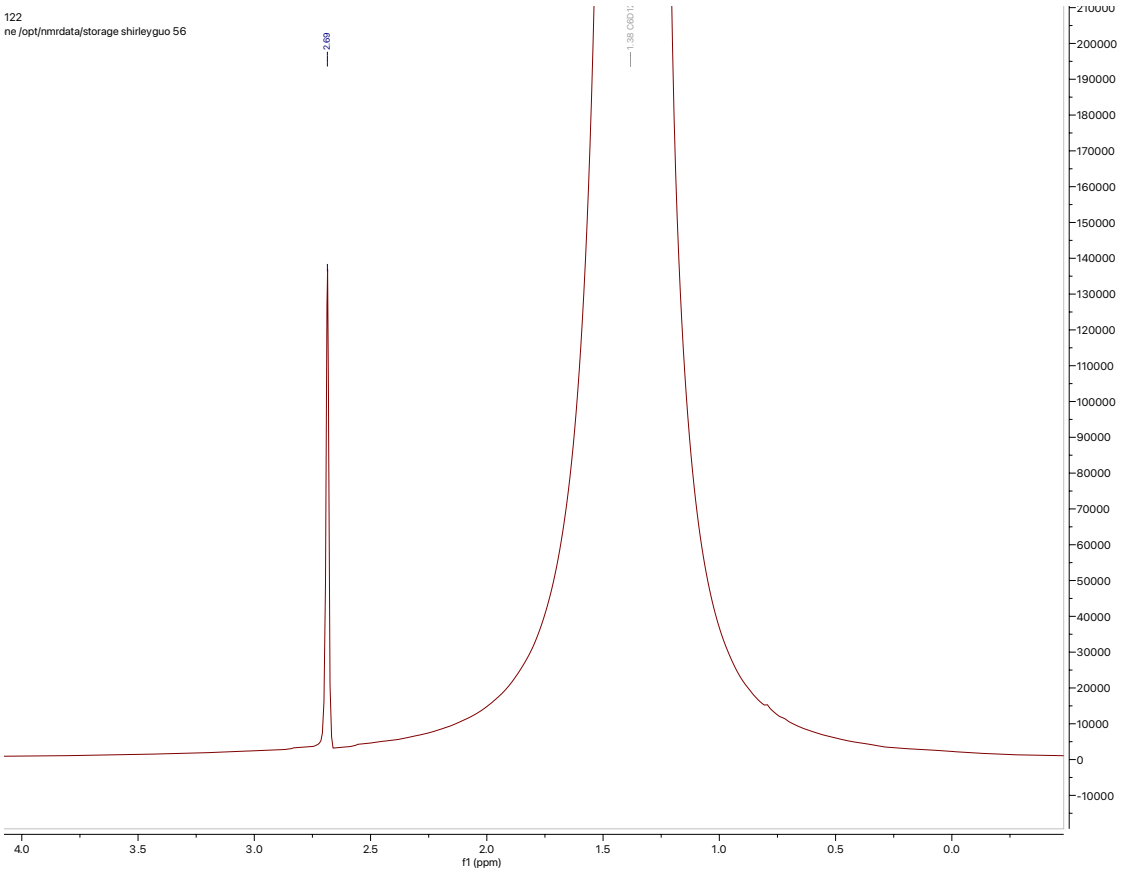

^{1}H-NMR (in cyclohexane)

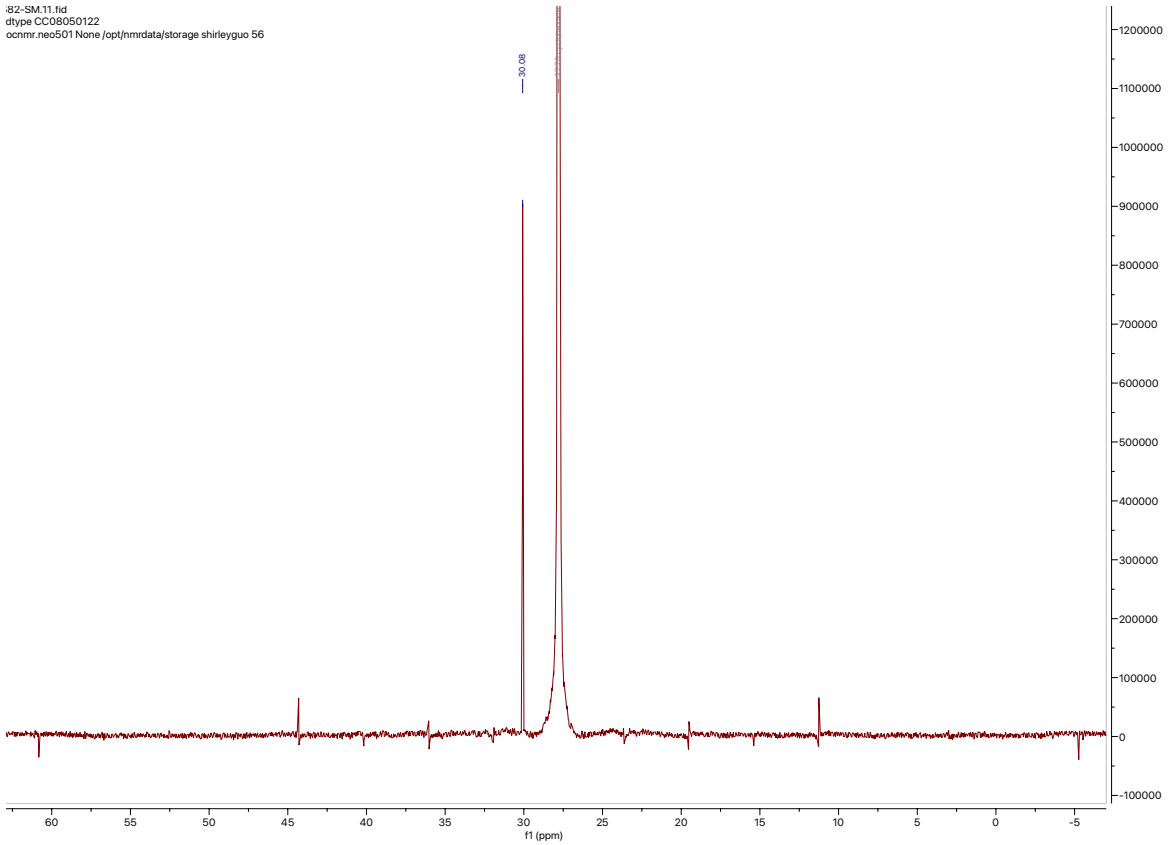

^{13}C-NMR (in cyclohexane)

[dihexylamine]

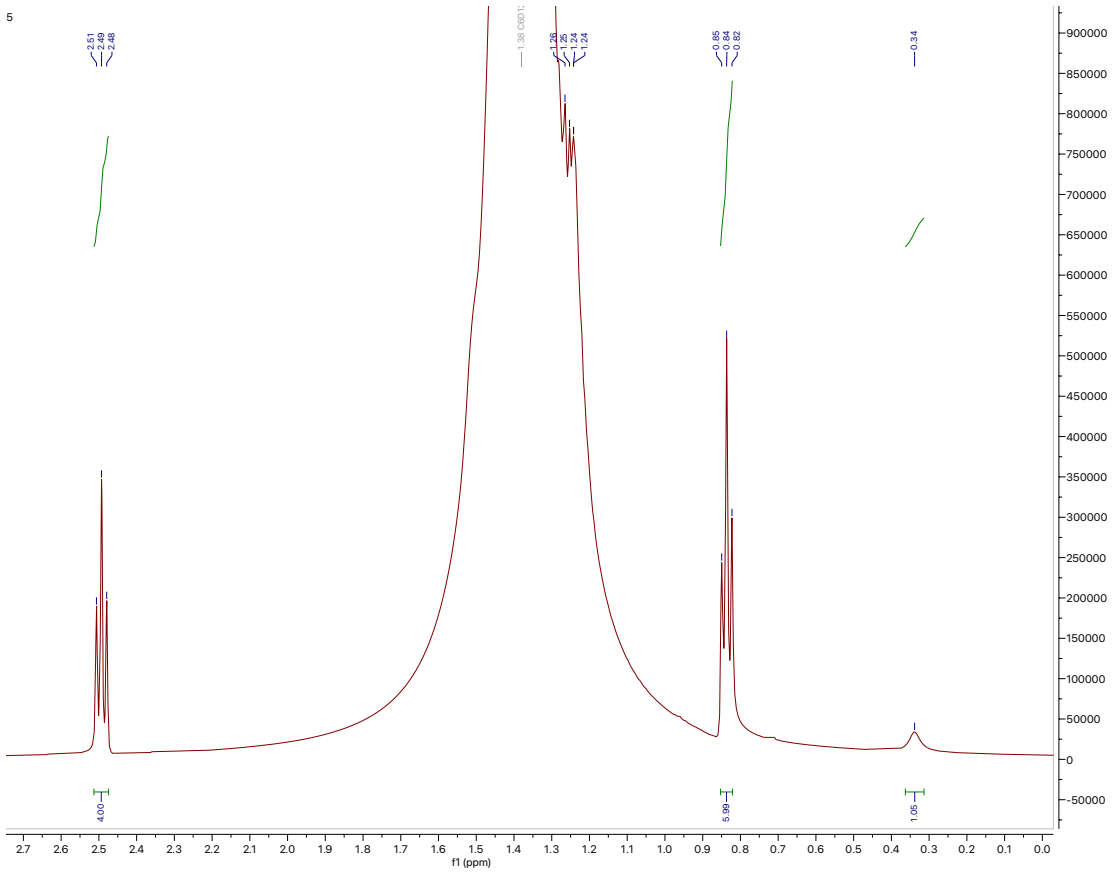

^{1}H-NMR (in cyclohexane)

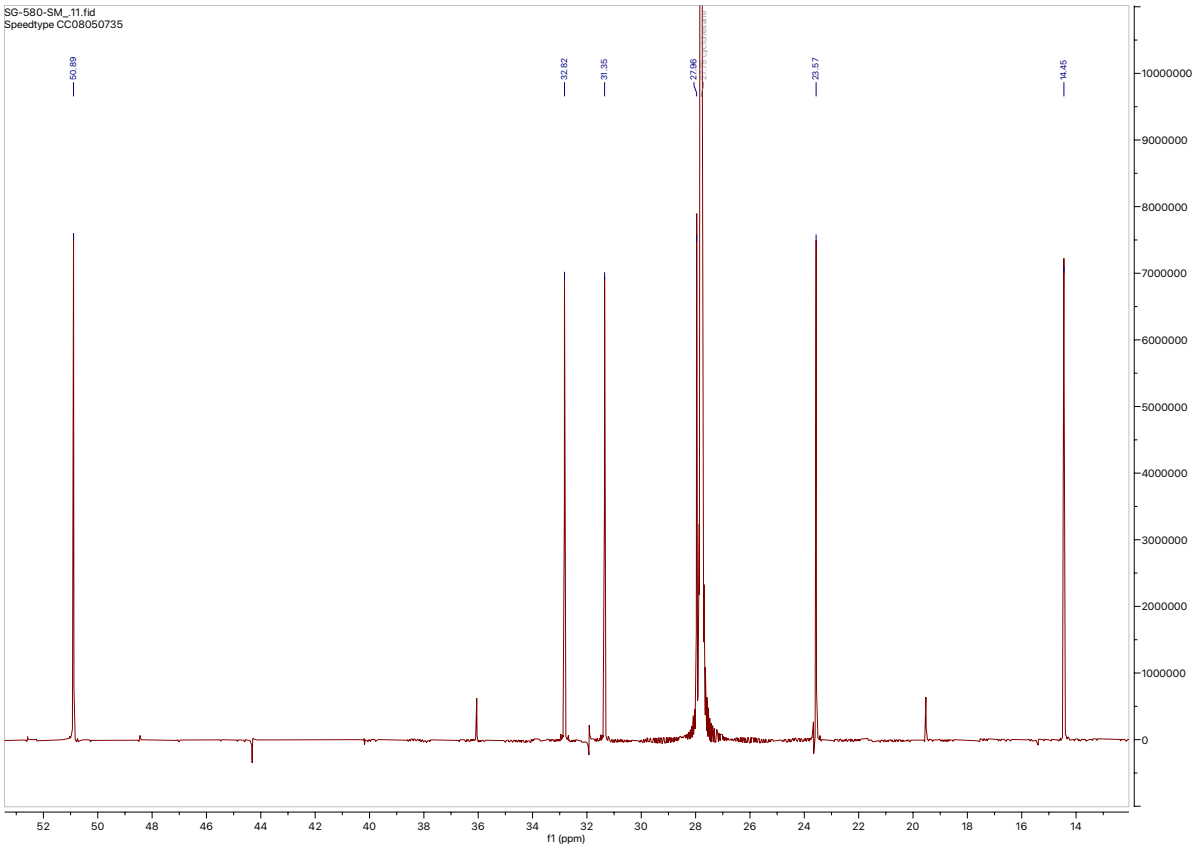

^{13}C-NMR (in cyclohexane)

[phenol]

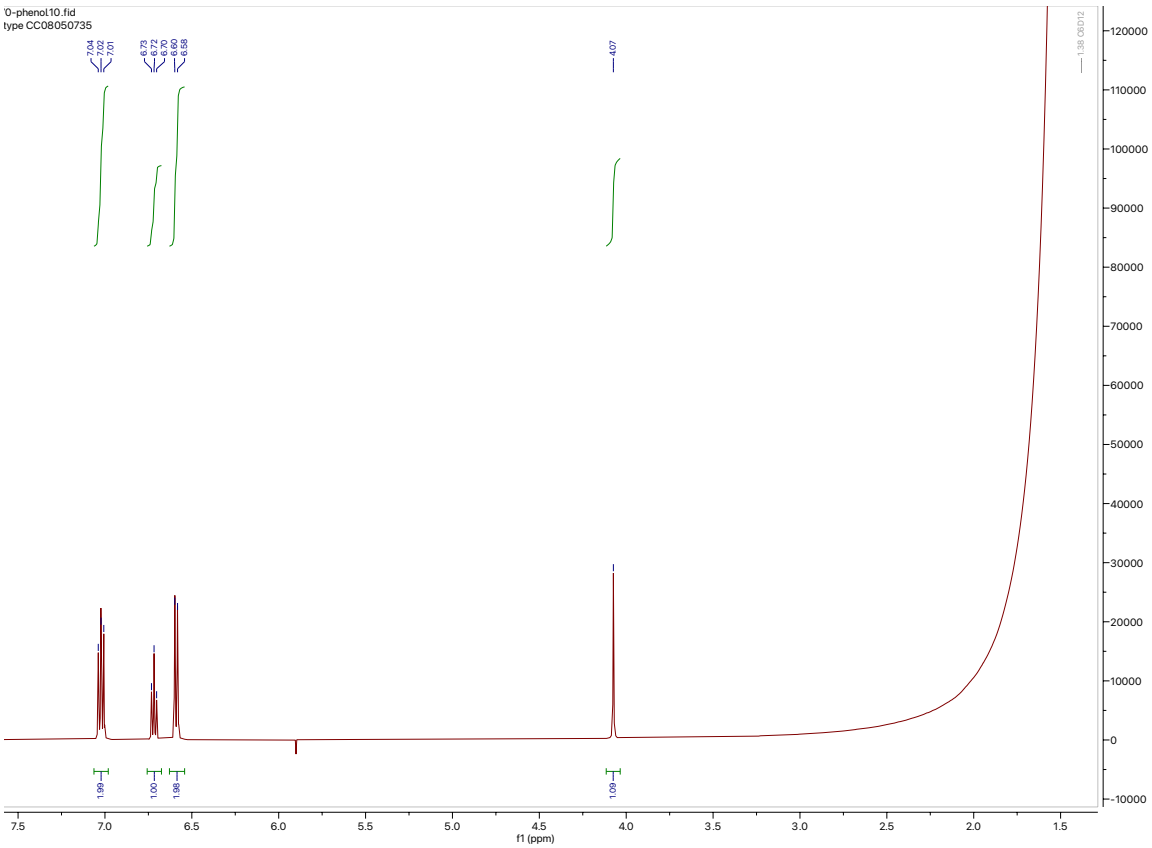

^{1}H-NMR (in cyclohexane-h_{12}/d_{12})

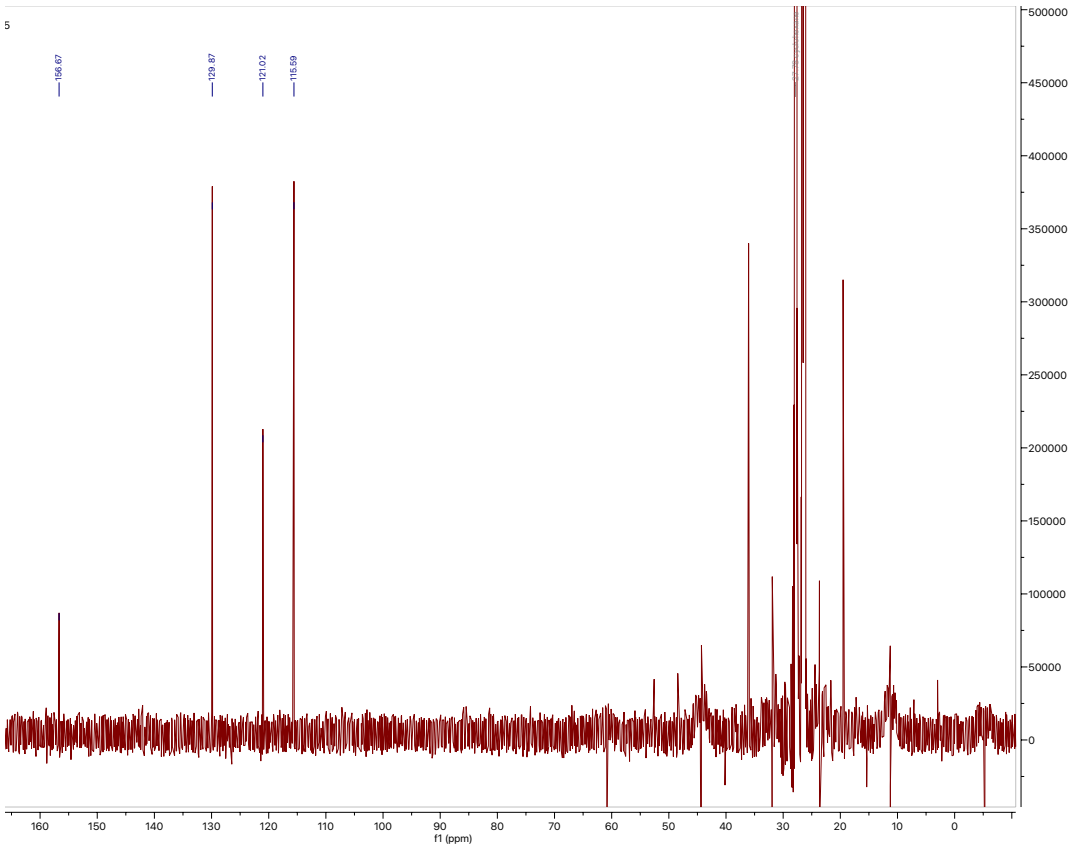

^{13}C-NMR (in cyclohexane-h_{12}/d_{12})

[aniline]

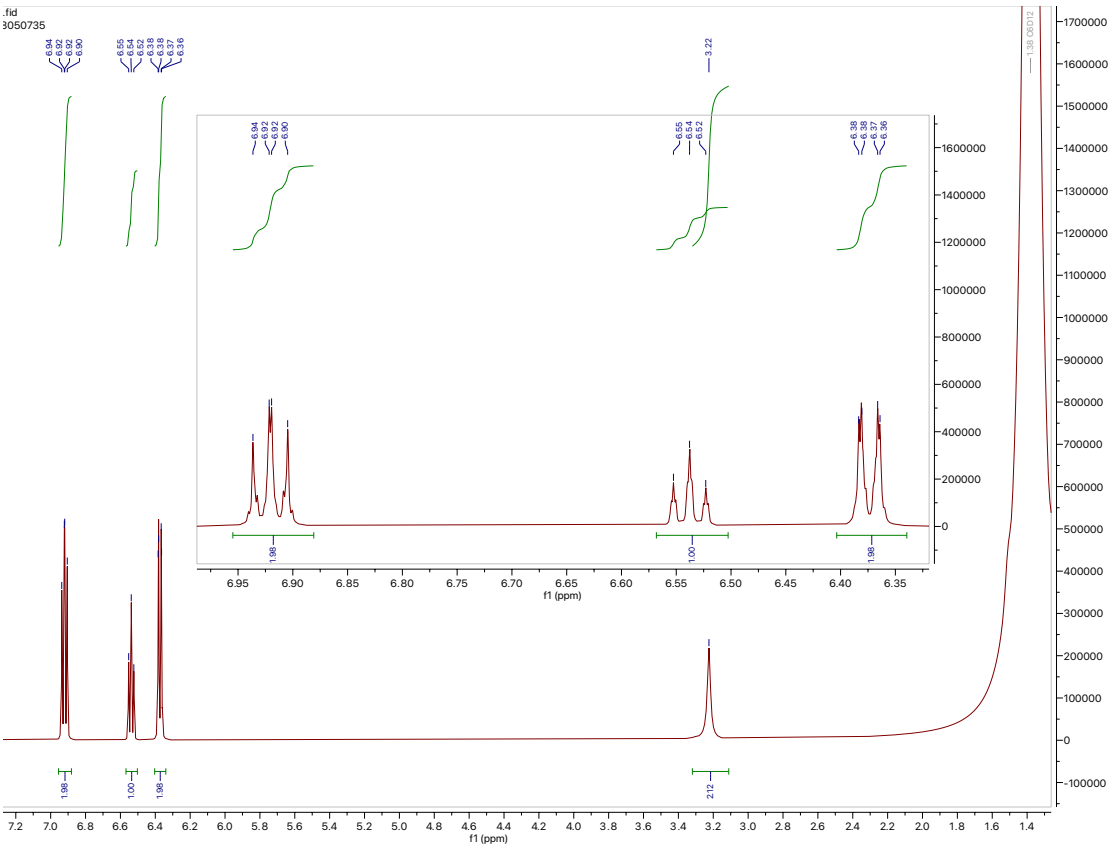

^{1}H-NMR (in cyclohexane)

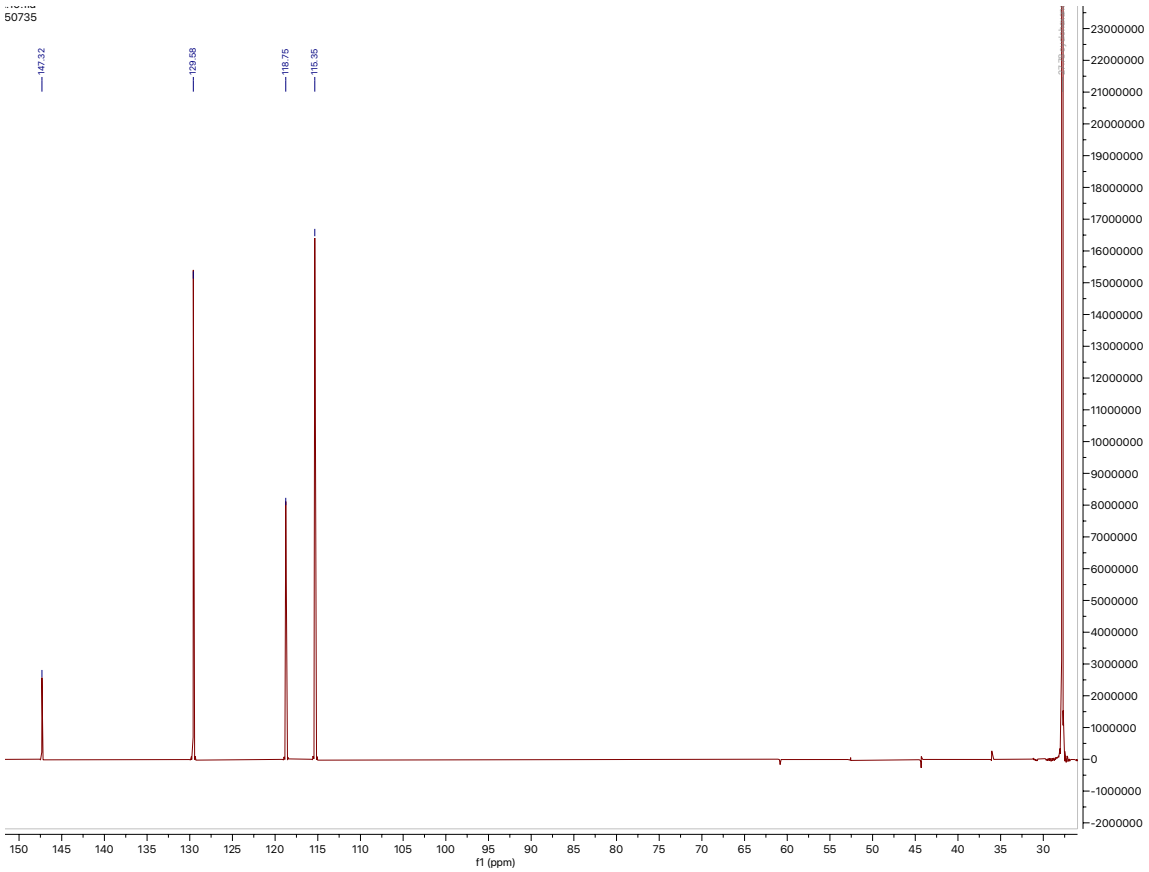

^{13}C-NMR (in cyclohexane)

[thiophenol]

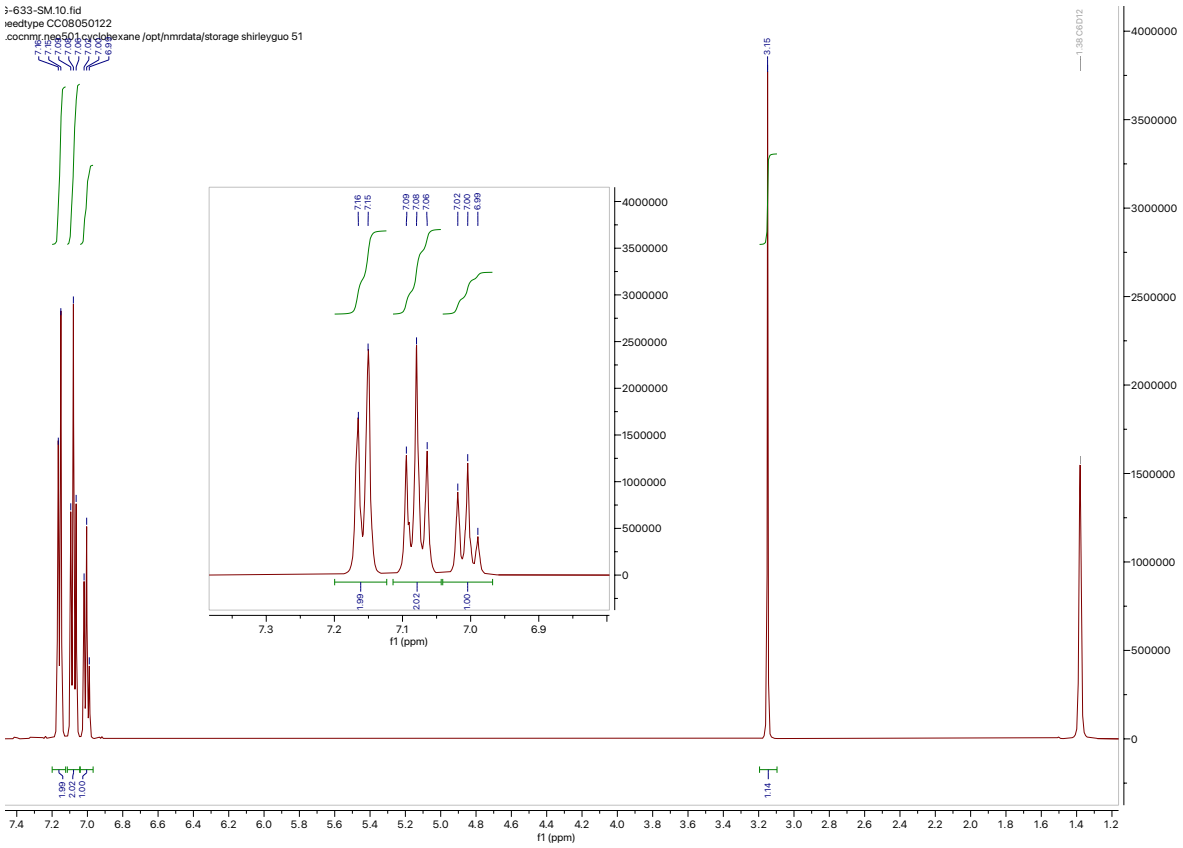

^{1}H-NMR

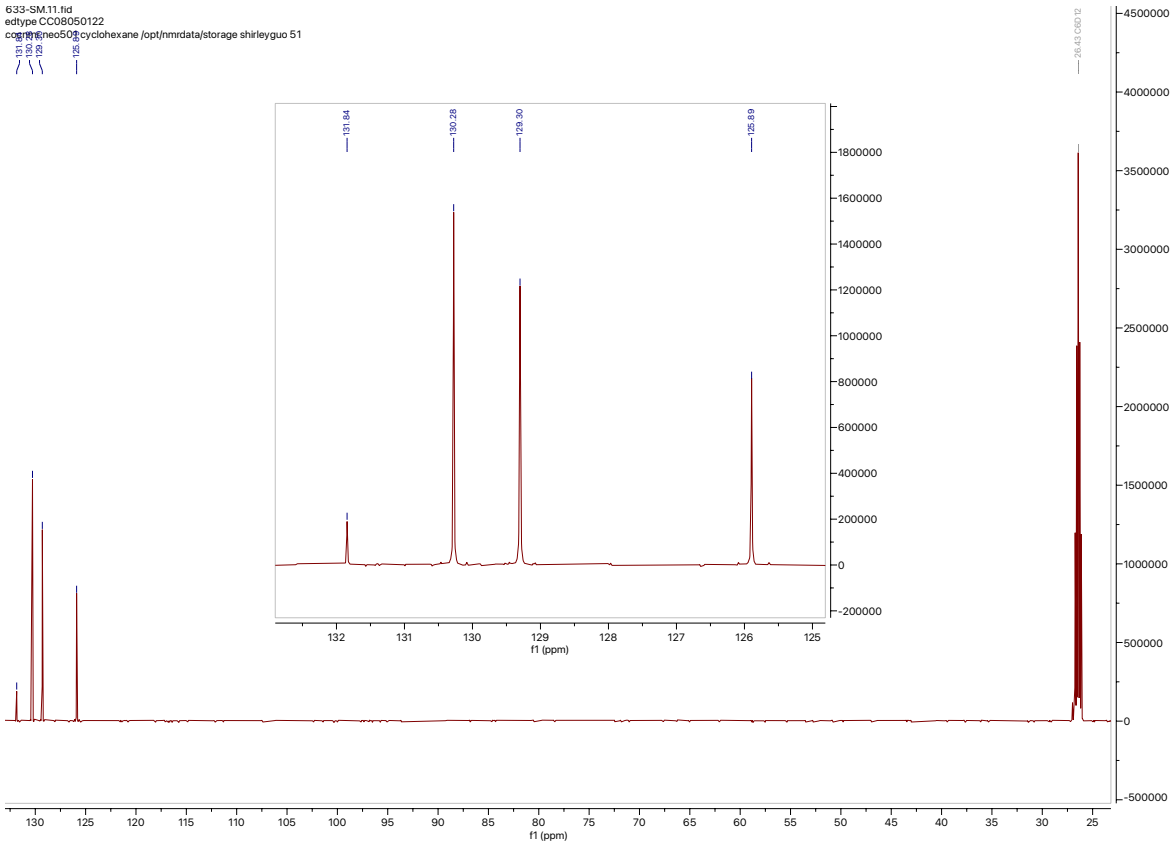

^{13}C-NMR

[3-methylpyridine]

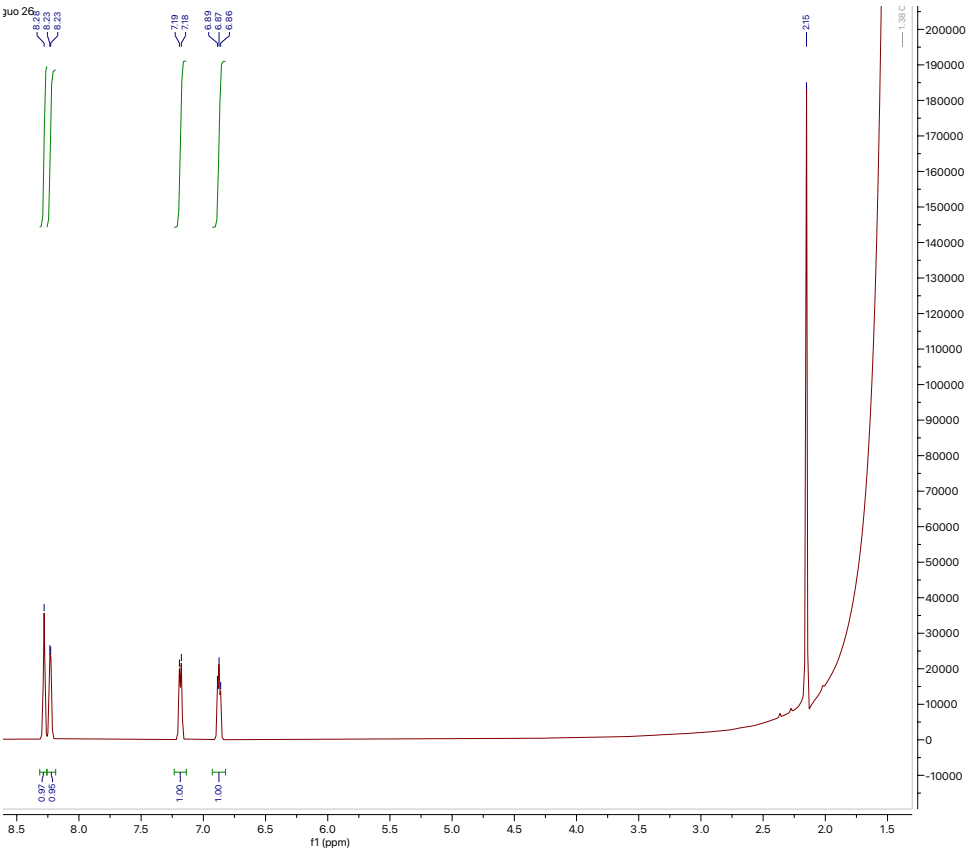

^{1}H-NMR (in cyclohexane)

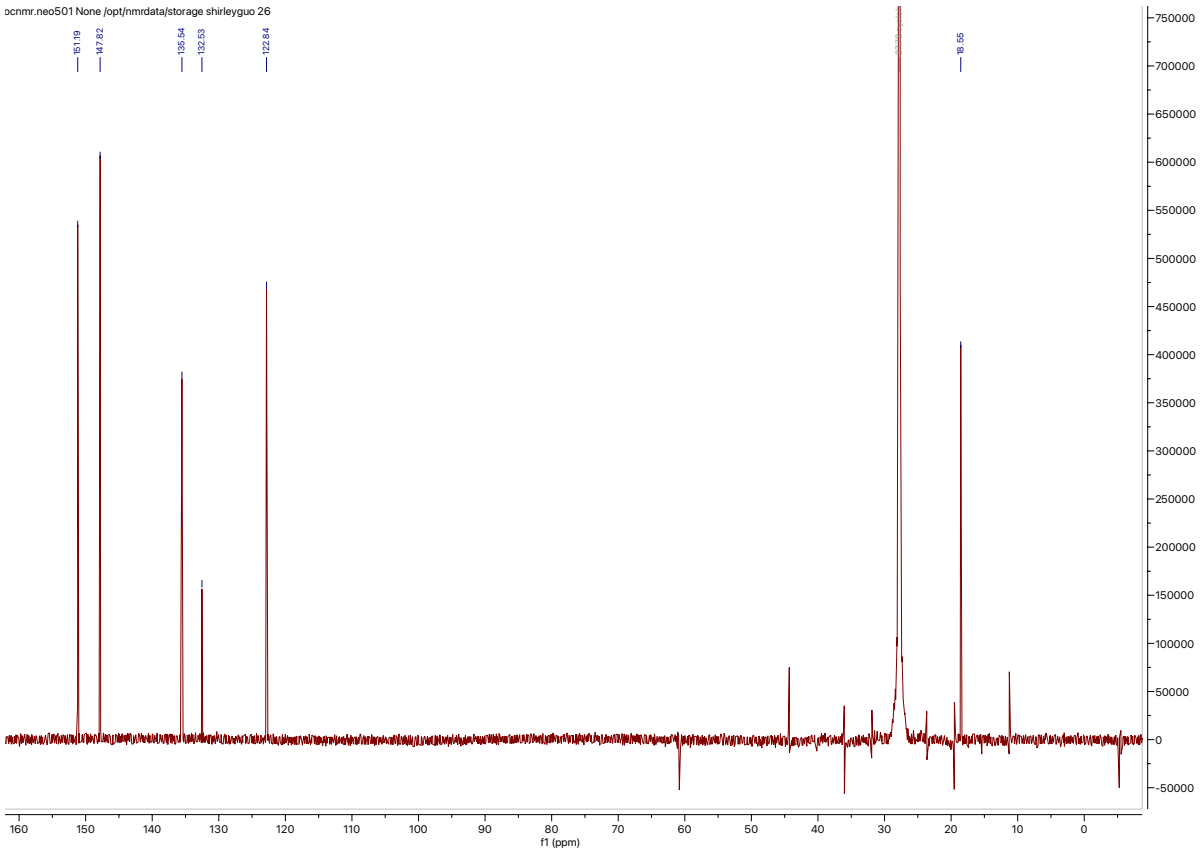

^{13}C-NMR (in cyclohexane)

[2-butyne]

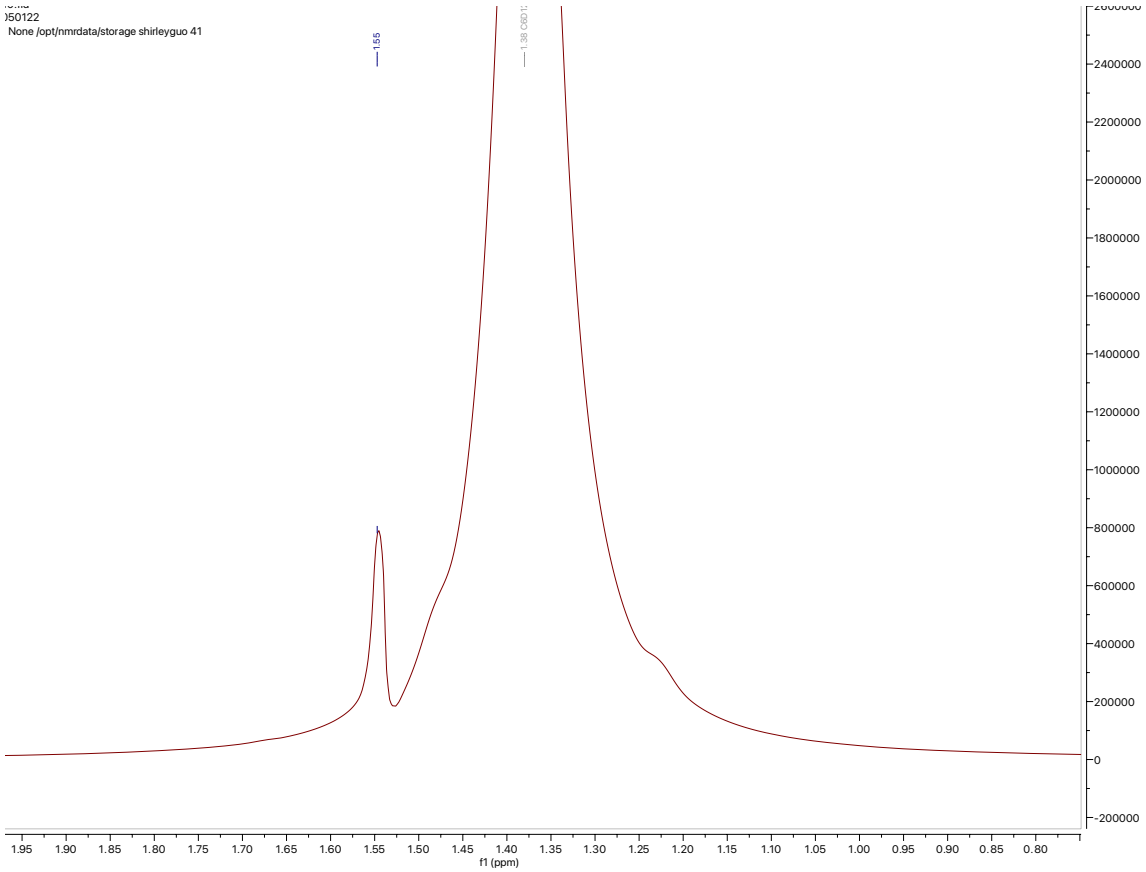

^{1}H-NMR (in cyclohexane)

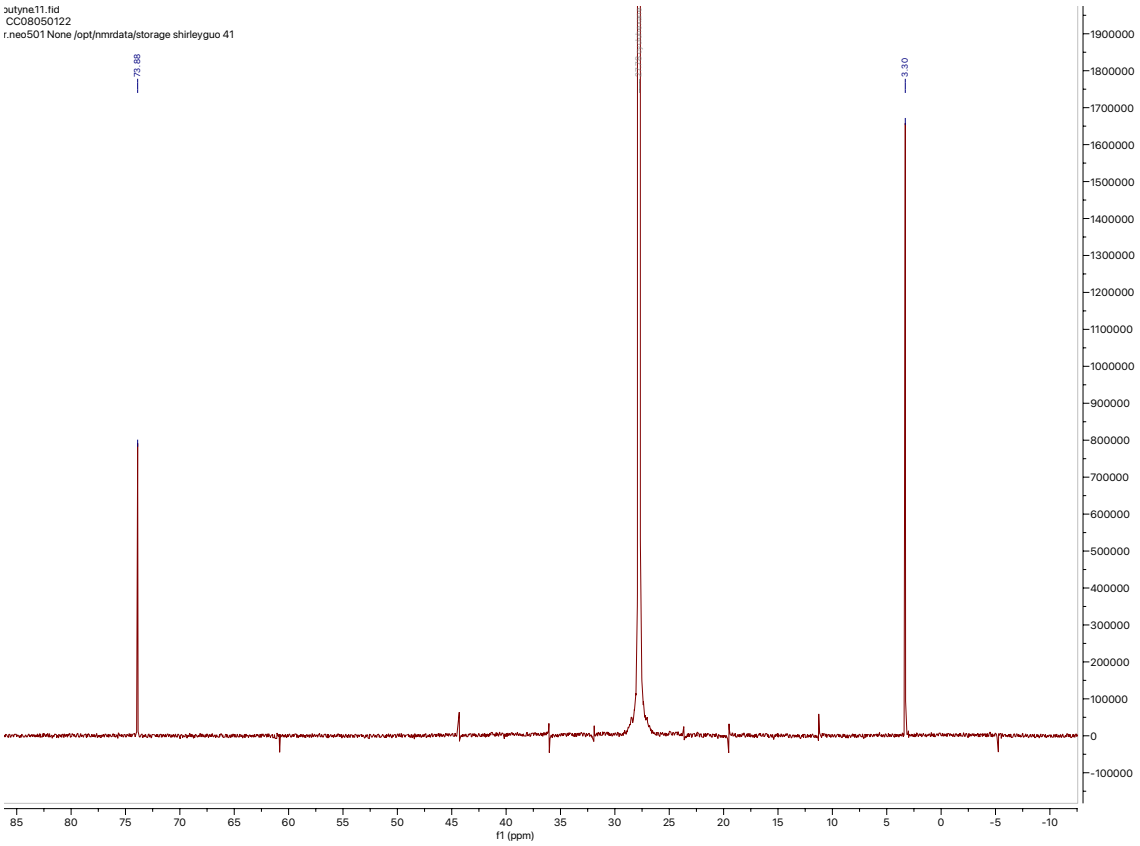

^{13}C-NMR (in cyclohexane)

[benzothiophene]

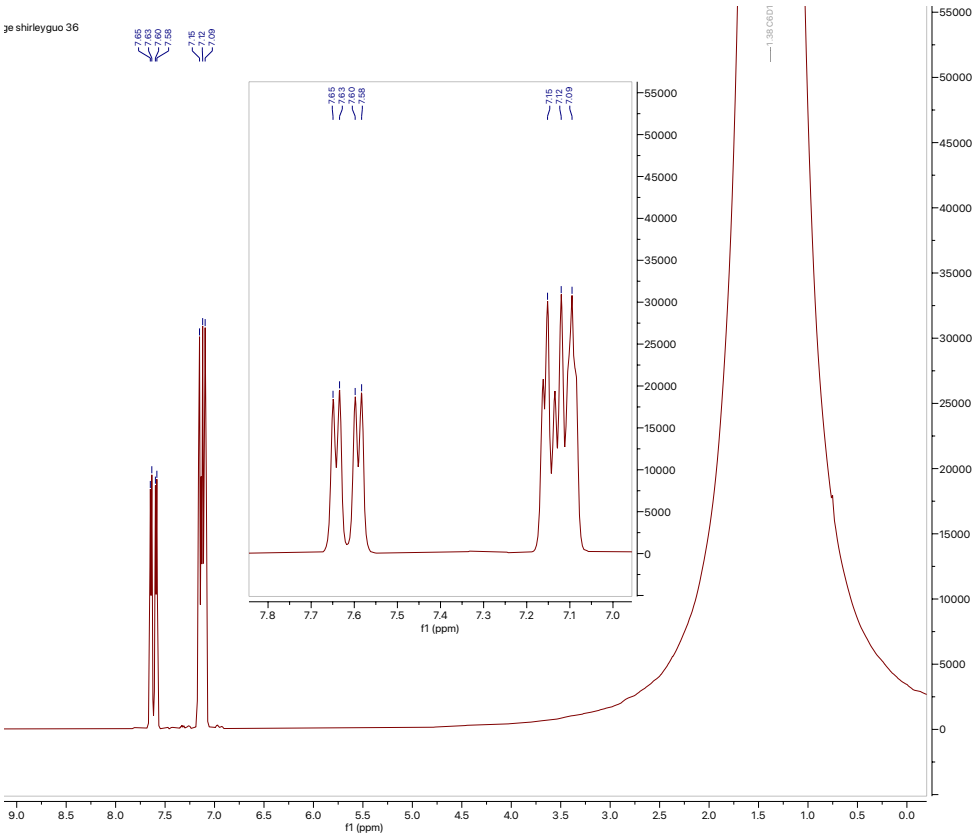

^{1}H-NMR (in cyclohexane)

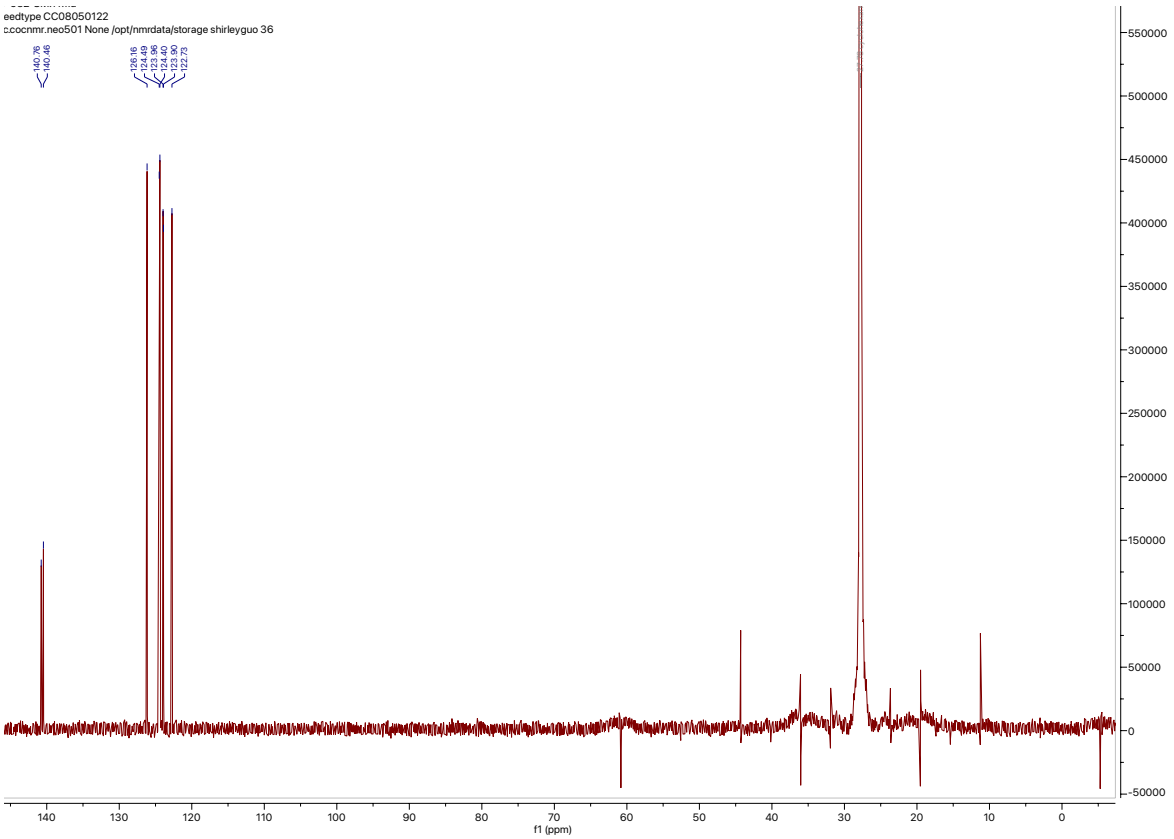

^{13}C-NMR (in cyclohexane)

[methylindole]

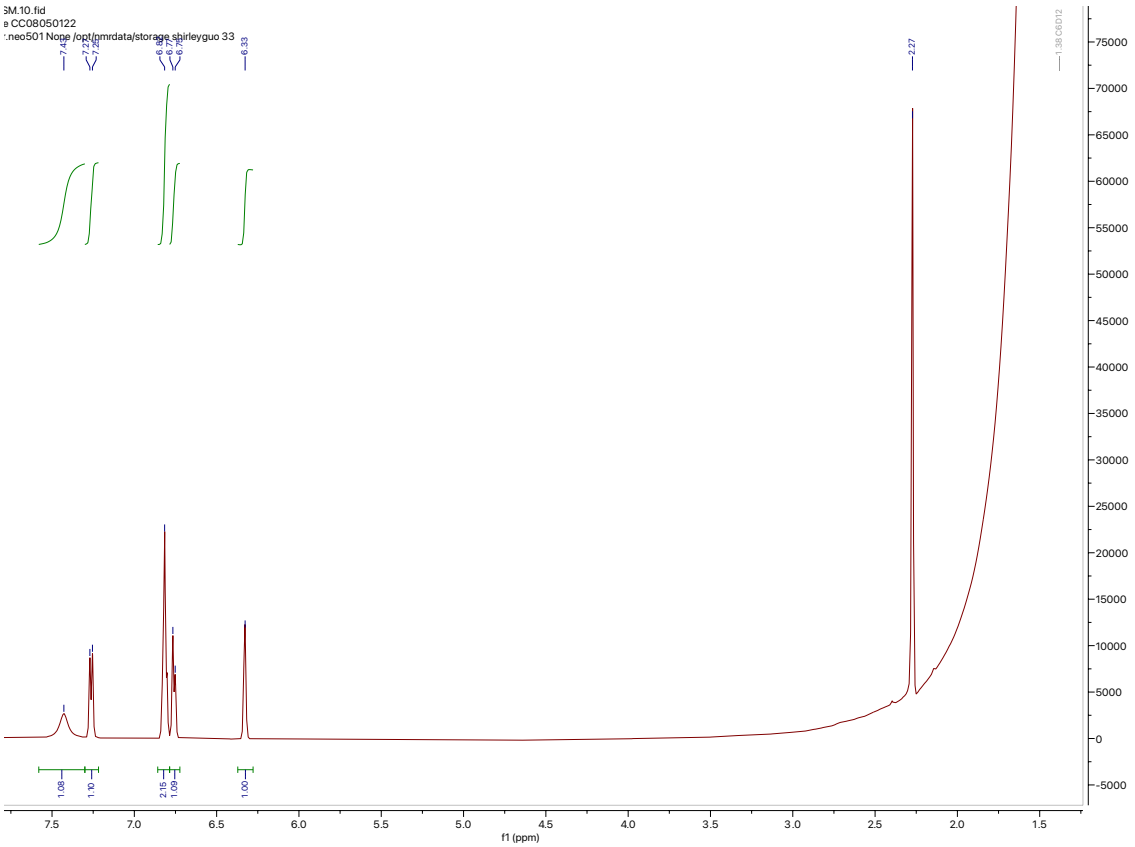

^{1}H-NMR (in cyclohexane)

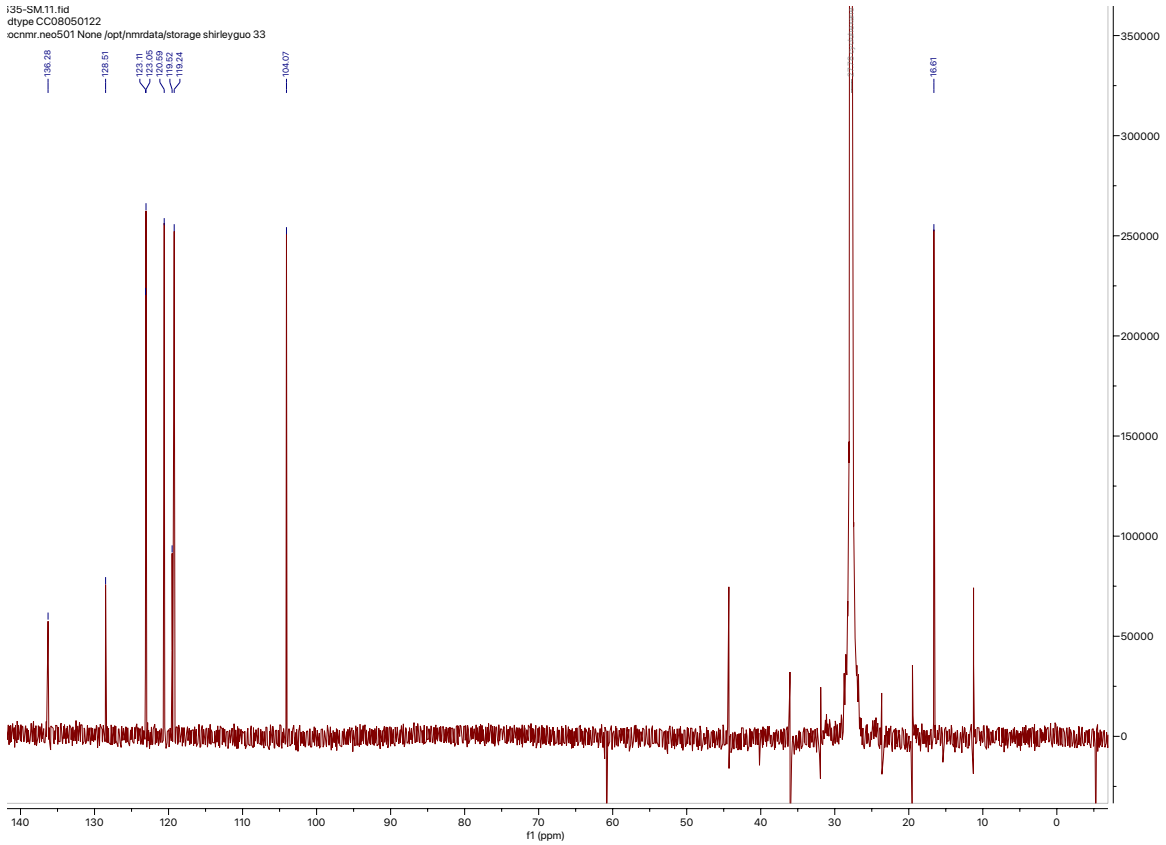

^{13}C-NMR (in cyclohexane)

1.4.6 Solutions for Additives which Impede the Catalytic C—H Borylation Reaction

Borylation of Octanethiol

In a glovebox, under an inert atmosphere of nitrogen, to a 4-mL vial equipped with a stir bar was added octanethiol (50 mg, 0.3 mmol). The vial was diluted with cyclohexane (650 uL). Then, pinacolborane (0.4 mL, 3 mmol) was added. The vial was sealed and allowed to stir at 100 °C for 17 h. The reaction was cooled to ambient temperature and then residual solvent was concentrated down with a Genevac. ^{1}H-NMR yield. Full conversion.

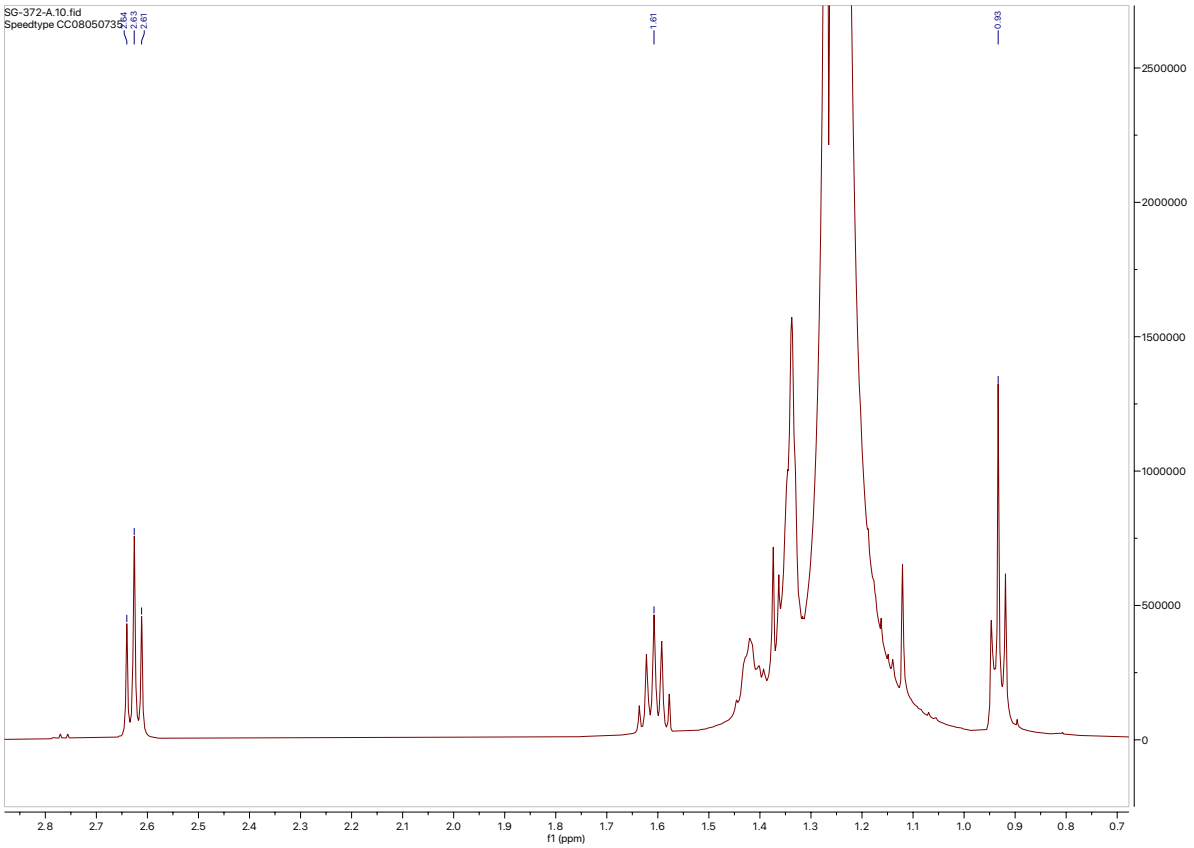
SG-372-A.10.fid
Speedtype CC08050735
2.64
2.63
2.61
1.61
0.93
2500000
2000000
1500000
1000000
500000
0
2.8 2.7 2.6 2.5 2.4 2.3 2.2 2.1 2.0 1.9 1.8 1.7 1.6 1.5 1.4 1.3 1.2 1.1 1.0 0.9 0.8 0.7
f1 (ppm)

^{1}H-NMR

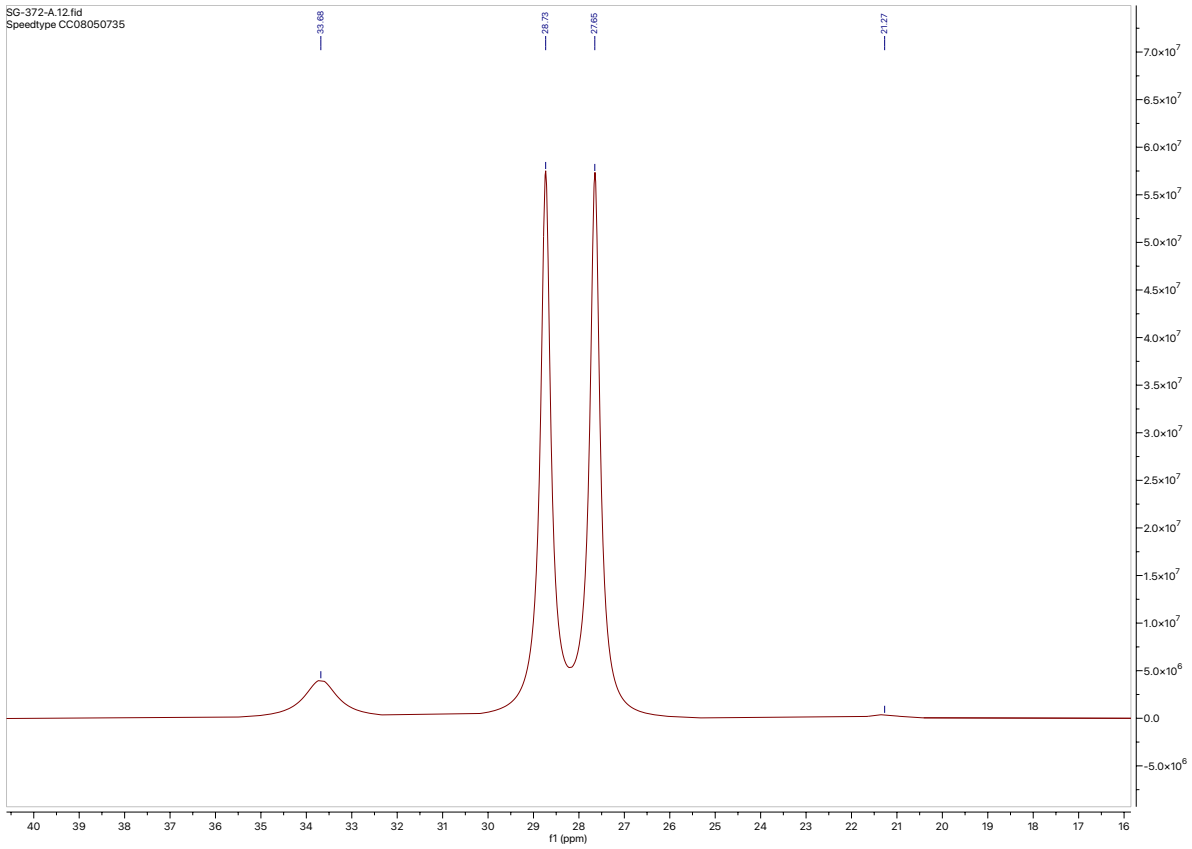

^{11}B-NMR

Deprotection of Borylated Octanethiol

In a glovebox, under an inert atmosphere of nitrogen, to a 4-mL vial equipped with a stir bar which contained the borylated octanethiol (80 mg, 0.3 mmol) was added 3-methylpentan-3-ol (300 mg, 3 mmol). Then, cyclohexane (600 uL) was added. The vial was sealed and allowed to stir at 100 °C for 19 h. The reaction was cooled to ambient temperature. ^{1}H-NMR yield, 90%.

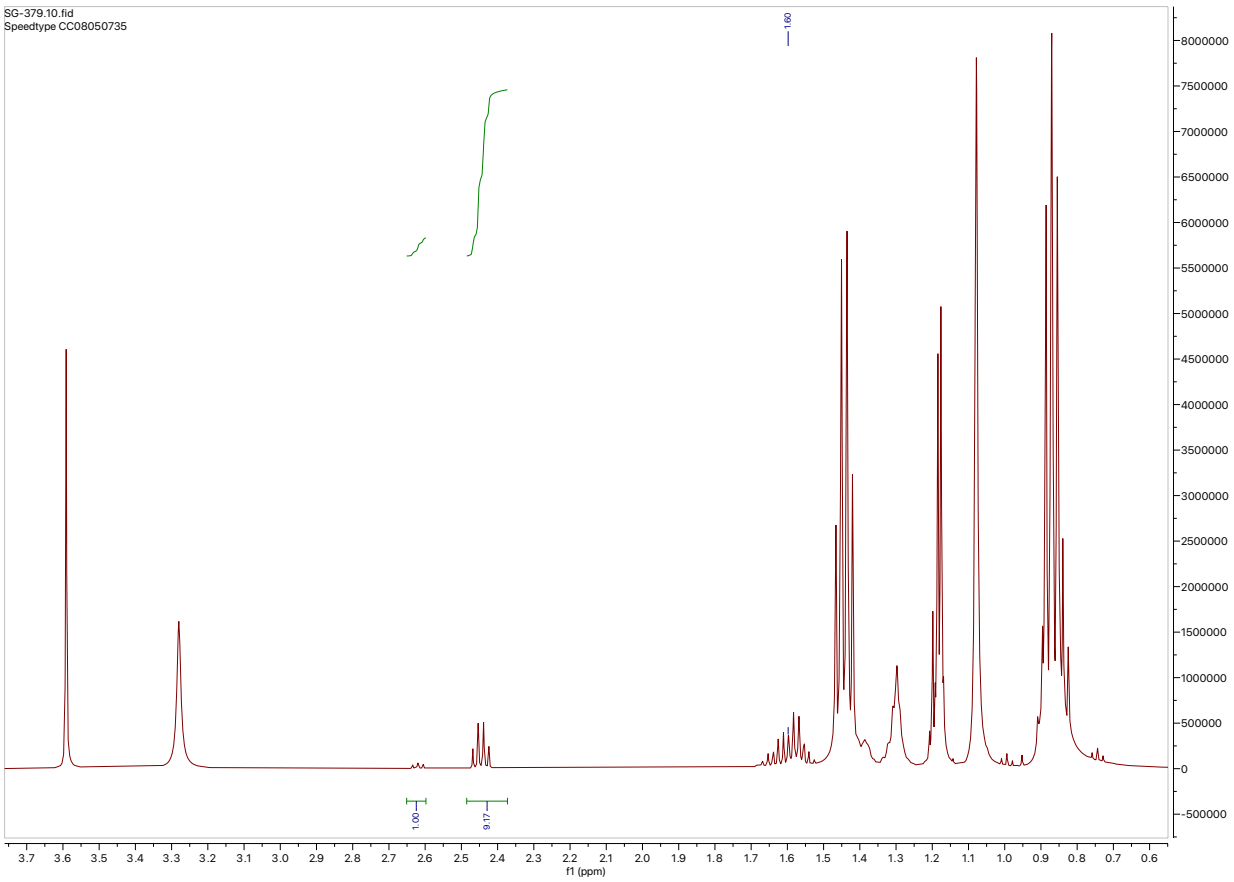

^{1}H-NMR

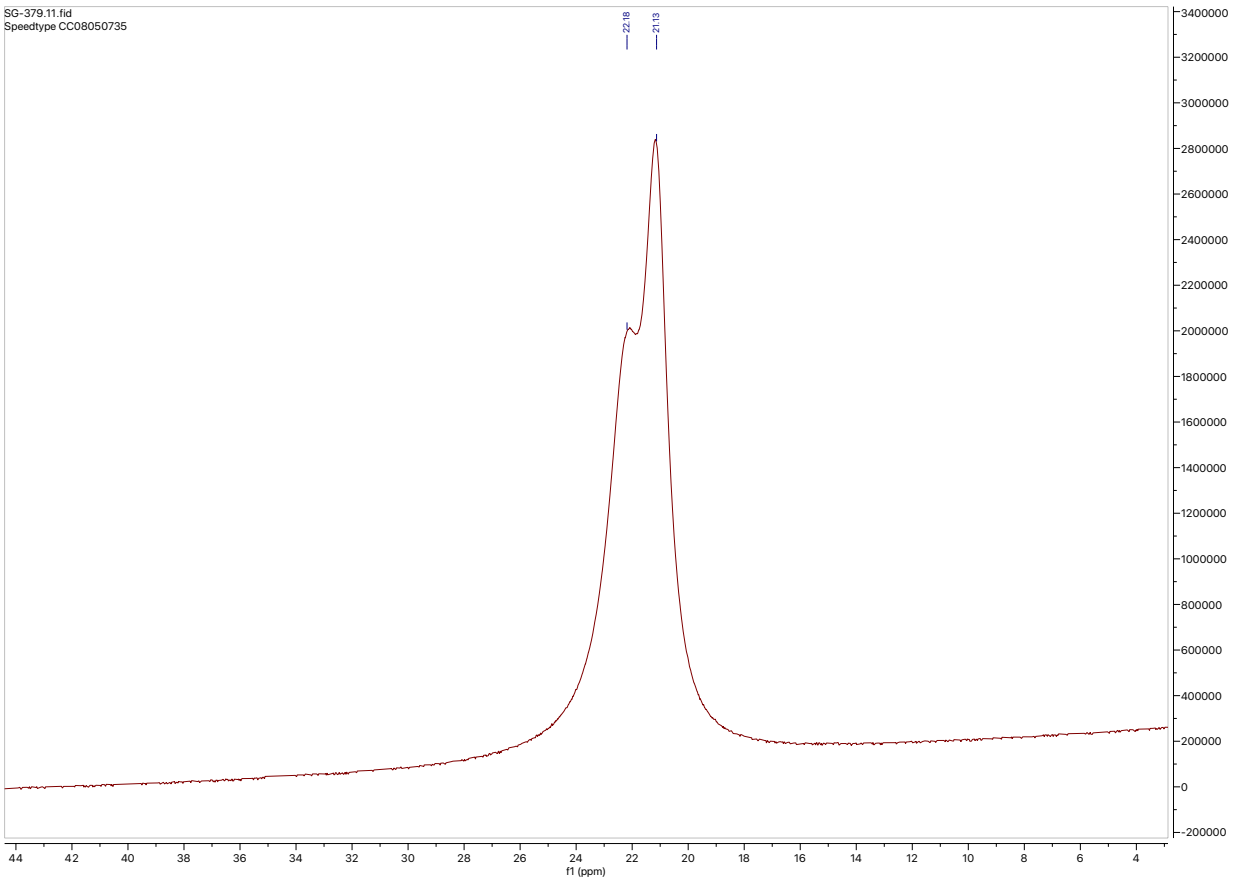

^{11}B-NMR

Catalytic Borylation of Arene 2 in the Presence of Octyliodide in C_6D_{12}

In a glovebox, under an inert atmosphere of nitrogen, to a 4-mL vial equipped with a stir bar was added bis(1,5-cyclooctadiene)di-μ-methoxydiiridium(I) (7 mg, 0.01 mmol, 0.025 equiv), 4,4'-di-tert-butyl-2,2'-dipyridyl (6 mg, 0.02 mmol, 0.055 equiv), and bis(pinacolato)diboron (100 mg, 0.4 mmol, 1 equiv). Then, cyclohexane (2 mL) was added. The vial was sealed and allowed to stir at 80 °C for > 1 h. The vial was then brought back into the glovebox to let cool to ambient temperature. This catalyst solution is a homogeneous dark red solution.

In a glovebox, under an inert atmosphere of nitrogen, to a separate 4-mL vial equipped with a stir bar was added 2-chloro-4-fluoro-1-methylbenzene (60 mg, 0.4 mmol, 1 equiv) and 1-iodooctane (90 mg, 0.4 mmol, 1 equiv). The catalyst solution was transferred to this vial which was then sealed and allowed to stir at 80 °C for 19 h. The reaction was cooled to ambient temperature. ^{1}H-NMR yield, 87%. Dioxane used as an external standard.

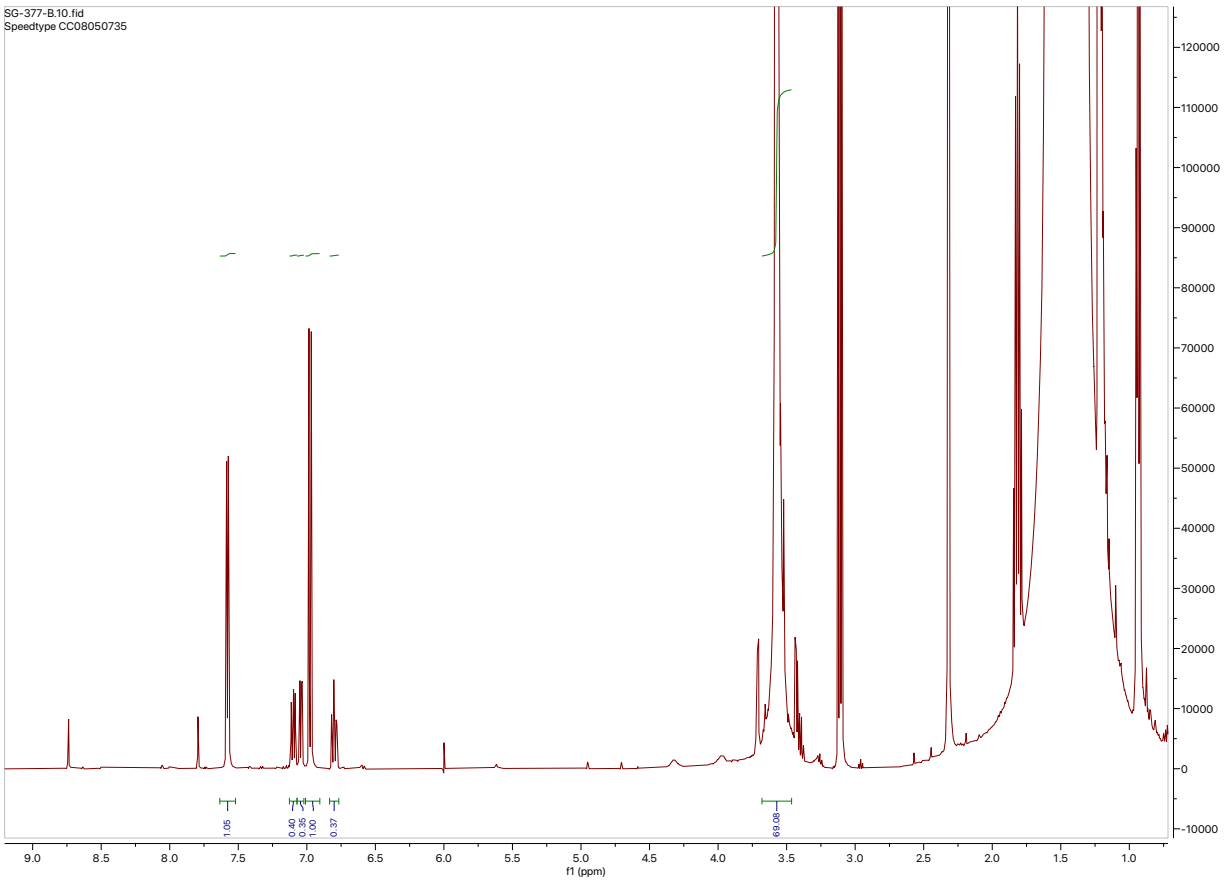
SG-377-B.10.fid
Speedtype CC08050735
1.05
0.40
0.35
1.00
0.37
69.08
f1 (ppm)

^{1}H-NMR

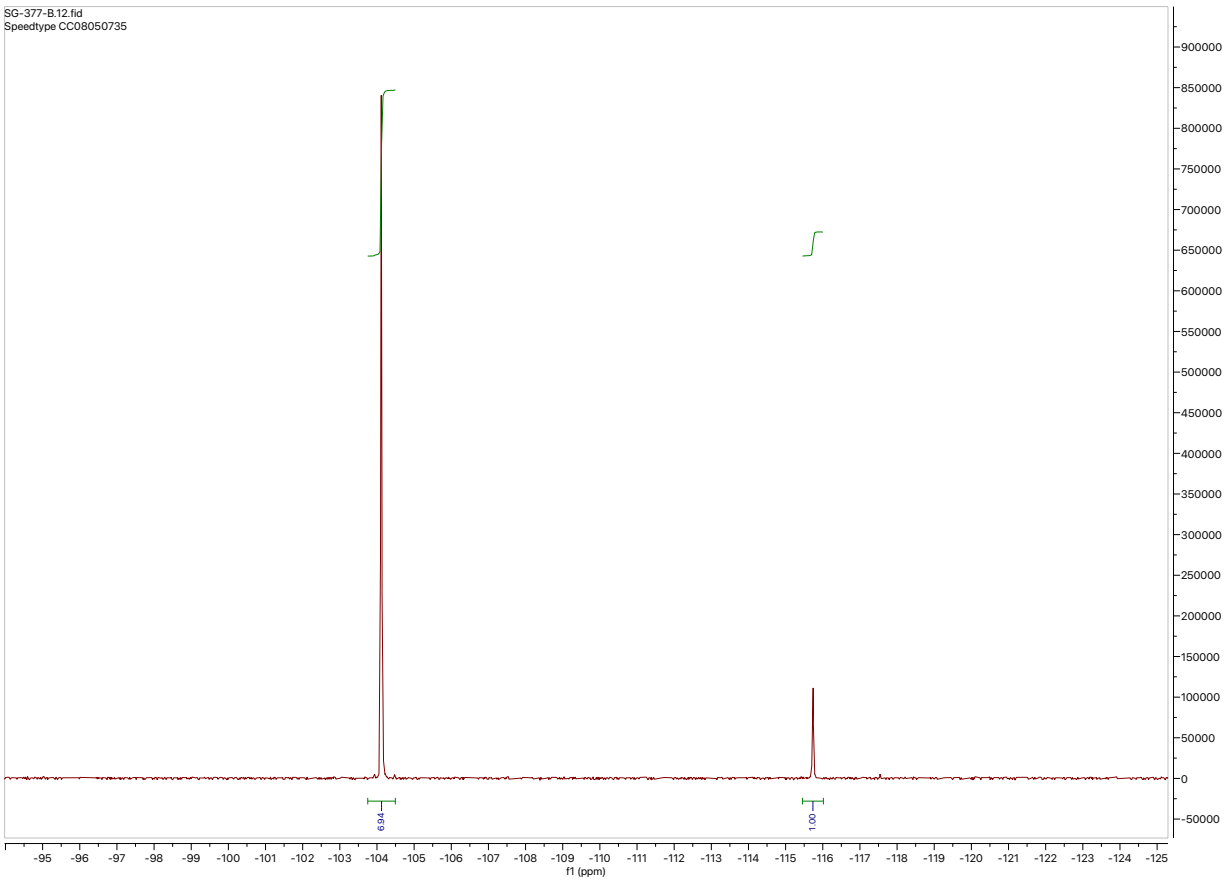

^{19}F-NMR

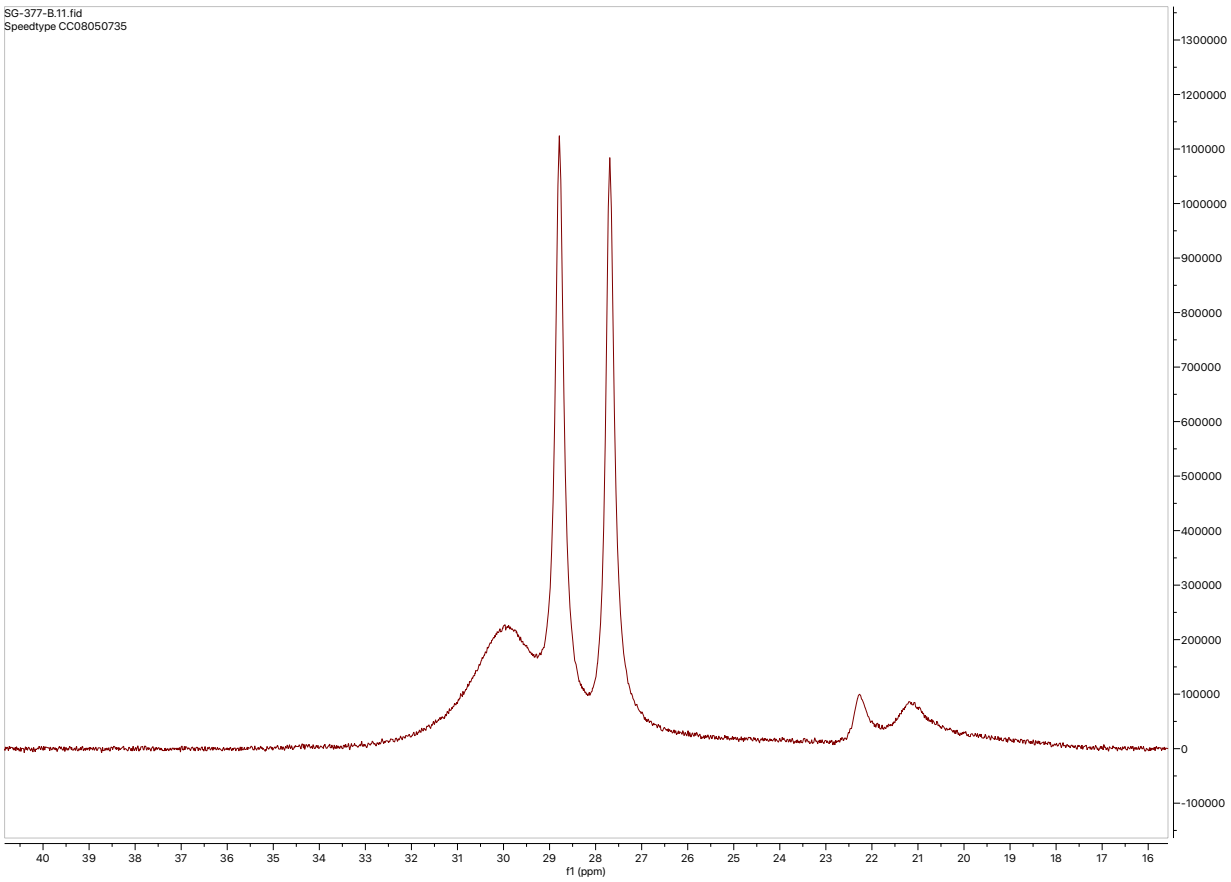

^{11}B-NMR

Catalytic Borylation of Arene 2 in the Presence of Octyliodide in THF-d_8

In a glovebox, under an inert atmosphere of nitrogen, to a 4-mL vial equipped with a stir bar was added bis(1,5-cyclooctadiene)di-μ-methoxydiiridium(I) (7 mg, 0.01 mmol, 0.025 equiv), 4,4'-di-tert-butyl-2,2'-dipyridyl (6 mg, 0.02 mmol, 0.055 equiv), and bis(pinacolato)diboron (100 mg, 0.4 mmol, 1 equiv). Then, THF (2 mL) was added. The vial was sealed and allowed to stir at 80 °C for > 1 h. The vial was then brought back into the glovebox to let cool to ambient temperature. This catalyst solution is a homogeneous dark red solution.

In a glovebox, under an inert atmosphere of nitrogen, to a separate 4-mL vial equipped with a stir bar was added 2-chloro-4-fluoro-1-methylbenzene (60 mg, 0.4 mmol, 1 equiv) and 1-iodooctane (90 mg, 0.4 mmol, 1 equiv). The catalyst solution was transferred to this vial which was then sealed and allowed to stir at 80 °C for 19 h. The reaction was cooled to ambient temperature. ^{1}H-NMR yield, 44%. Dioxane used as an external standard.

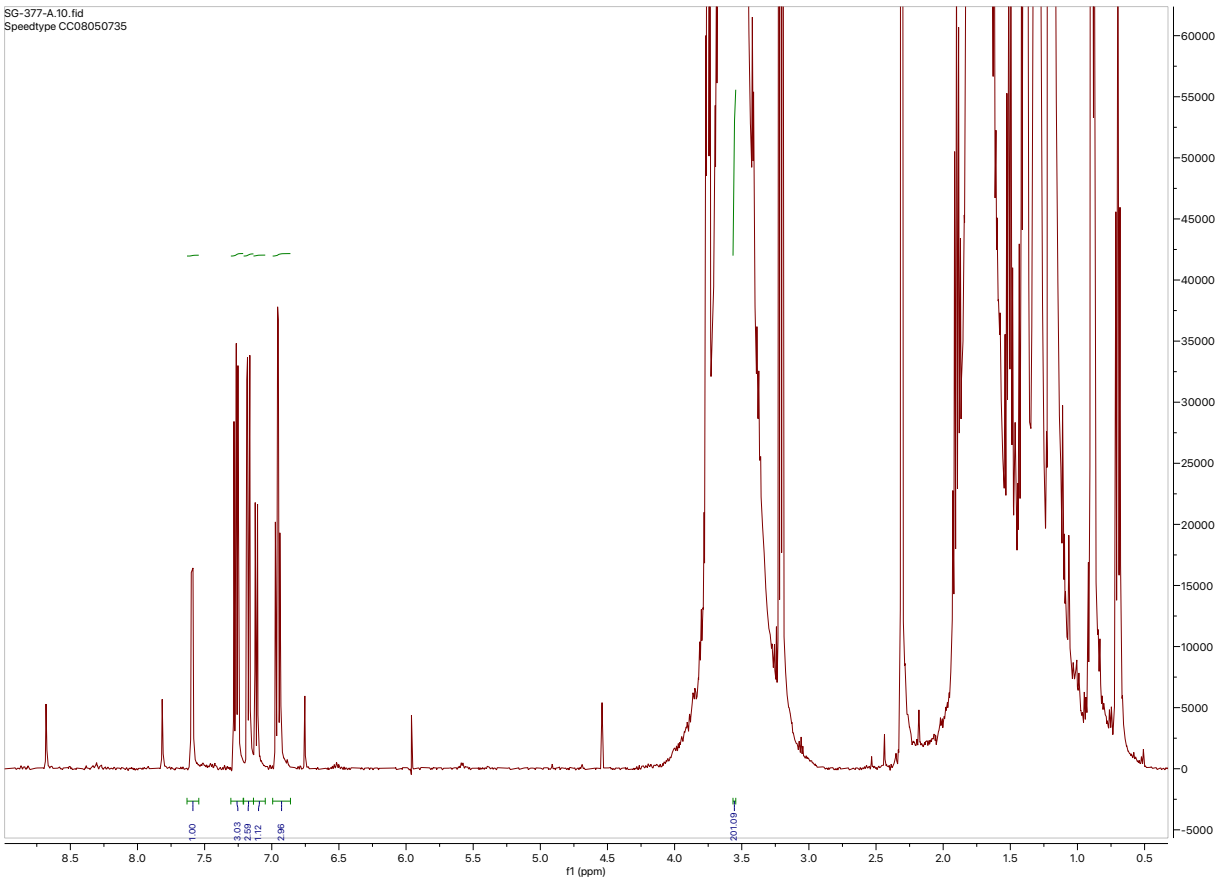
SG-377-A.10.fid
Speedtype CC08050735
1.00
3.03
2.69
1.12
2.96
201.09
f1 (ppm)

^{1}H-NMR

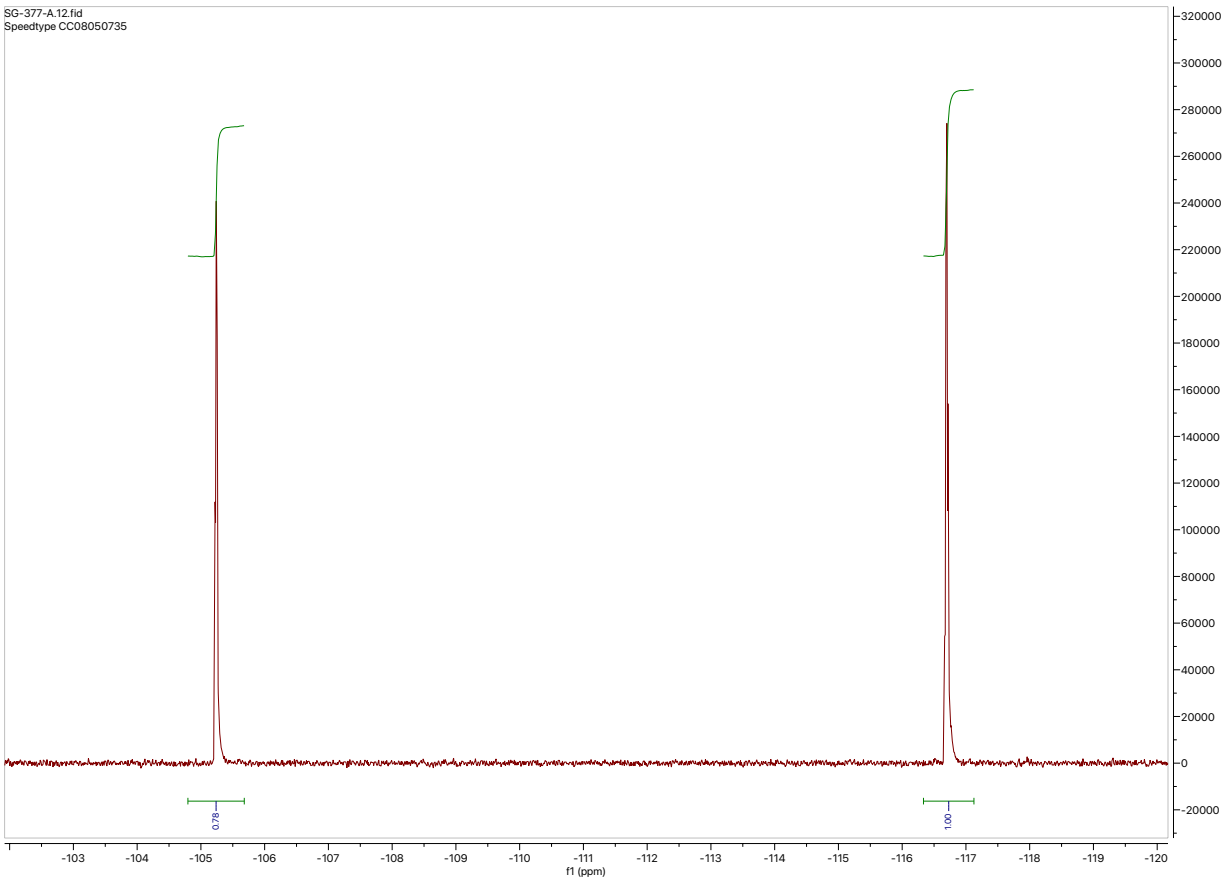
SG-377-A.12.fid
Speedtype CC08050735
320000
300000
280000
260000
240000
220000
200000
180000
160000
140000
120000
100000
80000
60000
40000
20000
0
-20000
0.78
1.00
-103
-104
-105
-106
-107
-108
-109
-110
-111
-112
-113
-114
-115
-116
-117
-118
-119
-120
f1 (ppm)

^{19}F-NMR

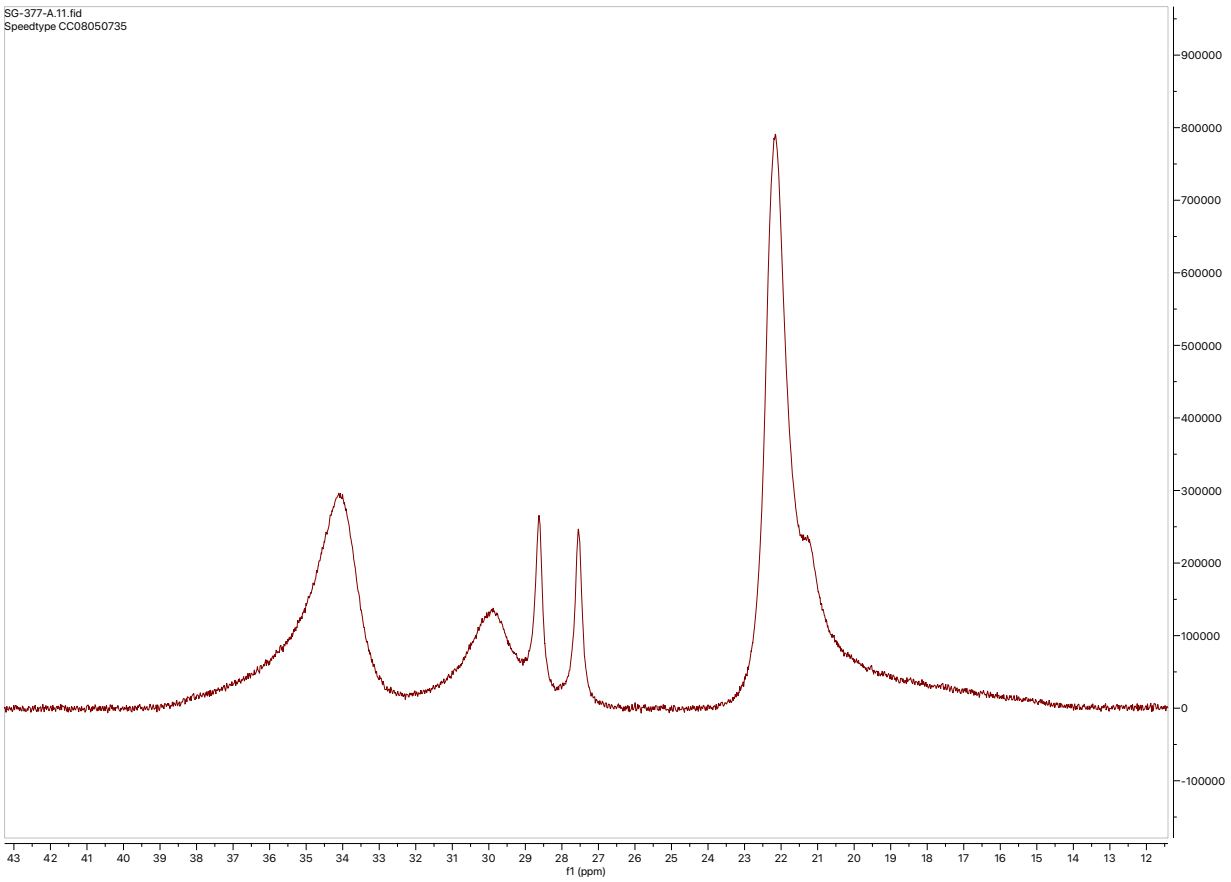

^{11}B-NMR

1.5 References

1. Isaac F. Yu, Jake W. Wilson and John F. Hartwig, Transition-Metal-Catalyzed Silylation and Borylation of C–H Bonds for the Synthesis and Functionalization of Complex Molecules. *Chem. Rev.* **2023**, *123(19)*, 11619-11663.
2. Jay S. Wright, Peter J. H. Scott and Patrick G. Steel, Iridium-Catalysed C—H Borylation of Heteroarenes: Balancing Steric and Electronic Regiocontrol. *Angew. Chem. Int. Ed.* **2021**, *60*, 2796 – 2821.
3. Chabush Haldar, Md Emdadul Hoque, Jagriti Chaturvedi, Mirja Md Mahamudul Hassan and Buddhadeb Chattopadhyay, Ir-catalyzed proximal and distal C–H borylation of arenes. *Chem. Commun.* **2021**, *57*, 13059 – 13074.
4. John F. Hartwig, Regioselectivity of the borylation of alkanes and arenes. *Chem. Soc. Rev.* **2011**, *40*, 1992–2002.
5. Sean M. Preshlock, Behnaz Ghaffari, Peter E. Maligres, Shane W. Krska, Robert E. Maleczka Jr. and Milton R. Smith III, High-Throughput Optimization of Ir-Catalyzed C–H Borylation: A Tutorial for Practical Applications. *JACS* **2013**, *135(20)*, 7572-7582.
6. Amanda Jane Lyons, Adam Clarke, Heidi Fisk, Bethany Jackson, Peter R. Moore, Samantha Oke, Thomas O. Ronson and Rebecca E. Meadows, Scaling up a C–H

Borylation: Addressing the Safety Concerns of an Iridium-Catalyzed Process for Multikilo Scale Manufacture. *Org. Process Res. Dev.* **2022**, *26(5)*, 1378-1388.
7. Tatsuo Ishiyama, Jun Takagi, Kousaku Ishida, Norio Miyaura, Natia R. Anastasi, and John F. Hartwig, Mild Iridium-Catalyzed Borylation of Arenes. High Turnover Numbers, Room Temperature Reactions, and Isolation of a Potential Intermediate. *JACS* **2002**, *124(3)*, 390-391.
8. C. N. Iverson and M. R. Smith, Stoichiometric and Catalytic B−C Bond Formation from Unactivated Hydrocarbons and Boranes. *JACS* **1999**, *121*, 7696–7697.
9. Timothy M. Boller, Jaclyn M. Murphy, Marko Hapke, Tatsuo Ishiyama, Norio Miyaura, and John F. Hartwig, Mechanism of the Mild Functionalization of Arenes by Diboron Reagents Catalyzed by Iridium Complexes. Intermediacy and Chemistry of Bipyridine-Ligated Iridium Trisboryl Complexes. JACS **2005**, 127(41), 14263–14278.
10. Raphael J. Oeschger, Matthew A. Larsen, Alessandro Bismuto, and John F. Hartwig, Origin of the Difference in Reactivity between Ir Catalysts for the Borylation of C–H Bonds. *JACS* **2019**, *141(41)*, 16479-16485.
11. Takayuki Furukawa, Mamoru Tobisu and Naoto Chatani, C–H Functionalization at Sterically Congested Positions by the Platinum-Catalyzed Borylation of Arenes. *JACS* **2015**, *137(38)*, 12211-12214.
12. Matthew A. Larsen and John F. Hartwig, Iridium-Catalyzed C–H Borylation of Heteroarenes: Scope, Regioselectivity, Application to Late-Stage Functionalization, and Mechanism. *JACS* **2014**, *136(11)*, 4287–4299.
13. Karl D. Collins and Frank Glorius, A robustness screen for the rapid assessment of chemical reactions. *Nat. Chem.* **2013**, *5*, 597 – 601.
14. William N. Olmstead, Zafra Margolin and Frederick G. Bordwell, Acidities of water and simple alcohols in dimethyl sulfoxide solution. *J. Org. Chem.* **1980**, *45*, 3295.
15. Frederick G. Bordwell, George E. Drucker and Herbert E. Fried, Acidities of carbon and nitrogen acids: the aromaticity of the cyclopentadienyl anion. *J. Org. Chem.* **1981**, *46*, 632.
16. Bordwell, F. G.; Hughes, D. L. Thiol Acidities and Thiolate Ion Reactivities toward Butyl Chloride in Dimethyl Sulfoxide Solution. The Question of Curvature in Brønsted Plots. *J. Org. Chem.* **1982**, *47*, 3224−3232.
17. F. G. Bordwell, J. A. Harrelson Jr., and Tsuei Yun Lynch, Homolytic bond dissociation energies for the cleavage of .alpha.-nitrogen-hydrogen bonds in carboxamides, sulfonamides, and their derivatives. The question of synergism in nitrogen-centered radicals. *J. Org. Chem.* **1990**, *55*, 3337.
18. Kuang Shen, Yao Fu, Jia-Ning Li, Lei Liu and Qing-Xiang Guo, What are the pKa values of C–H bonds in aromatic heterocyclic compounds in DMSO? *Tetrahedron* **2007**, *63*, 1568 – 1576.
19. Walter S. Matthews, Joseph E. Bares, John E. Bartmess, F. G. Bordwell, Frederick J. Cornforth, George E. Drucker, Zafra Margolin, Robert J. McCallum, Gregory J. McCollum, and Noel R. Vanier, Equilibrium acidities of carbon acids. VI. Establishment of an absolute scale of acidities in dimethyl sulfoxide solution. *JACS* **1975**, *97*, 7006.
20. Frederick G. Bordwell, Equilibrium acidities in dimethyl sulfoxide solution. *Acc. Chem. Res.* **1988**, *21(12)*, 456-463.

21. Xian Man Zhang, Frederick G. Bordwell, Michael Van Der Puy and Herbert E. Fried, Equilibrium acidities and homolytic bond dissociation energies of the acidic carbon-hydrogen bonds in N-substituted trimethylammonium and pyridinium cations. *J. Org. Chem.* **1993**, *58(11)*, 3060-3066.
22. Mark L. Hlavinka, Jeffrey F. Greco and John R. Hagadorn, The direct α-zincation of amides, phosphonates and phosphine oxides by H–Zn exchange. *Chem. Commun.* **2005**, *42*, 5304-5306.
23. Jay A. Labinger and John E. Bercaw, Understanding and exploiting C–H bond activation. *Nature* **2002**, *417*, 507–514.
24. Robin Larouche-Gauthier, Tim G. Elford and Varinder K. Aggarwal, Ate Complexes of Secondary Boronic Esters as Chiral Organometallic-Type Nucleophiles for Asymmetric Synthesis. *JACS* **2011**, *133(42)*, 16794-16797.
25. Carl W. Liskey and John F. Hartwig, Iridium-Catalyzed C–H Borylation of Cyclopropanes. *JACS* **2013**, *135(9)*, 3375-3378.
26. Per E. M. Siegbahn, Trends of Metal-Carbon Bond Strengths in Transition Metal Complexes. *J. Phys. Chem.* **1995**, *99(34)*, 12723-12729.
27. A. Ray Bulls, John E. Bercaw, Juan M. Manriquez and Mark E. Thompson, Relative bond dissociation energies for early transition metal alkyl, aryl, alkynyl and hydride compounds. Equilibration of metallated cyclopentadienyl derivatives of peralkylated hafnocene and scandocene with hydrocarbons and dihydrogen. *Polyhedron* **1988**, 7, 1409.
28. Raphael Oeschger, Bo Su, Isaac Yu, Christian Ehinger, Erik Romero, Sam He and John Hartwig, Diverse functionalization of strong alkyl C–H bonds by undirected borylation. *Science* **2020**, *368*, 736-741.
29. Carl W. Liskey and John F. Hartwig, Iridium-Catalyzed Borylation of Secondary C–H Bonds in Cyclic Ethers. *JACS* **2012**, *134(30)*, 12422-12425.
30. Margaret R. Jones, Caleb D. Fast and Nathan D. Schley, Iridium-Catalyzed sp3 C–H Borylation in Hydrocarbon Solvent Enabled by 2,2′-Dipyridylarylmethane Ligands. *JACS* **2020**, *142(14)*, 6488-6492.
31. Gautam Kumar, Zheng-Wang Qu, Soumen Ghosh, Stefan Grimme and Indranil Chatterjee, Boron Lewis Acid-Catalyzed Regioselective Hydrothiolation of Conjugated Dienes with Thiols. *ACS Catal.* **2019**, *9(12)*, 11627-11633.
32. Frederick G. Bordwell, Robert J. McCallum, and William N. Olmstead, Acidities and hydrogen bonding of phenols in dimethyl sulfoxide. *J. Org. Chem.* **1984**, *49(8)*, 1424-1427.
33. F. G. Bordwell, Donald Algrim, and Noel R. Vanier, Acidities of anilines and toluenes. *J. Org. Chem.* **1977**, *42(10)*, 1817-1819.
34. Carlos Hernandez-Tamargo, Alberto Roldan, and Nora H. de Leeuw, Tautomerization of Phenol at the External Lewis Acid Sites of Scandium-, Iron- and Gallium-Substituted Zeolite MFI. *J. Phys. Chem.* 2019, *123(13)*, 7604-7614.

35. Jwu-Ting Chen, Yu-Kun Chen, Jiane-Bond Chu, Gene-Hsiang Lee and Yu Wang, Coordination of Aniline to an (η^1-Allenyl)iridium Complex Leading to Hydroanilination. *Organometallics* **1997**, *16(7)*, 1476-1483.
36. Soocheta Jha, Souradeep Basu, Madison Bob and David R. Stuart, The Lewis basicity of amines on the Legault iodonium Lewis acidity scale. *Chem. Commun.* **2025**, Advance Article [doi: 10.1039/d5cc01711d]
37. Ivan Pietro Oliveri, Giuseppe Maccarrone and Santo Di Bella, A Lewis Basicity Scale in Dichloromethane for Amines and Common Nonprotogenic Solvents Using a Zinc(II) Schiff-Base Complex as Reference Lewis Acid. *J. Org. Chem.* **2011**, *76(21)*, 8879-8884.
38. Ibraheem A. I. Mkhalid, David N. Coventry, David Albesa-Jove, Andrei S. Batsanov, Judith A. K. Howard, Robin N. Perutz and Todd B. Marder, Ir-Catalyzed Borylation of CH Bonds in N-Containing Heterocycles: Regioselectivity in the Synthesis of Heteroaryl Boronate Esters. *Angew. Chem. Int. Ed.* **2006**, *45*, 489 – 491.
39. Robert R. Fraser, Tarek S. Mansour, and Sylvain Savard, Acidity measurements in THF. V. Heteroaromatic compounds containing 5-membered rings. *Can. J. Chem.* **1985**, *63(12)*, 3505-3509.
40. Laura Rubio-Pérez, E. A. Jaseer, Nestor García, Victor Polo, Manuel Iglesias and Luis A. Oro, Experimental and Computational Studies on the Reactivity and Binding Mode of Thiophene with N-Heterocyclic Carbene Iridium Complexes. *Organometallics* **2016**, *35(4)*, 569-578.
41. Christo S. Sevov, Jianrong (Steve) Zhou and John F. Hartwig, Iridium-Catalyzed, Intermolecular Hydroamination of Unactivated Alkenes with Indoles. *JACS* **2014**, *136(8)*, 3200-3207.
42. Shi-Chao Ren, Feng-Lian Zhang, Ai-Qing Xu, Yinuo Yang, Min Zheng, Xiaoguo Zhou, Yao Fu and Yi-Feng Wang, Regioselective radical α-borylation of α,β-unsaturated carbonyl compounds for direct synthesis of α-borylcarbonyl molecules. *Nat. Commun.* **2019**, *10*, 1934.
43. Sesha Kisan, Varadhan Krishnakumar and Chidambaram Gunanathan, Ruthenium-Catalyzed Deoxygenative Hydroboration of Carboxylic Acids. *ACS Catal.* **2018**, *8(6)*, 4772-4776.
44. Gaoli Hu, Qi Liu, Yi Zhou, Wei Yan, Yuqing Sun, Shuang Peng, Chengbin Zhao, Xiang Zhou and Hexiang Deng, Extremely Large 3D Cages in Metal–Organic Frameworks for Nucleic Acid Extraction. *JACS* **2023**, *145(24)*, 13181-13194.
45. Daniel W. Robbins and John F. Hartwig, A C–H Borylation Approach to Suzuki–Miyaura Coupling of Typically Unstable 2–Heteroaryl and Polyfluorophenyl Boronates. *Org. Lett.* **2012**, *14(16)*, 4266-4269.
46. Li Zhang and Lei Jiao, Pyridine-Catalyzed Radical Borylation of Aryl Halides. *JACS* **2017**, *139(2)*, 607-610.
47. Gabriel J. Lovinger, Mark D. Aparece and James P. Morken, Pd-Catalyzed Conjunctive Cross-Coupling between Grignard-Derived Boron “Ate” Complexes and C(sp2) Halides or Triflates: NaOTf as a Grignard Activator and Halide Scavenger. *JACS* **2017**, *139(8)*, 3153-3160.
48. Carl W. Liskey and John F. Hartwig, Iridium-Catalyzed C–H Borylation of Cyclopropanes. *JACS* **2013**, *135(9)*, 3375-3378.

49. Stephen J. Roseblade, Ivana Gazic Smilovic and Zdenko Casar, Study of chemoselective asymmetric hydrogenation of (1-bromo-1-alkenyl)boronic esters with iridium–PˆN complexes. *Tetrahedron* **2014**, *70*, 2654-2660.
50. Alessandro Bismuto, Michael J. Cowley and Stephen P. Thomas. Aluminum-Catalyzed Hydroboration of Alkenes. *ACS Catal.* **2018,** *8(3)*, 2001-2005.
51. Chun-I Lee, Jia Zhou and Oleg V. Ozerov, Catalytic Dehydrogenative Borylation of Terminal Alkynes by a SiNN Pincer Complex of Iridium. *JACS* **2013**, *135(9)*, 3560-3566.
52. Christopher J. Barger, Alessandro Motta, Victoria L. Weidner, Tracy L. Lohr and Tobin J. Marks, La[N(SiMe3)2]3-Catalyzed Ester Reductions with Pinacolborane: Scope and Mechanism of Ester Cleavage. *ACS Catal.* **2019**, *9(10)*, 9015-9024.
53. Zhi Yang, Mingdong Zhong, Xiaoli Ma, Karikkeeriyil Nijesh, Susmita De, Pattiyil Parameswaran and Herbert W. Roesky, An Aluminum Dihydride Working as a Catalyst in Hydroboration and Dehydrocoupling. *JACS* **2016**, *138(8)*, 2548-2551.
54. Étienne Rochette, Hugo Boutin and Frédéric-Georges Fontaine, Frustrated Lewis Pair Catalyzed S–H Bond Borylation. *Organometallics* **2017**, *36(15)*, 2870-2876.
55. Shang Gao, Meng Duan, Kendall N. Houk and Ming Chen, Chiral Phosphoric Acid Dual-Function Catalysis: Asymmetric Allylation with α-Vinyl Allylboron Reagents. *Angew. Chem. Int. Ed.* **2020**, *59*, 10540 – 10548.
56. Andy S. Tsai, Ming Chen and William R. Roush, Chiral Brønsted Acid Catalyzed Enantioselective Synthesis of anti-Homopropargyl Alcohols via Kinetic Resolution-Aldehyde Allenylboration Using Racemic Allenylboronates. *Org. Lett.* **2013**, *15(9)*, 2325-2325.
57. Zhi-Tao He, Haoquan Li, Alexander M. Haydl, Gregory T. Whiteker and John F. Hartwig, Trimethylphosphate as a Methylating Agent for Cross Coupling: A Slow-Release Mechanism for the Methylation of Arylboronic Esters. *JACS* **2018**, *140(49)*, 17197-17202.
58. Vignesh Palani, Melecio A. Perea, Kristen E. Gardner and Richmond Sarpong, A pyrone remodeling strategy to access diverse heterocycles: application to the synthesis of fascaplysin natural products. *Chem. Sci.* **2021**, *12*, 1528-1534.
59. Laura Falivene, Raffaele Credendino, Albert Poater, Andrea Petta, Luigi Serra, Romina Oliva, Vittorio Scarano, and Luigi Cavallo, SambVca 2. A Web Tool for Analyzing Catalytic Pockets with Topographic Steric Maps. *Organometallics* **2016**, *35(13)*, 2286-2293.
60. Henry E. Bryndza, Lawrence K. Fong, Rocco A. Paciello, Wilson Tam, and John E. Bercaw, Relative metal-hydrogen, -oxygen, -nitrogen, and -carbon bond strengths for organoruthenium and organoplatinum compounds; equilibrium studies of Cp*(PMe3)2RuX and (DPPE)MePtX systems. *JACS* 1987, *109(5)*, 1444-1456.

CHAPTER 2: Boronic Acid Selective Reactions Enabled by a Mild and Facile Bpin Deprotection

2.1 Introduction

The C—H borylation reaction exclusively furnishes boronate ester products. While boronate esters are highly useful, easily derivatized, synthetic handles there are a select number of derivatizations which do not perform well with boronate esters and instead select for boronic acids. A mild and facile bpin deprotection methodology would extend the utility of the C—H borylation reaction into boronic acid selective derivatizations. Such a deprotection methodology was published in 2019 by Hinkes and Klein[1] wherein methylboronic acid is employed (Figure 2.1). Methylboronic acid and its diol ester byproducts are volatile species, remnants of which are easily removed at the end of the deprotection by simple evaporation.[1] This facile purification enables a seamless transition from the boronate ester product of the C—H borylation reaction to its corresponding boronic acid as a substrate for boronic acid selective transformations.

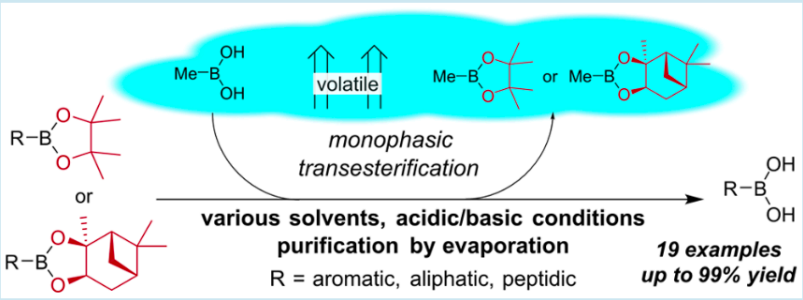

Figure 2.1 Deprotection of arylboronic esters to arylboronic acids with methylboronic acid[1]; Reprinted (adapted) with permission from Org. Lett. 2019, 21, 9, 3048–3052. Copyright 2019 American Chemical Society

A survey was taken of synthetically useful transformations that may be boronic acid selective to determine their efficacy on boronate esters versus their corresponding boronic acids. Many boronic acid selective reactions of high synthetic value were revealed thereby expanding the scope of the C—H borylation reaction.

2.2 Results and Discussion

2.2.1 Deprotection

2.2.1.1 Deprotection of Electron Rich Aryl BPin

Of the boronic esters successfully transformed into boronic acids by Hinkes and coworkers, 2-(3,5-dimethylphenyl)-4,4,5,5-tetramethyl-1,3,2-dioxaborolane was not included.[1] However, this deprotection of 2-(3,5-dimethylphenyl)-4,4,5,5-tetramethyl-1,3,2-dioxaborolane had been studied by Murphy and coworkers in their publication on the one-pot synthesis of arylboronic acids by Ir-catalyzed borylation of arenes (Figure 2.2).[2] Murphy and coworkers utilized aqueous $NaIO_4$ to afford the corresponding boronic acid in 66% yield. Utilizing methylboronic acid, however, drastically increased the yield of the boronic acid to 90%, and furthermore, allows for a facile workup procedure (Figure 2.2).

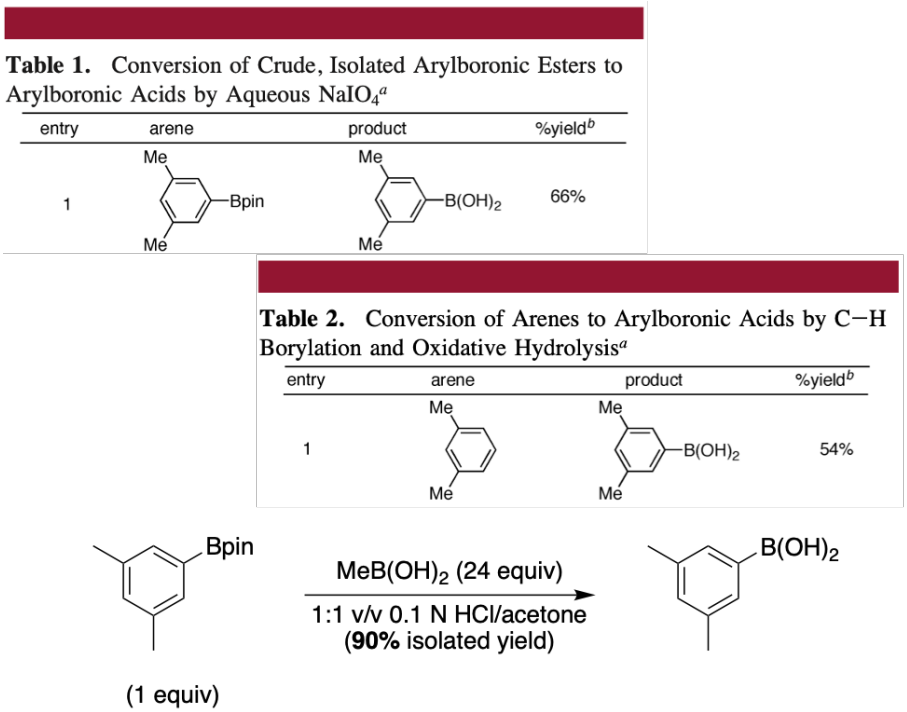

Figure 2.2 Deprotection of 2-(3,5-dimethylphenyl)-4,4,5,5-tetramethyl-1,3,2-dioxaborolane[2]; Reprinted (adapted) with permission from Org. Lett. 2007, 9, 5, 757–760. Copyright 2007 American Chemical Society

2.2.1.2 Deprotection of Electron Poor Aryl BPin

Of the boronic esters successfully transformed into boronic acids by Hinkes and coworkers, 2-(4-chlorophenyl)-4,4,5,5-tetramethyl-1,3,2-dioxaborolane was not included.[1] With methylboronic acid, the deprotection of 2-(4-chlorophenyl)-4,4,5,5-tetramethyl-1,3,2-dioxaborolane afforded the corresponding boronic acid in high yield (83%) (Figure 2.3).

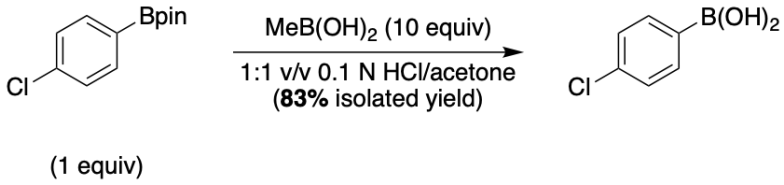

Figure 2.3 Deprotection of 2-(4-chlorophenyl)-4,4,5,5-tetramethyl-1,3,2-dioxaborolane

2.2.1.3 Deprotection of Heteroarenes

Lastly, few heteroarenes were included in the work by Hinkes and coworkers.[1] As heteroarenes are an important class of compounds for Ir-catalyzed borylations a survey of the deprotection of heteroarenes with methylboronic acid was taken (Figure 2.4). While most

heteroarylboronic esters were not stable to this deprotection methodology that of 2-(benzo[b]thiophen-2-yl)-4,4,5,5-tetramethyl-1,3,2-dioxaborolane (not represented in the work by Hinkes and coworkers[1]) was successful affording the corresponding boronic acid in 94% yield.

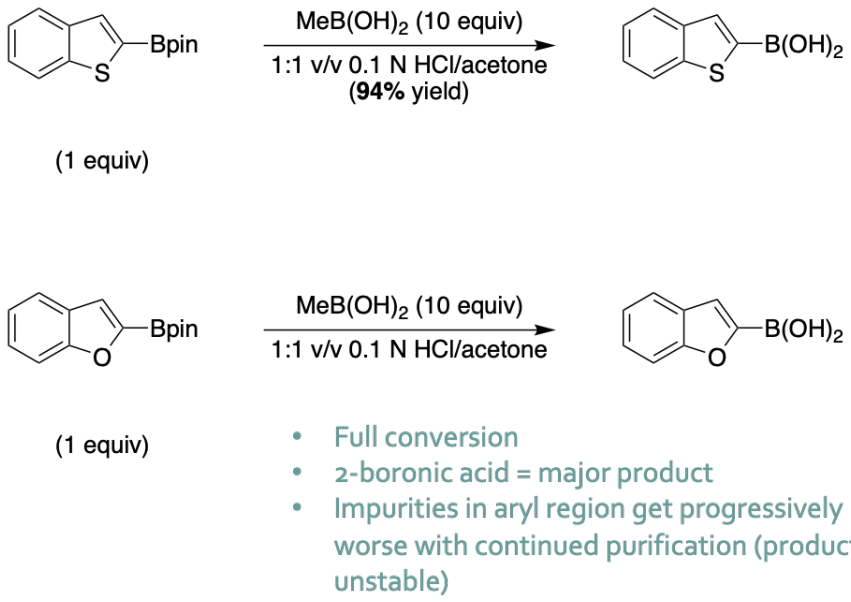

Figure 2.4 Deprotection of 2-(benzo[b]thiophen-2-yl)-4,4,5,5-tetramethyl-1,3,2-dioxaborolane versus that of 2-(benzofuran-2-yl)-4,4,5,5-tetramethyl-1,3,2-dioxaborolane

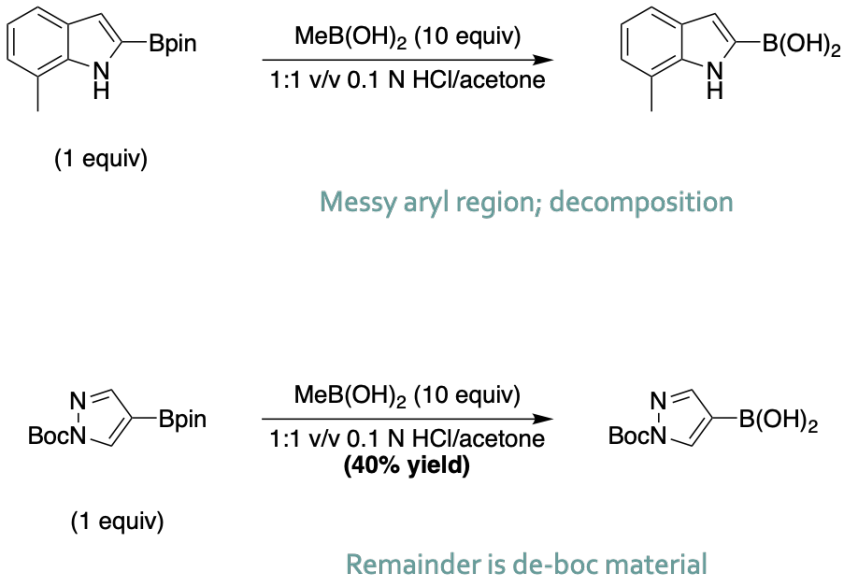

Figure 2.5 Unsuccessful deprotections of heteroarenes

2.2.2 Reactions

2.2.2.1 Catalyst-Free Petasis-Type Reaction: Decarboxylative Coupling of Boronic Acid with Proline & Salicylaldehyde for the Synthesis of Alkylaminophenols

In 2018, Kaboudin and coworkers developed the synthesis of alkylaminophenols via a three-component, catalyst-free decarboxylative coupling of proline with salicylaldehyde and boronic acids (Figure 2.6).[3] This boronic acid specific reaction was tested on both 2-(3,5-dimethylphenyl)-4,4,5,5-tetramethyl-1,3,2-dioxaborolane and its corresponding boronic acid (Figure 2.7). While 2-(3,5-dimethylphenyl)-4,4,5,5-tetramethyl-1,3,2-dioxaborolane did underperform in this Petasis-type reaction when compared to the boronic acid it only did so by 10% still providing a modest 55% yield of the corresponding alkylaminophenol. Therefore, this methodology is not boronic acid specific and is indeed tolerant of the designated electron rich boronic ester. The difference between the boronic ester and the boronic acid is more evident when this methodology was applied to 2-(4-chlorophenyl)-4,4,5,5-tetramethyl-1,3,2-dioxaborolane and its corresponding boronic acid. The electron poor boronic ester only provided 13% yield of the corresponding alkylaminophenol whereas the boronic acid provided a good yield of 65% of the alkylaminophenol. Therefore, the successful deprotection of 2-(4-chlorophenyl)-4,4,5,5-tetramethyl-1,3,2-dioxaborolane afforded by methylboronic acid (Figure 2.3) is important because this Petasis-type reaction is boronic acid specific for this electron poor aryl[B] compound.

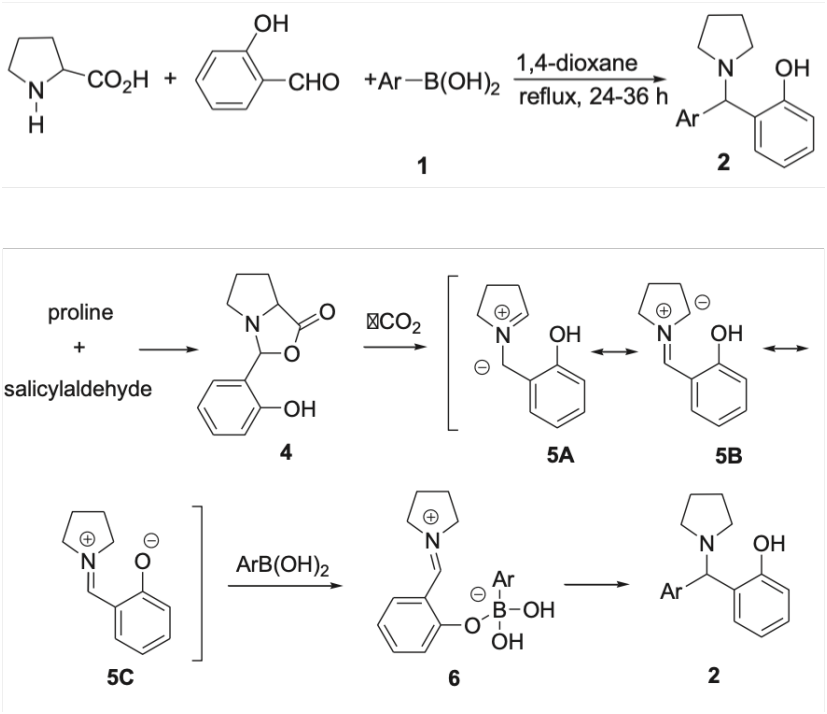

Figure 2.6 Catalyst-free Petasis-type reaction[3]; Reprinted (adapted) with permission from Tetrahedron Letters 2018, 59, 1046–1049. Copyright 2018 American Chemical Society

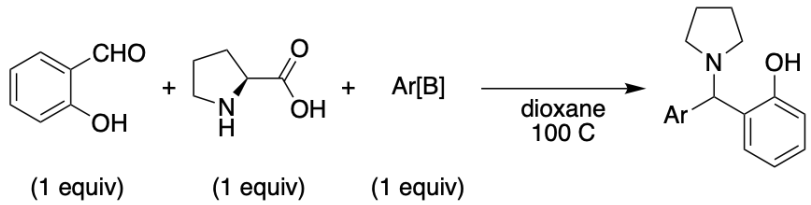

Ar[B]	^{1}H-NMR yield
3,5-dimethylphenyl**boronic acid**	65
3,5-dimethylphenyl**Bpin**	55
p-Cl-phenyl**boronic acid**	65
p-Cl-phenyl**Bpin**	13

Figure 2.7 Catalyst-free Petasis-type reaction as boronic acid selective reaction

2.2.2.2 Rhodium-Catalyzed Asymmetric 1,4-Addition of Arylboronic Acids to Enones

In 1998, Takaya and coworkers developed the rhodium-catalyzed asymmetric 1,4-addition of arylboronic acids to enones (Figure 2.8).[4] In this work, boronic acid selectivity was demonstrated for two substrates (Figure 2.9, green). While 2-(4-chlorophenyl)-4,4,5,5-tetramethyl-1,3,2-dioxaborolane only provided 10% yield of the corresponding beta-substituted ketone product the corresponding boronic acid was able to increase that yield to a modest 45%. Likewise, one equivalent of phenylboronic ester provided 25% yield of the corresponding beta-substituted ketone product while one equivalent of phenylboronic acid doubled this yield to 50%. Therefore, the successful deprotection of 2-(4-chlorophenyl)-4,4,5,5-tetramethyl-1,3,2-dioxaborolane (Figure 2.3) and of phenylboronic ester[1] afforded by methylboronic acid is important because this rhodium-catalyzed asymmetric 1,4-addition of arylboronic acids to enones is boronic acid specific for these aryl[B] compounds.

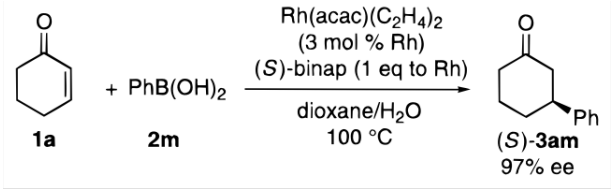

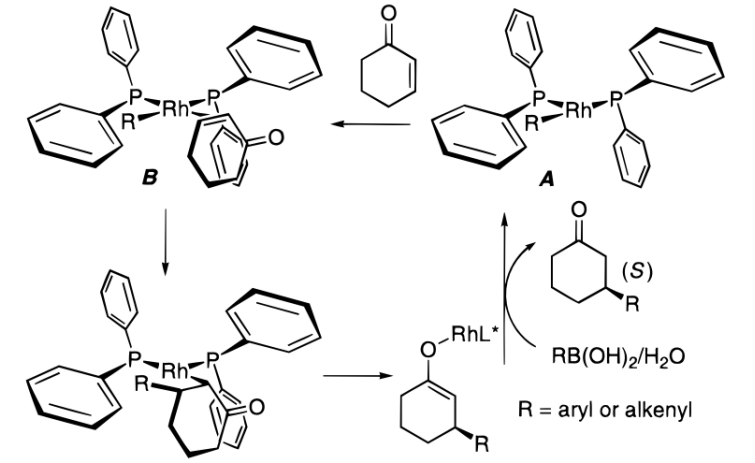

[a] The binaphthylene moiety in (*S*)-binap is omitted for clarity.

Figure 2.8 Rhodium-catalyzed asymmetric 1,4-addition of arylboronic acids to enones[4]; Reprinted (adapted) with permission from J. Am. Chem. Soc. 1998, 120, 22, 5579–5580. Copyright 1998 American Chemical Society

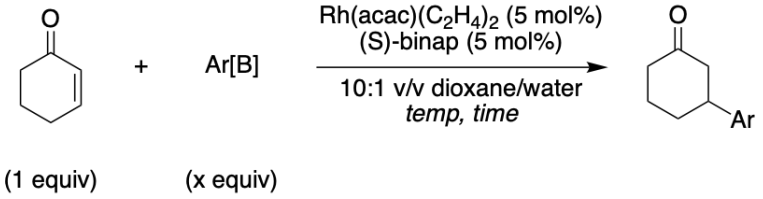

Ar[B]	Ar[B] equiv	temp (° C)	time (h)	^{1}H-NMR yield
p-Cl-phenylboronic acid	5	100	3	13
p-Cl-phenylBpin	5	100	3	17
p-Cl-phenylboronic acid	5	65	ovnt	45
p-Cl-phenylBpin	5	65	ovnt	10
phenylboronic acid	5	65	ovnt	80
phenylBpin	5	65	ovnt	80
phenylboronic acid	1	65	ovnt	50
phenylBpin	1	65	ovnt	25
3,5-dimethylphenylboronic acid	1	65	ovnt	25
3,5-dimethylphenylBpin	1	65	ovnt	43

Figure 2.9 Rhodium-catalyzed asymmetric 1,4-addition of arylboronic acids to enones as boronic acid selective reaction

2.2.2.3 Chan-Lam

In 2017, en route to the development of a catalytic Chan-Lam, Vantourout and coworkers described the boronic acid selective nature of the traditional Chan-Lam reaction (Figure 2.10).[5] Here, the boronic acid selective nature of the traditional Chan-Lam was also demonstrated for the electron poor para-chlorophenylboronic ester and acid compounds (Figure 2.11). Therefore, the successful deprotection of 2-(4-chlorophenyl)-4,4,5,5-tetramethyl-1,3,2-dioxaborolane (Figure 2.3) afforded by methylboronic acid is important because of the boronic acid selective nature of the traditional Chan-Lam reaction.

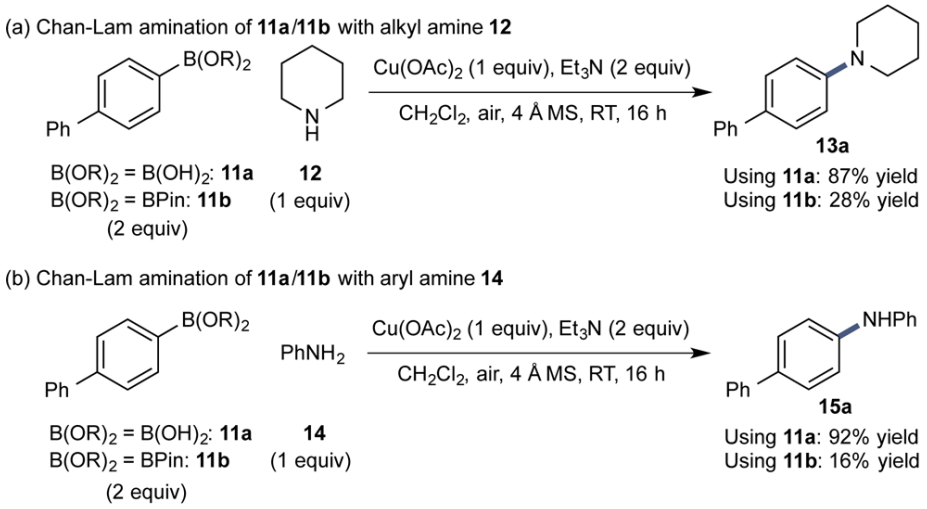

Figure 2.10 Chan-Lam[5]; Reprinted (adapted) with permission from J. Am. Chem. Soc. 2017, 139, 13, 4769–4779. Copyright 2017 American Chemical Society

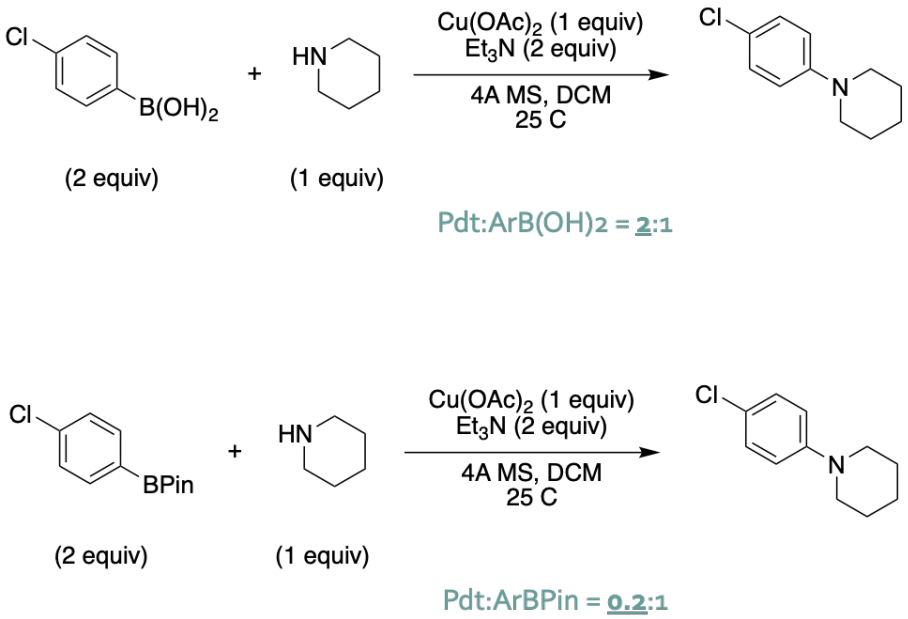

Figure 2.11 Chan-Lam as boronic acid selective reaction

2.2.2.4 Petasis

In 2010, Mandai and coworkers developed an improved protocol for the Petasis reaction of 2-pyridinecarbaldehydes evaluating a scope of both vinyl and aryl boronic acids.[6] Here, to demonstrate that the Petasis reaction is indeed boronic acid selective it was conducted with both (4-methoxyphenyl)boronic ester and (4-methoxyphenyl)boronic acid (Figure 2.12). The Petasis reaction with (4-methoxyphenyl)boronic ester did not provide the Petasis product. By contrast, the Petasis reaction with (4-methoxyphenyl)boronic acid fully converted to the Petasis product.

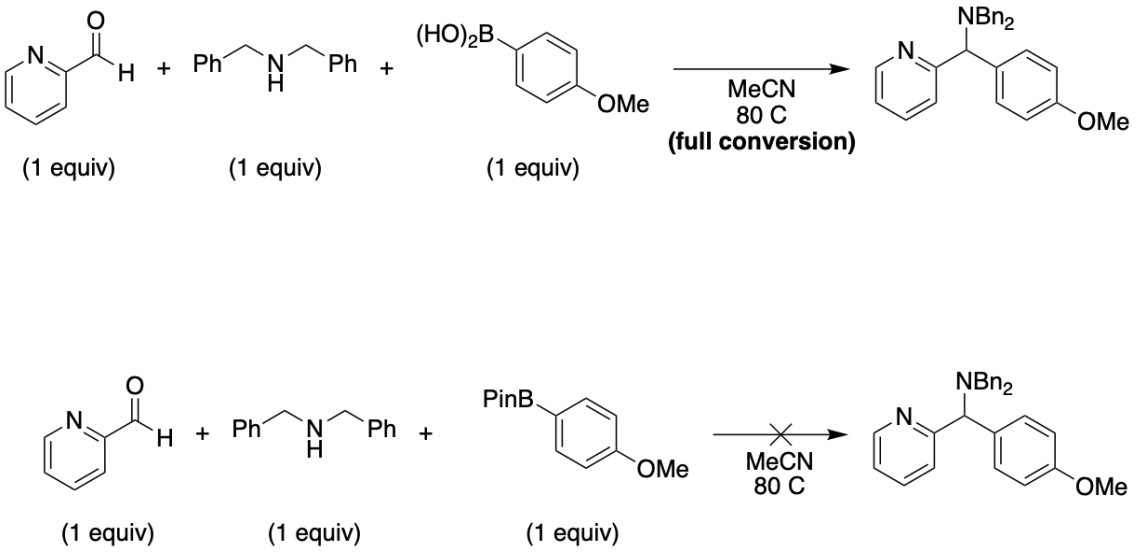

Figure 2.12 Petasis as boronic acid selective reaction

2.2.2.5 Carbon-Carbon Bond-Forming Reductive Coupling between Boronic Acids & Tosylhydrazones

In 2009, Barluenga and coworkers developed the metal-free carbon-carbon bond forming reductive coupling between boronic acids and tosylhydrazones (Figure 2.13).[7] Here, the boronic acid selective nature of the reaction was demonstrated in its comparison with the corresponding boronic ester (Figure 2.14). Therefore, the successful deprotection of phenylboronic ester[1] afforded by methylboronic acid is important because of the boronic acid selective nature of the reductive coupling.

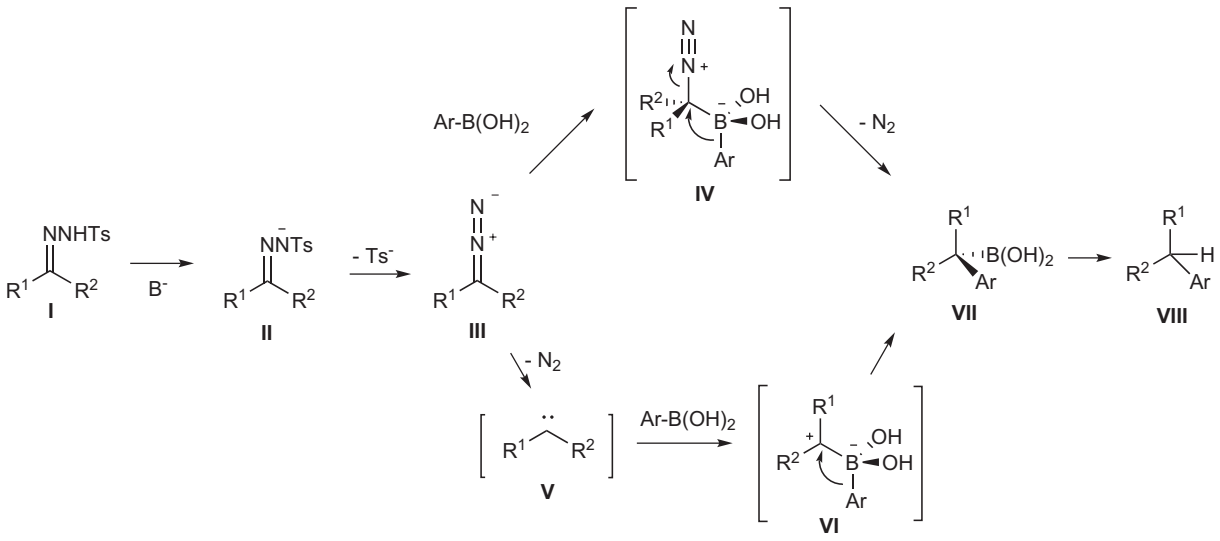

Figure 2.13 Carbon-carbon bond-forming reductive coupling[7]; Reprinted (adapted) with permission from Nature Chem 2009, 1, 494–499. Copyright 2009 American Chemical Society

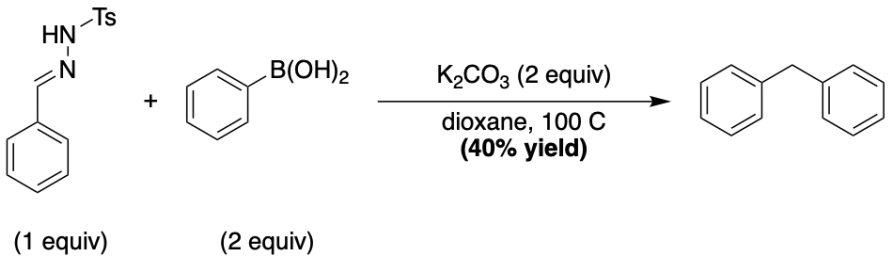

Figure 2.14 Carbon-carbon bond-forming reductive coupling as boronic acid selective reaction

2.3 Conclusion

A few arenes and heteroarenes not in the original publication by Hinkes and Klein were successfully deprotected and these substrates were utilized to screen for boronic acid selective

synthetic reactions. Five varied and synthetically valuable reactions were found to be boronic acid selective. These new substrates and boronic acid selective reactions extend the scope of utility of the arene C—H borylation reaction. Given the demonstrated ease of purification of the deprotection reaction, the extension of the arene C—H borylation reaction into these boronic acid selective reactions should be able to be accomplished via a telescope. Future work would include demonstration of the telescoping of these reactions as well as expansion of both substrates available to deprotection and other boronic acid selective reactions.

2.4 Experimental

2.4.1 Deprotections

Deprotection of 2-(3,5-dimethylphenyl)-4,4,5,5-tetramethyl-1,3,2-dioxaborolane with $MeB(OH)_2$

To a 20-mL vial equipped with a stir bar was added 2-(3,5-dimethylphenyl)-4,4,5,5-tetramethyl-1,3,2-dioxaborolane (586 mg, 2.5 mmol, 1 equiv) and methylboronic acid (3.6 g, 60 mmol, 24 equiv). Then, added a 1:1 v/v 0.1N HCl/acetone solution (10 mL). The vial was sealed and let stir at ambient temperature for 18 h. A clear homogeneous solution is obtained.

Residual solvents are removed via concentration in a Genevac. Then, iteratively, with a minimum of two cycles the crude was diluted with an excess of water/acetone and then concentrated in a Genevac to ensure full removal of residual methylboronic acid.

Yield was measured with ^{1}H-NMR spectroscopy against dioxane as an internal standard. Acetonitrile-d_3/D_2O solvents. The title compound was isolated as a white solid, 90%.

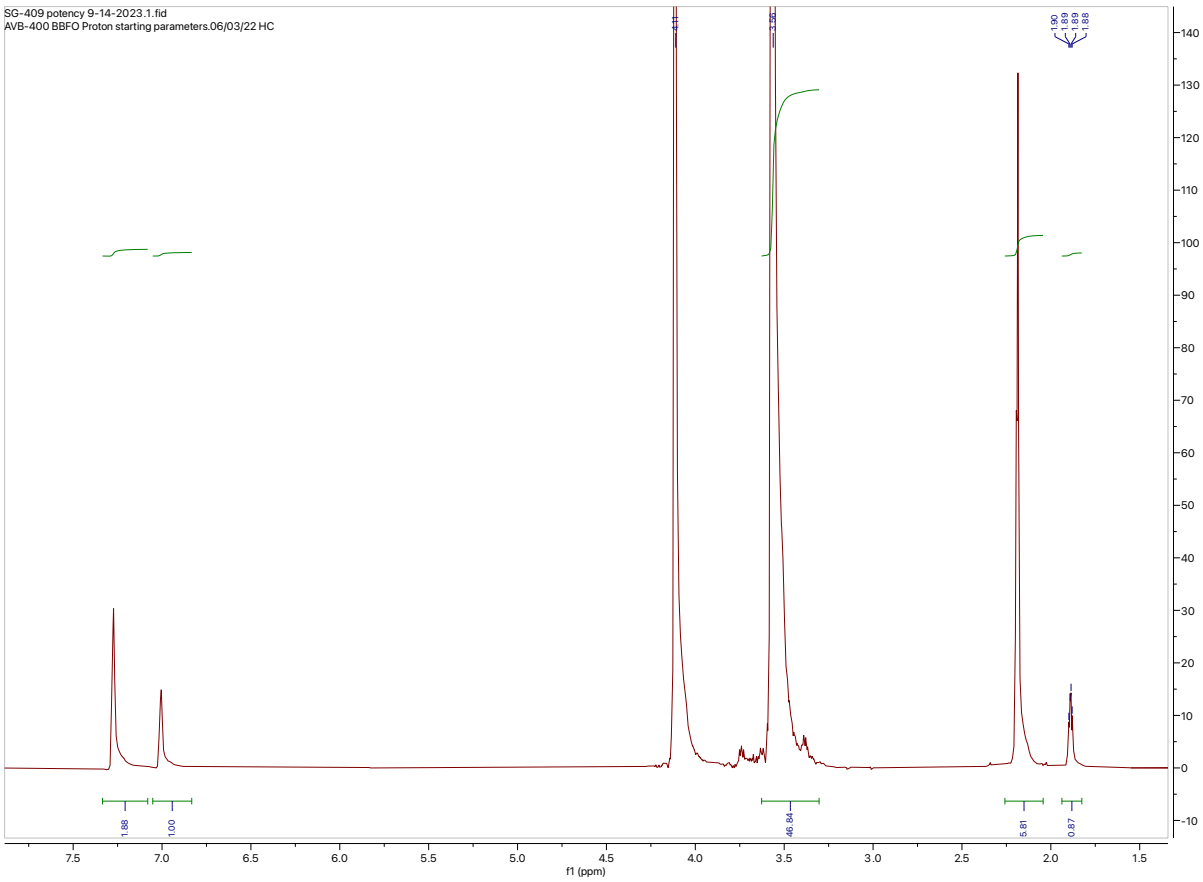

^{1}H-NMR

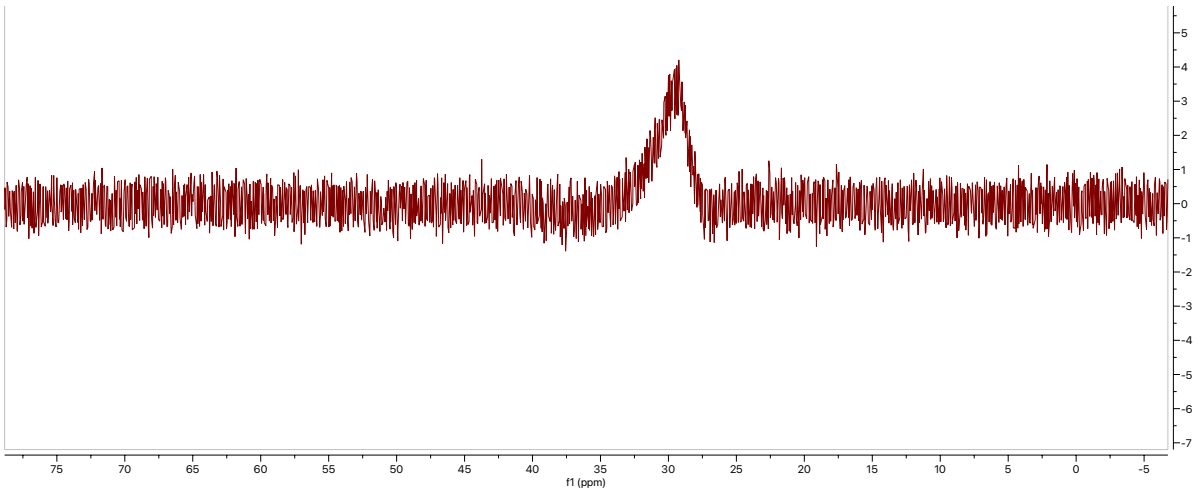

^{11}B-NMR

Deprotection of 2-(4-chlorophenyl)-4,4,5,5-tetramethyl-1,3,2-dioxaborolane with $MeB(OH)_2$

To a 20-mL vial equipped with a stir bar was added 2-(4-chlorophenyl)-4,4,5,5,-tetramethyl-1,3,2-dioxaborolane (298 mg, 1.25 mmol, 1 equiv) and methylboronic acid (0.75 g, 12.5 mmol,

10 equiv). Then, added a 1:1 v/v 0.1N HCl/acetone solution (5 mL). The vial was sealed and let stir at ambient temperature for 18 h. A clear homogeneous solution is obtained.

Residual solvents are removed via concentration in a Genevac. Then, iteratively, with a minimum of two cycles the crude was diluted with an excess of water/acetone and then concentrated in a Genevac to ensure full removal of residual methylboronic acid.

Yield was measured with ^{1}H-NMR against dioxane as an internal standard. The title compound was isolated as a solid, 83%.

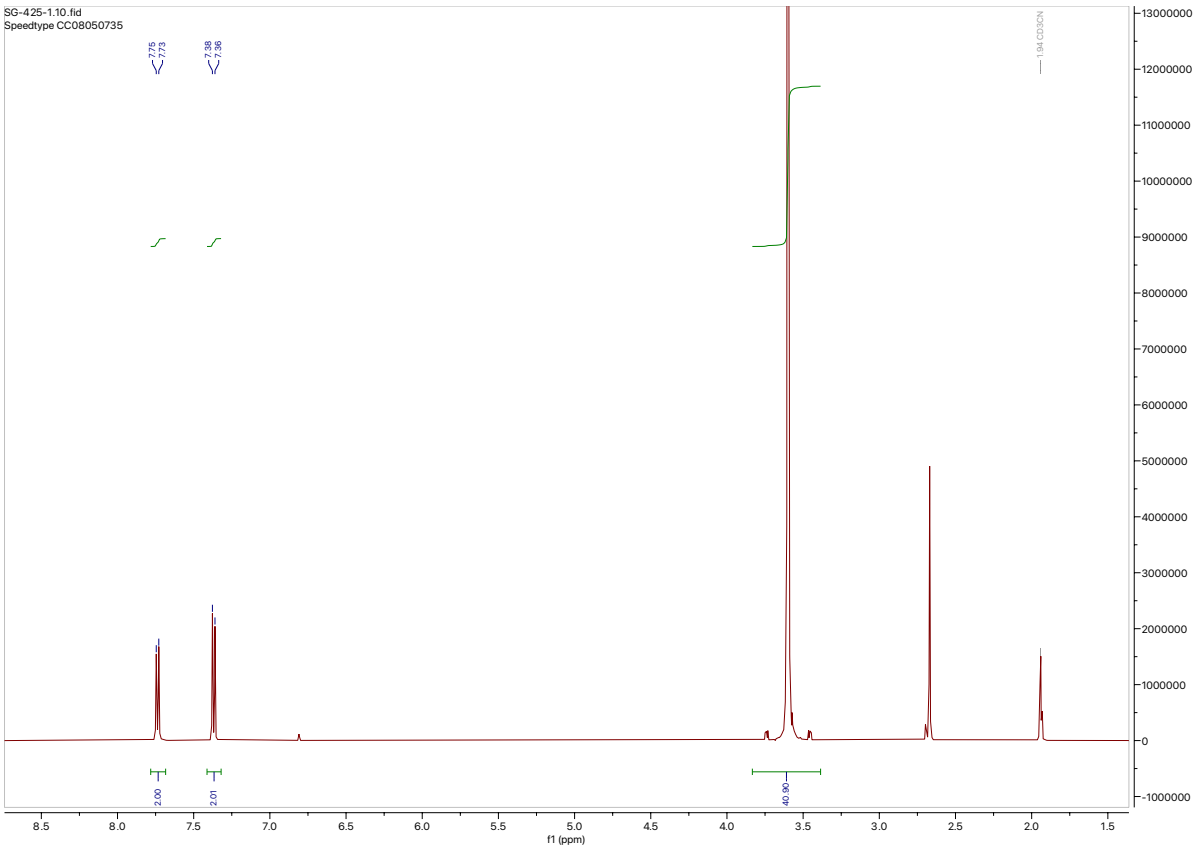

^{1}H-NMR

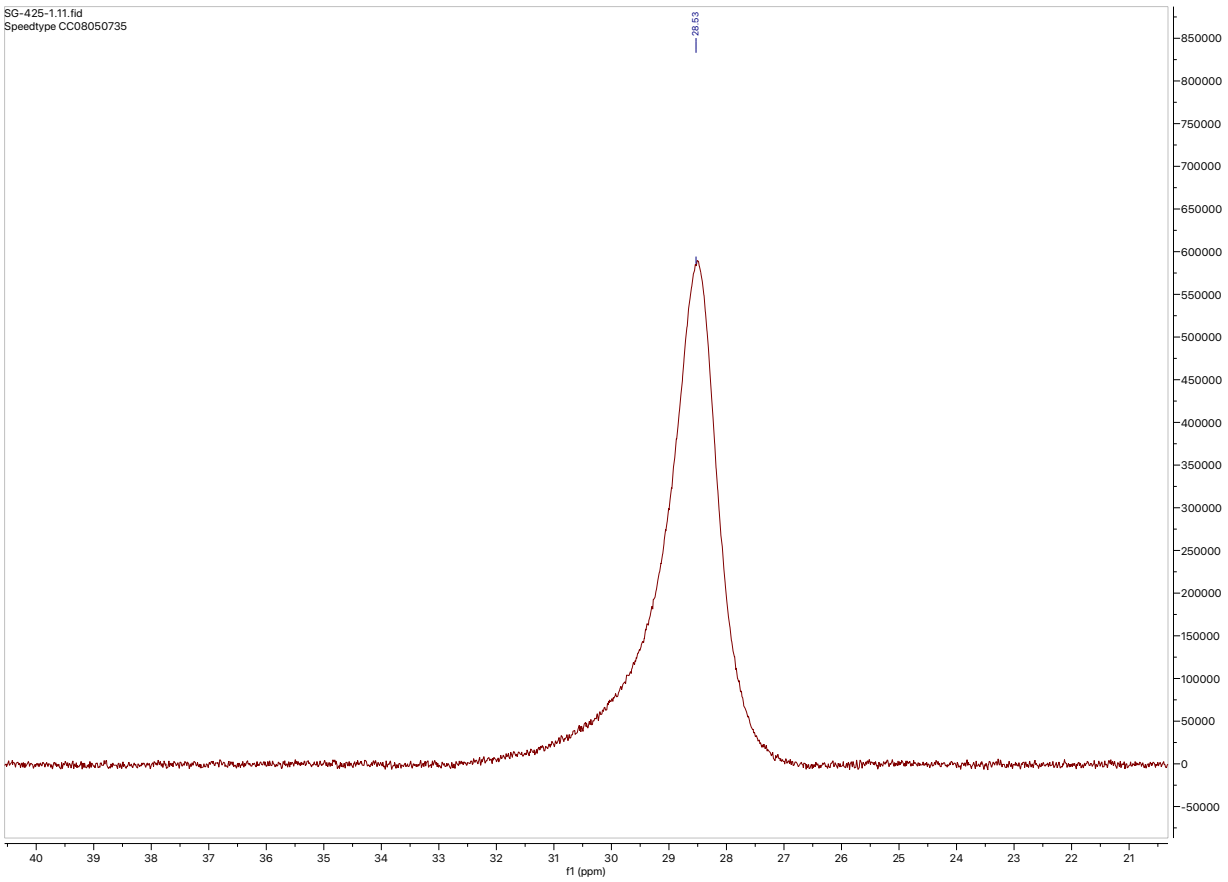

^{11}B-NMR

Deprotection of 2-(benzo[b]thiophen-2-yl)-4,4,5,5-tetramethyl-1,3,2-dioxaborolane

To a 20-mL vial equipped with a stir bar was added 2-(benzo[b]thiophen-2-yl)-4,4,5,5,-tetramethyl-1,3,2-dioxaborolane (91 mg, 0.35 mmol, 1 equiv) and methylboronic acid (0.21 g, 3.5 mmol, 10 equiv). Then, added a 1:1 v/v 0.1N HCl/acetone solution (5 mL). The vial was sealed and let stir at ambient temperature for 18 h. A clear homogeneous solution is obtained.

Residual solvents are removed via concentration in a Genevac. Then, iteratively, with a minimum of two cycles the crude was diluted with an excess of water/acetone and then concentrated in a Genevac to ensure full removal of residual methylboronic acid.

Yield was measured with ^{1}H-NMR against dioxane as an internal standard. The title compound was isolated as a solid, 94%.

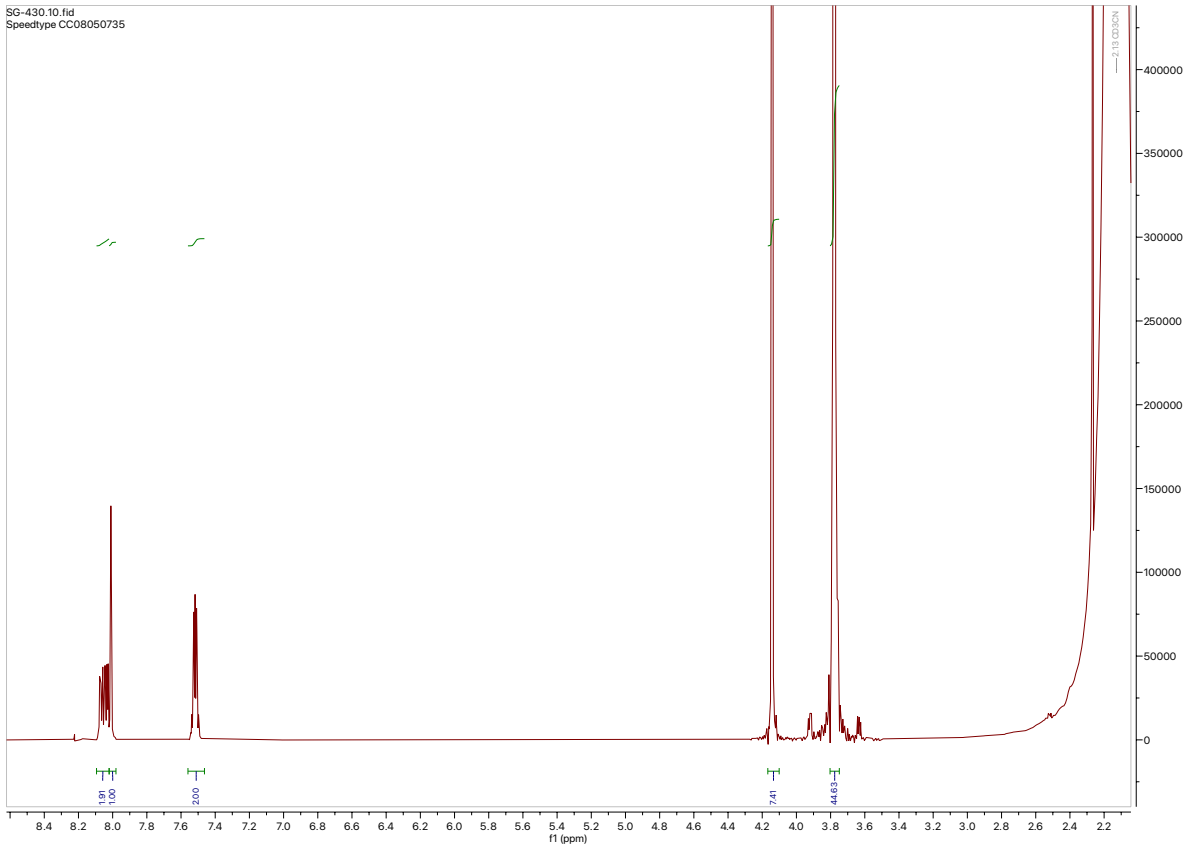
SG-430.10.fid
Speedtype CC08050735
2.13 CD3CN
400000
350000
300000
250000
200000
150000
100000
50000
0
1.91
1.00
2.00
7.41
44.63
8.4 8.2 8.0 7.8 7.6 7.4 7.2 7.0 6.8 6.6 6.4 6.2 6.0 5.8 5.6 5.4 5.2 5.0 4.8 4.6 4.4 4.2 4.0 3.8 3.6 3.4 3.2 3.0 2.8 2.6 2.4 2.2
f1 (ppm)

^{1}H-NMR

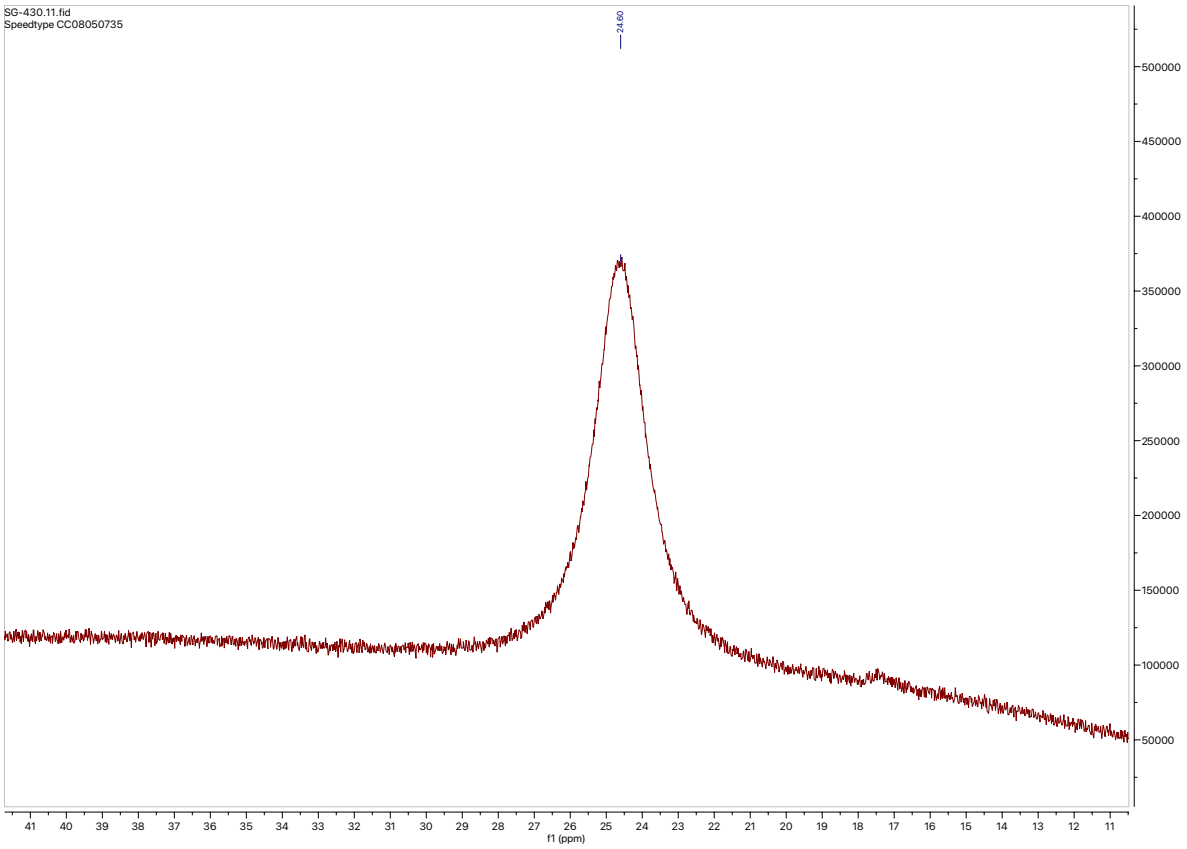

^{11}B-NMR

Deprotection of 2-(benzofuran-2-yl)-4,4,5,5-tetramethyl-1,3,2-dioxaborolane

To a 20-mL vial equipped with a stir bar was added 2-(benzofuran-2-yl)-4,4,5,5,-tetramethyl-1,3,2-dioxaborolane (305 mg, 1.25 mmol, 1 equiv) and methylboronic acid (0.75 g, 12.5 mmol, 10 equiv). Then, added a 1:1 v/v 0.1N HCl/acetone solution (5 mL). The vial was sealed and let stir at ambient temperature for 18 h. A homogeneous solution is obtained.

Residual solvents are removed via concentration in a Genevac. Then, iteratively, with a minimum of two cycles the crude was diluted with an excess of water/acetone and then concentrated in a Genevac to ensure full removal of residual methylboronic acid.

Initial ^{1}H-NMR showed full conversion to the desired product with some minor impurities present. However, continued purification (as described above) resulted in increased impurities formation. The title compound is unstable to the purification conditions.

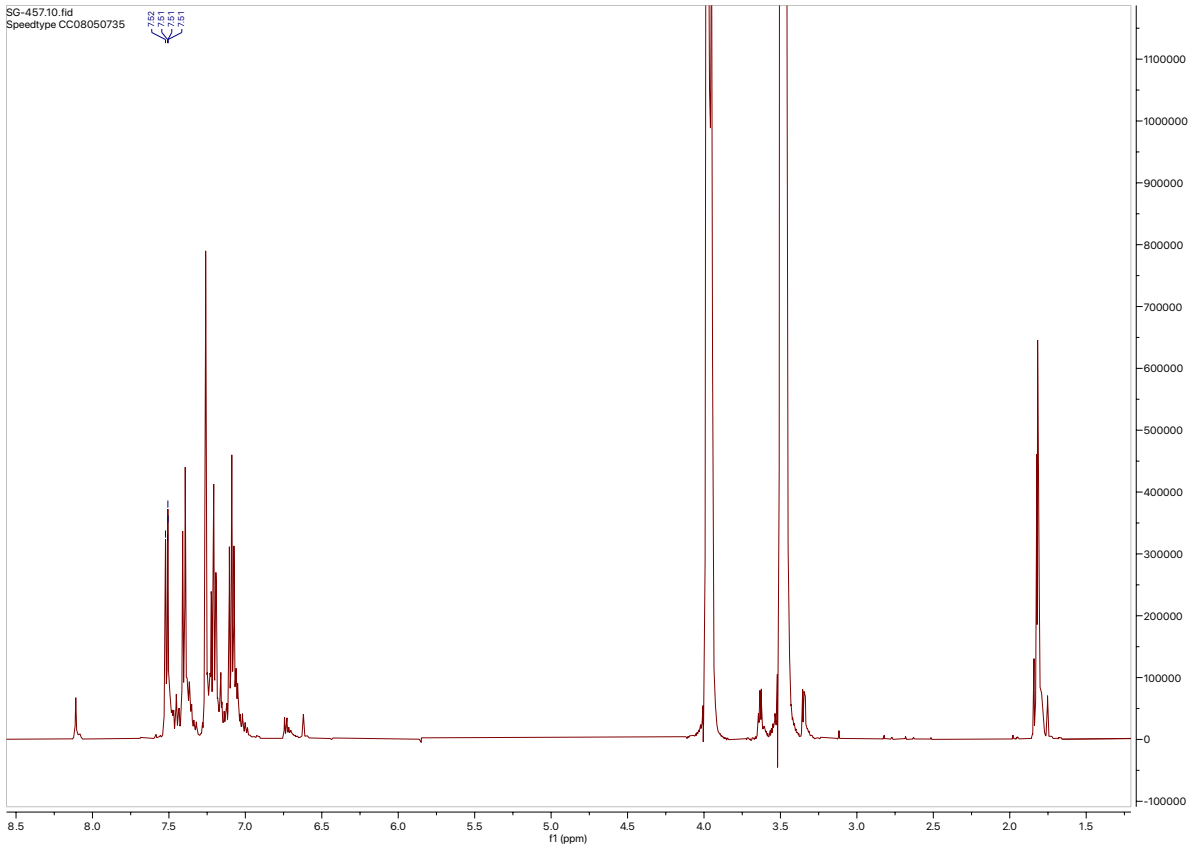

^{1}H-NMR [in-situ sample prior to purification]

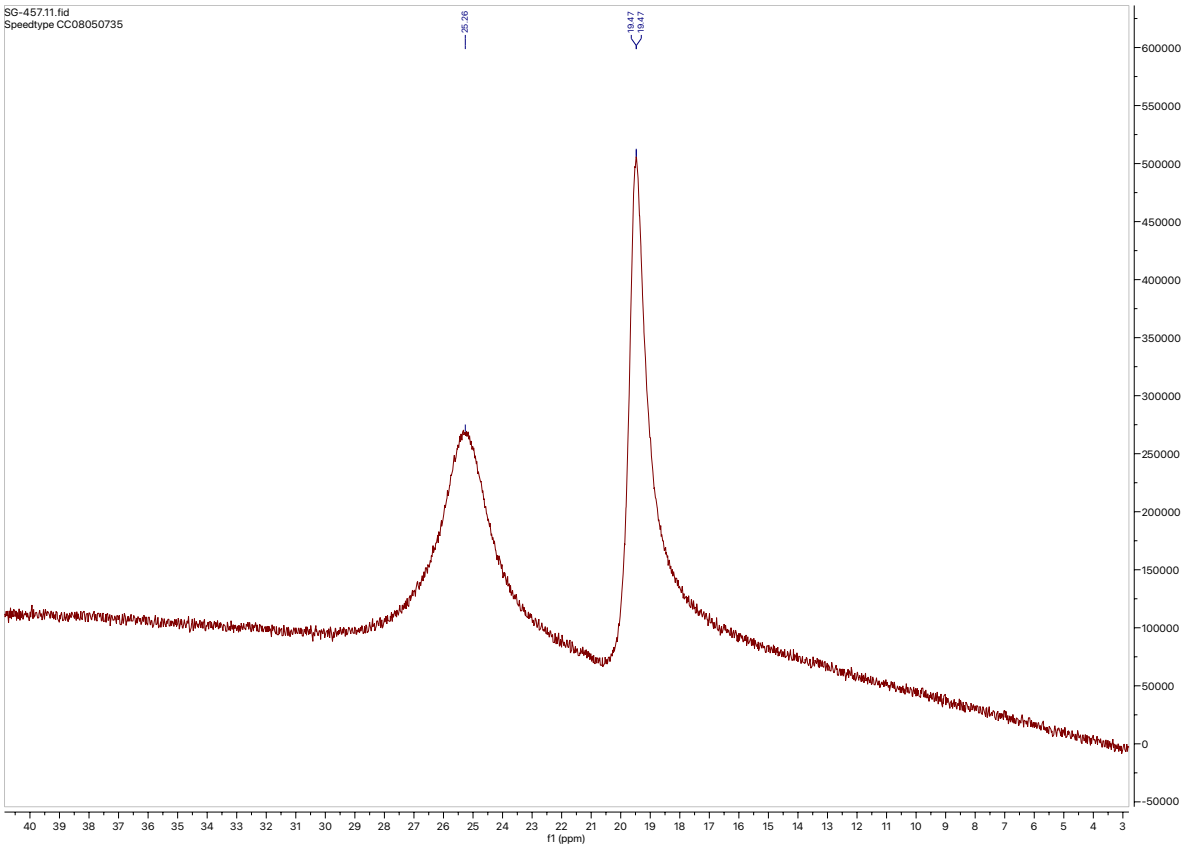

^{11}B-NMR [in-situ sample prior to purification]

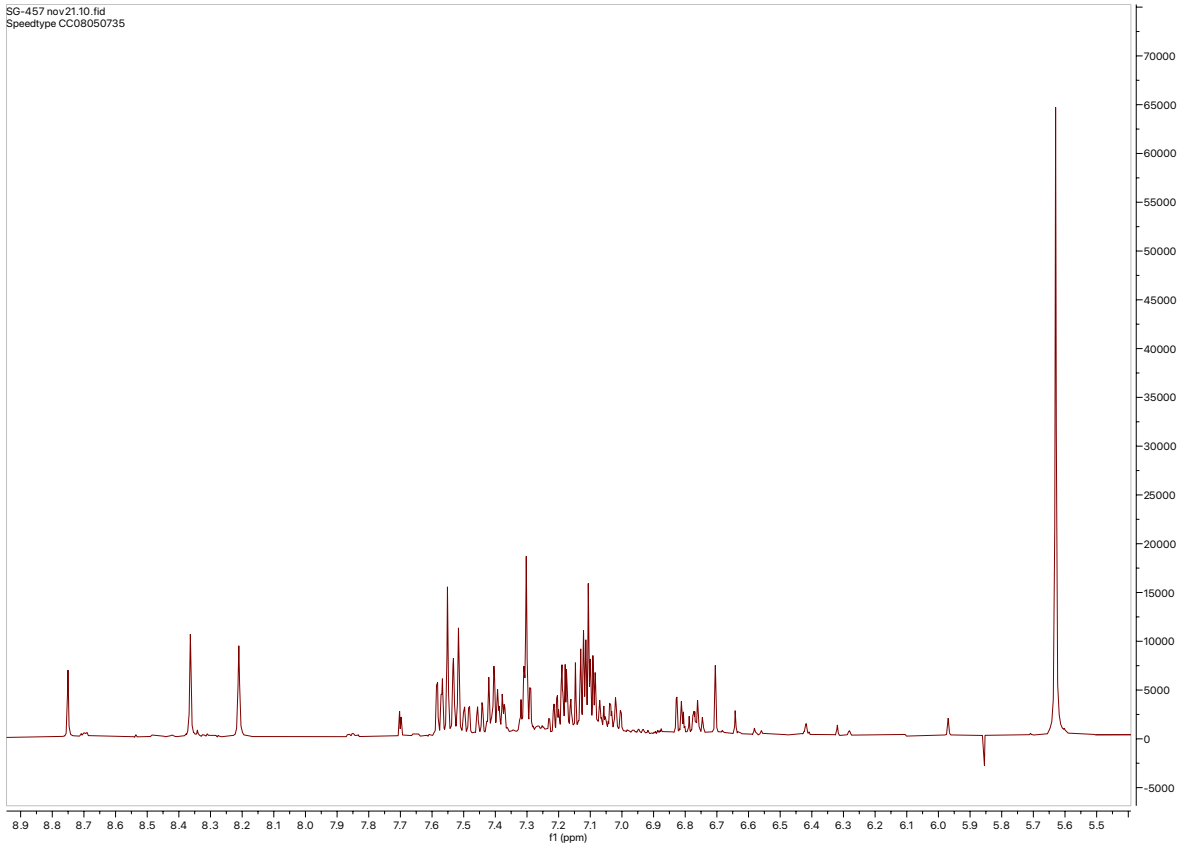

^{1}H-NMR [post purification]

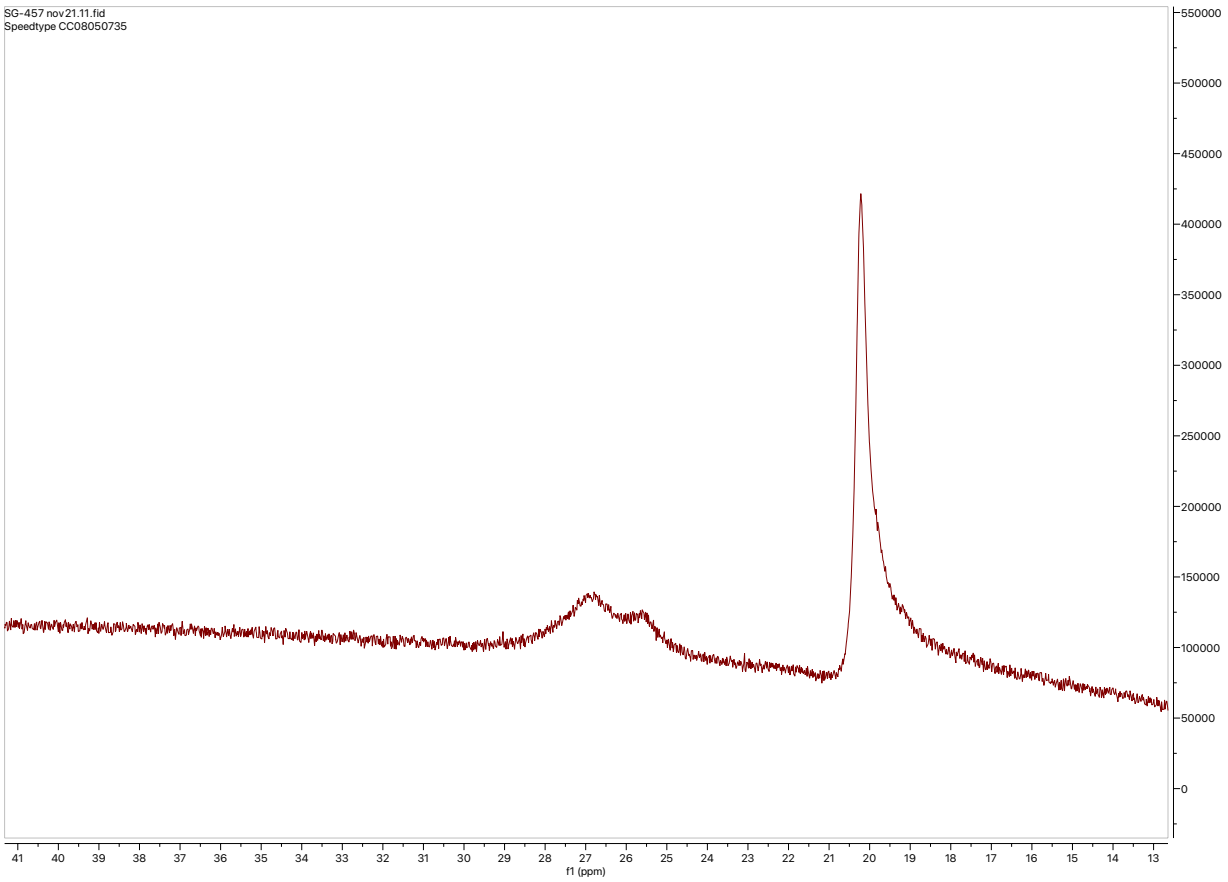

^{11}B-NMR [post purification]

Deprotection of 7-methyl-2-(4,4,5,5-tetramethyl-1,3,2-dioxaborolan-2-yl)-1H-indole

To a 20-mL vial equipped with a stir bar was added 7-methyl-2-(4,4,5,5,-tetramethyl-1,3,2-dioxaborolan-2-yl)-1H-indole (321 mg, 1.25 mmol, 1 equiv) and methylboronic acid (0.75 g, 12.5 mmol, 10 equiv). Then, added a 1:1 v/v 0.1N HCl/acetone solution (5 mL). The vial was sealed and let stir at ambient temperature for 18 h. A homogeneous solution is obtained.

Residual solvents are removed via concentration in a Genevac. Then, iteratively, with a minimum of two cycles the crude was diluted with an excess of water/acetone and then concentrated in a Genevac to ensure full removal of residual methylboronic acid.

The resulting ^{1}H-NMR shows a messy aryl region (decomposition).

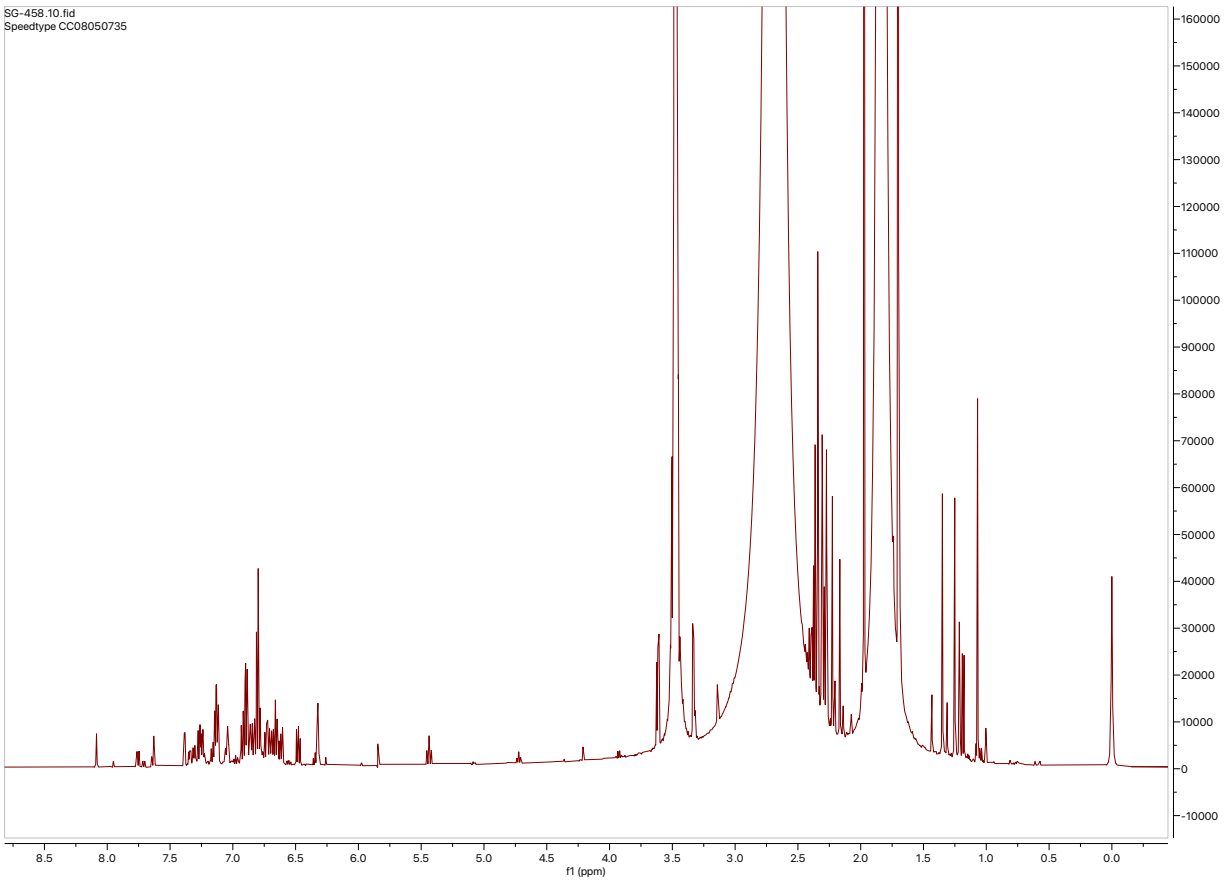
SG-458.10.fid
Speedtype CC08050735
160000
150000
140000
130000
120000
110000
100000
90000
80000
70000
60000
50000
40000
30000
20000
10000
0
-10000
8.5
8.0
7.5
7.0
6.5
6.0
5.5
5.0
4.5
4.0
3.5
3.0
2.5
2.0
1.5
1.0
0.5
0.0
f1 (ppm)

^{1}H-NMR

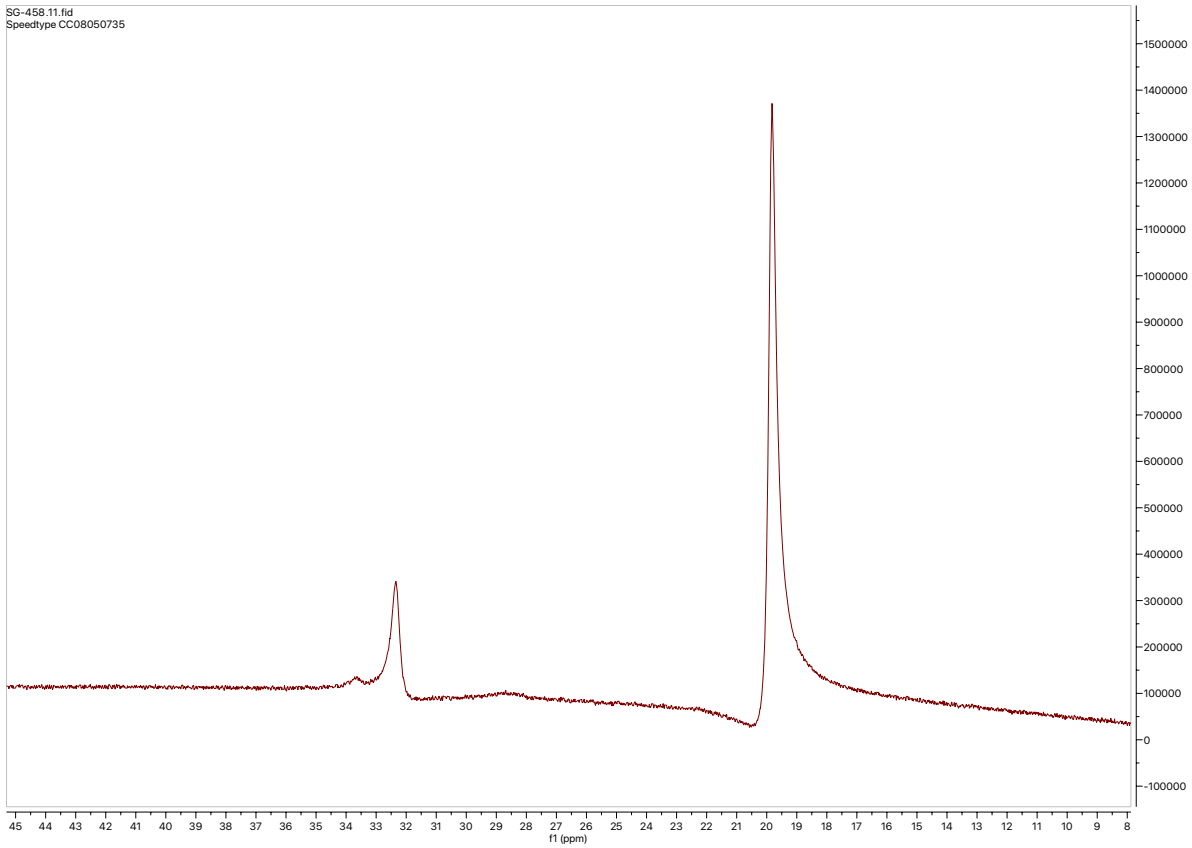

^{11}B-NMR

Deprotection of tert-butyl 4-(4,4,5,5-tetramethyl-1,3,2-dioxaborolan-2-yl)-1H-pyrazole-1-carboxylate

To a 20-mL vial equipped with a stir bar was added tert-butyl 4-(4,4,5,5,-tetramethyl-1,3,2-dioxaborolan-2-yl)-1H-pyrazole-1-carboxylate (368 mg, 1.25 mmol, 1 equiv) and methylboronic acid (0.75 g, 12.5 mmol, 10 equiv). Then, added a 1:1 v/v 0.1N HCl/acetone solution (5 mL). The vial was sealed and let stir at ambient temperature for 18 h. A heterogeneous mixture with white solids results.

Residual solvents are removed via concentration in a Genevac. Then, iteratively, with a minimum of two cycles the crude was diluted with an excess of water/acetone and then concentrated in a Genevac to ensure full removal of residual methylboronic acid.

Yield was measured with ^{1}H-NMR against dioxane as an internal standard. The title compound was formed in 40% yield (remainder is de-Boc material).

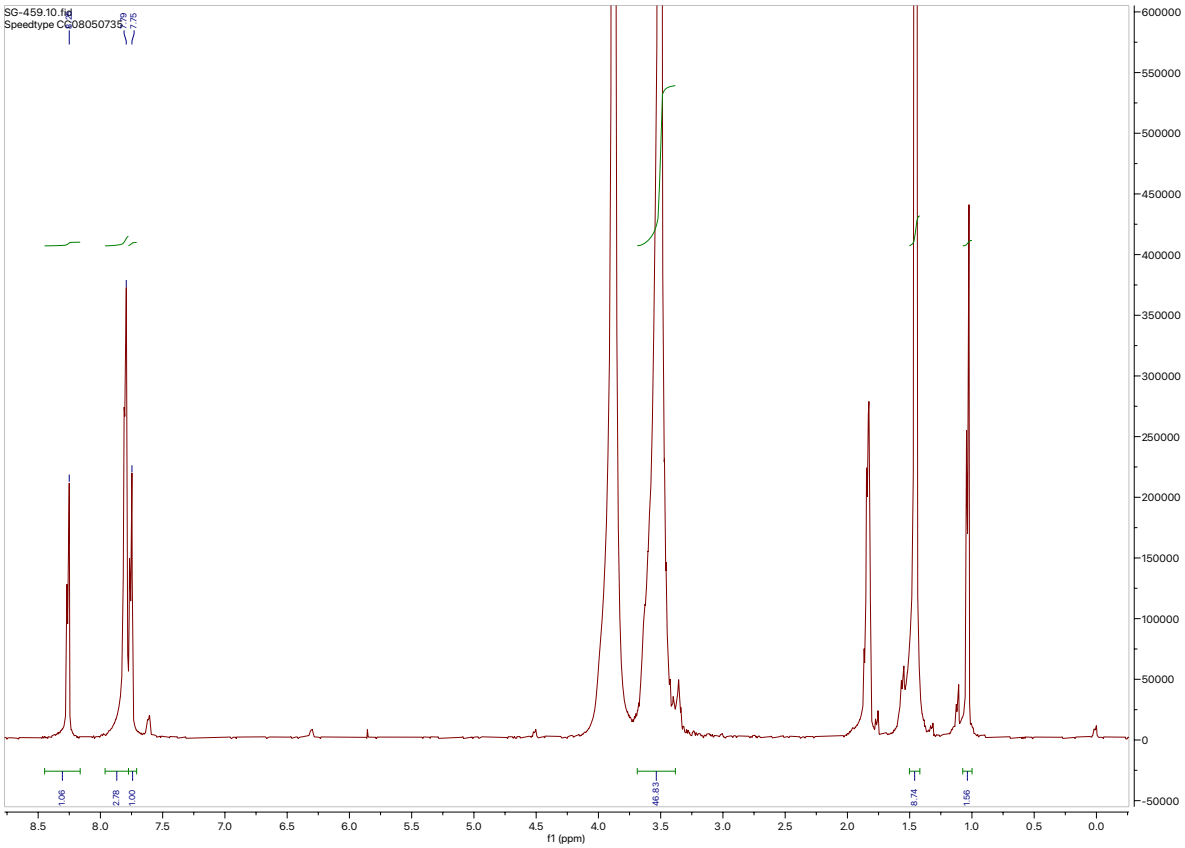
SG-459.10.fid
Speedtype CG08050735
7.79
7.75
1.06
2.78
1.00
46.83
8.74
1.56
f1 (ppm)

^{1}H-NMR

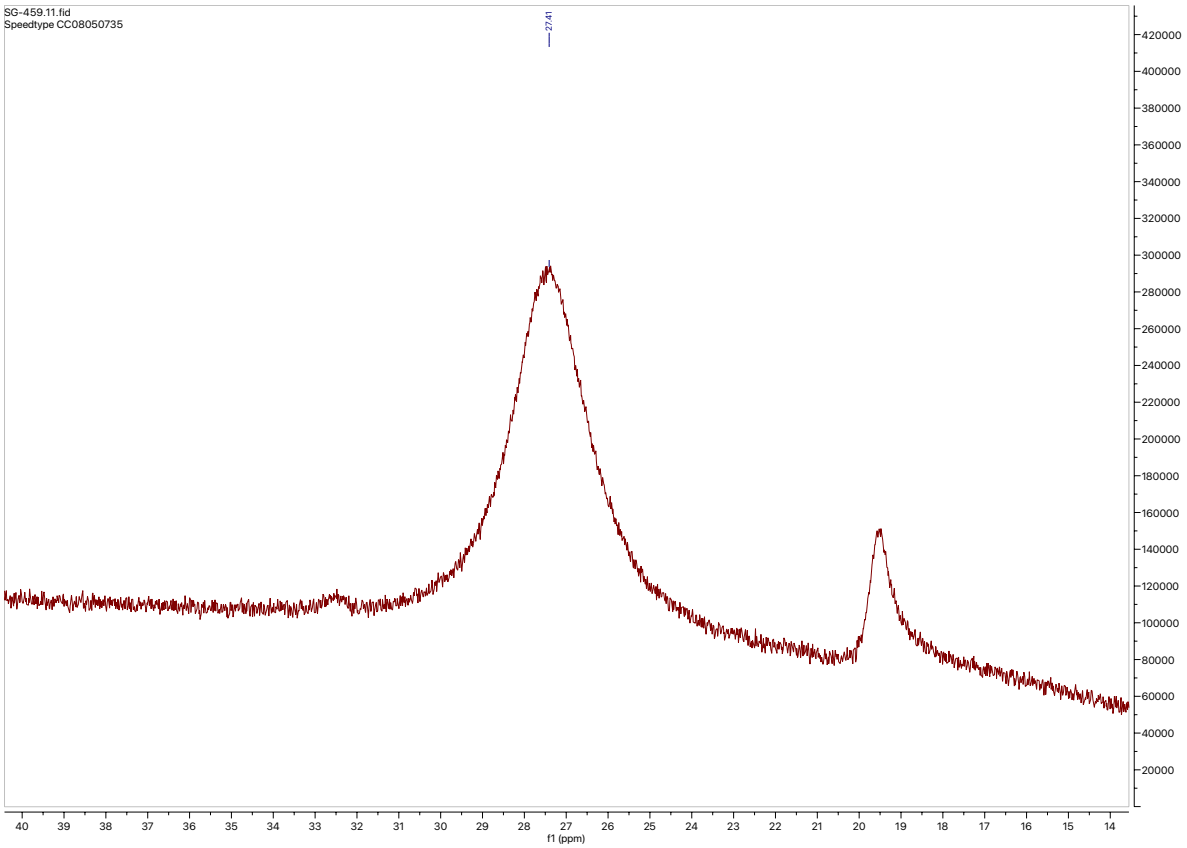

^{11}B-NMR

2.4.2 Reactions

Catalyst free petasis with 3,5-dimethylphenylboronic acid

To a 4-mL vial equipped with a stir bar was added (3,5-dimethylphenyl)boronic acid (30 mg, 0.2 mmol, 1 equiv), L-proline (25 mg, 0.2 mmol, 1.1 equiv), and 2-hydroxybenzaldehyde (20 mg, 0.2 mmol, 1.1 equiv). The vial was diluted with dioxane (1.6 mL) and the reaction was stirred at 100 °C for 23 h. The vial was cooled to ambient temperature to make for a homogeneous light orange solution.

^{1}H-NMR yield was measured against trimethoxybenzene as an internal standard, 65%.

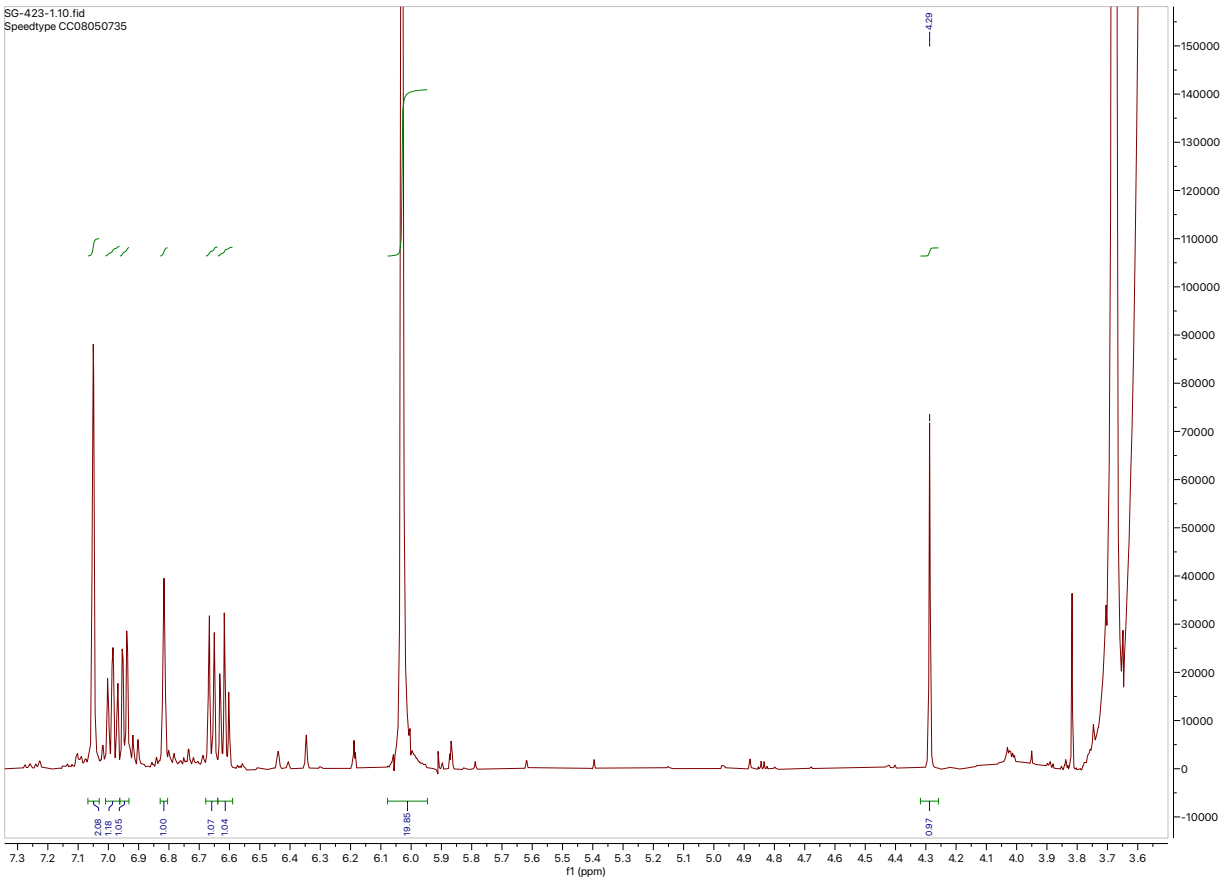

^{1}H-NMR

Catalyst free petasis with 2-(3,5-dimethylphenyl)-4,4,5,5-tetramethyl-1,3,2-dioxaborolane

To a 4-mL vial equipped with a stir bar was added 2-(3,5-dimethylphenyl)-4,4,5,5-tetramethyl-1,3,2-dioxaborolane (50 mg, 0.2 mmol, 1 equiv), L-proline (25 mg, 0.2 mmol, 1.1 equiv), and 2-hydroxybenzaldehyde (20 mg, 0.2 mmol, 1.1 equiv). The vial was diluted with dioxane (1.6 mL) and the reaction was stirred at 100 °C for 23 h. The vial was cooled to ambient temperature to make for a homogeneous light orange solution.

^{1}H-NMR yield was measured against trimethoxybenzene as an internal standard, 55%.

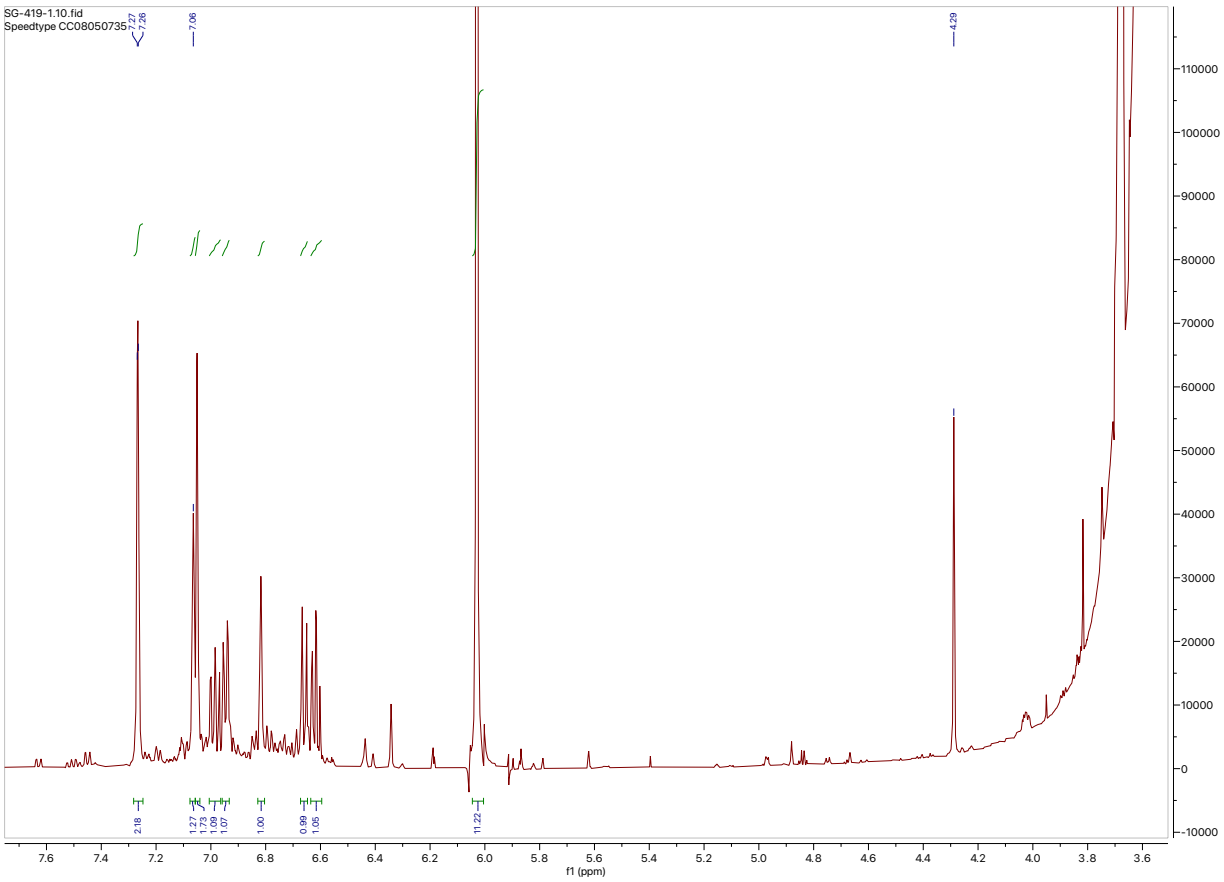

^{1}H-NMR

Catalyst free petasis with 4-Chlorophenylboronic acid

To a 4-mL vial equipped with a stir bar was added (4-chlorophenyl)boronic acid (30 mg, 0.2 mmol, 1 equiv), L-proline (25 mg, 0.2 mmol, 1.1 equiv), and 2-hydroxybenzaldehyde (20 mg, 0.2 mmol, 1.1 equiv). The vial was diluted with dioxane (1.6 mL) and the reaction was stirred at 100 °C for 23 h. The vial was cooled to ambient temperature to make for a homogeneous light orange solution.

^{1}H-NMR yield was measured against trimethoxybenzene as an internal standard, 65%.

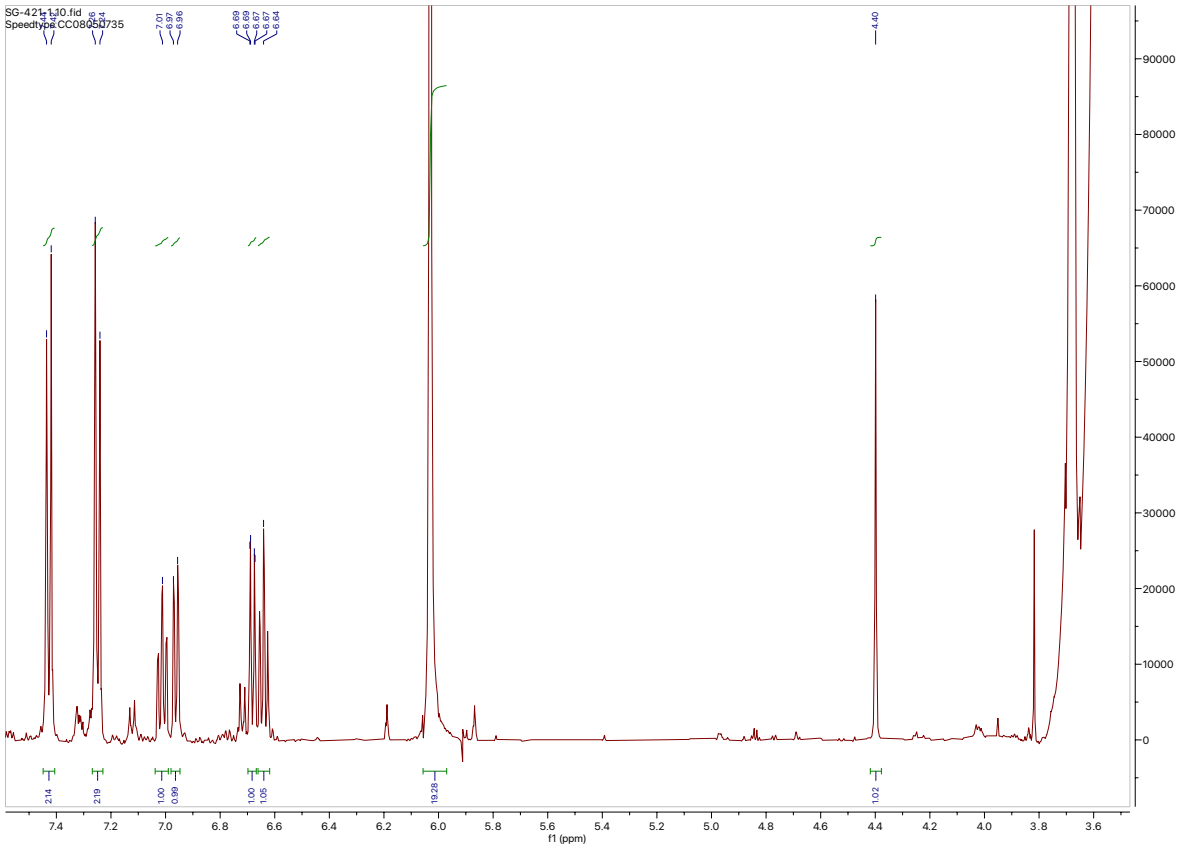

^{1}H-NMR

Catalyst free petasis with 4-chlorophenylboronic acid pinacol ester

To a 4-mL vial equipped with a stir bar was added 2-(4-chlorophenyl)-4,4,5,5-tetramethyl-1,3,2-dioxaborolane (50 mg, 0.2 mmol, 1 equiv), L-proline (25 mg, 0.2 mmol, 1.1 equiv), and 2-hydroxybenzaldehyde (20 mg, 0.2 mmol, 1.1 equiv). The vial was diluted with dioxane (1.6 mL) and the reaction was stirred at 100 °C for 23 h. The vial was cooled to ambient temperature to make for a homogeneous light orange solution.

^{1}H-NMR yield was measured against trimethoxybenzene as an internal standard, 13%.

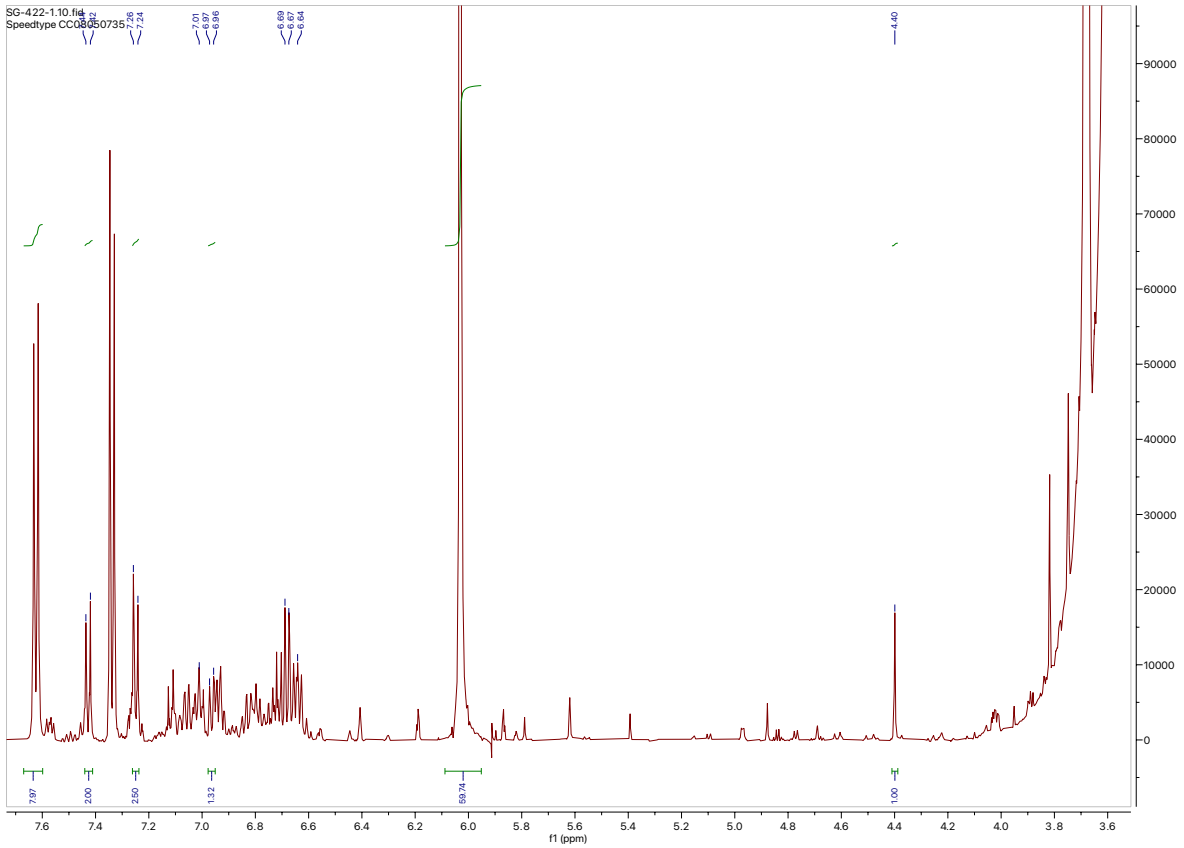

^{1}H-NMR

Rhodium-Catalyzed Asymmetric 1,4-Addition with p-Cl-phenylboronic acid

In a glovebox, under an inert atmosphere of nitrogen, to a 4-mL vial equipped with a stir bar was added acetylacetonatobis(ethylene) rhodium(I) (5 mg, 0.02 mmol, 0.05 equiv), S-(-)-2,2'-bis(diphenylphosphino)-1,1'-binaphthalene (0.02 mmol, 0.055 equiv), (4-chlorophenyl)boronic acid (2 mmol, 5 equiv) and cyclohex-2-en-1-one (0.4 mmol, 1 equiv). The vial was diluted with dioxane (2 mL) and water (0.2 mL) and the reaction was stirred at 65 °C for 17 h. The vial was cooled to ambient temperature. The solution was syringe filtered to remove black particulates.

^{1}H-NMR yield was measured against trimethoxybenzene as an internal standard, 45%.

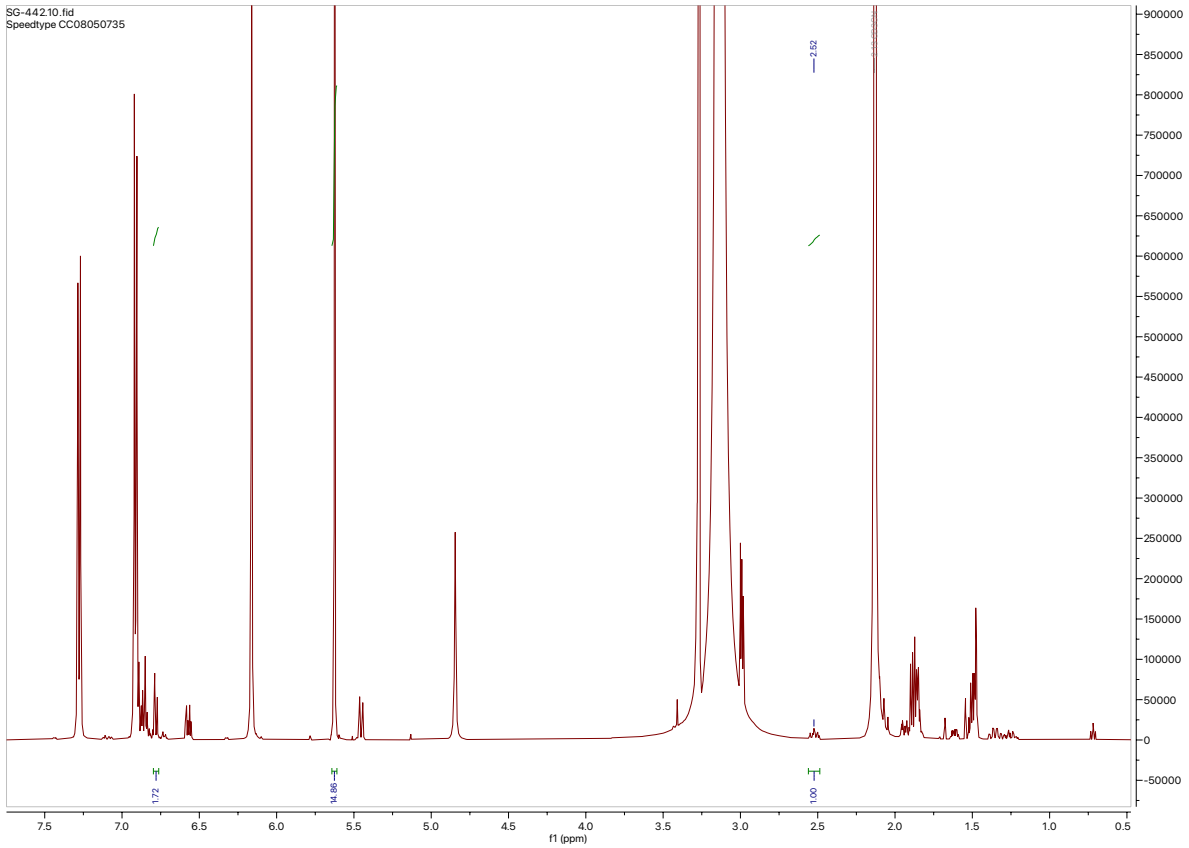

^{1}H-NMR

Rhodium-Catalyzed Asymmetric 1,4-Addition with p-Cl-phenylBpin

In a glovebox, under an inert atmosphere of nitrogen, to a 4-mL vial equipped with a stir bar was added acetylacetonatobis(ethylene) rhodium(I) (5 mg, 0.02 mmol, 0.05 equiv), S-(-)-2,2'-bis(diphenylphosphino)-1,1'-binaphthalene (0.02 mmol, 0.055 equiv), 2-(4-chlorophenyl)-4,4,5,5-tetramethyl-1,3,2-dioxaborolane (2 mmol, 5 equiv) and cyclohex-2-en-1-one (0.4 mmol, 1 equiv). The vial was diluted with dioxane (2 mL) and water (0.2 mL) and the reaction was stirred at 65 °C for 17 h. The vial was cooled to ambient temperature. The solution was syringe filtered to remove black particulates.

^{1}H-NMR yield was measured against trimethoxybenzene as an internal standard, 10%.

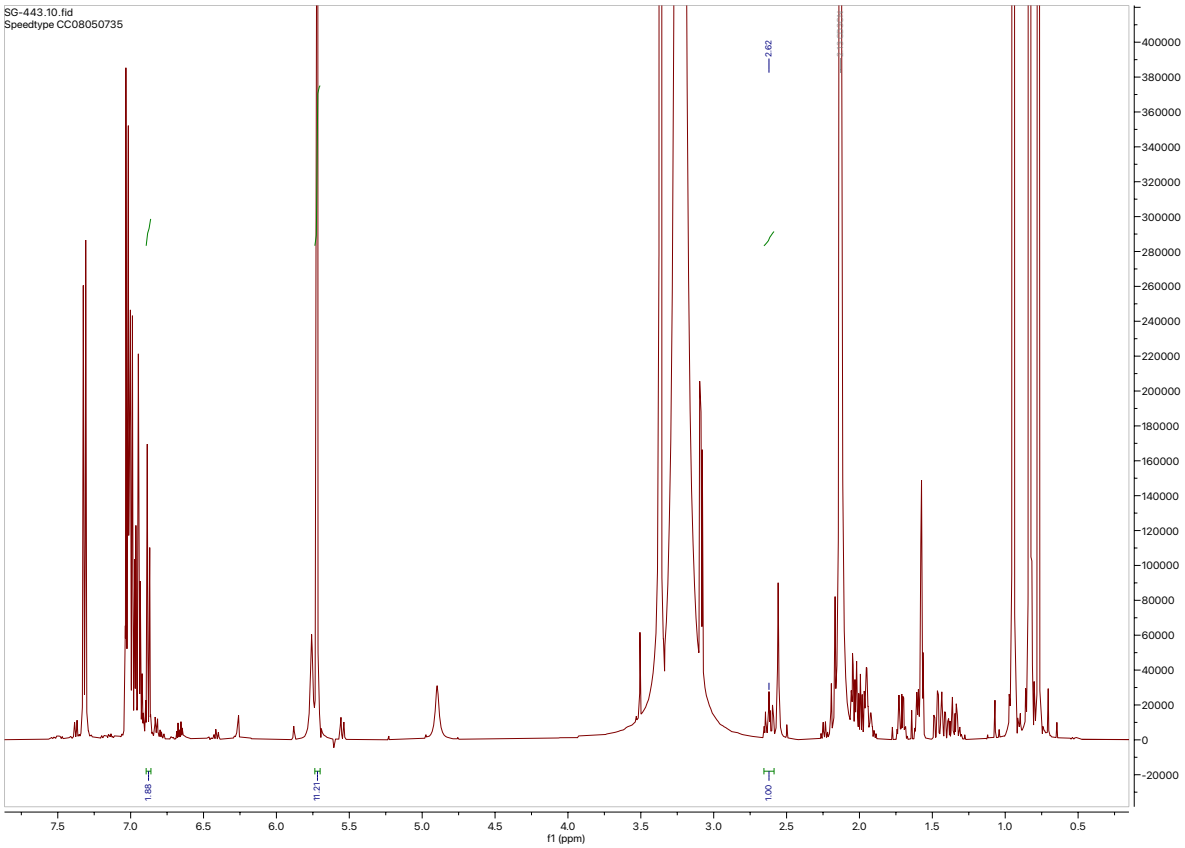

^{1}H-NMR

Rhodium-Catalyzed Asymmetric 1,4-Addition with phenylboronic acid

In a glovebox, under an inert atmosphere of nitrogen, to a 4-mL vial equipped with a stir bar was added acetylacetonatobis(ethylene) rhodium(I) (5 mg, 0.02 mmol, 0.05 equiv), S-(-)-2,2'-bis(diphenylphosphino)-1,1'-binaphthalene (0.02 mmol, 0.055 equiv), phenylboronic acid (0.4 mmol, 1 equiv) and cyclohex-2-en-1-one (0.4 mmol, 1 equiv). The vial was diluted with dioxane (2 mL) and water (0.2 mL) and the reaction was stirred at 65 °C for 18 h. The vial was cooled to ambient temperature.

^{1}H-NMR yield was measured against trimethoxybenzene as an internal standard, 50%.

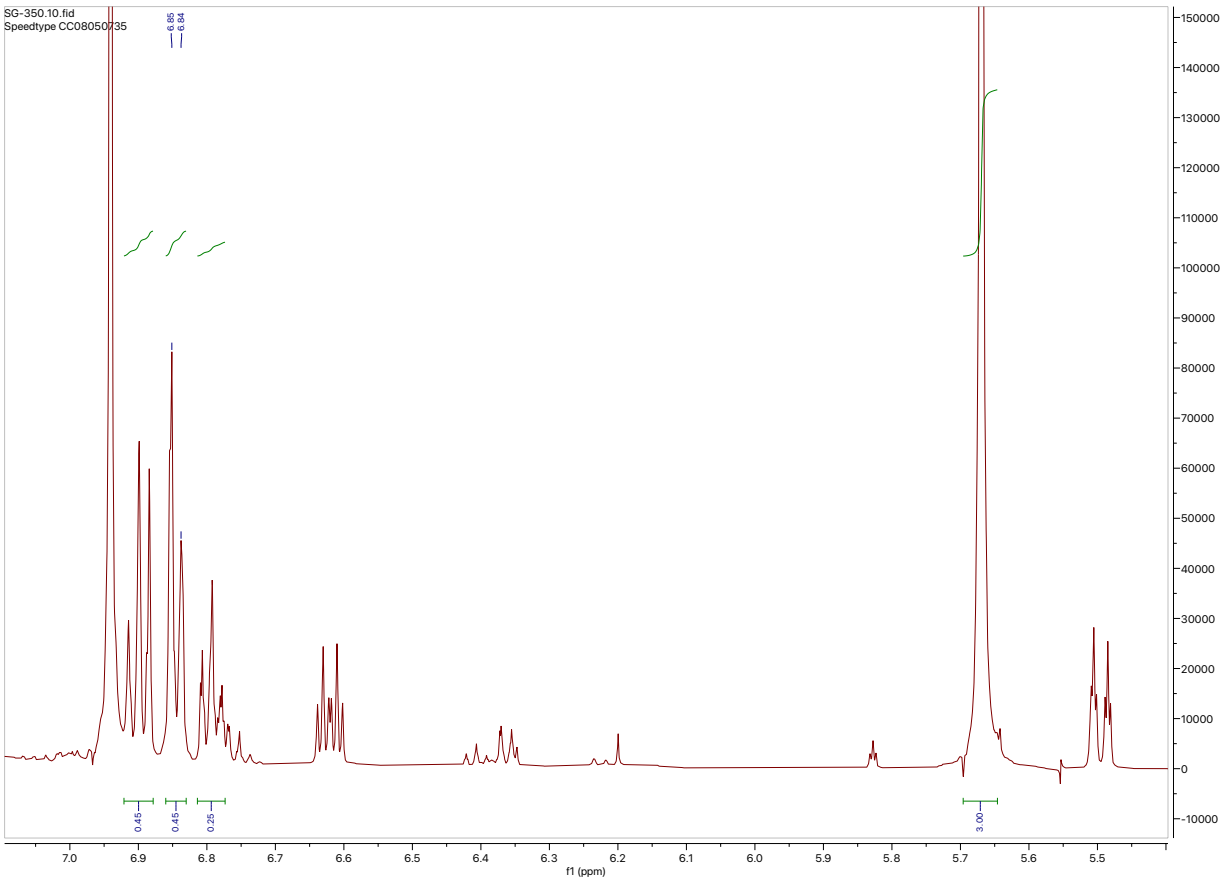

^{1}H-NMR

Rhodium-Catalyzed Asymmetric 1,4-Addition with phenylBpin

In a glovebox, under an inert atmosphere of nitrogen, to a 4-mL vial equipped with a stir bar was added acetylacetonatobis(ethylene) rhodium(I) (5 mg, 0.02 mmol, 0.05 equiv), S-(-)-2,2'-bis(diphenylphosphino)-1,1'-binaphthalene (0.02 mmol, 0.055 equiv), 4,4,5,5-tetramethyl-2-phenyl-1,3,2-dioxaborolane (0.4 mmol, 1 equiv) and cyclohex-2-en-1-one (0.4 mmol, 1 equiv). The vial was diluted with dioxane (2 mL) and water (0.2 mL) and the reaction was stirred at 65 °C for 18 h. The vial was cooled to ambient temperature.

^{1}H-NMR yield was measured against trimethoxybenzene as an internal standard, 25%.

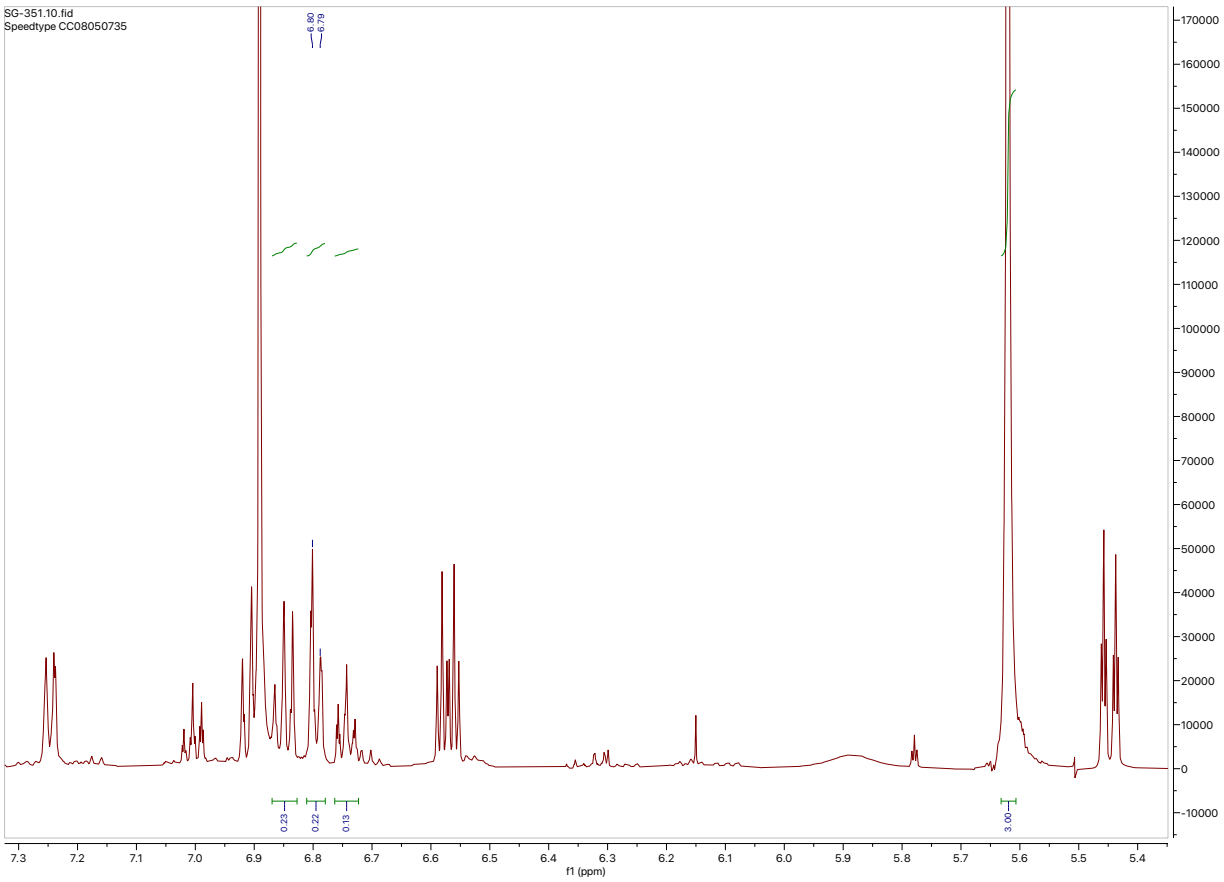

^{1}H-NMR

Chan-Lam with Piperidine and p-Cl-phenylboronic acid

To a 4-mL vial equipped with a stir bar was added copper diacetate (70 mg, 0.4 mmol, 1 equiv), triethylamine (0.8 mmol, 2 equiv), piperidine (0.4 mmol, 1 equiv) and (4-chlorophenyl)boronic acid (0.8 mmol, 2 equiv) and 4 A MS (400 mg). Then, diluted vial with dichloromethane (2 mL). Loosely capped vial and let stir at ambient temperature for 23 h. Reaction was filtered.

Product:$ArB(OH)_2$ = 2:1

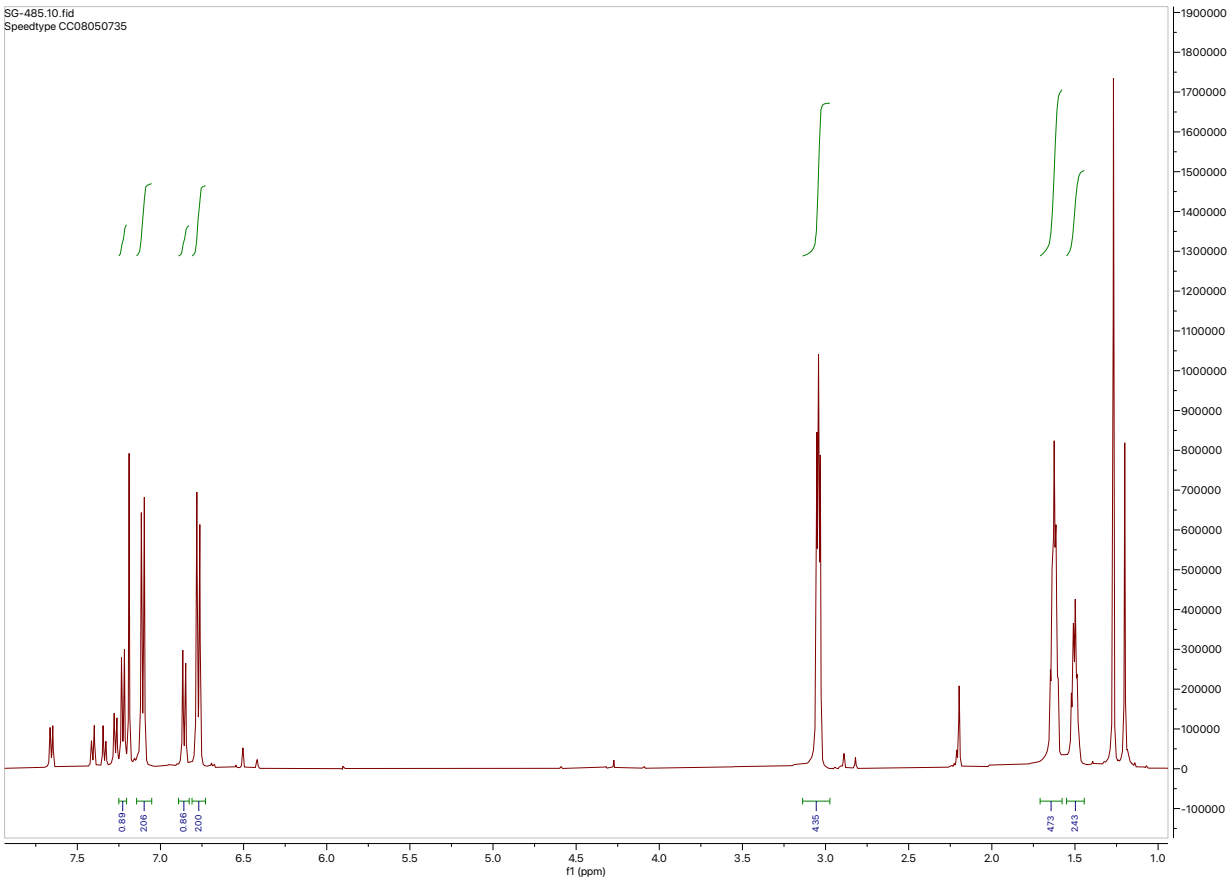

^{1}H-NMR

Chan-Lam with Piperidine and p-Cl-phenylBpin

To a 4-mL vial equipped with a stir bar was added copper diacetate (70 mg, 0.4 mmol, 1 equiv), triethylamine (0.8 mmol, 2 equiv), piperidine (0.4 mmol, 1 equiv) and 2-(4-chlorophenyl)-4,4,5,5-tetramethyl-1,3,2-dioxaborolane (0.8 mmol, 2 equiv) and 4 A MS (400 mg). Then, diluted vial with dichloromethane (2 mL). Loosely capped vial and let stir at ambient temperature for 23 h. Reaction was filtered.

Product:$ArB(OH)_2$ = 0.2:1

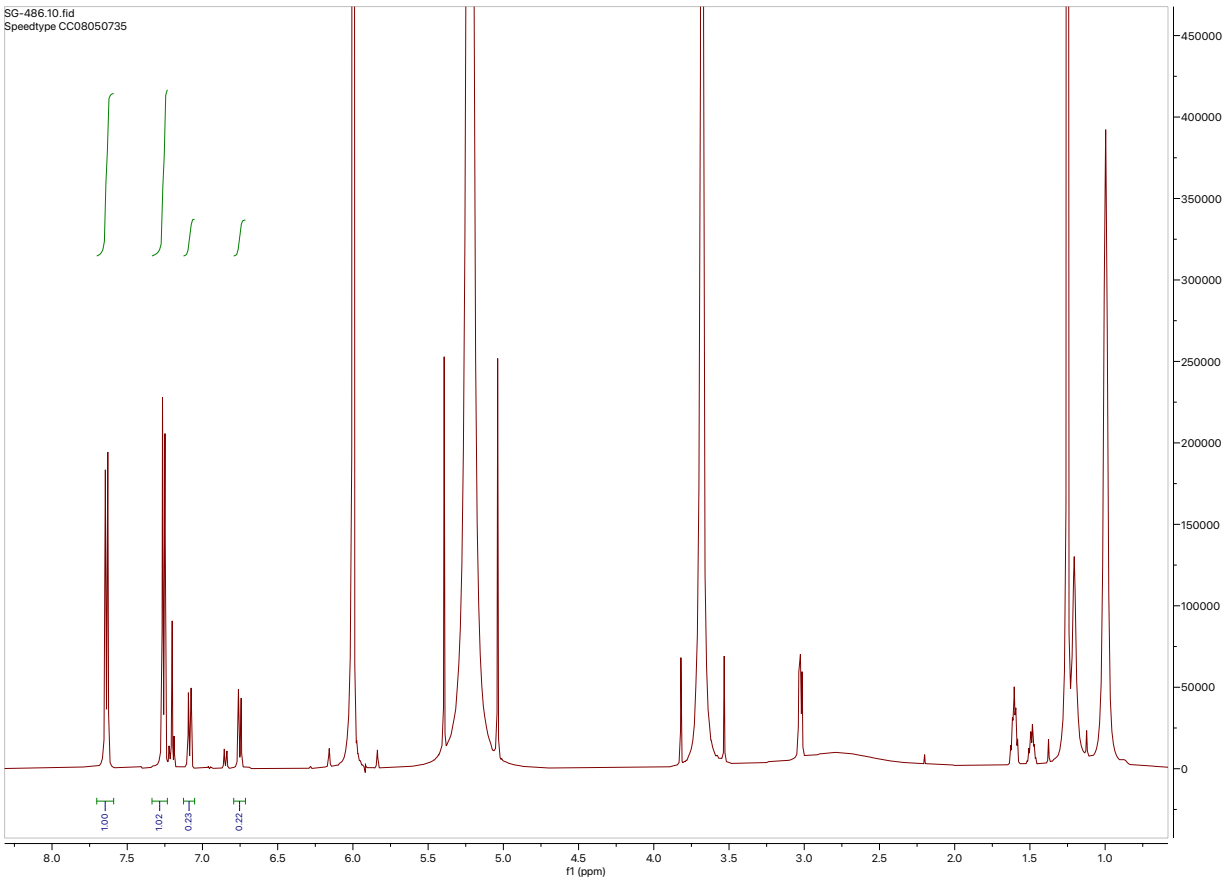

^{1}H-NMR

Petasis reaction of 2-pyridinecarbaldehyde with (4-methoxyphenyl)boronic acid

To a 4-mL vial equipped with a stir bar was added picolinaldehyde (0.4 mmol, 1 equiv) and dibenzylamine (0.4 mmol, 1 equiv). The contents were mixed briefly and then was added (4-methoxyphenyl)boronic acid (0.4 mmol, 1 equiv). The vial was diluted with acetonitrile (2 mL) and then was sealed and allowed to stir at 80 °C for 21 h. The vial was cooled to ambient temperature.

Full conversion to desired product.

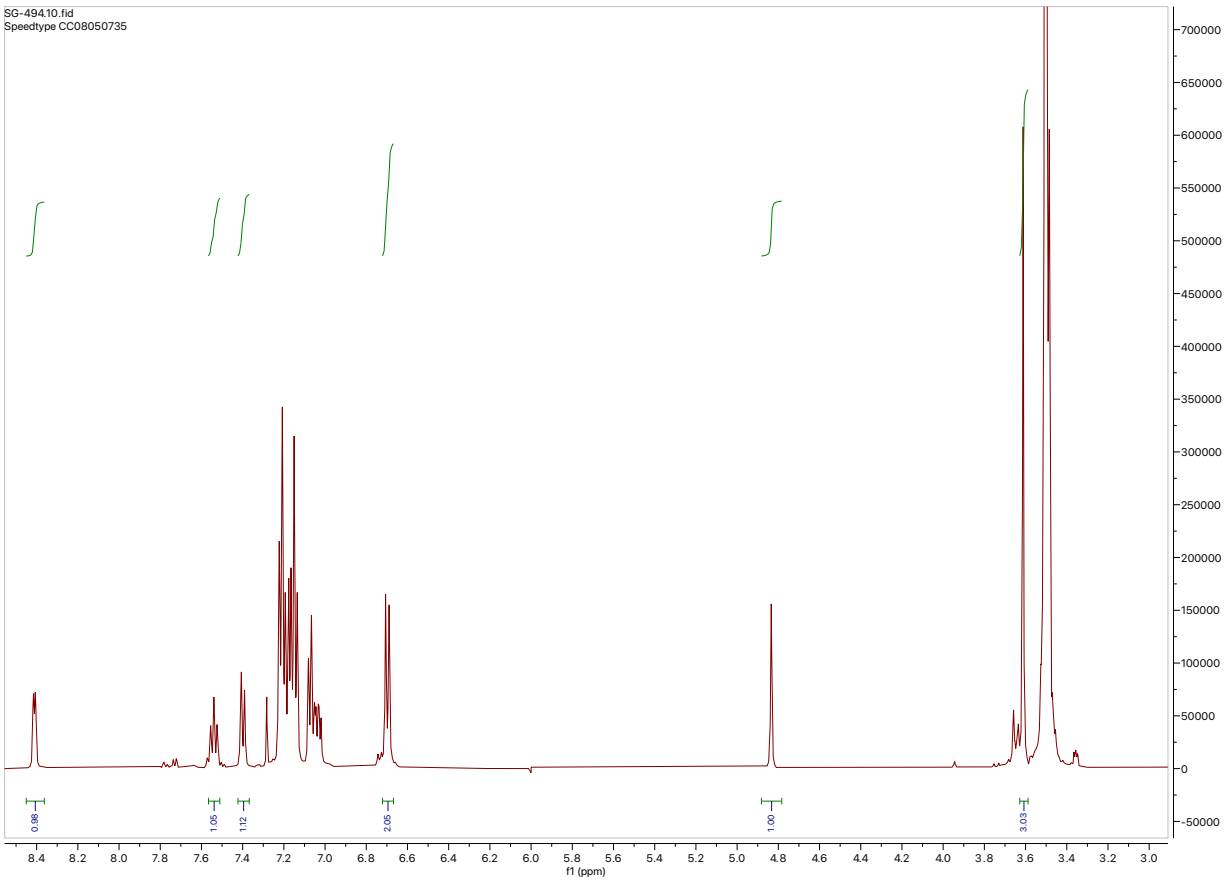

^{1}H-NMR

Petasis reaction of 2-pyridinecarbaldehyde with (4-methoxyphenyl)Bpin

To a 4-mL vial equipped with a stir bar was added picolinaldehyde (0.4 mmol, 1 equiv) and dibenzylamine (0.4 mmol, 1 equiv). The contents were mixed briefly and then was added 2-(4-methoxyphenyl)-4,4,5,5-tetramethyl-1,3,2-dioxaborolane (0.4 mmol, 1 equiv). The vial was diluted with acetonitrile (2 mL) and then was sealed and allowed to stir at 80 °C for 21 h. The vial was cooled to ambient temperature.

No conversion to desired product.

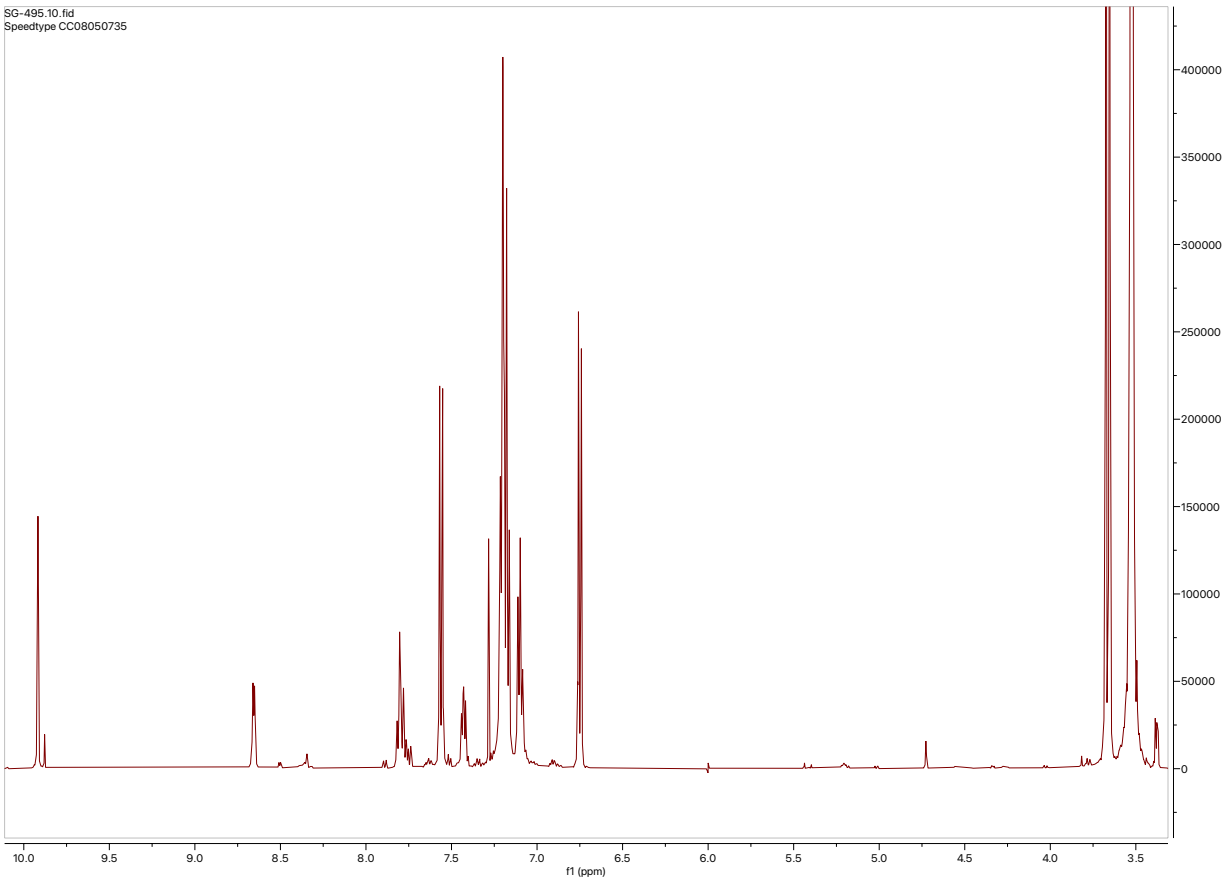

^{1}H-NMR

Reductive Coupling of Tosylhydrazones with Phenylboronic Acid

To a 4-mL vial equipped with a stir bar was added (E)-N'-benzylidene-4-methylbenzenesulfonohydrazide (0.5 mmol, 1 equiv), potassium carbonate (1.2 mmol, 2 equiv) and phenylboronic acid (1 mmol, 2 equiv). Then, vial was diluted with dioxane (2 mL) and then sealed and allowed to stir at 100 °C for 18 h. The vial was cooled to ambient temperature, and filtered.

^{1}H-NMR yield was measured against trimethoxybenzene as an internal standard, 40%. Acetone-d_6 NMR solvent.

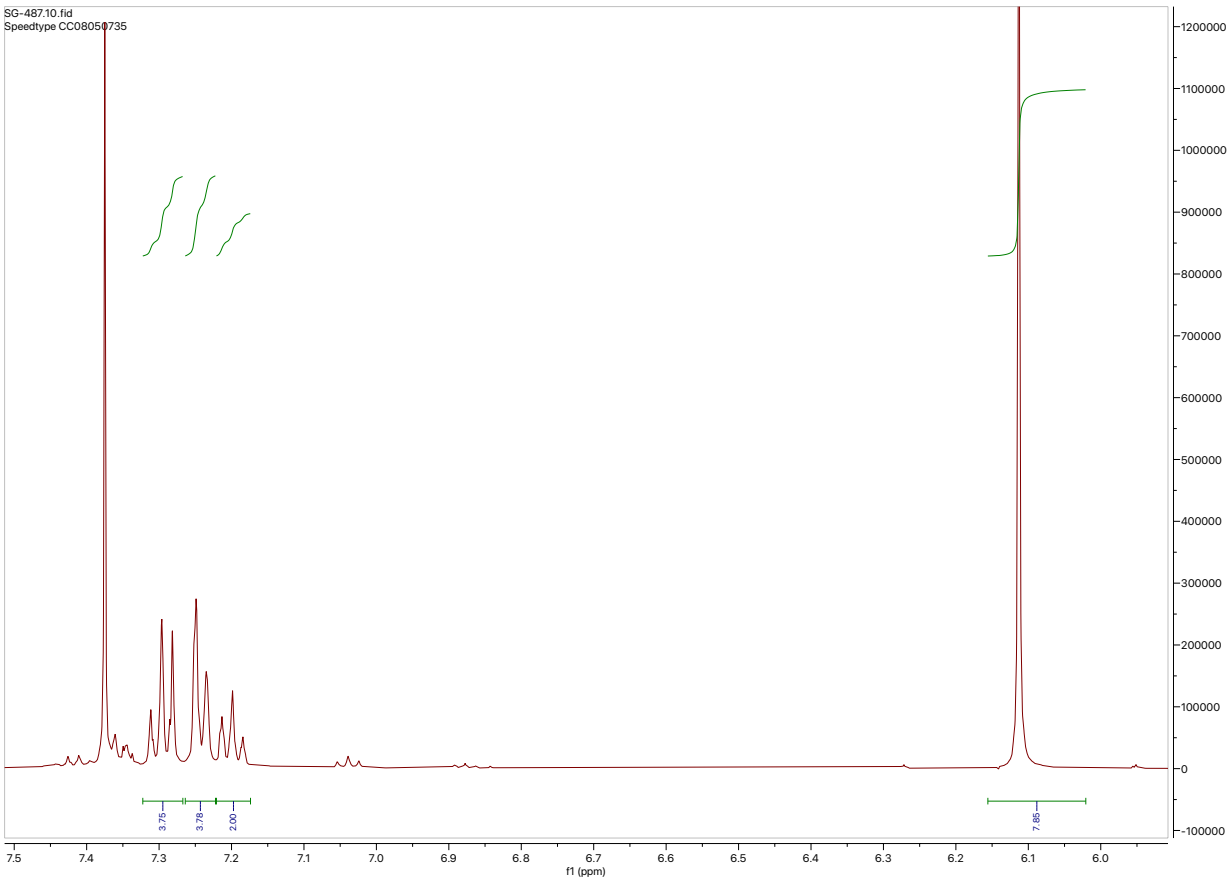

^{1}H-NMR

Reductive Coupling of Tosylhydrazones with PhenylBpin

To a 4-mL vial equipped with a stir bar was added (E)-N'-benzylidene-4-methylbenzenesulfonohydrazide (0.5 mmol, 1 equiv), potassium carbonate (1.2 mmol, 2 equiv) and 4,4,5,5-tetramethyl-2-phenyl-1,3,2-dioxaborolane (1 mmol, 2 equiv). Then, vial was diluted with dioxane (2 mL) and then sealed and allowed to stir at 100 °C for 18 h. The vial was cooled to ambient temperature, and filtered.

^{1}H-NMR yield was measured against trimethoxybenzene as an internal standard, 0%.

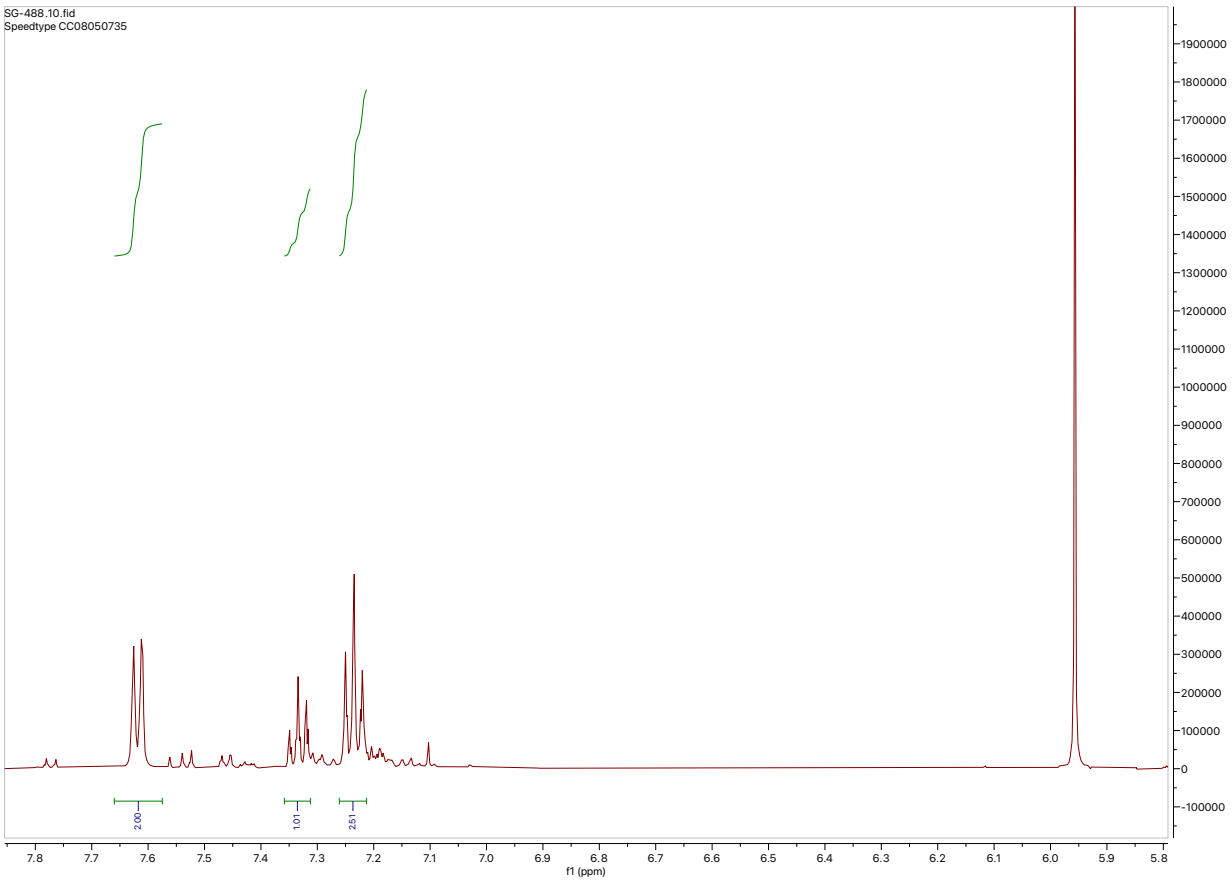

^{1}H-NMR

2.5 References

1. Stefan P. A. Hinkes and Christian D. P. Klein, Virtues of Volatility: A Facile Transesterification Approach to Boronic Acids. *Org. Lett.* **2019**, *21(9)*, 3048-3052.
2. Jaclyn M. Murphy, C. Christoph Tzschucke, and John F. Hartwig, One-Pot Synthesis of Arylboronic Acids and Aryl Trifluoroborates by Ir-Catalyzed Borylation of Arenes. *Org. Lett.* **2007**, *9(5)*, 757-760.
3. Babak Kaboudin, Ali Zangooei, Foad Kazemi and Tsutomu Yokomatsu, Catalyst-free Petasis-type reaction: Three-component decarboxylative coupling of boronic acids with proline and salicylaldehyde for the synthesis of alkylaminophenols. *Tet. Lett.* **2018**, *59*, 1046–1049.
4. Yoshiaki Takaya, Masamichi Ogasawara, Tamio Hayashi, Masaaki Sakai and Norio Miyaura, Rhodium-Catalyzed Asymmetric 1,4-Addition of Aryl- and Alkenylboronic Acids to Enones. *JACS* **1998**, *120(22)*, 5579-5580.
5. Julien C. Vantourout, Haralampos N. Miras, Albert Isidro-Llobet, Stephen Sproules, and Allan J. B. Watson, Spectroscopic Studies of the Chan–Lam Amination: A Mechanism-Inspired Solution to Boronic Ester Reactivity. *JACS Society* **2017**, *139(13)*, 4769-4779.
6. Hiroki Mandai, Kyouta Murota and Takashi Sakai, An Improved Protocol for Petasis Reaction of 2-Pyridinecarbaldehydes. *Tet. Lett.* **2010**, *51*, 4779–4782.

7. Jose Barluenga, Maria Tomas-Gamasa, Fernando Aznar and Carlos Valdes, Metal-Free Carbon–Carbon Bond-Forming Reductive Coupling between Boronic Acids and Tosylhydrazones. *Nat. Chem.* **2009**, *1*, 494–499.